

**TAXONOMY, TAPHONOMY AND SPATIAL DISTRIBUTION OF  
THE CERCOPITHECOID POSTCRANIAL FOSSILS FROM  
STERKFORTEIN CAVES**

Dipuo Winnie Mokokwe

A dissertation submitted to the Faculty of Science, University of the  
Witwatersrand, in fulfilment of the requirements for the higher degree of  
Doctor of Philosophy

July, 2016

## **DECLARATION**

I declare that this thesis is my own unaided work. It is submitted for the degree of PhD in the School of Geography, Archaeology and Environmental Studies, Faculty of Science at the University of the Witwatersrand, Johannesburg. It has not been submitted for any other degree or examination in other university.

---

Dipuo Winnie Mokokwe

\_\_\_\_\_ day of \_\_\_\_\_ 2016 \_\_\_\_\_

## ABSTRACT

Fossil primates are some of the most well represented fauna in South Africa's fossil Plio-Pleistocene cave sites. Sterkfontein preserves the largest number of fossil primates and a large portion of these are cercopithecoid remains. This research project provides a taxonomic analysis of the abundant fossil cercopithecoid post-cranial limb elements discovered at the site. One thousand five hundred fourteen identifiable fossil cercopithecoid postcrania from the Sterkfontein caves are analysed. From these, five genera are identified from morphologically diagnostic postcranial elements; these are *Papio*, *Parapapio*, *Theropithecus*, *Cercopithecoides* and *Cercopithecus*. *Theropithecus* is identified in Member 4, earlier than previously known. It is established that size, form and function are important factors in taxonomic studies. They play a major role in taxonomic examinations; however, they cannot be treated as disconnected facets of a taxonomic exercise. Each plays an essential role in taxonomic analyses. The study confirms that the Member 4 environment, which illustrates the turn from the Pliocene to the Pleistocene and the most mosaic of all the Plio-Pleistocene sites of the Cradle of Humankind World Heritage Site, samples the most faunal variability in the Sterkfontein Cave deposits. This research supports the hypothesis that carnivores were not the main accumulating agent for the cercopithecoid fossil remains within the caves. The carnivores, however, impacted the fossil cercopithecoid assemblage. Leopards and hyaenas are identified as some of the carnivores which accumulated the fossil cercopithecoids within the Sterkfontein caves. The research has opened a new scope for taxonomic analysis of isolated fossil cercopithecoid postcrania in the southern African fossil cave sites.

*To my kids: "all I do is for you"*

## ACKNOWLEDGEMENTS

The making of this thesis was by far the most challenging task of my life, however with the assistance and motivation of a number of people I was able to realize my dream of being a PhD holder. My supervisors, Associate Professor Ron Clarke and Professor Kathy Kuman were there since the first day, and their support inspired me to work hard. I thank them from the bottom of my heart. Professor Terry Harrison, Professor Leslea Hlusko, Dr Job Kibii and Dr Dominic Stratford commented on early scripts of the work. I cannot thank them enough for their support and assistance. Professor Lynn Wadley is one lecturer who always believed in me. Her words of motivation have gone a long way and contributed to my being here today. Thank you Prof Wadley, you are truly an inspiring human being. The following individuals allowed me access to their collections even at the most inconvenient of times, Dr Bernard Zipfel and Mr Sifelani Jirah of the ESI, as well as Ms Stephanie Potze and Dr Shaw Badenhorst of the Ditsong Museum of Natural History. I would also like to thank Professor Eric Delson of the New York Consortium of Evolutionary Primatology for providing me with access to the primate morphometrics data. Staff of the Evolutionary Studies Institute, as well as my colleagues at the Taung Skull World Heritage Site, Cradle of Humankind World Heritage Site: Blue IQ Projects and the Department of Science and Technology and their agencies were very supportive and always interested to hear about the making of this thesis.

My sister Keatlaretse Esther Mokokwe, brother Kegomoditswe Mokokwe, my uncles, Difako Sejwane, Michael Thaba Moremi and Nchipi Lechedi and my friend Ndukuyakhe Ndlovu were always inspiring me to reach for the stars, thank you very much. When my parents Irene Mamonnye Mokokwe and Jeremiah Bothata Mokokwe committed to educate their first daughter at whatever cost, they contributed to producing the first generation of literates in the family. It is through their commitment to my education that I am where I am today. I hope I have made them proud. Lastly, my loving husband Kereng

Kgotleng who kept motivating me to finish my thesis from the first day I registered, and who had to bear the brunt of being a homemaker when I was not able to due to commitments to my career. Thank you very much my love, you are one in a million.

The following financial institutions supported my PhD studies and I am grateful for their support:

Department of Science and Technology (DST);

Attaché for Science and Technology, Embassy of France in South Africa;

National Research Foundation, African Origins Platform grant; and

Palaeontology Scientific Trust (PAST)

Ms Andrea Leenen (PAST) and Mr. Vincent Baron (Attaché for Science and Technology Embassy of France in South Africa) deserve a special mention. They always came through when times were tough and were personally interested in ensuring that my studies were funded.

<b>CONTENTS</b>	<b>PAGE</b>
<b>DECLARATION</b>	<b>ii</b>
<b>ABSTRACT</b>	<b>iii</b>
<b>DEDICATION</b>	<b>iv</b>
<b>ACKNOWLEDGEMENTS</b>	<b>v</b>
<b>LIST OF FIGURES</b>	<b>xi</b>
<b>LIST OF TABLES</b>	<b>xiv</b>
<b>1. CHAPTER ONE - FOSSIL CERCOPITHECOIDEA OF THE STERKFontein CAVES</b>	<b>1</b>
1.1 The role of postcrania in understanding fossil cercopithecoid evolution in the Sterkfontein Caves	1
1.2 Identifying fossil cercopithecoid postcrania not associated with cranio-dental remains	3
1.3 The context of fossil cercopithecoid postcrania in primate evolution of the Sterkfontein Cave site	4
1.4 Research aims and objectives	5
1.5 Fossil cercopithecoid postcrania as behavioural and taxonomic indicators	6
1.6 Thesis Outline	7
<b>2. CHAPTER TWO - LITERATURE REVIEW</b>	
2.1. Study Area: Sterkfontein Cave site	9
2.1.1. <i>Member 1</i>	10
2.1.2. <i>Member 2</i>	11
2.1.3. <i>Member 3</i>	12
2.1.4. <i>Member 4</i>	12
2.1.5. <i>StW 53</i>	12
2.1.6. <i>Oldowan Infill</i>	13
2.1.7. <i>Member 5 West</i>	13
2.1.8. <i>Member 6</i>	13
2.1.9. <i>Post Member 6</i>	14
2.1.10. <i>Jacovec Cavern</i>	14
2.1.11. <i>Lincoln Cave</i>	14
2.2. The history of taxonomic classifications of the fossil cercopithecoids of the Sterkfontein Caves	15
2.3. Taxonomic re-assessments of some Sterkfontein fossil cercopithecoids	21
2.3.1. Genus <i>Cercopithecoides</i>	21

2.3.2. Genus <i>Parapapio</i> , Jones 1937	22
2.3.3. Genus <i>Papio</i> Erxleben 1777	23
2.3.4. Genus <i>Simopithecus</i> / <i>Theropithecus</i> Andrews 1916	23
2.3.5. Genus <i>Dinopithecus</i> . Broom 1937	23
2.3.6. Genus <i>Gorgopithecus</i> , Broom & Robinson 1949	24
<b>2.4. Analysis of the Sterkfontein Caves fossil cercopithecoid postcrania</b>	<b>25</b>
2.4.1 <i>Discriminant function analysis</i>	26
2.4.2 <i>Taxon free analysis</i>	26
<b>2.5. Form and function as indicators of locomotor and positional behavior</b>	<b>27</b>
<b>2.6. Inferring taxonomy on isolated postcranial elements</b>	<b>29</b>
<b>2.7. Spatial distribution of non-hominid fossil Primates at Sterkfontein Cave</b>	<b>38</b>
<b>2.8. Taphonomy of the fossil cercopithecoids of the Sterkfontein Caves</b>	<b>40</b>
<b>2.9. Identification of specific carnivore agents</b>	<b>43</b>
<b>3. CHAPTER THREE – MATERIALS AND METHODS</b>	<b>46</b>
<b>3.1 Materials</b>	<b>46</b>
3.1.1 <i>Excavated materials</i>	46
3.1.2. <i>Materials derived from the dumps</i>	47
3.1.3. <i>The condition of the collection</i>	48
3.1.4. <i>Comparative materials</i>	48
<b>3.2 Methods</b>	<b>51</b>
3.2.1. <i>Determining taxa of the Sterkfontein fossil cercopithecoid postcrania remains</i>	52
<b>3.3. Establishing diagnostic morphology from the modern skeleton: qualitative analysis</b>	<b>61</b>
a. Genus <i>Papio</i>	61
b. Genus <i>Cercopithecus</i>	64
c. Genus <i>Colobus guezara</i>	66
d. Genus <i>Mandrillus sphinx</i>	68
<b>3.4. Establishing diagnostic morphology from the modern skeleton: quantitative analysis:</b>	<b>70</b>
3.4.1 <i>Descriptive analysis</i>	70
3.4.2. <i>Results of the Bivariate Regression Analysis</i>	77
3.4.3. <i>Results for the Univariate Analysis of Variance (ANOVA)</i>	86
3.4.5. <i>Results of the Discriminant Function Analysis (DFA)</i>	87
3.4.6. <i>Summary of the statistical analysis</i>	95



3.5.	Identification of specific carnivore agents	97
3.6.	Skeletal element spatial clustering	98
4.	<b>CHAPTER FOUR - RESULTS: TAXONOMY OF THE STERKFORTEIN FOSSIL CERCOPITHECOID POSTCRANIA</b>	99
4.1.	<b>Systematic Palaeontology of the Sterkfontein fossil cercopithecoid postcrania</b>	99
4.1.1.	<i>Qualitative analysis</i>	99
4.1.2.	<i>Qualitative morphological comparison</i>	174
4.1.3.	<i>Quantitative analysis</i>	178
4.2.	<b>Quantitative analysis</b>	193
4.2.1.	<i>Bivariate regression</i>	193
4.2.2.	<i>Univariate analysis of variance</i>	201
4.3.	<b>Conclusions on the systematic palaeontology of the Sterkfontein fossil cercopithecoidea</b>	202
4.3.1.	<i>Form, function and taxonomy</i>	203
4.4.	<b>Fossil Cercopithecoid taxa identified per deposit within the Sterkfontein Caves</b>	205
4.4.1.	<i>Jacovec Cavern</i>	205
4.4.2.	<i>Silberberg Grotto</i>	206
4.4.3.	<i>Member 4</i>	207
4.4.4.	<i>Stw 53</i>	209
4.4.5.	<i>Oldowan infill</i>	210
4.4.6.	<i>Member 5 West</i>	210
4.4.7.	<i>Member 6</i>	210
4.4.8.	<i>Post Member 6</i>	211
5.	<b>CHAPTER FIVE - RESULTS: TAPHONOMY OF THE STERKFORTEIN FOSSIL CERCOPITHECOID POSTCRANIA</b>	212
5.1.	<b>Jacovec Cavern</b>	212
5.2.	<b>Silberberg Grotto</b>	215
5.3.	<b>Member 4</b>	217
5.4.	<b>StW 53</b>	222
5.5.	<b>Oldowan Infill</b>	223
5.6.	<b>Member 5 West</b>	224
5.7.	<b>Member 6</b>	226
5.8.	<b>Post Member 6</b>	226
5.9.	<b>Minimum numbers of individuals identified by taxa</b>	227
5.9.1.	<i>Jacovec Cavern</i>	227
5.9.2.	<i>Silberberg Grotto</i>	228
5.9.3.	<i>Member 4</i>	228
5.9.4.	<i>StW 53 Infill</i>	229
5.9.5.	<i>The Member 5 West deposit</i>	229

5.9.6. <i>The Oldowan Infill</i>	230
5.9.7. <i>The Member 6 deposit</i>	230
5.9.8. <i>The Post Member 6 deposit.</i>	230
<b>5.10. Carnivore tooth pit analysis</b>	<b>231</b>
<b>6. CHAPTER SIX RESULTS: SPATIAL DISTRIBUTION OF THE STERKFORTEIN FOSSIL CERCOPITHECOID POST-CRANIA</b>	<b>236</b>
6.1. <b>Jacovec Cavern</b>	<b>237</b>
6.2. <b>Silberberg Grotto</b>	<b>239</b>
6.3. <b>Member 4</b>	<b>241</b>
6.4. <b>STW 53</b>	<b>243</b>
6.5. <b>Oldowan Infill</b>	<b>244</b>
6.6. <b>Member 5 West</b>	<b>245</b>
6.7. <b>Member 6</b>	<b>247</b>
6.8. <b>Post Member 6</b>	<b>247</b>
6.9. <b>Sterkfontein deposits spatial patterns based on fossil cercopithecoid postcrania</b>	<b>248</b>
<b>7. CHAPTER SEVEN - DISCUSSION</b>	<b>249</b>
7.1. <b>Taxonomy of the fossil Cercopithecoidea of the Sterkfontein fossil cave site</b>	<b>249</b>
7.2. <b>Carnivore modification data</b>	<b>253</b>
7.3. <b>Taphonomy of the fossil cercopithecoidea of the Sterkfontein fossil cave site</b>	<b>254</b>
7.4. <b>Palaeoenvironmental and evolutionary implications of the Sterkfontein Caves fossil cercopithecoidea</b>	<b>257</b>
<b>8. CHAPTER EIGHT-CONCLUSION</b>	<b>259</b>
<b>9. REFERENCES</b>	<b>263</b>
<b>10. APPENDIX A: STERKFORTEIN FOSSIL CERCOPITHECOIDEA POSTCRANIA CATALOGUE</b>	<b>289</b>
<b>11. APPENDIX B: QUANTITATIVE ANALYSIS OF THE STERKFORTEIN FOSSIL CERCOPITHECOIDEA POSTCRANIA</b>	<b>357</b>
<b>12. APPENDIX C: TABLES</b>	<b>456</b>

LIST OF FIGURES	PAGE
Figure 2.1. Plan view of the main Sterkfontein fossil site to show the grid system	9
Figure 3.1. Plan of Sterkfontein site demonstrating the locality of the dumps in relation to the excavation sites	47
Figure 3.2. Illustration of measurements derived from the humerus	56
Figure 3.3. Illustration of measurements derived from the ulna	58
Figure 3.4. Illustration of measurements derived from the radius	59
Figure 3.5. Illustration of measurements derived from the femur	60
Figure 3.6. Modern <i>Papio</i> sp skeletal elements	61
Figure 3.7. Modern <i>Cercopithecus aethiops</i> skeletal elements	64
Figure 3.8. Modern <i>Colobus guezara</i> skeletal elements	66
Figure 3.9. Modern <i>Mandrillus sphinx</i> skeletal elements	68
Figure 3.10. Bivariate plot for 'anterior posterior length of humeral head and medio-lateral width of humeral head'	79
Figure 3.11. Bivariate plot for 'maximum proximo-distal length of olecranon fossa and maximum medio-lateral lateral length of olecranon fossa'	79
Figure 3.12. Bivariate plot for 'width of distal humeral articulation and bi-epicondylar width'.	80
Figure 3.13. Bivariate plot for 'humeral distal articulation and maximum medio-lateral breadth of olecranon fossa'.	80
Figure 3.14. Bivariate plot for 'width of humeral distal articulation and length of distal trochlea'.	81
Figure 3.15. Bivariate plot for 'ulna olecranon to anterior proximal trochlea notch and trochlea notch length'.	82
Figure 3.16. Bivariate plot for 'ulna proximo-distal height of olecranon and anterior-posterior length of olecranon process	83
Figure 3.17. Bivariate plot for 'olecranon proximo-distal length and trochlea notch proximo-distal length'.	83
Figure 3.18. Bivariate plot for ulna 'proximo-distal height of trochlea notch and medio-lateral breadth of trochlea notch'.	84
Figure 3.19. Bivariate plot for 'maximum diameter of radial head and perpendicular width of radial head'.	84
Figure 3.20. Bivariate plot for the 'radius neck anterior-posterior and medio-lateral breadth of radial neck'.	85
Figure 3.21. Bivariate plot for femur anterior-posterior neck breadth and medio-lateral neck width	86
Figure 3.22. Discriminant analysis plot for modern comparative humerus based on genera	88
Figure 3.23. Discriminant analysis plot for modern comparative ulna based on genera	90
Figure 3.24. Discriminant analysis plot for modern comparative radius based on genera	92
Figure 3.25. Discriminant analysis plot for modern comparative femur based on genera	94
Figure 4.1. SWP 504, a right proximal humerus and SWP 962, a left proximal humerus and BPI/C/541	105

Figure 4.2. From left to right, fossil specimens SWP 1141( <i>Papio/Parapapio</i> ), SWP 1271 ( <i>Papio/Parapapio</i> ), BPI/C/541 (modern <i>Papio</i> sp), UCMP 125868 ( <i>Papio izodi</i> ), UCMP 56693 ( <i>Procercocebus antiquus/Parapapio</i> ), SWP 1262 ( <i>Parapapio</i> ), SWP 1137 ( <i>Parapapio</i> ) and *KNM-ER 30298 (cf. <i>Parapapio</i> ).	105
Figure 4.3. On the left, the fossil SWP 523, a right <i>Parapapio</i> sp. proximal ulna and, on the right KNM-ER 30315 a left cf. <i>Parapapio</i> proximal ulna from Koobi Fora (Jablonski <i>et al.</i> 2008	107
Figure 4.4. BP/I/C/541, a modern <i>Papio ursinus</i> ulna	107
Figure 4.5. Figure 4.5. Top left insert, specimen EP 142/04, a <i>Parapapio ado</i> radius from Laetoli (After Harrison 2011). On the right, SWP 4243, a <i>Parapapio</i> radius and BPI/C 541, a modern <i>Papio</i> radius	109
Figure 4.6. A modern left <i>Papio ursinus</i> humerus and, on the right, SWP 2385, a right <i>Papio</i> sp proximal humerus.	113
Figure 4.7. SWP 4022, a fossil <i>Papio</i> radius specimen and BPI/C/541, a modern <i>Papio ursinus</i> radius.	120
Figure 4.8. BP/3/31923, a fossil <i>Papio</i> radius and BPI/C/541, a modern <i>Papio ursinus</i> radius	120
Figure 4.9. SWP 2792, a right proximal humerus demonstrating the head and the greater tuberosity which lie on the same level.	125
Figure 4.10. Left to right, BP/3/24000 (a left distal humerus) and BP/3/23016 (left distal humerus) demonstrating the elongated-ellipsoid shape of the olecranon fossa and a trochlea distal projection which is medially inclined.	126
Figure 4.11. SWP 853 a right proximal ulna.	134
Figure 4.12. SF 5496	138
Figure 4.13. On the left is SWP 1104, a left cf. <i>Theropithecus</i> proximal ulna and on the right is KNM-ER 1572, <i>Theropithecus oswaldi</i> from Koobi Fora.	145
Figure 4.14. A right modern <i>P. ursinus</i> ulna and SF 3418, a right proximal cf. <i>Theropithecus</i> sp ulna.	146
Figure 4.15. From left to right, cf. <i>Theropithecus</i> sp femora, SWP 4153, modern <i>Papio ursinus</i> BPI/C/541 and <i>Theropithecus</i> sp, SWP 4039 on the right.	149
Figure 4.16. SWP 1537, a left Papionini indet proximal femur.	168
Figure 4.17. SWP 738, a left Papionini indet proximal femur fragment.	168
Figure 4.18. On the left, SWP 4247, a proxima ulna Colobinae indet specimen and, on the right, a modern <i>Colobus guezara</i> ulna.	172
Figure 4.19. Extension of greater tuberosity relative to the humeral head.	175
Figure 4.20. Angle of the medial epicondyle.	191
Figure 4.21. Relative breadth of the medial epicondyle.	192
Figure 4.22. Relative length of radial neck index	193
Figure 4.23. Linear plot for maximum medio-lateral width of olecranon fossa (HDTROW) and width distal humeral articulation (HDTRWA).	195
Figure 4.24. Linear plot for humeral head diameter/medio-lateral width (HHDWTR) and humeral head anterior-posterior length (HHDWAP).	195
Figure 4.25. Linear plot for ‘maximum proximo-distal length of olecranon fossa and maximum medio-lateral length of olecranon fossa’.	196
Figure 4.26. Linear plot for ‘width distal humeral articulation (HDTRWA) and	196

width humeral trochlea (HDTRWT)'. Figure 4.27. Linear plot for 'width distal humeral articulation (HDTRWA) and anterior posterior distal humerus (HDTRWX)'.	197
Figure 4.28. Linear plot for 'ulna proximo-distal height of olecranon process and antero-posterior length of olecranon process'.	197
Figure 4.29. Linear plot for 'proximo-distal height of olecranon process and proximo-distal height of trochlea notch'.	198
Figure 4.30. Linear plot for 'maximum medio-lateral diameter of radial neck and anterior-posterior radius neck'.	198
Figure 4.31. Linear plot for 'femur anterior posterior length of femur head and medio-lateral breadth of femur head'.	199
Figure 4.32. Sterkfontein caves and Number of Identified Specimens (NISP) Minimum Number of Individuals (MNI) by taxa per deposit.	202
Figure 5.1 Jacovec Cavern fossil cercopithecoid postcranial skeletal element frequencies	213
Figure 5.2. Silberberg grotto fossil cercopithecoid postcranial skeletal element frequencies	216
Figure 5.3. Member 4 fossil cercopithecoid postcranial skeletal element frequencies	218
Figure 5.4. Example of the femur head fragments discovered within Member 4	221
Figure 5.5. Example of the femur head fragments discovered within Member 4.	221
Figure 5.6. StW 53 fossil cercopithecoid postcranial skeletal element frequencies	223
Figure 5.7. Oldowan Infill fossil cercopithecoid postcranial skeletal element frequencies	224
Figure 5.8. Member 5 West fossil cercopithecoid postcranial skeletal element frequencies	225
Figure 5.9. Post Member 6 fossil cercopithecoid postcranial skeletal element frequencies	227
Figure 5.10. SWP 1104, a left proximal cf. <i>Theropithecus</i> sp ulna with three carnivore tooth pits.	233
Figure 5.11. SWP 1140, a <i>Papio/Parapapio</i> distal humerus demonstrating carnivore toothpit marks	234
Figure 6.1. Sterkfontein Caves surface distribution demonstrating Member 4, Member 5 East, Member 5 West and the Post Member 6 infill.	237
Figure 6.2 Member 4 spatial distribution of skeletal elements based on age and size	240
Figure 6.3. StW 53 spatial distribution of skeletal elements based on age and size.	243
Figure 6.4. Oldowan Infill spatial distribution of skeletal elements based on age and size.	244
Figure 6.5. Member 5 West spatial distribution of skeletal elements based on age and size.	246

**LIST OF TABLES****PAGE**

Table 2.1. Primate taxa identified in southern African fossil cave sites	15
Table 2.2. Fossil cercopithecoid taxa identified in the Sterkfontein deposits based on crania and dentition	19
Table 2.3. Taxonomic reassignments of fossil cercopithecoidea which have been recorded at Sterkfontein Caves	23
Table 3.1. A list of comparative materials utilized in this study	49
Table 3.2. Comparative sample utilized from the PRIMO NYCEP	50
Table 3.3. Comparative materials from the literature	50
Table 3.4. Qualitative analysis of the proximal humerus	53
Table 3.5. Qualitative analysis of the distal humerus	54
Table 3.6. Qualitative analysis of the ulna	54
Table 3.7. Qualitative analysis of the radius	55
Table 3.8. Qualitative analysis of the femur	55
Table 3.9. Measurements derived from the humerus	57
Table 3.10. Measurements derived from the ulna	58
Table 3.11. Measurements derived from the radius	59
Table 3.12. Measurements derived from the femur	60
Table 3.13. Descriptive statistics of the humerus proximal medio-lateral breadth	70
Table 3.14. Descriptive statistics of the humeral head diameter	70
Table 3.15. Descriptive statistics of the humerus anterior posterior length of humeral head	70
Table 3.16. Descriptive statistics of the humerus anterior greater tuberosity diameter	71
Table 3.17. Descriptive statistics of the humerus bi-epicondylar breadth	71
Table 3.18. Descriptive statistics of the humerus medial trochlea flange length	71
Table 3.19. Descriptive statistics of the humerus lateral epicondyle to medial edge of trochlea	71
Table 3.20. Descriptive statistics of the humerus distal articular breadth	72
Table 3.21. Descriptive statistics of the humerus proximo-distal height of capitulum	72
Table 3.22. Descriptive statistics of the humerus maximum medio-lateral length of olecranon fossa	72
Table 3.23. Descriptive statistics of the humerus maximum proximo-distal length of olecranon fossa	72
Table 3.24. Descriptive statistics of the humerus axis of medial epicondyle	73
Table 3.25. Descriptive statistics of the ulna anterior-posterior length of olecranon process	73
Table 3.25. Descriptive statistics of the ulna proximo-distal height of olecranon process	73
Table 3.26. Descriptive statistics of the ulna medio-lateral breadth of olecranon process	73
Table 3.27. Descriptive statistics of the ulna Proximo-distal length of trochlea notch	74
Table 3.28. Descriptive statistics of the radius maximum dimension of radial head	74
Table 3.29. Descriptive statistics of perpendicular breadth of radial head	74
Table 3.30. Descriptive statistics of the radius proximo distal height of radial neck	74

Table 3.31. Descriptive statistics of the radius proximo distal height of radial neck and head	75
Table 3.32. Descriptive statistics of the femur anterior posterior head dimension	75
Table 3.33. Descriptive statistics of the femur medio-lateral breadth of femur head	75
Table 3.34. Descriptive statistics of the femur greater trochanter projection	75
Table 3.35. Descriptive statistics of the radius neck diameter	76
Table 3.36. Descriptive statistics of the femur medio-lateral neck diameter	76
Table 3.37. Descriptive statistics of the femur bi-epicondylar breadth	76
Table 3.38. Descriptive statistics of the radius neck shaft angle	76
Table 3.39. Descriptive statistics of the femur medial condyle width	77
Table 3.40. Descriptive statistics of the femur radius lateral condyle width	77
Table 3.41. Legend for the statistical plots.	78
Table 3.42. Eigenvalue and percent values for DFA results for modern comparative humerus based on genera	88
Table 3.43. Results for humerus, DFA Classification by genus	89
Table 3.44. Eigenvalue and percent values for DFA results for modern comparative ulna based on genera	90
Table 3.45. Results for ulna DFA Classification by genus	91
Table 3.46. Eigenvalue and percent values for DFA results for modern comparative radius based on genera.	92
Table 3.47. Results for radius DFA Classification by genus	93
Table 3.48. Eigenvalue and percent values for DFA results for modern comparative femora based on genera	94
Table 3.49. Results for femur DFA Classification by genus	94
Table 4.1. Qualitative assessment of the humerus based on taxa	176
Table 4.2. Qualitative assessment of the ulna based on taxa	177
Table 4.3. Qualitative assessment of the radius based on taxa	178
Table 4.4. Qualitative assessment of the femur based on taxa	179
Table 4.5. Descriptive statistics of the humerus anterior posterior length of humeral head	180
Table 4.6. Descriptive statistics of the humerus anterior greater tuberosity diameter	180
Table 4.7. Descriptive statistics of the humerus bi-epicondylar breadth	181
Table 4.8. Descriptive statistics of the humerus medial trochlea flange length	181
Table 4.9. Descriptive statistics of the humerus lateral epicondyle to medial edge of trochlea	181
Table 4.10. Descriptive statistics of the humerus distal articular breadth	182
Table 4.11. Descriptive statistics of the humerus proximo-distal height of capitulum	182
Table 4.12. Descriptive statistics of the humerus maximum medio-lateral length of olecranon fossa	182
Table 4.13. Descriptive statistics of the humerus maximum proximo-distal length of olecranon fossa	183
Table 4.14. Descriptive statistics of the humerus axis of medial epicondyle	183
Table 4.15. Descriptive statistics of the ulna anterior-posterior length of olecranon process	183
Table 4.16. Descriptive statistics of the ulna proximo-distal height of olecranon	184

process	
Table 4.17. Descriptive statistics of the ulna medio-lateral breadth of olecranon process	184
Table 4.18. Descriptive statistics of the ulna Proximo-distal length of trochlea notch	184
Table 4.19. Descriptive statistics of the radius maximum dimension of radial head	185
Table 4.20. Descriptive statistics of perpendicular breadth of radial head	185
Table 4.21. Descriptive statistics of the radius proximo distal height of radial neck	186
Table 4.22. Descriptive statistics of the radius proximo distal height of radial neck and head	186
Table 4.23. Descriptive statistics of the femur anterior posterior head dimension	186
Table 4.24. Descriptive statistics of the femur medio-lateral breadth of femur head	187
Table 4.25. Descriptive statistics of the femur greater trochanter projection	187
Table 4.26. Descriptive statistics of the femur neck diameter	187
Table 4.27. Descriptive statistics of the femur medio-lateral neck diameter	188
Table 4.28. Descriptive statistics of the femur bi-epicondylar breadth	188
Table 4.29. Descriptive statistics of the radius neck shaft angle	188
Table 4.30. Descriptive statistics of the femur medial condyle width	188
Table 4.31. Descriptive statistics of the femur radius lateral condyle width	189
Table 4.32. Descriptive statistics of the femur medial condyle width (MCW)	189
Table 4.33. Descriptive statistics of the femur lateral condyle width (LCW)	189
Table 4.34. Legend for the bivariate regression linear plots.	194
Table 4.35. Results of the ANOVA analysis	200
Table A1. Catalogue of specimens derived from Jacovec Cavern	288
Table A2. Catalogue of specimens derived from Silberberg Grotto	300
Table A3. Catalogue of specimens derived from Member 4	306
Table A4. Catalogue of specimens derived from StW 53	345
Table A5. Catalogue of specimens derived from the Oldowan Infill	349
Table A6. Catalogue of specimens derived from the Member 5 West	353
Table A7. Catalogue of specimens derived from the Member 6 and Post member 6	356
Table B1. Measurements derived from <i>Papio</i> sp humerus	357
Table B2. Measurements derived from <i>Papio</i> sp ulna	359
Table B3. Measurements derived from <i>Papio</i> sp radius	360
Table B4. Measurements derived from <i>Papio</i> sp tibia	361
Table B5. Measurements derived from <i>Papio</i> sp femur	362
Table B6. Measurements derived from <i>Cercopithecus aethiops</i> humerus	363
Table B7. Measurements derived from <i>Cercopithecus aethiops</i> ulna	364
Table B8. Measurements derived from <i>Cercopithecus aethiops</i> radius	365
Table B9. Measurements derived from <i>Cercopithecus aethiops</i> femur	366
Table B10. Measurements derived from <i>Cercopithecus aethiops</i> tibia	367
Table B11. Measurements derived from <i>Colobus</i> humerus	378
Table B12. Measurements derived from <i>Colobus</i> ulna	369
Table B13. Measurements derived from <i>Colobus</i> radius	370
Table B14. Measurements derived from <i>Colobus</i> femur	371
Table B15. Measurements derived from <i>Colobus</i> tibia	372
Table B16. Measurements derived from <i>Mandrillus sphinx</i> humerus	373



Table B17. Measurements derived from <i>Mandrillus sphinx</i> ulna	374
Table B18. Measurements derived from <i>Mandrillus sphinx</i> radius	375
Table B19. Measurements derived from <i>Mandrillus sphinx</i> femur	376
Table B20. Measurements derived from <i>Mandrillus sphinx</i> tibia	377
Table B21. List of abbreviations used in the PRIMO NYCEP database	379
Table B22a and b. Measurements derived from <i>Colobus</i> humeri	383
Table B23 Measurements derived from <i>Colobus</i> ulnae	384
Table B24 Measurements derived from <i>Colobus</i> radii	385
Table B25 Measurements derived from <i>Colobus</i> femora	386
Table B26a and b. Measurements derived from <i>Procolobus</i> humeri	388
Table B27 a and b. Measurements derived from <i>Procolobus</i> ulnae	389
Table B28. Measurements derived from <i>Procolobus</i> radii	390
Table B29. Measurements derived from the <i>Procolobus</i> femora	391
Table B30. Measurements derived from <i>Paracolobus</i> humeri	392
Table B31. Measurements derived from <i>Paracolobus</i> femur	393
Table B32. Measurements derived from <i>Rhinocolobus</i> humeri	394
Table B33. Measurements derived from <i>Cercopithecoides</i> humeri	395
Table B34a and b. Measurements derived from <i>Cercopithecoides</i> ulnae	396
Table B35 a and b. Measurements derived from <i>Chlorocebus</i> humeri	397
Table B36. Measurements derived from <i>Chlorocebus</i> radius	398
Table B37 a and b. Measurements derived from <i>Chlorocebus</i> ulnae	399
Table 38. Measurements derived from <i>Chlorocebus</i> femur	400
Table B39. Measurements derived from <i>Cercopithecus</i> humeri	401
Table B40 a and b. Measurements derived from <i>Cercopithecus</i> ulnae	404
Table B41. Measurements derived from <i>Cercopithecus</i> femora	405
Table B42. Measurements derived from <i>Papio</i> humeri	407
Table B43. Measurements derived from <i>Papio</i> radii	410
Table B43 a and b. Measurements derived from <i>Papio</i> ulnae	411
Table B45. Measurements derived from <i>Papio</i> femora	413
Table B46a and b. Measurements derived from <i>Mandrillus</i> humeri	416
Table B47. Measurements derived from <i>Mandrillus</i> radii	418
Table B48 a and b. Measurements derived from <i>Mandrillus</i> ulnae	419
Table B49. Measurements derived from <i>Mandrillus</i> femora	420
Table B50. Measurements derived from <i>Theropithecus</i> humeri	421
Table B51. Measurements derived from <i>Theropithecus gelada</i> radius	424
Table B52 a and b. Measurements derived from <i>Theropithecus</i> ulnae	425
Table B53. Measurements derived from <i>Theropithecus</i> femora	427
Table B54. Measurements derived from <i>Parapapio</i> humeri	429
Table B55. Measurements derived from <i>Parapapio</i> radii	430
Table B56. Measurements derived from <i>Parapapio</i> femora	432
Table B57a and b. Measurements derived from <i>Papio</i> humeri	433
Table B58. Measurements derived from <i>Papio</i> radii	436
Table B59. Measurements derived from <i>Papio</i> ulnae	437
Table B60a,b and c. Measurements derived from <i>Papio/Parapapio</i> humeri	438

Table B61a and b. Measurements derived from <i>Papio/Parapapio</i> ulna	442
Table B62. Measurements derived from <i>Papio/Parapapio</i> radii	444
Table B63a. Measurements derived from <i>Papio/Parapapio</i> femora	446
Table B64. Measurements derived from <i>Theropithecus</i> ulnae	447
Table B65. Measurements derived from <i>Theropithecus</i> femur	448
Table B66. Measurements derived from <i>Papionina</i> humerus	449
Table B67. Measurements derived from <i>Papionina</i> humerus	450
Table B68. Measurements derived from <i>Papionina</i> radius	451
Table B69. Measurements derived from <i>Papionina</i> femur	453
Table B70. Measurements derived from <i>Cercopithecus</i> sp radius	454
Table B71. Measurements derived from <i>Cercopithecoides</i> femur	455
Table C.1. Fossil cercopithecoid taxa identified in the Sterkfontein deposits based on post crania	457
Table C.2. Sterkfontein Caves combined skeletal frequencies, NISP	459
Table C.3. Jacovec Cavern skeletal frequencies, current study.	460
Table C.4. Jacovec Cavern skeletal frequencies by Kibii	460
Table C.5. Silberberg Grotto skeletal frequencies, current study	461
Table C.6. Member 2 Main excavation skeletal frequencies by Pickering <i>et al.</i>	461
Table C.7. Member 4 deposit skeletal frequencies, current study	462
Table C.8. Member 4 deposit skeletal frequencies by Kibii	462
Table C.9. StW 53 Infill skeletal frequencies, current study	463
Table C.10. StW 53 infill skeletal frequencies by Pickering	463
Table C.11. Oldowan Infill skeletal frequencies, current study	464
Table C.12. Oldowan Infill skeletal frequencies by Pickering	464
Table C.13. Member 5 West deposit skeletal frequencies, current stud	465
Table C.14. Member 5 West deposit skeletal frequencies by Pickering	465
Table C.15. Member 6 deposit skeletal frequencies, current study	466
Table C.16. Member 6 deposit skeletal frequencies by Ogola	466
Table C.17. Post Member 6 deposit skeletal frequencies, current study	467
Table C.18. Post Member 6 skeletal frequencies by Ogola	467
Table C.19. Sterkfontein fossil cercopithecoid postcrania carnivore modification tooth pit dimensions	469
Table C.20. Sterkfontein fossil cercopithecoid postcrania tooth pit true population mean	470
Table C21. Ordinary Least Squares Regression: maximum medio-lateral width of olecranon fossa (HDTROW) and width distal humeral articulation (HDTRWA)	471
Table C22. Ordinary Least Squares Regression: humeral head diameter/medio-lateral width (HHDWTR) and humeral head anterior-posterior length (HHDWAP).	471
Table C23. Ordinary Least Squares Regression: Maximum medio-lateral length of olecranon fossa-Maximum proximo-distal length of olecranon fossa	472
Table C24. Ordinary Least Squares Regression: HDTRWA-HDTRWT	472
Table C25. Ordinary Least Squares Regression: HDTRWX-HDTRWA	472
Table C26. Ordinary Least Squares Regression: Antero-posterior length of olecranon process and proximo distal height of olecranon process	473

Table C27. Ordinary Least Squares Regression: Proximo-distal height of olecranon process and proximo-distal height of trochlea notch	473
Table C28. Ordinary Least Squares Regression: Femur head anterior posterior length and femur medio-lateral width	473

## CHAPTER ONE

### FOSSIL CERCOPITHECOIDEA OF THE STERKFORTEIN CAVES

#### 1.1. The role of postcrania in understanding fossil cercopithecoid evolution in the Sterkfontein Caves

Southern African fossil hominin sites cover a very significant phase in the development of fossil primates and associated palaeoenvironments. This period is marked by environmental changes, climatic variability and survival through various adaptive mechanisms for these fossil primates (Jablonski & Leakey 2008). These transformations are particularly evident in the Sterkfontein fossil cave site which preserves the longest time span (4.17 My to 115,300) known for southern African fossil cave systems and has yielded the largest number of fossil primate remains. The site bears faunal evidence of these events from the Pliocene through to the late Pleistocene, therefore sampling the shift in faunal and palaeoclimatic events during that critical time in the southern African fossil record.

Fossil cercopithecoid remains have played a significant role in the development of palaeoanthropological studies in southern African fossil cave sites. The discovery of the first fossil hominin, *Australopithecus africanus* (i.e., the Taung skull), was set in motion by the numerous fossil cercopithecoid remains which were blasted out of the Taung limeworks by limeminers. A specimen of a fossil non-hominin primate was shown to Professor Raymond Dart, then head of the department of Anatomical studies at the University of the Witwatersrand, who, while taking keen interest in the fossil cercopithecoid remains, discovered a peculiar primate among breccia sent to him, which he named *Australopithecus africanus* (Dart 1925). This was to be one of the most prominent hominin discoveries of the 20<sup>th</sup> Century.

Fossil primates are some of the most researched and debated taxa in evolutionary studies and constitute the best represented fossil remains at Sterkfontein, particularly in Members 2 and 4.

Taxonomic analyses of the fossil cercopithecoids at Sterkfontein have mainly been based though not exclusively, on cranio-dental remains (Freedman 1957, Eisenhart 1974; Brain 1981; Kibii 2000, 2004; Pickering *et al* 2004a, Heaton 2006). This is justified as teeth are the most durable skeletal elements and are mainly reliable for taxonomic identification (Ciochon 1993). As a result, taxonomic analyses of postcranial remains have relied on association with cranio-dental specimens.

Few identified fossil cercopithecoid postcrania exist from southern African fossil cave sites. Research on the postcranial taxonomic identification has only recently been undertaken at Bolts Farm and Coopers cave sites (Gommery *et al.* 2008; De Silva *et al.* 2013). However, to date, there has been no fossil cercopithecoid postcranial remains directly associated with crania in southern African fossil cave sites. As a result, research on southern African fossil cercopithecoid has been very limited.

Most taxonomic descriptions of fossil cercopithecoid postcrania are made with reference to the East African cercopithecoids, the research on which is more advanced than in the southern African fossil cave sites. East African sites have sometimes preserved postcrania directly associated with taxonomically identifiable cranio-dental elements (Szalay & Delson 1979; Frost & Delson 2002; Jablonski *et al.* 2008; Harrison 2011). For example, the Hadar assemblage in Ethiopia and the Koobi Fora fossil sample from Kenya preserve a good sample of *Parapapio* postcrania with direct association to cranio-dental material in the East African Plio-Pleistocene (Frost & Delson 2002, Jablonski, Leakey & Anton 2008). In South Africa only the recently discovered post-crania material from Bolts Farm and Cooper's Cave have been taxonomically assigned to *Parapapio* (Gommery *et al.* 2008; De Silva *et al.* 2013). At Sterkfontein, only a few postcranial specimens from Member 4 have been investigated for taxonomic affinities (Ciochon 1993).

Although some of these have been the subject of several analyses, research theses and other publications (Pickering *et al.* 2004a, 2004b; Kibii 2000, 2004; Ogola 2009; Reynolds & Kibii 2011), only one known study by Ciochon (1993) has provided taxonomic analysis of a limited sample of the fossil cercopithecoid postcranial elements from the Sterkfontein Caves. The current study will be the first, at Sterkfontein, to provide an exclusive and comprehensive

analysis of the non-hominin fossil primate postcrania over time (from the earliest deposits, Member 2 and Jacovec Cavern to the youngest deposits such as Member 6 and Post-Member 6) at the Sterkfontein Caves. This study will provide a comprehensive morphological assessment of cercopithecoid postcranial specimens with preserved diagnostic traits within the various deposits.

The challenge posed by unassociated postcrania has to allow for possible regional species variation that could impact on comparability of specimens between regions. Specimens observed in the East African region could demonstrate variability from the southern African taxa and might not be directly comparable to southern African taxa. Secondly, unlike the East African material, the Sterkfontein postcrania sample consists of highly fragmented specimens impacted by rock fall, sediment compaction and blasting damage from lime mining, as well as by excavation damage by drilling and breccia breaking. This makes identification of anatomically distinguishable landmarks difficult and in many instances not feasible.

## **1.2. Identifying fossil cercopithecoid postcrania not associated with cranio-dental remains**

Studies have indicated that elbow joints are useful in identifying variation in primate locomotor modes and thus useful in taxonomic identification (Drapeau 2008). The anatomy of the primate elbow has received attention in the literature on morphology (e.g. Conroy 1976; Fleagle 1983; Rose 1973, 1974). This is because there are a number of morphological patterns in this area. In addition, the region is relatively well represented in the primate fossil record (Spoor *et al.*, 2007).

Two approaches will be undertaken to provide a thread between isolated postcranial elements and taxonomy. Independent assessments of the limb elements to make correlations to their functional significance and associated behavior will be the first methodological approach.

Comparative methods, which are also used in this study, make it possible to test the correspondence between skeletal traits and locomotor behaviour across a wide range of species while taking into account potential phylogenetic features (Spoor *et al.*, 2007). They allow inferences about individual behaviours that make up a locomotor profile, based on the most reliable indicators for behaviour (e.g., Silcox *et al.*, 2009). A comparative analysis will elucidate whether the extent to which form and associated function relate to the taxonomy of the fossil elements.

In the southern African context, fossil cercopithecoid postcranial remains have played little role in understanding taxonomic affinities, and in turn, phylogeny of the primates in the region. The abundance of fossil primate remains in the Sterkfontein deposits suggests that a large amount of data is missing from the understanding of the evolution of primates in South Africa. This has, in turn, led to reliance on data from other parts of the continent to determine a more comprehensive picture of the evolution of the fossil cercopithecoids in southern African sites. Data on the taxonomy of the postcrania will contribute to providing a more holistic overview of the Plio-Pleistocene ecosystem in the Sterkfontein valley area.

In this study I will test the hypothesis that taxonomic assignments can be made on isolated limb elements from the Sterkfontein fossil cercopithecoid assemblage. I will assess the lowest taxonomic rank to which the Sterkfontein fossil cercopithecoid postcranial elements can be assigned. The question of character combinations (qualitative assessment and size) as a predictor of function, and ultimately between taxa, will also be examined as a line of evidence for taxonomic analysis.

### **1.3. The context of fossil cercopithecoid postcrania in primate evolution of the Sterkfontein Cave site**

Taphonomic analyses of fossil fauna at Sterkfontein have indicated that carnivores have had an impact on their accumulation. In cases of carnivore accumulation, tooth-mark incidence is the only reliable indicator of a collecting agent in the Sterkfontein bone assemblages (Pickering *et al.* 2004b). There has been a debate on which carnivores may have been the likely agents in the

accumulation of the primate fossils, and how this could have affected their distribution within the cave system (Brain 1981; Pickering 1999). Though new techniques have been developed, such as tooth pit data, that aid in the identification of carnivores responsible for accumulation of a bone assemblage, no study has been conducted on the Sterkfontein fossil primate remains despite carnivores being implicated in the accumulation. Thus, analysis of the tooth pit data on the fossil cercopithecoid postcrania remains may reveal the identity of the predators.

The spatial study may help to detect clusters in distribution that inform about related fossil primate bone accumulation and the general mode of accumulation within the deposits. The study will add new dimensions and offer new insights into processes of cave deposit formation. In its entirety, this study will contribute towards ongoing research on fossil primate evolution in the Sterkfontein Valley area.

#### **1.4. Research aims and objectives**

A comprehensive taxonomic and taphonomic study of the fossil cercopithecoid postcrania in the Sterkfontein Caves has not previously been undertaken. The core of this project will be to provide taxonomic assignment to the abundant fossil cercopithecoid post-cranial limb elements discovered at the site. The project aims to provide a qualitative and quantitative assessment of morphologically diagnostic fossil cercopithecoid postcranial remains and assign them to family, genus and, where possible, species level.

The main research hypothesis is that taxonomic discrimination of skeletal elements at tribe level will be possible and morphological discrimination at genus level will be limited. The research will-

- 1) examine the extent to which Sterkfontein fossil cercopithecoid postcranial morphology can be linked to taxonomy and phylogeny;
- 2) determine if trait, size and shape can discriminate between taxa; and
- 3) establish the lowest taxonomic level to which these postcranial elements can be assigned.



Secondary to the taxonomic analysis, the taphonomy of the Sterkfontein fossil primates is assessed to attempt to determine the causal agent(s) responsible for accumulating the abundant fossil primate remains concentrated in Member 2, Jacovec Cavern, Member 4, StW 53 Infill, Member 5, Member 6 and Post-Member 6 infill. This will be achieved through tooth-pit analysis of the carnivore modification marks. The research project also seeks to provide an analysis of the spatial patterning of the fossil cercopithecoid postcrania remains that will aid in the interpretations of site formation processes.

### **1.5. Fossil cercopithecoid postcrania as behavioural and taxonomic indicators**

Through isolated skeletal elements it is possible to infer anatomical behavioural and environmental adaptations (Elton *et al.* 2003; Patel *et al.* 2007). Morphological analysis coupled with size assessments enable inferences to be made on behavior and taxonomic affiliations of the skeletal elements as demonstrated through a study undertaken on isolated cervical vertebrae from an early Pleistocene site of Pirro Nord Italy (Patel *et al.* 2007). In this study, morphological variation will be examined for implications on behavioural and taxonomic classification, and these will be compared to existing records on fossil cercopithecoid postcranial remains from East African sites.

## **1.6. Thesis Outline**

The thesis will undertake an investigation of the fossil cercopithecoid post-crania in seven chapters.

In the introduction (Chapter 1) taxonomy, taphonomy and the spatial analysis of the Sterkfontein fossil cercopithecoids are introduced to provide the reader with a background to the thesis. The research goal is outlined as addressing taxonomy, taphonomy and spatial clustering of the fossil cercopithecoids of Sterkfontein caves including the question of the significance of trait, form and function.

Chapter 2 provides a review of the literature on studies undertaken on the fossil cercopithecoids of the site and demonstrates the gaps in the research. The link between trait, form and function is explored in detail. The extent to which postcrania can be linked to form and function and ultimately taxonomy is examined.

In Chapter 3, comparative materials and specimens under study are described. Qualitative morphological assessment of the limb elements which will lead to correlations to their functional significance and associated behavior is undertaken. This analysis is supplemented by statistical correlation with existing data on taxonomically classified postcrania to make assumptions on their possible taxonomic affinities. Bivariate linear analysis is undertaken to determine the relationship among variables. The measurements are also analysed with a Univariate Analysis of Variance (ANOVA) to assess statistical differences of the identified traits among taxonomic groups. For a broader understanding of the context of these remains in relation to the mode of accumulation, tooth pit analysis methods are presented in order to assess the nature of carnivores involved.

Chapter 4 provides the results of the morphological analysis in two sections. In section 4.1 the reader is presented with the outcome of the qualitative examination of the limb elements to provide a basis for interpretations on locomotor adaptation. The second part (section 4.2)

demonstrates the results of the statistical analysis, Linear Regression and Discriminant Function Analysis) and makes comparisons to existing statistical data on similar elements. The concluding part of this Chapter (Section 4.3) uses these results to make inferences on the taxonomic affinities of the Sterkfontein fossil cercopithecoid postcrania. Five genera are identified within the assemblage which relate to cranio-dental fossil remains previously identified within the site.

Chapter 5 provides an outline of taphonomic interpretation of the fossil remains. The most crucial aspect of this chapter is data derived from tooth pit analysis which points to the identity of some of the carnivores that participated as accumulating agents at the site. Taphonomy of the fossil cercopithecoids is compared to existing data on hominins to elucidate whether these discriminate between cercopithecoids and hominins, and the impact of these taphonomic processes is compared against bovid and carnivore remains.

Chapter 6 outlines of the spatial clustering of fossil primate remains in the Sterkfontein Caves. Spatial clustering is illustrated to search for any spatial patterns that correlate with taxonomic and size classifications.

In Chapter 7, the author provides the discussion on the taxonomy and taphonomy of the fossil cercopithecoids of the Sterkfontein Caves. The role of the cercopithecoids in the evolution of primates in the Sterkfontein Valley and South African fossil cave sites is discussed.

In the concluding chapter (Chapter 8) the author concludes that trait, size and shape are important factors in taxonomic assessments of isolated skeletal elements. The research established that isolated fossil cercopithecoid postcrania can be assigned to taxonomic level, however, in the current context, not to the lowest taxonomic level, species. The possibility of more than one *Parapapio* species within the assemblage is found. Tooth pit analysis undertaken has revealed that hyenas and leopards are the main agents involved in the accumulation of the cercopithecoid fossil remains. The spatial arrangement of the postcrania has indicated variation over time.

## CHAPTER TWO

### LITERATURE REVIEW

#### 2.1. Study Area: Sterkfontein Cave site

The Sterkfontein fossil site is situated northwest of Johannesburg in the Gauteng Province of South Africa, within an area commonly known as Cradle of Humankind World Heritage Site. The site has yielded the largest concentrations of fossil primate remains in southern Africa (Pickering *et al.* 2004a, 2004b; Kibii 2000, 2004; Ogola 2009; Reynolds & Kibii 2011). Of these, the largest quantities are the fossil cercopithecoid remains, which outnumber fossil hominin remains, and are dominated by cranio-dental elements. The observed quantity and variety of species represented has implications for primate evolutionary research not only in the Sterkfontein Valley but in the southern African Plio-Pleistocene.

The main fossil-yielding area of the Sterkfontein Cave System contains infills (Figure 2.1) that were divided into six members within the Sterkfontein Formation (Partridge 1978). Stratigraphic analysis of the cave deposits demonstrated that although the succession of infills is complex, they appear discernable (Partridge 1978; Partridge & Watt 1991). A study of the lithostratigraphy showed that each infill preserves concentrations of rock, clay and sand usually different from overlying, underlying or adjacent strata (Partridge 1978). Below is a brief outline of the stratigraphic sequence as described by Clarke (2006), as well as some dates which have been provided for the deposits. Research in recent years has determined that although Partridge's stratigraphy provides a basic framework, there are many complications in the history of deposition and these are currently being investigated in greater detail (Stratford 2009).

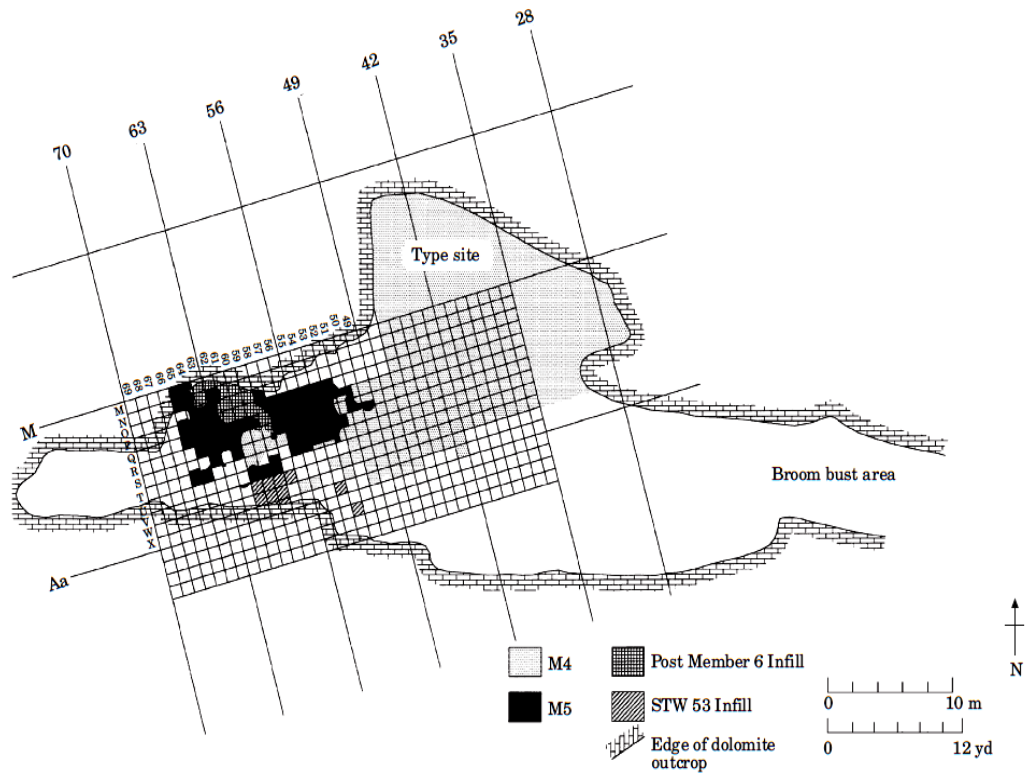


Figure 2.1. Plan view of the main Sterkfontein fossil site to show the grid system (From Kuman & Clarke 2000).

#### 2.1.1. Member 1

The Member 1 deposit, which mainly occurs on the floor of the Silberberg Grotto, was the first deposit to be formed prior to the cave surface opening (Partridge 1978). It consists of collapsed dolomite and chert blocks cemented with calcium carbonate and it bears no fossil or cultural material (Stratford 2008). Partridge (1978) demonstrated that Member 1 is older than the Member 2 deposits, which were later dated by the cosmogenic nuclide burial method using Aluminum-26 and Beryllium-10 to ca.  $4.17 \pm 0.14$  My (Partridge *et al.* 2003). Pickering and Kramers (2010) subsequently used flowstone in corings from the site and estimated that Member 1, being older than Member 2, would be  $>2.8$  Ma based on the Uranium Lead dating of Member 2. However, their date for Member 2 is now known to be erroneous (Bruxelles *et al.* 2014).

### 2.1.2. Member 2

Member 2 formed when sediments entered from a surface opening into the Silberberg Grotto (Clarke 2002, 2008). This was accompanied by deposition of faunal material which accumulated as a result of animals falling into the cavern and being trapped or killed in the fall (Pickering *et al.* 2004a). Palaeomagnetic analysis of the Member 2 flowstones in the Silberberg Grotto had estimated them to be between 3.60 and 3.22 My (Partridge *et al.* 1999). However, this infill was subsequently dated by Aluminum<sup>26</sup> and Beryllium<sup>10</sup> burial dates to ca  $4.17 \pm 0.14$  My (Partridge *et al.* 2003). Some other studies suggest younger dates, for example, U-Pb dates on the flowstone estimate Member 2 to be between 2.8-2.6 My and, according to Pickering and Kramers (2010), the duration of this deposition is uncertain. Herries and Shaw (2011) also undertook palaeomagnetic analysis of speleothems in the Sterkfontein Caves. Their study suggests that the STW 573 skeleton within Member 2 cannot be older than 2.58 My. This viewpoint is rejected by Bruxelles *et al.* (2014), who point out that all above dates on speleothems were on flowstones which were formed as infills within voids left by subsidence of breccia subsequent to the deposition of the hominin skeleton infill. A new study by Granger *et al.* (in press) now places Member 2 at well over 3 My.

Fauna represented in these deposits include cercopithecoids and remains of Felidae, Hyaenidae and Bovidae (Pickering *et al.* 2004a). Fossil cercopithecoid remains are the best represented skeletal elements within the Member 2 faunal assemblage, followed by Felidae skeletal elements (*ibid.*). In addition to an almost complete *Australopithecus* skeleton, there are articulating sets of specimens in the bovid and felid sub-assemblages. Due to their relative abundance in the infill, Member 2 is one of the deposits which points to the importance of fossil cercopithecids in the taphonomic history of the Sterkfontein cave fossil site. The abundance of fossil cercopithecoid remains over felids in the deposit has implications for the taphonomic history of the infill.

### 2.1.3. Member 3

This deposit lies beneath Member 4 and is exposed only within the Silberberg Grotto where it banked up against a large stalagmite boss that has since been removed by lime miners. It is one of the unexcavated deposits within the site. It is 8 metres thick and contains fossil faunal remains (Partridge & Watt 1991).

### 2.1.4. Member 4

Member 4 is the deposit in which Broom (1936) found the first adult *Australopithecus* specimen. It is described as a huge underground chamber filling consisting of calcified and partly calcified deposits (Kuman and Clarke 2000). It accumulated in an underground cavern extending from east to west of the site, with a later phase extending further west (Robinson 1962; Kuman & Clarke 2000; Ogola 2009). This deposit has proved to contain a large number of fossil primates including *Australopithecus* fossils and other fauna (Kibii 2004). It was labeled 'Lower Breccia' by Robinson (1962), then Member 4 by Partridge (1978). Its stratigraphy is currently being investigated by Stratford and Bruxelles. Pickering and Kramers (2010) dated a Member 4 flowstone to between  $2.65 \pm 0.30$  and  $2.01 \pm 0.05$  My. Palaeomagnetic analysis of Member 4 speleothem by Herries and Shaw (2011) suggests a date between 2.58 and 2.16 My. According to Bruxelles' ongoing research, however, all of the dated flowstones are post-depositional crack infills and therefore younger than the surrounding fossiliferous breccia (Clarke pers comm.).

### 2.1.5. StW 53 Infill

This infill is situated south of the Member 5 deposits (Kuman and Clarke 2000). The StW 53 deposit dates between Member 4 and the Oldowan stone tool infill of Member 5; it is likely to be younger than 2.6 My and older than 2 My (Kuman & Clarke 2000). The deposit preserves the hominin cranium, StW 53, which bears cutmarks on the zygomatic arch consistent with deliberate disarticulation (Pickering *et al.* 2000). This, however, has

been challenged by Clarke (2013) who considers the cuts to have been made naturally by pressure of a sharp edged chert rock within the deposit.

#### *2.1.5. Oldowan infill*

The Oldowan Infill developed through a centrally located vertical shaft (Kuman and Clarke 2000). The instability of the dolomite floor below this area appears to have led to the collapse of some of the Oldowan breccia into the underlying Name Chamber cavern (Clarke 1994; Kuman & Clarke 2000; Stratford 2008). The deposit is restricted to a 4 m (15 feet) horizontal surface, which suggests that the materials accumulated through a narrow vertical shaft. It preserves Oldowan style stone tools, various grassland fossil fauna remains (Pickering 1999) and lies at a level underlying the Acheulian infill. The Oldowan also preserves remains of *Paranthropus robustus* (Pickering 1999; Kuman & Clarke 2000)

#### *2.1.6. Member 5 West*

The Acheulian deposits accumulated subsequent to the Oldowan infill across the western part of the site, but the best preserved breccia is Member 5 West (Kuman & Clarke 2000; Ogola 2009). This infill has Early Acheulean stone tools including two bifaces and some large flakes, as well as remains of *Homo ergaster* (*ibid.*).

#### *2.1.7. Member 6*

Formerly known as the Upper Breccia (Robinson 1962), the Member 6 deposit filled a limited area between the dolomite roof and the underlying Member 5 breccia (Kuman & Clarke 2000). It preserves faunal remains belonging to the Orders- Primate, Artiodactyla and Carnivora (Ogola 2009), although primates are not common.



#### 2.1.8. Post Member 6

Subsequent to the deposition of Member 6, part of Member 5 was eroded in the northern area and left a channel that became filled with the post-Member 6 infill (*ibid.*). This infill, which bears Middle Stone Age artifacts, lies between the intact Member 5 West breccia and the eastern portion of Member 5 (Ogola 2009), which is not discussed here due to its poor context. Post Member 6 has remains of bushbuck, springbok, lechwe and waterbuck, (*ibid.*). The latter two species are water-dependent taxa, suggesting a swamp environment. Primate remains are the least represented fossil fauna in this younger infill.

#### 2.1.9. Jacovec Cavern

This cavern is located underground and seems unconnected to the main deposits. It is situated lower than and to the east of the main breccias exposed in the surface excavations (Wilkinson 1973). The cavern contains the deepest deposits in the Sterkfontein cave system consisting of an older orange breccia and a younger brown breccia (Partridge *et al.* 2003; Kibii 2000, 2004). The orange breccia has been dated by cosmogenic nuclide dating to ca.  $4.02 \pm 0.27$  while the brown breccia was dated to ca.  $3.76 \pm 0.26$  (Partridge *et al.* 2003). The dates are, however, no longer considered reliable by Darryl Granger who first calculated them (Clarke pers. comm.). Jacovec Cavern deposits preserve faunal remains belonging to the families Homininae, Cercopithecidae, Felidae and Bovidae (Kibii 2004). D. Stratford is currently conducting new excavations in this cavern and refining the stratigraphic interpretation.

#### 2.1.10. Lincoln Cave

The Lincoln Cave, which forms part of the Lincoln-Fault Cave System, is situated adjacent to the Sterkfontein Cave system (Reynolds *et al.* 2003). Two sections of the cave have been excavated: Lincoln Cave North and Lincoln Cave South. The excavated deposits have been dated using Uranium Series to between  $252,600 \pm 35,600$  and  $115,300 \pm 7,700$  years old on two flowstones present in Lincoln Cave North). These deposits,

which also contain intrusive fauna and artefacts eroded from Member 5, have yielded faunal remains belonging to *Homo ergaster*, four carnivore species (*Felis sp.*, *Canis sp.*, *Suricata sp.*, and an indeterminate hyena), four bovid species *Megalotragus sp.*, *Hippotragus sp.*, *Tragelaphus scriptus* and an indeterminate small duiker (Reynolds *et al.* 2007). Some diagnostic MSA stone artefacts have also been excavated from the deposits in Lincoln Cave North (Reynolds & Kibii 2011), which undoubtedly was once joined with the Lincoln Cave South breccias prior to disturbance by lime miners (Reynolds *et al.* 2007).

## **2.2. The history of taxonomic classifications of the fossil cercopithecoids of the Sterkfontein Caves.**

Research on the fossil cercopithecoid remains at Sterkfontein began in 1935 when T.R. Jones (1937) undertook the first known description of fossil primates from lime miners' blasting of what is now Member 4 in the Sterkfontein Caves. Since then large numbers of primate fossils have been uncovered at the site and numerous researchers have paid attention to fossil primate remains from the Sterkfontein deposits, which include the following provenances: Member 2 (Clarke, 1998; 1999; 2002; Clarke & Tobias 1995, Pickering *et al.* 2004a; Heaton 2006), Jacovec Cavern (Kibii 2000, 2004; Partridge *et al.* 2003); Member 4 (Broom 1936, 1937; Broom 1940; Freedman 1957; Freedman & Stenhouse 1972; Eisenhart 1974; Brain 1981; Delson 1984; Delson *et al.* 2000; Clarke 1988; Moggi-Cecchi *et al.* 1998; Elton 2001; Kibii & Clarke 2003; Pickering *et al.* 2004b; Kibii 2004; El Zaatari *et al.* 2005, Heaton 2006); Member 5 deposits (Hughes & Tobias 1977; Clarke 1994; Pickering 1999; Kuman & Clarke 2000; Pickering *et al.* 2000; Curnoe & Tobias 2006; Clarke 2008); as well as Member 6 and Post Member 6 (Robinson 1962; Ogola 2009) and Lincoln Cave (Reynolds 2000; Reynolds *et al.* 2007). Table 2.1 provides a synopsis of the fossil cercopithecoid taxa identified in southern African fossil cave sites.

Table 2.1.Cercopithecoid taxa identified in southern African fossil cave sites

<b>Taxon</b>	<b>Type Site</b>	<b>Holotype</b>	<b>Reference</b>	<b>Appearance at other sites</b>
<i>Parapapio antiquus</i>	Taung	Sts 5364	Haughton 1925	N/A
<i>Parapapio broomi</i>	Sterkfontein M4	Sts 564	Jones 1937	Makapansgat and Bolts Farm
<i>Parapapio jonesi</i>	Sterkfontein M4	Sts 565	Broom 1940 Freedman, 1957, 1970; Freedman and Brain, 1977	Swartkrans, Taung, Kromdraai, and Makapansgat
<i>Parapapio whitei</i>	Sterkfontein M4	Sts 563	Broom 1940; Brain, 1981; Delson, 1984	Taung, Swartkrans, Bolts' Farm and Makapansgat
<i>Papio izodi</i>	Taung	TP 7	Gear 1926	Sterkfontein
<i>Papio robinsoni</i>	Swartkrans	SK 555	Freedman 1957	Sterkfontein
<i>Papio angusticeps</i>	Kromdraai	KA 194	Broom 1940	Haasgat and Cooper's Cave, Minaar's Cave
<i>Papio spelaeus</i>	Pretoria	Unnumbered	Broom 1936	N/A
Genus <i>Cercocebus</i>			Geoffroy 1812	Sterkfontein
<i>Simopithecus (Theropithecus) darti</i>	Makapansgat	M 201,1326/1	Broom & Jensen 1946	Sterkfontein
<i>Simopithecus danieli</i> sp nov	Swartkrans	TMP 563	Freedman 1957	
<i>Theropithecus oswaldi</i>	Kanjera Kenya	BM A M 11539	Andrews 1916	Swartkrans; Sterkfontein and Hopefield
Genus <i>Dinopithecus</i>			Broom 1937	
<i>Dinopithecus ingens</i>	Schuverberg, Pretoria	SB 7	Broom 1937	Swartkrans
<i>Gorgopithecus major</i>	Kromdraai A		Broom & Robinson 1948	N/A
<i>Cercopithecoides williamsi</i>	Makapansgat	AD 1326	Mollet 1947	Bolts Farm, Haasgat, Swartkrans and Sterkfontein
<i>Cercopithecoides haasgati</i>	Haasgat	HGD 1165	Mckee <i>et al.</i> 2011	Haasgat

When Jones (1937) undertook the first analysis of fossil Cercopithecoidea at Sterkfontein Caves, he named the genus and species *Parapapio broomi*. Although he suggested the presence of a second species or genus within the collection, he did not identify the said taxon at the time (*ibid.*). Later, Broom (1940) analysed the Sterkfontein cercopithecoid collection and stated that the genus *Parapapio* consisted of three species: *Parapapio jonesi*; *Parapapio whitei* and *Parapapio broomi*. *Parapapio whitei* is the larger bodied of the three, and *Parapapio jonesi* is the smallest sized member (*ibid.*). Robinson (1952) referred to the presence of *Parapapio* in the Sterkfontein Lower Breccia (Member 4) and its absence in the nearby underground part of the cave known as the Graveyard site, which preserves *Papio* specimens indistinguishable from the modern *Papio ursinus*.

Freedman (1957) undertook a comprehensive study of the fossil cercopithecoid primates. According to him, 550 cercopithecoid specimens from Sterkfontein were recorded in the 1950's (Freedman 1957). Of these, he noted, only half were studied and the other half were either very small or very badly damaged fragments which offered no clues to their taxa. Freedman was referring to cranio-dental materials which seem to have occurred in larger quantities compared to the postcranial specimens. According to his observation there were a few postcranial bones within the collection (*ibid.*). Freedman (1957) also undertook a metric assessment of the cranio-dental materials in comparison to extant *Papio ursinus*. He validated the presence of the three *Parapapio* species at Sterkfontein as initially suggested by Broom.

Eisenhart (1974) also produced a detailed assessment of the fossil cercopithecoid sample. He observed that the diversity of the Sterkfontein materials is greater than the identified *Parapapio* species as most of the studies relied on dental size which is an unreliable indicator for taxonomic classification when used without any other additional data. Some of the materials identified as *Parapapio* he demonstrated to be *Cercocebus* remains and he also assigned some materials to the species *Papio wellsi* with characteristics similar to *Papio* specimens from Taung as initially identified by Freedman (Eisenhart 1974).

In the 1980s Delson undertook a different approach to determining taxonomic occurrences of fossil Cercopithecoidea at Sterkfontein and other African sites. He embarked on biochronological assessment of the African Plio-Pleistocene fossil cercopithecoids from which he made correlations between East and southern African fossil hominin sites (Delson 1984). The temporal framework applied in his study sought to create cercopithecoid faunal zonation based on co-occurrence of taxa. Twenty cercopithecoid taxa sequences and their geographic ranges were analysed, and the results demonstrated the presence of seven main zones defined by the presence of taxa and their relative frequency. Even though the framework is not best correlated to southern African fossil sites, fossil cercopithecoids from Sterkfontein Member 4 were classified in the African cercopithecoid (AC) 3 zone or the *Parapapio* acme-zone (*ibid.*). This zone occurs around 2.5 My in East Africa, and is accompanied by *Theropithecus darti*, *Theropithecus brumpti*, *Cercopithecoides williamsi* and *Papio hamadryas robinsoni*. A smaller, unidentified *Papio* or *Cercocebus* which also occurs at Makapansgat Members 2 and 4 is linked to this *Parapapio* acme zone (Delson 1984).

In the late 1990s Pickering (1999) undertook a study of the fossil remains from the western portion of the Sterkfontein excavations in the StW 53 infill and the Member 5 deposits, and found that primate numbers are less represented than in the older infills. He referred to the presence of *Theropithecus oswaldi* which Clarke identified based on dental specimens. A number of taxonomically indeterminate cercopithecines was also recovered from both infills. Within the StW 53 deposit dental remains of *Cercopithecoides williamsi* were also identified (Pickering 1999). Around the same period in the late 1990s Clarke and colleagues examined faunal remains occurring in the Member 2 deposit. A distinct feature of this member is that cercopithecines form the bulk of the faunal remains in the deposit. This is a taphonomic issue which will be explored later in this thesis. Member 2 has yielded a large concentration of fossil cercopithecoid remains and one complete skeleton of an *Australopithecus*, a mandible belonging to the extinct *Cercopithecoides williamsi*, and several crania belonging to *Parapapio jonesi*, *Parapapio broomi* and *Papio izodi* (Clarke 1998, 1999, 2002; Pickering *et al.* 2004a). At the turn of the 21<sup>st</sup> century fossil faunal remains from Jacovec Cavern were analysed by Kibii

(2000). Three hundred thirteen cercopithecoid cranio-dental and postcranial specimens belonging to fossil cercopithecoids were recorded. Kibii's analysis of the fossil cercopithecoid cranio-dental material identified the presence of four species: *Parapapio jonesi*, *Parapapio broomi*, *Papio izodi*, and a colobine as well as a taxonomically indeterminate cercopithecine.

Later Heaton (2006) reassessed taxonomic classifications of the Sterkfontein Cercopithecinae, in particular the tribe Papionini of Members 2 and 4. The study entailed a cranio-dental classification of fossils within the *Papio* and *Parapapio* genera and the intra and inter-specific variation thereof. Heaton (2006) noted the fragmentary nature of the Sterkfontein sample and that, despite many years of excavation, many of the elements recovered still remained too fragmentary to have a larger sample identified to the lowest taxonomic level, i.e. species level. Heaton's (2006) cranio-dental taxonomic categorization included quantitative and qualitative analysis of the sample. This study concluded that the fossil cercopithecoid species composition in Members 2 and 4 is similar and that only two species of *Parapapio* and one of *Papio* exist in Sterkfontein Members 2 and 4-*Parapapio broomi*, *Parapapio jonesi* and *Papio izodi*. Much younger than Members 2 and 4 are some deposits in Lincoln Cave adjacent to the main Sterkfontein cave system. Lincoln Cave preserves scant primate remains. In the two identified Lincoln Cave deposits (Lincoln Cave North and South) only five fossil cercopithecoid postcranial specimens were preserved (Reynolds 2000; Reynolds *et al.* 2003, 2007).

All the above taxonomic assignments were based on cranio-dental identifications and none attempted to identify the fossil Cercopithecoidea postcrania to taxa (Table 2.2). There are to date two studies by Elton (2000, 2001) and Ciochon (1993) which have examined some of the Sterkfontein fossil cercopithecoid postcrania. Of these two Elton (2000) provided a habitat classification of the specimens, and Ciochon (1993) assigned the specimens taxonomically.

Table 2.2. Fossil cercopithecoid taxa identified in the Sterkfontein deposits based on crania and dentition.

<b>Taxa</b>	<b>M2</b>	<b>Jacovec</b>	<b>M4</b>	<b>StW53</b>	<b>Oldowan</b>	<b>M5West</b>	<b>M6</b>	<b>Lincoln</b>
<i>Papio sp</i>			x					x
<i>Papio izodi</i>	x	x	x					
<i>Parapapio broomi</i>	x	x	x					
<i>Parapapio jonesi</i>	x	x	x					
<i>Parapapio whitei</i>			x					
<i>Theropithecus oswaldi</i>				x	x			
<i>Cercopithecus sp</i>							x	
<i>Cercopithecus aethiops</i>						x		
<i>Cercopithecoides</i>		x	x		x	x		
<i>Cercopithecoides williamsi</i>	x		x	x				
<i>Colobinae indet</i>			x					
<i>Colobus sp</i>		x						

### 2.3. Taxonomic re-assessments of some Sterkfontein fossil cercopithecoids.

Taxonomic classification of fossil specimens is an on-going exercise which relies heavily on availability (quality and quantity) of data to support the conclusions. As the Sterkfontein fossil fauna has been collected and studied for over eighty years it should be expected that the inventory of the specimens and the context of the fossil assemblage have changed over time, impacting on various taxonomic interpretations. The section below delves into the taxonomic status of fossil Cercopithecoidea occurring at Sterkfontein Caves and how these have transformed and, in some cases, resulted in re-classification of materials or assemblages. Table 2.3 provides a summary of these. The details of this debate in relation to papionini occurring in Sterkfontein Members 2 and 4 can be found in Heaton (2006). The history of taxonomic assignments of fossil cercopithecids at Sterkfontein, as at other sites, demonstrates that differing views on classification are a reflection of the availability and or paucity of diagnostic samples as well as trends in classification systems. Five genera which have been named at Sterkfontein Caves are discussed. It is these currently accepted assignments which will be followed in this study. The following taxonomic scheme will be pursued-for the genus *Cercopithecoides*, *Cercopithecoides williamsi* will be adopted; where, and if applicable, *Procercocebus antiquus* is recognized as suggested by Gilbert *et al.* (2016) and *Parapapio whitei* will be classified into *Parapapio broomi*; the only fossil *Papio* recognised is *Papio izodi*; specimens previously referred to as *Simopithecus* will be classed as *Theropithecus*; the genus *Dinopithecus* is not recognized at Sterkfontein; *Gorgopithecus* has not been described at Sterkfontein, as a result, it does not form part of discussion.

#### 2.3.1. Genus *Cercopithecoides* Mollet, 1947

The taxon *Cercopithecoides molletti* was first assigned to fossil colobine specimens from Swartkrans by Freedman (1957). He designated a new species because of morphological and size variation. However, it was later considered that the variation in dental specimens from the Swartkrans and Makapansgat assemblages pointed to intraspecific variety rather than a separate species (Freedman 1960). *Cercopithecoides molletti* thus has subsequently been classified as *Cercopithecoides williamsi* (Freedman 1960; Frost & Delson 2002).



### 2.3.2. Genus *Parapapio*. Jones 1937

Subsequent to Jones' (1937) naming of the species *Parapapio broomi*, other new species of this genus were assigned based on dental size variation. Eisenhart (1974) however found that there was an overlap in dental dimensions between some of the Sterkfontein cercopithecoids, emphasizing that dental size alone was not an accurate criterion for species identification. Moreover, Eisenhart (1974) observed that dental variations observed in these samples are not congruent with observed cranial variations. All of this information was later examined by Heaton (2006) in his doctoral thesis which undertook to re-assess taxonomic assignments of Papionini from Sterkfontein Member 2 and Member 4. In his study, Heaton concluded that *Parapapio broomi* demonstrated more variability than had been previously considered. He invalidated *Parapapio antiquus* and *Parapapio whitei* as independent species and included them as subspecies of *Parapapio broomi*. Gilbert (2007), however, rejected this conclusion on the basis that Heaton did not include extant taxa in his study. According to Gilbert (2007; 2013), fossils classed as *Pp. antiquus* have more affinities to the early *Cercocebus* lineage than to *Parapapio* and should thus be removed from the latter genus. Jablonski and Frost (2010) argue that *Pp. antiquus* shares affinities with *Cercocebus* and Mandrills and they also assign it to the *Cercocebus* lineage (*Procercocobus*).

Even though other scholars have provided distinguishing characteristics between *Parapapio whitei* and *Parapapio broomi* (e.g. Freedman 1957; Szalay & Delson 1979), Heaton (2006) invalidates *Parapapio whitei* and suggests that its type specimen, Sts 563, shares more affinities with male *Parapapio broomi*. According to Heaton (2006), specimens representing *Papio hamadryas robinsoni* were erroneously assigned to this species based on large dentition identified in the post-1966 sample without other supporting characteristics. Taxonomists were lumping specimens based on ambiguous traits, size and locality with limited classification methods and sample sizes. Specimens previously assigned to *P. hamadryas robinsoni* have subsequently been assigned to either *Parapapio broomi* or *Papio izodi* (Heaton 2006). Contrary to Heaton's analysis, Jablonski and Frost (2010) recognize the presence of *P. robinsoni*, in addition to *P. izodi* and *P. angusticeps*. They argue that *P. izodi* is a distinct species from modern *P. hamadryas* and *P. robinsoni* is a subspecies of the living *P. hamadryas*.

### 2.3.3. Genus *Papio*. Erxleben 1777

Since most materials from Sterkfontein had been identified as *Parapapio*, Eisenhart's (1974) study indicated more variability in the fossil cercopithecoid sample and suggested the presence of a different species at Sterkfontein. Some of the materials he noted to share affinities with cranio-dental remains that had been previously identified at Taung, *Papio wellsi*. The identification of this species at Sterkfontein has since been questioned due to lack of convincing characteristics on identified specimens and they were re-assigned to *Papio izodi* (Szalay & Delson 1979; McKee 1993).

### 2.3.4. Genus *Simopithecus*/*Theropithecus*. Andrews 1916

*Simopithecus oswaldi* was first described by Andrews (1916) based on dental remains from Homa (Kanjera), Kenya. Andrews was the first author, in 1916, to demonstrate similarities in tooth morphology between *Simopithecus* species and the extant *Theropithecus gelada* (Maier 1972). Maier (1970, 1972) and Jolly (1970, 1972) considered that *Simopithecus* and *Theropithecus* show the same specialization and share many significant features. Maier (1972) contended that the two genera be retained as separate genera within a related lineage. However, there is now consensus *Simopithecus* should be classed within the genus *Theropithecus* (Jolly 1972; Freedman 1976). Jablonski and Frost (2010) argue that *Theropithecus* derives from a papionin ancestor around 3.5Ma and 4 Ma.

### 2.3.5. Genus *Dinopithecus*. Broom 1937

*Dinopithecus* was initially described from Schurveberg 1, in the then Transvaal (South Africa) by Broom (1937). Some fossils from Swartkrans Member 1 were later assigned to this genus and noted to exhibit large rugged skulls with considerable sexual dimorphism and fairly long muzzles in the females (Freedman 1957). The use of this taxon was abandoned and materials assigned to this genus from Omo are now placed in *Theropithecus* (Simons & Delson 1978). Later assessments of this genus suggest that *Dinopithecus* has affinities to *Papio quadratiostris* and should be included in the *Papio* genus as a sub-species (Delson & Dean, 1993). Although Gilbert (2013) finds that there is little similar morphology to link *Dinopithecus* to the

*Soromandrillus quadratiostris* clade (with *Mandrillus/Cercocebus/Procercocebus*) or the *Theropithecus* clade, he argues that *Dinopithecus* is a stem African papionin.

#### 2.3.6. Genus *Gorgopithecus*. Broom & Robinson 1949

The type specimen for this genus is *Gorgopithecus major* identified at Kromdraai A (Broom & Robinson 1949). It is a medium to large sized papionin. Recently the genus has been identified at Olduvai Gorge in Tanzania among fossil remains previously identified as cf. *Papio* sp (Gilbert *et al.* 2015).

Table 2.3. Taxonomic reassignments of fossil Cercopithecoidea which have been recorded at Sterkfontein Caves

Genus/Species	Conclusion	Re-assignment	Reference
<i>Parapapio antiquus</i>	Not the same as <i>Parapapio</i>	<i>Cercocebus</i> lineage	Gilbert 2007, 2013 and 2016; Jablonski & Frost 2010
<i>Papio hamadryas</i>	Subspecies of <i>P. robinsoni</i>	<i>P. hamadryas robinsoni</i>	Jablonski & Frost 2010
<i>Parapapio whitei</i>	Invalidated	<i>P. broomi</i>	Heaton 2006
<i>Parapapio makapania</i>	Invalidated	<i>P. broomi</i>	Freedman 1957
<i>Parapapio angusticeps</i>	Not <i>Parapapio</i>	<i>Papio angusticeps</i>	Freedman 1957; Jablonski & Frost 2010
<i>Papio spelaeus</i>	Same morphology as <i>P. ursinus</i>	<i>Papio</i> cf. <i>ursinus</i>	Freedman 1975
<i>Papio robinsoni</i>	Invalidated	<i>Papio izodi</i> and <i>Parapapio broomi</i>	Heaton 2006
<i>Papio wellsi</i>	Invalidated	<i>P. izodi</i>	Szalay & Delson 1979; Mckee 1993
<i>Cercopithecoides molletti</i>	Re-assigned to <i>C. williamsi</i>	<i>C. williamsi</i>	Freedman 1961
<i>Simopithecus</i>	Same genus as <i>Theropithecus</i>	<i>Theropithecus</i>	Stark & Frick 1958; Maier 1972

#### 2.4. Analysis of the Sterkfontein cave fossil cercopithecoid postcrania

Some approaches have been applied which have provided an indication of the taxonomic variation of some of the non-hominin fossil primate postcrania at Sterkfontein Caves. Two prominent studies have used discriminant functional analysis and taxon free analysis. These research projects sampled some of the Sterkfontein fossil cercopithecoid postcrania to determine either the taxa or habitat preferences based on locomotor data derived from limb elements. These studies form the foundation for fossil cercopithecoid postcrania taxonomic investigations at Sterkfontein Caves.

a) *Discriminant function analysis*

Ciochon (1993) undertook a multivariate analysis of postcrania of southern African fossil Cercopithecoidea and described functional and systematic differences in the extant cercopithecoid forelimb. The study entailed application of standard and novel multivariate statistical techniques to quantify patterns of variation in the forelimb of 20 species of living and extinct cercopithecoids. In this analysis he noted that even though the law of closest living relative is applied to his study, Pliocene taxa share little affinity to any extant members of his comparative sample.

Ciochon (1993) analysed 27 postcranial elements from Sterkfontein Member 4 and other materials from Makapansgat, Taung, Swartkrans and Kromdraai. His results suggest the presence of some previously un-identified taxa within the Sterkfontein Caves. Some of his results resonate with Eisenhart's 1974 study and also correlate with Delson's (1984) conclusions on biochronological assessment of Sterkfontein fossil Cercopithecoidea. From the 27 elements studied from Member 4, Ciochon (1993) identified five genera (*Theropithecus darti*, *Papio cf robinsoni*, *Parapapio indet*, *Cercopithecoides* and *Cercocebus sp*). *Theropithecus darti* is the peculiar one which had not been previously identified at Sterkfontein prior to this study.

Ciochon (1993) identified an early form of *Papio* which he states had been previously misidentified as a *Parapapio*, and he classified one skeletal element, STS 1087, as *Cercocebus*, a genus which had also been previously identified by Eisenhart on cranial fossils. Ciochon (1993) identified *Papio cf robinsoni* from the postcrania and *Theropithecus darti* which had not been previously identified at Sterkfontein.

b) *Taxon free analysis*

Elton (2000) undertook a locomotor and habitat classification study by examining post-cranial morphology of the fossil cercopithecoids of Sterkfontein Member 4, Bolt's Farm and Swartkrans. She employed a taxon-free multivariate study in which statistical discriminant function study was used to determine variation between bony elements which would ultimately determine the variability in habitat and locomotor preferences (Elton 2000, 2001). Although the

study did not necessarily assign the specimens to taxonomic groups, the habitat and locomotor data derived are useful in determining the ecology of the area. The habitat categories identified are: 'forest arboreal', which relates to forest living quadrupeds; 'open mixed' suggesting a mix of arboreal and terrestrial quadrupeds; and open habitat quadrupeds represented by the 'open terrestrial' category.

The bony elements used were the proximal and distal humerus, the proximal ulna, and the distal femur (Elton 2000, 2001). Only 'well preserved' specimens were included in the analysis which therefore excluded much of the Sterkfontein non-hominin fossil primate postcrania. Twenty five specimens from Sterkfontein were assigned to the following habitat categories: four to 'forest arboreal' 15 to 'open mixed' and six to 'open terrestrial'. The highest percentage of locomotor type discovered from Sterkfontein Member 4 was assigned to the 'open mixed' category. Due to the limited sample in the study, Elton used the percentages of categories only to suggest the presence of habitat types found during accumulation of Member 4, and thus there might not necessarily be a complete representation of the Sterkfontein Member 4 fossil monkey habitat. These two studies provide a sample of fossil Cercopithecoidea taxa and habitat preferences available in the Sterkfontein cave sites. Of the two, Ciochon's study demonstrates the importance of functional elements as possible taxonomic indicators which can provide data not yet derived from cranio-dental remains.

## **2.5. Form and function as indicators of locomotor and positional behavior**

To date, little is known about the degree to which taxonomic assignments can be made to isolated postcranial skeletal elements (Elton *et al.* 2003, Patel *et al.* 2007). Skeletal remains with identifiable morphological traits are the only evidence which can be used to make interpretations on function, behaviour and, where comparative materials exist, related taxonomic links. Limb elements particularly are the main postcranial skeletal parts which can shed light on the subject.

Even in light of the little evidence which shows the degree to which taxonomic assignments can be made to fossil cercopithecoid postcranial elements, studies have been undertaken which examine the monkey's behavioural preferences. Such data enables researchers to make inferences about the locomotor behavior of fossil remains from skeletal shape variations that are

associated with behaviour, which can then be used to interpret the palaeobiology of fossil primates.

Various postcranial elements have been utilised to theorize on monkey locomotor preferences. Rein *et al* (2015) established a predictive model which can be applied to infer significance of behaviours. They were able to demonstrate that shape exploration and predictive analysis can be applied to limb bones and to other positional behaviours in order to uncover those aspects. In their field study of locomotor patterns for extant new world monkeys, Youlatos and Meldrum (2011) utilise the talus to hypothesize that platyrrhine species have ecological niches. They found that these monkeys have a range of locomotor adaptations. This ranges from small bodied monkeys with morphological adaptation for claw climbing and leaping, medium sized variation with adaptation for generalised locomotion and large bodies animals with adaptation for climbing and suspension (Youlatos & Meldrum 2011). Ruff (2002) established the relationship between long bone epiphyses and diaphyses structural proportions and found that movement or limb positioning is related to long bone structure. Species with slow cautious movements have larger articular to cross section shaft proportions and species with more forelimb suspensory movements show relatively larger and stronger forelimbs while stronger and or larger forelimbs are observed in species with an emphasis on leaping; however, structure and function did not always covary with taxonomy (Ruff 2002, 2003). Ruff (2003) also indicates that some morphological dimensions, such as the medio-lateral breadth of the proximal tibia are not the best locomotor predictors. In the context of Sterkfontein fossil cercopithecoid postcrania, this lack of direct correlation between structure/function and taxonomy suggests that isolated postcrania can be linked to function, however, taxonomic assignments have to be made independently of functional or behavioural assumptions. A study of locomotor differentiation in mangabey morphology demonstrates that limb anatomy, particularly in the humerus and femur, shows differences between arboreal and terrestrial species (Nakatsukasa 1996). The same variation is found in colobine limb morphology. Egi *et al.*'s (2007) study of the distal humerus and ulna of *Parapresbytis*, a colobine from the Russian Pliocene, showed structural differences between terrestrial colobines. According to Gebo (1993) all arboreal cercopithecoid monkeys are secondarily arboreal as few adaptations can be seen in the foot. He asserts that old world monkeys were arboreal, went through a terrestrial phase and regained arboreality recently (Gebo 1993).

## **2.6. Inferring taxonomy on isolated postcranial elements**

Ruff's (2002) analysis has indicated that structure and function do not always covary with taxonomy. However, there is a link which can be made between specific taxa and a suite of characteristics which can enable estimations to be made on taxonomic affinities. Analysis of morphological variations and morphometric relationships and establishing exclusions enables calculated assumptions to be made on the taxonomic affinities of skeletal elements. The discovery of fossil cercopithecoid postcranial skeletal remains associated with cranio-dental remains in East African sites provides a foundation for these taxonomic approximations.

As observed by Ciochon (1993), limb elements make valuable contributions to the understanding of phyletic affinities and palaeoecology of extinct primates and, due to their functional significance, are a good basis for taxonomic investigations. Due to the relatively higher frequency of isolated cercopithecoid limb elements in the Sterkfontein fossil faunal assemblage, the current research thesis will focus on limb elements discovered at the site and their usefulness as gauges for taxonomic classification.

Two approaches will be undertaken to provide a thread between isolated postcranial elements and taxonomy. Independent assessments of the limb elements to make correlations to their functional significance and associated behavior will be the first methodological approach.

Comparative methods make it possible to test the correspondence between skeletal traits and locomotor behaviour across a wide range of species while taking into account potential phylogenetic features (Spoor *et al.*, 2007). They allow inferences about individual behaviours that make up a locomotor profile, based on the most reliable indicators for behaviour (e.g., Silcox *et al.*, 2009). A comparative analysis will elucidate whether the extent to which form and associated function relate to the taxonomy of the fossil elements.

In the southern African context, fossil cercopithecoid postcranial remains have played little role in understanding taxonomic affinities, and in turn, phylogeny of the primates in the region. The abundance of fossil primate remains in the Sterkfontein deposits suggests that a large amount of data is missing from the understanding of the evolution of primates in South Africa. This has, in turn, led to reliance on data from other parts of the continent to determine a more comprehensive



picture of the evolution of the fossil cercopithecoids in southern African sites. Data on the taxonomy of the postcrania will contribute to providing a more holistic overview of the Plio-Pleistocene ecosystem in the Sterkfontein valley area.

Studies have indicated that elbow joints are useful in identifying variation in primate locomotor modes and thus useful in taxonomic identification (Nakatsukasa 1994, 1996; Ruff 2002, 2003; Drapeau 2008; Patel 2007). In addition, authors such as Jablonski *et al.* (2008) developed comprehensive landmark analysis data to evaluate variation in species occurring at Koobi Fora. Other authors have provided detailed morphological descriptions of fossil cercopithecoid postcrania which occur in the African Plio-Pleistocene fossil record. Frost and Delson (2002) have described postcranial remains of *Theropithecus*, *Parapapio*, *Rhinocolobus*, *Cercopithecoides meaveae* and *Cercopithecoides kimeui* from Hadar, Ethiopia. Harrison (2011) has illustrated fossil cercopithecoid remains of *Parapapio ado*, *Parapapio* sp., *Cercopithecoides* sp. and *Rhinocolobus* sp. from Laetoli in Tanzania. Nakatsukasa (1994) provides a detailed analysis of *Cercopithecus* and *Cercocebus* limb bone elements which occur in African sites.

Subfamily	Cercopithecinae Gray 1921
Tribe	Papionini Burnett 1828
Subtribe	Papionina Burnett 1828
Genus	<i>Parapapio</i> . Jones 1937

*Parapapio* is a small to medium sized fossil papionin which occupied South and East Africa during the Pliocene. The smallest of the *Parapapio* genus in southern African fossil caves, *Pp jonesi* females from Sterkfontein are estimated to have weighed between 9.5kg and 13.5kg while their male counterparts are estimated at 14kg and 20kg (Delson *et al.* 2000). The fossil *Parapapio cf jonesi* sample from Hadar also has size ranges similar to the southern African fossils. *Parapapio whitei* specimens from Makapansgat, which Heaton (2006) recently assigned to male *Parapapio broomi*, suggest that it was heavier. Males belonging to *Pp. broomi* are estimated to have weighed between 20kg and 30kg (Delson *et al.* 2000). *Parapapio ado* from Laetoli is estimated to have been similar in weight to *Parapapio jonesi*; males are approximated to have weighed between 17kg and 25kg while females range between 10kg and 14kg (*ibid.*).

Unlike *Papio*, *Parapapio*'s fossil history is relatively better known and postcranial remains of *Parapapio* species (*ado* and *jonesi*) have been identified, particularly in East African sites such as Laetoli (Leakey & Delson 1987; Harrison 2011), Koobi Fora (Jablonski, Leakey & Anton 2008) and Hadar (Frost & Delson 2002). In South African sites fossil *Parapapio* cranio-dental materials have been intensely studied (e.g. Freedman 1957; Thackeray & Myer 2004; Heaton 2006). However, very few studies have focused on postcranial remains. Known research on fossil *Parapapio* postcrania in South Africa is based on material studied by Gommery *et al.* (2008) from Bolt's Farm Waypoint 160 and fossil remains from Cooper's Cave (De Silva *et al.* 2013). Bolt's Farm *Parapapio* postcranial material is preserved in the same breccia block with dentition belonging to the same genus and is presumed to belong to the same individual (Gommery *et al.* 2008). This occurrence is a rarity in the South African fossil cave sites.

Conclusions on *Parapapio sp.* postcrania from Waypoint 160 suggest that it was a terrestrial to semi-terrestrial monkey. *Parapapio ado* skeletal remains from Laetoli also indicate that the species was a slender and agile semi-terrestrial monkey (Harrison 2011). Koobi Fora *Parapapio* anatomy points to their generalist nature in terms of habitat; the elbow joints in these specimens

lack extreme arboreality or terrestrially adapted morphology while cranio-dental material points to a generalist herbivore diet (Jablonski & Leakey 2008). *Parapapio* fossil remains from Bolt's Farm, specimens WP1 and WP2, are considered but are too fragmentary to be used for comparison in this study.

Subfamily	Cercopithecinae Gray 1921
Tribe	Papionini Burnett 1828
Subtribe	Papionina Burnett 1828
Genus	<i>Papio</i> . Eerxleben, 1777

*Papio* is a medium to large terrestrially adapted cercopithecoid. According to a body mass index study undertaken by Delson *et al.* (2000), the estimated body mass from the dentition of specimens previously assigned to *Papio hamadryas robinsoni* from Bolt's Farm ranges between 22kg and 34kg in males and 15kg and 23kg in females. Average weights of fossil *Papio izodi* are estimated at 22kg for males and 17kg for females (*ibid.*). Their East African fossil counterparts are estimated to have higher body mass. Male *Papio quadratiostris* from Omo, Ethiopia and Leba in Angola average between 30kg and 53kg while the weight of females is estimated to be between 16kg and 25kg (Delson *et al.* 2000). Locomotor assignment of *Papio* is to a ground stander and walker (Rose 1973). Modern *Papio* occupies a wide variety of environments in Africa, including gallery forest, rainforest, thorn scrub, semi-deserts, grassland and woodland savannas (Rowe 1996; Codron *et al.* 2005). Its functional anatomy demonstrates adaptation towards a terrestrial habitat.

Modern baboons are generally opportunistic feeders with a high variability of diets across the continent (Codron *et al.* 2005). Codron *et al.* (2005) suggest that *Papio h. robinsoni* from Swartkrans Member 1 and 2 primarily subsisted on a diet of fruits, and leaves were a secondary food source. *Papio (Dinopithecus) ingens* from Swartkrans Members 1 and 2 consumed more fruits than leaves. Therefore compared to its modern counterparts such as *Papio ursinus*, fossil *Papio* had a greater utilisation of grass foods and more variability in diet. The suggested faunal age of the Swartkrans Member 1 *Papio* fossils is between 1.9Mya and 1.8Mya (Pickering *et al.* 2012), or possibly slightly older (Gibbon *et al.* 2014).

The fossil history of *Papio* is not as well known as that of other papionins. A few sites are currently known to preserve *Papio* fossil remains in the Middle Pleistocene (Szalay & Delson, 1979; Kalb *et al.*, 1980; Jablonski, 2008). Even fossil-rich East African sites such as Koobi Fora and Hadar rarely preserve fossil *Papio* remains (Frost & Delson 2002; Jablonski *et al.* 2008). The rarity of identified fossil *Papio* postcrania from other sites significantly impacts on this

research and has led to a reliance on modern *Papio* remains for comparison with the Sterkfontein fossils.

Subfamily	Cercopithecinae Gray 1921
Tribe	Papionini Burnett 1828
Subtribe	Papionina Burnett 1828
Genus	<i>Theropithecus</i> .

*Theropithecus* is one of the most studied non-hominin fossil primate genera in Africa. Its abundance in the East African fossil sites makes it one of the most well known fossil cercopithecoids. *Theropithecus* fossil remains are known from sites such as Olduvai Gorge (Hopwood 1934; Leakey 1965), Olorgesailie (Jolly 1972; Leakey & Leakey 1973, Shipman, Bosler & Davis 1981), Koobi Fora (Leakey 1976; Jablonski, Leakey & Anton 2008), Lomekwi in West Turkana Kenya (Jablonski *et al.* 2002), Luangwa Valley, Zambia (Elton *et al.* 2003), Hadar and Omo in Ethiopia (Eck 1976; Frost & Delson 2002) Afar in Ethiopia (Frost *et al.* 2014). In South Africa, *Theropithecus* has been identified in Sterkfontein (Pickering 1999), Swartkrans (Freedman 1957; Freedman & Brain 1977), Makapansgat (Maier 1972) and tentative assignments to this genus have been made on some specimens from Coopers Cave (De Silva *et al.* 2013). Sterkfontein preserves a very limited sample of *Theropithecus* with only two individuals identified from the StW53 breccia and the Oldowan Infill (Pickering 1999; Kuman & Clarke 2000).

The fossil genus is comprised of two groupings: *Theropithecus darti* connected with *Theropithecus oswaldi*, and *Theropithecus brumpti* and its predecessors (Jablonski 1993). *Theropithecus gelada* is an extant form, the fossil history of which is generally unknown (*ibid.*). *Theropithecus* is a large (weighing between 20kg and 43 kg), heavily built and sexually dimorphic papionin (Delson *et al.* 2000; Jablonski *et al.* 2002). The genus shares a number of traits with *Papio* suggesting close alignment in locomotion and posture (Krentz 1993). Modern *Theropithecus* has the ability to manipulate objects and is characterized by ground standing and walking (Rose 1974). As observed by Krentz (1993), *Theropithecus gelada* and *Theropithecus oswaldi* share more similar postcranial morphology than either does with *Theropithecus brumpti*. *Theropithecus oswaldi* demonstrates features of a terrestrial quadruped with shuffling behaviours and an opposable thumb for manual foraging (Krentz 1993). *Theropithecus brumpti* differs from other theropithecines in that it possesses a suite of characters which suggest that it spent some time in trees (Krentz 1993). According to Jablonski *et al.* (2002), *T. brumpti* was also adapted for

propulsive locomotion. In East Africa *T. darti* is represented by small sample sizes and its locomotor tendencies are not as well known (Krentz 1993). From the known postcrania, East African *T. darti* was the smallest species of the genus, had a stable shoulder joint, opposable first and second digits and was also a generalised terrestrial quadruped which spent time in trees (*ibid.*).

Criticism has been leveled against Krentz' (1993) taxonomic identification of *Thereopithecus brumpti*. The postcranial specimens from the Shungura Formation that he assigned to different species of *Theropithecus* were not directly associated with cranio-dental material (Guthrie 2011). His description of *Theropithecus brumpti* as arboreal has been disproved by recent discoveries. *Theropithecus brumpti* forelimb and hindlimb remains from Tugen Hills and West Turkana suggest that the species was terrestrially adapted, similar to modern *Papio* and was capable of moving in tress (Jablonski *et al.* 2002, Gilbert *et al.* 2011).

El Zaatari *et al.* (2011) suggest that fossil *Theropithecus oswaldi* had a different diet from extant *Theropithecus gelada*. Microwear data extracted from fossil *Theropithecus* specimens from Swartkrans indicate a diet which includes grass, leaves and fruit unlike modern *Theropithecus gelada* which is a grass and leaf eater (El Zaatari *et al.* 2011). *T. darti* on the other hand could have been mainly subsisting on grasses and leaves (*ibid.*).

Subfamily	Cercopithecinae Gray 1821
Tribe	Cercopithecini
Genus	<i>Cercopithecus</i> sp. Brunnich, 1772

Jablonski, Leakey & Anton (2008) suggest that fossil *Cercopithecus* is best represented at Koobi Fora. Even though this site represents the best evidence of *Cercopithecus*, the fossil remains for this genus are rare and the reasons for their rarity are yet to be explored (Jablonski, Leakey & Anton 2008). *Cercopithecus aethiops* has been assigned to fossil cercopithecoid remains occurring in the Post Member 6 Infill at Sterkfontein (Ogola 2009). These assignments were based on the presence of *C. aethiops* cranio-dental remains.

*Cercopithecus* is a small cercopithecine, a guenon, the females of which weigh between 3.5 kg and 4.5kg and males weigh between 4.5kg and 7.5kg (Delson *et al.* 2000). All guenons use arboreal environments, but diversity in the use of arboreal substrates is apparent (Gebo & Sargis 1994). *Cercopithecus aethiops* is a quadruped classified as a 'branch sitter and walker' and is an open woodland terrestrial guenon (Napier & Napier 1967; Rose 1973). The species, however, has been found to 'exhibit fewer morphological adaptations characteristic of a terrestrial lifestyle' (Gebo & Sargis 1994:1). It retains arboreal features while demonstrating that it frequents terrestrial substrates (Gebo & Sargis 1994; Nakatsukasa 1994).



Subfamily	Colobinae Jerdon 1867
Tribe	Colobini Blyth 1875
Subtribe	Colobina
Genus	<i>Cercopithecoides</i> . Mollet 1947

*Cercopithecoides williamsi* is the most commonly occurring fossil colobine in South African fossil cave sites. It is a large fossil colobine with females thought to have weighed an average of 15kg and males weighing 21kg on average (Delson *et al.* 2000; Jablonski *et al.* 2008). Postcrania belonging to *C. williamsi* have been identified at Koobi Fora by Jablonski *et al.* (2008). Postcrania belonging to this species demonstrate a colobine with full adaptation to terrestrial locomotion and posture (*ibid.*). It bears relatively long forelimbs and hindlimbs compared to *Papio*. The long bones also demonstrate an emphasis on flexion, extension movements during locomotion and a highly flexible hip joint (Jablonski *et al.* 2008).

Dental microwear studies on *C. williamsi* from Koobi Fora suggest that this colobine subsisted on unripe fruits and young leaves (El-Zaatari *et al.* 2005; Jablonski *et al.* 2008). Isotopic composition of *C. williamsi* material from Sterkfontein Member 4 and Swartkrans Members 1 and 2 indicate that the species spent considerable time foraging on a terrestrial substrate (Codron *et al.* 2005). In South Africa a new species of *Cercopithecoides* has been named from cranio-dental specimens, *C. haasgati* (McKee *et al.* 2011). The morphology demonstrates variation from known South African and East African *Cercopithecoides* and it is relatively smaller (*ibid.*).

## **2.7. Spatial distribution of fossil cercopithecids at Sterkfontein Caves**

Patterns of spatial distribution of fossils in cave systems such as Sterkfontein are crucial for taphonomic assessment, palaeoenvironmental reconstruction, and site formation processes during and subsequent to deposition of the infills. Sterkfontein cave site formation is of particular interest due to the complex nature of the history of deposition of the infills.

Jacovec Cavern is a deep cave bearing deposits at a depth of at least 30 meters (Wilkinson 1973). It has three components: an older, hominin-bearing *in situ* hanging remnant in the cavern which is the orange breccia; a younger brown breccia visible as a talus cone; and a mixed brown and

orange breccia in the floor of the cavern resulting from the collapse of both breccias (Partridge *et al.* 2003, Kibii 2004, Reynolds & Kibii 2011). Member 2 lies within the Silberberg Grotto above the oldest Sterkfontein deposit, Member 1 (Partridge 2000). The deposit is a talus cone oriented northeast to southwest.

Kuman and Clarke (2000) investigated stratigraphic associations of the Sterkfontein Member 4-5 infills by analyzing the taxa represented in the according to their distribution in space relative to site plan (Figure 1), which is divided into squares by yard. They discovered that there are inherent patterns that distinguish different infills, and these patterns also provide some insight into the taphonomic history of the site and relationships of the deposits.

Previously, Clarke (1985) had plotted the distribution of the hominins and artefacts within Member 4 and 5 and suggested that they demonstrate a pattern. The distribution in Member 4 suggests that the infill possibly accumulated through different phases, with the southern end likely deposited later than the rest of the infill, and possibly under different conditions (Partridge & Watt 1991; Moggi-Cecchi *et al.* 1998; Kuman & Clarke 2000). Later, Ogola (2009) determined that Member 4 extends to the western and southern end of the cavern where it was covered by a stalagmite curtain. The Member 5 deposits lie against this curtain (Ogola 2009).

The StW 53 Infill is a hanging remnant of Member 4 against the south wall of the surface exposures and in the western area of the breccias excavated at surface. The *Australopithecus* cranium StW53 was found partially in solid breccia forming the wall of a solution pocket and partially in decalcified breccia within the solution pocket (Hughes and Tobias 1977; Pickering 1999). Further east within the site, such decalcified pockets of this infill were removed during excavations by Hughes and Tobias (Kuman & Clarke 2000).

The Oldowan deposit lies within the eastern portion of the Member 5 deposits from ca 22 feet below datum and occupies cavities and erosion channels from the collapse of Member 4 in that area (Kuman & Clarke 2000). The Member 5 West deposit, like the Oldowan Infill, also occurs within similar cavities but in the western part of the Member 5 deposits (Kuman & Clarke 2000). These deposits are covered by a flowstone ‘cap’ in the north-western end (Robinson 1962; Ogola 2009).

The Member 6 deposit lies on top of this flowstone that caps Member 5. The Post Member 6 deposit is preserved today in the northern section of the site, just east of this flowstone (Kuman and Clarke 2000; Ogola 2009). The two breccias identified within the Lincoln Cave system consist of a hard calcified breccia (Lincoln Cave North) and a deposit consisting of both decalcified and hard breccia (Lincoln Cave South) divided by a fill of lime miners rubble (Reynolds et al. 2007).

The spatial distribution of the cercopithecoid postcrania in these deposits is undertaken in this study. It will add to interpretations of the modes of accumulation of the materials in the Sterkfontein Caves deposits. This will be particularly useful for deposits with more complex taphonomic histories, such as Member 4.

## **2.8. Taphonomy of the fossil cercopithecoids of the Sterkfontein Caves**

Fossil primates form the majority of faunal remains within the older Sterkfontein Cave deposits and their presence thus has significant implications relevant to the modes of accumulation of the infills. The taphonomic history of fossil primates at the site is a significant factor in determining the depositional history of the site and the general fauna in the Sterkfontein vicinity. Below is an account of taphonomic studies undertaken on the fossil primates at the Sterkfontein Caves.

Member 2, one of the earliest deposits, contains faunal collections dominated by fossil remains of cercopithecids and felids. The collection is comprised of partial skeletons across all taxonomic groups that includes a full representation of skeletal elements, in addition to the presence of a complete skeleton of *Australopithecus* (Pickering *et al.* 2004a). The Member 2 deposit suggests that the infill accumulated as a result of a death trap whereby animals fell into the cave and were either killed by the fall or were unable to exit (*ibid.*). Some rare carnivore tooth damage represented by scores, pits, punctures and crenulation are present in the primate assemblage, but their paucity does not support significant carnivore involvement in the accumulation of the primate assemblage (Pickering *et al.* 2004a).

C.K. Brain (1981) initiated taphonomic studies of the Member 4 macro-vertebrate fossil assemblage. This assemblage preserves the largest collection of fossil primates at Sterkfontein

and it has been reported that 3400 fossil primate specimens have been recovered from the infill (Kuman & Clarke 2000). The results of Brain's study suggested involvement of porcupines and a possibility of carnivore accumulation of the assemblage (Brain 1981). The presence of carnivore modification marks represented by scores, pits, punctures and crenulation in Member 4 also suggests a carnivore ingested assemblage. The identity of the specific carnivores that could have accumulated the fossil primate remains could not be ascertained. Brain (1981: 213) suggested that carnivores represented in the sample--leopard, *Dinofelis*, *Megantereon*, hunting hyaenas (*Chasmoporthetes*) and spotted hyaena (*Crocuta*)--could have been the major contributors to the fossil assemblage.

Pickering *et al.* (2004b) revisited the fossil primate assemblage to explain their high frequencies in the Member 4 deposit. The authors examined the skeletal part representation and the minimum number of individuals, and they analysed the surface modifications on limb bones of all hominin specimens. Assessment of the ratio of NISP: MNE (Number of Identified Specimens: Minimum Number of Elements) indicated that carnivores other than hyaena accumulated the hominin sample (Pickering *et al.* 2004b). The NISP: MNE ratio of 1.00 to 1.04 is apparent for bone accumulations by leopards and lions, while hyaenas produce higher ratios of around 5.90 (Richardson 1980). Carnivore tooth marks with intense damage are also reported to be scant in the assemblage. The tooth mark frequency on the limb bones is also not equivalent to that inflicted by hyaenas. Pickering *et al.* (2004b) then concluded that large carnivores were responsible for the accumulation of the hominin assemblage in Member 4.

Additional research on the taphonomy of Member 4 fossil primates conducted by Kibii (2004) supported Pickering *et al.*'s research. Kibii (2004) examined the bone surface modification and assemblage formation in light of primate body size, age, locomotor habits, the presence of predators and, predator hunting range. Not all primate specimens that were recovered in the Member 4 infill were assessed for bone surface modification. Thus, Kibii (2004: 67) notes that the taphonomy of the primates in Member 4 can only be 'considered with the incorporation of all the specimens recovered from the infill'. Medium sized primate individuals have a higher representation in the Member 4 assemblage and could have thus been prey to the majority of carnivore predators in the Member 4 fossil assemblage (Kibii 2004). Moreover, a death trap scenario is also one of the modes of accumulation suggested by the presence of a full range of fossil primate skeletal elements in the infill. This research will attempt to address the concern

raised by Kibii by providing a comprehensive study of the primate fossil remains from all Sterkfontein cave deposits.

Kibii (2000) also studied the Jacovec Cavern primate assemblage and concluded it was most likely accumulated as a result of a combination of processes such as surface slope wash, carnivore action and gravitational slump. Three hundred thirteen fossil cercopithecoid specimens have been recovered from Jacovec Cavern. In terms of carnivore activity, the skeletal part representation is consistent with leopard ravaged carcasses in a refuse assemblage and 3% of fossil primate collection possesses carnivore related modification marks.

Younger deposits studied by Brain (1981) and later by Pickering (1999), such as the Member 5 deposits, demonstrate a decline in the frequency of fossil primate individuals relative to bovids. The predominance of dry-broken bone and the rarity of dense skeletal parts in the StW 53 deposit led Pickering (1999) to suggest that part of the infill represented in the excavated sample was impacted on by post-depositional processes such as sediment compaction and rock fall. The StW 53 infill preserves a low portion of chewed and digested bone (*ibid.*).

The Oldowan infill preserves a full range of cercopithecoid post-cranial elements including fragile ribs and vertebrae (Pickering 1999). Skeletal element representation in this infill suggests that the cave was a death trap at some point, and some surface wash of materials from areas surrounding the cave entrance is also indicated by abrasion of the bone remains (*ibid.*).

In the Member 5 West assemblage primates are represented by limb bones, axial skeletons and cranial pieces (Pickering 1999). Pickering (1999) suggests that the whole faunal assemblage in the Member 5 West infill accumulated as a possible result of hyaena accumulation, porcupine collection and materials washing in from the surface of the cave. Hyaena accumulation is inferred from the abundance of hyaena remains, including young hyaenas, and the absence of hominin-inflicted bone damage in the assemblage (Pickering 1999).

Lincoln Cave preserves the least number of fossil primate remains in the whole Sterkfontein Cave system. Only four fossil *Papio* individuals are preserved in the deposits (Reynolds *et al.* 2007). Reynolds' (2000) taphonomic analysis of the Lincoln Cave deposits, which preserves high percentages of carnivore damage, suggests that carnivores were active in the surface catchment area during the time of deposition.

The Member 6 fossil cercopithecoid collection consists of only two elements. The general skeletal element representation of the fauna in the deposit is poor with only compact elements represented. Ogola (2009) concluded that the Member 6 fossil faunal assemblage could be partly attributed to carnivore predation. In the Post Member 6 assemblage non-hominin fossil primate postcrania are better represented with 13 specimens (44% of the post Member 6 fossil primate NISP) compared to the Member 6 deposits. Cranio-dental remains dominate the assemblage. The taphonomic factor implied in the accumulation of some of the Post Member 6 collection is that they could have been the result of a death trap (Ogola 2009).

Taphonomic interpretations of assemblages in Member 2, Jacovec Cavern, Member 4, StW 53 infill, Oldowan Infill, Member 5 West, Member 6, Post Member 6 infills and Lincoln Cave indicate the presence of carnivore involvement to varying degrees. Only Pickering (1999) in his study of Member 5 West suggested a specific carnivore, a hyaena. However, this interpretation is based on the Member 5 West assemblage that consists of various animal taxa and in which primate remains are less represented. Most of the taphonomic interpretations using criteria such as body size and taxa, skeletal element representation and type of bone surface modification can only suggest the involvement of carnivores in general rather than a specific genus. This study supplements these aforementioned criteria with a new method of analyzing tooth pit dimensions in order to better identify the carnivores that could have accumulated the primate bone assemblages.

## **2.9. Identification of specific carnivore agents**

Previous research indicates that carnivore modification is present on fossils from the Sterkfontein deposits and various criteria have been used to determine the carnivores involved. Dominguez-Rodrigo and Piqueras' (2003) model measures tooth pit marks on the limb bone specimens to determine which carnivores could have imparted those marks, and is based on tooth pit variations of modern carnivore taxa. Even though their study is based on modern taxa, it is the only model of its kind that applies data from extant carnivores to tooth pit dimensions of extinct carnivore taxa. Selvaggio (1994) makes inferences regarding tooth pit dimensions produced by extinct carnivore taxa such as *Dinofelis*, *Homotherium* and *Megantereon*. The difference between Selvaggio (1994) and Dominguez-Rodrigo and Piqueras' (2003) models is

that Selvaggio used pit length and breadth ratios which yielded many overlaps on the measurements, while the latter analysed these variables separately, which provided clearer distinction between taxa. It is for this reason that Dominguez-Rodrigo and Piqueras' (2003) model is preferred.

Pits are 'bone surface modifications imparted by animal chewing and appear as discrete, roughly circular marks in plan view, resulting from scarring bone without inward crushing of bone cortex' (Pickering & Wallis 1997: 1120). These authors provide detailed measurements of pits produced by:

- spotted hyaena,
- jackal,
- dog,
- lion,
- leopard, and
- cheetah.

Epiphyses and diaphyses are treated separately, as carnivore teeth impact differently on spongy bone (epiphyses) and dense bone (diaphyses), and data on them is recorded as such:

Table 2.4. Carnivore tooth pit size distribution on epiphyses

Length	Breadth
1. <4mm: small canids.	<2mm: medium sized felids.
2. 4-6mm: middle sized carnivores except felids.	2-4mm: most carnivores.
3. >6mm: large sized carnivores and felids.	>4mm: hyaenas and lions.

Table 2.5. Carnivore tooth pit size distribution on diaphyses

Length	Breadth
1. <2mm: small carnivores to medium felids	1.5mm: small carnivores
>4mm: hyaenas dogs or lions	>2mm: hyaenas, dogs or lions

When the whole sample of tooth pits from epiphyses and diaphyses and their ranges of variation are established, a good basis for identification of carnivore taxa using tooth mark sizes will be achieved (Dominguez-Rodrigo & Piqueras 2003). This method was applied by Pickering *et al.*

(2004c) on carnivore tooth pits in the Swartkrans Member 3 fossil assemblage. Their results led them to note that there are taxon-specific carnivore tooth marks. Dominguez-Rodrigo and Piqueras (2003) further suggest that tooth pit size should be complimented by other methods, such as analysis of skeletal element frequencies and taphonomic analysis to provide a comprehensive analysis of observed results.

Generally found on cancellous bone, furrows, or what other authors (e.g. Binford, 1981; Brain 1981) refer to as scooping or hollowing out, occur as a result of removal of soft tissue (Bonnichsen 1973; Maguire *et al.* 1980). Bone furrowing patterns are characteristic of individual carnivores (Dominguez-Rodrigo & Piqueras 2003). Intense bone furrowing of epiphyses is likely to be produced by hyaenids, leopards and canids (*ibid.*). Proximal and distal parts of upper limbs particularly suffer furrowing from lion teeth (Haynes 1983). Non-intensive furrows are generally associated with lions (Dominguez-Rodrigo & Piqueras 2003).



## CHAPTER THREE

### MATERIALS AND METHODS

#### 3.1 Materials

Materials utilised in this research are the Plio-Pleistocene cercopithecoid postcrania collections from Sterkfontein Caves of South Africa. The assemblage consists of materials collected from the lime miners' dumps and those from *in situ* material processed from ongoing excavations at the site (see Appendix A for a catalogue of the fossil cercopithecoid postcrania assemblage from Sterkfontein according to their respective infills). These materials include fossil Cercopithecoidea postcrania housed at Sterkfontein, the Ditsong Museum of Natural History in Pretoria (formerly known as the Transvaal Museum), and, during this study, at the primate laboratory of the School of Anatomical Sciences at the University of the Witwatersrand. Kuman & Clarke (2000) report that more than 3400 fossil primate (hominid and non-hominid) skeletal remains have been uncovered from Sterkfontein Member 4 only. They include both fossil cranio-dental and postcranial specimens. Fossil cercopithecoidea postcrania from Sterkfontein, including those from Member 2, Jacovec Cavern, Member 4, StW 53 Infill, Oldowan infill, Member 5 West, Member 6, Post Member 6 and Lincoln Cave deposits, are analysed. The sum of identifiable fossil non-hominid primate postcranial materials examined in this study is 1514.

##### *3.1.1. Excavated materials*

Excavated materials used in this study were first obtained by Robert Broom between 1936 and 1945. Excavations were continued by Broom and John Robinson between 1945 and 1949 and, by Robinson and Revil Mason in the 1950s. Alun Hughes excavated large numbers of primate fossils between 1966 and 1991, the year when he retired. He was succeeded by Ronald Clarke and excavations have continued until the present.

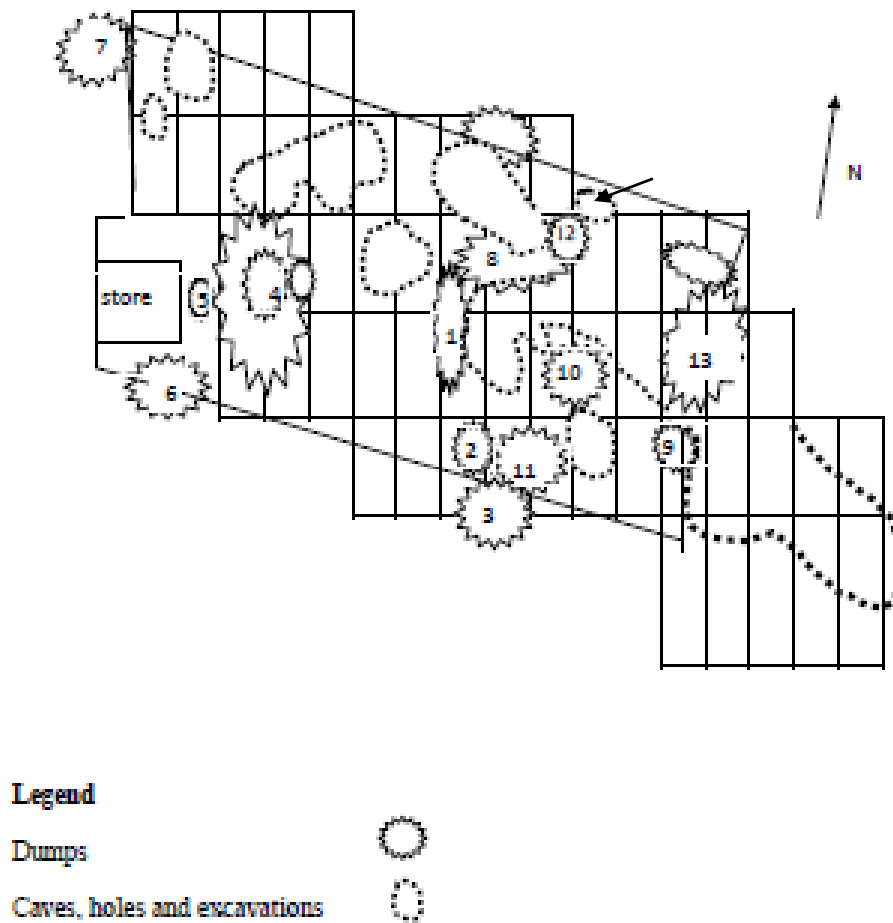


Figure 3.1. Plan of Sterkfontein site demonstrating the locality of the dumps in relation to the excavation sites (adapted from Hughes and Tobias 1969). Dump 18 is underground and is indicated with an arrow.

### 3.1.2. *Materials derived from the dumps*

After the opening of systematic excavations by Hughes and Tobias in 1966 at Sterkfontein Caves, one of their first tasks was to process rubble dumps left at various localities by the lime miners who were extracting the stalagmites and stalactites from the caves. Hughes and Tobias (1969) numbered these dumps and then labeled them on a site plan (Figure 3.1). The fossils in the dumps derive from areas quarried by the lime-miners.

The miners did not move the quarried materials far from the area they were working; therefore it was possible to relate dump material from Dumps 10, 12, 13, 14, 15, 17 and 18 to the various infills of the cave system (Heaton 2006). These materials were stored at four locations: on site at the Sterkfontein Caves, at the School of Anatomical Sciences and the Bernard Price Institute at the University of the Witwatersrand (the latter two now moved to the Evolutionary Studies Institute), and the Ditsong Museum of Natural History (formerly known as the Transvaal Museum). Large quantities of primates and other fossils came from the breccia that was labeled Member 4 of the Sterkfontein Formation by Partridge (1978). Dump 20 is not shown in Figure 3.1 as it was located underground in the Silberberg Grotto and contained primates from Members 2 and 3 (*ibid.*).

#### 3.1.3. *The condition of the collection*

The Sterkfontein fossil faunal sample consists of highly fragmented materials mainly due to rock fall caused by collapse and other pressures within the deposits. The samples from lime miners' dumps are also generally highly fragmented, largely due to being blasted out of their original context. As a result the Sterkfontein fossil primate assemblage is dominated by incomplete elements; complete bones are a rare occurrence in the sample. The provenance of the specimens is noted and the impact on the taphonomic history of the sample is addressed in Chapter 5. The fragmented nature of the Sterkfontein materials reduced the diagnostic sample size of the assemblage and impacted on taxonomic assignment of the specimens. This is discussed in Chapter Five of the thesis.

#### 3.1.4. *Comparative materials*

Modern comparative samples from the School of Anatomical Sciences in the Raymond Dart Collection (RDC) and the Evolutionary Studies Institute (ESI) at the University of the Witwatersrand, the Vertebrate Palaeontology department of the Ditsong Museum of Natural History (DMNH) and the Primate Morphometrics Online (PRIMO) Database of the New York Consortium in Evolutionary Primatology (NYCEP) are used in this study. A complete list of the modern comparative skeletal remains is attached in Table 3.1 and

Table 3.2. Various literature on taxonomic descriptions of cercopithecoid post-crania from East African and southern African sites also forms the basis for consultation on taxonomic identification of the fossil cercopithecoid postcrania from Sterkfontein (e.g. Harrison 1989; Delson *et al.* 1993; Leakey 1993; Jablonski & Chaplin 2008). Frost & Delson (2002) provide detailed descriptions and measurements of cranial and postcranial morphology of *Parapapio*, *Papio*, *Cercopithecoides* and *Theropithecus*, which are genera previously identified in the South African fossil cercopithecoid cranial specimens. Jablonski, Leakey and Anton (2008) provide a detailed qualitative descriptive analysis of Cercopithecoidea from the Koobi Fora region in Kenya, which the author assessed at the Nairobi Museum in Kenya. Eisenhart (1957, 1960, 1961), Freedman (1974) and Heaton (2006) have also provided descriptions of crania and dentition from Sterkfontein, Makapansgat and Taung.

**Table 3.1. A list of comparative materials utilised in this study**

Number	Location	Catalogue no	Elements	Taxon
1.	ESI	BP1/C 295	Humerus, Radius, Ulna, Femur, Tibia	<i>Cercopithecus aethiops</i>
2.	RDC	V33	Humerus, Radius, Ulna, Femur, Tibia	<i>Cercopithecus aethiops</i>
3.	RDC	Za 12S	Humerus, Tibia	<i>Cercopithecus aethiops</i>
4.	RDC	Za 862	Humerus, Radius, Ulna, Femur, Tibia	<i>Cercopithecus aethiops</i>
5.	RDC	Za 864	Humerus, Radius, Ulna, Femur, Tibia	<i>Cercopithecus aethiops</i>
6.	RDC	Za 973	Ulna, Radius, Tibia	<i>Cercopithecus aethiops</i>
7.	RDC	Za 968	Humerus, Radius, Ulna, Femur, Tibia	<i>Cercopithecus aethiops</i>
8.	RDC	Za 1129	Humerus, Femur	<i>Cercopithecus aethiops</i>
9.	RDC	Za 1244	Humerus, Radius, Ulna, Femur, Tibia	<i>Cercopithecus aethiops</i>
10.	RDC	Za 1226	Humerus, Radius, Ulna, Femur, Tibia	<i>Papio sp</i>
11.	RDC	Za 1357	Humerus, Radius, Ulna, Femur, Tibia	<i>Papio sp</i>
12.	RDC	Za 11232	Humerus, Radius, Ulna, Femur, Tibia	<i>Papio sp</i>
13.	RDC	Za 1299	Humerus, Radius, Ulna, Femur, Tibia	<i>Papio sp</i>
14.	RDC	Za 1360	Humerus, Radius, Ulna, Femur, Tibia	<i>Papio sp</i>
15.	RDC	Za 740	Humerus, Radius, Ulna, Femur, Tibia	<i>Papio sp</i>
16.	RDC	Za 1231	Humerus, Radius, Ulna, Femur, Tibia	<i>Papio sp</i>
17.	ESI	BP1/C 541	Humerus, Radius, Ulna, Femur, Tibia	<i>Papio ursinus</i>
18.	RDC	Za 1226	Humerus, Radius, Ulna, Femur, Tibia	<i>Papio sp</i>
19.	RDC	Za 1227	Humerus, Radius, Ulna, Femur, Tibia	<i>Papio sp</i>
20.	RDC	Za 1228	Humerus, Radius, Ulna, Femur, Tibia	<i>Papio sp</i>
21.	DMNH	Az/981	Humerus, Radius, Ulna, Femur, Tibia	<i>Colobus guezara</i>
22.	DMNH	Az/807	Humerus, Radius, Ulna, Femur, Tibia	<i>Colobus guezara</i>

23.	DMNH	Az/155	Humerus, Radius, Ulna, Femur, Tibia	<i>Colobus guezara</i>
24.	DMNH	Az/1437	Humerus, Radius, Ulna, Femur, Tibia	<i>Colobus guezara</i>
25.	DMNH	Az/971	Radius, Ulna, Femur	<i>Mandrillus sphinx</i>
26.	DMNH	Az/972	Humerus, Radius, Ulna, Femur, Tibia	<i>Mandrillus sphinx</i>

Table 3.2. Comparative sample utilised for the quantitative analysis derived from the PRIMO NYCEP database.

Genus	N
<i>Colobus</i>	29
<i>Procolobus</i>	10
<i>Paracolobus</i>	3
<i>Rhinocolobus</i>	2
<i>Cercopithecoides</i>	3
<i>Chlorocebus</i>	3
<i>Cercopithecus</i>	56
<i>Papio</i>	57
<i>Mandrillus</i>	13
<i>Theropithecus</i>	29

Table 3.3. Comparative materials from the literature

	Reference	Specimen no	Elements	Taxon
1.	Frost & Delson, 2002	AL 363-12	Humerus	cf. <i>Parapapio jonesi</i>
2.	Jablonski <i>et al</i> , 2008	KNMER 861	Humerus	cf. <i>Parapapio</i> ,
3.	Jablonski <i>et al</i> , 2008	KNM-ER 30315	Ulna	cf. <i>Parapapio</i> ,
4.	Jablonski <i>et al</i> , 2008	KNMER 30298	Humerus	<i>Parapapio</i> sp. indet
5.	Jablonski <i>et al</i> 2008	KNMER 3013	Humerus, Ulna, Femur	<i>Theropithecus brumpti</i>
6.	Jablonski <i>et al</i> , 2008	KNMER 18197	Humerus, Ulna, Radius	<i>Theropithecus oswaldi</i>
7.	Jablonski <i>et al</i> , 2008	KNMER 5491	Humerus, Ulna	<i>Theropithecus oswaldi</i>
8.	Elton <i>et al</i> , 2003	Zambian specimen	Femur	<i>Theropithecus</i> cf. <i>darti</i>
9.	Jablonski <i>et al</i> , 2008	KNMER 974	Femur	<i>Cercopithecoides</i> cf. <i>williamsi</i>
10.	Jablonski <i>et al</i> , 2008	KNMER 4420	Femur	<i>Cercopithecoides williamsi</i>
11.	Jablonski <i>et al</i> , 2008	KNMER 44361	Humerus	<i>Cercopithecus</i> sp. indet

### 3.2 Methods

Excavations at the Sterkfontein site in the mid 1950's and from 1966 onwards were undertaken systematically. The provenance of excavated fossils was recorded in feet (‘) and inches (‘‘) of depth below datum and in 3 foot x 3 foot (90cm x 90cm) grid squares given successive letters from north to south and consecutive numbers from east to west. See Figure 3.1 for grid square numbers.

Data on the specimens are recorded as:

- specimen number,
- skeletal element,
- element portion,
- side,
- taxon,
- size class, and
- the maturation age of the individual.

As applied in most research on taphonomy, the following is also recorded: weathering stage, with reference to Behrensmeyer's work (1978), and bone surface modifications of all the fossil primate bone specimens (Binford 1981; Blumenschine & Selvaggio 1988, 1991; Shipman 1981; Pickering 1999). In order to measure skeletal element and individual abundance the following were calculated: the number of identified specimens (NISP), the minimum number of elements (MNE), and the cumulative number of individuals (cMNI) (Grayson 1989; Bunn 1982, 1986; Klein & Cruz-Urbe 1984; Bunn & Kroll 1986; Pickering 1999).

Size classes were allocated according to the following classification.

- Small: <11 Kg (smaller than modern adult *Papio ursinus*)
- Medium: 11-29Kg (Comparable in size to a modern adult *Papio ursinus*)

- Large:  $\geq 30\text{Kg}$  (Primates equal to or larger in size than a modern adult *Papio ursinus*)

Two approaches are adopted to analyse the Sterkfontein cercopithecoid limb elements. Qualitative and quantitative analyses are undertaken on the humeri, radii, ulnae and femora which dominate the fossil cercopithecoid postcrania assemblage.

### **3. 2.1. Determining taxa of the Sterkfontein Caves fossil cercopithecoid postcranial remains**

Qualitative and quantitative approaches are applied to the Sterkfontein Cave fossil cercopithecoid postcrania to determine their taxonomic affiliations. These two methods are combined to determine the behaviours of the Sterkfontein fossil cercopithecoids. In addition to the qualitative data, statistical analyses are applied to determine the variables which discriminate between genus and, where possible, species level.

#### **a) *Qualitative analysis***

The qualitative taxonomic study undertaken in this thesis is adapted from this comprehensive examination. Additional data for qualitative analysis is adapted from literature sources which provide different measures for variation on postcranial skeletal elements (e.g. Szalay & Delson 1979; Harrison 1989; Leakey 1993; Frost & Delson 2002; Thackeray & Myer 2004). Qualitative data focus on unique landmarks and anatomical traits which are aligned to functional morphology. To establish variation, a suite of 36 anatomical landmarks from the humerus, ulna, radius and femur were qualitatively analysed from specimens which preserve determinant landmarks. These are adapted Harrison 1989; Leakey 1993; Frost & Delson 2002 and Jablonski, Leakey & Anton 2008. Their variation in the form of shape, position and size relative are described. A comprehensive list of these is attached as Appendix B. Three important regions for locomotion and postural behaviors are considered in this study:

- The upper fore-arm

The upper humerus:

Variation of the humeral greater and lesser tuberosity, which are attachment sites for the rotator cuff muscles of the shoulder, are associated with variation in locomotor habits (Krentz 1993). According to Krentz (1993), disparity in their morphology mirrors the importance towards stability of the shoulder joint. The shape of the humeral head and greater tuberosity, the size of the greater tuberosity relative to the humeral head structurally define the movement of the shoulder joint (Harrison 1993). Therefore the upper humerus is an essential component for understanding locomotor preferences which are associated with different taxa. Table 3.4. provides a list of morphological traits assessed on proximal humeral specimens,

Table 3.4. Qualitative analysis of the proximal humerus

1.	Head shape
2.	Head shape and lesser tuberosity separated by a groove
3.	Superior extension of greater tuberosity relative to the humeral head
4.	Greater tuberosity lateral surface area shape
5.	Size of greater tuberosity relative to lesser tuberosity

- The lower fore-arm (Figure 3.5)

The distal humerus is one of the most occurring fossil remains in the Sterkfontein cercopithecoid assemblage. This anatomical part is important in distinguishing between arboreal and terrestrially adapted locomotion (Krentz 1993). Variation in morphology of the distal humerus reflects differing requirements for stability, forearm movement and digit dexterity (*ibid.*). The medial epicondyle and its varying degrees of orientation, the distal shaft walls, the olecranon fossa, height of olecranon process and the shape of radial head provide useful information as indicators of locomotor type. Harrison's (1989) analysis of *Victoriapithecus* remains from Maboko Island, Kenya has demonstrated a wide range of



morphological indices which can be applied to determine taxa and he concludes that the distal humerus provides the best evidence to determine taxa at the site.

Table 3.5. Qualitative analysis of the lower humerus

6.	Distal shaft thickness
7.	Distal shaft symmetry
8.	Distal shaft dorsal pillar shape above medial and lateral epicondyle
9.	Medial epicondyle orientation
10.	Size of medial epicondyle relative to lateral epicondyle
11.	Lateral epicondyle morphology
12.	Olecranon fossa shape
13.	Length of medial lip distal projection
14.	Capitulum shape

The proximal ulna (Table 3.6) and radius (Table 3.7)

The height of the olecranon process is different between colobines and terrestrial cercopithecines and quadrupedal arboreal and semi-terrestrial cercopithecines (Harrison 1993). Not much variation exist in the proximal radius, the main difference can be observed on the length of the neck which can discriminate between colobines and semi-terrestrial and terrestrial monkeys (*ibid.*)

Table 3.6. Qualitative analysis of the Ulna

15.	Olecranon superior aspect morphology
16.	Olecranon orientation
17.	Olecranon superior projection relative to trochlea notch
18.	Anconeal process articular surface
19.	Olecranon lateral aspect relative to medial aspect
20.	Sigmoid notch shape
21.	Coronoid process articular surface
22.	Ulna shaft groove distal to coronoid process
23.	Shaft shape

Table 3.7. Qualitative analysis of the radius

24.	Head shape
25.	Head orientation
26.	Bicipital tuberosity surface
27.	Shaft shape

- The hind-limb

The hip joint (Figure 3.8)

The proximal femur morphology holds specializations for the hip joint which are indicative of hip abduction and rotation capabilities (Nakatsukasa 1994). Distal to the hip joint, i.e. the distal femur and tibia, there is less variation in morphology within cercopithecoids. As a result, the distal tibia is not included in this study.

Table 3.8. Qualitative analysis of the femur

28.	Head shape
29.	Extension of greater trochanter relative to the head
30.	Greater trochanter lateral surface area
31.	Position and shape of fovea capitis
32.	Neck size
33.	Depth of intertrochanteric fossa
34.	Lesser trochanter shape and orientation
35.	Shaft shape
36.	Size of medial condyle relative to lateral condyle

b). *Quantitative and Statistical analysis*

Standard digital caliper measurements are recorded for quantitative analysis on specimens with diagnostic anatomical landmarks. Measurements are taken on anatomical landmarks on the basis of their functional significance and their potential to distinguish size variation. The quantitative study provides a morphometric analysis of the anatomical

landmarks and measurements, and these are compared to established means and ranges of skeletal elements of identified taxa. Collectively, 35 measurements deriving from the humerus, ulna, radius and femur are recorded which are compared against existing comparative materials and literature. Detailed results of these are attached in Appendix B. To avoid bias of taxonomic alignment of postcrania based on the available cranio-dental data in an infill, descriptions of fossil specimens are initially undertaken without reference to their chronological or spatial origin within the Sterkfontein Cave site.



Figure 3.2. Illustration of measurements derived from the humerus

Table 3.9. Measurements derived from the humerus

<b>NUMBER</b>	<b>ACRONYM</b>	<b>REGION</b>
<b>1</b>	<b>PMLD</b>	Proximal medio-lateral dimension
<b>2</b>	<b>HHD</b>	Humeral head diameter
<b>3</b>	<b>APLHH</b>	Anterior- posterior length of humeral head
<b>4</b>	<b>GTD</b>	Greater tuberosity diameter
<b>5</b>	<b>MMLLO</b>	Maximum medio-lateral length of olecranon fossa
<b>6</b>	<b>MPDLO</b>	Maximum proximo-distal length of olecranon fossa
<b>7</b>	<b>DAB</b>	Distal articular breadth
<b>8</b>	<b>BEB</b>	Bi-epicondylar breadth
<b>9</b>	<b>MTFL</b>	Medial trochlea flange length
<b>10</b>	<b>PDHC</b>	Proximo-distal height of capitulum
<b>11</b>	<b>LEMET</b>	Lateral epicondyle to medial edge of trochlea
<b>12</b>	<b>AME</b>	Angle of medial epicondyle relative to axis of distal articular surface

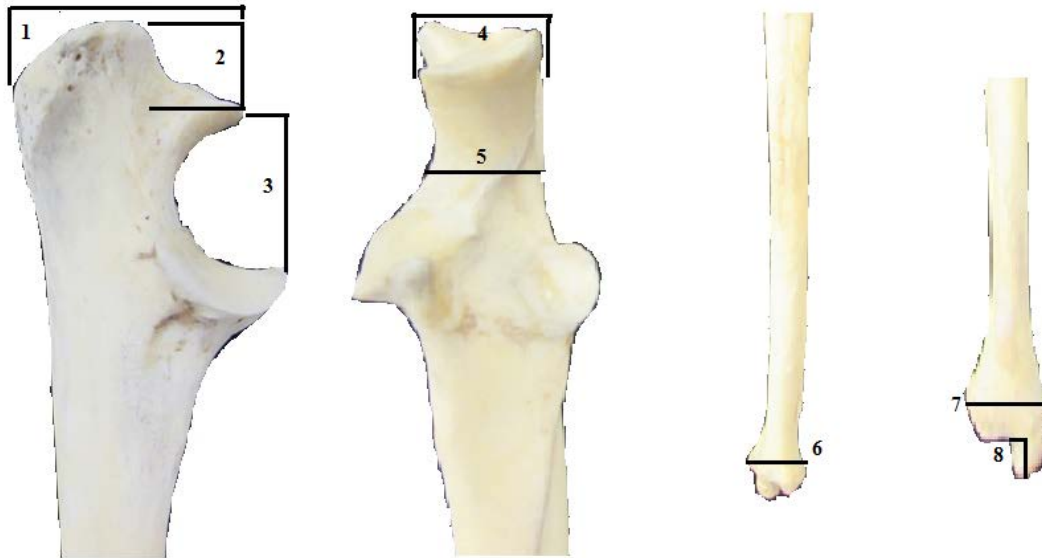


Figure 3.3. Illustration of measurements derived from the ulna

Table 3.10. List of measurements derived from the ulna

NUMBER	ACRONYM	REGION
1	APLOP	Anterior-posterior length of olecranon process
2	PDHOP	Proximo distal height of olecranon process
3	PDLTN	Proximo-distal length of trochlear notch
4	MLBOP	Medio-lateral breadth of olecranon process
5	MLBTN	Medio-lateral breadth of trochlea notch
6	DAPW	Distal antero-posterior width
7	DMLB	Distal medio-lateral breadth
8	LUS	Length of ulna styloid

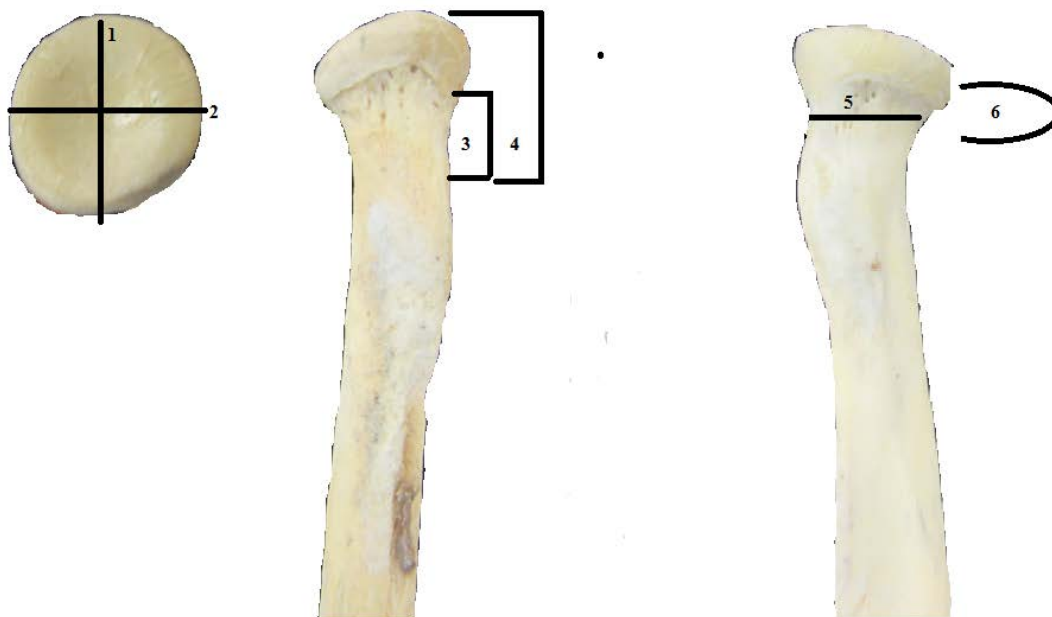


Figure 3.4. Illustration of the measurements derived from the radius

Table 3.11. Radius

NUMBER	ACRONYM	REGION
1	<b>MDRH</b>	Maximum diameter of radial head
2	<b>PBRH</b>	Perpendicular breadth of radial head
3	<b>PDHRN</b>	Proximo distal height of radial neck
4	<b>PDHRNH</b>	Proximo-distal height of radial neck and head
5	<b>MLBRN</b>	Medio-lateral breadth of radial neck
6	<b>APWRN</b>	Anterior-posterior width of radial neck

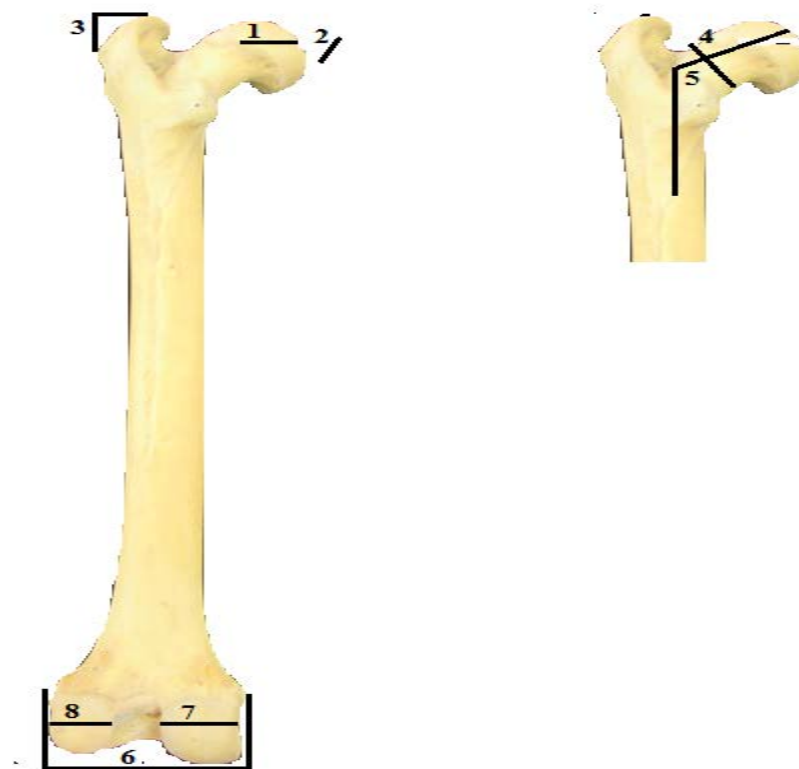


Figure 3.5. Illustration of measurements derived from the femur.

Table 3.12. Measurements derived from the femur

NUMBER	ACRONYM	REGION
1	MLBFH	Medio-lateral breadth of femur head
2	APHD	Anterior-posterior head diameter
3	GTP	Greater trochanter projection
4	ND	Neck diameter
5	NSA	Neck-shaft angle
6	BB	Bi-condylar breadth
7	MCW	Medial condyle width
8	LCW	Lateral condyle width
9	PSRH	Patella surface rim height

The Sterkfontein assemblage is highly fragmented. Within the whole Sterkfontein fossil cercopithecoid limb sub-assemblage, only one element is complete and no other

specimen preserves a full suite of characters. However, statistical methods are applied to skeletal elements to estimate taxonomic affinities. Linear measurements are run through a bivariate linear regression analysis to assess the relationship between variables and the significance of the association. Univariate Analysis of Variance (ANOVA) is applied to reveal the traits which are significantly different among taxonomic groups. To determine if groups are statistically significant Discriminant Function Analysis (DFA) is applied. These are undertaken using the Paleontological Statistics Programme (PAST) Version 3.6 (Hammer *et al.* 2001).

### 3.3. Establishing diagnostic morphology from the modern skeleton: qualitative analysis

Diagnostic morphology for determining features which distinguish between taxa of the comparative specimens is established through qualitative and quantitative and statistical analysis. Postcranial elements of three genera (*Papio*, *Cercopithecus* and *Colobus*) are analysed for qualitative traits.

a. Subfamily Cercopithecinae Gray 1921

Tribe Papionini Burnett 1828

Subtribe Papionina Burnett 1828

Genus *Papio* Eerxleben, 1777



Figure 3.6. Modern *Papio ursinus* (BPI/C/541) skeletal elements a) humerus; b) ulna; c) radius; and d) femur.



a) The humerus

The head is proximo-distally compressed. The head and the lesser trochanter are continuous. The greater trochanter is significantly larger than the lesser trochanter and its superior extension lies above the level of humeral head. Its lateral surface area is slightly convex. The shoulder mobility is restricted in this genus. The tuberosities vary in size with the greater tuberosity being significantly larger than the lesser tuberosity. The shaft is approximately straight. Distally, the shaft morphology is asymmetrical, thick and rounded in the coronal plane. The medial epicondyle is retroflexed and approximately equal in size to the lateral epicondyle. The lateral epicondyle has a small dorsal face and projects slightly above the level of the olecranon fossa. The trochlea breadth is narrow. Its medial lip distal projection is short. It is also medially inclined relative to shaft. The capitulum is rounded and its medio-lateral width is even in the proximo-distal axis. The olecranon fossa is shallow and has an elongated-ellipsoid shape.

b) The ulna

The anconeal process is in horizontal plane with no significant proximal extension. The coronoid process is also in horizontal plane with no significant distal extension. The trochlea notch is crescentic. The olecranon is less than the trochlea notch length. The centre of the olecranon process is retroflexed. In medial view, the anconeal process is sharply projecting dorsally; it is flattened in the antero-posterior dimension. In medial view, the posterior portion of the olecranon process rises sharply. The shaft is approximately straight. The styloid process is a rounded globular projection with a rounded facet laterally.

c) The radius

In superior view, the radius head is ovoid and slightly depressed. Its medial and lateral borders are slightly unequal in height. The bicipital tuberosity is bulbous and elongated proximo-distally. In lateral view, it extends out of the shaft and has a longitudinal groove laterally. The bicipital tuberosity is mainly rugose, and it protrudes laterally. The neck is

also relatively short. The radial shaft in *Papio* is superiorly dorso-ventrally flattened and approximately straight. The styloid process is a sharp distally oriented projection.

d) The femur

The head has a superior orientation. The fovea capitis is located centrally on the anterior head surface. The femoral head bears obvious dorsal extension towards the greater trochanter. The greater trochanter has a blunt apex and has a slight medial orientation. On anterior view, the proximal neck is a medially tilted u-shaped slope. The intertrochanteric fossa shape is large and deeply cavitated. It is located at the same level as the femoral head and is narrow with parallel margins. The lesser trochanter is long with a parabolic profile and faces more medially than dorsally. The neck is short. The shaft is nearly straight. Distally, the lateral condyle is smaller than the lateral condyle. They are splayed with a deep inter-condylar fossa.

b. Subfamily Cercopithecinae Gray, 1821  
Tribe Cercopithecini Gray, 1821  
Genus *Cercopithecus* Brunnich, 1772



Figure 3.7. Modern *Cercopithecus aethiops* (BPI/C/295) skeletal elements a) humerus; b) radius; c) ulna; and d) femur.

a) The humerus

The humerus head is hemi-spherical. The greater tuberosity lies at the same level as the head. The greater tuberosity is larger than the lesser tuberosity. The shaft has a lateral

bow. Distally, the humerus shaft is symmetrical. It has a shallow, high and rounded olecranon fossa. In specimen Za 973 the olecranon fossa has a centrally located fenestra. The medial epicondyle is retroflexed. The trochlea medial lip distal projection is very short and projects medially. The dorsal pillars are wider and thicker above the lateral epicondyle. The capitulum is relatively flatter than in *Papio*. The medial epicondyle is larger than the lateral epicondyle.

b) The ulna

The shaft is approximately straight. In medial view the olecranon is slightly concave. The olecranon superior projection is almost equal to the trochlea notch height. The radial notch is a rounded facet which lies against the disto-medial trochlea notch. Distal to the radial notch the supinator crest and the ulna tuberosity are form defined ridges.

c) The radius

The head shape is ovoid. It bears a deep rounded depression for accommodation of the capitulum. The lateral aspect is higher than the medial aspect. The bicipital tuberosity is half circular with a nodule on its distal corner. The neck is long compared to *Papio*. The neck and the shaft are medio-laterally flattened. The shaft has a slight lateral bow.

d) The femur

The head is superiorly oriented. The greater trochanter has a blunt apex and is superiorly oriented. The lesser trochanter is dorsally oriented. The superior neck extension is reduced towards the head; it has more surface area distally than superiorly. The intertrochanteric groove is deep and elongated proximo-distally. The greater trochanter lateral surface area is rugose. Distally the lateral condyle is narrower than the medial condyle.

*Cercopithecus aethiops* is used to identify specimens of modern taxa which are provenanced as such in their catalogues from University of the Witwaterand. For ease of reference and consistency with their cataloguing, the species *Cercopithecus aethiops* is retained.

is

c. Subfamily Colobinae Jerdon, 1867

Tribe Colobini Blyth, 1875

Genus *Colobus* Illiger, 1811

Species *Colobus guezara*



Figure 3.8. Modern *Colobus guezara* specimens, a) humerus, b) ulna, c) radius, d) femur, and e) tibia.

a) The humerus

The humeral head is rounded on anterior view. The greater and lesser tuberosities are almost equal in size. The greater tuberosity superior extension lies below the level of the head. Lesser tuberosity and head are continuous. Unlike in the cercopithecines, the

proximal humeral shaft in *Colobus*, the delto-triceps-brachialis and the deltoid crest are very pronounced. The bicipital tuberosity is shallow. Its medial and lateral edges are not defined. The shaft has a slight posterior curvature. The medial epicondyle is retroflexed. The olecranon fossa is deep and oval in shape. Distally, the shape is symmetrical in dorso-ventral view. The medial epicondyle has an extreme medial protuberance. The capitulum is bulbous and prominent. The trochlea distal projection is very short.

b) The ulna

The olecranon process is long and does not bear the same retroflexion seen in the papionins; it is straight. The olecranon bears a superiorly inclined medial flange which is another feature not seen in the papionins. On medial aspect, the olecranon superior portion is deeply cavitated creating a medial flange posteriorly. The trochlea notch proximo-distal height is almost the same as the proximal extension of the olecranon notch. The radial notch has an inverted triangle shape. The shaft has a slight lateral bow. The ulna styloid is blunt.

c) The radius

The head is oval with an extreme anterior-posterior compression unlike what is seen in the Cercopithecines. The head superior aspect has a deep depression. The radial neck is dorso-ventrally flattened. The bicipital tuberosity is a square-like eminence. The shaft is laterally bowed.

d) The femur

The femur head is supero-inferiorly compressed. The greater trochanter projects above the level of the head and is almost medially inclined. The lesser trochanter is small and medially inclined. It has a parabolic profile. The intertrochanteric groove is a small rounded fossa which lies at the same level of the head. The neck is very short and stout. The femur shaft resembles that of papionins; it is straight and symmetrical in the dorso-ventral plane. The condyles are splayed and are almost equal in size.

d. Subfamily Cercopithecinae Gray 1921

Tribe Papionini Burnett 1828

Subtribe Papionina Burnett 1828

Genus: *Mandrillus* Ritgen 1824

Species *Mandrillus sphinx*



Figure 3.9. Modern *Mandrillus sphinx* specimens, a) humerus, b) radius, c) ulna, d) tibia and e) femur.

a) The humerus

The humerus looks very similar to *Colobus*. The head shape is rounded on anterior view. On the proximal shaft, the delto-triceps-brachialis and the deltoid crest are distinct, however not as marked as seen in *Colobus*. The greater tuberosity is almost at the same level as the head. It is almost equal in size to the lesser tuberosity. Distally, the shaft is asymmetrical (as seen in cercopithecines). The distal lateral wall is wider and thicker

above the lateral epicondyle. The olecranon is deep with a triangular shape. The medial epicondyle is retroflexed. The trochlea distal lip is long. The capitulum is rounded, however it is modestly protuberant compared to *Colobus*.

b) The ulna

The ulna resembles papionin ulnae. The olecranon is short and has anterior retroflexion. On anterior view, the anconeal process forms a pronounced beak, with the lateral aspect more elevated compared to the medial aspect. The radial notch is medio-laterally elongated, it forms an oval shape. The trochlea notch has a crescentic outline in the supero-inferior axis. The ulna tuberosity and the supinator crest form defined ridges creating a depression distal to the radial notch. The ulna shaft is approximately straight. Distally, the styloid process is blunt.

c) The radius

The bicipital tuberosity bears a slit-like furrow in its centre. Unlike *Colobus*, the head is thicker in the proximo-distal axis. Similar to colobines, the superior aspect of the radial head bears a deep indentation for accommodation of the capitulum. The neck is thicker than *Colobus* and oval in cross section. The shaft has a lateral bow. The radial styloid process is blunt.

d) The femur

The intertrochanteric groove on the *Madrillus* lies at the same level as the head. The lesser trochanter is flanked by a shallow depression on its supero-lateral aspect. The lesser trochanter is medially facing with a rough surface. It does not possess the groove seen in papionins. The neck is very short. The greater trochanter is elevated above the head; however it is short and faces supero-medially. The greater trochanter surface area is almost flat with a rough surface. The shaft is nearly straight as seen in other cercopithecines. The distal condyles are not as splayed as seen in *Colobus*. On anterior view, the lateral condyle is narrower than the medial condyle.



### 3.4. Establishing diagnostic morphology: quantitative analysis:

Three approaches are undertaken for the quantitative analysis. The first involves descriptive statistics of the comparative sample to illustrate variation present in the sample. Only the proximal epiphyseal joints of the ulna, the radius and the femur are subjected to statistical analysis. Descriptive statistics provide Bivariate regression analysis demonstrates correlations between variables. Multivariate Analysis of Variance (ANOVA) is applied to the measurement set to determine where the differences lie between the taxa. Bivariate regression analysis suggests strong linear correlation among morphological traits of the humerus, the ulna and the femur. Results of the Analysis of Variance (ANOVA) point to limited statistical significance. Only traits on the proximal radius and the proximal femur demonstrate differences among taxa.

Table 3.13. Descriptive statistics of the humerus proximal medio-lateral breadth (PMLB)

<b>Taxa</b>	<b>N</b>	<b>Minimum</b>	<b>Maximum</b>	<b>Mean</b>	<b>SD</b>	<b>CV</b>
<i>Papio sp</i>	10	25	34	39	2.8643	9.87
<i>Cercopithecus aethiops</i>	9	15	18.3	17.14	1.2164	7.9
<i>Colobus guezara</i>	4	20	26	23.675	2.6094	11.02
<i>Mandrillus sphinx</i>	1	26	26	26		

Table 3.14. Descriptive statistics of the humeral head diameter (HHD)

<b>Taxa</b>	<b>N</b>	<b>Minimum</b>	<b>Maximum</b>	<b>Mean</b>	<b>SD</b>	<b>CV</b>
<i>Papio sp</i>	10	12.69	26	21.539	3.8419	17.83
<i>Cercopithecus aethiops</i>	10	10.91	14.9	13.946	4.4058	31.359
<i>Colobus guezara</i>	4	15.5	19.9	18.3	2.0607	11.2608
<i>Mandrillus sphinx</i>	1	21	21	21		

Table 3.15. Descriptive statistics of the humerus anterior posterior length of humeral head (APLHH)

<b>Taxa</b>	<b>N</b>	<b>Minimum</b>	<b>Maximum</b>	<b>Mean</b>	<b>SD</b>	<b>CV</b>
<i>Papio</i>	10	23.2	28.31	25.252	2.5001	9.900

<i>Cercopithecus aethiops</i>	7	13.36	15.5	14.7386	0.67	4.545
<i>Colobus guezara</i>	4	17.21	20.1	19.05	1.8267	9.588
<i>Mandrillus sphinx</i>	1	22.6	22.6			

Table 3.16. Descriptive statistics of the humerus greater tuberosity diameter (GTD)

<i>Taxa</i>	<b>N</b>	<b>Minimum</b>	<b>Maximum</b>	<b>Mean</b>	<b>SD</b>	<b>CV</b>
<i>Papio</i>	10	15	19.8	17.202	2.3422	13.6157
<i>Cercopithecus aethiops</i>	9	9	12	10.7156	1.268	11.832
<i>Colobus guezara</i>	4	12.9	16.4	14.4	1.6912	11.744
<i>Mandrillus sphinx</i>	1	13	13			

Table 3.17. Descriptive statistics of the humerus bi-epicondylar breadth (BEB)

<i>Taxa</i>	<b>N</b>	<b>Minimum</b>	<b>Maximum</b>	<b>Mean</b>	<b>SD</b>	<b>CV</b>
<i>Papio</i>	10	31	44	34.659	3.7652	10.837
<i>Cercopithecus aethiops</i>	9	17	23.1	20.9367	2.1136	10.0954
<i>Colobus guezara</i>	4	26	34.9	30.275	9.9246	12.963
<i>Mandrillus sphinx</i>	1	33	33			

Table 3.18. Descriptive statistics of the humerus medial trochlea flange length (MTFL)

<i>Taxa</i>	<b>N</b>	<b>Minimum</b>	<b>Maximum</b>	<b>Mean</b>	<b>SD</b>	<b>CV</b>
<i>Papio sp</i>	10	16.17	18.9	17.786	2.0851	11.723
<i>Cercopithecus aethiops</i>	9	8	12.1	10.45	1.1951	11.428
<i>Colobus guezara</i>	4	9.1	12.3	11.075	1.3913	12.562
<i>Mandrillus sphinx</i>	1	13.2	13.2			

Table 3.19. Descriptive statistics of the humerus lateral epicondyle to medial edge of trochlea (LEMET)

<i>Taxa</i>	<b>N</b>	<b>Minimum</b>	<b>Maximum</b>	<b>Mean</b>	<b>SD</b>	<b>CV</b>
<i>Papio sp</i>	10	28	34.9	31.31	2.8196	9.0052
<i>Cercopithecus aethiops</i>	9	14.7	19.4	17.5533	1.5181	8.6448
<i>Colobus guezara</i>	4	21	28	25.025	2.9556	11.8107
<i>Mandrillus sphinx</i>	1	26	26			

Table 3.20. Descriptive statistics of the humerus distal articular breadth (DAB)

<i>Taxa</i>	<b>N</b>	<b>Minimum</b>	<b>Maximum</b>	<b>Mean</b>	<b>SD</b>	<b>CV</b>
<i>Papio sp</i>	10	23.4	30	25.525	2.3284	9.12
<i>Cercopithecus aethiops</i>	9	11	16.2	13.4467	1.6191	12.0411
<i>Colobus guezara</i>	4	17.1	24.9	20.525	3.3521	15.8443
<i>Mandrillus sphinx</i>	1	22.6	22.6			

Table 3.21. Descriptive statistics of the humerus proximo-distal height of capitulum (PDHC)

<i>Taxa</i>	<b>N</b>	<b>Minimum</b>	<b>Maximum</b>	<b>Mean</b>	<b>SD</b>	<b>CV</b>
<i>Papio sp</i>	10	13.69	18	14.949	1.3462	9.005
<i>Cercopithecus aethiops</i>	9	7.38	18	9.9289	3.341	33.364
<i>Colobus guezara</i>	4	8	14.9	10.75	2.9331	27.285
<i>Mandrillus sphinx</i>	1	11	11			

Table 3.22. Descriptive statistics of the humerus maximum medio-lateral length of olecranon fossa (MMLLO)

<i>Taxa</i>	<b>N</b>	<b>Minimum</b>	<b>Maximum</b>	<b>Mean</b>	<b>SD</b>	<b>CV</b>
<i>Papio sp</i>	8	12.1	26.2	15.0589	4.5809	3.04
<i>Cercopithecus aethiops</i>	9	9.02	14.2	11.35	1.9182	16.900
<i>Colobus guezara</i>	4	11	14.2	13.325	1.5521	11.648
<i>Mandrillus sphinx</i>	1	12.3	12.3			

Table 3.23. Descriptive statistics of the humerus maximum proximo-distal length of olecranon fossa (MPDLO)

<i>Taxa</i>	<b>N</b>	<b>Minimum</b>	<b>Maximum</b>	<b>Mean</b>	<b>SD</b>	<b>CV</b>
<i>Papio sp</i>	9	9.8	19	11.9956	3.1772	26.48
<i>Cercopithecus aethiops</i>	8	4.9	9.62	6.8	1.5097	22.201
<i>Colobus guezara</i>	4	8	11	9.2	1.4697	15.974
<i>Mandrillus sphinx</i>	1	11				

Table 3.24. Descriptive statistics of the humerus axis of medial epicondyle (AME)

<i>Taxa</i>	<b>N</b>	<b>Minimum</b>	<b>Maximum</b>	<b>Mean</b>	<b>SD</b>	<b>CV</b>
<i>Papio sp</i>	10	30	40	38	3.496	9.200
<i>Cercopithecus aethiops</i>	9	34	44	38.555	2.9202	7.574
<i>Colobus guezara</i>	4	23	30	27	3.559	13.181
<i>Mandrillus sphinx</i>	40	40	40			

### The Ulna

Table 3.25. Descriptive statistics of the ulna anterior-posterior length of olecranon process (APLOP)

	<b>N</b>	<b>Minimum</b>	<b>Maximum</b>	<b>Mean</b>	<b>SD</b>	<b>CV</b>
<i>Papio sp</i>	8	22	34	25.7013	3.5746	13.908
<i>Cercopithecus aethiops</i>	7	7.9	16.9	12.5829	3.2918	26.160
<i>Colobus guezara</i>	4	7.4	16.1	12.7	3.8549	30.353
<i>Mandrillus sphinx</i>	2	6	10.3	8.15	3.0406	37.307

Table 3.25. Descriptive statistics of the ulna proximo-distal height of olecranon process (PDHOP)

	<b>N</b>	<b>Minimum</b>	<b>Maximum</b>	<b>Mean</b>	<b>SD</b>	<b>CV</b>
<i>Papio sp</i>	8	10	16.15	3.1255	3.1255	25.996
<i>Cercopithecus aethiops</i>	7	6	10.82	8.5514	2.606	30.474
<i>Colobus guezara</i>	4	7.4	16.1	12.7	3.8549	30.353
<i>Mandrillus sphinx</i>	2	6	10.3	8.15	3.0406	37.3071

Table 3.26. Descriptive statistics of the ulna medio-lateral breadth of olecranon process (MLBOP)

	<b>N</b>	<b>Minimum</b>	<b>Maximum</b>	<b>Mean</b>	<b>SD</b>	<b>CV</b>
<i>Papio sp</i>	8	11	15	12.8588	1.3093	10.182
<i>Cercopithecus aethiops</i>	7	7.24	9.48	7.95	0.7302	9.183
<i>Colobus guezara</i>	4	9.5	11.8	10.75	0.9469	8.808
<i>Mandrillus sphinx</i>	2	10.2	11	10.6	0.5657	5.336

Table 3.27. Descriptive statistics of the ulna Proximo-distal length of trochlea notch (PDLTN)

	<b>N</b>	<b>Minimum</b>	<b>Maximum</b>	<b>Mean</b>	<b>SD</b>	<b>CV</b>
<i>Papio sp</i>	7	14.2	18.9	17.0262	1.9085	11.209
<i>Cercopithecus aethiops</i>	6	7.6	11.8	9.765	1.407	14.4680
<i>Colobus guezara</i>	4	11.2	14.1	12.325	1.242	10.0768
<i>Mandrillus sphinx</i>	2	13	13	13		

The radius

Table 3.28. Descriptive statistics of the radius maximum dimension of radial head (MDRH)

	<b>N</b>	<b>Minimum</b>	<b>Maximum</b>	<b>Mean</b>	<b>SD</b>	<b>CV</b>
<i>Papio sp</i>	9	14.2	18	16.437	1.2932	7.86
<i>Cercopithecus aethiops</i>	8	8.5	9.1	9.4387	0.6062	6.4226
<i>Colobus guezara</i>	8	7.9	16	13.3	3.6615	27.5301
<i>Mandrillus sphinx</i>	2	15	15.2	15.1	0.1414	0.936

Table 3.29. Descriptive statistics of perpendicular breadth of radial head (PBRH)

	<b>N</b>	<b>Minimum</b>	<b>Maximum</b>	<b>Mean</b>	<b>SD</b>	<b>CV</b>
<i>Papio sp</i>	9	9.5	16.8	15.0544	2.1927	14.564
<i>Cercopithecus aethiops</i>	8	7.8	9.37	8.6563	0.571	6.595
<i>Colobus guezara</i>	4	11	13.4	11.975	1.034	8.6346
<i>Mandrillus sphinx</i>	2	13.1	14	13.55	0.6364	4.6966

Table 3.30. Descriptive statistics of the radius proximo distal height of radial neck (PDHRN)

	<b>N</b>	<b>Minimum</b>	<b>Maximum</b>	<b>Mean</b>	<b>SD</b>	<b>CV</b>
<i>Papio sp</i>	8	4.9	8	6.57	0.9121	13.882
<i>Cercopithecus aethiops</i>	8	4	8.5	5.7525	1.4849	25.813
<i>Colobus guezara</i>	4	6	13.3	7.875	3.617	45.929
<i>Mandrillus sphinx</i>	2	5.9	7	6.45	0.7778	12.059

Table 3.31. Descriptive statistics of the radius proximo distal height of radial neck and head (PDHRNH)

	N	Minimum	Maximum	Mean	SD	CV
<i>Papio sp</i>	8	12	15.41	12.8889	1.1756	9.1213
<i>Cercopithecus aethiops</i>	8	7.1	13	9.4112	1.7394	18.482
<i>Colobus guezara</i>	4	7.2	15	10.65	3.2919	30.909
<i>Mandrillus sphinx</i>	2	12	12			

The femur

Table 3.32. Descriptive statistics of the femur anterior posterior head dimension (APHD)

	N	Minimum	Maximum	Mean	SD	CV
<i>Papio sp</i>	10	20.9	25	22.222	1.7871	8.0421
<i>Cercopithecus aethiops</i>	7	10.9	13.23	12.134	0.9391	7.7390
<i>Colobus guezara</i>	4	16	17.8	17.05	0.7937	4.6552
<i>Mandrillus sphinx</i>	2	17.5	17.9	17.7	0.2828	15.9798

Table 3.33. Descriptive statistics of the femur medio-lateral breadth of femur head (MLBFH)

	N	Minimum	Maximum	Mean	SD	CV
<i>Papio sp</i>	10	17.5	22	18.739	1.324	7.0655
<i>Cercopithecus aethiops</i>	7	8.2	10.98	10.2286	0.9629	9.4138
<i>Colobus guezara</i>	4	12.8	15.7	14.025	1.2121	8.642
<i>Mandrillus sphinx</i>	2	14.9	19.9	17.4	3.5355	20.3191

Table 3.34. Descriptive statistics of the femur greater trochanter projection (GTP)

	N	Minimum	Maximum	Mean	SD	CV
<i>Papio sp</i>	9	9.5	14	11.5433	1.408	12.1973
<i>Cercopithecus aethiops</i>	8	4.6	7.97	5.795	1.225	21.1397
<i>Colobus guezara</i>	4	6	9.1	7.1	1.3736	19.345
<i>Mandrillus sphinx</i>	2	6.6	7.4	7	0.5657	8.081

Table 3.35. Descriptive statistics of the radius neck diameter (ND)

	<b>N</b>	<b>Minimum</b>	<b>Maximum</b>	<b>Mean</b>	<b>SD</b>	<b>CV</b>
<i>Papio sp</i>	10	9.11	21	15.867	3.1955	20.141
<i>Cercopithecus aethiops</i>	8	3.8	12.6	8.3288	2.4907	29.904
<i>Colobus guezara</i>	4	9	16	13.5	3.1091	23.030
<i>Mandrillus sphinx</i>	2	8.7	9	8.85	0.2121	2.396

Table 3.36. Descriptive statistics of the femur medio-lateral neck diameter (MLND)

	<b>N</b>	<b>Minimum</b>	<b>Maximum</b>	<b>Mean</b>	<b>SD</b>	<b>CV</b>
<i>Papio sp</i>	10	4	12.1	8.444	2.3671	28.0334
<i>Cercopithecus aethiops</i>	8	4	12.6	5.9463	2.915	49.0221
<i>Colobus guezara</i>	5	6.5	13.2	7.92	3.2813	41.430
<i>Mandrillus sphinx</i>	2	6	7	6.5	0.7071	10.878

Table 3.37. Descriptive statistics of the femur bi-epicondylar breadth (BEB)

	<b>N</b>	<b>Minimum</b>	<b>Maximum</b>	<b>Mean</b>	<b>SD</b>	<b>CV</b>
<i>Papio sp</i>	10	28.5	42	35.477	3.6518	10.2933
<i>Cercopithecus aethiops</i>	7	18	22.38	20.72	1.5918	7.6822
<i>Colobus guezara</i>	4	28	32.5	30.6	1.8815	6.148
<i>Mandrillus sphinx</i>	2	29	31.3	30.15	1.6262	5.394

Table 3.38. Descriptive statistics of the radius neck shaft angle (NSA)

	<b>N</b>	<b>Minimum</b>	<b>Maximum</b>	<b>Mean</b>	<b>SD</b>	<b>CV</b>
<i>Papio sp</i>	10	120	145	128.7	8.4202	6.542
<i>Cercopithecus aethiops</i>	8	100	145	117.625	15.9458	13.5564
<i>Colobus guezara</i>	4	127	140	133	5.7155	4.2973
<i>Mandrillus sphinx</i>	2	125	135	133	5.7155	4.2973

Table 3.39. Descriptive statistics of the femur medial condyle width (MCW)

	N	Minimum	Maximum	Mean	SD	CV
<i>Papio sp</i>	10	11	18	12.244	2.9415	24.024
<i>Cercopithecus aethiops</i>	8	5.5	8.54	7.2275	0.8526	11.7966
<i>Colobus guezara</i>	4	8.1	11.6	10.375	1.5543	14.9811
<i>Mandrillus sphinx</i>	2	13	17.5	15.25	3.182	20.8654

Table 3.40. Descriptive statistics of the femur radius lateral condyle width (LCW)

	N	Minimum	Maximum	Mean	SD	CV
<i>Papio sp</i>	10	8	12	10.22	1.263	12.357
<i>Cercopithecus aethiops</i>	8	5	7.9	6.5363	0.8658	1.2245
<i>Colobus guezara</i>	4	8.1	11	10.175	1.3961	13.7211
<i>Mandrillus sphinx</i>	2	8.2	9.7	8.95	1.0607	11.8509

### 3.4.2. Results of the Bivariate Regression Analysis

Bivariate regression analysis was run to establish the relationship and strength of association between skeletal traits found in the Sterkfontein fossil cercopithecoid postcranial assemblage.

#### a) The humerus

Five humeral traits were assessed for strength of correlation: the anterior posterior length of humeral head and medio-lateral width of humeral head; maximum proximo-distal length of olecranon and maximum medio-lateral breadth of olecranon; humeral distal articulation and maximum medio-lateral breadth of olecranon fossa; the width of distal humeral articulation and bi-epicondylar width and; width of distal humeral articulation and width of distal trochlea.

Bivariate analysis for the anterior posterior length of humeral head and medio-lateral width of humeral head (Fig. 3.10) suggests a strong positive relationship ( $r = 0.9$ ) between the two traits. Data for the medio-lateral width of the olecranon fossa and proximo-distal length of olecranon fossa was only derived from 10 specimens. Bivariate



analysis of maximum proximo-distal length of olecranon and maximum medio-lateral breadth of olecranon (Fig. 3.11) led to a correlation ( $r$ ) of 0.605, which suggests a positive linear correlation. The same analysis for the width of distal humeral articulation and bi-epicondylar width (Fig. 3.12) shows a strong positive Correlation ( $r = 0.9$ ) between the two traits. The fourth index, humeral distal articulation and maximum medio-lateral breadth of olecranon fossa (Fig. 3.13) shows a strong positive relationship,  $r = 0.8$ . Bivariate analysis of the fifth index, width of distal humeral articulation and length of distal trochlea (Fig. 3.14) shows a strong positive relationship between the distal articulation and the width of the trochlea.

Table 3.41. Legend for the statistical plots.

Tribe	Colour	Symbol	Genus
Colobines	red	dot	<i>Colobus</i>
	red	square	<i>Procolobus</i>
	red	open square	<i>Rhinocolobus</i>
	red	x (letter)	<i>Cearcopithecoides</i>
Cercopithecini	black	diamond	<i>Cercopithecus</i>
	black	star	<i>Chlorocebus</i>
Papionins	black	triangle	<i>Papio</i>
	black	inverted triangle	<i>Parapapio</i>
	black	Fill triangle	<i>Theropithecus</i>
	black	dash	<i>Mandrillus</i>
Papionins (Sterkfontein Fossils)	aqua	bar	<i>Papionin</i>
	aqua	triangle	<i>Papio</i>
	aqua	inverted triangle	<i>Parapapio</i>
	aqua	Fill inverted triangle	<i>Papio/parapapio</i>
	aqua	Fill triangle	<i>Theropithecus</i>

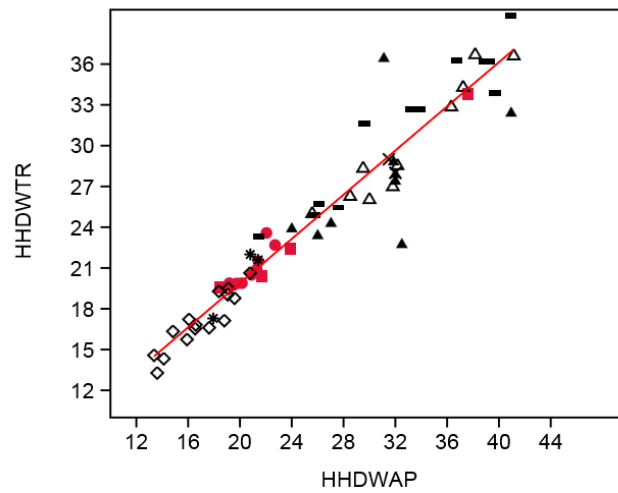


Figure 3.10. Bivariate plot for ‘anterior posterior length of humeral head (HHDWAP) and medio-lateral width of humeral head (HHDWTR)’.

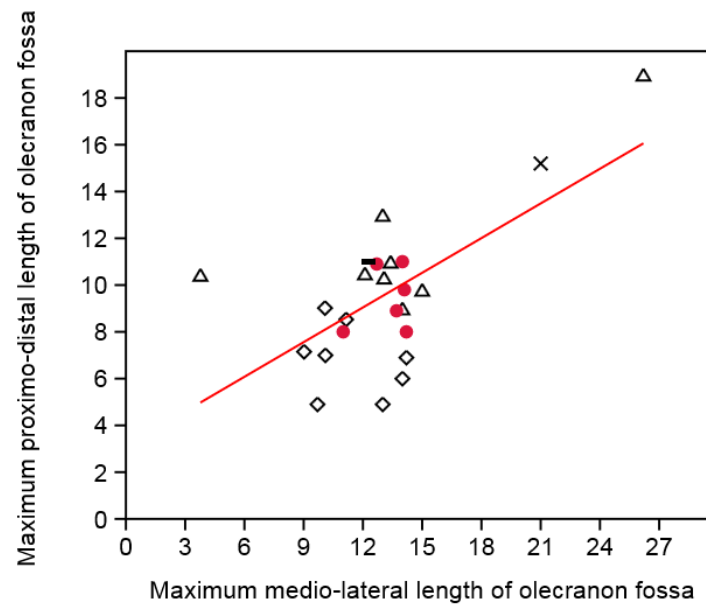


Figure 3.11. Bivariate plot for ‘maximum proximo-distal length of olecranon fossa and maximum medio-lateral lateral length of olecranon fossa’.

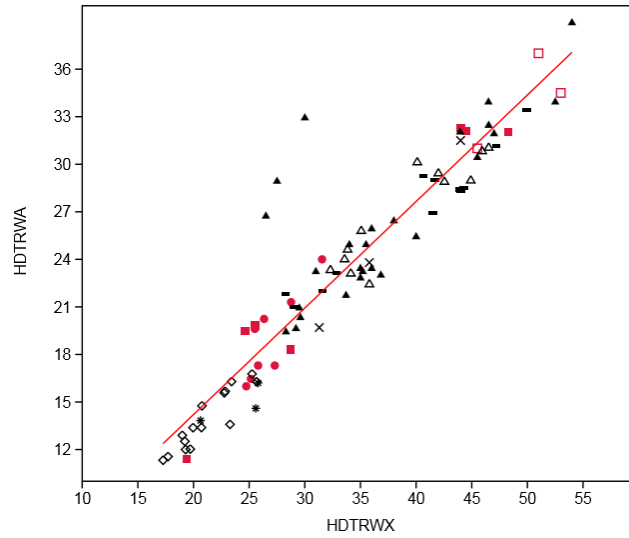


Figure 3.12. Bivariate plot for ‘width of distal humeral articulation (HDTRWA) and bi-epicondylar width (HDTRWX) ’.

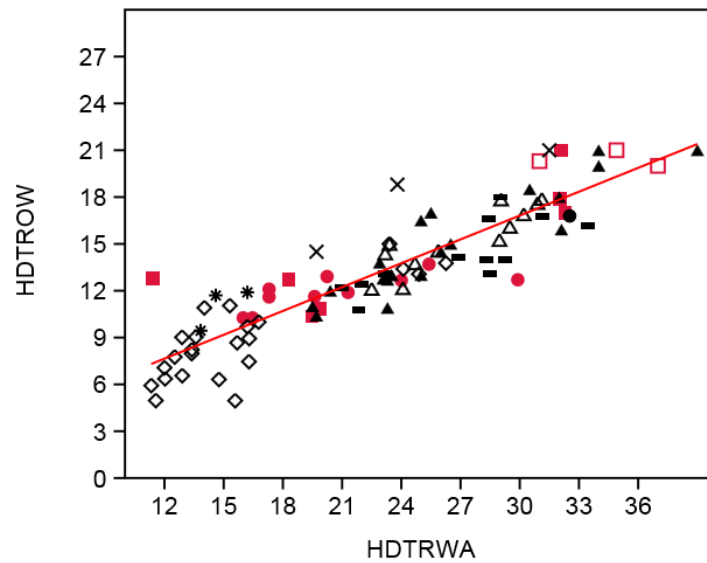


Figure 3.13. Bivariate plot for ‘humeral distal articulation (HDTRWA) and maximum medio-lateral breadth of olecranon fossa (HDTROW)’.

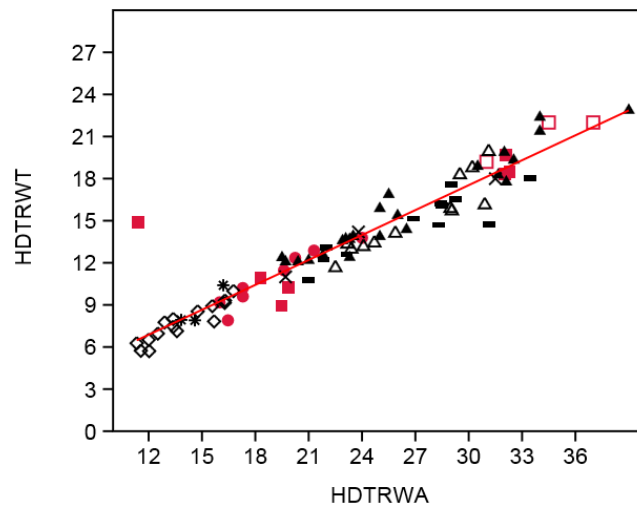


Figure 3.14. Bivariate plot for ‘width of distal humeral articulation and length of distal trochlea’.

b. The ulna

Bivariate regression analysis of the ulna olecranon height and trochlea notch length (Fig. 3.15) shows a strong positive correlation ( $r = 0.86$ ) between the two traits. A similar analysis for ulna proximo-distal height of olecranon and anterior-posterior length of olecranon (Fig 3.16) shows a very weak correlation ( $r = 0.3$ ). The same weak correlation of  $r = 0.3$  was reached when undertaking a bivariate regression analysis of olecranon proximo-distal length and trochlea notch proximo-distal length (Fig 3.17). On the ulna, other traits which demonstrate a strong positive correlation ( $r = 0.9$ ) are the trochlea notch proximo-distal height and medio-lateral breadth (Fig 3.18).

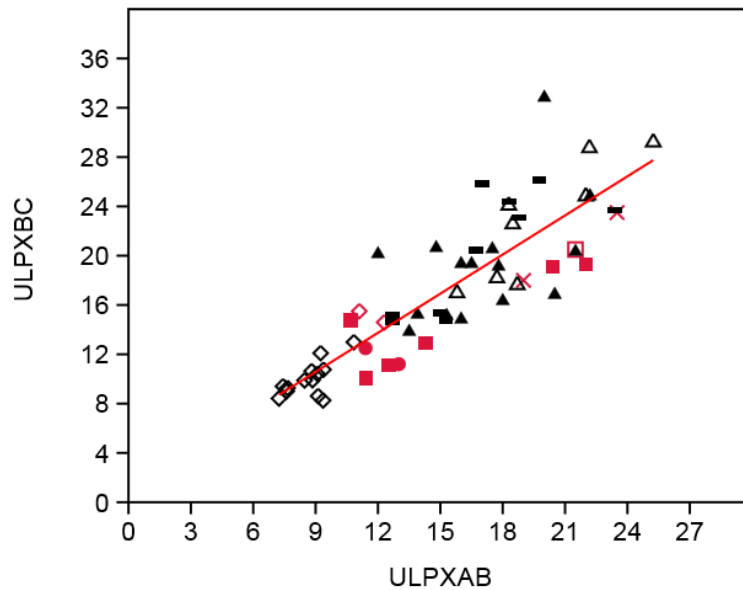


Figure 3.15. Bivariate plot for 'ulna olecranon to anterior proximal trochlea notch and trochlea notch length'.

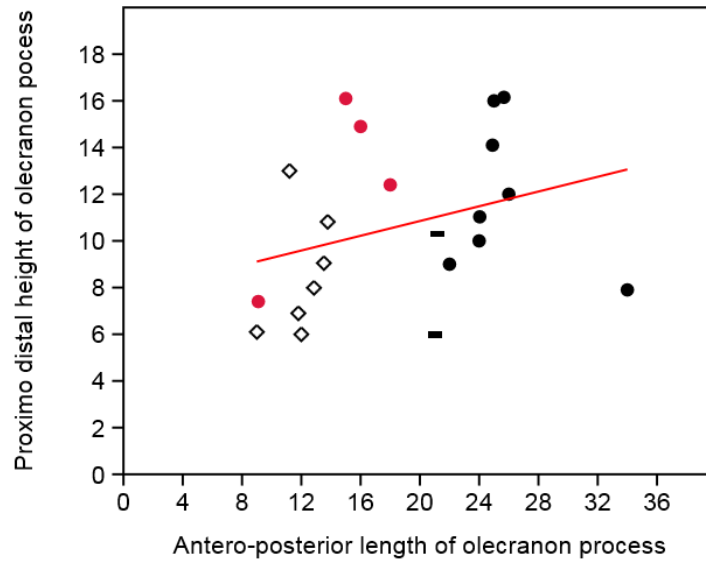


Figure 3.16. Bivariate plot for 'ulna proximo-distal height of olecranon and anterior-posterior length of olecranon process'.

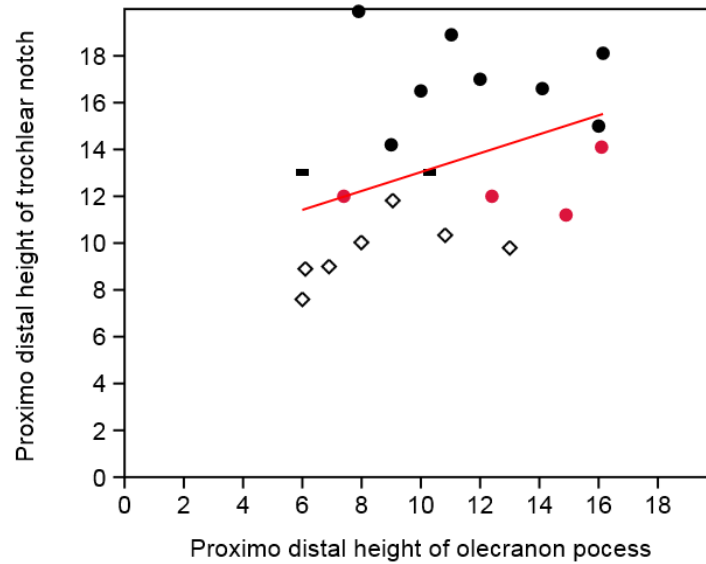


Figure 3.17. Bivariate plot for 'olecranon proximo-distal length and trochlea notch proximo-distal length'.

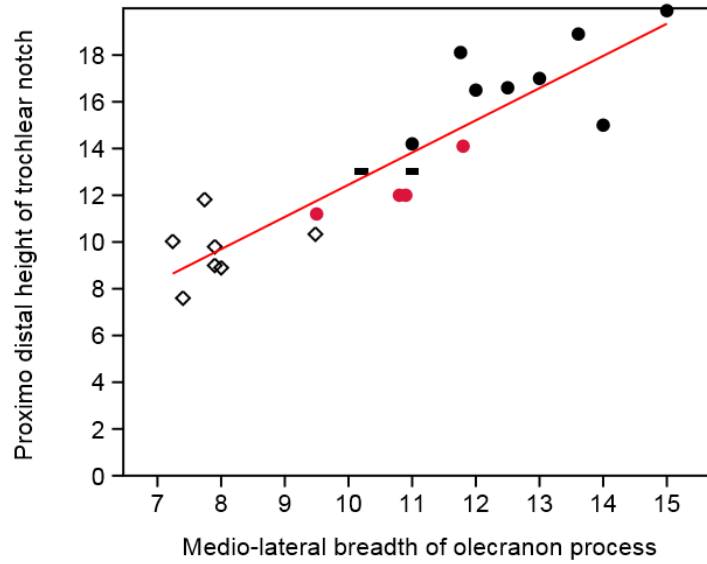


Figure 3.18. Bivariate plot for ulna 'proximo-distal height of trochlea notch and medio-lateral breadth of trochlea notch'.

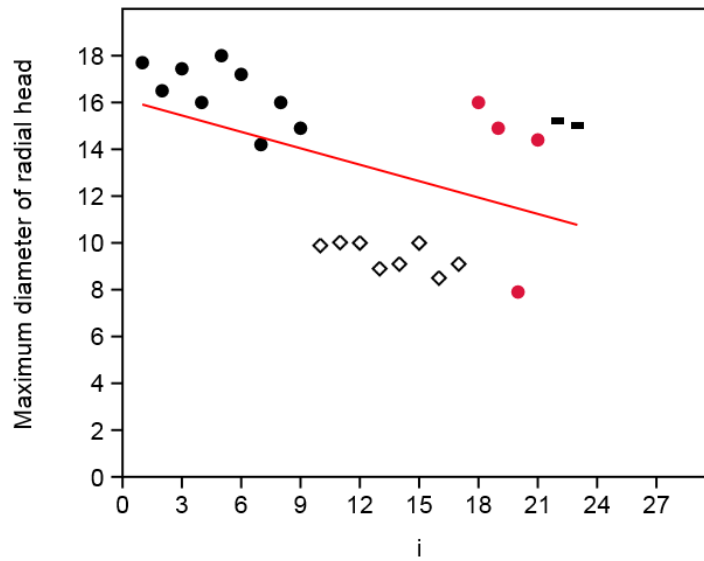


Figure 3.19. Bivariate plot for 'maximum diameter of radial head and perpendicular width of radial head'.

### The radius

No strong correlation exists in the radius indices studied. The maximum diameter of radial head and perpendicular breadth of radial head (Fig.3.19) have a moderate negative correlation ( $r = -0.45$ ). The radius neck anterior-posterior and medio-lateral breadth bivariate analysis (Fig. 3.20) illustrated a positive relationship between the two variables,  $r = 0.5$ .

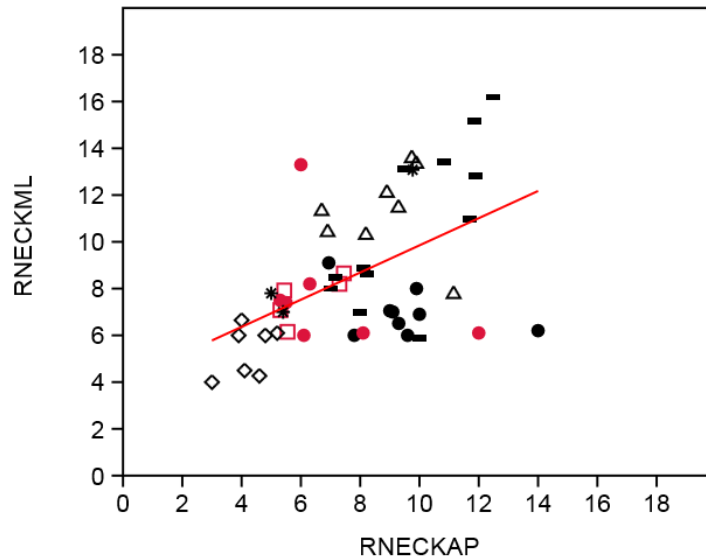


Figure 3.20. Bivariate plot for the 'radius neck anterior-posterior and medio-lateral breadth of radial neck'.



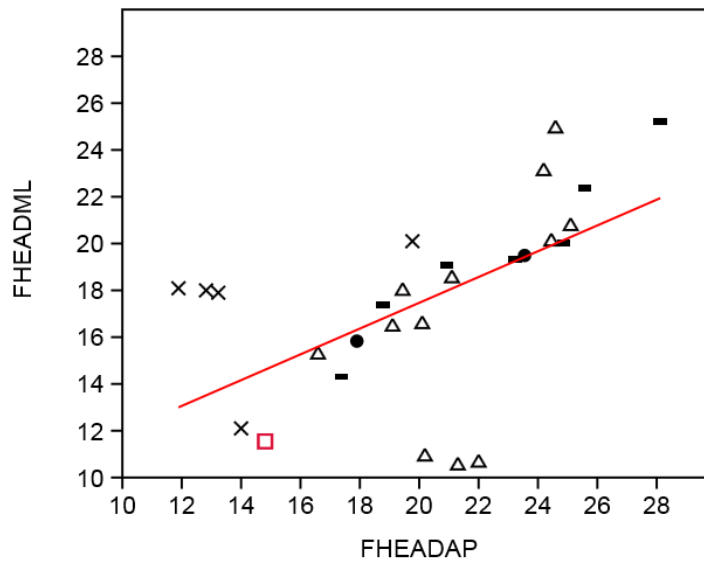


Figure 3.21. Bivariate plot for femur anterior-posterior neck breadth and medio-lateral neck width'.

c) The femur

Only one index showed a positive correlation on the femur. Bivariate analysis for the femur head medio-lateral width and anterior-posterior neck breadth (Fig 3.21) demonstrated a moderate positive correlation,  $r = 0.5$ .

### 3.4.3. Results for the Univariate Analysis of Variance (ANOVA)

a) Humerus

The following variables were tested for statistical significance and none were found to indicate statistical significance among the four genera (*Colobus*, *Cercopithecus*, *Mandrillus* and *Papio*): humeral head anterior-posterior length, and humeral head medio-lateral breadth; width of distal humerus and width of distal humerus articulation; width of humeral trochlea and humeral trochlea length and distal humerus anterior-posterior width and maximum medio-lateral width of olecranon fossa. The lateral epicondyle breadth to medial edge of trochlea and distal articular breadth at  $p < 0.05$  ( $p = 0.0103$ ;  $F = 7.097$ ). Bonferroni corrected  $p$  values are at 0.0081 for both the lateral epicondyle breadth to medial edge of trochlea and the distal articular breadth.

b) Ulna

On the ulna, none of the following variables demonstrated statistical significance, ( $p > 0.05$ ): the ulna olecranon height and olecranon anterior posterior length; the ulna trochlea notch height and ulna length from coronoid process to proximal olecranon. For control and to establish if other traits on the ulna, which are not necessarily preserved in the fossil remains, are capable of showing statistical significance, the ulna length and trochlea notch height was also run through ANOVA and the same conclusion (not statistically significant;  $p > 0.05$ ) was also reached. The olecranon proximo-distal height and trochlea proximo-distal height shows statistical significance ( $p = 0.01121$ ;  $F = 7.039$ ). Bonferroni corrected p values are at 0.0169 for both traits.

c) Radius

On the radius, the proximo-distal height of radial neck and head and the radial neck medio-lateral width demonstrated a significant positive relationship ( $p = 0.0278$ ;  $F = 5.208$ ). Bonferroni corrected values are ( $p$ ) 0.03634 for both traits. Significance is also found for the anterior posterior radius shaft and medio-lateral radial diameter ( $P = 0.00215$ ;  $F = 10.69$ ). Bonferroni corrected p values are 0.01016 for both traits. No statistical significance is recorded for radial length and proximo-distal length of radius from bicipital tuberosity to distal styloid process. ( $p > 0.05$ ). No significance was also found for radius neck anterior posterior length and neck medio lateral breadth ( $p > 0.05$ )

d) Femur

On the femur, only the antero-posterior length of head and medio-lateral width of head index point to positive statistical significance,  $p = 0.03095$ ,  $F = 4.909$ . Bonferroni  $p = 0.03117$ .

3.4.5. *Results of the Discriminant Function Analysis (DFA)*

DFA undertaken on the humerus from modern comparative monkeys suggest that a large percentage of the specimens were classified correctly (92.86%). The DFA plot shows

separation between the different genera (Figure 3.22). Higher variation in the groups is observed in axis one which is at 84% (Table 3.42).

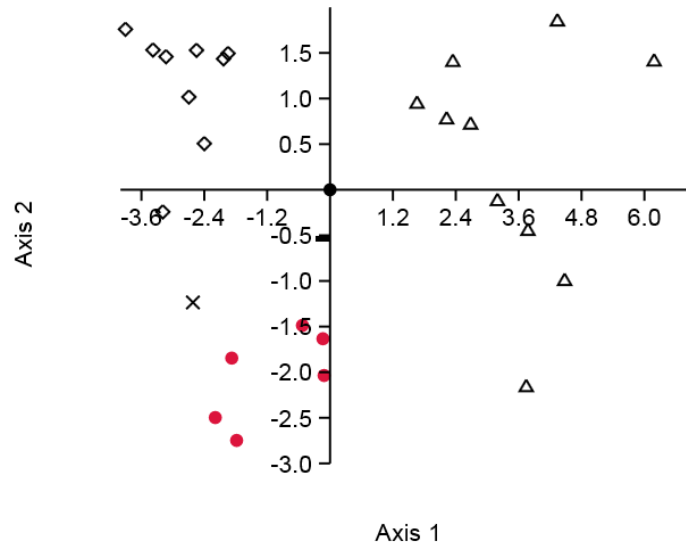


Figure 3.22. Discriminant analysis plot for modern comparative humerus based on genera

Table 3.42. Eigenvalue and percent values for DFA results for modern comparative humerus based on genera

Axis	Eigenvalue	Percent
1	8.552	84.27
2	1.457	14.39
3	0.13609	1.344

Table 3.43. Results for humerus, DFA Classification by genus

Point	Given group	Classification	Jackknifed
<i>Papio</i> sp	1	1	1
<i>Papio</i> sp	1	1	1
<i>Papio</i> sp	1	1	1
<i>Papio</i> sp	1	1	1
<i>Papio</i> sp	1	1	1
<i>Papio</i> sp	1	1	1
<i>Papio</i> sp	1	1	1
<i>Papio</i> sp	1	1	1
<i>Papio</i> sp	1	1	1
<i>Papio</i> sp	1	1	1
<i>Cercopithecus aethiops</i>	2	2	2
<i>Cercopithecus aethiops</i>	2	2	2
<i>Cercopithecus aethiops</i>	2	2	2
<i>Cercopithecus aethiops</i>	2	2	2
<i>Cercopithecus aethiops</i>	2	2	2
<i>Cercopithecus aethiops</i>	2	2	2
<i>Cercopithecus aethiops</i>	2	2	2
<i>Cercopithecus aethiops</i>	2	2	2
<i>Cercopithecus aethiops</i>	2	2	2
<i>Cercopithecoides williamsi</i>	2	3	3
Colobinae indet	3	3	3
Colobinae indet	3	3	3
<i>Colobus guezara</i>	3	4	4
<i>Colobus guezara</i>	3	3	4
<i>Colobus guezara</i>	3	3	3
<i>Colobus guezara</i>	3	3	3
<i>Mandrillus sphinx</i>	4	4	4
<i>Mandrillus sphinx</i>	4	4	3

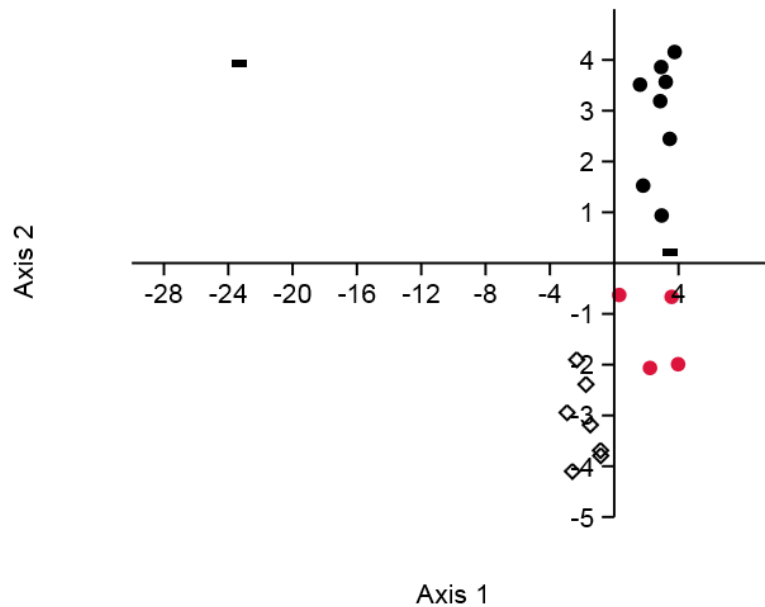


Figure 3.23. Discriminant analysis plot for modern comparative ulna based on genera

On the ulnae all of the specimens were correctly classified at 100%. The box plot (Fig 3.23) demonstrates distinction between the genera. Eigenvalues suggest (Table 3.43) that higher variability is observed in axis 1 at 79%.

Table 3.44. Eigenvalue and percent values for DFA results for modern comparative ulna based on genera

Axis	Eigenvalue	Percent
1	39.197	79.79
2	9.2422	18.81
3	0.68762	1.4

Table 3.45. Results for ulna DFA Classification by genus

Specimen no	Genus	Given group	Classification	Jackknifed
ZA 1227	<i>Papio</i> sp	1	1	3
Za 1226	<i>Papio</i> sp	1	1	1
Za 1228	<i>Papio</i> sp	1	1	1
Za 1299	<i>Papio</i> sp	1	1	1
Za 740	<i>Papio</i> sp	1	1	1
Za 1357	<i>Papio</i> sp	1	1	1
Za 1232	<i>Papio</i> sp	1	1	3
Za 1231	<i>Papio</i> sp	1	1	3
Za12s	<i>Cercopithecus aethiops</i>	2	2	2
V33	<i>Cercopithecus aethiops</i>	2	2	2
Za 973	<i>Cercopithecus aethiops</i>	2	2	2
Za 968	<i>Cercopithecus aethiops</i>	2	2	2
Za 1224	<i>Cercopithecus aethiops</i>	2	2	2
Za 864	<i>Cercopithecus aethiops</i>	2	2	2
Za 862	<i>Cercopithecus aethiops</i>	2	2	2
A2 981	<i>Colobus guezara</i>	3	3	3
A2 1437	<i>Colobus guezara</i>	3	3	3
A2/807	<i>Colobus guezara</i>	3	3	2
A2/155	<i>Colobus guezara</i>	3	3	2
A2/1971	<i>Colobus guezara</i>	3	3	1
A2/1972	<i>Mandrillus sphinx</i>	4	4	2

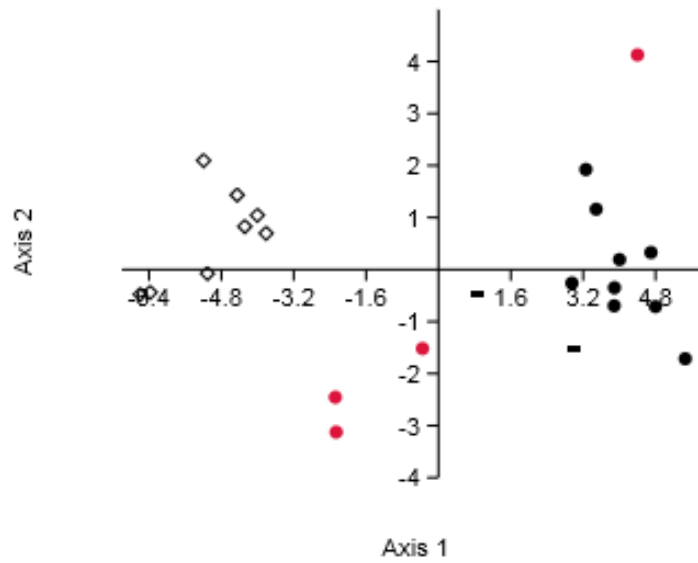


Figure 3.24. Discriminant analysis plot for modern comparative radius based on genera

The discriminant function for radii showed a perfect score, with 100% of the specimens correctly classified. More variation is observed in axis one which accounts for 96% of the difference (Fig 3.24; Table 3.46).

Table 3.46. Eigenvalue and percent values for DFA results for modern comparative radius based on genera.

Axis	Eigenvalue	Percent
1	11.986	96.34
2	0.4581	3.656

Table 3.47. Results for radius DFA Classification by genus

Point	Given group	Classification	Jackknifed
<i>Papio</i> sp	1	1	1
<i>Papio</i> sp	1	1	1
<i>Papio</i> sp	1	1	1
<i>Papio</i> sp	1	1	1
<i>Papio</i> sp	1	1	1
<i>Papio</i> sp	1	1	1
<i>Papio</i> sp	1	3	3
<i>Papio</i> sp	1	1	3
<i>Papio</i> sp	1	1	1
<i>Cercopithecus</i> <i>aethiops</i>	2	2	2
<i>Cercopithecus</i> <i>aethiops</i>	2	2	2
<i>Cercopithecus</i> <i>aethiops</i>	2	2	2
<i>Cercopithecus</i> <i>aethiops</i>	2	2	2
<i>Cercopithecus</i> <i>aethiops</i>	2	2	2
<i>Cercopithecus</i> <i>aethiops</i>	2	2	2
<i>Cercopithecus</i> <i>aethiops</i>	2	2	2
<i>Cercopithecus</i> <i>aethiops</i>	2	2	2
<i>Cercopithecus</i> <i>aethiops</i>	2	2	2
<i>Colobus</i> guezara	3	3	2
<i>Colobus</i> guezara	3	3	3
<i>Colobus</i> guezara	3	3	2
<i>Colobus</i> guezara	3	3	1
<i>Mandrillus sphinx</i>	3	1	1
<i>Mandrillus sphinx</i>	3	3	3



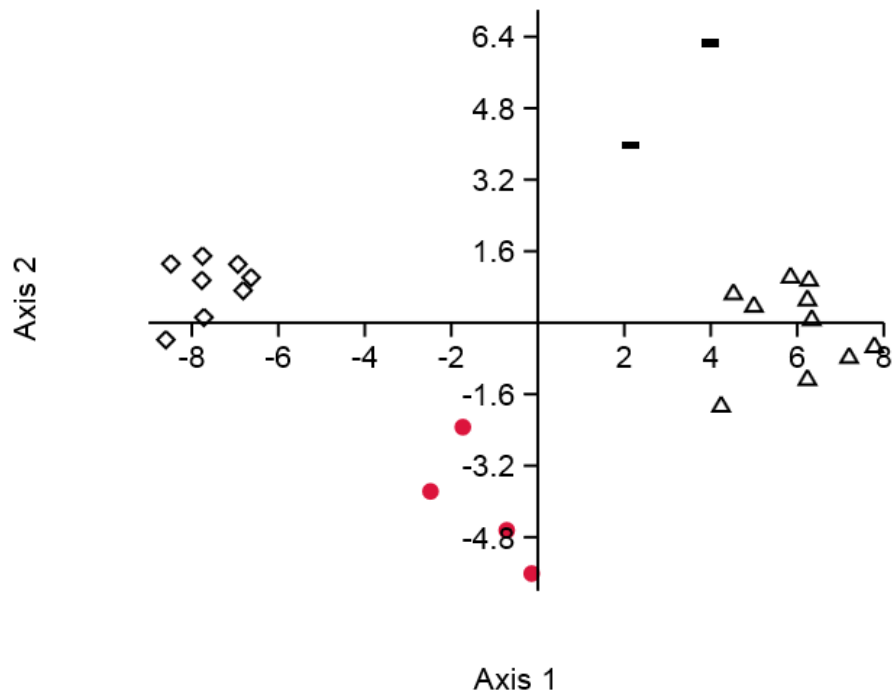


Figure 3.25. Discriminant analysis plot for modern comparative femur based on genera

Results of the discriminant function for the femur showed a 100% score for the classification. More distinction is observed in Axis one which is 86% of the variation (Fig 3.25; Table 3.48).

Table 3.48. Eigenvalue and percent values for DFA results for modern comparative femora based on genera

Axis	Eigenvalue	Percent
1	22.42	86.98
2	2.3034	8.936
3	0.85187	3.305
4	0.1931	0.7492

Table 3.49. Results for femur DFA Classification by genus

Point	Species	Given group	Classification	Jackknifed
Za 1227	<i>Papio</i> sp	1	1	1
Za 1226	<i>Papio</i> sp	1	1	1
Za 1228	<i>Papio</i> sp	1	1	1
BPI/C 541	<i>Papio</i> sp	1	1	1
Za 1360	<i>Papio</i> sp	1	1	1
Za 740	<i>Papio</i> sp	1	1	1
Za 1357	<i>Papio</i> sp	1	1	33
Za 1232	<i>Papio</i> sp	1	1	1
Za 1231	<i>Papio</i> sp	1	1	1
V33	<i>Cercopithecus aethiops</i>	2	2	22
Za 973	<i>Cercopithecus aethiops</i>	2	22	22
BPI/C 294	<i>Cercopithecus aethiops</i>	2	22	22
Za 12s	<i>Cercopithecus aethiops</i>	2	2	22
Za 968	<i>Cercopithecus aethiops</i>	2	22	22
Za 1244	<i>Cercopithecus aethiops</i>	22	22	2
Za 864	<i>Cercopithecus aethiops</i>	2	2	2
Za 862	<i>Cercopithecus aethiops</i>	2	2	2
Az/981	<i>Colobus guezara</i>	3	3	22
Az 1437	<i>Colobus guezara</i>	3	3	4
Az 807	<i>Colobus guezara</i>	3	3	2
A2/155	<i>Colobus guezara</i>	33	33	1
A2/1971	<i>Mandrillus sphinx</i>	4	4	1
A2/1972	<i>Mandrillus sphinx</i>	4	4	4

#### 3.4.6. Summary of the statistical analysis

Quantitative analysis undertaken through bivariate regression analysis suggests positive correlation of the traits studied on the humerus, the ulna, the radius and the femur. However, the humerus and the ulna are the only two skeletal elements with traits which are strongly associated. On the humerus, all indices showed a positive correlation. However, strong correlation was observed on the following variables a) width of distal humeral articulation and bi-epicondylar width; b) humeral distal articulation and maximum medio-lateral breadth of olecranon fossa, and c) width of distal humeral articulation and length of distal trochlea.

On the ulna, only two indices proved to have a strong positive relationship: a) the ulna olecranon height and trochlea notch length, and, b) the trochlea notch proximo-distal height and medio-lateral breadth. No strong correlation exists in the radius indices studied. The radius neck anterior-posterior and medio-lateral breadth bivariate analysis showed a moderate correlation. The femur head medio-lateral breadth and anterior-posterior length was the only femur index studied, and it showed positive association.

The Univariate Analysis of Variance demonstrated statistical significance on one index of the humerus (distal articular breadth and medial trochlea flange length) and one of the ulna (the trochlea notch proximo-distal height and olecranon process proximo-distal height). The radial neck (anterior posterior diameter and medio-lateral width as well as the neck height and neck and head length) proved statistically significant among the genera. The femur neck, anterior posterior width and medio-lateral length also showed statistical significance.

The discriminant function analysis of the modern comparative materials establishes that all analysed skeletal elements show success of classification and variability among the four genera. These complement skeletal parts are fully preserved, which is a different scenario from the highly fragmented Sterkfontein cercopithecoid remains. A multivariate analysis such as DFA will not be possible to conduct as it requires multiple variables and more than two groups to conduct.

### 3.5. Identification of specific carnivore agents

The methodology follows Dominguez-Rodrigo & Piqueras (2003) model for assessing tooth-pith data. This method was applied by Pickering *et al.* (2004c) on carnivore tooth pits in the Swartkrans Member 3 fossil assemblage.

Digital calipers are used to measure tooth pits and scores. These were categorized based on size and location (either occurring on the diaphysis or occurring on the epiphysis) on the bone. Carnivore categories considered in this study are small canids, middle sized carnivores, felids, large sized carnivores, hyaenas and dogs.

For the length on epiphyses

- Pits less than 4mm are assigned to small canids;
- Pits which range between 4mm and 6mm are assigned to middle sized carnivores and felids were excluded from this category; and
- All pits larger than 6mm were assigned to large carnivores and felids.

For the pit breadth of epiphysis

- Pits less than 4mm are assigned to small canids;
- Pits which range between 4mm and 6mm are assigned to middle sized carnivores and felids were excluded from this category; and
- All pits larger than 6mm are assigned to large carnivores and felids.

Measurements derived from tooth pits which occur in the diaphyses are grouped according to the length and breadth and each have two categories:

For tooth pit length-

- Pits less than 2mm are assigned to small carnivores to medium felids; and
- Pits which measure above 4mm are assigned to hyaenas, dogs and lions

For tooth pit breadth-

- Pits less than 1.5mm are assigned to small carnivores; and

- Pits which measure above 2mm are assigned to hyaenas, dogs and lions

In addition to tooth pit sizes, other taphonomic factors such as analysis of skeletal element frequencies are considered to provide a comprehensive assessment of the observed results.

### **3.6. Skeletal element spatial clustering**

Fossil cercopithecoid assemblages from Member 2, Jacovec Cavern, Member 4, StW 53 infill, Member 5 and Member 6 and Post Member 6 are investigated for spatial distribution within each infill. Even though squares do not necessarily reflect any discrete palaeoenvironmental spatial arrangement, data derived from spatial clustering is useful for taphonomic investigations. Temporal and chronological spatial clustering of all specimens is plotted to determine the spatial arrangement of the specimens in their respective deposits within the cave system. The relationship between the original cave opening at the time of accumulation, the taphonomic imprint within the assemblage and the spatial clustering patterns are discussed.

## CHAPTER FOUR

### RESULTS: TAXONOMY OF THE STERKFORTEIN FOSSIL CERCOPITHECOID POSTCRANIA

#### 4.1. Systematic Palaeontology of the Sterkfontein fossil cercopithecoid postcrania

##### 4.1.1. Qualitative Analysis

Anatomical descriptions and comparative observations made in the qualitative analysis point to the Sterkfontein fossil cercopithecoid postcrania assemblage which comprises of a minimum of two subfamilies, Cercopithecinae and Colobinae and five genera, *Papio*, *Parapapio*, *Theropithecus*, *Cercopithecoides* and *Cercopithecus*. Sixty-three elements, which constitute 24% of the NISP, cannot be differentiated between *Papio* and *Parapapio*, and therefore a general category *Papio/Parapapio* is utilised. Due to the high fragmentation level of the Sterkfontein fossil cercopithecoid assemblage no specimens could be identified to species level.

The most common genera identified are lumped into the *Papio/Parapapio* category with an NISP of 63. This is followed by *Papio* with 41 specimens identified. Humeri constitute the largest percentage of identified elements with an NISP of 85, constituting 32% of the total identified NISP, while femora are the least identified at NISP of 30, constituting 11 % of the total NISP. *Parapapio* specimens identified from the Sterkfontein assemblage display similar morphology, albeit with differing sizes, to known East African materials. Colobines are very limited in the assemblage; however, *Cercopithecoides* sp is tentatively assigned to one specimen.

Subfamily	Cercopithecinae Gray 1921
Tribe	Papionini Burnett 1828
Subtribe	Papionina Burnett 1828
Genus	<i>Parapapio</i> . Jones 1937

##### a) The humerus

Sixteen humeri are assigned to the *Parapapio* genus. These share the following fifteen characteristics; 1) the head has a hemi-spherical shape; 2) the greater tuberosity lies below the head; 3) the lateral surface of the greater tuberosity is convex; 4) the greater tuberosity is equal to or larger than the lesser tuberosity; and 5) the bicipital groove is shallow. On the distal humeri- 6) on the coronal plane the distal shaft medial and lateral aspects are asymmetrical; 7) on the coronal plane the distal shaft is thick and rounded; 8) the distal shaft's dorsal pillars are wider and thicker above the lateral epicondyle; 9) the medial epicondyle is narrower than the lateral epicondyle; 10) the medial epicondyle angle is retroflexed; 11) the lateral epicondyle has a large dorsal face with a tall wall facing the olecranon fossa; 12) the trochlea breadth is narrow; 13) the trochlea medial lip distal projection is long and perpendicular to the shaft; 14) the capitulum is rounded and has an even width in the proximal-distal axis; it is not as protruding as observed in *Colobus* specimens 15) the olecranon fossa is deep with a triangular shape. These morphological traits are also observed on specimen KNM-ER 30322 assigned to *Parapapio cf. ado*, from Koobi Fora (Jablonski, Leakey & Anton 2008) and specimen EP 399/98 from Laetoli (Harrison 2011). Based on the morphological similarities and equal sizes of *Parapapio* and *Papio* specimens, the large size and extent of elevation of the greater tuberosity and the shape of the olecranon fossa are used to distinguish the humeri of the two genera.

- SWP 504 is a right proximal humerus with less than a third of the shaft preserved:  
The specimen head is broken off on the anterior-medial portion of the head. The head shape is hemi-spherical and is separated from the lesser tuberosity by a narrow groove. The greater tuberosity lateral surface is slightly convex. The superior extension of the greater tuberosity lies slightly below the head and is also larger in size than the lesser tuberosity.
- SWP 959 is a right proximal humerus:  
The head shape on this specimen is hemi-spherical. The bicipital groove is narrow. The lateral surface of the greater tuberosity is slightly convex. The superior extension of the greater tuberosity lies slightly below the head. It is larger in size than the lesser tuberosity.
- SWP 962, a left proximal humeral head with greater and lesser tuberosity:

The head shape is hemi-spherical and is separated from the lesser tuberosity by a narrow groove. The lateral surface of the greater tuberosity is slightly convex. The superior extension of the greater tuberosity lies slightly below the head. The greater tuberosity is larger than the lesser tuberosity, and it lies at the same level as the head.

- STS 2219, a right proximal humeral head with both the greater and lesser tuberosities preserved:

The posterior portion of the specimen is embedded in breccia. The head shape is also hemi-spherical and is separated from the lesser tuberosity by a narrow groove. The lateral surface of the greater tuberosity is slightly convex. The superior extension of the greater tuberosity lies slightly below the head and is also larger in size than the lesser tuberosity.

- SWP 1137, a left distal humerus:

The distal shaft's medial and lateral edges are asymmetrical. The distal shaft is also thick and rounded. The distal shaft's dorsal pillars are wider and thicker above the lateral epicondyle. The medial epicondyle is narrower than the lateral epicondyle and is retroflexed. The lateral epicondyle has a large dorsal face with a tall wall facing the olecranon fossa. The trochlea breadth is narrow. The capitulum is pitted from possible carnivore chewing and its shape is therefore not easily discernible. The olecranon fossa is deep and triangular in shape.

- SWP 1262, a left distal humerus:

The distal shaft's medial and lateral edges are oriented asymmetrically. The distal shaft is thick and rounded. The dorsal pillars are wider and thicker above the lateral epicondyle. The medial epicondyle is retroflexed. The lateral epicondyle has a large dorsal face with a tall wall facing the olecranon fossa. The trochlea is narrow and its distal projection is short and medially inclined in relation to humeral shaft. Viewed from the proximo-distal axis, the capitulum medio-lateral width is distally narrowed. The olecranon fossa is triangular in shape.

- SWP 1287, a left distal humerus:



This specimen's medial and lateral edges are oriented asymmetrically. The distal shaft is thick and rounded and its distal dorsal pillars are wider and thicker above the lateral epicondyle. The medial epicondyle is approximately equal in width to the lateral epicondyle and is retroflexed. The lateral epicondyle has a large dorsal face with a tall wall facing the olecranon fossa. The trochlea breadth is narrow and its medial lip distal projection is short and medially inclined relative to the humeral shaft. In the proximo-distal axis, the capitulum's medio-lateral width is distally narrowed. The olecranon fossa is rounded ellipsoid.

- SWP 1540, a left distal humerus with less than a third of the shaft preserved distally:  
The proximal part of the shaft is missing; however the shaft is straight. Its dimensions are average for the Sterkfontein cercopithecoid humeri. The distal shaft is rounded and wider and thicker above the lateral epicondyle. The medial epicondyle is approximately equal in width to the lateral epicondyle and is retroflexed. The lateral epicondyle has a large dorsal face with a tall wall facing the olecranon fossa. Trochlea breadth is narrow. Its medial lip distal projection is short and medially inclined relative to the medial shaft. The capitulum's medio-lateral width is distally narrowed in the proximo-distal axis. The olecranon fossa has a triangular shape.
- SWP 1589, a left distal humerus:  
This specimen is missing the medial epicondyle. The olecranon fossa is triangular. The distal shaft is thick and rounded. The lateral epicondyle has a small dorsal face with minimum projection above the olecranon fossa.
- SWP 4081, left distal humerus with more than half of the shaft preserved proximally:  
The shaft is approximately straight and the distal portion is thick and rounded. The dorsal pillars are wider and thicker above the lateral epicondyle. The supinator crest is sharply raised and approximately a third of the humeral shaft length. The medial epicondyle is narrower than the lateral epicondyle. It is retroflexed. The lateral epicondyle has a large dorsal face with a tall wall facing the olecranon fossa. The trochlea breadth is narrow and its medial lip distal projection is long and perpendicular

to the humeral shaft. In the proximo-distal axis, the capitulum's medio-lateral width is narrower distally. The olecranon fossa has a triangular shape.

- SWP 1165, a right distal humerus:

The specimen has medial and lateral edges which are asymmetrically oriented. The distal shaft is rounded and its dorsal pillars are wider and thicker above the lateral epicondyle. The olecranon fossa has a triangular shape. The medial epicondyle is retroflexed. The lateral epicondyle has a large dorsal face with a tall wall facing the olecranon fossa. The trochlea breadth is narrow. The medial lip distal projection is short and medially inclined relative to the humeral shaft. The capitulum has an even medio-lateral width in the proximo-distal axis.

- SWP 4006, a right distal humerus with less than a third of its shaft preserved distally:

The humerus distal shaft morphology is thick and rounded, and the distal shaft's dorsal pillars above the lateral epicondyle are wider and thicker than they are above the medial epicondyle. The medial epicondyle is approximately equal in width to the lateral epicondyle. The specimen is one of the relatively larger specimens in the assemblage. The medial epicondyle is retroflexed. The trochlea breadth is narrow. The trochlea flange distal projection is short and medially inclined relative to the humeral shaft. The capitulum has an even medio-lateral width in the proximo-distal plane. The olecranon fossa shape is triangular.

- SWP 4036, a right distal humerus with distal shaft:

The distal humeral shaft is thick and rounded. Its medial and lateral edges are asymmetrical. Dorsally, the lateral pillar is wider and thicker above the lateral epicondyle than it is above the medial epicondyle. The medial epicondyle is narrower than the lateral epicondyle and is retroflexed. The lateral epicondyle has a large dorsal face with a tall wall facing the olecranon fossa. The trochlea breadth is narrow. The trochlea medial lip is short and is medially inclined relative to humeral shaft. The capitulum medio-lateral width is distally narrowed when viewed in the proximo-distal axis. The olecranon fossa is triangular in shape.

- SWP 4047, right distal humerus:

The distal shaft's medial and lateral edges are asymmetrical. The distal shaft dorsal pillars are wider and thicker above the lateral epicondyle. The medial epicondyle is narrower than the lateral epicondyle and is retroflexed. The lateral epicondyle has a large dorsal face with a tall wall facing the olecranon fossa. The trochlea breadth is narrow; its medial lip distal projection is short and is medially inclined relative to the humeral shaft. The capitulum has a narrower medio-lateral width on its distal end. The olecranon fossa is triangular in shape.

- SWP 4248, a left distal humerus

The distal shaft is asymmetrical. The distal lateral wall is wider and thicker above the lateral epicondyle. The olecranon is filled with breccia, however, it is deep with a triangular shape. The medial epicondyle is retroflexed. The trochlea distal lip is long and pronounced. The capitulum is rounded and defined, however it is modestly protuberant compared to *Colobus*.

Un-sided distal humerus

- SWP 1211, an unsided distal humerus with a shaft fragment:

The medial and lateral edges of this specimen are oriented asymmetrically. The distal shaft is thick and rounded. The distal shaft dorsal pillar is wider and thicker above the lateral epicondyle. The medial epicondyle is narrower than the lateral epicondyle and is retroflexed. The lateral epicondyle has a large dorsal face with a tall wall facing the olecranon fossa. The trochlea breadth is narrow, and its medial lip is short and medially inclined relative to the humeral shaft. In the proximo-distal axis, the capitulum is medio-laterally narrowed in its distal end. The olecranon fossa has a triangular outline.

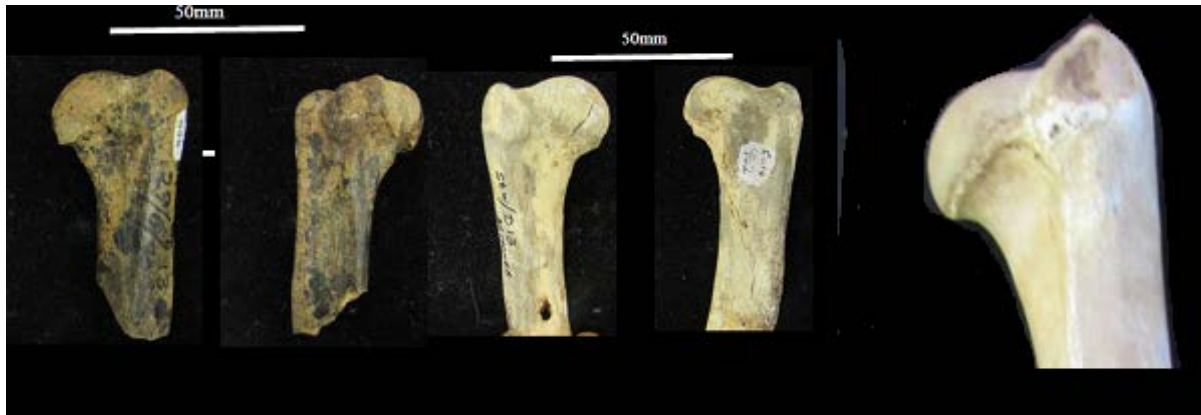


Figure 4.1. SWP 504, a right proximal humerus and SWP 962, a left proximal humerus and BPI/C/541, a modern *Papio ursinus* humerus.



Figure 4.2. From left to right, fossil specimens SWP 1141(*Papio/Parapapio*), SWP 1271 (*Papio/Parapapio*), BPI/C/541 (modern *Papio* sp), UCMP 125868 (*Papio izodi*), UCMP 56693 (*Procercocebus antiquus/Parapapio*), SWP 1262 (*Parapapio*), SWP 1137 (*Parapapio*) and KNM-ER 30298 (cf. *Parapapio*). Note that *Parapapio* specimens have a high triangular olecranon fossa, compared to the four specimens on the left with more elongated ellipsoid olecranon fossae. Data and images derived from Gilbert *et al.* 2016 and Jablonski *et al.* (2008).

---

b) Ulna

Two proximal ulnae within the Sterkfontein assemblage as assigned to *Parapapio*. These have the following morphology- 1) the centre of the olecranon process is retroflexed; 2) the anconeal process articular surface is in horizontal plane with some proximal extension; 3) on medial view, the anconeal process is a blunt beak which is extensive proximally and flattens out posteriorly 5) the trochlea notch shape is crescentic 6) the coronoid process articular surface is in horizontal plane with no significant distal extension 7) the shaft has a groove distal to the coronoid process and 8) a deep depression distal to the radial notch is present; 9) the shaft is nearly straight proximo-distally. Only a single *Parapapio* ulna specimen is known, specimen KNM-ER 30315 from Koobi Fora. Modern *Papio* ulnae are also used for comparison. Jablonski *et al.* 2008 indicate that the specimen is identical to *Papio*. They also state that this ulna has a deep olecranon, which based on my observation, is consistent with the deep olecranon fossa seen in the *Parapapio* humerus. The main difference that could be established between these and *Papio* specimens is the distinction of the anconeal process in medial view, which, in *Parapapio* specimens, is thick and reduced.

- BP/3/23257, a right proximal ulna which preserves less than a third of the shaft proximally:

The centre of the olecranon process is retroflexed. The anconeal process articular surface is in horizontal plane with proximal extension. In medial view, the anconeal process is not as defined as in *Papio* sp ulnae. It rises into a steep angle antero-posteriorly and the posterior most portion is flat. The trochlea notch shape is crescentic. The coronoid process articular surface is in horizontal plane with no significant distal extension. The shaft groove distal to the coronoid process is present. The deep depression distal to the radial notch is present. The shaft is nearly straight proximo-distally.

- SWP 523, (Fig. 4.3) a right proximal ulna with more than half of the shaft preserved proximally:

This specimen's anterior anconeal process is broken off. The olecranon superior aspect is flattened. Its lateral aspect is higher than the medial. The olecranon superior projection is less than the trochlea notch. The shaft groove distal to the coronoid process is present but is cracked. The shaft is nearly straight.



Figure 4.3. On the left, the fossil SWP 523, a right *Parapapio* sp. proximal ulna and, on the right KNM-ER 30315 a left cf. *Parapapio* proximal ulna from Koobi Fora (Jablonski *et al.* 2008). Note that the beak of the olecranon is not as pronounced as observed in *Papio*.



Figure 4.4. BP/I/C/541, a modern *Papio ursinus* ulna. Note the pronounced olecranon beak on the *Papio* specimen and the continuous anconeal process which is not separated from the posterior olecranon on the fossil *Parapapio* specimen.

c) Radius

Six proximal radii reflect the following characteristics- 1) on superior view the head is ovoid; 2) it has a depression for accommodation of the capitulum; 3) the head lateral aspect lies lower than the medial aspect; 4) the neck is relatively longer than *Papio* sp neck; 5) the bicipital/radial tuberosity is a lateral bulge with a centrally located furrow. These characteristics are consistent with specimen EP142/04 from upper Laetoli beds in Laetoli, Tanzania (Harrison 2011). The radius head shape is similar to other papionins. It is ovoid. The most distinguishing feature is the relatively longer neck and the bicipital tuberosity which usually (but not always) preserves a central furrow. Variation on the presence of a furrow on the bicipital tuberosity is observed in this group of specimens. However the constant feature is the relative extension of the neck.

- SWP 515, a left proximal radius:

The head shape on this specimen is ovoid with a defined rim. In superior view it has a deep depression for insertion of the capitulum, more so than in *Papio* specimens. The neck is relatively longer. There is a proximo-distally elongated bicipital tuberosity which bears a longitudinal furrow located in its centre. The lateral aspect of the head is lower than the medial aspect. The specimen has the longest neck of all cercopithecoid radii in the Sterkfontein. This is not a factor of size. The specimen is medium sized and similar in size to specimens within the assemblage.

- SWP 1204, a left proximal radius:

The head is chipped off on the medial anterior side. The head is ovoid in shape and its lateral aspect is lower than the medial. The bicipital tuberosity has a centrally located longitudinal furrow.

- SWP 1219, a left proximal radius:

The shape of the head is nearly round and has a depression in superior view. The lateral aspect of the head is on the same level as the medial aspect. The bicipital tuberosity is elongated proximo-distally and bears a longitudinal furrow in its centre.

- SWP 784, a right proximal radius:  
The specimen's head is broken on the posterior dimension. Only the anterior head and proximal portion of the shaft preserved. The medial edge of the head is higher than the lateral aspect. The bicipital tuberosity does not bear a longitudinal furrow.
- SWP 802, a right proximal radius:  
The head shape is ovoid and the lateral aspect is inferior to the medial aspect. The bicipital tuberosity bears a longitudinal furrow.
- SWP 4243, a right proximal radius with more than a third of the shaft preserved proximally:  
The head is ovoid. On superior view the head is depressed. The head's lateral aspect lies lower than the medial aspect. The bicipital tuberosity bears a furrow centrally and does not have the extreme lateral projection seen in *Papio*. The neck is relatively long. The shaft is nearly straight.



Figure 4.5. Top left insert, specimen EP 142/04, a *Parapapio ado* radius from Laetoli (After Harrison 2011). On the right, SWP 4243, a *Parapapio* radius and BPI/C 541, a modern *Papio* radius. Note the shallow furrow on the centre of the fossil specimen



d) Femur

One femur is described as *Parapapio* sp.

- SWP 1300, a left proximal femur with more than a third of the shaft preserved proximally:

The greater trochanter on this specimen extends superior to the head 1) and points medially. 2) The lateral surface area of the greater trochanter is flat. 3) The intertrochanteric fossa is deep and lies at the same level as the head. 4) The lesser trochanter faces medially. This femur specimen resembles AL 363 from Hadar, Ethiopia (Frost & Delson 2002).

*Locomotor adaptation of specimens identified as Parapapio sp*

The Sterkfontein *Parapapio* specimens demonstrate morphology that is consistent with semi-terrestrial locomotion. The upper humerus with a greater tuberosity that lies below the head points to a shoulder joint with rotary capabilities (Harrison 1989). The distal humerus (with a retroflexed medial epicondyle, the trochlea medial lip which is distally projecting) bears features consistent with terrestrially adapted motion. Retroflexion of the humeral medial epicondyle assists in stabilization of the elbow joint (Jolly 1972). The proximal radius has not been proved to have locomotor or behavioural differences; however, the relatively elongated radial neck is generally observed in colobines and cercopithecins (Harrison 2011). Therefore it is a trait usually associated with arboreally and semi-terrestrially adapted monkeys. The proximal ulna and the only femur identified both preserve characteristics consistent with an adaptation to terrestrial substrates.

---

Subfamily	Cercopithecinae Gray 1921
Tribe	Papionini Burnett 1828
Subtribe	Papionina Burnett 1828
Genus	<i>Papio</i> . Eerxleben, 1777

#### a) Humerus

Seventeen humeri reflect *Papio* sp characteristics. They possess the following traits- 1) a hemi-spherical head shape; 2) the head and the lesser tuberosity are continuous; 3) the greater tuberosity is significantly larger than the lesser tuberosity; 4) the greater tuberosity superior extension lies above the level of humeral head; 5) the greater tuberosity has a slightly convex lateral surface area; 6) the tuberosities are separated by a narrow groove; 7) the shaft is nearly straight; distally, 8) the shaft is thick and rounded in coronal plane; 9) the medial epicondyle is retroflexed 10) the lateral epicondyle is smaller than the medial epicondyle; 11) the trochlea distal lip is short; 12) the trochlea is medially inclined relative to the humeral shaft; 13) the trochlea breadth is narrow 14) in the proximo-distal axis, the capitulum's medio-lateral width is distally narrowed 15) the olecranon fossa is shallow and nearly rounded or elongated-ellipsoid. These bear similarities to specimen UCMP 125868, a *Papio izodi* humerus identified from Taung by Gilbert *et al.* (2016).

- BP/3/22757 is a head with a greater tuberosity with less than a third of the proximal shaft preserved:  
The head is proximo-distally compressed. The head and the lesser tuberosity are continuous. The greater tuberosity is significantly larger than the lesser tuberosity and its superior extension lies above the level of humeral head. Its lateral surface area is slightly convex.
- SWP 960, a proximal humerus:  
The specimen's head is proximo-distally compressed. The head and the lesser tuberosity are continuous. The greater tuberosity is significantly larger than the lesser tuberosity. Its superior extension lies above the level of the humeral head.

- SWP 1201, a head with the lesser and greater tuberosities:  
The head has a hemi-spherical shape. The head and the lesser tuberosity are continuous. The greater tuberosity is significantly larger than the lesser tuberosity and its superior extension lies above the level of humeral head. The greater tuberosity's lateral surface area is slightly convex. This specimen is abraded on the medial and lateral aspect of the intertubercular groove, such that this morphology cannot be ascertained on this particular specimen.
- SWP 830, a right proximal humerus fragment:  
The specimen preserves less than a third of the shaft proximally and is part of a cluster of fore-limb specimens embedded in a breccia block. The head shape is hemi-spherical. The greater tuberosity lies above the level of the head.
- S94-10064, a right proximal humerus head:  
The head has a hemispherical shape. The greater tuberosity is chipped off proximally. However, it is sufficiently preserved to determine that its superior extension is significantly larger than the lesser tuberosity.
- SWP 1276, a right proximal humerus:  
This specimen is chipped proximo-medially but the head shape is discernable is nearly round. The greater tuberosity is significantly greater than the lesser. The greater tuberosity is chipped off proximally and has a slightly convex lateral surface area. The intertubercular groove/sulcus is deep with sharply defined lateral and medial margins.
- SWP 1406, a right proximal humerus:  
The specimen's greater tuberosity is broken off in the proximo-distal plane. The greater tuberosity lies significantly above the head. The bicipital groove is shallow.
- SWP 2385, a right proximal humerus:  
The head shape is hemispherical; it is proximo-distally compressed. The head and lesser tuberosity are continuous. The greater tuberosity is significantly greater than the

lesser tuberosity. The intertubercular groove is deep with sharply defined lateral and medial margins.



Figure 4.6. A modern left *Papio ursinus* humerus and, on the right, SWP 2385, a right *Papio* sp proximal humerus.

- BP/3/23389, a left distal humerus:  
The humeral shaft shape is approximately straight. The medial epicondyle is retroflexed and is wider than the lateral epicondyle which is slightly covered in breccia. The trochlea is medially inclined relative to the humeral shaft. The trochlea breadth is narrow. In the proximo-distal axis, the capitulum's medio-lateral width is distally narrowed. Similar to other specimens in this category, the olecranon fossa is rounded ellipsoid.
- SWP 511, a left distal humerus:  
This specimen's distal shaft morphology is asymmetrical, thick and rounded. The medial epicondyle is approximately equal in size to the lateral epicondyle and is retroflexed. The lateral epicondyle has a small dorsal face with minimum projection above the level of the olecranon fossa. The trochlea breadth is narrow. Its medial lip distal projection is short. The capitulum's medio-lateral width is even in the proximo-distal axis. The olecranon fossa shape is elongated-ellipsoid.
- SWP 1176, a left distal humerus:

SWP 1176 has a thick and rounded distal shaft. The medial and lateral edges are oriented asymmetrically. The medial epicondyle is approximately equal to the lateral epicondyle and is retroflexed. The lateral epicondyle has a small dorsal face with minimum projection above the level of the olecranon fossa. The trochlea projects distally. It has a narrow breadth with a distal projection of the medial lip which is short and medially inclined relative to shaft. The capitulum's medio-lateral width is even in the proximo-distal axis. The olecranon fossa is elongated-ellipsoid.

- SWP 2810, a left distal humerus:

This is one of the medium sized specimens within the Sterkfontein assemblage. The distal shaft's medial and lateral edges are oriented asymmetrically. The distal shaft is thick and rounded. The medial epicondyle is approximately equal to the lateral epicondyle and is retroflexed. The lateral epicondyle has a small dorsal face and projects minimally above the level of the olecranon fossa. The trochlea breadth is broken off. The capitulum's medio-lateral width is even in the proximo-distal axis. The olecranon fossa is elongated-ellipsoid.

#### Right distal humeri

- BP/3/31691, a right distal humerus with less than a third of the shaft preserved distally:  
The distal shaft on this specimen is relatively straight and thick and rounded. The medial epicondyle is wider than the lateral epicondyle and is retroflexed. The lateral epicondyle has a small dorsal face with minimum projection above the level of the olecranon fossa. The trochlea breadth is narrow; its medial distal lip projection is short and medially inclined relative to the humeral shaft. In the proximo-distal axis, the capitulum has a narrowed medio-lateral width distally. The olecranon fossa is deep and elongated-ellipsoid.
- SWP 911, a right distal humerus:  
This specimen's distal shaft's medial and lateral edges are oriented asymmetrically. The distal shaft is thick and rounded. The supinator crest is sharply raised and is approximately a third of the humeral shaft length. The medial epicondyle is approximately equal to the lateral epicondyle and is retroflexed. The lateral epicondyle

has a small dorsal face with minimum projection above the level of the olecranon fossa. The trochlea breadth is narrow and its medial lip distal projection is short and is medially inclined relative to shaft. The medio-lateral breadth of the capitulum is even on the proximo-distal axis. The olecranon fossa has an elongated-ellipsoid shape.

- SWP 1120, a right distal humerus:

This specimen has no epicondyles preserved; therefore no bi-epicondylar breadth is recorded. The olecranon fossa is elongated-ellipsoid and perforated. Some *Papio* species preserve an elongated-ellipsoid olecranon fossa or a rounded one and in others it is perforated.

- SWP 1584, a right distal humerus:

This specimen is covered in breccia and the bone surface is highly flaked. It is one of the larger *Papio* humerus specimens in the Sterkfontein assemblage. The humeral distal shaft is thick and rounded; the medial and lateral edges are asymmetrical. The medial epicondyle is narrower than the lateral epicondyle and is retroflexed. The lateral epicondyle has a large dorsal face with a tall wall facing olecranon fossa. The trochlea breadth is narrow. The trochlea medial distal lip and capitulum are broken off distally. The olecranon fossa is elongated-ellipsoid in shape; it is wider medio-laterally.

- SWP 4246, a right distal humerus:

The olecranon fossa is elongated-ellipsoid. The trochlea breadth is narrow. The lateral epicondyle morphology has a small dorsal face with minimal projection above the level of the olecranon fossa. The medial epicondyle is retroflexed and is wider than lateral epicondyle. The distal shaft is thick and rounded. The medio-lateral breadth of the capitulum is narrowed distally in the proximo-distal axis.

---

b) Ulna

Nine proximal ulnae are attributed to *Papio* sp. These have 1) an anconeal process which is in horizontal plane with no significant proximal extension; 2) the coronoid process is also in

horizontal plane with no significant distal extension; 3) the trochlea notch has a crescentic shape; 4) the olecranon is less than the trochlea notch length; 5) the centre of the olecranon process is retroflexed 6) in medial view, the anconeal process is flattened in the antero-posterior dimension; 8) and the posterior portion of the olecranon process rises sharply. All eight proximal ulnae demonstrate this feature. These vary from *Parapapio* by having a defined beak (in the medial and lateral views) of the anconeal process.

- SWP 1208, a left proximal ulna with less than a third of the shaft preserved proximally:  
The ulna is very slender, medio-laterally flattened and elongated more than other ulnae in the assemblage. The olecranon superior aspect morphology is flat with lateral and medial edges at approximately equal heights. The olecranon in colobines is short and straight (Jablonski & Leakey 2008). Its projection is less than the trochlea notch. A short olecranon indicates mechanical advantage for the *m. triceps brachii* muscles, a feature observed in arboreal cercopithecoids (*ibid.*). The centre of the process is aligned with the long axis of the ulna. The trochlea notch is shallow and does not bear a waist. It has a crescentic shape. The coronoid process' articular surface is in horizontal plane with no significant distal extension. The anconeal process is also in horizontal plane and quite small compared to other ulnae in the assemblage. The shaft groove distal to the coronoid process is present but relatively smaller than that observed in Papionins. Preservation of the shaft is not sufficient to determine the shaft shape.
- SWP 814, a right proximal ulna:  
The posterior portion of the olecranon process is broken off. The anconeal process is in horizontal plane with no significant proximal extension. The coronoid process is also in horizontal plane with no significant distal extension. The trochlea notch has a crescentic shape. The olecranon is less than the trochlea notch length. The centre of the olecranon process is retroflexed. In medial view, the anconeal process is sharply projecting dorsally; it is flattened in the antero-posterior dimension.
- SWP 830, a right proximal ulna fragment:  
This specimen is part of an upper arm preserved in a breccia block. The olecranon is retroflexed. Its superior extension is less than the trochlea notch length. The anconeal process is in horizontal plane with no significant proximal extension. The coronoid

process is also in horizontal plane with no significant distal extension. The trochlea notch is crescentic in shape.

- SWP 1572, a right proximal ulna which preserves less than a third of the shaft proximally:

The olecranon process is only partly preserved on the medial side and its whole posterior aspect is chipped off. The olecranon is retroflexed. The trochlea height is more than the olecranon superior projection. The depression below the radial notch is present.

- BP/3/23257, a right proximal ulna:

The olecranon is retroflexed. Its medial and lateral aspects are unequal in height. The olecranon superior projection is less than the trochlea height. The coronoid process is in horizontal plane with no significant distal extension.

- SWP 824, a right proximal ulna without a shaft:

The specimen's olecranon process is retroflexed.. The proximal extension of the olecranon is less than the trochlea notch. The coronoid process lies in horizontal plane with no significant distal extension.

- SWP 2788, a right proximal ulna without a shaft:

The ulna has a retroflexed olecranon process with a spherical trochlear notch. Proximally, the olecranon medial and lateral edges are unequal in height; the lateral aspect is higher than the medial aspect.

- SWP 1155, a left proximal ulna without a shaft:

This specimen is fragmented on the proximal olecranon. The coronoid process is in horizontal plane with no significant distal extension.

- SWP 1577, a left proximal ulna:

The olecranon process is broken off proximally. The anconeal process is abraded but is in horizontal plane with no significant proximal extension. The trochlea notch is crescentic. The coronoid process is also in horizontal plane with no significant distal



extension. The ulna shaft groove disto-medial to coronoid process is present. The deep depression distal to the radial notch is present.

---

c) Radius.

Fifteen radii are identified as *Papio* sp. These demonstrate the following features- 1) the head superior view is ovoid and slightly depressed; 2) the head lateral aspect lies lower than the medial aspect 3) the bicipital tuberosity is a proximo-distal protrusion which does not bear a central groove 4) the neck is also relatively shorter, compared to *Parapapio* sp 5) the radial shaft in is superiorly dorso-ventrally flattened and approximately straight.

- BP/3/23235, a left proximal radius:

In superior view, the radius head is ovoid and slightly depressed. Its medial and lateral borders are slightly unequal in height. The bicipital tuberosity is bulbous and elongated proximo-distally, suggesting a large insertion for *m. biceps brachii*. In lateral view, it extends out of the shaft and has a longitudinal groove laterally which is not centrally located as observed in *Parapapio* sp. The bicipital tuberosity is mainly rugose rather than having a furrow run through it centrally. The neck is also relatively shorter, compared to *Parapapio* sp. The radial shaft in is superiorly dorso-ventrally flattened and approximately straight.

- BP/3/31923, a left small proximal radius :

This specimen belongs to a small juvenile and the head is therefore missing. The bicipital tuberosity is bulbous and elongated proximo-distally. In lateral view, it extends out of the shaft and has a laterally projecting bicipital tuberosity. The neck is short. The radial shaft and neck are superiorly dorso-ventrally flattened and the shaft almost straight.

- BP/3/23453, a right proximal radius with more than a third of the shaft preserved proximally:

The head shape is ovoid. The lateral aspect of the head lies inferior to the medial aspect. The bicipital tuberosity is elongated with a lateral projection.

- SWP 514, a right proximal radius with more than a third of the shaft preserved proximally:

The shape of the head is ovoid. The lateral aspect lies inferior to the medial aspect. In superior view it bears a slight depression. The bicipital tuberosity is wider than the body in medial view and has no ridges.

- SWP 793, a right proximal radius:

The head shape is slightly medio-laterally compressed. The head is tilted laterally. The bicipital tuberosity is wide medio-laterally but still elongated. It bears a longitudinal furrow and has a deep ridge antero-medially.

- SWP 4022, a left proximal radius:

The shape of the head is ovoid. The lateral aspect lies inferior to the medial aspect. In superior view it bears a slight depression. The neck is short. The bicipital tuberosity protrudes laterally and bears no furrow.



Figure 4.7. SWP 4022, a fossil *Papio* radius specimen and BPI/C/541, a modern *Papio ursinus* radius.



Figure 4.8. BP/3/31923, a fossil *Papio* radius and BPI/C/541, a modern *Papio ursinus* radius.

- SWP 803, a right proximal radius  
In superior view, the head has an ovoid shape. It also bears a slight depression for accommodation of the capitulum. The lateral aspect of the head is lower than the medial aspect. The neck is relatively long; it is one of the longest necks in the assemblage. The bicipital tuberosity is elongated proximo-distally and has an elongated furrow on its antero-medial side.
- SWP 1418, a right proximal radius:  
This specimen's head has a nearly round shape. The head lateral aspect lies inferior to the medial aspect. The neck is relatively short. The bicipital tuberosity is proximo-distally elongated and bulbous.
- SWP 1552, a right proximal radius:  
This radial head shape is ovoid. The head's lateral aspect is lower than the medial. The bicipital tuberosity bears a longitudinal furrow on the medial side.
- SWP 2200 is a right proximal radius with the neck and bicipital tuberosity:  
The head shape is ovoid. The bicipital groove is fractured, however it is bulbous with a strong lateral projection.
- SWP 798, a right proximal radius:  
The radial head is chewed off on the whole anterior aspect of this specimen; however, the head is ovoid and is depressed in superior view. The lateral aspect is on the same level as the medial aspect. The bicipital tuberosity is wider than the body medio-laterally, and does not have a furrow centrally. It only has a depression on its anterior side.
- SWP 4042, a left proximal radius:  
This specimen preserves the same features as seen in other specimens. It has an ovoid head. In superior view the head has a shallow depression. The lateral aspect is lower than the medial aspect. The neck is short. The bicipital tuberosity has a lateral bulge and does not preserve a furrow in its centre.

- SWP 517, a left proximal radius with less than a third of the shaft preserved proximally:  
The head shape is ovoid. The lateral aspect lies at the same level as the medial aspect. The bicipital tuberosity is elongated proximo-distally and bears a longitudinal furrow and extends out of the body. Behind it antero-medially is a ridge with a sharp crest.
- SWP 791, a left proximal radius with less than a third of the shaft preserved proximally:  
The head is rounded to ovoid and is depressed in superior view. The neck is short. The bicipital tuberosity has an extreme lateral projection.
- SWP 4249, a left proximal radius with less than a third of the shaft preserved proximally:  
The radial head superior view has a slight depression. The neck is short, and, it is oval on the dorso-ventral plane. The bicipital tuberosity has an extensive lateral protrusion.

The differences between the femur of *Parapapio* sp and *Papio* sp are not established in this research. As a result, all femora are assigned to the *Papio/Papio* sp category.

#### *Locomotor adaptation of specimens identified as Papio sp*

Skeletal elements identified as *Papio* sp preserve morphology consistent with terrestrial adaptation. The humerus, which is the most occurring specimen in the assemblage points to a cercopithecoid adapted to terrestrial locomotion. Proximally, it has a greater tuberosity which extends above the level of the head; distally it preserves characters linked to restricted quadrupedal activities such as a deep olecranon fossa and a short retroflexed medial epicondyle and distally projecting trochlea lip (Youlatos & Meldrum 2011). The ulna specimen possesses a retroflexed olecranon, a feature common in papionins. The radius head is very similar to the semi-terrestrial *Parapapio* but the radial the neck is relatively shorter compared to what is observed in arboreal monkeys.

Subfamily	Cercopithecinae Gray 1921
Tribe	Papionini Burnett 1828
Subtribe	Papionina Burnett 1828
Genus	<i>Papio/Parapapio</i> sp.

The Sterkfontein fossil cercopithecoid postcranial assemblage consists of specimens which, due to ambiguous character states and or fragmentation of defining morphology, cannot be confidently assigned to either group. The most defining features in the humerus of the two groups (*Parapapio* sp and *Papio* sp), the projection of the greater tuberosity and the shape of the olecranon, are ambiguous and cannot be clearly distinguished and assigned to either group. The main ulna feature which could not be determined to separate the specimens between the two genera is the dorso-ventral elevation of the olecranon superior aspect. The specimens classed into this group do not preserve sufficient morphology to determine the olecranon superior structure. On the radius, the relative size of the neck and the central furrow on the bicipital tuberosity which are used to distinguish between *Papio* and *Parapapio* could not be differentiated and, as a result, radii which do not preserve sufficient morphology to discriminate between these are lumped into the *Papio/Parapapio* group. There is no sufficient evidence of *Parapapio* femur in the literature to differentiate this genus from *Papio*. Specimen AL 363-1c, a proximal femur specimen from Hadar in Ethiopia (Frost & Delson 2002), assigned to *Parapapio jonesi* could not be contrasted to *Papio* specimens.

#### a) Humerus

Humeri which bear the combination of *Parapapio* and *Papio* sp features and are too fragmented to assign to genus are lumped in the *Papio/Papio* sp category. These specimens bear features which are consistent with both *Parapapio* sp and *Papio* sp morphology: 1) the proximal humerus has a globular head; 2) the tuberosity sizes are relatively similar and in some specimens the greater tuberosity is larger than the lesser tuberosity; 3) the greater tuberosity lies at the same level as the head; 4) the distal shaft is asymmetrical in the dorso-ventral plane; 5) the dorsal pillars are wider and thicker above the lateral epicondyle; 6) distally the olecranon fossa is deep and rounded-ellipsoid. These specimens do not display

the same robust masculinity observed in *Theropithecus* specimens. Twenty-nine humeri specimens are discussed.

- ST (number is invisible), a left proximal humerus head:

The humeral head shape on this specimen is proximo-distally compressed as seen in *Papionins*. The head and lesser tuberosity are continuous. The greater tuberosity is significantly larger than the lesser tuberosity

- SWP 2792, a right proximal humerus:

The humeral head shape on this specimen is proximo-distally compressed as seen in *Papionins*. The head and lesser tuberosity are continuous. The greater tuberosity is significantly larger than the lesser tuberosity. The humeral head and lesser tuberosity are at the same level. The sizes of the trochantae and the proximal extension of the greater trochantae have a combination of features which can either be part of *Parapapio* sp (which preserves a greater tuberosity which lies at same level as the head) or *Papio* sp (which has trochantae of unequal size). The greater tuberosity surface is slightly convex.

- BP/3/24000 , a left distal humerus:

This specimen preserves a distal shaft which is nearly straight. It is thick and rounded on its most distal end. The distal shaft's medial and lateral edges are asymmetrical. The distal shaft dorsal pillars are wider and thicker above the lateral epicondyle. The medial epicondyle is retroflexed. The lateral epicondyle has a small dorsal face with minimal projection above the level of the olecranon fossa. The trochlea is broken off. The capitulum medio-lateral width is distally narrowed in the proximo-distal axis. This specimen preserves a rounded ellipsoid olecranon fossa.

- BP/3/18382, a left distal humerus:

This specimen's medial epicondyle is approximately the same size as the lateral epicondyle. The medial epicondyle is retroflexed. The lateral epicondyle has a small dorsal face with a tall wall facing the olecranon fossa. The trochlea breadth is narrow with a medial lip distal projection is short and medially inclined. In the proximo-distal

axis, the capitulum medio-lateral width is distally narrowed. The olecranon fossa is deep and is nearly rounded.

- BP/3/23016 left distal humerus condyles:

The specimen is similar to others in this class. It is medium in size. The medial epicondyle is wider than the lateral epicondyle. The medial epicondyle is retroflexed. The trochlea breadth is narrow. The trochlea medial lip distal projection is short, and is medially inclined. The capitulum's width is medio-laterally even when viewed in the proximo-distal axis. The full olecranon shape cannot be determined as it is missing its proximal portion.

- STS 1504, a left distal humerus:

This specimen is largely covered in matrix. Only the trochlea and capitulum are visible. The trochlea is short and medially inclined. It has a narrow breadth. The capitulum has an even medio-lateral width in the proximo-distal axis.

- SWP 510, a left distal humerus:

SWP 510's medial epicondyle is approximately equal in size to the lateral epicondyle and is retroflexed. The lateral epicondyle has a small dorsal face with minimum projection above the level of the olecranon fossa. The trochlea breadth is narrow and its medial lip distal projection is short and medially inclined relative to the shaft. The capitulum's medio-lateral width is even in the proximo-distal axis. The olecranon fossa is rounded ellipsoid.



Figure 4.9. SWP 2792, a right proximal humerus demonstrating the head and the greater tuberosity which lie on the same level.



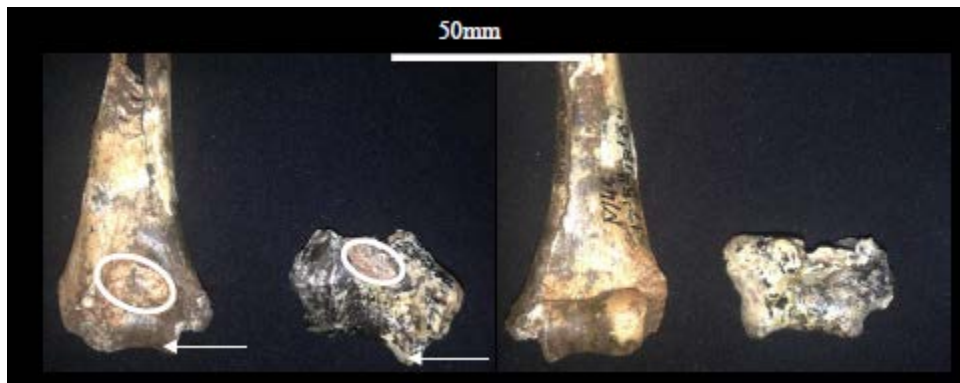


Figure 4.10. Left to right, BP/3/24000 (a left distal humerus) and BP/3/23016 (left distal humerus) demonstrating the elongated-ellipsoid shape of the olecranon fossa and a trochlea distal projection which is medially inclined.

- SWP 562, a left humerus without the head:

This specimen is one of the larger specimens in this class. It preserves the whole shaft and distal humerus and is only missing the head. The shaft is approximately straight. The medial and lateral edges are asymmetrical. The distal shaft is thick and rounded. The distal shaft dorsal pillars are asymmetrical and rounded above the lateral and medial edges. The supinator crest is sharply raised and approximately a third of the humeral shaft length. The medial epicondyle is retroflexed and approximately equal in size to the lateral epicondyle. The lateral epicondyle has a small dorsal face with minimum projection above the level of the olecranon fossa. The trochlea breadth is narrow and its medial lip distal projection is short and medially inclined relative to the shaft. The capitulum is broken off distally. The olecranon fossa shape is rounded ellipsoid.

- SWP 995, a left distal humerus with more than a third of the shaft preserved:

The humeral shaft is approximately straight. The medial and lateral edges are asymmetrical. The distal shaft is thick and rounded above the lateral and medial epicondyles. The medial epicondyle is retroflexed. The lateral epicondyle has a small dorsal face with minimum projection above the level of the olecranon fossa. The trochlea breadth is narrow and missing the distal portion. The capitulum's medio-lateral width is even in the proximo-distal axis. The olecranon fossa is rounded.

- SWP 1410, a left distal humerus:

This specimen has a thick and rounded distal shaft. The distal dorsal shaft pillars are wider and thicker above the lateral epicondyle. The medial epicondyle is narrower than the lateral epicondyle. The medial epicondyle is retroflexed while the lateral epicondyle has a large dorsal face with a tall wall facing the olecranon fossa. The trochlea breadth is narrow and its medial lip distal projection is short and medially inclined relative to the humeral shaft. Viewed in the proximo-distal axis, the capitulum's medio-lateral width is distally narrowed. The olecranon fossa is elongated-ellipsoid.

- SWP 4019, a right distal humerus:

Distally, the shaft is thick and rounded. It is asymmetrical in dorso-ventral view. The distal dorsal shaft pillars are wider and thicker above the lateral epicondyle. The medial epicondyle is narrower than the lateral epicondyle. The medial epicondyle is retroflexed while the lateral epicondyle has a large dorsal face with a tall wall facing the olecranon fossa. The trochlea breadth is narrow and its medial lip distal projection is short and medially inclined relative to the humeral shaft. Viewed in the proximo-distal axis, the capitulum's medio-lateral width is distally narrowed. The olecranon fossa is elongated-ellipsoid.

- SWP 4038, a left distal humerus:

The medial and lateral edges are oriented asymmetrically. Distally, the shaft is rounded. The distal shaft dorsal pillars are wider and thicker above lateral epicondyle. The shaft is broken but the supinator crest is sharply raised and a third of humeral shaft length. The medial epicondyle is narrower than lateral epicondyle and is retroflexed. The lateral epicondyle has a large dorsal face with tall wall facing the olecranon fossa. The trochlea breadth is narrow. Trochlea medial lip distal projection is short and medially inclined. The capitulum's medio-lateral width is distally narrower when viewed in the proximo-distal plane. The olecranon fossa shape cannot be ascertained, as it is covered with breccia.

- SWP 4041, a left distal humerus:  
This specimen's distal shaft is thick and rounded. The medial and lateral edges are oriented asymmetrically. The distal shaft dorsal pillars are wider and thicker above the lateral epicondyle. The medial epicondyles are narrower than lateral epicondyle and are retroflexed. The trochlea breadth is narrow and its medial lip distal projection is long and perpendicular to humeral shaft. The medio-lateral breadth of the capitulum is narrowed distally on the proximo-distal axis. The olecranon fossa is elongated-ellipsoid.
- SWP 1199, a right proximal humerus:  
The head shape on this specimen is nearly round. The greater tuberosity is broken off proximally and is slightly larger than the lesser tuberosity. Therefore its length relative to the head is indeterminate. The intertubercular groove is deep with sharply defined medial and lateral margins.
- SWP 1542, a right proximal humerus:  
This specimen preserves a greater tuberosity and a head which is broken medially. The whole specimen is broken on its posterior side. No shaft is on preserved. The head and greater tuberosity are continuous.
- BP/3/24053, a right, highly fragmented distal humerus:  
The lateral portion of the specimen is missing. The medio-lateral breadth of the capitulum is narrowed distally. The medio-lateral breadth of the capitulum is even in the proximo-distal axis. The medial epicondyle is narrower than the lateral epicondyle. The medial epicondyle is retroflexed.
- SWP 4239, a right distal humerus:  
The specimen is highly flaked . It preserves more than half of the shaft distally. The distal shaft is rounded and its shaft dorsal pillars are thick and rounded above the lateral epicondyle. The medial and lateral epicondyles are roughly equal in size. The trochlea breadth is narrow and its medial lip distal projection is perpendicular to the shaft. In proximo-inferior view, the medio-lateral breadth of the capitulum is narrowed distally. The olecranon fossa has a rounded-ellipsoid shape.

- SWP 507, a right distal humerus:

The distal shaft's medial and lateral edges are asymmetrically oriented. The distal shaft is rounded. The medial epicondyle is approximately equal to the lateral epicondyle and is retroflexed. The lateral epicondyle has a small dorsal face with minimum projection above the olecranon fossa. The trochlea is narrow. Its medial lip distal projection is short and medially inclined relative to the shaft. In the proximo-distal axis, the capitulum's medio-lateral width is distally narrowed. The olecranon is perforated and is almost rounded.

- STS 377c, a right distal humerus:

The specimen distal shaft is dorso-ventrally asymmetrical. The distal shaft is rounded and its shaft dorsal pillars are thick and rounded above the lateral epicondyle. The medial and lateral epicondyles are roughly equal in size. The trochlea breadth is narrow and its medial lip distal projection is perpendicular to the shaft. In the proximo-distal axis, the medio-lateral breadth of the capitulum is narrowed distally. The olecranon fossa has a rounded-ellipsoid shape.

- SWP 912, a right distal humerus:

This specimen medial epicondyle is approximately equal to the lateral epicondyle and is dorsally inclined (retroflexed). The lateral epicondyle has a small dorsal face with minimum projection above the level of the olecranon fossa. The trochlea breadth is narrow and its medial lip distal projection is short and is medially inclined relative to shaft. The medio-lateral breadth of the capitulum is even on the proximo-distal axis. The olecranon fossa shape is rounded-ellipsoid.

- SWP 1016, a right distal humerus:

This specimen's shaft is approximately straight. The medial and lateral edges are asymmetrical. The distal shaft is thick and rounded. The medial epicondyle is broken off. The lateral epicondyle has a small dorsal face with minimum projection above the level of the olecranon fossa. The trochlea breadth is narrow and its medial distal lip projection is short and medially inclined relative to the shaft. The capitulum is broken

off medially and therefore its width is not discernable. The olecranon fossa shape is rounded-ellipsoid.

- SWP 1140, a right distal humerus:

This specimen is the largest humerus in this category. The medial and lateral edges of this specimen's distal shaft are asymmetrical. The medial epicondyle is approximately equal in width as the lateral epicondyle and is retroflexed. The lateral epicondyle has a small dorsal face with minimum projection above the level of the olecranon fossa. The trochlea breadth is narrow and its medial lip distal projection is short and medially inclined relative to humeral shaft. In the proximo-inferior view, the medio-lateral breadth of the capitulum is narrowed distally. The olecranon fossa is shallow and elongated-ellipsoid.

- SWP 1141, a right distal humerus:

This specimen is glued together which extends its length; therefore no reliable measurements could be derived from this specimen. The medial and lateral edges are oriented asymmetrically. The distal shaft is thick and rounded. The supinator crest is broken off. The epicondyles are also chipped off on this specimen. The trochlea breadth is narrow and its medial lip distal projection is short and medially inclined relative to shaft. The capitulum distal end is missing. The olecranon fossa shape is rounded-ellipsoid.

- SWP 1205, a right distal humerus:

This specimen's shaft is approximately straight. The medial and lateral edges are symmetrical. The distal shaft is thick and rounded, and wider and thicker above the lateral epicondyle. The medial epicondyle is retroflexed. The lateral epicondyle has a small dorsal face with minimum projection above the level of the olecranon fossa. The trochlea breadth is narrow and its medial distal lip projection is short and medially inclined relative to the shaft. The medio-lateral width of the capitulum is even in the proximo-distal axis. The olecranon fossa shape is rounded-ellipsoid.

- SWP 1582, a right distal humeral condyle:

Only the lateral epicondyle, the distal articular surface and the distal half of the olecranon fossa are preserved on this specimen. The trochlea breadth is narrow. The medial lip distal projection is long and medially inclined. The medio-lateral breadth of the capitulum is narrowed distally. The olecranon fossa has an elongated-ellipsoid shape.

- SWP 2816, right distal humeral condyles:

This specimen only preserves the capitulum and the medial and lateral condyles, however, with features consistent with *Parapapio* sp and *Papio* sp morphology. In superior view, the medio-lateral breadth of the capitulum is narrowed distally. The medial epicondyle is narrower than the lateral epicondyle and is retroflexed.

#### Unsidled humeri

- STS 377D, a distal humerus fragment:

This specimen is in a very flaky condition and is embedded in breccia. The olecranon fossa shape is elongated-ellipsoid. The distal shaft is rounded and asymmetrical. It is also thicker and wider above the lateral epicondyle.

- SWP 1119 is an unsided distal humerus fragment without a shaft:

The specimen's distal shaft medial and lateral edges are oriented asymmetrically. The distal shaft is also thick and rounded with dorsal pillars which are wider and thicker above the lateral epicondyle. The medial epicondyle is retroflexed. The lateral epicondyle has a large dorsal face with a tall wall facing the olecranon fossa. The trochlea is narrow. The trochlea medial lip's distal projection is medially inclined relative to the humeral shaft. The capitulum's medio-lateral width is even in the proximo-distal axis. The olecranon fossa is rounded-ellipsoid in shape.

- SWP 2537, a distal humerus:

The distal shaft medial and lateral edges are oriented asymmetrically. The distal shaft is also thick and rounded and its dorsal pillars are wider and thicker above the lateral epicondyle. The medial epicondyle is wider than the lateral epicondyle, and is retroflexed. The lateral epicondyle has a large dorsal face with a tall wall facing the

olecranon fossa. The olecranon fossa is filled with breccias and its shape cannot be determined. The capitulum has an even medio-lateral width in the proximo-distal axis.

---

b) Ulna

Due to the fragmented state of preservation of the ulna sample resulting in some of the diagnostic anatomical parts as missing, some ulnae cannot be positively distinguished between *Parapapio* sp and *Papio* sp. The main feature which could not be determined to separate the specimens between the two genera is the dorso-ventral elevation of the olecranon superior aspect. These specimens do not preserve sufficient morphology to determine the olecranon superior structure. However, they preserve the following traits 1) the olecranon superior extension is less than the trochlea length; 2) the trochlea has a crescentic shape; 3) the coronoid process lies in horizontal plane without significant distal extension; 4) the radial notch is rounded to accommodate an ovoid radial head; and 5) they are not robust as seen in *Theropithecus* sp specimens. Fifteen proximal ulnae are included within the *Papio/Papio* sp category. No distal ulnae are identified within this group.

- BP/3/23271, a left proximal ulna:
- The olecranon superior aspect morphology is concave with the lateral aspect higher than the medial aspect. The olecranon superior projection is less than the trochlea notch length. The olecranon is retroflexed. The anconeal process is in coronal plane with no significant proximal extension. The trochlea notch is crescentic. The coronoid process articular surface is in horizontal plane with no significant distal extension. There shaft groove distal to the coronoid process is present.
- BP/3/23336, a left proximal ulna:  
This specimen is fully preserved proximally and is missing the shaft. The olecranon superior aspect morphology is concave with the lateral aspect higher than the medial aspect. The olecranon superior projection is less than the trochlea notch length. The olecranon is retroflexed. The anconeal process is broken off. The trochlea notch is

crescentic. The coronoid process articular surface is in horizontal plane with no significant distal extension. There is a shaft groove distal to the coronoid process.

- SWP 1569, a left proximal ulna:

The superior olecranon on this specimen is broken off. The coronoid process is in horizontal plane with no significant distal extension.

- SWP 4008, a left proximal ulna with more than a third of the shaft preserved proximally:

The superior aspect of the olecranon is broken off. The trochlea notch is crescent shaped. There is an elongated proximo-distal groove distal to the coronoid process. The coronoid process is extensive and extends medially creating a depression postero-medially to it. The depression below the radial notch is present with pillars on both the medial and lateral sides with the lateral pillar creating a proximo-distal ridge. The shaft shape is nearly straight.

- BP/3/23357, a right proximal ulna with less than a third of the proximal shaft preserved:

The olecranon superior aspect is concave and inclined with the lateral aspect higher than the medial aspect. The superior aspect is less than the trochlea notch length. The olecranon is retroflexed. The trochlea notch is crescentic. The coronoid process articular surface is in horizontal plane without significant distal extension. The anconeal process articular surface also lies in horizontal plane with no significant proximal extension. The ulna shaft groove distal to coronoid process is present and the shaft fracture starts immediately where the depression starts.

- SWP 524, a right proximal ulna with more than a third of the shaft preserved:

The specimen is broken off on the posterior olecranon process. The olecranon superior length is less than the trochlea notch. The trochlea notch is crescentic in shape. The coronoid process articular surface is in horizontal plane with no significant distal extension. The anconeal process' articular surface is in horizontal plane with no significant proximal extension. The ulna shaft groove disto-medial to the coronoid



process is present. The shaft is not fully preserved, is nearly straight. The depression distal to the radial notch is present.

- SWP 853, a right proximal ulna with less than a third of the shaft preserved:  
The olecranon is broken off medially on this specimen. The centre of the process is retroflexed. The trochlea notch is crescentic. The coronoid process is broken off anteriorly but is in horizontal plane with no significant distal extension. The anconeal process is broken off posteriorly and is also in horizontal plane with no significant proximal extension. There is a deep proximo-distal ridge below the radial notch.
- SWP 1568, a right proximal ulna:  
The olecranon process is broken off. The trochlea notch is crescent shaped. There is an elongated proximo-distal groove distal to the coronoid process. The coronoid process is extensive and extends medially; it emphasises the postero-medial depression.

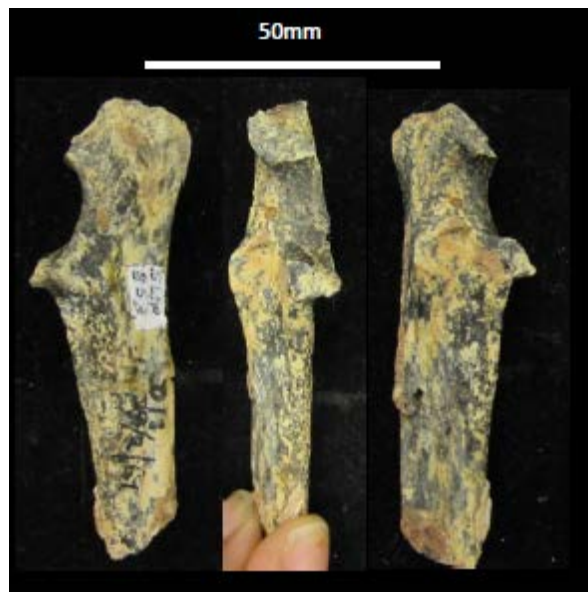


Figure 4.11. SWP 853 a right proximal ulna. The anconeal process is not fully preserved on this specimen.

- SWP 1570, a right proximal ulna:  
The olecranon is retroflexed. The superior aspect of the olecranon is smaller than the trochlea notch. The proximo-distal groove distal to the coronoid process is present. The coronoid process projects significantly medial to the rest of the ulna. The

depression below the radial notch is present with pillars on both the medial and lateral sides with the lateral pillar creating a proximo-distal ridge.

- SWP 1571: a right proximal ulna:  
The specimen's olecranon process is slightly broken off posteriorly. The olecranon is retroflexed. The superior aspect of the olecranon is very small, and much less than the trochlea notch. The proximo-distal groove distal to coronoid process is present. The coronoid process lies in horizontal plane with no significant distal extension.
- SWP 1576, a right proximal ulna:  
This specimen is missing the whole posterior aspect. The radial notch is rounded and has a depression distally.
- SWP 1580, a right proximal ulna:  
The olecranon on this specimen is missing the posterior superior portion. The superior aspect of the olecranon is less than the trochlea notch.
- SWP 1590, a right proximal ulna:  
The anconeal process is missing on this specimen. The superior aspect of the olecranon is, however, less than the trochlea notch.
- BP/3/31175, a right proximal ulna without shaft:  
This specimen's posterior portion of the olecranon process is broken off. The anconeal process lies in horizontal plane. The olecranon superior aspect is concave and the lateral aspect projects higher than the medial aspect. The remaining portion of the olecranon superior projection is less than the trochlea length. The coronoid process articular surface is in horizontal plane with no significant distal extension.
- SWP 2296, a right proximal ulna:  
The olecranon superior aspect is concave with the lateral aspect higher than medial. Its superior projection is less than the trochlea notch length. The olecranon is retroflexed. The trochlea notch is crescentic. The coronoid process articular surface is in horizontal plane without significant distal extension. The anconeal process articular surface also

lies in horizontal plane with no significant proximal extension. The ulna shaft groove distal to the coronoid process is present.

---

c) Radius

Ambiguity of diagnostic traits and fragmentary nature of the specimens prevented assignment to either *Parapapio* sp or *Papio* sp. 1) the head is not as robust as observed in *Theropithecus* sp specimens; 2) the head is ovoid in shape and its medial and lateral aspects are unequal in height. In the absence of a well preserved bicipital tuberosity combined with either a long or short neck, it is difficult to discern between these two genera. Five of these radii are therefore included in the *Papio/Papio* sp category.

- BP/3/24043, a left proximal radius:  
This specimen's head is broken off on its dorsal and ventral portions. The head shape, however, is ovoid, unlike that which is observed in colobines. The bicipital tuberosity is also broken off ventrally and bears a longitudinal furrow in its centre.
- SWP 518, a left proximal radius:  
The head is depressed in superior view. It is ovoid in shape. The lateral and medial aspects are approximately on the same level.
- SWP 1368, a left proximal radius:  
The specimen has the head broken off on its anterior side and medial aspect. Therefore The only undisturbed morphology is the bicipital tuberosity with has a furrow on the medial side.
- SWP 1519, a right proximal radius:  
The head is broken off on the posterior aspect. The head shape is ovoid and is depressed in superior view. The neck is 8.16mm long in the proximo-distal axis. The bicipital tuberosity is elongated proximo-distally but does not preserve a furrow.

- SWP 2177, right proximal radius:

A portion of the head is broken off on the posterior side. The head is ovoid and is depressed in superior view. The deep depression on the head could suggest that this specimen similar to *Parapapio* sp specimens; however the neck size is too short. The bicipital tuberosity is covered in breccia.

---

#### d) Femur

There is no sufficient evidence of *Parapapio* femur in the literature to differentiate this genus from *Papio*. The main known *Parapapio* femur is specimen AL 363-1c, a proximal femur from Hadar in Ethiopia (Frost & Delson 2002). This specimen could not be contrasted to *Papio* specimens. It preserves the following features: it has a long neck, the head is not cranially oriented; the neck shaft angle overlies with many other species; the greater trochanter is elevated superiorly to the head and is medially; the lesser trochanter is also medially oriented; the fovea capitis is short and oval. The fossil femora specimens which are identified as part of the *Papio/Parapapio* group preserve the following characteristics: 1) the greater tuberosity extends above the head; 2) it is medially oriented and not as robust as in *Theropithecus* sp specimens; 2) its lateral surface is not as rugose and concave as that of *Theropithecus* sp specimens. 3) the lesser trochanter is long with a parabolic profile and faces more medially than dorsally 4) The neck is short. The length of the neck is the only feature which could be of significance to differentiating between the two genera. However, because the neck shaft angle of the *Papio jonesi* (AL 363-1c) specimen overlaps many species, it cannot be used to isolate between the two. Seventeen proximal femora are assigned to *Papio/Papio* sp category.

- SF 5496 (Fig. 4.12), a left proximal femur with less than a third of the shaft preserved proximally:

The head has a superior orientation. The fovea capitis is located centrally on the anterior head surface. The femoral head bears obvious dorsal extension towards the greater tuberosity. The greater trochanter has a blunt apex and is oriented superiorly. The intertrochanteric fossa shape is large and deeply cavitated. It is located at the same

level as the femoral head and is narrow with parallel margins. The lesser trochanter is long with a parabolic profile and faces more medially than dorsally. The neck is short.

- SWP 1404, a right proximal femur:

The femur is slender. The greater trochanter is elevated above the level of the head. It is superiorly pointed. The greater trochanter lateral surface is almost flattened. Proximo-laterally, the *linear aspera* is sharp and creates a flange on the lateral side. The femur shaft is proximally asymmetrical. The lesser trochanter is reduced with a triangular profile and is medially facing. Its supero-medial face has a large flat facet for attachment of *m. psoas major*. The intertrochanteric fossa is small and deeply cavitated and is located at the same level as the head. The *fovea capitis* is oval and elongated dorso-ventrally. The intertrochanteric groove is relatively narrow with parallel margins.

- SWP 1700, a left proximal femur with most of the shaft preserved:

The head of this specimen is fragmented. The greater trochanter is bluntly pointed and is superiorly oriented relative to the femoral head. The intertrochanteric fossa is small and deeply cavitated and lies at same level as the head. The intertrochanteric groove is relatively narrow with parallel margins. The lesser trochanter has a long base with a parabolic profile and faces more medially than dorsally.



Figure 4.12. SF 5496. Note the superior extension, and inclination of the greater tuberosity (a), a large deeply cavitated intertrochanteric fossa (b) located at the same level as the head, (c) and a medially facing lesser tuberosity.

- SWP 526, a left proximal femur:  
The greater trochanter is not preserved. The intertrochanteric groove is deep and lies at the same level as the head. The lesser trochanter is medially facing.
- SWP 746, a left proximal femur:  
The specimen is missing the head and both trochantae. It is flaked and cracked. The intertrochanteric groove is deep, small and at the same level as the head. The lesser trochanter is medially facing.
- SWP 1(invisible number)85, a left proximal femur:  
The greater trochanter is broken off on this specimen. It only preserves the head and lesser trochanter.
- SWP 1171, a left proximal femur:  
The specimen is highly fragmented. The greater trochanter is missing its proximal surface. The intertrochanteric groove is deep and at the same level as the head. The lesser trochanter is dorsally facing.
- SWP 1203, a left proximal femur:  
The femoral head articular surface lacks obvious dorsal extension towards greater trochanter. The greater trochanter is slightly broken off proximally; it is oriented parallel to the femoral head. The intratrochanteric fossa is small and deeply excavated and lies at same level as femoral head. The intratrochanteric groove is narrow with parallel margins. The lesser trochanter has a long base, a parabolic profile and is oriented dorsally.
- SWP 1263, a left proximal femur:  
The proximal greater trochanter is not preserved on this specimen. The intertrochanteric groove is deep and at the same level as the head. The lesser trochanter is medially oriented.

- SWP 1385, a left proximal femur:  
The intertrochanteric groove is flaked off. The femoral head articular surface lacks obvious dorsal extension towards the greater trochanter. The greater trochanter is blunt superiorly, and is oriented parallel to femoral head. The lesser trochanter has a long base with a parabolic profile. The region of the intertrochanteric groove is filled with breccia. The lesser trochanter faces more medially than dorsally.
- SWP 1206, a left proximal femur head fragment:  
The specimen preserved is a head fragment; however it is consistent with *Papio/Papio* sp morphology. The head has a spherical shape. The *fovea capitis* is postero-distally located. It is elongated in the medio-lateral axis.
- SWP 1698, a left proximal femur fragment:  
The intertrochanteric groove and fossa are fragmented and filled with breccia. The femoral head articular surface lacks obvious dorsal extension to the greater trochanter. The greater trochanter has a sharply pointed apex and is parallel to the femoral head. The lesser trochanter is fragmented but has a long base with parabolic profile and faces more medially than dorsally.
- SWP 531, a right proximal femur:  
The greater trochanter is missing its proximal surface. The intertrochanteric groove is deep and at the same level as the head. The lesser trochanter is medially facing.
- SWP 532, a right proximal femur:  
The specimen has robust muscle attachments. The greater trochanter is elevated above the head and faces medially. The lesser trochanter is dorsally facing and very stout. The intertrochanteric fossa is deep.
- SWP 533, a right proximal femur:  
The greater trochanter is missing its proximal surface. The intertrochanteric groove is deep and lies at the same level as the head. The lesser trochanter is medially facing. The fovea capitis is rounded and anterior facing.

- SWP 1008, a right proximal femur:  
The specimen is missing the trochantae. The intertrochanteric fossa is deeply cavitated and lies at the same level as the head. The fovea capitis is posterior facing and oval.
- SWP 4103, a right proximal femur:  
The greater trochanter is broken off proximally and was glued such that no diagnostic assessment can be made from this portion of the specimen. The femoral head articular surface bears no obvious dorsal extension toward the greater trochanter. The intertrochanteric groove and fossa are covered by breccia and are fragmented. The lesser trochanter has a long base with parabolic profile and faces more medially than dorsally.

*Locomotor adaptation of specimens identified as Papio/Parapapio sp*

The fossil remains assigned to the *Papio/Parapapio* sp class have character traits which could not be designated to either genus but can be differentiated from other papionins discovered at the Sterkfontein cave site. The major characters mainly point to terrestrial locomotion. The proximal humerus, which, in this study, is used to distinguish between the two genera bore ambiguous traits, the greater tuberosity lies on the same level as the head or is missing. The distal humerus the medial trochlea distal lip extends distally, a feature associated with terrestrial locomotion, contrary to a distal lip which is moderately developed as seen in semi-terrestrial and arboreal monkeys (Benefit *et al.* 2008). The radii do not possess the distinctive furrow in the bicipital tuberosity and demonstrate terrestrial features observed in other papionins. The ulna superior olecranon is missing on these specimens. The femur, one of the skeletal elements whose morphology covaries with locomotion, possesses a greater trochanter which projects superior to the head, a feature consistent with powerful hind limb extension motion (Harrison & Harris 1996; Hlusko 2007)



Subfamily	Cercopithecinae Gray 1921
Tribe	Papionini Burnett 1828
Subtribe	Papionina Burnett 1828
Genus	cf. <i>Theropithecus</i> . I. Geoffroy, Saint-Hilaire 1843

Within the assemblage there is a subset of specimens which are, on average, larger than the three groups already discussed, and, they possess very robust muscular attachments. These are tentatively classed as cf. *Theropithecus* sp.

---

a) Ulna

Ten ulnae form part of the assemblage. These specimens are different from other specimens in the assemblage. They are robust with defined muscular attachments. These have the following features 1) The olecranon superior aspect morphology is concave and inclined with lateral aspect higher than the medial aspect; 2) the olecranon superior projection is elevated but less than trochlea notch length; 3) the centre of the olecranon process is retroflexed 4) the trochlea notch shape is crescentic; 5) the coronoid process is in horizontal plane with no significant distal extension and 6) the anconeal process articular surface is oriented in horizontal plane with no significant proximal extension; 7) the trochlea notch preserves a curved ridge in its lateral corner; 8) medially, the olecranon is deeply concave for attachment of extensive *m. flexor carpi ulnaris* and the *m. flexor digitorum profundus* muscles. 9) All specimens bear a robust ulna shaft groove distal to the coronoid process; 10) the radial notch is bean-shaped and bears a deep groove distally. All these features are consistent with ulnae described as *Theropithecus*, e.g., KNM-ER 1572 from the upper Burgi member of Koobi Fora (Jablonski *et al.* 2008)

- SWP 822, a left proximal ulna:

This specimen is chipped off on the posterior olecranon process. The olecranon process superior aspect morphology is flat with medial and lateral aspects of roughly equal heights. The olecranon superior projection is less than trochlea notch length, and even though the shaft is absent, the centre of the process is retroflexed. The trochlea

notch is crescentic in shape. The coronoid process is in horizontal plane with no significant distal extension. The anconeal process articular surface is oriented in horizontal plane with no significant proximal extension.

- SWP 1104, a left proximal ulna:

The olecranon superior morphology is flat with the lateral aspect slightly elevated than the medial aspect. Its projection is less than trochlea notch length and even though the shaft is absent, the centre of the process is retroflexed. The trochlea notch is crescentic in shape. The coronoid process is in horizontal plane with no significant distal extension. The anconeal process is oriented in horizontal plane with no significant proximal extension.

- SWP 1110, a left proximal ulna:

The olecranon process superior aspect morphology is concave with the lateral aspect elevated higher than the medial aspect. The anconeal process is in horizontal plane with no significant proximal extension. Olecranon superior projection is less than trochlea notch length and even though the shaft is absent, the centre of the process is to be aligned with the long process of the ulna. The trochlea notch is crescentic in shape. The coronoid process is in horizontal plane with no significant distal extension.

- SWP 1156, a left proximal ulna:

The olecranon process superior aspect morphology is flat with medial and lateral aspects of roughly equal heights. The olecranon superior projection is less than trochlea notch length and is retroflexed. The trochlea notch is crescentic in shape. The coronoid process is in horizontal plane with no significant distal extension. The anconeal process lies in horizontal plane with no significant proximal extension.

- SF 3418 (Fig 4.14), a right proximal ulna:

The olecranon superior aspect morphology on this specimen is concave and inclined with lateral aspect higher than medial. The anconeal process is in horizontal plane with no significant proximal extension. The olecranon superior aspect is less than the trochlea notch length and is retroflexed. The trochlea notch is crescentic in shape. Medially, the olecranon is deeply concave for attachment of *m. flexor carpi ulnaris*

and the *m. flexor digitorum profundus* muscles but fades away immediately distal to the coronoid process. The coronoid process is in horizontal plane with no significant distal extension. The ulna shaft groove distal to the coronoid process is present. The radial notch is bean-shaped and has the deep groove below it. The lateral edge has a groove on the lateral side. The trochlea notch preserves a curved ridge in its lateral corner.

- SWP 825, a right proximal ulna:

The olecranon process is chipped off on the proximo-posterior aspect. The olecranon process height is less than the trochlea notch. The trochlea notch is crescentic. The coronoid process is in horizontal plane with no significant distal extension. The anconeal process articular surface is in horizontal plane with no significant proximal extension. The deep depression below the radial notch is present. The lateral aspect of the trochlea notch bears a curved proximo-distally oriented ridge.

- SWP 1148, a right proximal ulna:

The olecranon is missing its superior aspect. The trochlea notch is crescentic. The coronoid process is in horizontal plane with no significant distal extension. The anconeal process articular surface is in horizontal plane with no significant proximal extension. The deep depression below the radial notch is present. The lateral aspect of the trochlea notch bears a curved proximo-distally oriented ridge.

- SWP 1578, a right proximal ulna:

The olecranon superior aspect is concave and inclined with the lateral aspect higher than the medial aspect. The anconeal process is in horizontal plane with no significant proximal extension. The olecranon superior aspect is less than the trochlea notch length and its posterior aspect is retroflexed. The trochlea notch is crescentic in shape. The coronoid process is in horizontal plane with significant distal extension. The ulna shaft groove distal to coronoid process is present. The radial notch is bean-shaped and has the deep groove below it. The trochlea notch preserves a curved ridge in its lateral corner.

- SWP 4001, a right proximal ulna:

The olecranon superior aspect morphology of this specimen is concave with its lateral aspect higher than the medial aspect. The anconeal process is in horizontal plane with no significant proximal extension. The olecranon superior aspect is less than the trochlea notch length and is retroflexed. The trochlea notch is crescentic in shape. The coronoid process is in horizontal plane with significant distal extension. The ulna shaft groove distal to coronoid process is present. The radial notch is bean-shaped and has the deep groove below it. The trochlea notch preserves a curved ridge in its lateral corner.

- SWP 4084, a right proximal ulna:

The olecranon superior aspect morphology of this specimen is concave with the lateral aspect elevated higher than the medial aspect. The olecranon postero-superior aspect is retroflexed. The trochlea notch is crescentic in shape. The trochlea notch and the olecranon superior projection are almost the same height. The coronoid fossa and anconeal process are in horizontal plane. The coronoid process is in horizontal plane and is flattened. The anconeal process is also in horizontal plane with significant proximal extension. The ulna shaft groove distal to the coronoid process is present. The radial notch is bean-shaped and has the deep groove below it.



Figure 4.13. On the left is SWP 1104, a left cf. *Theropithecus* proximal ulna and on the right is KNM-ER 1572, *Theropithecus oswaldi* from Koobi Fora. SWP 1104 demonstrates the superior projection of the olecranon (a), the concave medial face of the olecranon (b) and the deep ridge distal to the coronoid fossa (c).

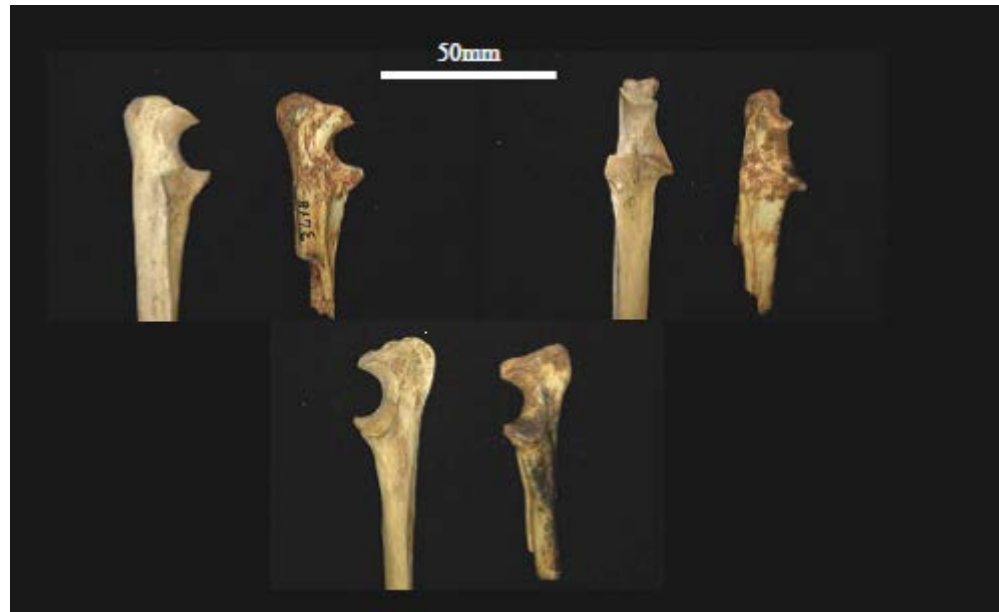


Figure 4.14. A right modern *P. ursinus* ulna and SF 3418, a right proximal *cf. Theropithecus sp* ulna.

b) Femur

Three proximal femora are tentatively assigned to cf. *Theropithecus* sp. Common features in these femora include- 1) a large greater trochanter with a proximal tip that lies above the head; it is higher in *Theropithecus* sp than in *Papio* sp.; 2) the superior extension of the greater trochanter points medially; 3) the lateral border of the greater trochanter is concave it is a distally oriented u-shape and is located slightly lower than the intertrochanteric fossa, whereas in *Papio* sp this feature is mainly rugose and is located more superiorly than in *Theropithecus* sp. 4) there is no obvious dorsal extension from the greater trochanter to the head; 5) The superior surface between the neck and the head is wider, more open, and flattened than in *Papio* sp. 6) the femoral head faces superiorly; 7) the neck is relatively long 8) the lesser trochanter is short with a parabolic profile and; 9) it faces dorso-medially; 10) the shaft is convex anteriorly and angles laterally.

- SWP 528, a left proximal femur:

The greater trochanter is large and its proximal tip lies above the head and points medially. The femoral head faces superiorly. The neck is very long.. The supero-lateral border of the greater tuberosity is concave. The superior surface between the neck and the head is flat. The lesser tuberosity is short with a parabolic profile and faces dorsally. The shaft is convex anteriorly and angles laterally.

- SWP 4039, a left proximal femur, and SWP 4153, a right proximal femur (Fig. 4.15):

These specimens are very similar and are likely to be from the same individual. The femoral heads are superiorly inclined. The *foveae capitis* are horizontally elongated with a slight nodule on the superior surface. The femoral head articular surface lacks obvious dorsal extension toward the greater tuberosity. The greater trochantae have a blunt apex and are medially inclined. The antero-medial border of the greater tuberosity is very shallow, unlike that of *Papio* sp, which is deep. The lateral border of the greater trochanter is concave. The intertrochanteric fossa is long and deeply excavated and lies on the same level as the femoral head. It is relatively narrow with parallel margins. The lesser trochanter has a long base with a parabolic profile and is

oriented more medially than dorsally. SWP 4039 preserves a shaft which has a slight - lateral bow.

*Locomotor adaptation of specimens identified as cf. Theropithecus sp*

The Sterkfontein fossil *Theropithecus* is a large, robust and highly terrestrial cercopithecoid which, based on the sizes of the specimens, most likely towered above other cercopithecines in the environment. No humerus specimens are identified for this genus; therefore no assumptions are made about the shoulder joint. The ulna morphology resembles other papionins and suggests that the specimens belonged to individuals who frequented terrestrial niches (Fleagle 1983). The upper femur has a head which lies below the greater trochanter, restricts hip abduction and is therefore associated with terrestrial adaptations (Smith & Savage 1956).

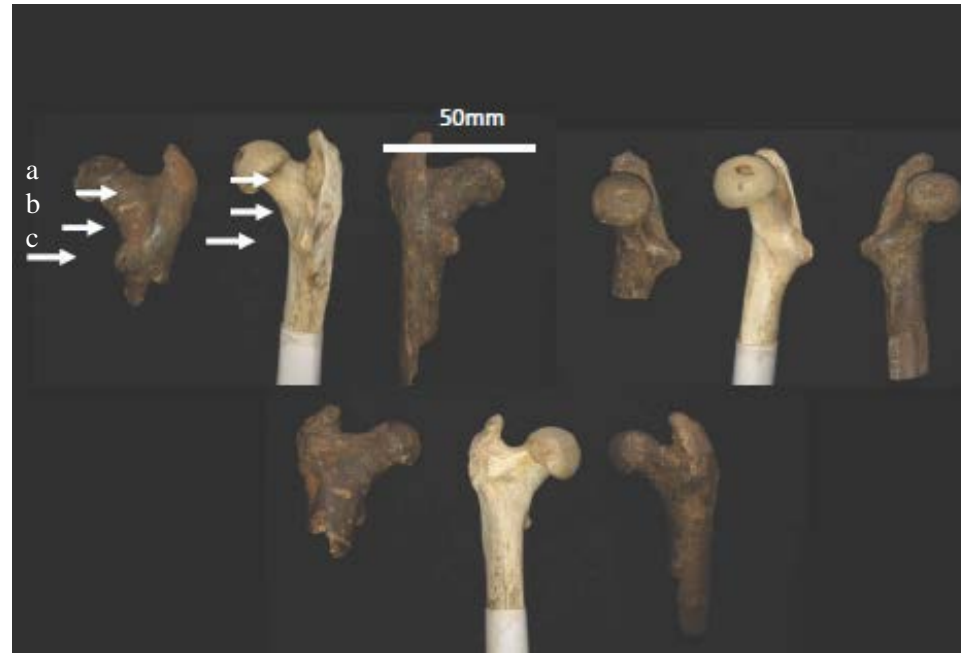


Figure 4.15. From left to right, cf. *Theropithecus sp* femora, SWP 4153, modern *Papio ursinus* BPI/C/541 and *Theropithecus sp*, SWP 4039 on the right. The arrows demonstrate a medially facing greater trochanter (a), an extensive intertrochanteric groove in *Theropithecus* (b) and a medially facing lesser trochanter which is more dorsally facing in *Papio* (c) and a laterally inclined shaft in *Theropithecus* (d).



Subfamily Cercopithecinae Gray 1921

Tribe Papionini. Burnett 1828

This sub-assemblage preserves features which are generally consistent with the first four groups, however, due to limited preservation of diagnostic morphological traits', they are categorised as a separate group.

a) Humerus

Eighteen humeri form part of this group. These specimens have varying degrees of preservation; they however preserve general papionin characteristics. They are highly fragmented and do not preserve sufficient morphology to assign them to a genus. The specimens have 1) a hemispherical head shape; 2) the lesser tuberosity is continuous from the head; 3) the shaft is approximately straight 4) distally, the shaft is thick and rounded; 5) they also preserve a retroflexed medial epicondyle; 6) the dorsal pillars are wider and thicker above the lateral epicondyle; 7) the trochlea is narrow; 8) its medial distal lip is medially oriented; 9) the capitulum is rounded. These features are consistent with papionin morphology.

- SWP 993, a right proximal humerus:

The specimen preserves a greater tuberosity and head fragment. The head shape is hemi-spherical. The greater tuberosity surface is convex, therefore excluding it from being a theropithecine. The intertubercular groove is deeply excavated with sharply defined medial and lateral edges.

- STS 2185, a right proximal humeral lateral head fragment:

The specimen only preserves the lateral aspect of the head. The head is hemi-spherical in shape.

- SF 4610, a right distal humerus fragment:

Only the distal shaft and proximal part of the olecranon fossa are preserved on this specimen. The distal shaft is thick and rounded.

- SWP 726, a right distal humerus fragment:  
This specimen is similar to specimen SF 4610. It is a fragment preserving the shaft and no condyles. The distal shaft is thick and rounded.
- SWP 1539, a right distal humerus fragment:  
Only the capitulum and lateral epicondyle are preserved on this specimen. The lateral epicondyle has a small dorsal surface with minimum projection above the level of the olecranon fossa. In the proximo-distal axis, the capitulum's medio-lateral width is narrowed distally.
- SWP 963, a left proximal humerus fragment:  
The head is proximo-distally compressed. The specimen only preserves the head fragment.
- SWP 965, a left proximal humerus fragment:  
The head is proximo-distally compressed as observed in other specimens.
- S94-9257, a left proximal humerus head fragment:  
The head is proximo-distally compressed.
- STS 2074, a left distal humerus:  
This is a highly broken specimen with only the lateral epicondyle and less than a third of the distal shaft preserved. The distal shaft is rounded and asymmetrical.
- SWP 1544, an unsided proximal humerus fragment:  
This specimen is a humerus head fragment with a greater tuberosity. The head is hemispherical in shape. The greater tuberosity superior extension is lower than the level of the humeral head. The specimen is highly fragmented.
- SWP 727, a left distal humerus fragment:  
The distal shaft is thick and rounded. As seen in *Papionins*, the distal dorsal pillars are wider and thicker above the lateral epicondyle.

- SWP 729, a left distal humerus:  
The specimen preserves less than a third of the shaft distally. The distal shaft is thick and rounded. The distal dorsal pillars are wider and thicker above the lateral epicondyle. The medial and lateral edges of the shaft are oriented asymmetrically.
- SWP 1543, a left distal humerus:  
Only the distal articular surface and medial epicondyle are preserved. The capitulum is broken off on its lateral aspect. The medial epicondyle is retroflexed. The lateral epicondyle is not preserved. The trochlea is narrow and its medial lip distal projection is short and in straight line with the humeral shaft.
- SWP 1581, a left distal humerus:  
The epicondyles and the trochlea are broken off. The capitulum is narrowed distally. The olecranon fossa is triangular.
- SWP 1583, a left distal humerus:  
This specimen preserves a fragment of the distal shaft, the epicondyles and the olecranon fossa. It is the second largest humerus specimen in the whole Sterkfontein assemblage. This character state is observed in *Papionins* (Jablonski *et al.* 2002). The medial epicondyle is larger and retroflexed. The lateral epicondyle has a small face with minimal projection above the level of the olecranon fossa. The trochlea breadth is narrow, and its medial lip distal projection is short and medially inclined relative to the humeral shaft. The capitulum is rounded and it has an uneven width in the proximo-distal axis. It also bears an extensive surface area for radial articulation. The capitulum shape and position are indicative of the level or ability of upper arm movement. The olecranon fossa is triangular in shape. The triangular ridges of this specimen are very defined and the outline is more open. This specimen is very robust compared to other specimens identified in the Sterkfontein fossil cercopithecoid sub-assemblage. The specimen resembles specimen KNM-ER 17723 from Koobi Fora, which is *Theropithecus oswaldi* (Jablonski *et al.* 2008). However, due to its small size, it is assigned to *Papionini*.

- SWP 4099, a left distal humerus:

This specimen preserves a lateral condyle and less than a third of the shaft distally. Its morphology shows a large dorsal face with a tall wall facing the olecranon fossa. The olecranon is broken off proximo-distally.

- STS 1264, a left distal humerus:

This humerus is embedded in breccias. It preserves the distal condyles and more than a third of the shaft distally. Therefore most of the morphology cannot be ascertained. It has a rounded and asymmetrical distal shaft.

- STS 27(invisible number), a left distal humerus:

This specimen is a distal humerus fragment without condyles. The distal shaft is asymmetrical and rounded. It is wider and thicker above the lateral epicondyle.

---

#### b) Ulna

Twenty-nine ulnae are discussed below. These have the following traits, 1) the trochlea notch is crescentic in shape; 2) the surface orientation of the anconeal process is in horizontal plane with no significant proximal extension; 3) the coronoid process lies in horizontal plane with no significant distal extension; 4) distal to the coronoid process, the ulna bears a shaft groove; 5) the olecranon superior aspect morphology is concave with the lateral aspect higher than medial; 6) the olecranon superior projection is less than the trochlea notch length and it is retroflexed; 7) the radial notch has a deep groove distally.

- d) SWP 817, a left proximal ulna with less than a third of the shaft preserved proximally:  
The olecranon proximo-distal length is less than the trochlea height.

- SWP 1(invisible number)79: a left proximal ulna with less than a third of the shaft preserved proximally:

The olecranon and proximal portion of the trochlea are broken off.

- SWP 1513, a left proximal ulna with less than a third of the shaft preserved proximally:  
This specimen is highly fragmented. The olecranon is retroflexed.
- SWP 1566, a left proximal ulna with less than a third of the shaft preserved proximally:  
This specimen's olecranon is retroflexed. Its whole proximal aspect is fragmented.
- SWP 1567, a left proximal ulna fragment with less than a third of the shaft preserved proximally:  
The ulna is missing the proximal olecranon. The olecranon is retroflexed. The trochlea notch shape is crescentic.
- SWP 1575, a left proximal ulna fragment with less than a third of the shaft preserved proximally:  
This specimen is highly fragmented. The proximal olecranon is missing; however the rest of the olecranon is retroflexed.
- SWP 1604, a right proximal ulna:  
The olecranon is concave with lateral aspect higher than medial. Its antero-posterior length is 27.32mm. The specimen is disintegrated. The olecranon superior projection is less than the trochlea notch length and is retroflexed. The anconeal process is in horizontal plane with no significant proximal extension. The trochlea notch is crescentic. The shaft does not have a groove distal to the coronoid process.
- BP/3/23028, a left proximal ulna with less than a third of the shaft preserved proximally:  
The specimen is missing the proximal olecranon process. The coronoid process is in horizontal plane with no significant distal extension. The shaft groove below the coronoid process is present.
- BP/3/23093, a left proximal ulna with less than a third of the shaft preserved proximally:

This specimen is also missing the proximal olecranon process. The coronoid process is in horizontal plane with no significant distal extension. The shaft groove below the coronoid process is present.

- SF 4611, a left proximal ulna with less than a third of the shaft preserved proximally:  
The proximal olecranon process is not preserved. The coronoid process is in horizontal plane with no significant distal extension. The shaft groove below the coronoid process is present.
- SWP 1197, a left proximal ulna with less than a third of the shaft preserved proximally:  
This specimen is also missing the proximal olecranon process. The coronoid process is in horizontal plane with no significant distal extension. The shaft groove below the coronoid process is present.
- SWP 1285, a left proximal ulna with less than a third of the shaft preserved proximally:  
The olecranon proximo-distal height is much smaller than the trochlea notch length. The coronoid process is in horizontal plane with no significant distal extension. The shaft groove below the coronoid process is present.
- SWP 1560, a left proximal ulna with less than a third of the shaft preserved proximally:  
This specimen is also missing the proximal olecranon process. Only the radial notch, a fragment of the shaft distal to the trochlea notch and a fragment of the coronoid process are preserved. The coronoid process is in horizontal plane with no significant distal extension. The shaft groove below the coronoid process is present.
- S94-13152, a left proximal ulna fragment with less than a third of the shaft preserved proximally:  
S94-13152 is highly fragmented; only the coronoid process and distal end of trochlea notch are preserved. The coronoid process is in horizontal plane with no significant distal extension. The shaft groove below the coronoid process is present.

- SWP 4015, a left proximal ulna:  
This specimen is very muscular suggesting that it belongs to a robust *Papionin*. The olecranon superior aspect morphology is slightly rounded with the lateral and medial aspects which are roughly equal in height. The olecranon is retroflexed. The olecranon superior projection is less than trochlea notch length. The robust nature of this specimen suggests that it belongs to a robust papionin.
- BP/3/23718, a right proximal ulna fragment:  
BP/3/23718 preserves the trochlea notch, the coronoid process, and less than a third of the shaft distally. The trochlea notch is crescentic. The coronoid process articular surface is in horizontal plane with no significant distal extension. The shaft groove distal to the coronoid process is present.
- SF 1465, a right proximal ulna fragment:  
The anterior surface of the specimen is missing. The coronoid process is also partly preserved, but it is chipped off laterally.
- SWP 815, a right proximal ulna:  
This specimen only preserves the coronoid process, the radial notch and less than a third of the shaft. The coronoid process is in horizontal plane with no significant distal extension. The deep depression below the radial notch is also present. .
- SWP 1213, a right proximal ulna:  
The olecranon is missing the proximal and anterior aspect. The trochlea notch has a crescentic shape. The coronoid process is broken off medially. Its articular surface orientation is in horizontal plane with no significant distal extension. The depression below the radial notch is present.
- SWP 1291, a right proximal ulna missing the olecranon superior aspect:

The olecranon process is broken off on the superior and the lateral aspect of the specimen. The coronoid process is missing proximally; distally it does not preserve significant distal extension. It has a depression below the radial notch. .

- SWP 1574, a right proximal ulna missing the olecranon superior aspect:  
The specimen is highly flaked. The anconeal process is in horizontal plane with no significant proximal extension. Only the trochlea notch and the anconeal process are discernible. The trochlea notch is crescentic in shape.
- SWP 2813, a right proximal ulna missing the olecranon superior aspect:  
The surface orientation of the anconeal process is in horizontal plane with no significant proximal extension. The shaft groove distal to the coronoid process is absent. The wide groove below the radial notch is present and flanked by ridges on both the medial and lateral side.
- SWP 561, a right proximal ulna:  
This specimen is highly fragmented. The superior olecranon, the coronoid process and the radial notch are broken off. The remaining portion of the olecranon is retroflexed. The radial notch is bean-shaped and distal to it are deep medial and lateral ridges.
- SWP 813, a right proximal ulna:  
The specimen does not preserve the superior olecranon. The olecranon is retroflexed. The trochlea notch has a crescentic shape.
- SWP 816 a right proximal ulna:  
SWP 816 does not preserve even a small portion of the proximal shaft. It preserves features which suggest that it belonged to a robust papionin. The trochlea notch is broken off proximally. The coronoid process is reduced medially. The radial notch is bean-shaped and has a deep, sharp proximo-distal ridge laterally. The lateral aspect of the olecranon is concave. The deep ridge lateral to the trochlea notch is present.
- SWP 1561, a right proximal ulna:



The anconeal process is broken off. The olecranon superior aspect morphology is concave; the lateral aspect is higher than the medial aspect. The olecranon superior projection is less than trochlea notch length and is retroflexed. The trochlea notch shape is crescentic. The coronoid process articular surface is in horizontal plane with no significant distal extension. The deep groove below the radial notch is present.

- SWP 1563, a right proximal ulna:

The anconeal process is broken off but is to be in horizontal plane with no significant proximal extension. The olecranon superior aspect morphology is concave with lateral aspect higher than medial. The olecranon superior projection is less than the trochlea notch length and it is retroflexed. The trochlea notch is crescentic. The coronoid process articular surface is in horizontal plane with no significant distal extension. The deep groove below the radial notch is present.

- SWP 1573, a right proximal ulna:

This specimen is highly fragmented. It is missing the anconeal process and the anterior trochlea notch. The ulna shaft groove distal to the coronoid process and the shaft groove distal to the radial notch are present. In lateral view, the olecranon process has a shaft groove posterior to the trochlea notch.

- e) SWP 4098, a right proximal ulna:

The specimen is highly fragmented and cemented together by breccia. The olecranon process is less than the trochlea notch length. The coronoid process is the most diagnostic morphology preserved; it is in horizontal plane with no significant distal extension. The trochlea notch has a proximo-distal groove on the lateral corner. Below the radial notch, there is a deep and defined depression.

- 
- c) Radius

Twenty-nine radii specimens are identified which preserve papionin characteristics. The specimens grouped in this category preserve little diagnostic morphology to be assigned to a

genus. The general radial morphology observed is that 1) the head shape is ovoid; 2) the lateral aspect lies lower than the medial aspect 3) the neck is relatively short; 4) the bicipital tuberosity is a rough lateral projection. The specimens are discussed below.

- BP/3/23235, a left proximal radius:

The head shape is slightly medio-laterally compressed. The lateral aspect is lower than the medial aspect. The shaft is nearly straight. The bicipital tuberosity is elongated proximo-distally.

- SF 2689, a left proximal radius:

The specimen is a radius shaft which is missing the head. The bicipital tuberosity is a proximo-distally elongated protuberance with a furrow antero-laterally. The head is broken off. The shaft is nearly straight.

- SWP 808, a left proximal radius:

This specimen is highly flaked, only the anterior and posterior aspects of the head are preserved. In superior view the head has a depression. The angle of the lateral aspect indicates that it is lower than the medial aspect. The shape of the head is ovoid. The shaft is nearly straight.

- SWP 4087, a left proximal radius:

The specimen is broken off on the proximo-medial side. The head shape is ovoid. The shaft is nearly straight.

- BP/3/31553, a left proximal radius without a shaft:

The head shape is ovoid.

- SF 1553, a left radius head without a shaft:

The head is chipped off posteriorly and has a nearly round shape. .

- SWP 4063, a left radius head without a shaft:

The radius' whole medial portion is missing. The head shape is ovoid.

- SWP 1139, a right proximal radius:  
This specimen is missing the unfused head. It is a juvenile right radius shaft with an elongated bicipital tuberosity which preserves a furrow antero-medially.
- SF 3484, a right proximal radius with at least a third of the shaft preserved proximally:  
The radius is broken off distally below longitudinal tuberosity. Its head shape is nearly round. The lateral aspect is lower than the medial. The bicipital tuberosity is a proximo-distal protuberance which has an antero-medial furrow.
- SWP 799, a right proximal radius with at least a third of the shaft preserved proximally:  
This is a flaky specimen with the anterior portion of the head missing. The head shape is nearly round. The lateral aspect is lower than the medial aspect. The bicipital tuberosity is missing.
- SWP 4059, an unsided radius head:  
The head is ovoid. The lateral aspect and the medial aspect lie approximately on the same level.
- SWP 797, an unsided radius head:  
The specimen is chipped off on the lateral aspect. The head is ovoid. The lateral aspect and the medial aspect are approximately on the same level.
- SWP 255, an unsided radius head:  
The head has a deep depression in superior view. It is ovoid in shape. The lateral aspect and medial aspect lie approximately on the same level.
- SWP 506, an unsided radius head:  
The head is ovoid in shape and has a deep depression in superior view. The lateral aspect and medial aspect lie approximately on the same level.
- SWP 4005, an unsided radius head with a fragment of the neck

The head has a deep depression proximally. It is ovoid in shape. The medial and the lateral aspects lie on the same level.

- Unnumbered STS, a right proximal radius with less than a third of the shaft preserved proximally:

This is one of the radii with robust papionin characteristics. The head shape is ovoid. The lateral aspect is lower than the medial aspect. The bicipital tuberosity is very pronounced.

- SWP 516, a right proximal radius:

The shape of the head is ovoid. Similar to other radial heads, its proximal attachment has a deep depression. The lateral aspect of the head is lower than the medial aspect. The bicipital tuberosity is elongated proximo-distally and bears a furrow on its antero-medial side.

- SWP 519, a left proximal radius:

The head proximal articulation has a deep depression. It is nearly rounded. The lateral aspect is lower than the medial aspect. The bicipital tuberosity is elongated proximo-distally.

- SWP 979, a right proximal radius:

The radius head is depressed in superior view and is nearly rounded. The lateral aspect is lower than the medial aspect. The bicipital tuberosity is elongated proximo-distally and bears a furrow antero-medially.

- SWP 1125, a right proximal radius:

The shape of the head is nearly round. The lateral aspect of the head is broken off; however the head angle suggests that it lay lower than the medial aspect. In superior view, the head is depressed. The bicipital tuberosity surface is elongated proximo-distally and bears a longitudinal furrow on its antero-medial side.

- SWP 1306 (this specimen is missing the posterior portion of the head):  
The head is depressed in superior view. It is nearly rounded and broken off on the lateral aspect. The lateral aspect is missing but as observed in specimen SWP 1125 the angulation of the head suggests that the lateral aspect was lower than the medial aspect. The bicipital tuberosity is elongated proximo-distally.
- SWP 1416, a right proximal radius:  
The shape of the head is ovoid to nearly round. In superior view, the head is depressed. The lateral aspect of the head is lower than the medial aspect. The bicipital tuberosity surface is elongated proximo-distally.
- SWP 520, a left proximal radius:  
This specimen preserves the head and neck only. The head shape is ovoid. It has a small neck.
- SWP 792, a left proximal radius:  
This specimen is broken off posteriorly. Head shape is ovoid. The lateral and medial aspects are approximately on the same level. The bicipital tuberosity is broken off distally; however, it is elongated proximo-distally.
- SWP 806, a left proximal radius:  
The radius head is completely chewed off, and only the postero-lateral aspect is preserved. The bicipital tuberosity is elongated proximo-distally.
- SWP 972, a left proximal radius:  
In superior view the head has a deep depression and has an ovoid shape. Its lateral aspect is approximately on the same level as the medial aspect. The bicipital tuberosity is broken off.
- SWP 1198, a left proximal radius:  
This specimen does not preserve a head. The bicipital tuberosity is elongated proximo-distally as observed.

- SWP 1308, a left proximal radius:  
Similar to SWP 1198 and SWP 806, no head is preserved on this specimen. The bicipital tuberosity is elongated proximo-distally.
  - SWP 1162, an unsided proximal radius:  
This specimen is a very large radial head which is highly flaked, fragmented and is missing its lateral part. The head is ovoid in shape. The head slopes laterally.
- 

#### d) Femur

Twenty-four femora with characteristics consistent with Papionini indet. morphology, are identified. 1) the Sterkfontein Papionini indet. femur has a lesser trochanter which faces medially; 2) the head articular surface lacks obvious dorsal extension toward the greater trochanter; 3) the intertrochanteric fossa is small, deeply cavitated, and 4) lies at the same level as the femoral head 5) the lesser trochanter has a long base with a parabolic or triangular profile; 6) the *fovea capitis* is located medial to the head and extends dorsally 7) it is deep and rounded in shape 8) the medial condyle surface area exceeds the lateral condyle 9) the condyles are splayed; 10) the femur distal shaft morphology is thick and rounded.

- SWP 527, a left proximal femur:  
The head on this specimen is broken off on the whole anterior portion. The greater trochanter is also broken off on its superior aspect. The lesser trochanter is medially facing. The greater trochanter lateral surface is lightly concave.
- SWP 529, a left proximal femur:  
The greater tuberosity is not preserved on this proximal femur. The lesser trochanter is medially facing. The intertrochanteric fossa is very shallow and almost non-existent. The neck is flat antero-posteriorly.
- SWP 530, a left proximal femur:  
The specimen preserves the head and neck only. The *fovea capitis* is oval and deep.

- SWP 738, a left proximal femur:  
The specimen is missing the head. The lesser trochanter is laterally facing due to cracking of the specimen and subsequent cementing with breccia. The intertrochanteric fossa is deep and lies at the same level as the head. The greater trochanter lateral surface has robust muscle attachment. The fovea capitis preserves a flange on its proximal aspect.
- SWP 743, a left proximal femur:  
The specimen preserves only the lesser trochanter and less than a third of the shaft. The lesser trochanter is extensive and faces dorso-medially.
- SWP 1154, a left proximal femur:  
This specimen only preserves a fragment of the neck, greater trochanter and intertrochanteric fossa which is deeply cavitated.
- SWP 1536, a right proximal femur with less than a third of the shaft preserved proximally:  
The greater trochanter is robust, extensive and pointed superiorly. The superior extension of the greater trochanter is higher. There is no obvious dorsal extension from the greater trochanter to the head. The superior surface between the neck and the head is more flattened than in *Papio* which bears a u-shaped surface. The lateral border of the greater trochanter is concave and defined in a distally oriented u-shape located slightly lower than the intertrochanteric fossa. The lesser trochanter is dorso-medial facing with a parabolic profile.
- SWP 1537, a left proximal femur:  
The greater trochanter is large and robust; it lies above the head and is medially oriented. The femoral head faces superiorly. The supero-lateral border of the greater trochanter is concave and has robust muscle attachments for the *gluteus medius* tendons. The superior surface between the neck and the head is flat. The lesser trochanter is short with a parabolic profile. It also faces dorsally.

- SWP 1697, a right proximal femur with less than a third of the shaft preserved proximally:  
The greater trochanter is also big and medially facing rather than superiorly inclined. There is no obvious dorsal extension between the greater trochanter and head. The superior surface between the neck and the head is more flattened. The lateral surface of the greater trochanter is concave. The lesser trochanter is broken off. The deep proximo-distally elongated groove distal to the coronoid process is present.
- SWP 1699, a left proximal femur:  
Only the head, neck, base of the lesser trochanter and a bit of the shaft are preserved on this specimen. The whole lateral portion of the specimen is missing. The head bears no obvious dorsal extension to the greater trochanter. The lesser trochanter is more medially inclined than dorsal.
- SWP 1706, a left proximal femur:  
All the epiphyses are chipped off. Only the shaft fragment, intertrochanteric fossa and distal portion of the neck are preserved. The intertrochanteric fossa is deeply cavitated and is positioned at the same level as the head. The lesser trochanter base is medio-dorsally facing.
- SWP 4035, a left proximal femur:  
The greater trochanter is broken off and preserves less than a third of the shaft proximally. The lesser trochanter is medially facing. The femoral head articular surface lacks obvious dorsal extension toward the greater tuberosity. The intertrochanteric fossa is broken off proximally but it is small, deeply cavitated, and lies at the same level as the femoral head. The lesser trochanter has a long base with a parabolic profile.
- SWP 742, a right proximal femur:  
The specimen is broken off on the whole proximal aspect. It preserves only the distal portion of the head, the lesser trochanter and less than a third of the shaft proximally. The lesser trochanter is extensive and faces dorso-medially.
- SWP 745, a right proximal femur:



This specimen is a femur head and neck which are broken off medio-laterally and glued together on the neck. The *fovea capitis* is rounded and deep. It preserves a flange on its proximal aspect.

- SWP 754, a right proximal femur:

This specimen preserves only the intertrochanteric fossa and a lesser trochanter. The intertrochanteric groove is deep and lies at the same level as the head.

- SWP 900, a right proximal femur:

This specimen is a femur head with a proximal greater trochanter. The *fovea capitis* is located on the posterior portion of the head. It is deep and oval with a flange on its proximal aspect.

- SWP 905, a right proximal femur:

The lesser trochanter and less than a third of the shaft constitute this specimen. The lesser trochanter tip is chipped off and is medially facing.

- SWP 1514, a right proximal femur:

This specimen is similar to SWP 905. It preserves the lesser trochanter and less than a third of the shaft. The lesser trochanter is dorso-medially facing. The intertrochanteric fossa is deep and elongated proximo-distally.

- SWP 1355, a right proximal femur:

This specimen is weathered and missing the proximal greater trochanter and proximal portion of the head. It preserves the lesser trochanter and less than a third of the shaft. The lesser trochanter base is medially facing.

- SWP 1384, a right proximal femur:

This specimen is a head, intertrochanteric fossa and is missing both the greater and lesser trochantae. The neck is broken off proximally. The *fovea capitis* is rounded and anterior facing.

- SWP 1704, a right proximal femur:

The femoral head articular surface bears obvious dorsal extension towards the greater trochanter. The greater trochanter is blunt and pointed superiorly. The intertrochanteric fossa is covered in breccia. The intertrochanteric groove is small, deeply cavitated and at same level as the femoral head. The lesser trochanter has a long base with a parabolic profile and it faces more dorsally than medially.

- SWP 1534, a left distal femur:

This specimen is missing the lateral anterior condyle. The medial condyle surface area exceeds the lateral condyle. The condyles are splayed. The femur distal shaft morphology is thick and rounded.

- SWP 1532, a right distal femur:

The distal shaft on this specimen is asymmetrically flattened superior to the condyles. The condyles are splayed, and the medial condyle is larger than the lateral condyle.

- SWP 753, a right proximal femur:

The femur head is spherical. The greater trochanter is robust and projects superior to the femur head. The *fovea capitis* is located medial to the head and extends dorsally. It is deep and rounded in shape. The lesser trochanter has a triangular outline. The intertrochanteric fossa is small, rounded, deeply cavitated and lies at the same level as the head.

#### *Locomotor adaptation of specimens identified as Papionini indet*

They are highly fragmented and do not preserve sufficient morphology to assign them to genus level. The general papionin morphology observed includes a hemispherical head shape, an approximately straight humeral shaft which is thick and rounded distally; they also preserve a retroflexed medial epicondyle; and a rounded capitulum. On the ulna, the trochlea notch is crescentic in shape, the olecranon superior aspect morphology is concave with the lateral aspect higher than medial; the olecranon superior projection is less than the trochlea notch length and it is retroflexed. These features are consistent with terrestrial papionin morphology (Rose 1974, 1997; Fleage 1983; Harrison 1989). The femur bears a lesser trochanter which faces medially while the medial condyle surface area exceeds the lateral condyle.



Figure 4.16. SWP 1537, a left Papionini indet proximal femur. Note the greater trochanter which is elevated superior to the head, its medial orientation and a lesser trochanter which is also medially oriented.

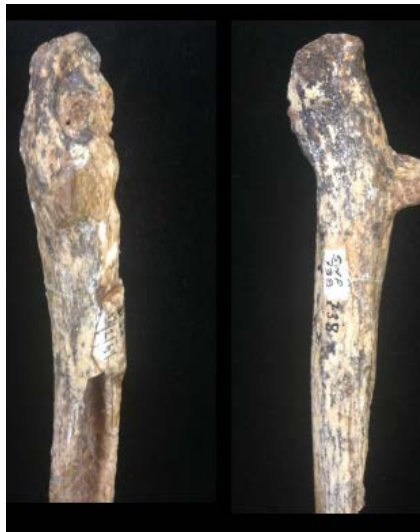


Figure 4.17. SWP 738, a left Papionini indet proximal femur fragment.

Subfamily	Cercopithecinae Gray, 1821
Tribe	Cercopithecini Gray, 1821
Genus	<i>Cercopithecus</i> . Brunnich, 1772

In the assemblage, two specimens that likely represent the same individual, are assigned to *Cercopithecus* sp. The *Cercopithecus* sp. specimens point to gracile individuals.

a) Humerus

BP/3/34170, a left distal humerus fragment:

The olecranon fossa is shallow. The medial epicondyle is retroflexed. The trochlea medial lip distal projection is very short compared to *Papio* sp and projects medially. The shaft distal dorsal pillars are wider and thicker above the lateral epicondyle. This fossil element has a very high and rounded olecranon fossa. The capitulum is relatively flatter than in *Papio*.

b) Radius

SWP 4012, a proximal radius:

The head is ovoid. In superior view, it bears a deep rounded depression. The lateral aspect is lower than the medial aspect. The bicipital tuberosity is half circular with a flange distally. The neck is relatively long. The neck and the shaft are medio-laterally flattened. The shaft has a slight lateral bow.

*Locomotor adaptation of specimens identified as Cercopithecus sp*

The fossil *Cercopithecus* points to a small individual with a combination of terrestrial adaptations with arboreal capabilities. The humerus lacks the proximal aspect therefore assumptions about the shoulder joint cannot be made. The retroflexed medial epicondyle shows similarities to what is seen in terrestrial quadrupeds (Harrison 1989). The reduced distal projection of the trochlea is similar to *Cartelles* which occupy arboreal habitats, which is different from what is observed in papionins (Halenar & Rosenberger 2013). The longer radial neck increases the lever arm for the biceps, which is consistent with semi-terrestrial and arboreal locomotion seen in suspensory *Ateles* (Jones 2008).

Subfamily     Colobinae, Jerdon 1867  
Tribe           Colobini Blyth 1875  
Genus          cf. *Cercopithecoides*. Mollet 1947

One specimen, a femur, compares to *Cercopithecoides* sp.

- SWP 883, a left proximal femur:

The specimen has a very long neck. The posterior aspect of the neck has an oval proximo-laterally angled fossa. Above this fossa is a flange which faces proximo-posterior to the head. The specimen's anterior surface is very flat. The intertrochanteric fossa is small, rounded, deeply cavitated and lies at the same level as the head.

*Locomotor adaptation of specimens identified as Cercopithecoides sp*

The *Cercopithecoides* femur points to a specimen which belonged to a terrestrially adapted fossil monkey. The long femoral neck length relates to increased mechanical advantage of the lesser gluteal muscles by lengthening their lever arm, a feature consistent with terrestrial locomotion seen in terrestrial papionins (Harrison and Harris 1996).

Subfamily	Colobinae Jerdon 1867
Tribe	Colobini Blyth 1875
Subtribe	Colobina indet.

a) Ulna

Four ulnae are assigned to Colobina indet. These specimens are highly fragmented. 1) the olecranon superior aspect is the same length as the trochlea notch; and 2) it is retroflexed. 3) the olecranon process is concave and the lateral aspect is higher than the medial; 4) the trochlea notch is big and crescentic in shape; 5) the coronoid process is in horizontal plane with no significant distal extension; 6) the anconeal process is also in horizontal plane with no significant proximal extension, 7) the anconeal process and the coronoid process are robust and create a deeply crescentic trochlea notch.

- S94-10836, a right proximal ulna:

The olecranon superior aspect is less than the trochlea notch; it is almost non-existent. The trochlea notch has a half circular shape. The coronoid process is in horizontal plane with no significant distal extension. The anconeal process is also reduced in appearance. The olecranon process is flat superiorly; however, the lateral aspect is higher than the medial aspect.

- S94 13505, a left proximal ulna:

The olecranon superior aspect is less than the trochlea notch; it is almost non-existent and it is retroflexed. The olecranon process is flat superiorly but the lateral aspect is slightly higher than the medial. This is different from papionin specimens, which have a superior projection which is highly unequal in height. The trochlea notch is big and crescentic in shape. The coronoid process is in horizontal plane with no significant distal extension. The anconeal process is also in horizontal plane with no significant proximal extension. The anconeal process and the coronoid process are robust and create a deeply crescentic appearance for the trochlea notch interiorly.

- SWP 1258, right proximal ulna fragment:

This specimen only preserves a small distal portion of the coronoid process and less than a third of the proximal shaft. The specimen's shaft is very flat anterior-posteriorly. The coronoid process articular surface is in horizontal plane with no significant distal extension. The radial notch is very deep and has a circular outline.

- SWP 4247

The olecranon process is long. It is not as retroflexed as observed in Cercopithecines. The olecranon bears a superiorly inclined medial flange. On the medial aspect, the olecranon superior portion is deeply with a medial flange posteriorly. The trochlea notch proximo-distal height is almost the same as the proximal extension of the olecranon notch. The radial notch is oval. The shaft is flat medio-laterally.

4



Figure 4.18. On the left, SWP 4247, a proximal ulna Colobinae indet specimen and, on the right, a modern *Colobus guezara* ulna.

---

b) Radius

SF 2567, a left proximal radius with more than a third of the shaft preserved proximally:

This specimen is one of the largest radii in the Sterkfontein cercopithecoid assemblage. The head is ovoid in shape with the lateral aspect higher than the medial aspect. The radius is thin. Colobines have thin radii compared to cercopithecines (Krentz 1993). This indicates a larger range of pronation and supination (*ibid.*). The neck is short relative to the size of the specimen. The shaft is laterally bowed.

---

c) Femur

SWP 1163, a left proximal femur which preserves a lesser trochanter, intertrochanteric fossa and less than a third of the shaft:

The lesser trochanter on this specimen has a relatively short base with a triangular profile. It is medially oriented rather than dorso-medially. The intertrochanteric fossa is deep.

*Locomotor adaptation of specimens identified as Colobina indet*

The upper arm on the identified fossil colobine specimens from Sterkfontein points to arboreal locomotion. The extensive olecranon process seen in SWP 4247 is consistent with arboreally adapted monkeys; this feature is also observed in Miocene *Aegyptopithecus* (Rose 1997). Other specimens have a short olecranon which is not retroflexed. A short olecranon process which is aligned to the long axis of the ulna, which provides for rotational ability in the gleno-humeral joint, is recorded for arboreal adapted colobines (Mcphee & Horovitz 2002). The extent and orientation of the olecranon process, combined with a wide trochlea notch are features also seen in arboreal species such as *Paracolobus* from Lemudong'o in Kenya (Hlusko 2007). Therefore, from the locomotor repertoire a minimum of two different species are likely represented in the indeterminate colobines.



#### 4.1.2. Qualitative morphological comparisons

Taxonomic analyses of primate postcranial remains in the Plio-Pleistocene have relied on association with cranio-dental specimens. To date, within the Stekfontein caves fossil cercopithecoid assemblage, there has been no fossil cercopithecoid postcranial remains directly associated with crania in southern African fossil cave sites. This section provides a morphological comparison of these limb bones.

##### a) *The humerus- projection of the greater tuberosity relative to the head*

Ten specimens are assessed for the level of the greater tuberosity in relation to the humeral head. The first group (*Papio*) consists of six proximal humeri (BP/3/22757, SWP 960, SWP967, SWP 1201, SWP 1276 and SWP 1406). On all these specimens the greater tuberosity projects above the level of the head. The second group of specimens classed as *Parapapio* (SWP 504, SWP 959 and SWP 962) have a greater tuberosity which lies below the level of the head. This implies a flexible scapula-humeral joint associated with arboreal movements (Fleagle and Simons 1982), which is in contrast to the first group. Specimen SWP 2792 is separate from the first two groups and has a greater tuberosity which lies at the same level as the head.

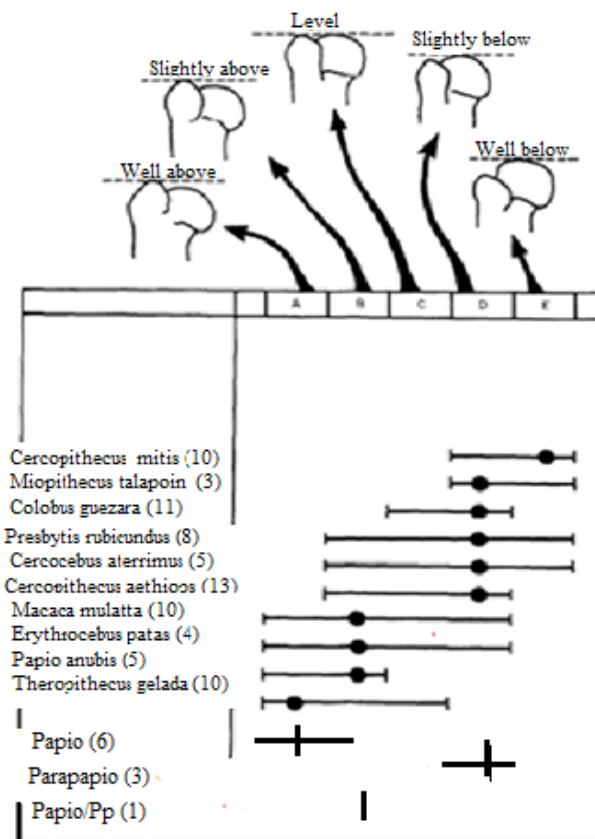


Figure 4.19. Extension of greater tuberosity relative to the humeral head. Data on taxa follows Harrison 1989)

Table 4.1. Qualitative assessment of the humerus based on taxa

<b>Trait</b>	<i>Parapapio</i> sp	<i>Papio</i> sp	<i>Papio/Papio</i> sp	<i>Papionini</i> indet.	<i>Cercopithecus</i> sp.
<b>Head shape</b>	hemi-spherical	hemi-spherical	hemi-spherical	hemi-spherical	
<b>Greater tuberosity relative to lesser</b>	larger	larger	larger	larger	
<b>Projection of greater tuberosity relative to head</b>	below	above	same level		
<b>Shaft shape</b>	nearly straight	nearly straight	nearly straight	nearly straight	
<b>Distal shaft dorsal wall above lateral epicondyle</b>	thick	thick	thick	thick	thick
<b>Medial epicondyle size relative to lateral epicondyle</b>	narrower	narrower	narrower	equal	narrower
<b>Retroflexion of medial epicondyle</b>	retroflexed	retroflexed	retroflexed	retroflexed	retroflexed
<b>Trochlea medial lip distal projection</b>	long	long	long	long	short
<b>Trochlea medial lip alignment</b>	medial	medial	medial	medial	medial
<b>Olecranon fossa shape</b>	triangular	elongated-ellipsoid	rounded		rounded
<b>Capitulum shape</b>	rounded	rounded	rounded		flatter

Table 4.2. Qualitative assessment of the ulna based on taxa

	<i>Parapapio</i> <b>sp</b>	<i>Papio</i> <b>sp</b>	<i>Papio/Papio</i> <b>o sp</b>	<i>Theropithecus</i> <b>s sp</b>	<i>Papionini</i> <b>indet.</b>	<i>Cercopithecoidea</i> <b>s sp.</b>	<i>Colobinae</i> <b>e sp.</b>
<b>Olecranon superior shape</b>	concave	concave	concave	flat	concave	rounded	concave
<b>Olecranon lateral and medial aspect height</b>	unequal	unequal	unequal	equal	unequal	equal	unequal
<b>Olecranon superior projection</b>	retroflexed	retroflexed	retroflexed	retroflexed	retroflexed	straight	straight
<b>Olecranon height vs trochlea notch height</b>	less	less	less	slightly less	less	less	same
<b>Trochlea notch shape</b>	crescentic	crescentic	crescentic	crescentic	crescentic	crescentic	deeply crescentic
<b>Anconeal process on medial view</b>	anconeal is sharp	anconeal is thick		anconeal is thick and flat anteriorly		flat	extensive
<b>Proximal olecranon medial view</b>	flat	flat	flat	concave	flat	rounded	
<b>Coronoid process</b>	flat	flat	flat	flat		flat	extensive

Table 4.3. Qualitative assessment of the radius based on taxa

	<i>Parapapio</i> sp	<i>Papio</i> sp	<i>Papio/Papio</i> sp	<i>Theropithecus</i> sp	Papionini indet.	<i>Cercopithecus</i> sp.
Head shape	ovoid	ovoid	ovoid	Ovoid	Ovoid	ovoid
Head lateral aspect vs medial	lower	lower	lower	lower	lower	lower
Neck height	long	short	short	short		Short
Bicipital tuberosity	central furrow	No furrow		No furrow		Half circular with a nodule

Table 4.4. Qualitative assessment of the femur based on taxa

	<i>Parapapio</i> sp	<i>Papio/Parapio</i> sp	<i>Theropithecus</i> sp	<b>Papionini</b> <b>indet.</b>	<i>Cer</i> <i>opithecoides</i>	<i>Colobini</i>
<b>Greater trochanter superior projection</b>	Above	Above	Above			above
<b>Greater trochanter orientation</b>	Medial	Proximal	Medial			medial
<b>Greater trochanter lateral surface area</b>	Flat	Flat	Concave	Concave		
<b>Lesser trochanter surface area flattened</b>		Medial	Dorsal	Medial and dorsal		Medial
<b>Intertrochanteric fossa</b>		Deep	Deep	Shallow and deep	Deep rounded	Deep
<b>Shaft shape</b>		Approximately straight	bowed	Approximately straight		

Tables 4.5-4.33 provide descriptive statistics of the humerus, ulna, radius and femur in the Sterkfontein fossil cercopithecoid assemblage (in bold font) compared to descriptive statistics of the modern comparative samples in normal font. All measurements are in millimetres

Table 4.5. Descriptive statistics of the humerus proximal medio-lateral breadth (PMLB)

<b>Taxa</b>	<b>N</b>	<b>Minimum</b>	<b>Maximum</b>	<b>Mean</b>	<b>SD</b>	<b>CV</b>
<i>Parapapio</i>	<b>3</b>	<b>27.93</b>	<b>32.92</b>	<b>29.57</b>	<b>2.89552</b>	<b>9.79</b>
<i>Papio</i>	<b>3</b>	<b>21.03</b>	<b>24.06</b>	<b>27.56</b>	<b>2.6865</b>	<b>13.6</b>
<i>Papio sp</i>	10	25	34	39	2.8643	9.87
<i>Papio/Parapapio</i>	<b>1</b>	<b>22.35</b>	<b>22.35</b>	<b>22.35</b>		
<i>Papionin</i>	<b>1</b>	<b>37.54</b>	<b>37.54</b>	<b>37.54</b>		
<i>Cercopithecus aethiops</i>	9	15	18.3	17.14	1.2164	7.9
<i>Colobus guezara</i>	4	20	26	23.675	2.6094	11.02
<i>Mandrillus sphinx</i>	1	26	26	26		

Table 4.6. Descriptive statistics of the humerus head diameter (HHD)

<b>Taxa</b>	<b>N</b>	<b>Minimum</b>	<b>Maximum</b>	<b>Mean</b>	<b>SD</b>	<b>CV</b>
<i>Parapapio</i>	<b>3</b>	<b>15.86</b>	<b>17.35</b>	<b>16.07</b>	<b>1.1845</b>	<b>7.369</b>
<i>Papio</i>	<b>7</b>	<b>24.5</b>	<b>30.64</b>	<b>25.81</b>	<b>3.02579</b>	<b>9.8</b>
<i>Papio sp</i>	10	12.69	26	21.539	3.8419	17.83
<i>Papio/Parapapio</i>	<b>11</b>	<b>17.45</b>	<b>30.26</b>	<b>27.75</b>	<b>4.328</b>	<b>15.5</b>
<i>Cercopithecus aethiops</i>	10	10.91	14.9	13.946	4.4058	31.359
<i>Colobus guezara</i>	4	15.5	19.9	18.3	2.0607	11.2608
<i>Mandrillus sphinx</i>	1	21	21	21		

Table 4.7. Descriptive statistics of the humerus anterior posterior length of humeral head (APLHH)

<i>Taxa</i>	<b>N</b>	<b>Minimum</b>	<b>Maximum</b>	<b>Mean</b>	<b>SD</b>	<b>CV</b>
<i>Parapapio</i>	<b>3</b>	<b>17.69</b>	<b>20.94</b>	<b>19.29</b>	<b>1.62531</b>	<b>8.423</b>
<i>Papio</i>	<b>3</b>	<b>16.4</b>	<b>20.86</b>	<b>21.74</b>	<b>4.1138</b>	<b>19.715</b>
<i>Papio sp</i>	10	23.2	28.31	25.252	2.5001	9.900
<i>Papio/Parapapio</i>	<b>1</b>	<b>14.95</b>	<b>14.95</b>	<b>14.95</b>		
<i>Cercopithecus aethiops</i>	7	13.36	15.5	14.7386	0.67	4.545
<i>Colobus guezara</i>	4	17.21	20.1	19.05	1.8267	9.588
<i>Mandrillus sphinx</i>	1	22.6	22.6			

Table 4.8. Descriptive statistics of the humerus. greater tuberosity diameter (GTD)

<i>Taxa</i>	<b>N</b>	<b>Minimum</b>	<b>Maximum</b>	<b>Mean</b>	<b>SD</b>	<b>CV</b>
<i>Parapapio</i>	<b>3</b>	<b>16.39</b>	<b>20.68</b>	<b>18.06</b>	<b>2.19477</b>	<b>12.015</b>
<i>Papio</i>	<b>7</b>	<b>13</b>	<b>16.32</b>	<b>19.03</b>	<b>2.28179</b>	<b>13.978</b>
<i>Papio sp</i>	10	15	19.8	17.202	2.3422	0.136157
<i>Papio/Parapapio</i>	<b>1</b>	<b>15.57</b>	<b>15.57</b>	<b>15.57</b>		
<i>Cercopithecus aethiops</i>	9	9	12	10.7156	1.268	11.832
<i>Colobus guezara</i>	4	12.9	16.4	14.4	1.6912	11.744
<i>Mandrillus sphinx</i>	1	13	13			

Table 4.9. Descriptive statistics of the humerus bi-epicondylar breadth (BEB)

<i>Taxa</i>	<b>N</b>	<b>Minimum</b>	<b>Maximum</b>	<b>Mean</b>	<b>SD</b>	<b>CV</b>
<i>Parapapio</i>	<b>7</b>	<b>27.09</b>	<b>35.36</b>	<b>30.2</b>	<b>3.06243</b>	<b>10.121</b>
<i>Papio</i>	<b>7</b>	<b>18.4</b>	<b>24.54</b>	<b>31.69</b>	<b>4.87972</b>	<b>19.88</b>
<i>Papio sp</i>	10	31	44	34.659	3.7652	10.837
<i>Papio/Parapapio</i>	<b>1</b>	<b>34.79</b>	<b>34.79</b>	<b>34.79</b>		
<i>Cercopithecus aethiops</i>	9	17	23.1	20.9367	2.1136	10.0954
<i>Colobus guezara</i>	4	26	34.9	30.275	9.9246	12.963
<i>Mandrillus sphinx</i>	1	33	33			



Table 4.10. Descriptive statistics of the humerus medial trochlea flange length (MTFL)

<i>Taxa</i>	<b>N</b>	<b>Minimum</b>	<b>Maximum</b>	<b>Mean</b>	<b>SD</b>	<b>CV</b>
<i>Parapapio</i>	<b>8</b>	<b>10.27</b>	<b>19.34</b>	<b>15.92</b>	<b>3.13503</b>	<b>20.048</b>
<i>Papio</i>	<b>7</b>	<b>15.34</b>	<b>20.23</b>	<b>25.08</b>	<b>3.2149</b>	<b>15.891</b>
<i>Papio sp</i>	10	16.17	18.9	17.786	2.0851	11.723
<i>Papio/Parapapio</i>	<b>11</b>	<b>11.3</b>	<b>18.31</b>	<b>15.23</b>	<b>2.77</b>	<b>18.2</b>
<i>Papionin</i>	<b>2</b>	<b>15.11</b>	<b>16.45</b>	<b>15.78</b>	<b>0.9475</b>	<b>6.133</b>
<i>Cercopithecus aethiops</i>	9	8	12.1	10.45	1.1951	11.428
<i>Colobus guezara</i>	4	9.1	12.3	11.075	1.3913	12.562
<i>Mandrillus sphinx</i>	1	13.2	13.2			

Table 4.11. Descriptive statistics of the humerus lateral epicondyle to medial edge of trochlea (LEMET)

<i>Taxa</i>	<b>N</b>	<b>Minimum</b>	<b>Maximum</b>	<b>Mean</b>	<b>SD</b>	<b>CV</b>
<i>Parapapio</i>	<b>7</b>	<b>25.2</b>	<b>33.24</b>	<b>27.26</b>	<b>2.79231</b>	<b>10.243</b>
<i>Papio</i>	<b>7</b>	<b>20.27</b>	<b>27.1</b>	<b>32.64</b>	<b>4.514</b>	<b>13.82</b>
<i>Papio sp</i>	10	28	34.9	31.31	2.8196	9.0052
<i>Papio/Parapapio</i>	<b>11</b>	<b>21.46</b>	<b>33.64</b>	<b>26.82</b>	<b>3.662</b>	<b>13.653</b>
<i>Papionin</i>	<b>1</b>	<b>32.06</b>	<b>32.06</b>	<b>32.06</b>		
<i>Cercopithecus aethiops</i>	9	14.7	19.4	17.5533	1.5181	8.6448
<i>Colobus guezara</i>	4	21	28	25.025	2.9556	11.8107
<i>Mandrillus sphinx</i>	1	26	26			

Table 4.12. Descriptive statistics of the humerus. distal articular breadth (DAB)

<i>Taxa</i>	<b>N</b>	<b>Minimum</b>	<b>Maximum</b>	<b>Mean</b>	<b>SD</b>	<b>CV</b>
<i>Parapapio</i>	<b>8</b>	<b>18.52</b>	<b>24.55</b>	<b>21.005</b>	<b>2.34561</b>	<b>11.167</b>
<i>Papio</i>	<b>3</b>	<b>8.73</b>	<b>12.19</b>	<b>15.77</b>	<b>3.52137</b>	<b>28.879</b>
<i>Papio sp</i>	10	23.4	30	25.525	2.3284	9.12
<i>Papio/Parapapio</i>	<b>13</b>	<b>15</b>	<b>26.74</b>	<b>19.76</b>	<b>3.103</b>	<b>15.52</b>
<i>Papionin</i>	<b>2</b>	<b>15.68</b>	<b>22.72</b>	<b>19.2</b>	<b>4.978</b>	<b>25.92</b>
<i>Cercopithecus aethiops</i>	9	11	16.2	13.4467	1.6191	12.0411
<i>Colobus guezara</i>	4	17.1	24.9	20.525	3.3521	15.8443
<i>Mandrillus sphinx</i>	1	22.6	22.6			

Table 4.13. Descriptive statistics of the humerus proximo-distal height of capitulum (PDHC)

<i>Taxa</i>	<b>N</b>	<b>Minimum</b>	<b>Maximum</b>	<b>Mean</b>	<b>SD</b>	<b>CV</b>
<i>Parapapio</i>	<b>7</b>	<b>12.38</b>	<b>15.79</b>	<b>13.22</b>	<b>1.27407</b>	<b>9.415</b>
<i>Papio</i>	<b>4</b>	<b>18.7</b>	<b>21.98</b>	<b>25.33</b>	<b>3.03285</b>	<b>13.798</b>
<i>Papio sp</i>	10	13.69	18	14.949	1.3462	9.005
<i>Papio/Parapapio</i>	<b>14</b>	<b>10</b>	<b>15.1</b>	<b>11.22</b>	<b>1.947</b>	<b>17.34</b>
<i>Papionin</i>	<b>5</b>	<b>5.68</b>	<b>15.02</b>	<b>11.612</b>	<b>3.502</b>	<b>30.18</b>
<i>Cercopithecus aethiops</i>	9	7.38	18	9.9289	3.341	0.33364
<i>Colobus guezara</i>	4	8	14.9	10.75	2.9331	0.27285
<i>Mandrillus sphinx</i>	1	11	11			

Table 4.14. Descriptive statistics of the humerus maximum medio-lateral length of olecranon fossa (MMLLO)

<i>Taxa</i>	<b>N</b>	<b>Minimum</b>	<b>Maximum</b>	<b>Mean</b>	<b>SD</b>	<b>CV</b>
<i>Parapapio</i>	<b>7</b>	<b>11.23</b>	<b>15.79</b>	<b>13.06</b>	<b>1.38616</b>	<b>10.609</b>
<i>Papio</i>	<b>9</b>	<b>10.02</b>	<b>13.13</b>	<b>14.5</b>	<b>1.68971</b>	<b>12.865</b>
<i>Papio sp</i>	8	12.1	26.2	15.0589	4.5809	3.04
<i>Papio/Parapapio</i>	<b>11</b>	<b>8.01</b>	<b>14</b>	<b>11.2</b>	<b>1.706</b>	<b>15.22</b>
<i>Papionin</i>	<b>1</b>	<b>14.32</b>	<b>14.32</b>	<b>14.32</b>		
<i>Cercopithecus aethiops</i>	9	9.02	14.2	11.35	1.9182	16.900
<i>Colobus guezara</i>	4	11	14.2	13.325	1.5521	11.648
<i>Mandrillus sphinx</i>	1	12.3	12.3			

Table 4.15. Descriptive statistics of the humerus maximum proximo-distal length of olecranon fossa (MPDLO)

<i>Taxa</i>	<b>N</b>	<b>Minimum</b>	<b>Maximum</b>	<b>Mean</b>	<b>SD</b>	<b>CV</b>
<i>Parapapio</i>	<b>7</b>	<b>7.02</b>	<b>14.64</b>	<b>10.07</b>	<b>2.41498</b>	<b>22.719</b>
<i>Papio</i>	<b>10</b>	<b>4.41</b>	<b>8.8</b>	<b>11.9</b>	<b>1.91651</b>	<b>21.779</b>
<i>Papio sp</i>	9	9.8	19	11.9956	3.1772	26.48
<i>Papio/Parapapio</i>	<b>10</b>	<b>4.41</b>	<b>13.36</b>	<b>10.06</b>	<b>2.564</b>	<b>25.4</b>
<i>Papionin</i>	<b>1</b>	<b>10.44</b>	<b>10.44</b>	<b>10.44</b>		
<i>Cercopithecus aethiops</i>	8	4.9	9.62	6.8	1.5097	22.201
<i>Colobus guezara</i>	4	8	11	9.2	1.4697	15.974
<i>Mandrillus sphinx</i>	1	11				

Table 4.16. Descriptive statistics of the humerus axis of medial epicondyle (AME)

<i>Taxa</i>	<b>N</b>	<b>Minimum</b>	<b>Maximum</b>	<b>Mean</b>	<b>SD</b>	<b>CV</b>
<i>Parapapio</i>	<b>7</b>	<b>25</b>	<b>46</b>	<b>35.57</b>	<b>7.11471</b>	<b>20.001</b>
<i>Papio</i>	<b>8</b>	<b>31</b>	<b>41</b>	<b>36.371</b>	<b>3.7773</b>	<b>10.38</b>
<i>Papio sp</i>	10	30	40	38	3.496	9.200
<i>Papio/Parapapio</i>	<b>11</b>	<b>18</b>	<b>40</b>	<b>30.54</b>	<b>8.248</b>	<b>27.9</b>
<i>Papionin</i>	<b>2</b>	<b>21</b>	<b>43</b>	<b>32</b>	<b>15.556</b>	<b>48.61</b>
<i>Cercopithecus aethiops</i>	9	34	44	38.555	2.9202	7.574
<i>Colobus guezara</i>	4	23	30	27	3.559	13.181
<i>Mandrillus sphinx</i>	40	40	40			

Table 4.17. Descriptive statistics of the ulna anterior-posterior length of olecranon process (APLOP)

	<b>N</b>	<b>Minimum</b>	<b>Maximum</b>	<b>Mean</b>	<b>SD</b>	<b>CV</b>
<i>Parapapio</i>	<b>2</b>	<b>26.5</b>	<b>19.96</b>	<b>23.23</b>	<b>4.62448</b>	<b>19.907</b>
<i>Papio</i>	<b>5</b>	<b>17.01</b>	<b>26.50</b>	<b>21.81</b>	<b>3.78145</b>	<b>17.34</b>
<i>Papio sp</i>	8	22	34	25.7013	3.5746	13.908
<i>Papio/Parapapio</i>	<b>5</b>	<b>18.34</b>	<b>24.51</b>	<b>22.07</b>	<b>7.9295</b>	<b>13.27</b>
<i>Theropithecus</i>	<b>10</b>	<b>15.91</b>	<b>28.03</b>	<b>23.088</b>	<b>4.2517</b>	<b>18.41</b>
<i>Papionin</i>	<b>4</b>	<b>19.24</b>	<b>25.31</b>	<b>22.042</b>	<b>3.1061</b>	<b>14.0</b>
<i>Cercopithecus aethiops</i>	7	7.9	16.9	12.5829	3.2918	26.160
<i>Colobus guezara</i>	4	7.4	16.1	12.7	3.8549	30.353
<i>Mandrillus sphinx</i>	2	6	10.3	8.15	3.0406	37.307

Table 4.18. Descriptive statistics of the ulna proximo-distal height of olecranon process (PDHOP)

	<b>N</b>	<b>Minimum</b>	<b>Maximum</b>	<b>Mean</b>	<b>SD</b>	<b>CV</b>
<i>Parapapio</i>	<b>2</b>	<b>12.8</b>	<b>9.89</b>	<b>11.345</b>	<b>2.05768</b>	<b>18.137</b>
<i>Papio</i>	<b>5</b>	<b>6.81</b>	<b>12.8</b>	<b>9.09</b>	<b>2.45103</b>	<b>26.97</b>
<i>Papio sp</i>	8	10	16.15	3.1255	3.1255	25.996
<i>Papio/Parapapio</i>	<b>7</b>	<b>3.98</b>	<b>10.17</b>	<b>7.8</b>	<b>2.156</b>	<b>27.62</b>
<i>Theropithecus</i>	<b>10</b>	<b>8.3</b>	<b>14.34</b>	<b>10.028</b>	<b>2.948</b>	<b>29.39</b>
<i>Papionin</i>	<b>4</b>	<b>6.03</b>	<b>10.38</b>	<b>8.15</b>	<b>2.1771</b>	<b>26.7</b>
<i>Cercopithecus aethiops</i>	7	6	10.82	8.5514	2.606	30.474
<i>Colobus guezara</i>	4	7.4	16.1	12.7	3.8549	30.353
<i>Mandrillus sphinx</i>	2	6	10.3	8.15	3.0406	37.3071

Table 4.19. Descriptive statistics of the ulna medio-lateral breadth of olecranon process (MLBOP)

	N	Minimum	Maximum	Mean	SD	CV
<i>Parapapio</i>	2	10.5	8.99	9.745	1.06773	10.957
<i>Papio</i>	5	9.11	11.71	10.32	0.97549	9.449
<i>Papio sp</i>	8	11	15	12.8588	1.3093	10.182
<i>Papio/Parapapio</i>	12	7.16	11.94	10.14	1.332	13.12
<i>Theropithecus</i>	10	6.23	14.41	11.025	2.1172	19.14
<i>Papionin</i>	7	9.72	11.94	10.92	0.7156	6.55
<i>Cercopithecus aethiops</i>	7	7.24	9.48	7.95	0.7302	9.183
<i>Colobus guezara</i>	4	9.5	11.8	10.75	0.9469	8.808
<i>Mandrillus sphinx</i>	2	10.2	11	10.6	0.5657	5.336

Table 4.20. Descriptive statistics of the ulna proximo-distal length of trochlea notch (PDLTN)

	N	Minimum	Maximum	Mean	SD	CV
<i>Parapapio</i>	2	17.2	10.96	14.08	4.41235	31.33
<i>Papio</i>	5	13.66	17.2	15.05	1.48361	9.85
<i>Papio sp</i>	7	14.2	18.9	17.0262	1.9085	11.209
<i>Papio/Parapapio</i>	10	11.37	20.36	14.71	2.5533	16.84
<i>Theropithecus</i>	10	8.07	20.36	14.577	3.5109	24.08
<i>Papionin</i>	8	10.15	16.93	13.79	2.5537	85.1
<i>Cercopithecus aethiops</i>	6	7.6	11.8	9.765	1.407	14.4680
<i>Colobus guezara</i>	4	11.2	14.1	12.325	1.242	10.0768
<i>Mandrillus sphinx</i>	2	13	13	13		

The radius

Table 4.21. Descriptive statistics of the radius maximum dimension of radial head (MDRH)

	N	Minimum	Maximum	Mean	SD	CV
<b><i>Parapapio</i></b>	<b>5</b>	<b>14.26</b>	<b>17.73</b>	<b>15.198</b>	<b>1.61077</b>	<b>10.119</b>
<b><i>Papio</i></b>	<b>10</b>	<b>13.3</b>	<b>18.06</b>	<b>15.346</b>	<b>1.59561</b>	<b>10.398</b>
<i>Papio sp</i>	9	14.2	18	16.437	1.2932	7.86
<b><i>Papio/Parapapio</i></b>	<b>3</b>	<b>14.74</b>	<b>17.08</b>	<b>15.81</b>	<b>1.182</b>	<b>7.48</b>
<b><i>Papionin</i></b>	<b>19</b>	<b>13.25</b>	<b>19.52</b>	<b>16.144</b>	<b>1.3449</b>	<b>0.08.51</b>
<i>Cercopithecus aethiops</i>	8	8.5	9.1	9.4387	0.6062	6.4226
<i>Colobus guezara</i>	8	7.9	16	13.3	3.6615	27.5301
<i>Mandrillus sphinx</i>	2	15	15.2	15.1	0.1414	0.936

Table 4.22. Descriptive statistics of the radius perpendicular breadth of radial head (PBRH)

	N	Minimum	Maximum	Mean	SD	CV
<b><i>Parapapio</i></b>	<b>3</b>	<b>12.74</b>	<b>15.4</b>	<b>14.46</b>	<b>1.49171</b>	<b>10.316</b>
<b><i>Papio</i></b>	<b>8</b>	<b>12.82</b>	<b>15.87</b>	<b>14.062</b>	<b>1.0525</b>	<b>07.484</b>
<i>Papio sp</i>	9	9.5	16.8	15.0544	2.1927	14.564
<b><i>Papio/Parapapio</i></b>	<b>3</b>	<b>13.15</b>	<b>15.31</b>	<b>14.353</b>	<b>1.1</b>	<b>7.67</b>
<b><i>Papionin</i></b>	<b>9</b>	<b>12.28</b>	<b>16.16</b>	<b>14.12</b>	<b>1.3921</b>	<b>9.85</b>
<i>Cercopithecus aethiops</i>	8	7.8	9.37	8.6563	0.571	6.595
<i>Colobus guezara</i>	4	11	13.4	11.975	1.034	8.6346
<i>Mandrillus sphinx</i>	2	13.1	14	13.55	0.6364	4.6966

Table 4.23. Descriptive statistics of the ulna proximo distal height of radial neck (PDHRN)

	N	Minimum	Maximum	Mean	SD	CV
<b><i>Parapapio</i></b>	<b>6</b>	<b>4.72</b>	<b>11.14</b>	<b>7.75</b>	<b>2.40687</b>	<b>30.957</b>
<b><i>Papio</i></b>	<b>10</b>	<b>5.4</b>	<b>9.74</b>	<b>6.99</b>	<b>1.29586</b>	<b>18.539</b>
<i>Papio sp</i>	8	4.9	8	6.57	0.9121	13.882
<b><i>Papio/Parapapio</i></b>	<b>1</b>	<b>8.16</b>	<b>8.16</b>	<b>8.16</b>		
<b><i>Theropithecus</i></b>						
<b><i>Papionin</i></b>	<b>18</b>	<b>4.72</b>	<b>10.41</b>	<b>7.433</b>	<b>1.8466</b>	<b>24.64</b>
<i>Cercopithecus aethiops</i>	8	4	8.5	5.7525	1.4849	25.813
<i>Colobus guezara</i>	4	6	13.3	7.875	3.617	45.929
<i>Mandrillus sphinx</i>	2	5.9	7	6.45	0.7778	12.059

Table 4.24. Descriptive statistics of the radius proximo distal height of radial neck and head (PDHRNH)

	N	Minimum	Maximum	Mean	SD	CV
<i>Parapapio</i>	<b>5</b>	<b>11.75</b>	<b>17.65</b>	<b>14.598</b>	<b>2.67943</b>	<b>18.355</b>
<i>Papio</i>	<b>10</b>	<b>10.31</b>	<b>16.15</b>	<b>12.76</b>	<b>1.83301</b>	<b>14.36</b>
<i>Papio sp</i>	8	12	15.41	12.8889	1.1756	9.1213
<i>Papio/Parapapio</i>	<b>1</b>	<b>10.22</b>	<b>10.22</b>	<b>10.22</b>		
<i>Papionin</i>	<b>14</b>	<b>10.69</b>	<b>17.28</b>	<b>13.759</b>	<b>1.8534</b>	<b>13.46</b>
<i>Cercopithecus aethiops</i>	8	7.1	13	9.4112	1.7394	18.482
<i>Colobus guezara</i>	4	7.2	15	10.65	3.2919	30.909
<i>Mandrillus sphinx</i>	2	12	12			

---

## Femur

Table 4.25. Descriptive statistics of the femur anterior posterior head dimension (APHD)

	N	Minimum	Maximum	Mean	SD	CV
<i>Papio/Parapapio</i>	<b>10</b>	<b>16.1</b>	<b>19</b>	<b>18.168</b>	<b>0.8617</b>	<b>4.7</b>
<i>Theropithecus</i>						
<i>Papionin</i>						
<i>Papio sp</i>	10	20.9	25	22.222	1.7871	8.0421
<i>Cercopithecus aethiops</i>	7	10.9	13.23	12.134	0.9391	7.7390
<i>Colobus guezara</i>	4	16	17.8	17.05	0.7937	4.6552
<i>Mandrillus sphinx</i>	2	17.5	17.9	17.7	0.2828	15.9798

Table 4.26. Descriptive statistics of the femur medio-lateral breadth of femur head (MLBFH)

	N	Minimum	Maximum	Mean	SD	CV
<i>Papio/Parapapio</i>	<b>10</b>	<b>13.82</b>	<b>17.18</b>	<b>15.96</b>	<b>1.2041</b>	<b>7.5</b>
<i>Papio sp</i>	10	17.5	22	18.739	1.324	7.0655
<i>Theropithecus</i>	<b>2</b>	<b>17.43</b>	<b>18.8</b>	<b>18.115</b>	<b>0.9687</b>	<b>5.34</b>
<i>Papionin</i>	<b>7</b>	<b>12.22</b>	<b>17.93</b>	<b>15.11</b>	<b>2.2153</b>	<b>14.66</b>
<i>Cercopithecus aethiops</i>	7	8.2	10.98	10.2286	0.9629	9.4138
<i>Colobus guezara</i>	4	12.8	15.7	14.025	1.2121	8.642
<i>Mandrillus sphinx</i>	2	14.9	19.9	17.4	3.5355	20.3191

Table 4.27. Descriptive statistics of the femur greater trochanter projection (GTP)

	N	Minimum	Maximum	Mean	SD	CV
<b><i>Papio/Parapapio</i></b>	<b>4</b>	<b>8.35</b>	<b>9</b>	<b>8.66</b>	<b>0.2891</b>	<b>3.3</b>
<i>Papio sp</i>	9	9.5	14	11.5433	1.408	12.1973
<b><i>Theropithecus</i></b>	<b>2</b>	<b>12.14</b>	<b>13.06</b>	<b>12.6</b>	<b>0.6505</b>	<b>5.16</b>
<b><i>Papionin</i></b>	<b>1</b>	<b>7.72</b>	<b>7.72</b>	<b>7.72</b>		
<i>Cercopithecus aethiops</i>	8	4.6	7.97	5.795	1.225	21.1397
<i>Colobus guezara</i>	4	6	9.1	7.1	1.3736	19.345
<i>Mandrillus sphinx</i>	2	6.6	7.4	7	0.5657	8.081

Table 4.28. Descriptive statistics of the femur neck diameter (ND)

	N	Minimum	Maximum	Mean	SD	CV
<b><i>Papio/Parapapio</i></b>	<b>11</b>	<b>7.07</b>	<b>17.53</b>	<b>13.6</b>	<b>3.8742</b>	<b>28.4</b>
<i>Papio sp</i>	10	9.11	21	15.867	3.1955	20.141
<b><i>Theropithecus</i></b>	<b>2</b>	<b>16.8</b>	<b>16.93</b>	<b>16.865</b>	<b>0.0919</b>	<b>0.5</b>
<b><i>Papionin</i></b>	<b>6</b>	<b>13.33</b>	<b>17.21</b>	<b>15.23</b>	<b>1.6595</b>	<b>10.89</b>
<i>Cercopithecus aethiops</i>	8	3.8	12.6	8.3288	2.4907	29.904
<i>Colobus guezara</i>	4	9	16	13.5	3.1091	23.030
<i>Mandrillus sphinx</i>	2	8.7	9	8.85	0.2121	2.396

Table 4.29. Descriptive statistics of the femur medio-lateral neck diameter (MLND)

	N	Minimum	Maximum	Mean	SD	CV
<i>Papio sp</i>	10	4	12.1	8.444	2.3671	28.0334
<b><i>Papio/Parapapio</i></b>						
<b><i>Theropithecus</i></b>						
<b><i>Papionin</i></b>						
<i>Cercopithecus aethiops</i>	8	4	12.6	5.9463	2.915	49.0221
<i>Colobus guezara</i>	5	6.5	13.2	7.92	3.2813	41.430
<i>Mandrillus sphinx</i>	2	6	7	6.5	0.7071	10.878

Table 4.30. Descriptive statistics of the femur bi-epicondylar breadth (BEB)

	N	Minimum	Maximum	Mean	SD	CV
<b><i>Papio/Parapapio</i></b>	<b>1</b>	<b>34.83</b>	<b>34.83</b>	<b>34.83</b>		
<i>Papio sp</i>	10	28.5	42	35.477	3.6518	0.102933
<i>Cercopithecus aethiops</i>	7	18	22.38	20.72	1.5918	0.076822
<i>Colobus guezara</i>	4	28	32.5	30.6	1.8815	0.06148
<i>Mandrillus sphinx</i>	2	29	31.3	30.15	1.6262	0.05394

Table 4.31. Descriptive statistics of the femur neck shaft angle (NSA)

	N	Minimum	Maximum	Mean	SD	CV
<b><i>Papio/Parapapio</i></b>	<b>8</b>	<b>104</b>	<b>125</b>	<b>114.25</b>	<b>6.8191</b>	<b>5.96</b>
<i>Papio sp</i>	10	120	145	128.7	8.4202	6.542
<b><i>Theropithecus</i></b>	<b>2</b>	<b>100</b>	<b>100</b>	<b>100</b>	<b>0</b>	<b>0</b>
<b><i>Papionin</i></b>	<b>2</b>	<b>112</b>	<b>120</b>	<b>116</b>	<b>5.6569</b>	<b>4.87</b>
<i>Cercopithecus aethiops</i>	8	100	145	117.625	15.9458	13.5564
<i>Colobus guezara</i>	4	127	140	133	5.7155	4.2973
<i>Mandrillus sphinx</i>	2	125	135	133	5.7155	4.2973

Table 4.32. Descriptive statistics of the femur medial condyle width (MCW)

	N	Minimum	Maximum	Mean	SD	CV
<b><i>Papio/Parapapio</i></b>	<b>1</b>	<b>11.65</b>	<b>11.65</b>	<b>11.65</b>		
<i>Papio sp</i>	10	11	18	12.244	2.9415	24.024
<b><i>Papionin</i></b>	<b>1</b>	<b>11.65</b>	<b>11.65</b>	<b>11.65</b>		
<i>Cercopithecus aethiops</i>	8	5.5	8.54	7.2275	0.8526	11.7966
<i>Colobus guezara</i>	4	8.1	11.6	10.375	1.5543	14.9811
<i>Mandrillus sphinx</i>	2	13	17.5	15.25	3.182	20.8654

Table 4.33. Descriptive statistics of the femur lateral condyle width (LCW)

	N	Minimum	Maximum	Mean	SD	CV
<b><i>Papio/Parapapio</i></b>	<b>2</b>	<b>11</b>	<b>14.23</b>	<b>12.61</b>	<b>2.284</b>	<b>18.1</b>
<i>Papio sp</i>	10	8	12	10.22	1.263	12.357
<b><i>Papionin</i></b>	<b>2</b>	<b>13</b>	<b>14.23</b>	<b>13.615</b>	<b>0.8697</b>	<b>6.38</b>
<i>Cercopithecus aethiops</i>	8	5	7.9	6.5363	0.8658	1.2245
<i>Colobus guezara</i>	4	8.1	11	10.175	1.3961	13.7211
<i>Mandrillus sphinx</i>	2	8.2	9.7	8.95	1.0607	11.8509



## Morphological comparisons, quantitative analysis

### a) *The humerus- long axis of the medial epicondyle*

The long axis of the medial epicondyle observed in the Sterkfontein cercopithecoid assemblage suggests the presence of terrestrial to semi-terrestrial locomotor preference. The first group of specimens labelled as *Parapapio* sp (BP/3/23389, BP/3/24000, BP/3/3169, SWP 511, SWP 1176, SWP 1584, and SWP 4246) have a medial epicondyle axis which lies within the range of terrestrial and semi-terrestrial cercopithecoids, however, at a lower range than modern *Papio anubis* recorded in Harrison's (1989) study. All seven specimens have a medial epicondyle angle above 31°. The mean value for the epicondyle angle is 35°. The second group of specimens labelled as *Papio* sp (SWP 1165, SWP 1211, SWP 1262, SWP 1287, SWP 1540, SWP 4006 and SWP 4047) have a medial epicondyle with similar ranges. The third group, *Papio/Parapapio* sp (BP/3/23016, SWP 4041, SWP 1410, SWP 562, STS 377C, SWP 507, SWP 1140, SWP 995, SWP 995, SWP 912 and SWP 1016) have a mean angle of 30°. The fourth group consists of specimens classified as *Papionin* indet, (SWP 1543 and SWP 1583) which, morphologically could not be grouped with the other specimens. These two specimens have a medial epicondyle axis between 41° and 43°.

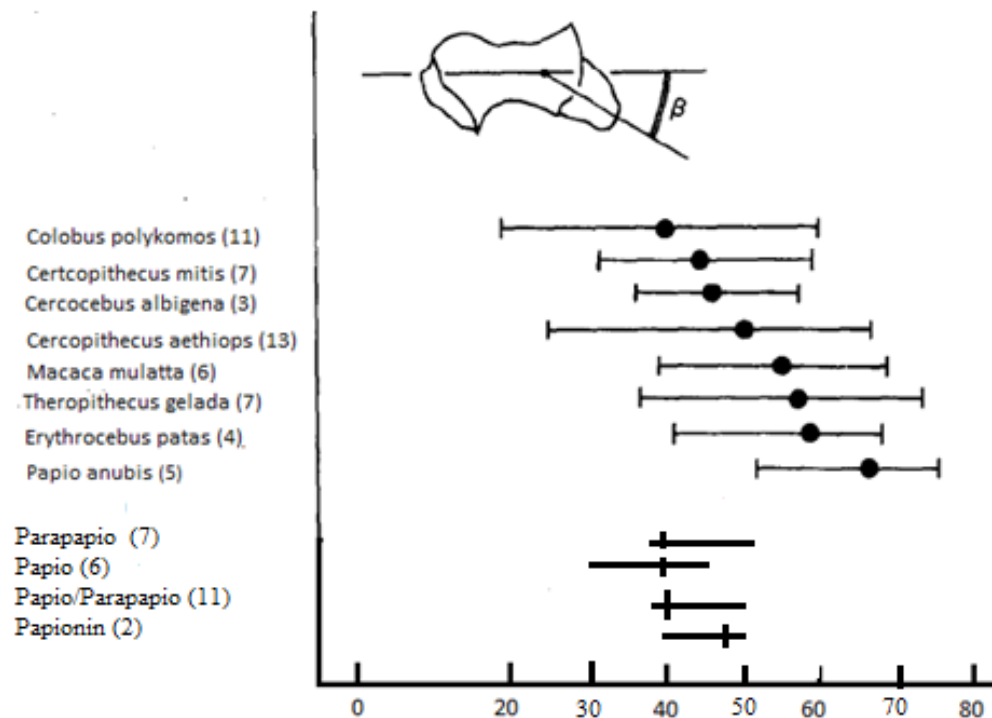


Figure 4.20. Angle of the medial epicondyle. Data on taxa follows Harrison, 1989.

b) *The humerus-relative breadth of the medial epicondyle*

The breadth of the medial epicondyle is demonstrated in Figure 4.20. Twenty three specimens are analysed. They are comparable to terrestrial locomotion observed in papionins. *Parapapio* specimens, (SWP 511, SWP 1137, SWP 1176, SWP 1584, SWP 2810 and SWP 4246) have a medial epicondyle breadth with a mean of 9.2mm. The seven *Papio* specimens (SWP 1165, SWP 1211, SWP 1262, SWP 1287, SWP 1540, SWP 4006 and SWP 4047) have a mean breadth of 9.6. *Papio/Parapapio*'s mean is 7.5. The group consists of SWP 4041, SWP 1410, SWP 562, STS 377C, SWP 507, SWP 1140, SWP 912, SWP 1016 and SWP 4038. SWP 1583, which is the only specimen identified as Papionin indet., has a medial epicondyle breadth of 7.8. This index is aligned to the ranges observed in *Papio*.

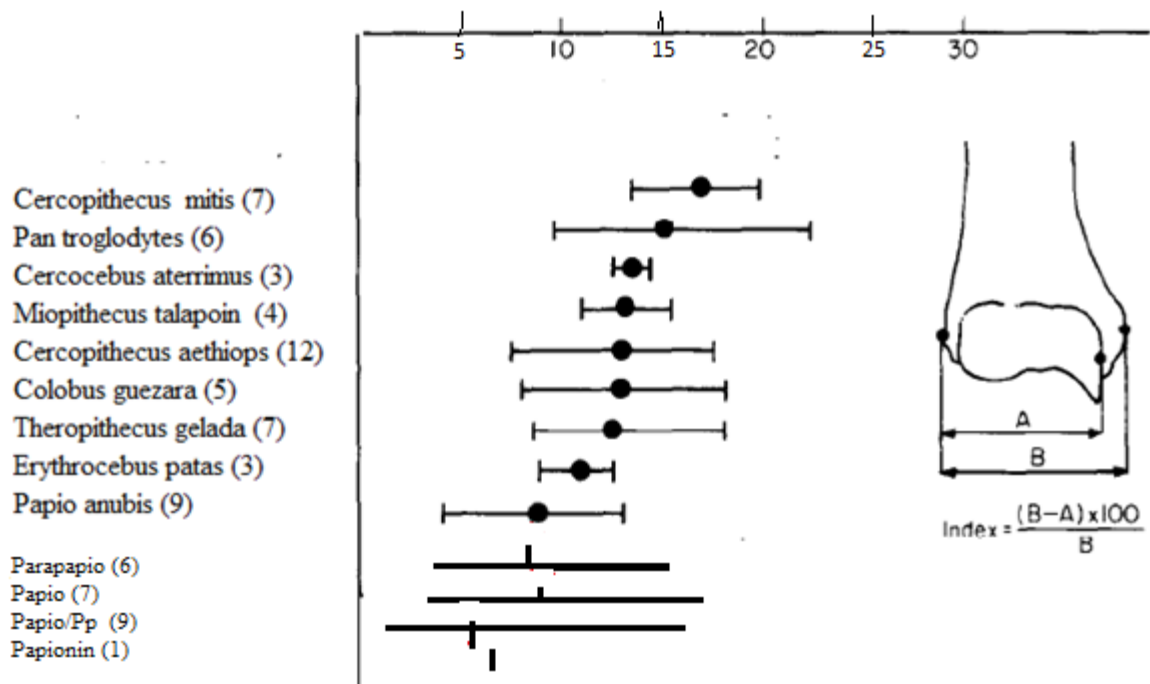


Figure 4.21. Relative breadth of the medial epicondyle. Data on taxa follows Harrison 1989.

c) *The radius- relative length of radial neck*

The specimens analysed for the relative length of radial neck index suggests proclivity to terrestrial to semi-terrestrially adapted locomotion. The *Papio* group consists of 10 specimens; BP/3/23453, SWP 1552, SWP 514, SWP 517, SWP 791, SWP 798, SWP 793, SWP 803, SWP 1418 and SWP 4042. The relative length of radial neck is consistent with cercopithecine radii index. Their mean ratio is very similar to Harrison's (1989) *Papio*, suggesting that they are within the range of terrestrial monkeys. *Parapapio* specimens (SWP 515, SWP 784, SWP 802, SWP 1204 and SWP 1219) which preserve a relatively longer neck, have a higher neck index of 51. They, however, do not fall directly within the range of colobines but display the same range as *Macaca*. The *Papio/Parapapio* class (STS unnumbered, SWP 516, SWP 519, SWP 520, SWP 792, SWP 799, SWP 808, SWP 972, SWP 979, SWP 1125, SWP 1306 and SWP 1416) has a similar head neck ratio as the first group of specimens. They have a mean ratio of 48.9 which is closer to *Papio* than to the colobines.

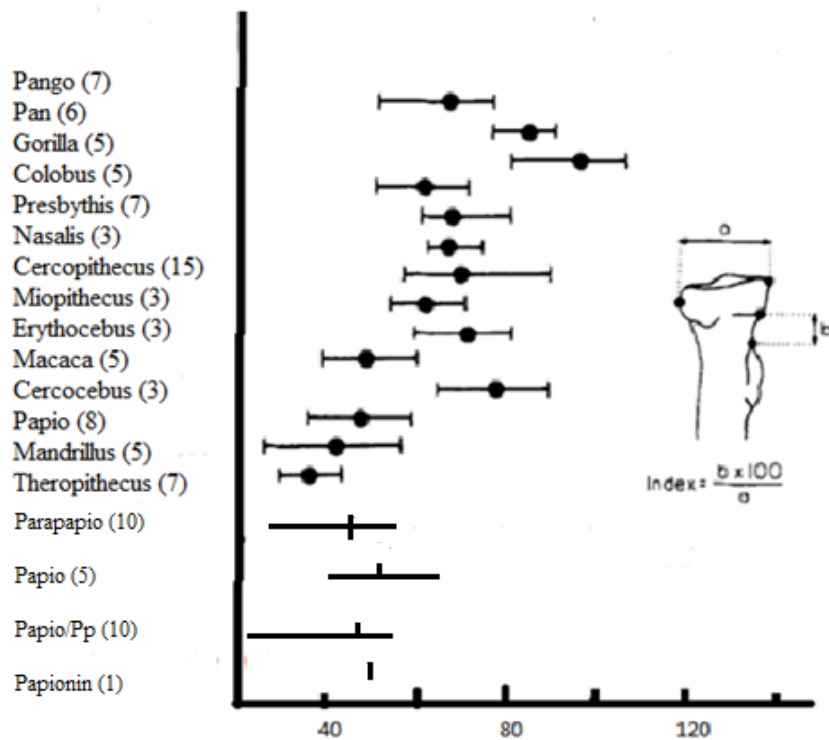


Figure 4.22. Relative length of radial neck index. Data on taxa follows Harrison 1989

#### 4.1.3. Quantitative analysis

Qualitative observations are used as the basis for the statistical examinations. The results of the quantitative analysis are outlined through three analyses: a). Descriptive statistics are provided to illustrate variation present in the sample; b). The bivariate linear regression analysis points to correlation between morphological traits; and the Univariate Analysis of Variance (ANOVA) points to statistically significant differences among taxa.

#### 4.1.4. Bivariate regression analysis

To assess the significance of the relationships between traits, bivariate linear regression analysis is applied to, five indices on the humerus and a couple of traits on ulna, the radius and the femur each.

a) Humerus

Six indices on the humerus were run through the bivariate regression analysis. Bivariate analysis for humeral distal articulation and maximum medio-lateral breadth of olecranon fossa (Fig 4.23) shows a strong positive relationship;  $r = 0.87$ . The anterior posterior length of humeral head and medio-lateral width of humeral head (Fig 4.24) suggests a strong positive correlation ( $r = 0.9$ ) between the two traits. Data for the maximum proximo-distal length of olecranon and maximum medio-lateral breadth of olecranon (Fig 4.25) indicates a correlation ( $r$ ) of 0.4 which suggests a weak positive statistical correlation. Bivariate analysis of the width of distal humeral articulation and bi-epicondylar width shows a strong positive correlation ( $r = 0.9$ ) between the two traits. The fifth index, bivariate analysis of the fifth index, width of distal humeral articulation and width of distal trochlea (Fig 4.26) shows a strong positive relationship  $r = 0.9$ . Width distal humeral articulation and anterior posterior distal humerus (Fig 4.28) also have a positive correlation  $r=0.9$ .

Table 4.34. Legend for the bivariate regression linear plots.

Tribe	Colour	Symbol	Genus
Colobines	red	dot	<i>Colobus</i>
	red	square	<i>Procolobus</i>
	red	open square	<i>Rhinocolobus</i>
	red	x (letter)	<i>Cearcopithecoides</i>
Cercopithecini	black	diamond	<i>Cercopithecus</i>
	black	star	<i>Chlorocebus</i>
Papionins	black	triangle	<i>Papio</i>
	black	inverted triangle	<i>Parapapio</i>
	black	Fill triangle	<i>Theropithecus</i>
	black	dash	<i>Mandrillus</i>
Papionins (Sterkfontein Fossils)	aqua	bar	<i>Papionin</i>
	aqua	triangle	<i>Papio</i>
	aqua	inverted triangle	<i>Parapapio</i>
	aqua	Fill inverted triangle	<i>Papio/parapapio</i>
	aqua	Fill triangle	<i>Theropithecus</i>

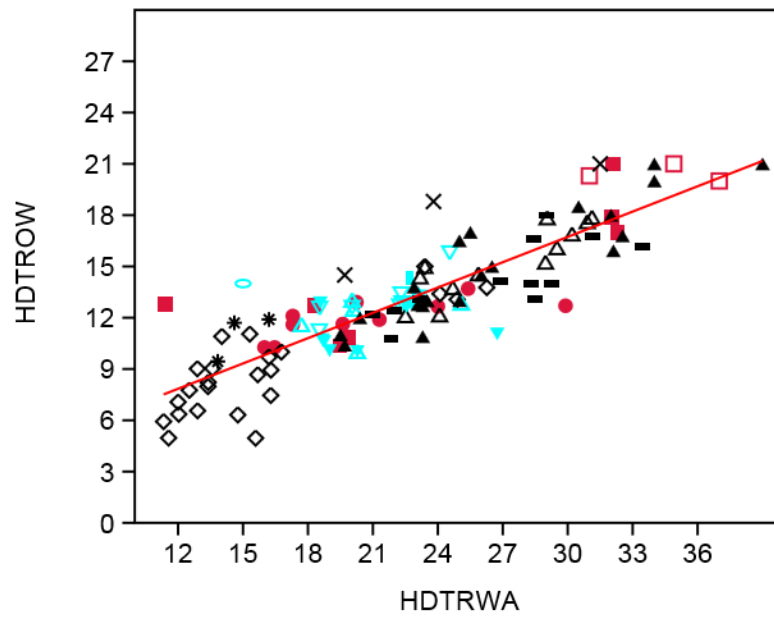


Figure 4.23. Linear plot for maximum medio-lateral width of olecranon fossa (HDTROW) and width distal humeral articulation (HDTRWA).

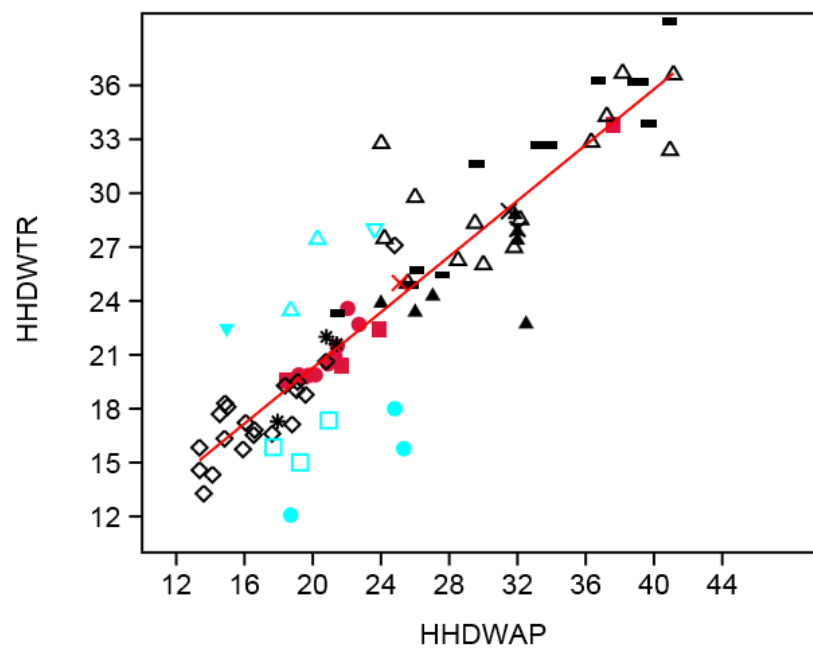


Figure 4.24. Linear plot for humeral head diameter/mediolateral width (HHDWTR) and humeral head anterior-posterior length (HHDWAP).

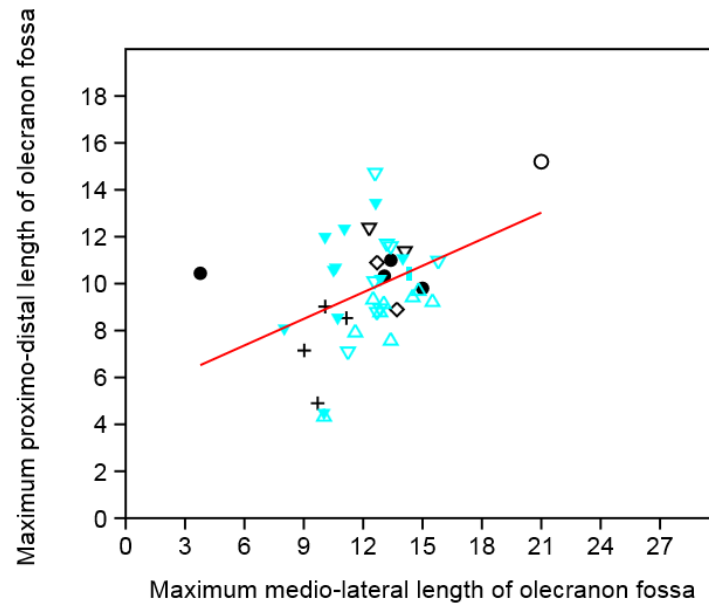


Figure 4.25. Linear plot for ‘maximum proximo-distal length of olecranon fossa and maximum medio-lateral length of olecranon fossa’.

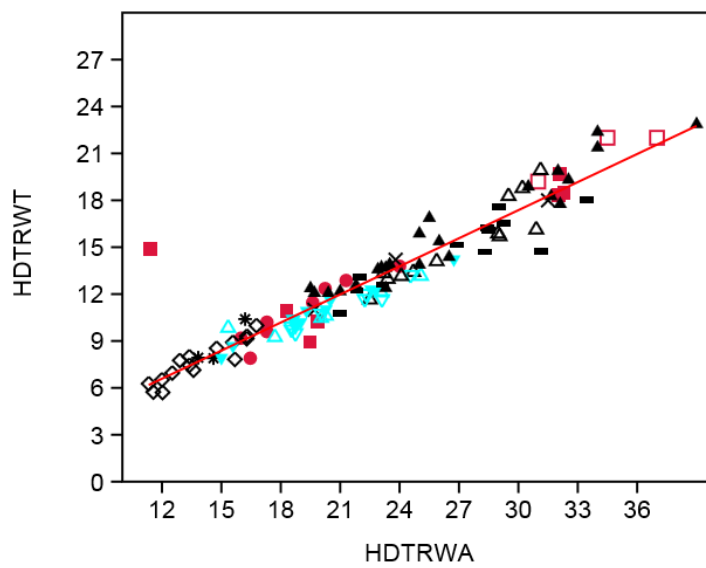


Figure 4.26. Linear plot for ‘width distal humeral articulation (HDTRWA) and width humeral trochlea (HDTRWT)’.

\

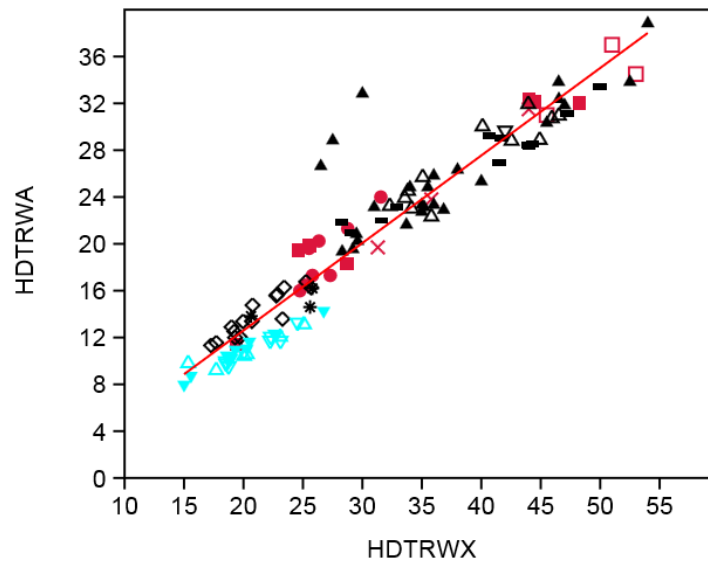


Figure 4.27. Linear plot for 'width distal humeral articulation (HDTRWA) and anterior posterior distal humerus (HDTRWX)'.

b)

c) Ulna

Bivariate regression analysis of the ulna proximo-distal height of olecranon process and antero-posterior length of olecranon process (Fig 4.28) shows a negative correlation ( $r = -0.3$ ). Examination of the ulna proximo-distal height of olecranon process and trochlea notch height (Fig. 4.29) proved to have a negative correlation ( $r = -0.003$ )

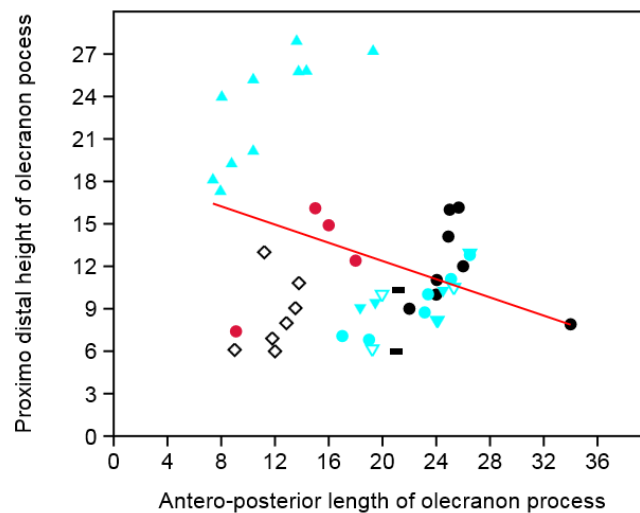


Figure 4.28. Linear plot for 'ulna proximo-distal height of olecranon process and antero-posterior length of olecranon process'.



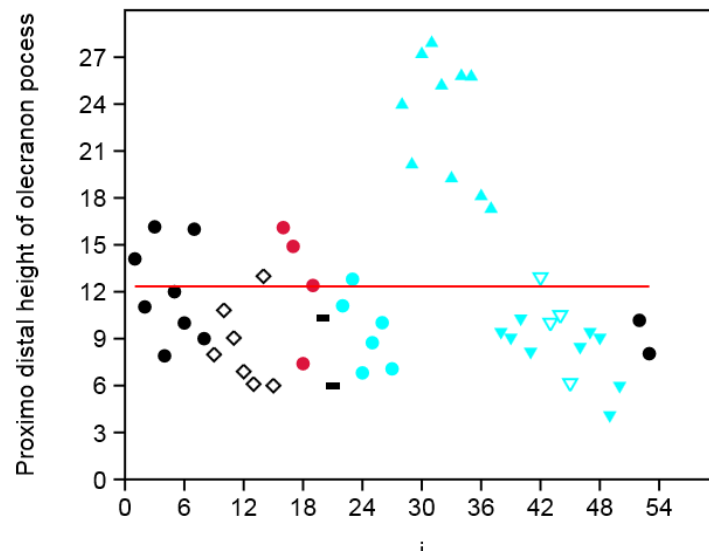


Figure 4.29. Linear plot for 'proximo-distal height of olecranon process and proximo-distal height of trochlea notch'.

#### d) Radius

Regression analysis for maximum diameter of radial head and proximo-distal height of radial neck points to a modest positive relationship between the two variables. The maximum medio-lateral diameter of radial neck and antero-posterior radius neck shows a positive correlation (Fig. 4.30).

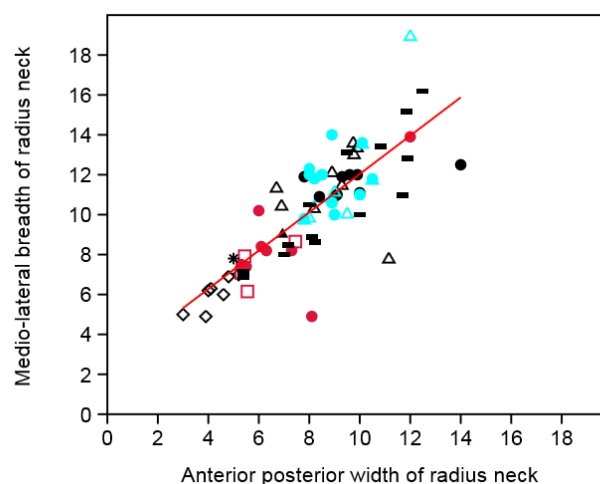


Figure 4.30. Linear plot for 'maximum medio-lateral diameter of radial neck and antero-posterior radius neck'.

e) Femur

Bivariate linear regression for femur anterior posterior length of femur head and medio-lateral breadth of femur head (Fig 4.31) shows a moderate positive correlation;  $r=0.6$ .

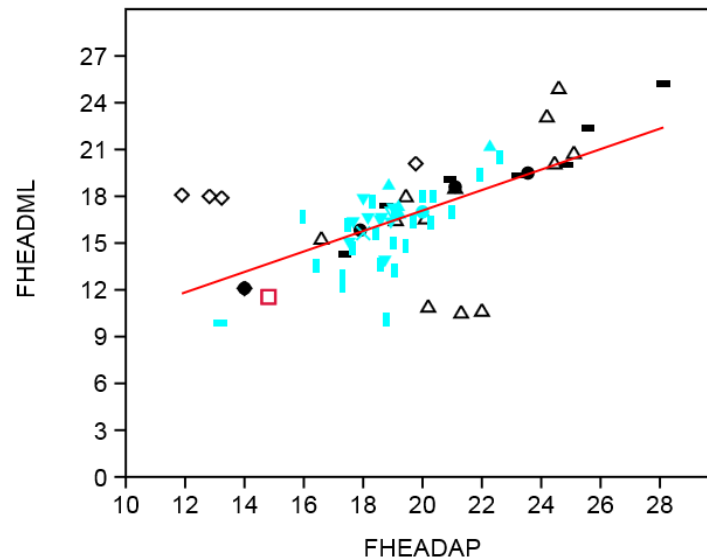


Figure 4.31. Linear plot for 'femur anterior posterior length of femur head and medio-lateral breadth of femur head'.

Table 4.35 results of the ANOVA analysis

<b>Character Traits</b>	<b>Sum of squares</b>	<b>df</b>	<b>Mean Square</b>	<b>F</b>	<b>Significance</b>
Maximum medio-lateral width of olecranon fossa (HDTROW) and width distal humeral articulation (HDTRWA)	693.557	1	693.557	20.64	0.0002881
Lateral epicondyle breadth to medial edge of trochlea and the medial trochlea flange length	649.626	1	649.626	15.69	0.0001491
Proximo-distal height of olecranon process and trochlea notch height	102.43	1	102.43	4.312	0.0403
Proximo-distal height of olecranon process and antero-posterior length of olecranon process	649.626 1			15.69	0.0001491

#### 4.1.5. Results of the Univariate Analysis of Variance (ANOVA). See Table 4.35.

##### a) Humerus

Five variables on the humerus did not yield positive results. No significant differences ( $p > 0.05$ ) were found for 1) head diameter, 2) olecranon width and height, 3) bi-epicondylar breadth; 4) humeral distal articulation and maximum medio-lateral breadth of olecranon fossa, and 5) humeral olecranon maximum medio-lateral width and olecranon maximum proximo-distal length.

The ANOVA test results suggest that two indices are statistically significant at  $p < 0.05$ , the lateral epicondyle to medial edge of trochlea and the medial trochlea flange length and Maximum medio-lateral width of olecranon fossa and width distal humeral articulation.

##### b) Ulna

The ulna trochlea notch height and olecranon to anterior trochlea notch shows no statistical significance ( $p > 0.05$ ). ANOVA test results for olecranon proximo-distal height and olecranon anterior posterior length shows statistical significance ( $p = 0.0001$ ). The trochlea notch proximo-distal height and olecranon process proximo-distal height is statistically significant among the different genera ( $p = 0.04248$ ).

##### c) Radius

The radius neck proximo-distal height of neck and head and proximo-distal height of neck index did not demonstrate statistical significance ( $p > 0.05$ ) between genera. The radius anterior-posterior length and medio-lateral breadth of neck also did not prove to be statistically significant.

##### d) Femur

For the femur, significance ( $p > 0.05$ ) is not observed for neck anterior-posterior length and neck medio-lateral breadth. Femur anterior posterior length of femur head and medio-lateral breadth of femur head proved not to have statistical significance ( $p > 0.05$ ).

### 4.3 Conclusions on the systematic palaeontology of the fossil cercopithecoid postcrania of the Sterkfontein Caves

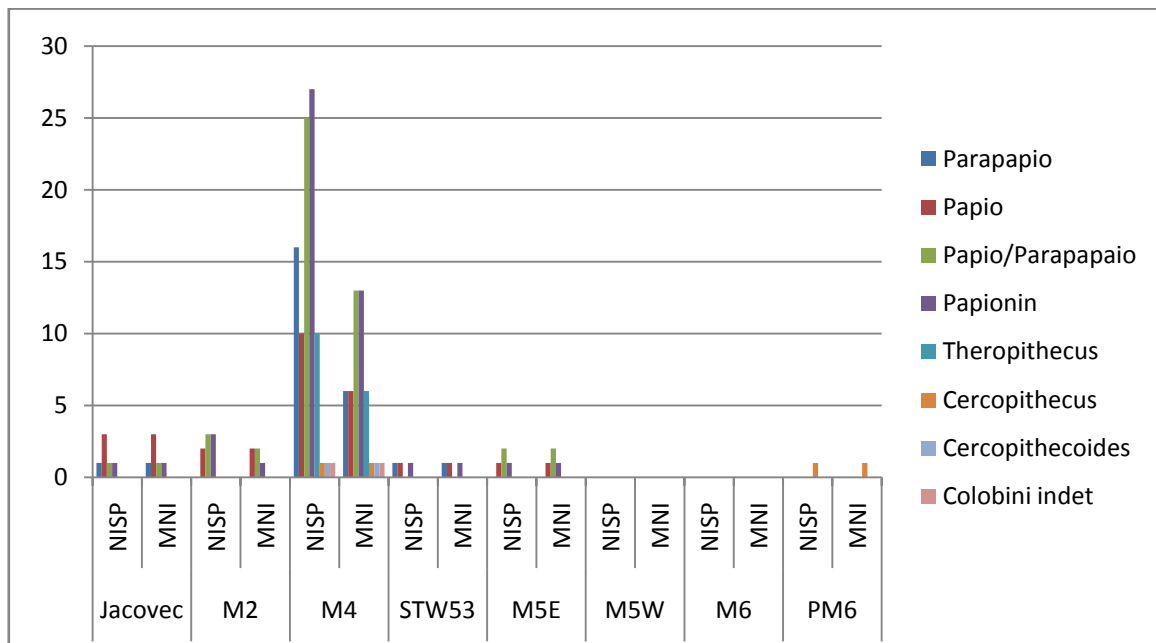


Figure 4.32. Sterkfontein caves and Number of Identified Specimens (NISP) Minimum Number of Individuals (MNI) by taxa per deposit.

Qualitative analysis of the sterckfontein postcrania indicates that the four limb bones, the humerus, the ulna, the radius and the femur can be used to distinguish between taxa. The following traits proved to be significantly different on, the humerus, the extension of the greater trochanter distinguishes between *Parapapio* and *Cercopithecus* and *Papio*. Distally, comparisons of the shape of the olecranon fossa suggest differences between the same two groups. Variation at species level could not be ascertained from all fossil skeletal elements under study.

Statistical assessment of all but one of the humeral traits could not distinguish between taxa. Therefore the humeral epiphyses are weak indicators for taxa among the family Cercopithecoidea. From the results of this analysis it can be assumed evident that the humerus bears little taxonomic signals in primate cercopithecoid genera. Examination of

most of the morphological traits of the ulna show the olecranon proximo-distal height and olecranon anterior posterior length and the trochlea notch proximo-distal height and olecranon process proximo-distal height are positive indicators for genera and are statistically significant.

More statistically significant traits observed are on the radius and the femur. The radius neck supero-inferior length and the radius neck and head length index suggest statistical significance. The same significance applies for the radius neck, based on the antero-posterior width and medio-lateral width index. The femur antero-posterior length of head and medio-lateral breadth of head width did not show statistical significance among the different genera.

From the quantitative morphological analysis it is evident that the radial neck (neck height versus neck and head height, and neck antero-posterior width versus medio-lateral breadth) and the femur head (anterior-posterior head length and medio-lateral head width) can be used to discriminate between cercopithecoid genera.

#### 4.3.1. *Form, function and size of the fossil cercopithecoid postcrania of the Sterkfontein Caves*

Research on postcrania remains has demonstrated its applicability to provide information on cercopithecoid locomotion (e.g. Elton 2000, 2001). In cercopithecoids, the difference in the proximal and distal humerus, proximal ulna, and proximal femur have proven to yield significant information on the locomotor habitus (Harrison 1989; Hlusko 2007).

This study has supports research which argues that that functional adaptation and morphology does not necessarily, always, translate to taxonomy. The results of the taxonomic analysis indicate that anatomical form is not the best discriminator between various taxa. On the humerus, the humeral greater tuberosity extension does not discriminate at any taxonomic level. The level of greater tuberosity superior projection of the greater tubercle varies among members of the same family and tribes, and the trait is also shared among various genera and locomotor groups. The elevated greater tuberosity serves to restrict movement at the gleno-humero joint, a feature seen in more terrestrially adapted cercopithecids (Jolly, 1967; Harrison 1989). Terrestrially (and semi-terrestrial) adapted

morphology and locomotion is known in papionins (*Papio*, *Theropithecus*), Cercopithecines (*Cercopithecus aethiops*) and in fossil Colobines (*Cercopithecoides williamsi*, *Cercopithecoides kimeui*). However, within this locomotor group, morphological and size differences are discernable. The humeral head shape varies between the cercopithecines, papionins and colobines. Cercopithecines have a hemispherically (proximo-distally compressed) shaped head compared to old world monkey whose humeral heads are more proximo-distally elongated (oval) on anterior view. The medial epicondyle is more retroflexed in *Papio* and *Cercopithecines* than in the colobines. The olecranon fossa shape has also proved not to have any discriminatory properties. On the ulna, the extension of the olecranon process varies between arboreal forms and terrestrial forms. The olecranon in arboreal colobines is short and is not retroflexed while terrestrial papionins such as *Papio*, have a longer and retroflexed olecranon.

Size is an important discriminatory factor in taxonomic analyses. Various studies (e.g. Gingerich 1981; Conroy 1999; Spoor & Manger 2007; Sears *et al.*, 2008) have been undertaken which estimate body mass based on cranio-dental data. Postcranial skeletal element sizes, particularly in adult individuals, are a better approximation of body mass (Payseur *et al.* 1999). They have a close association with body size and mass. Descriptive statistics, demonstrate numerous overlaps in size between different genera but groups according to body size or mass. As a result, and as seen in this study, size is one of the elements which can be utilised to discriminate between possible taxonomic groups. However, size in isolation, has not proved to be useful as a distinguishing variable in taxonomic studies.

Form, function and size are important factors in taxonomic studies. They play a major role in taxonomic examinations; however, they cannot be treated as disconnected facets of a taxonomic exercise. Each plays an essential role in taxonomic analyses.

#### 4.4 Fossil cercopithecoid taxa identified per deposit within the Sterkfontein Caves

Taxonomic groups identified within the Sterkfontein Cave infills demonstrate variability over time. The Silberberg Grotto preserves the same taxonomic groups (mainly Papionins) as those identified within the Member 4 deposit; however, Member 4 preserves more taxonomic diversity than the older Silberberg Grotto and Jacovec Cavern. Primate taxa are drastically reduced in the deposits younger than Member 4.

##### 4.4.1. *Jacovec Cavern*

The Jacovec Cavern is the deepest fossil-bearing deposit in the cave system, but is one of the least fossil-yielding deposits (Wilkinson 1973; Kibii 2000). The possible causes are discussed in the taphonomy section in Chapter 5.

Only papionins are taxonomically identified in the Jacovec Cavern. Fourteen specimens represent these papionins. Five *Papio* individuals are present in the cavern. There is also a small and a medium sized *Papio/Parapapio* as well as two specimens which could only be identified to the tribe papionini. The morphological analysis has demonstrated that these fossil *Papio* specimens are very similar to modern *Papio*. The morphology is consistent with terrestrial locomotion.

The small to medium sized fossil *Papio* specimens discovered in this infill display terrestrially adapted morphology. They demonstrate an upper arm and a stable shoulder joint restricted in the sagittal plane. The morphology and size (particularly of the medium specimen, BP/3/23257) does not deviate from the modern *Papio* anatomy. They have similar morphology and are comparable in size.

The small and medium *Papio* species identified, based on fossil cercopithecoid postcrania in the Jacovec Cavern mixed breccia, correspond to Kibii's (2000) conclusion that *Papio izodi* is present in the assemblage. *Papio izodi* was a medium sized primate; therefore, there is likelihood that the two *Papio* individuals identified in this study are *Papio izodi*. *Papio izodi* demonstrates affinities towards a more primitive form and towards *Parapapio broomi*



(McKee 1993). Morphologically these resemble the humerus UCMP 125858 (which is identified as *Papio izodi*) identified from taung by Gilbert *et al*, 2016.

The medium sized *Papio/Parapapio* specimens identified within the deposit cannot be linked to cranio-dental *Parapapio* specimens. The medium *Pp. broomi* identified within Jacovec demonstrates different morphological traits to modern *Papio* (Kibii 2004). The only link that the *Parapapio broomi* mandible has with the postcrania in the *Papio/Parapapio* category is the medium size. This is not sufficient data to infer correlations between the two specimens. The Sterkfontein *Parapapio* forelimb shares some affinities with *Parapapio jonesi* from Hadar as described by Frost and Delson (2000). No other comparative postcranial material from this species or other fossil monkeys occurring in southern or East Africa exists. Therefore the materials are assigned to *Parapapio* sp. Taxonomic conclusions derived from cercopithecoid postcrania correspond to cranio-dental taxonomic data recorded by Kibii (2004) which suggest the dominance of papionins within the deposit. Kibii (2004) also identified a colobine which is not identified postcranially.

#### 4.4.2. Silberberg Grotto

Papionini dominate the Member 2 fossil cercopithecoid assemblage. These are represented by small and medium sized *Parapapio* and *Papio* as well as large papionins. The taxa and the associated morphology of the Silberberg Grotto fossil cercopithecoids remains are similar to the Jacovec cercopithecoids. However, the average individual size within the Silberberg Grotto is medium. When considering cranio-dental data, the Silberberg Grotto fossil cercopithecoids demonstrate more taxonomic diversity than Jacovec Cavern. This is probably due to the much smaller sample size from the Jacovec Cavern thus far.

The Silberberg Grotto preserves *Cercopithecoides williamsi*, *Parapapio broomi*, *Parapapio jonesi* and *Papio izodi* (Pickering *et al*. 2004a). Jacovec Cavern has yielded remains of *Parapapio broomi*, *Parapapio jonesi* and *Papio izodi* and an unidentified colobine. No *C. williamsi* has been recorded from Jacovec, although this is an uncommon taxon overall at Sterkfontein. The morphology of the fossil cercopithecoid remains does not vary from the Jacovec specimens. The link between the *Papio* and *Parapapio* postcrania and the fossil

species identified in the cranio-dental material cannot be ascertained by the current study. *Australopithecus* is the only hominid genus discovered within both deposits.

The similarity of the taxa preserved within the Silberberg Grotto and the Jacovec Cavern suggests comparable palaeoenvironmental conditions during accumulation. However, Member 2 has a high predominance of primates and felids. The two common morphological features between these two taxonomic groups are the similar body sizes and their agility. Felids and primates are agile animals and their equivalent frequency in the Silberberg Grotto is likely to be related to this factor, in contrast with bovids that occur in lesser frequencies within the deposit. The closed wooded environment in which these taxa co-existed in such large numbers was suitable for their dominance. Pickering *et al.* (2004a: 279) state that the Member 2 palaeoenvironment was characterised by ‘rolling, rock-littered and brush- and scrub-covered hills’ with some tree cover--the sort of environment which supports agile body forms. Kibii (2004) suggests that Jacovec Cavern had a mosaic of open and closed habitats with a riverine gallery forest. On average, however, the number and percentage of small individuals is less in Member 2 compared to Jacovec Cavern, which has higher frequencies of small sized cercopithecoids. The latter environment is reconstructed as relatively open, with a permanent water supply in the vicinity (Pickering *et al.* 2004a).

#### 4.4.3. Member 4

Member 4 preserves more taxonomic diversity in fossil cercopithecoid postcrania. *Papionins* disproportionally dominate the assemblage with an NISP of 242, which constitutes 92 % of the total NISP of identified taxa and 23% of the Member 4 fossil cercopithecoid postcrania assemblage. The papionins identified are similar to Member 2 papionins; these are *Parapapio*, *Papio*, and an unidentified papionin. *Cercopithecus aethiops* is present in the deposit. The tribe Colobini as well as the most common and large colobine in the southern African fossil deposits, *Cercopithecoides*, also form part of the assemblage. The *Parapapio* and *Papio* sizes range from small to large. There are indeterminate *Theropithecus* individuals in the deposit identified from postcranial remains.

The morphology of the papionins identified within the Member 4 assemblage point to a suite of characters. The Sterkfontein fossil *Parapapio* upper arm is flexible with rotational

abilities while retaining terrestrial tendencies in the hind limb. The East African *Pp. ado* is highly terrestrial in nature; however its shoulder joint preserves anatomy which is more arboreally inclined (Jablonski *et al.* 2008), a feature similar to South African *Parapapio*. Based on the limited nature of *Parapapio* postcrania fossil remains in the East African context, this data is used with caution. Studies of East African *Parapapio ado* suggests that the species had a generalist-type of locomotion with most of its time spent on the ground (*ibid.*). The relationship between the South African *Parapapio* and the East African *Pp. ado* is currently unclear. However, morphological and quantitative analysis of the Sterkfontein *Parapapio* suggests that the genus is similar to the East African variant of the genus.

Cranio-dental data has not revealed *Theropithecus* within Member 4. *Theropithecus* postcranial specimens in the deposit represent robust medium to large individuals. Delson's biochronology (1984) study suggests that Member 4 is a zone occupied by *Theropithecus darti*, *Theropithecus brumpti*, *Cercopithecoides williamsi*, *Parapapio* and *Papio hamadryas robinsoni*. However, not all these species are represented at Sterkfontein. *Theropithecus darti* is identified in Makapansgat Members 2, 3 and 4 (Freedman 1965; Maier 1970). Makapansgat Member 2 is dated by faunal correlation to 3.2-2.7 My (Reed 1997; Tobias 2000), palaeomagnetism dates suggest that Member 3 and 4 are 3.03 -2.58 My (Partridge 1979). The presence of *Theropithecus* in the Member 4 landscape is highly plausible and a lack of recorded cranio-dental materials could be due to factors other than its absence from the Sterkfontein environment (i.e., sampling or taphonomic issues)during the accumulation of Member 4. This genus was identified by Ciochon (1993) within the Member 4 fossil cercopithecoid postcranial sample. He identified remains of *T. darti*, although this study questions these identifications. *Theropithecus oswaldi* in Sterkfontein is also identified by T.R Pickering in Member 5.

*Cercopithecoides* identified in the Sterkfontein deposits is a medium-sized individual. Von Mayer's (1999) assertion that Sterkfontein Member 4 *Cercopithecoides* is a small variant of the genus, adapted to woodland environments, cannot be corroborated by this study. The upper arm of this species suggests a terrestrially inclined fossil monkey, particularly in the forearm; its femur suggests it had a flexible hind limb joint, although movement was restricted to the sagittal plane. The specimens are slightly smaller than the *C. williamsi*

Koobi Fora specimen; however, they are similar in size to the Laetoli specimen which is a *Cercopithecoides* sp. Only two specimens are assigned to *Cercopithecoides*, therefore statements on this genus' postcrania in the Sterkfontein caves are tentative.

The presence of *Parapapio*, a generalist herbivore (and *Parapapio jonesi* which subsisted on a mixed diet consisting of grasses, leaves and fruits) suggests that they existed in a mosaic of open and closed wooded environments (El Zaatari *et al.* 2005, Jablonski & Leakey 2008). Hatchett (2011) states that *Theropithecus* relied on a C<sup>4</sup> diet which it supplemented with fruits and leaves. Member 4 and the Member 5 East infill indicate the presence of a wooded to moderately wooded environment until about 2.0-1.8 My (Luyt & Lee-Thorp 2003). Data indicate a shift to open environments with the accumulation of the Member 5 West infill (*ibid.*). The terrestrial habitat preference of *Papio* and *Cercopithecoides* support the presence of an open environment near to the forested valley. The extreme terrestrial nature of *Theropithecus* and the domination of terrestrial papionins over colobines in Member 4 point to the existence of an open grassland near to the caves at the time of accumulation of the deposit. The presence of arboreal primates also suggests there was some tree cover in the Sterkfontein valley area during the Member 4 period.

Papionins constitute 92 % of identified taxa within the Member 4 assemblage. When cranio-dental specimens are also considered, data still indicate that papionins dominate colobines. 95% of individuals within the deposit are papionins, compared to 5% colobine individuals (Kibii 2004). This relates to an environment conducive to their complex social structure and the reproductive success of the papionins in the African Plio-Pleistocene. The lack of abrupt changes in the taxa between Members 2 and 4 is noteworthy. The similarity of papionins identified in this deposit to the Silberberg papionins suggests some continuity between these two deposits.

#### 4.4.4. StW 53

The difference in the taxonomic content of the Member 5 deposits suggests that the StW 53 infill is unique from the other two infills. The StW 53 deposit has been suggested to be a probable later phase of Member 4 (Kuman & Clarke 2000). The presence of *Theropithecus* and a colobine in StW 53, which are also found in Member 4 and the Oldowan infill and not

in Member 5 West, suggests a relationship between Member 4 and StW 53. The Member 5 West deposit and its taxonomic composition of papionins differ from the latter's taxonomic pattern. The apparent decline of primate frequencies between Member 4 and the StW 53 deposit partially supports that conclusion, although the StW 53 infill is a very small deposit. The presence of an *Australopithecus* in that latter infill which is similar to the ones identified in Member 4. Clarke (2013) points this to be a deposit different from the rest of Member 5.

#### 4.4.5. Oldowan Infill

The only recorded taxon from the Oldowan infill fossil cercopithecoid postcranial assemblage is a *Papio* specimen which resembles modern *Papio ursinus* in morphology. The Member 5 deposits preserve the *Papio/Parapapio* specimens. The likelihood of *Parapapio* occurring during the accumulation of this deposit is very low as *Parapapio* possibly occupied a mosaic of a closed environment with some open habitats (El Zaatari *et al.* 2005), which are more associated with earlier deposits. Therefore the likelihood that the specimens identified as *Papio/Parapapio* are *Papio* is high. The fragmentary nature of these specimens hinders conclusive taxonomic assignment to either genus.

#### 4.4.6. Member 5 West

These deposits also demonstrate a radical reduction in fossil primate quantities. The low primate numbers in these deposits is attributed to the changing environment after 1.7 Ma, which saw the decline in primate variability in the fossil record.

#### 4.4.7. Member 6

Within the Member 6 deposit only the cercopithecoid family is identified and these are not identified to tribe. The Member 6 deposit primate assemblage is very small. The two cercopithecoid postcranial specimens in the deposit have not been identified to taxa.

#### 4.4.8. *Post Member 6 deposit*

The Post Member 6 assemblage retains some of the *Papionin* taxa identified within the earlier deposit, albeit at a reduced scale, which is expected, due to the changing environment during the accumulation of this deposit. The deposit preserves a very small range of primates and as a result few taxa are represented. A small *Cercopithecus* as well as a small *Papio* individual are identified. Taxonomic identification of the Sterkfontein fossil *Cercopithecus* specimens was based on modern comparative materials which are assigned to the genus *Cercopithecus*. Further examination of the humerus and the radius specimens could not be assigned to species level. According to the literature, the species *aethiops* has been moved to *Chlorocebus* and the genus *Cercopithecus* is still under revision. The genus *Cercopithecus* is still a valid genus. For purposes of this thesis, the Sterkfontein fossil specimens are identified only to genus level. The relative prominence and sudden appearance of the small bodied *Cercopithecus* in the Post Member 6 assemblage is likely a factor of the changing cave structure Reynolds *et al.* (2007) report an increase in small carnivores in the younger deposits (Member 6, Post-Member 6 and Lincoln Caves) of Sterkfontein. After the deposition of Member 5, the cave entrance was too low. (Ogola 2009) suggests that carnivores could have been able to access, and accumulates bone into the cave. This correlates with the increase in small monkeys, particularly the cercopithecines, observed in the cercopithecoid assemblage.

**CHAPTER FIVE**  
**RESULTS: TAPHONOMY OF THE STERKFORTEIN FOSSIL**  
**CERCOPITHECOID POSTCRANIA**

The Sterkfontein non-hominid fossil primate post-crania assemblage examined in this study consists of 1514 identified specimens (NISP). Appendix A provides a detailed list of the skeletal elements from each deposit. Femora constitute the most identified skeletal element at 29% of NISP, while only four carpals were identified in the whole assemblage constituting 0.2 % of the NISP. In all skeletal elements, shafts constitute the most identified anatomical parts while distal portions are the least. This chapter provides the taphonomic descriptions and analysis, but detailed interpretations are presented in Chapter Seven.

**5.1. Jacovec Cavern**

Jacovec cavern preserves 12% (NISP: 181) of the total Sterkfontein non hominid primate postcrania assemblage. One hundred and fifty seven elements are identified, constituting a high NISP:MNE ratio. All skeletal body parts are represented in the assemblage; extremities are the highest represented in terms of NISP and MNE (Fig. 5.1). Phalanges and metapodials have a combined NISP (54) which is 29% of the total Jacovec NISP, and 33% of total MNE.

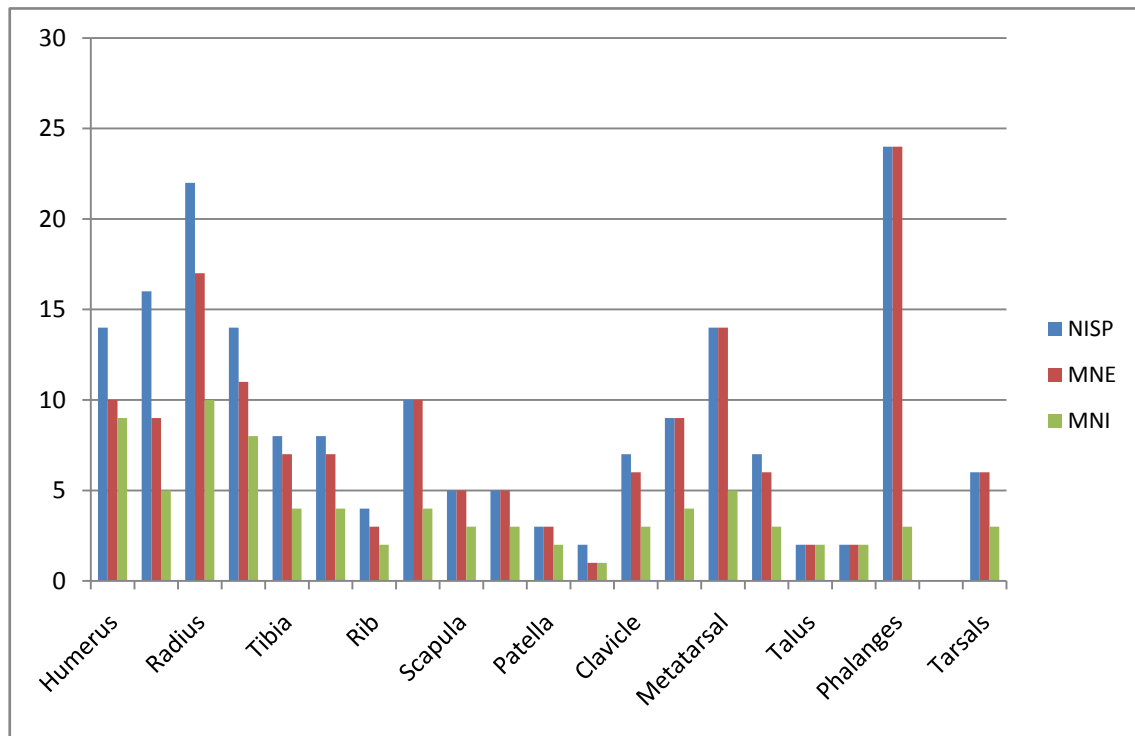


Figure 5.1. Jacovec Cavern fossil cercopithecoid postcranial skeletal element frequencies.

Fore limbs dominate in terms of the minimum number of individuals preserved and they constitute the second largest proportion of preserved NISP. The largest MNI within the fore limb category is represented by the radius. Radii suggested the presence of at least ten individuals. These are: one medium sized juvenile represented by a proximal left radius (BP/3/31553); five medium sized adults are represented by two right proximal radii (BP/3/23235 and BP/3/31923); two radii shafts (BP/3/22494 and BP/3/31388) as well as additional five radius shafts (BP/3/22575, BP/3/23232, BP/3/23715, BP/3/31354 and BP/3/31382). Four small sized individuals are represented by two left proximal radii (BP/3/22613 and BP/3/23453) two left radii shafts (BP/3/22456 and BP/3/31922) and three more unsided shafts (BP/3/22660, BP/3/23191 and BP/3/23237). In addition there is a small juvenile individual (BP/3/22456), a small sub-adult (BP/3/31661) and a medium sized sub-adult (BP/3/31691). The hind limb suggests there is an additional individual, a large adult represented by a left proximal tibia (BP/3/22520).



The age distribution of the elements preserved also suggests a normal distribution of a primate community. When assessing the age distribution within the Sterkfontein fossil cercopithecoid postcrania assemblage using radii, adults constitute 90% of the MNI population, juveniles constitute 10% of the MNI and there are no sub-adult radii preserved. The size distribution also suggests the same trend. Sixty percent are medium sized individuals (MNI) and 30% are small sized individuals. The dominant percentage of preserved skeletal element portions per NISP are shafts and proximal portions are the least preserved. Only seven percent of the specimens could be identified to genus level.

The pattern of skeletal element representation in the Jacovec Cavern is unlike the other deposits. The domination of fore limbs, phalanges and podials over hind limbs is peculiar as the general pattern observed within other deposits is that hind limbs are preserved in greater quantities compared to fore limbs. Extremities are the smaller skeletal elements. This scenario suggests movement of skeletal elements into the cave. Tumbling and surface slopewash of bones into this cavern are suggested by the high representation of extremities and the presence of abraded and trampled specimens preserved in the assemblage.

During the slump of the brown breccia talus, all the smaller juvenile primates as well as a large percentage of the fossil cercopithecoid specimens were washed and tumbled into the cavern floor where admixture of materials from the brown and orange breccias occurred. Kibii (2004) suggests that various processes played a role in the accumulation of the Jacovec Cavern skeletal remains. Carnivore modification marks, combined with evidence of tumbling, suggests that the assemblage was impacted by carnivores and only later tumbled into the deposit (Kibii 2004). The hominid material, along with some cercopithecoids, was accumulated in the cave through water action during deposition of the (earlier) orange breccia. The majority of the monkeys was washed in during the accumulation of the younger brown breccia. The absence of hominid remains during the deposition of the brown breccia could suggest that the hominids may not have been active around the vicinity of the cave, compared to the earlier stage when the orange breccia formed.

## **5.2. The Silberberg Grotto**

All materials from the Silberberg Grotto (Members 2 and 3) included in this study are from Dump 20. The assemblage is the third largest fossil cercopithecoid primate postcrania assemblage in the Sterkfontein deposits after Member 4 and Jacovec Cavern. It preserves 9% (NISP: 137) of the Sterkfontein fossil cercopithecoid postcrania assemblage. Materials from this dump contain a full range of skeletal parts, including limbs, parts of the axial skeleton and extremities (Fig. 5.2). It even preserves one set of articulating distal humerus with a proximal ulna (SWP 1585). Limbs dominate the assemblage at 78% of the postcranial NISP. The femur is the dominant skeletal element; it is 40% of the Silberberg fossil cercopithecoid postcrania. This is followed by the humerus at 16% of the Member 2/3 NISP.

A minimum of 14 individuals is represented in this assemblage. There is a small juvenile individual represented by a humerus (SWP 1588), while the femurs suggest a minimum of 13 individuals: one small adult (SWP 1617), two large individuals (SWP 1534, SWP 1605), one medium juvenile (SWP 1367), one medium sub-adult (SWP 1697) and 15 medium adults represented by ten left proximal femora (SWP 1785, SWP 1385, SWP 1414, SWP 1537, SWP 1612, SWP 1698, SWP 1699, SWP 1700, SWP 1705, SWP 1709).

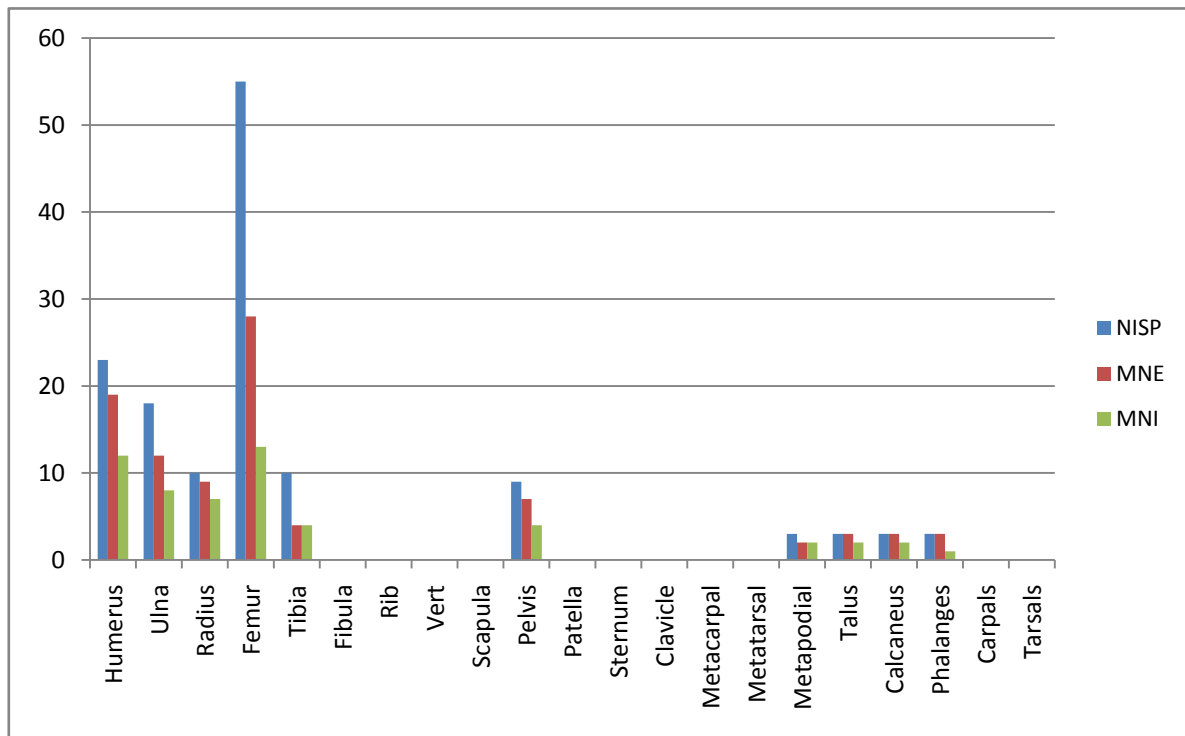


Figure 5.2. Silberberg Grotto fossil cercopithecoid postcranial skeletal element frequencies.

The Silberberg Grotto cercopithecoid materials are missing much of the postcranial axial skeletal elements; however, cranio-dental materials are well represented. The state of preservation of the in situ Member 2 fossil assemblage, as reported by Pickering *et al.* (2004a), indicates that the fossil primates are represented by a full range of skeletal elements. Although some of the materials from Dump 20 could possibly derive from Member 3, the general pattern is still consistent with the materials from the in situ Member 2 excavations.

The high frequency of fossil cercopithecoid remains with a full range of skeletal elements preserved, articulated fossil cercopithecoid and hominid specimens, as well as the large numbers of carnivores within Member 2/3 strongly suggest a death trap as a mode of accumulation. This situation suggests that the Member 2/3 fossil faunal assemblage accumulated as a result of an aven scenario where animals accidentally fall down a shaft in a closed environment and are trapped within the cave (Pickering *et al.* 2004a).

Femora are highly fragmented and are the most represented skeletal elements in the dump. Twenty-eight femoral elements are represented by 55 specimens. It is the only element within the dump with an average ratio of 1:2. The average NISP: MNE ratio within the dump is less, at 1:1.5. Therefore, representation of the femur is exaggerated due to fragmentation. The proximal and distal portions of the femur are also highly represented. Sampling is a likely causal factor for this phenomenon. The dump material derives from lime mining operations.

Pickering et al. (2004a) suggest that the deposit gathered as a result of different death trap scenarios. Both hominids and cercopithecoids are agile animals that could have entered the cave through an accidental, either being killed in the fall or being unable to exit. Both the *Australopithecus* skeleton (ibid.) and the fossil cercopithecoid remains are, in some cases, represented by articulating skeletal parts, which confirms the deathtrap scenario.

### **5.3. Member 4**

This assemblage contains the largest number of identified specimens and individuals within the Sterkfontein fossil non-hominid primate postcrania (Fig. 5.4). It preserves 67% (NISP: 1013) of the Sterkfontein fossil Cercopithecoidea postcrania assemblage. A significant percentage (39%, NISP: 400) of specimens in the Member 4 assemblage are derived from the associated dumps and 292 (28% of NISP) of these are from Dump 13. Dump 18 has the second largest NISP (48) and Dumps 10 and 12 preserve the least at 10 specimens each. Forty-three specimens (4% of Member 4 NISP) are from the Type Site locality.

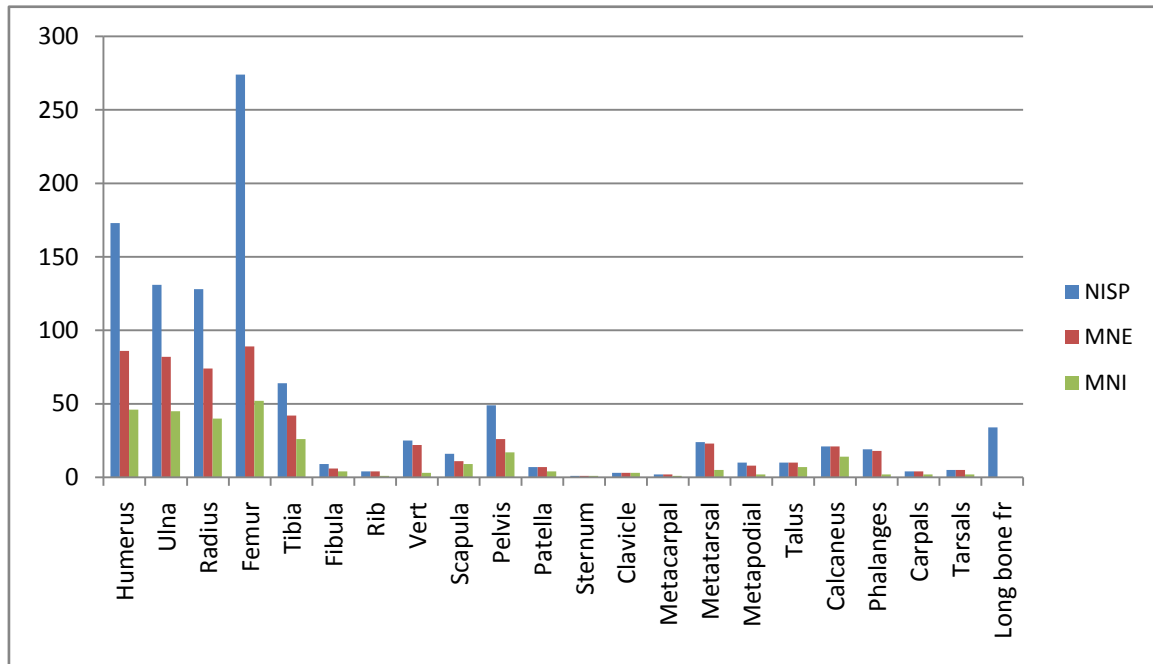


Figure 5.3. Member 4 fossil cercopithecoid postcranial skeletal element frequencies.

A full range of skeletal body parts is present in the Member 4 assemblage. The most discerning feature about the M4 deposit is that the limbs are disproportionately dominant compared to other body parts. Fore limbs specifically dominate in terms of NISP/MNE/MNI ratios. The femur is the largest occurring element at 27% (NISP: 274). Research on carnivore assemblages has demonstrated that hand and foot bones are normally swallowed whole and as a result the limb elements will be the remaining elements in a scat assemblage (Pickering 1999). The rock fall on the Member 4 talus would have crushed the more delicate elements such as fibulae and radii, and some small elements would have filtered through the rocks into cavities lower down in the talus. Therefore the limb elements such as the femur and humerus will have a higher survival rate. This is also evident from the head fragments discovered in the deposit (Fig. 5.5).

There are at least 52 individuals identified. These are based on the femur. They include four small individuals (a juvenile, a sub-adult and two adults), 45 medium adult individuals (which include a single *Theropithecus* individual represented by two femur elements), one large juvenile and two large adults.

The large frequency of limb NISP overshadows the number of skeletal elements preserved within the Member 4 deposit. The femur, the largest preserved skeletal element in the deposit, is represented by 274 specimens consisting of 52 individuals. This number points to fracture of the Sterkfontein fossil primate limb elements. The fragmentation of these elements is largely fresh and this points to post-depositional factors (Kibii 2004). However, the numbers of individuals represented by the limb elements also suggest higher values than the cranio-dental remains, as discussed by Kibii (2004). The high frequency of limb elements, along with the trampling and abrasion marks observed on the postcrania, point to the suggestion that the remains travelled a distance prior to being incorporated into the infill. Therefore surface slope wash of materials explains the presence of numerous quantities of limbs in the deposit. Kibii (2004) also suggests that some of the fossil cercopithecoids entered the cave and died naturally. This is supported by the presence of articulating specimens within the deposit (e.g. Fig 5.6).

The most diversity in primate taxa within the Sterkfontein Cave deposits is found in Member 4. This large diversity of papionins, colobines and Cercopithecini in the Member 4 deposit, coupled with the diversity observed in the preservation of felids and bovids (Kibii 2000), could be the result of two factors: the long excavation period of the deposit, from Broom's 1947 excavations to Clarke's excavations which still continue today; or the large variety of primates which existed within the Member 4 habitat. Although the latter explanation is likely, Member 4 has yielded the largest number of fossil specimens and 67% of the non-hominid fossil primate postcrania assemblage within the Sterkfontein Caves. Materials derived from this deposit are from the deepest excavation at 10 meters depth, and it covers the largest space in the cave at more than 30 meters wide. The size of this deposit and the commensurate quantities of materials it yields attract scholarly investigations. It is demonstrated by O'Regan and Reynolds (2009) that the Member 4 carnivore assemblage represents a time-averaged palimpsest. They suggest that sites preserving relatively few species of fossil carnivore remains than Member 4 better demonstrate fossil carnivore communities. Therefore the diversity observed in Member 4 is due to the long duration of accumulation.

Primates coupled with felids in fossil cave sites are large constituent animal groups in death trap scenarios of closed environments where agile animals comprise a large percentage of the animal community (Pickering, Heaton & Clarke 2004). The agility of primates and carnivores lends them to the danger of falling into caves. Baboons sleep in caves, and that situation would attract carnivore predation in the cave locales (Brain 1981). Fossil carnivore remains are also present in the Member 4 deposit; however they are not the second highest representation in terms of species and minimum numbers of individuals. In Member 4, bovids are the second most numerous occurring animals in the fossil deposits (Kibii 2004). The domination of bovids, which do not frequent cave sites, suggests that several other factors played a role in the accumulation of Member 4 fauna. According to Kibii (2004) bovids and primates, particularly the small postcranial elements which occur in Member 4, were accumulated through multiple agents, such as carnivore voiding, as well as water action washing in skeletal remains from the surface around the cave entrance.

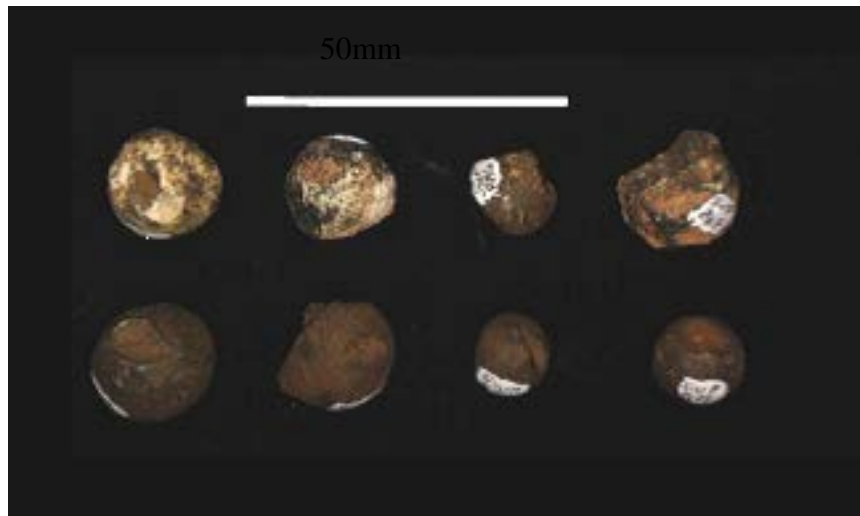


Figure 5.4. Example of the femur head fragments discovered within Member 4. Top row from left, SWP 876, SWP 892, SWP886 and SWP 869. Bottom row from left, SWP 879, SWP 877, SWP 874 and SWP 895.



Figure 5.5. SWP 1585, an articulated fore limb embedded in breccia from Dump 13 (Member 4).



#### 5.4. STW 53 Infill

The STW 53 Infill preserves 25% (NISP: 39) of the total Member 5 fossil non-hominid primate postcrania assemblage. Medium sized adults dominate this infill at NISP 87% of the assemblage. Juveniles are 12% and only one sub-adult specimen is present. Small specimens occur at 10% and no large individuals have been identified in this assemblage. Fore limbs dominate this assemblage in terms of NISP, MNE and MNI frequencies (Fig.5.7). Hind limbs, axial skeleton and extremities are also represented in the assemblage. The radius is the most dominant skeletal element. It represents four individuals, two medium sized *theropithecines* (SWP 1198 and SWP 1204), one small juvenile (SWP 1308) and one medium unidentified cercopithecine (SWP 1279). In addition, five more individuals are present in this assemblage: four juvenile elements (SWP 1308; SWP 2376; SWP 2377 and SWP 23870) represent one medium sized juvenile individual within this deposit. There is a *Papio* (SWP 2385) and a colobine (SWP 1163). One sub-adult is present (SWP 2797) and one small individual derives from four elements (SWP 1308; SWP 2377; SWP 2796 and SWP 2696). Therefore a total of nine individuals is in this assemblage. It contains *Theropithecus* postcranial specimens. This genus has not been identified postcranially either in the Member 5 West deposits or in the Oldowan Infill. However, *Theropithecus* has been identified from dental remains in the Oldowan Infill (Pickering 1999). The only colobine postcrania discovered in the StW 53 deposit is located in square X53, at the eastern edge of the identified distribution of this infill. Carnivore accumulation has been inferred by Pickering (1999), and data derived from primate postcrania also support the presence of carnivore impact on the assemblage.

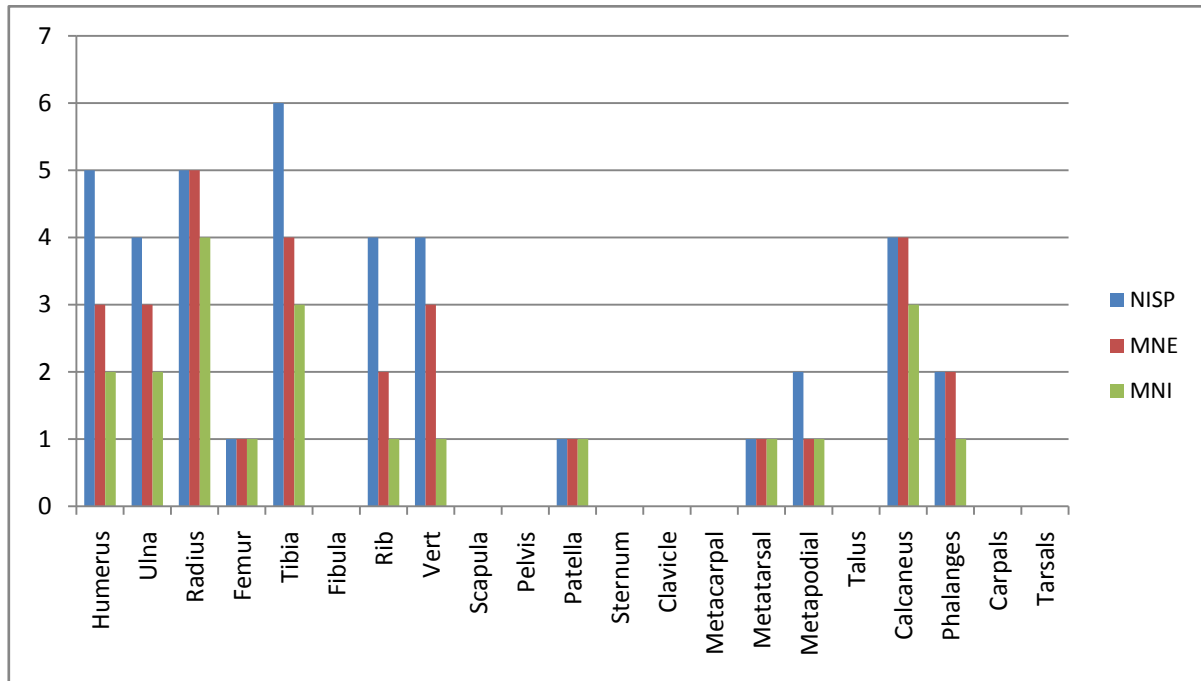


Figure 5.6. StW 53 fossil cercopithecoid postcranial skeletal element frequencies

### 5.5. The Oldowan Infill

The Oldowan Infill preserves the largest percentage (61%) of specimens within the Member 5 deposits with an NISP of 96. The full range of skeletal body parts is represented in the infill (Fig. 5.8). The axial skeleton has the largest NISP. These, however, comprise a single individual. There is a minimum of 7 (cMNI) individuals represented by four medium sized right proximal ulnae (SWP 2184, SWP 2193, SWP 2194 and SWP 2296) one small individual (SWP 2477), a single large individual (SWP 2779) and a medium sized juvenile (SWP 2481).

The high concentration of cercopithecoids in squares R51 and Q51 is at the interface with the Member 4 squares where there is an irregular contact between Members 4 and 5 (see Fig 1), and hence these fossils most likely derive from Member 4. Thus 57% of the primates in the Oldowan Infill are likely to be from an area of interface where it was difficult during excavation to separate the eastern margin of the Oldowan Infill from

Member 4. All body parts are represented in the area of the Member 4, Member 5 interface, which would be consistent with a the presence of a death trap scenario.

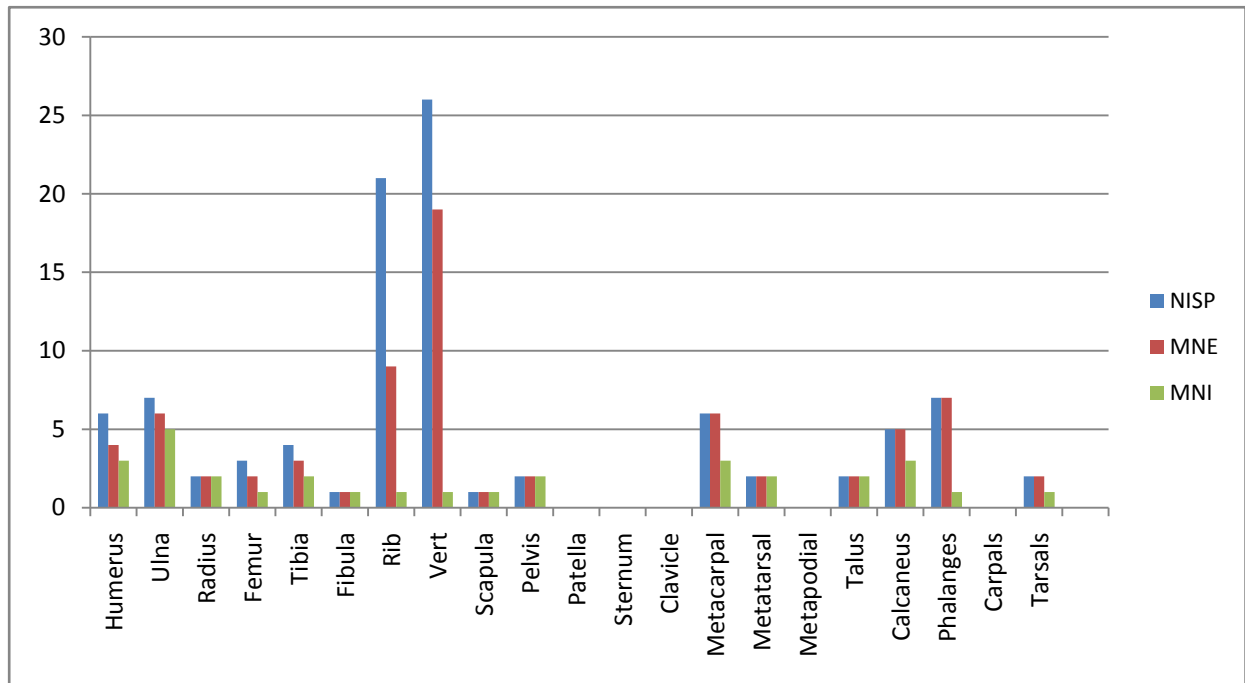


Figure 5.7. Oldowan Infill fossil cercopithecoid postcranial skeletal element frequencies

## 5.6. Member 5 West

Member 5 West preserves 11% (NISP: 19) of the Member 5 fossil postcranial remains. Even with a limited assemblage, the deposit preserves a full range of skeletal elements: fore limb, hind limb, axial skeleton and extremities are present in the sample. Tarsals have the highest representation in terms of NISP/MNE/MNI (Fig. 5.9). Four individuals (MNI) are present in this deposit: two small adults represented by two small adult tali (SWP 1284, SWP 2805) and two medium adults represented by two left calcanei (SWP 2741, SWP 2742).

According to Pickering (1999), the Member 5 West assemblage mainly accumulated as a result of hyaenas. Surface slope wash of materials and porcupines also played a role in the formation of the deposit (Pickering 1999). Surface slope wash of materials into the cave is supported by the domination of tarsals in the deposit.

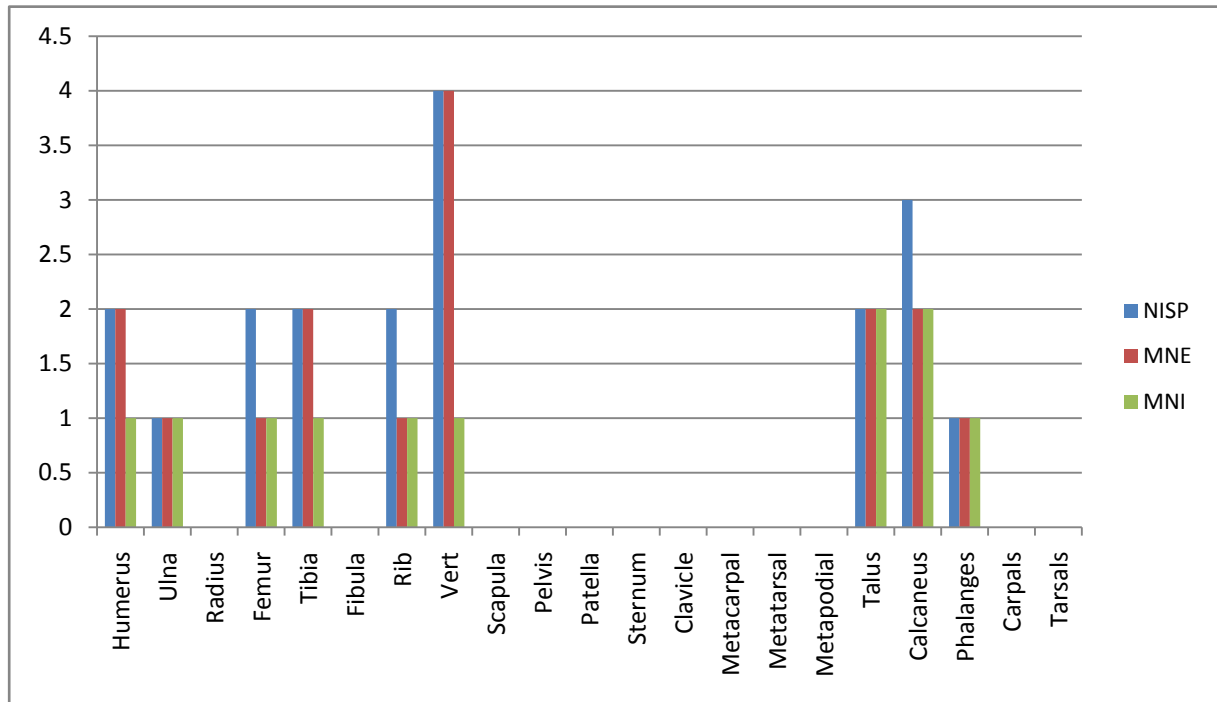


Figure 5.8. Member 5 West fossil cercopithecoid postcranial skeletal element frequencies

### **5.7. The Member 6 deposit**

The Member 6 deposit is the most primate deficient faunal assemblage in the whole Sterkfontein Cave system. It is the only deposit within the Sterkfontein caves without hominid remains and with only two cercopithecoid specimens. Ogola (2009) suggests that there was a significant time gap between the Early Pleistocene Acheulian infill and the Member 6 deposit, which is considered to be Mid Pleistocene. Brain (1981) describes Member 6 as a very small deposit with a small faunal sample that cannot provide much taphonomic information. It fills a small space under the cave roof and rests conformably on the capping flowstone of Member 5 (L. Bruxelles, pers. com. to K. Kuman).

### **5.8. The Post Member 6 deposit**

This deposit demonstrates an environmental shift from the Member 5 deposit. It constitutes 1.4% of the Sterkfontein fossil non-hominid primate assemblage at NISP of 22. Fore limbs dominate in terms of skeletal part representation (Fig. 5.10). The ulna and the humerus collectively constitute 41% of the total NISP in the assemblage. Nineteen elements are identified within the assemblage. A minimum of four individuals within the Post Member 6 infill consist of a medium sized juvenile individual (BP/3/19236), a small juvenile *Papio* represented by a humerus head fragment (S94-10064), and a distal humerus (SWP 1111) representing a different genus.

The Post Member 6 was accumulated by multiple accumulating agents at the same time or through one or more entrances (Ogola 2009). These include carnivores, porcupines, hominids and death traps (ibid.).

The L63 deposit was partly accumulated by porcupines (Reynolds et al. 2007). The discovery of hyaena coprolites in the deposit implies that hyaena used the cave or part of the cave as a den at the time of accumulation (ibid.). This deposit contains stone artefacts

which are not diagnostic to a specific industry but suggest to be younger than the Acheulian industry found in the Member 5 West (Reynolds 2003).

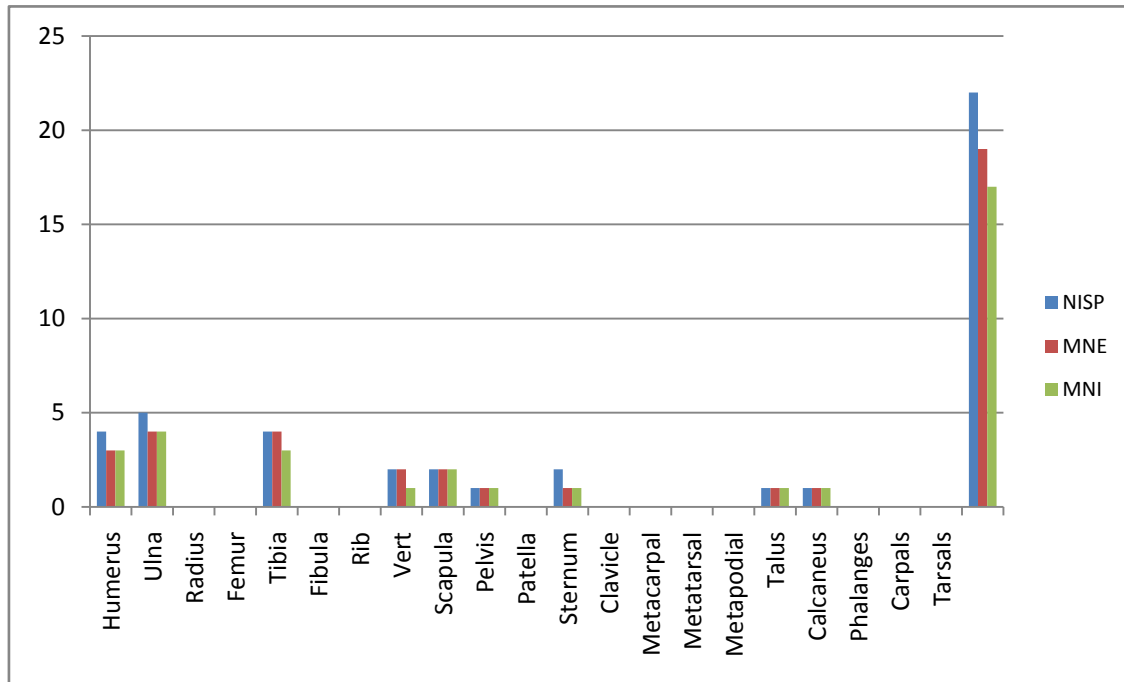


Figure 5.9. Post Member 6 fossil cercopithecoid postcranial skeletal element frequencies

## 5.9. Minimum number of individuals represented within the cercopithecoid postcranial assemblage, identified by taxa

### 5.9.1. Jacovec Cavern

Jacovec Cavern has a minimum of ten taxonomically identifiable cercopithecoid individuals. Only one is from the Orange breccia while the rest are from the mixed breccia found on the floor of the cavern.

Six *Papio/Parapapio* specimens which make up three individuals are found within the Jacovec. Two medium adults correspond with two left ulnae (BP/3/23271 and BP/3/23336). One of these adults is from the Orange Breccia while the second is from the

mixed breccia. A small adult *Papio/Parapapio* individual is identified from a proximal ulna (BP/3/21175) and a distal humerus (BP/3/18382).

Five *Papio* individuals are recognised. These are preserved within the mixed breccia only. These are: one medium juvenile individual identified from one left medium juvenile humerus head (BP/3/22757); one medium sub-adult left distal humerus (BP/3/31691); two medium adults are represented by two right proximal radii (BP/3/23235 and BP/3/1923) and a left distal humerus (BP/3/23389) signifies the presence of a small adult individual.

Two papionin individuals are also present in the mixed breccia. These are based on one medium adult, inferred from a right proximal ulna (BP/3/23718) and a medium juvenile suggested by a left proximal radius (BP/3/31553).

#### 5.9.2. Silberberg Grotto

A minimum number of 13 individuals identifiable to taxa, is observed in the Silberberg Grotto. There are at least two *Parapapio* individuals recognised from two left distal humeri (SWP 1540 and SWP 1589). Six *Papio/Parapapio* individuals emanate from five left medium sized adult proximal femora (SWP 1785, SWP 1385, SWP 1404, SWP 1698 and SWP 1700) and one small adult individual from a left proximal ulna (SWP 1594).

Two *Papio* radii specimens (SWP 1418 and SWP 1552) belong to one *Papio* individual. Seventeen *Papionini* indet elements suggest the presence of four individuals: one large individual derives from a right proximal radius (SWP 1416), a distal femur (SWP 1534) and a right proximal ulna (SWP 1604); a single medium sub-adult is inferred from a right proximal femur (SWP 1697) and two medium adult individuals are represented by two left proximal femora (SWP 1537 and SWP 1699).

#### 5.9.3. Member 4

*Papio* sp has a NISP of 20 specimens. These comprise of a minimum of four individuals. One small sized adult individual is inferred from a right proximal radius (SWP 798); and three medium sized adults are deduced from three right proximal radii (SWP 793, SWP 803 and SWP 4243). Eighteen specimens (NISP) are assigned to *Parapapio* sp. *Papionini* indet is represented by 73 specimens which constitute a minimum of 17 individuals. cf. *Theropithecus* has an NISP of 14 comprising of a minimum of six individuals. These are observed from six right proximal ulnae (SF 3418, SWP 828, SWP 1148, SWP 1578, SWP 4001 and SWP 4084). Two colobine specimens are present in the deposit and two individuals are identified from these. These are: one large individual (inferred from the presence of SWP 13505, a large proximal ulna), and a small individual inferred from S94 10836, a right proximal ulna. One medium adult *Cercopithecoides* sp individual corresponds to the two specimens (SWP 1208, a left proximal ulna and SWP 883, a left proximal femur) recorded in the Member 4 assemblage.

#### 5.9.4. The StW 53 Infill

Six individuals are taxonomically identified within the StW 53 Infill. One specimen of an adult colobine (a left proximal femur, SWP 1163) is present. One left proximal radius (SWP 1198) of a single *Theropithecus* adult is recognised. One medium *Parapapio* individual is indicated by a left proximal radius (SWP 1204). SWP 2385 (a right proximal humerus) suggests the presence of one medium adult *Papio*. Two *Papionin* individuals (a small juvenile and medium adult) are represented by left unfused proximal radius (SWP 1308) and a right proximal radius (SWP 1306) respectively.

#### 5.9.5 The Member 5 West deposit

The Member 5 West deposit only preserves two specimens which are identified to the tribe, *Papionini*. A left proximal femur (SWP 1154) is the only specimen attributed to a medium adult *Papionini* indet. SWP 1119, a distal humerus of a medium adult is the only specimen belonging to *Papio/Parapapio*



#### 5.9.6. *The Oldowan Infill*

A minimum of three individuals are estimated from the Oldowan Infill. *Papio/Parapapio* has an NISP of 4 (BP/3/18382, a left distal humerus; SWP 2177, a right proximal radius; SWP 2296, a right proximal ulna; and SWP 2792, a right proximal humerus) which suggests the presence of one medium adult individual. *Papio* sp has an NISP of three (SWP 1120, a right distal humerus; SWP 2200, a right proximal radius; and SWP 2788, a right proximal ulna fragment). These consist of a minimum of one individual.

#### 5.9.7. *The Member 6 deposit*

The Member 6 deposit preserves only two cercopithecoid postcrania which are not identifiable to taxa.

#### 5.9.8. *The Post Member 6 deposit*

In the Post Member 6 deposit five cercopithecoid specimens are identified which indicate the presence of four individuals. A small juvenile *Papio* individual is distinguished by a right proximal humerus (SWP 10064). SWP 1285 (a left proximal ulna) corresponds to a small papionin adult individual. One medium adult colobine is represented by a right proximal ulna (SWP 1258), and two adult *Cercopithecus* specimens (SWP 1111 and SWP 1112) indicate the presence of a single adult individual.

### 5.10. Carnivore tooth pit analysis

Sixteen specimens are confirmed to have carnivore modification and can be assessed. These are discussed below.

SF 4217 from Member 4 is a left distal radius with two pits and a single score.

- a. the first pit is located medially on the most antero-proximal corner of the medial malleolus, on the epiphysis. It has a length of 4.73mm and a breadth 4.3mm,
- b. the second pit lies on the epiphysis on the most distal and posterior portion of the specimen. It is 4.98mm long and 4.39mm wide, and
- c. the score is located on the epiphysis. It starts from the proximo-posterior-medial corner of the medial malleolus. It has a length of 7.54mm and a breadth of 4.77mm.

SF 1465 is a right proximal ulna belonging to a papionin individual. It possesses a pit located on its antero-proximal corner of the olecranon process with the following measurements, 5.68mm long and 4.88mm wide.

SWP 377d, a *Papio* or *Parapapio* distal humerus has three pits on the diaphysis, on the anterior lateral corner.

- a. the first pit is 2.9mm long and 2.2mm wide,
- b. the second pit's length is 2.1mm and the breadth is 1.9mm, and
- c. the third pit has a length of 5.0mm and a breadth of 3.5mm

SWP 526, an unidentified left proximal femur, has a pit located on the posterior surface of the head, on the corner of the neck. Its pit, located on the diaphysis, has a length of 3.74mm and a breadth of 2.18mm.

SWP 531 is a *Papio/Parapapio* right proximal femur with three pits:

- a. the first pit on this specimen is located on the diaphysis, on the anterior central portion of the femur neck. It has a length of 2.95mm and a breadth of 2.83mm,

- b. the second pit measures 3.42mm long and 2.56mm wide; it lies below the neck on the diaphysis,
- c. the third pit is located on the epiphysis, on the anterior corner of the greater trochanter, and, it measures 3.44mm long and 2.43mm wide.

SWP 756, an unidentified right proximal femur, has a score on the diaphysis and anterior surface of the head which is 9.06mm long and 5.67mm wide.

SWP 896 is an unidentified femur head with a score located on the diaphysis, on the distal ridge of head. It has a length of 8.46mm and a breadth of 1.45mm.

SWP 1104 (Fig. 5.10), a left cf. *Theropithecus* proximal ulna. It possesses three pits located on the diaphysis in a proximo-distal linear fashion:

- a. the most proximal pit is situated on the lateral posterior portion of the olecranon. Its longest axis is 7.76mm and it is 4.51mm wide.
- b. below pit a. is a second pit on the medial portion of olecranon. It is 4.51mm long and 3.74mm wide, and
- c. the most distal pit has a length measuring 5.34mm and a breadth measuring 4.47mm.

SWP 1119, a *Papio/Parapapio* distal humerus possesses a pit located above the olecranon fossa on the anterior surface. It is 3.94mm long and 2.20 wide.

SWP 1137 is a *Papio* distal humerus with two pits:

- a. the first pit is located on the anterior medial epicondyle, it is positioned proximo-distally in a linear manner. It is 5.94mm long and 4.99mm wide, and
- b. the second pit is located posterior on the proximal portion of the trochlea covering most of the trochlea; it is 6.99mm long and 4.02mm wide.



Figure 5.10. SWP 1104, a left proximal cf. *Theropithecus* sp ulna with three carnivore tooth pits.

SWP 1140 (Fig 5.11), a *Papio/Parapapio* right distal humerus: This specimen possesses 3 pits-

- a. on the anterior portion of the lateral epicondyle, located on the corner of the anterior proximal corner of the trochlea fossa (with a length of 7.01mm and a breadth of 5.02mm),
- b. the second pit is located on the distal portion of the first pit and measures 6.99mm long and 5.02mm wide, and
- c. the last and most distal pit is positioned on the anterior of the capitulum. It is 7.99mm long and 5.01mm wide.

SWP 1206, a left femur head of a *Papio/Parapapio*, has two pits located on the femoral head.

- a. the first pit has a length of 7.63mm and breadth of 5.66mm.
- b. the second pit is 5.66mm long and 1.66mm wide.

SWP 1263, a *Papio/Parapapio* left distal humerus has a pit located on the trochlea, on the anterior surface; its length is 6.13mm and its breadth 4.86mm.

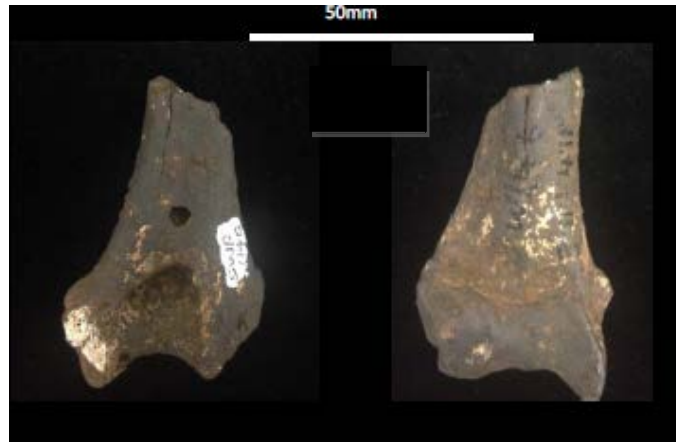


Figure 5.11. SWP 1140, a *Papio/Parapapio* distal humerus demonstrating carnivore toothpit marks

SWP 1271, a *Papio/Parapapio* right distal humerus; two pits are observed on this specimen.

- a. the first is located on the posterior proximal corner of the trochlea; it has a length measuring 6.18mm and a breadth which measures 5.09mm, and
- b. the second and distal pit is located on the inferior portion of the lateral epicondyle; it is 7.01mm long and 4.98mm wide.

SWP 1351, an indeterminate cercopithecoid right proximal femur: one pit is observed in this specimen on the anterior neck between the head and the lesser trochanter, it is 5.90mm long and 4.34mm wide.

SWP 1416, a *Papionini* indet right proximal radius with a pit on the diaphysis, on the medial side above radial notch, it is 7.25mm long and 6.66mm wide.

From the above sample, a pattern is observed in the location of the pits on humeral specimens. The pits are concentrated on the trochlea and capitulum. The results of the tooth pit data are outlined in Appendix C, Figures C19-20. Pits which occur on the epiphyses of the postcrania identified suggest that they were imparted by middle sized carnivores and hyaenas; lions are implicated by the breadth size. The length (>4mm) and

breadth size ( $>2\text{mm}$ ) on the diaphysis, which is larger than indicate that they were inflicted by hyenas, dogs and or lions. Data derived from scores is inconclusive as the true population range is too wide and the sample size is too small to infer any meaningful conclusions.

## **CHAPTER SIX**

### **RESULTS: SPATIAL DISTRIBUTION OF THE STERKFORNTEIN FOSSIL CERCOPITHECOID POSTCRANIA**

The complex periods of deposition, collapse and re-deposition of materials into the Sterkfontein caves are evident in the lack of distinct spatial clusters and clustering of primate fauna in possible mixed deposits. The various depositional processes recorded in Member 2 and Member 4 do not demonstrate taxonomic spatial bias among the primate remains. Jacovec Cavern's spatial separation of the hominids from the majority of the fossil cercopithecoids is interpreted as a result of hominid use at the time of accumulation. Member 4 primates demonstrate the least movement around the cave subsequent to deposition. The northern part of the StW 53 infill suggests that it is of a closer time frame to Member 4 due to the higher preservation of fossil primates in that corner and to the similar cercopithecoid taxonomic composition to Member 4. The drastic decline in primate frequencies in the younger Member 5, Member 6 and post Member 6 deposits has not yielded any spatial patterns. This chapter provides the description of spatial distribution patterns of cercopithecoid fossils and initial interpretations on the modes of accumulation which led to the accumulation of the fossil monkeys. The specimens are studied out of their original context; these were not digitally recorded. As a result, only the excavation squares and levels are examined for the spatial clustering.

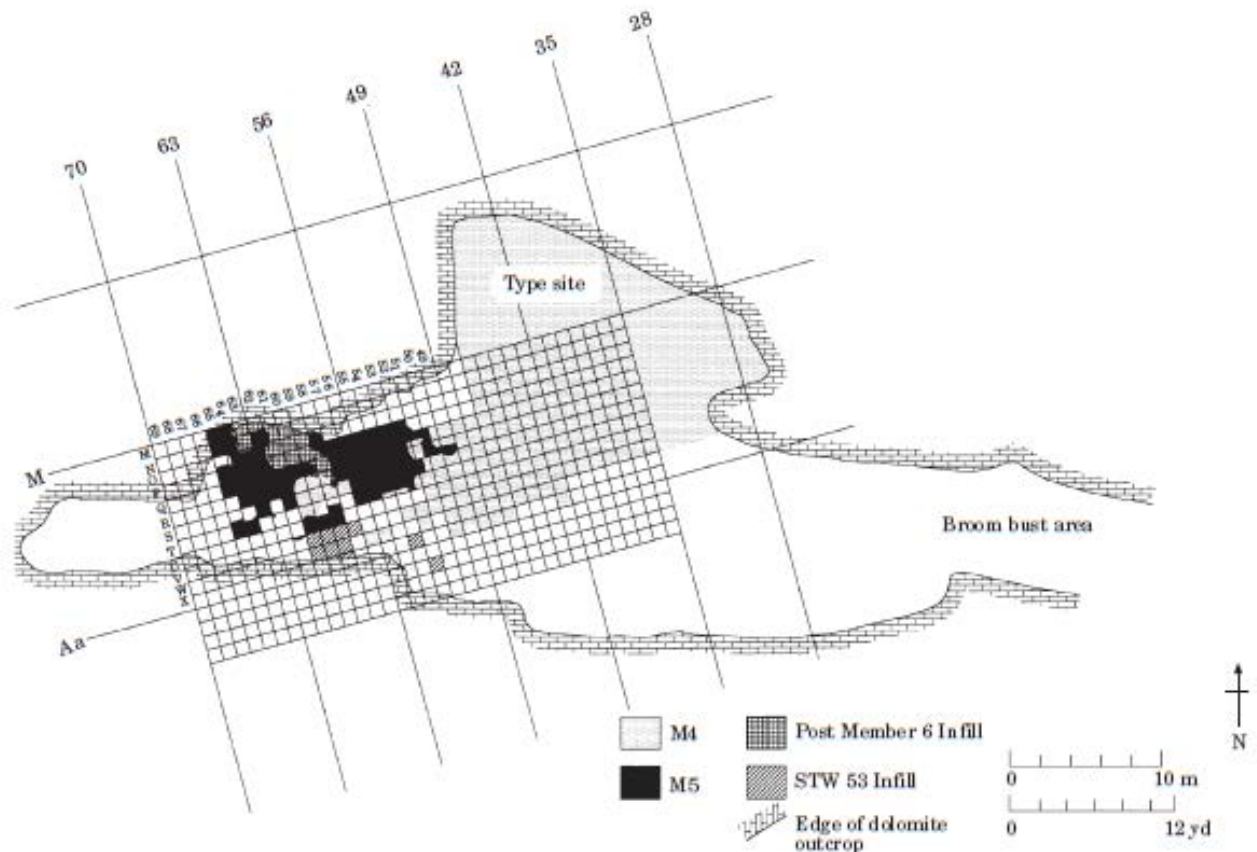


Figure 6.1. Sterkfontein Caves surface distribution demonstrating Member 4, Member 5 East, Member 5 West and the Post Member 6 infill. (after Kuman & Clarke 2000).

## 6.1. Jacovec Cavern

The Jacovec Cavern fossiliferous infills have formed through a number of depositional processes (Partridge 2003). The cave shaft opening, which is currently blocked, was located in the eastern end of Cavern. The ceiling and walls are covered by stony breccia with a patch of the older, orange breccia exposed in the ceiling. The orange breccia which is about 3 m



deep and has yielded remains of a hominid skull (STW 578). A younger westward sloping dark-brown, slightly calcified deposit which is about 1 m deep completely fills the eastern end of the Cavern (*ibid.*). On the floor, there is evidence of a collapsed orange breccia mixed with the younger dark-brown breccia, which yielded hominid fragments and cercopithecoid remains. Other taxa identified within the deposit include members of the Bovidae, Viverridae, Herpestidae, Felidae, Hyaenidae and Canidae families. Also preserved are *Pedetes capensis* (spring hare), *Potamochoerus porcus* (bushpig) and *Lepus capensis* (the Cape hare). These deposits were subsequently filled by a calcite flowstone which formed over these sediments (Partridge 2003). The *Australopithecus* partial cranium, StW 578, was excavated *in situ* from the orange breccia which is exposed in the roof (*ibid.*). The rest of the materials were recovered *ex situ* from the mixed breccia on the floor of the chamber (Kibii 2004)

The orange breccia contains only 5% (10 NISP) of the total Jacovec Cavern fossil cercopithecoid postcrania assemblage. Only two of these are long bones (one ulna and one femur), there are also two clavicles and six extremities. The *in situ* orange breccia also preserves 12 hominid specimens which represent six *Australopithecus* individuals (Kibii 2004). The small sample recovered in this part of the infill does not have much implication in terms of spatial distribution of skeletal elements as they were only provenanced to breccias type.

The younger brown breccia which is visible as a talus cone preserves 8% (NISP: 14) of the Jacovec Cavern fossil cercopithecoid post-crania sub-assemblage; the rest of which were discovered on the floor of the cavern. Neither juvenile cercopithecoids nor the hominids are found in this section of the cavern. Axial skeletal elements are limited, with the exception of two clavicles.

Based on the current study sample the orange breccia bears the least amount of primate remains within the Jacovec Cave System, but preserves all of the hominid assemblage. Most (NISP: 157, 86%) of the Jacovec fossil cercopithecoid postcrania lie on the cavern floor in the combined breccia. This could suggest that the majority of the cercopithecoid specimens in the orange breccia were spatially separated from the hominids which remained intact after the slump of the deposit. Kibii (2004) concluded that Jacovec Cavern primates accumulated

as a result of surface slopewash of the materials which were within the catchment area around the cave. A possible scenario therefore is that the hominids were within the collection close to the cave entrance in the east of the cave during the accumulation of the orange breccia. When the brown breccia accumulated cercopithecoids were the dominant primates within the catchment area.

## **6.2. Silberberg Grotto**

Member 2 formed through different ‘facies’ (Partridge 2000; Clarke 2002, Bruxelles *et al.* 2014). A rocky talus cone which dips to the west formed underneath the roof of the Silberberg Grotto; this is the same infill which contained the StW 573 skeleton (Clarke 1999). Over a long period, this deposit was cemented by calcium carbonate water. However other sediments were slightly cemented and remain ‘silty and soft’ (Bruxelles *et al.* 2014:46) Water entered the cave from the entrance. Cavities also formed within the breccia as a result of erosion. These cavities would cause collapse of the roof above them. Calcite was deposited and flowstone covered the collapsed part of the StW 573. Some of the cavities were filled with flowstone floors from the bottom to the ceiling while others remained unfilled (Bruxelles *et al.* 2014).

Between 1978 and the 1980s, Alun Hughes’ team removed lime miners’ breccia from Dump 20 that covered the floor of the Silberberg Grotto. This included Member 2 and some parts of the Member 3 deposit. These were accumulated through an aven, in the roof of the Silberberg Grotto. Within the eastern region, which is highly fossiliferous, carnivores, some bovid remains and other taxa form part of the Silberberg Grotto (specifically the Member 2) faunal assemblage (Clarke 1999; Pickering *et al.* 2004a). The *Australopithecus prometheus* skeleton was located on the western face of the infill at the base of a steep slope with fossil cercopithecoid remains (Clarke 1999; Pickering *et al.* 2004a). The Member 2 *in situ* fossils, where most of the fossil cercopithecoid remains were recovered, were excavated by controlled blasting in the eastern end by Clarke in 1997 (Pickering *et al.* 2004). No spatial patterns are detected within and between the two facies, but the excavated areas are very limited.

	Small	Medium	Large
Adult	■	●	▲
Subadult	■	●	▲
Juvenile	■	●	▲

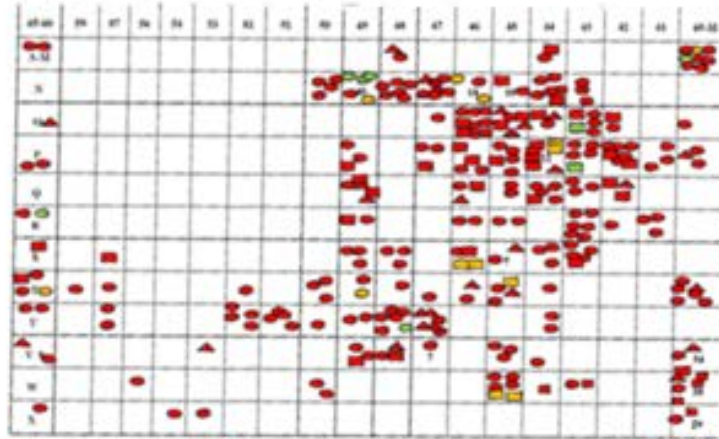


Figure 6.2 Member 4 spatial distribution of skeletal elements based on age and size

### 6.3. Member 4

The main cave opening at the time of accumulation of Member 4 was south-east of the cave (Partridge 1978). This shaft cavity was disturbed by successive roof collapses which led to the enlargement of the original shaft opening. Member 4 was a large underground chamber which was deposited as a talus and is now exposed due to weathering of the dolomite roof (Robinson 1962). The south-western part of the deposit collapsed leaving a void which was filled by subsequent deposits such as Member 5 deposits (Ogola 2009). A hanging remnant of Member 4 (the StW 53 sediments) is exposed in the western end of the cavern's southern wall. Partridge's (1978) stratigraphic analysis of the Member 4 deposit suggests the presence of four beds, A-D. Bed A is a red calcified sandy silt which contains some bone fragments and measures 2 to 3 m. Bed B is a reddish brown sandy loam which is exposed in the lower levels of the Extension site and the Type Site. It contains remains of *Australopithecus*. Bed B is also an *Australopithecus* bearing deposit; it has yielded the "Mrs Ples" crania. Bed C lies on top of an eroded section of Bed B. It is 0.5-2m reddish brown silty sand. Bed D is a laminated flowstone deposit (Partridge 1978).

The Member 4 assemblage is more widespread relative to other deposits in the Sterkfontein Caves (Figure 6.1). The excavation starts from 1.2 m (four feet) down to 9 m (30 plus feet) below the datum line in squares e.g. N45, P42-45, R43-45 and T43. The northerly parts of Member 4 preserve the least (2.8%; NISP, 29) of the fossil cercopithecoid postcrania in Member 4. Only one small sized specimen was discovered from this part of the deposit. The largest concentration of the fossil cercopithecoids is in the more central to westerly located within Member 4. Dump 13 preserves the most specimens compared to other dumps from Member 4. The fossil cercopithecoid postcrania suggest that the western and the southwestern end of Member 4 (where the original cave opening was located at the time of accumulation) are possibly a different phase of the whole Member 4 deposits as this part of the cave preserves the highest frequency of cercopithecoids compared to other parts. The western-most part of Member 4, where it interfaces with Member 5 is very sparse in fossil cercopithecoids and preserves large sized skeletal elements at 6% of NISP, whereas these large sized monkeys are absent in the StW 53 deposit. Squares east of line 50 within

Member 4 are rich in fossil monkeys and preserve a large variety of size and age classes. This is very different from line 50 and the squares situated westerly of this line. High frequencies of fossil cercopithecoid specimens within the former squares are related to high numbers of hominids within the same region of the deposit. Hominid remains dominate and are the only primates in squares H42, Q40, U46, U45, V46, W46, W47, U43 and V43. These hominid remains however, are still concentrated in the same region (even though they are not the same squares) as the cercopithecoids, which is central to westerly of the deposit.

This concentration of the hominids in particular, is aligned with the north-westerly dip of the deposit. It also suggests that once the hominid fossil remains entered the cave, they, either did not tumble far from the entrance or the accumulation was through different phases. The distribution of fossil cercopithecoids also points to the same scenario. There is no spatial separation or clustering between cercopithecoid taxa within the deposit. Cranio-dental remains of the large colobine, *Cercopithecoides*, in the Member 4 deposit were recovered with other tribes, from the D13 and D14 dumps as well as from the main 'Type Site' as recorded in the Broom and Robinson's excavations.

Three different phases are detected from the spatial clustering in terms of the depth. Large concentrations of specimens are found in the upper levels of the Member 4 deposit and the very lower levels of the deposit, while the middle levels (between 18" and 25" below datum) preserve the least numbers of specimens. This clustering supports the hypothesis by Kuman and Clarke (2000) that Member 4 accumulated through different phases and probably through a relatively longer time span. Partridge (1978) identifies four beds within the deposit; however, analysis based on fossil primates currently distinguishes three periods.

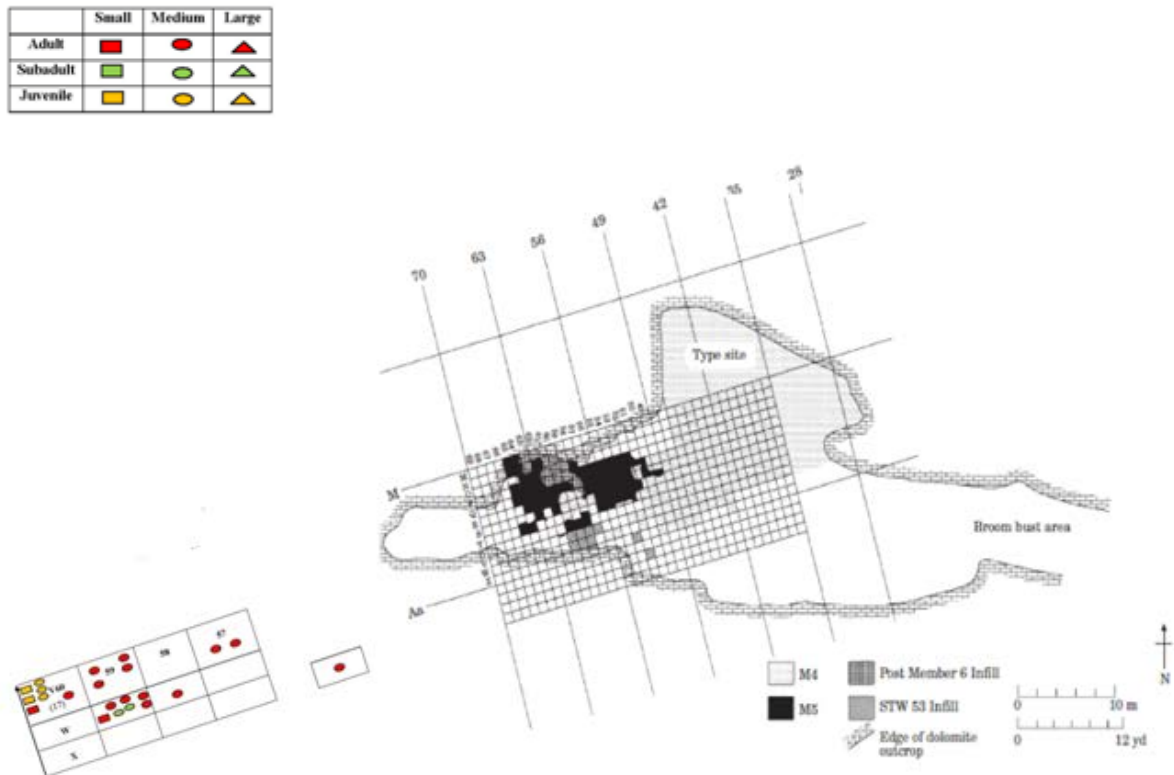


Figure 6.3. StW 53 spatial distribution of skeletal elements based on age and size.

#### 6.4. STW 53 Infill

The collapse and erosion of the Member 4 deposit in the western and central areas left a hanging remnant of Member 4 which filled the cracks with an *in situ* solid breccia, StW 53 (Kuman and Clarke 2000). The entrance at the time of deposition was located in the south east (*ibid*). The excavation of the specimens is spread through a 3 meters (10 feet) depth and there is no visible pattern chronologically. This deposit is characterised by *Theropithecus* specimens. All *Theropithecus* specimens are concentrated in the W-V 59-60 squares. The genera *Papio* and *Parapapio* have also been identified in this deposit and they are more spread throughout the deposit compared to *Theropithecus*. The square X53, located south east of the StW 53 deposit and isolated from the main StW 53 deposit, preserves one specimen and the only *Colobine sp* in this assemblage. The square is currently isolated as the squares in between are currently under investigation. Most of the specimens (63% NISP of

the cercopithecoid postcrania assemblage and 88% NISP of the total fossil primate assemblage) lie in the north-western corner of the deposit, in square V60. This is followed by Square W59 and V59 which have four and six specimens respectively. The large concentration of the primate fossil remains entered the cave in the south east and, moved and aligned with the northwest dip of the infill to fill the northwest corner of the deposit. This suggests different phases of accumulation.

Clarke (1994) maintained that there is a stratigraphic separation between StW 53 and the Member 5 deposits. The difference between these deposits is also supported by faunal content (Pickering 1999, Kibii 2004). Taxonomic composition of StW 53 demonstrates a very different pattern from the Member 5 West deposit. The high concentration of specimens in the north western corner of the StW 53 deposit demonstrates a link between Member 4 and StW 53. The rest of StW 53 deposit is not as abundant with primate remains as the square V60 corner. StW 53 was formed after 2.6My, a period associated with a change towards a drier conditions and the decline of primate numbers. The corner possibly represents the earliest materials which accumulated at the early stages of StW53 deposition

	Small	Medium	Large
Adult	■	●	▲
Subadult	■	●	▲
Juvenile	■	●	▲

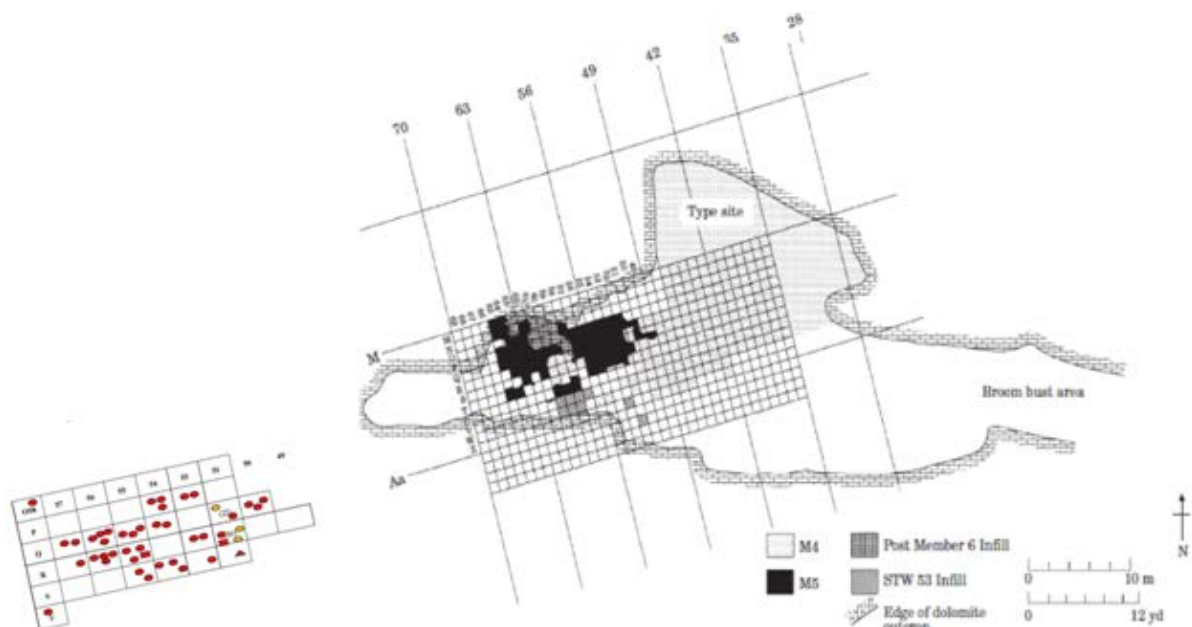


Figure 6.4. Oldowan Infill spatial distribution of skeletal elements based on age and size.

### 6.5. Oldowan Infill

The Oldowan infill accumulated in a small area as a result of the collapse and erosion of the Member 4 breccia (Kuman & Clarke 2000). The deposit is limited to a 4 m (15 feet) horizontal surface in the Member 5 East, and lies 6 to 9 m (22 to 36) feet below datum in the deepest square which suggests that the materials accumulated through a narrow vertical shaft (*ibid.*).

The pattern of preservation of fossil cercopithecoid postcrania within these deposits in the Member 4 erosion channels supports the spatial and temporal separation of these deposits from either StW53 or the earlier Member 4 assemblage (see Figure 6.1). Based on present data, the spatial separation of this westerly deposit from the eastern Oldowan deposit is not clear. The majority of the postcranial specimens are concentrated in the R51 and Q51 (34% and 23% of NISP), accounting for more than half of the cercopithecoid postcranial assemblage. These squares are at the north easterly end of the Member 5 East deposits and at the junction with Member 4. This concentration does not discriminate based on body part or on size. Both squares, R51 and Q51, have a full range of skeletal elements. However, these two squares only form NISP 33% of the whole fossil primate assemblage. The cranio-dental remains, which form 55% of the Oldowan primate NISP, are spread throughout the deposit. However the archaeology shows them to be distinct as Member 5 West contains early Acheulian artefacts (Kuman & Clarke 2000).



	Small	Medium	Large
Adult	■	●	▲
Subadult	■	●	▲
Juvenile	■	●	▲

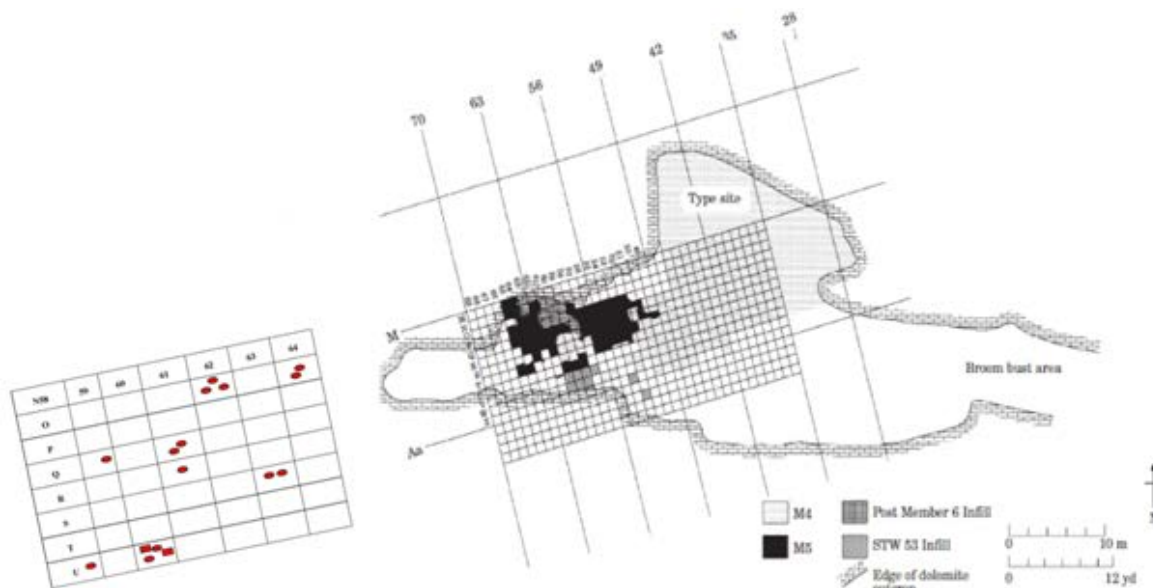


Figure 6.5. Member 5 West spatial distribution of skeletal elements based on age and size.

## 6.5. Member 5 West

The Member 5 West breccias (Figure 6.1) formed within the collapsed area of Member 4 (Ogola 2009). It is sandwiched between two flowstones, one overlying it and the other one curtaining Member 4 on the southern end. Two facies of Member 5 West have been identified (Ogola 2009). The earliest deposit consists of a fine brown breccia which lies against the Member 4 curtaining flowstone and was subsequently covered by a coarse pinkish breccia. Both sediments bear stone tools (Kuman & Clarke 2000). The pinkish breccia is covered by a capped flowstone to the north, and a yellowish microfauna breccia to the south. Square U60, located in the south, has a larger concentration (33% NISP) of the Member 5 West materials. This is within the pinkish breccia in the north. This is also where the only two small specimens within the deposit were discovered. There is neither a distinct pattern observed in the body part distribution within the deposit nor is there a pattern in the age profiles. The only two taxonomically identified specimens *Parapapio* (SWP 1119) and a

*Papionin* (SWP 1154) in the sample come from square Q59 which is in the south-east and square U58 at the south of the deposit. The specimens are spread between spits 17'9"-18'9" and 9'5"-10'5".

## **6.6. Member 6**

Subsequent to the Member 5 deposits a flowstone cap formed in the north-western portion (Ogola 2009). The Member 6 breccia formed on top of this flowstone, beneath the cave roof. Ogola (2009) argues that the Member 6 cave was vertically restricted. Following this formation, parts of the Member 5 and Member 6 breccia were eroded away (Kuman & Clark 2000; Ogola 2009). Member 6 only preserves two cercopithecoid postcrania. These were discovered in the same decalcified deposit alongside bovids, carnivores, equids and hyraxes (Ogola 2009). Therefore no specific spatial information can be derived from the fossil primate faunal data. The near-absence of primates in this deposit is linked to taphonomic factors discussed in Chapter 7.

## **6.7. Post Member 6**

The concentration of the skeletal remains within the Post-Member 6 deposit suggests that they predominantly accumulated in the early stages of formation of the deposit, as they are more concentrated in the lower levels, and abruptly ceased to accumulate towards the end of the deposit.

The erosion of the Member 5 and Member 6 breccia was followed by filling with the post-Member 6 deposit in a large area in the northern part of the cavern. It lies horizontally and is decalcified (Kuman & Clarke 2000; Ogola 2009). Within the Order Primates, there are no observed taxonomic spatial clustering preferences. The single *Homo sapien* specimen was discovered alongside fossil cercopithecoid remains (Kuman & Clarke 2000; Ogola 2009). Chronological distribution of the Post Member 6 primate assemblage indicates that 99% of the specimens derive from the lower levels (between 13'9" - 14'9" and 21'10" - 22'10") while only 1 primate specimen is from the upper level (8'1" – 9'1"). However, other taxa (e.g.

bovids and carnivores constitute 99% of the fauna NISP) are represented in the younger upper levels of the deposit.

#### **6.8. Sterkfontein deposits spatial patterns based on fossil cercopithecoid postcrania**

Spatial analysis of the Sterkfontein fossil cercopithecoid postcrania does not demonstrate any considerable spatial patterns. Complex geological processes of deposition, roof collapse and refilling of deposits point to complex taphonomic factors which have influenced the spatial arrangements of the assemblage at the time of recovery. Member 2 points to different taphonomic events which led to different facies of site formation as indicated by Bruxelles *et al.* (2014). The discovery of the majority of the specimens in the mixed breccia on the floor of the Jacovec Cavern, which is *ex situ*, points to a mosaic of events which led to the configuration of the Jacovec Cavern breccias.

Member 4, however, suggests different phases of accumulation represented in the deposit. Temporal variability in the accumulation of the deposit is proposed by the three phases discerned from the fossil cercopithecoid assemblage. Faunal occurrence of the northern corner of the StW 53 deposit demonstrates to be closer in time to the Member 4 deposit. This is the deposit which Kuman and Clarke (2000) have suggested to be a hanging remnant of Member 4. The decreased primate frequencies in Member 5 deposits, even in the deep Oldowan Infill, point more to a changing environment than to spatial patterning.

The depiction provided by examination of the fossil cercopithecoid spatial arrangement of the Sterkfontein Cave deposits is that of complex processes of deposition, collapse and re-deposition which have rendered most of the materials *ex situ*, and as a result provides little significant data on spatial patterns within the cave.

## CHAPTER SEVEN

### DISCUSSION

#### 7.1. Taxonomy of the fossil Cercopithecoidea of the Sterkfontein fossil cave site

Three papionin genera are identified from the Sterkfontein Caves fossil postcrania, *Parapapio*, *Papio* and *Theropithecus*. A Cercopithecini, *Cercopithecus* is present in the assemblage. Colobines are present and so is the large fossil colobine, *Cercopithecoides* sp. The fragmentary nature of the Sterkfontein fossil cercopithecoid postcranial remains has impacted on the study by reducing the percentage of identifiable Rock fall, sediment compaction, lime mining activities and excavation damage have contributed to the fragmentation of the assemblages. None of the cercopithecoid postcrania could be indisputably linked to cranial remains from the same deposit.

Cranio-dental data demonstrate a more varied picture of taxa which were accumulated into the Sterkfontein Caves deposits. Seven genera and eight species have been identified from fossil cranio-dental remains: *Papio izodi*, *Parapapio broomi*, *Parapapio jonesi*, *Chlorocebus aethiops*, *Theropithecus oswaldi*, *Cercopithecoides williamsi*, *Colobus* sp. and *Cercocebus*. However, none of the postcranial elements could be confidently assigned to species level. The poor state of preservation of the skeletal elements and the general rareness of identified fossil postcrania which can be utilised as comparative materials also contributed to the restriction in identifying the specimens to the lowest (i.e. species) possible level. The distinction between *Papio* and *Parapapio* skeletal elements was also hindered by fragmented skeletal elements. A quarter of identified specimens could not be differentiated between *Papio* and *Parapapio*, and therefore a general category *Papio/Parapapio* was created. This is also the most commonly occurring taxa. The difficulty in delineating between the *Papio* and *Parapapio* genus has been part of Sterkfontein papionin classifications as early as the 1970's. Eisenhart (1974) stated that

*Parapapio* dentition is not easily distinguishable from *Papio*. The nasal side profile has been applied as a distinguishing trait between the two genera (Eisenhart 1974; Brain 1981). Even the validity of this character as a marker between *Papio* and *Parapapio* has been questioned (e.g. Jones 1978). The debate surrounding this distinction demonstrates the morphological overlaps between the two genera. Even in this study, the author could not make distinction between the two genera.

Sterkfontein preserves skeletal elements which are assigned to the *Parapapio* genus, and a large contingent of skeletal remains which are very similar to *Papio*. The sizes identified within *Parapapio* are also variable. Data derived from fossil cercopithecoid postcrania remains in the Sterkfontein deposits suggest the presence of small, medium and large sized *Parapapio*. This range of sizes and the variable upper forearm morphology are a likely indicator of different species as suggested by Jablonskii *et al.* (2008). However, due to the incomplete nature of the specimens, none of these could be identified to species level.

Even in the light of a very fragmented and limited postcranial assemblage, *Parapapio* morphological traits assessed in this study are consistent with East African *Parapapio* and also point to a generalist with a mosaic of morphological traits. The generalist nature of *Parapapio*'s forearm suggests that the genus navigated various substrates in the ecosystem. Therefore a generalist *Parapapio* would have survived the changing environment of Sterkfontein from the Pliocene to the Early Pleistocene.

South Africa's fossil *Papio* is regarded as ancestral to modern *Papio*, as suggested by Gilbert and colleagues (2016) in their assessment of fossil humeri of *Procercocebus* and *Papio* from Taung, South Africa. The fossil *Papio* postcranial remains from Sterkfontein have demonstrated commonality with the modern *Papio* species, suggesting some relationship between the modern and fossil variants of the genus *Papio*. The genus *Papio* on the other hand seems to have survived major environmental shifts which took place from the Plio-Pleistocene to the present day and outlived most fossil cercopithecoid counterparts in southern Africa. *Papio* occupies the widest parts of modern day Africa

with varied species constituting the genus (Napier & Napier 1967). The relationship between fossil and modern *Papio* species in Africa is yet to be investigated.

The long time span of *Papio* and *Parapapio* genera in the Sterkfontein caves fossil record supports the conclusion reached by numerous authors (Heaton 2006; Williams *et al.*, 2007; Gilbert 2008) that the changes in the Sterkfontein palaeoenvironment were gradual and that the habitat was quite variable, accommodating different primate species. Future research on the Member 3 deposit and its contents could shed more light on the transition between Member 2 and Member 4.

Twenty-two percent of identified postcrania in the Member 4 cercopithecoid sample assessed by Ciochon (1993) were *T. darti* specimens. No fossil cranio-dental remains have been assigned to *Theropithecus* earlier than Member 5 deposits. However, this does not exclude the presence of *Theropithecus* in the environment at the time. *Theropithecus* is present in Gladysvale between 2.5 My and 1.7 My (Berger *et al.* 1993).

The dominance of papionins over other members of the Cercopithecidae family correlates with data derived from cranio-dental remains. Colobines are present in the Sterkfontein fossil record, although in limited numbers. Their scant numbers are likely to be a factor of the environment within which these primates existed. Even terrestrial *Cercopithecoides* is not as abundant as terrestrial papionins. The *Cercopithecoides* identified in the Sterkfontein sample is probably *C. williamsi*. However, data derived from this study is not sufficient to attribute the specimens to the species.

Taxonomic variability is demonstrated by primate postcrania over time. Papionins dominate the earliest deposits. Jacovec Cavern and the Silberberg Grotto preserve comparable fossil cercopithecoid taxa. Continuity of these is observed in Member 4, which is the most complex and lengthy accumulation of deposits within the Sterkfontein Cave system. The largest taxonomic variability is observed in the Member 4 deposit, followed by Member 2 and the Jacovec Cavern. Papionins are less represented in the

younger Pleistocene deposits, and this is also marked by the appearance of small sized fossil primates, e.g. *Cercopithecus*.

El Zaatari and colleagues' (2011) study on molar micro-wear and dietary reconstruction of Sterkfontein Cercopithecoidea shows that there is no visible distinction between the earlier wooded deposits and the later more open ones in terms of the dietary habits of the fossil cercopithecoid taxa. The consistency of the dietary habits among fossil cercopithecoids is an indication of consistency in available and accessible food sources in the Sterkfontein valley area.

O'Regan and Reynolds (2011) hypothesis for time averaging represented within the Member 4 deposits is suggested as an explanation for the large primate taxonomic diversity observed in Member 4. Member 4 is the only deposit that preserves such a large contingent of cercopithecoid taxa in the whole Sterkfontein Cave system. Time averaging is likely, however, it cannot be established by the current study.

*Theropithecus* species in the southern African fossil record also occupy a specialised period during the Plio-Pleistocene and do not occur in that part of Africa by the late Pleistocene. The morphology and body size of *Theropithecus* are different from *Parapapio*. The large and robust form of *Theropithecus* contrasts with *Parapapio* which has a smaller and more gracile frame. However, the smaller *T. darti* is recorded alongside *Parapapio* and *Papio*, while the larger *T. oswaldi* is coupled with *Papio* to the exclusion of *Parapapio*. Even though these genera are contemporaneous, the demands that the environment placed on them for their survival were probably not comparable. Predation from carnivores and availability of food sources would have had an impact on their survival in the Sterkfontein region.

*Parapapio broomi* and *Parapapio jonesi* had a mixed diet (El-Zaatari *et al.* 2005). Makapansgat *Theropithecus darti* had a diet similar to modern *Theropithecus gelada*; it was a grass and leaf eater. *Theropithecus oswaldi* had a varied diet which consisted of grass leaves and fruit, *Papio robinsoni* at Swartkrans probably subsisted on grass and/or

leaves (*ibid.*) El- Zaatari *et al.*'s study demonstrates that there is no distinction between the dietary habits of the earlier *Parapapio* and *Theropithecus* taxa over time. The lack of changes between earlier and younger taxa suggests that environmental shifts which occurred in southern African fossil cave sites were gradual and the change the environmental change was observed between 3Ma and 1.8Ma (Luyt & Lee-Thorp 2003).

In this study, the role that postcrania can play in taxonomic identification of fossil cercopithecoids is elucidated. However reliance on previous taxonomic studies and association with cranio-dental data is emphasised for a fuller picture.

## **7.2. Carnivore modification data**

Tooth pit data sourced from the Sterkfontein fossil cercopithecoid postcrania assemblage are very limited. The nature of the method of analysis excluded a relatively larger sample of carnivore modified marks which were not manifested as pits or scores or which are covered by matrix.

The results of the tooth pits data suggest that they were mainly imparted by medium sized carnivores, hyenas and lions. *Panthera pardus*, *Chasmaporthetes* and an indeterminate hyaena are the common medium sized carnivores identified within all the Sterkfontein cave deposits (Kibii 2004; Pickering *et al.* 2004; Ogola 2009). *Panthera leo* is also part of the carnivore community represented in Sterkfontein fossil fauna assemblages, particularly in Jacovec Cavern, Member 2, Member 4 and the Member 5 deposits (Pickering 1999; Pickering *et al.* 2004a; Kibii 2004). The length of the pits excludes the possibility of large sized carnivores as the cause of the pit.

Hyenas and leopards are known to use caves as breeding areas, dens and places of retreat (Simons 1966; Brain 1981; Lam 1992; Klein *et al.* 1999). Hyaena and leopard-accumulated assemblages are characterised by a high proportion of carnivores and primates (Simons 1966; Pickering 2002). This is the case for the Member 2 assemblage.



However, it is expected that hyaena collections will preserve coprolites and juvenile carnivore remains as they leave behind their young in dens when hunting. Brown hyenas (*Hyaena brunnea*), in particular, are known to prey on small carnivores for their young and transport the food back to the den (Brain 1981; Mills & Mills 1977). Therefore, carnivore juvenile remains will form a significant component of an assemblage collected by hyaenas and leopards in a den scenario. This is not supported by data from the Sterkfontein fossil faunal assemblages. Carnivore juveniles and coprolites are absent in Members 2, 4 and 6 (Kibii 2004; Pickering *et al.* 2004; Ogola 2009). Post Member 6 preserves carnivore juveniles and coprolite remains (Ogola 2009). Prior to that time the vertical alignment and depth of the entrance shaft would have made caves generally inaccessible for use as dens. Therefore a den scenario is not suggested for the earlier deposits.

Kibii's (2004) faunal analysis suggests that carnivore accumulation in Jacovec Cavern and Member 4 occurred as a result of resident carnivores which occupied the vicinity of the cave, above and around the entrances. Therefore leopards and hyaenas were likely using the cave localities as areas for retreat, as suggested by Simons (1966).

### **7.3. Taphonomy of the fossil cercopithecoids of the Sterkfontein Cave site**

The taphonomy of the Sterkfontein fossil cercopithecoid community has indicated an array of processes which have impacted on the fossil remains. This is more so in the Jacovec Cavern and Member 4 deposit.

The absence of large juveniles and large sub-adult individuals is a distinct feature in the taphonomic history of the Sterkfontein Cave non-hominid primates. These age groups are present in other faunal size categories. The fact that other fauna preserve all age groups suggests that this is likely the result of taphonomic factors

The social organisation of *Theropithecus gelada*, the sole surviving species of this genus, is such that the females (and their young) have a strong coalition with each other and tend to remain in their 'reproductive units', while the males are 'socially peripheral' (Dunbar

1993: 432). Therefore females will most likely remain in a social group with juveniles, while males wander off without the young to join 'non breeding male groups' or to be part of another 'band' or 'herd' (Dunbar 1993). Reproductive units tend to avoid areas where risk of predation by carnivores is high, unless they can join herds and the prospective habitat is rich in food sources (*ibid.*). Therefore the likelihood that the catchment areas for the caves were further from these 'reproductive units' or similar organisations of these large primates is possible. However, the presence of these age groups in other families suggests that this could be the result of taphonomic bias.

The multiple scenarios which have impacted on the primate assemblages include surface slope wash, tumbling, sediment compaction, carnivore accumulation and death traps. The most common mode of accumulation, surface slope wash, is indicated in Jacovec Cavern, Member 4 and the Member 5 West deposits, even through other taphonomic processes took place within these deposits. Some of the Member 2 and Member 4 fossil primate remains fell into the cave and eventually died in the cave.

No two deposits preserve the same taphonomic package and no post-depositional feature is exclusive to a specific deposit. Due to the extent of the deposit and associated quantities, Member 4 preserves the widest range of accumulation patterns over the longest period of time. Member 4 is the only deposit which, based on fossil cercopithecoid fauna, demonstrates different patterns of accumulation (Kibii 2004). Locomotor habitat classification of the Member 4 cercopithecoid postcrania indicated the presence of three habitat types, forest, open woodland and grassland (Elton 2001).. O'Regan and Reynolds (2009) propose that Member 4 is a long, time-averaged sample. Member 4 accumulated through a period spanning around 300,000 years (Partridge 1978). This is sufficient time for different modes of accumulation to take place through time or even different cave entrances which were opened due to processes such as dissolution of dolomite and voids caused by collapse of the breccia.

Cercopithecoids in the Member 5 deposits are outnumbered by carnivores, bovids and other macro-mammalian taxa (Pickering 1999). This trend is also observed in Member 6 and Post Member 6 (Ogola 2009). In the southern African fossil record, the tendency is

also observed in Swartkrans and Kromdraai. The Early Pleistocene of Swartkrans (Member 3) only preserves *Papio robinsoni* and *Theropithecus oswaldi*; Coopers (A and B) preserves a wider variety of cercopithecoid taxa (*Papio*, *Cercopithecoides* and *Theropithecus*). However, after the climatic changes associated with the time of the early Acheulian industry and *Homo ergaster* on the landscape, these primates are significantly reduced due to the reduction or increased patchiness of more wooded, closed conditions.

Previous studies of the Sterkfontein fossil faunal assemblages had indicated that carnivores have played a role in the accumulation of fauna in Jacovec Cavern, Member 4, StW 53 and Member 5 West (Kibii 2000; Kibii 2004; Pickering 1999). Even through tooth pit data analysis undertaken in Chapter Five, the current study has demonstrated that, medium-sized carnivores, leopard and hyaena, are the main carnivores which have imparted tooth pits and scores on the primate remains mainly from the Member 4 deposit. The identification of these carnivores from the actual tooth pit sizes is a new perspective on the taphonomy of the Sterkfontein cave. Previous studies had recognised the involvement of these carnivores from the types of assemblages and not necessarily from analysis of the actual tooth imprints. No differences are inferred between the various deposits as the sample size is too small to make any generic statements about the deposits.

Post-depositional fragmentation of the limb elements has rendered a large portion of the assemblages unidentifiable. As a result, the larger limb elements in the Sterkfontein fossil cercopithecoid postcranial assemblages dominate. Humeri constitute the largest percentage of identified elements with an NISP of 85, comprising 32% of the total identified NISP, while femora are the least identified at NISP of 30 (11% of the total NISP). Pickering and Carlson's (2002) study of baboon bone mineral density at Swartkrans has concluded that primate skeletal representation is not the result of bone density but of an assortment of other factors such as size, length, shape and body mass destructibility. Stated simply, the larger and longer limb elements are the postcranial elements with a higher survival rate in fossil faunal assemblages.

#### **7.4. Palaeoenvironmental and evolutionary implications of the Sterkfontein Caves fossil Cercopithecoidea**

Non-hominid primates have played a significant role in interpreting African Plio-Pleistocene palaeoenvironments. Due to their relative abundance in fossil cave sites, analysis of fossil primate remains has provided a glimpse into African palaeoenvironments. The observed transformation of the primate community over time (from the older moister through to the younger and drier environments) is observed in terms of taxonomic variation and body size. It suggests that these cercopithecoids, and primates in general, played a very significant ecological role in the Plio-Pleistocene environments at Sterkfontein. The cercopithecoids in the region were likely able to co-exist by adopting seasonal feeding patterns, or alternatively their diets were less similar than the data currently suggest (Fulwood 2012).

The evolution of the Sterkfontein fossil cercopithecoids suggests predominance of the papionins (*Papio* and *Parapapio*) in the earlier deposits, Member 2 and Jacovec Cavern. They are also the most common taxa in the younger Member 4 deposits. The Member 5 deposits associated with a drier open environment coincide with a decline in primate representation and the disappearance from Sterkfontein of the *Australopithecus* genus. The environmental shift to more open habitats in Member 5 is emphasised by the reduction of the taxonomic variation and number of primates that was preserved in Member 4.

Data derived from fauna and stable isotope analysis suggest that the shift from Member 4 to Member 5 habitats is marked by more open environments with some woodland cover (Reed 1997; Kuman & Clarke 2000; Luyt 2001; Lee-Thorp *et al.* 2007). The shift from closed woodland to more open environments was observed from around 3 Ma and 1.8 Ma (Luyt & Lee-Thorp 2003). Luyt and Lee-Thorp (2003) have applied the ratio of C4 grazing bovids to C3 browsing bovids to determine the variability of grasslands during the Plio-Pleistocene. This change to more open environments is observed particularly well in the younger Member 5 Acheulean deposits, coinciding with a drastic reduction in

primates in the environment. This shift is evident in the C<sub>4</sub> grass biomass, which saw a boost in the quantity of grazers between 1.8Ma and 1.7Ma (Luyt and Lee-Thorp 2003).

## **CHAPTER EIGHT**

### **CONCLUSION**

Isolated fossil postcrania of non-hominid primates are common in the southern African fossil record. Attempts at taxonomic identification of these isolated elements have been undertaken; however, none has assumed a comprehensive analysis of the postcrania in the Sterkfontein cave site. The current research hypothesis has established that taxonomic discrimination of skeletal elements at genus level is feasible. This research has examined the extent to which Sterkfontein's isolated fossil cercopithecoid postcranial morphology can be linked to taxonomy and phylogeny by undertaking qualitative combined with quantitative assessments. Assigning the taxa to species level is more complicated considering the fragmented state of the Sterkfontein fossil cercopithecoid remains and the paucity of available comparative taxa in the fossil record. However, the research has established that trait, size and shape are important factors in taxonomic assessments of isolated skeletal elements to at least genus level. The Sterkfontein cave deposits preserve a large assemblage of fossil primate remains compared to other South African fossil Plio-Pleistocene sites. For the first time, the fossil cercopithecoid postcrania are identified to taxa and correlated to cranio-dental taxa which have previously been the only source for conclusions on fossil monkey identifications in the Sterkfontein Caves.

Through the use of comparative modern cercopithecoid postcranial specimens and data from East African sites, this study was able to make taxonomic assessments of the Sterkfontein fossil cercopithecoid postcrania. This study relied on comparative taxa from East African sites which yield postcrania associated with crania and dentition. Sterkfontein site does not preserve fossil cercopithecoid postcrania belonging with taxonomically identifiable cranio-dental specimens. This lack of association has, in the past, obstructed identification of cercopithecoid postcrania in southern African fossil sites.

Data derived from fossil cercopithecoid postcrania support the large diversity of primate taxa in Member 4, which, according to O'Regan and Reynolds (2009), is a 'time-averaged palimpsest'. This context also resulted in a drastic increase of primate taxa compared with

the earlier Member 2 deposit (ca 3.67 My) and the Jacovec Cavern. Surface slope wash and gravitational slump which occurred in the accumulation of Jacovec Cavern (Kibii 2000) influenced the preservation pattern of macro vertebrates and resulted in limited numbers of primates. Current research has also confirmed the subsequent radical reduction in numbers of fossil monkeys in the younger infills such as the StW53, Member 5, Member 6 and Post Member 6 deposits. In these deposits the same taphonomic processes took place which influenced the scant preservation of the primates. These also formed within more limited periods compared to the longer duration seen in the accumulation of Member 4.

The quantitative and qualitative analysis of the Sterkfontein fossil cercopithecoid postcrania in this thesis has provided evidence of the probability of more fossil cercopithecoid diversity than was previously reported. For example, the existence of *Theropithecus* in Sterkfontein Member 4 is suggested, even though there is a lack of cranio-dental remains for the genus in the deposits, which had suggested its absence. The presence of *Theropithecus* interpreted from postcrania provides a different perspective on the evolution of the genus in South Africa. The abundance of *Theropithecus* fossils in the Pliocene at Makapansgat and the early Pleistocene at Swartkrans suggests that one might also expect it to have been present in the Sterkfontein Valley landscape in the early Pleistocene. This is now indicated by the identification of the genus, based on postcranial remains in Member 4. More cranio-dental data on the presence of *Theropithecus* in Member 4 will possibly shed more light into the evolution of this genus in the Plio-Pleistocene.

The predominance of fossil cercopithecoid remains over hominids in the Sterkfontein deposits is attributed to the success of the fossil monkeys, in particular, the papionins, during the Plio-Pleistocene. This has also resulted in the large numbers of cercopithecoid remains in the cave deposits.

The cercopithecoid postcrania were identified to tribe and genus level and none of the specimens could be confidently assigned to species level. *Parapapio* demonstrated variability in the shoulder joint. The size and morphological variation observed in the taxonomic analysis of *Parapapio* postcrania indicate the possibility of more than one species. The Sterkfontein fossil *Parapapio* possesses similar functional anatomy and relative size as the East African *Parapapio*. The genus *Papio* has had no record of comparable fossil postcrania. Plio-Pleistocene *Papio* fossil history in East Africa is virtually unknown; some of

the remains previously identified as *Papio* have been subsequently allocated to *Parapapio* (Jablonski *et al.* 2008). This had implications for the thesis. First, no record of fossil *Papio* postcrania is available for comparative purposes. Secondly, it demonstrates that there is a large overlap of morphological traits between the two genera. As a result of this ambiguity, which was also observed in the current investigation, a general class of *Papio* and *Parapapio* was created. The fossil *Papio* postcrania remains from Sterkfontein have demonstrated commonality with the modern *Papio* form, therefore suggesting a close relationship between the modern and fossil variants of the genus in southern Africa.

Taxonomic analysis of the fossil cercopithecoid postcrania demonstrates locomotor capabilities of Sterkfontein fossil monkeys, which in turn have contributed to palaeoenvironmental reconstructions of the region in the Plio-Pleistocene. The large contingent of taxa with generalist locomotor capabilities such as *Parapapio* and *Papio* and their long time span, from the Pliocene through to the early Pleistocene, points to an environment with a mosaic of habitats.

The general Sterkfontein faunal assemblage is highly fragmented due to rock fall, sediment compaction and blasting damage from lime mining as well as excavation damage. The Sterkfontein cave deposits' taphonomic history of collapse and re-deposition of infills has impacted on the high fragmentation of the limb elements and resulted in relatively large NISP relative to MNI numbers. The high representation of femora over others limb elements is the result of such taphonomic factors.

Tooth pit data analysis implicates medium sized carnivores, lions, canids and hyaena as the pre-dominant agents which accumulated the fossil monkeys, and possibly, the hominins. Earlier research on the taphonomy of various deposits of the Sterkfontein caves indicated that carnivores, in combination with other taphonomic processes such as surface slope-wash, death trap and porcupine collection, were active agents in the accumulation of the cercopithecoids of Jacovec Cavern, Member 2, Member 4 and the younger deposits, StW 53, Member 5 west and the Member 6 and Post Member 6 deposits (Brain 1981, Pickering 1999, Kibii 2000, 2004, Pickering *et al.* 2004, Ogola 2009). Tooth-pit analysis undertaken in this research supports the hypothesis that carnivores were not the main accumulator of the cercopithecoid fossil remains overall within the caves. The carnivores, however, did have an impact on the fossil cercopithecoid assemblage. Tooth pit analysis has revealed that, based



on the size of the pits on the diaphyses and epiphyseal ends, the general group of medium sized carnivores, hyenas, lions and dogs are the main agents involved in the accumulation of the cercopithecoid fossil remains. This research, has, for the first time, revealed the nature of the carnivores which have accumulated the fossil monkey postcrania through various deposits.

The spatial arrangement of the postcrania has indicated variation over time. The complex Member 4 deposits only demonstrate large concentrations of fossil cercopithecoid specimens in the upper and the very lower levels of the deposit. This clustering supports the hypothesis by Kuman and Clarke (2000) which states that Member 4 accumulated through different phases and probably through a relatively longer time span and by different agencies. The large concentration of fossil primate remains within the north-westerly part of Member 4 demonstrates alignment with the stratigraphic dip of the deposits. The same conclusion is reached for the north-western corner of the StW53 deposit, which possibly represents the earliest deposition subsequent to the Member 4 period.

This study has provided new scope for cercopithecoid postcrania taxonomy in southern African fossil cave sites. The research has given context to the numerous cercopithecoid postcrania which have been discovered in Sterkfontein caves. It has demonstrated the importance of considering postcranial remains as part of a suite of cercopithecoid and primate taxonomic studies.

## REFERENCES

- Andrews, C.W. (1916). Note on a new baboon (*Simopithecus oswaldi* gen.et sp.n.) from the Pliocene of British East Africa. *The Annals and Magazine of Natural History, Including Zoology, Botany and Geology*, **18**: 410-419.
- Avery, D.M. (2001). The Plio-Pleistocene vegetation and climate of Sterkfontein and Swartkrans, South Africa, based on micromammals. *Journal of Human Evolution*, **41**:113–132.
- Berger, L.R., Keyser, A.W. and Tobias, P.V. (1993). Gladysvale: first early hominid site discovered in South Africa since 1948. *American Journal of Physical Anthropology*, **92**: 107-111.
- Benefit, B.R. and McCrossin, M.L. (1989). New primate fossils from the middle Miocene of Maboko Island, Kenya. *Journal of Human Evolution*, **18**: 493-497.
- Benefit, B.R., McCrossin, M. Boaz, N.T., and Pavlakis, P. (2008) *New Fossil. Cercopithecoids from the Late Miocene of As Sahabi, Libya*. In N.T. Boaz, A. El-Aranouti, P. Pavlakis and M.Salem (eds.), *Circum- Mediterranean Geology and Biotic Evolution During the Neogene Period: The Perspective from Libya*, pp.265-282. Garyounis Scientific Bulletin, Special Issue No. 5.
- Behrensmeyer, A.K. (1978). Taphonomic and ecologic information from bone weathering. *Paleobiology*, **4**: 150-162.
- Binford, L.R. (1981). *Bones, Ancient Man and Modern Myths*. New York: Academic Press.

- Blumenschine, R.J. and Selvaggio, M.M. (1988). Percussion marks on bone surfaces as diagnostic criteria of hominid behavior. *Nature* **333**: 763-765.
- Blumenschine, R.J. and Selvaggio, M.M. (1991). On the marks of bone marrow processing by hammerstones and hyaenas: their anatomical patterning and archaeological implication. In Clark, J.D. (ed.). *Cultural Beginnings: Approaches to Understanding Early Hominid Lifeways in the African Savannah*, pp 17-31. Union Internationale des Sciences Prehistoriques et Protohistoriques Monographien Band 19.
- Bonnichsen, R. (1973). Some operational aspects of human and animal bone alteration. In Gilbert, M. (ed.). *Mammalian Osteo-Archaeology: North America*, pp. 9-24. Colombia: Missouri Archaeological Society.
- Brain, C.K. (1981). *The Hunters or the Hunted? An Introduction to the African Cave Taphonomy*. Chicago and London: University of Chicago Press.
- Brain, C.K. (1993). *Swartkrans: a Cave's Chronicle of Early Man*. Pretoria: Transvaal Museum Monograph no 8. Pretoria
- Broom, R. (1936). A new fossil anthropoid skull from South Africa. *Nature*, **138**: 486–488.
- Broom R. (1937). On some new Pleistocene mammals from limestone caves of the Transvaal. *South African Journal of Science* **33**: 750–768.
- Broom, R. (1940). The South African Cercopithecoid Apes. *Annals of the Transvaal Museum*, **20**: 89-100.
- Broom, R., and Jensen, J. S. (1946). A new fossil baboon from the caves at Potgietersrus. *Annals of the Transvaal Museum*, **20**: 337–340.

- Broom, R. and Robinson, J.T. (1948) "A new type of fossil baboon, *Gorgopithecus major*". *Proceedings of the Zoological Society of London*, **119** (2): 379–386.
- Bruxelles, L., Clarke, R.J., Maire, R., Ortega, R. and Stratford, D. (2014). Stratigraphic analysis of the Sterkfontein StW 573 *Australopithecus* skeleton and implications for its age. *Journal of Human Evolution*, **70**: 36-48.
- Bunn, H.T. (1982). *Meat-eating and Human Evolution: Studies on the Diet and Subsistence Patterns of Plio-Pleistocene Hominids in East Africa*. Ph.D. dissertation. University of California, Berkeley.
- Bunn, H.T. (1986). Patterns of skeletal part representation and hominid subsistence activities at Olduvai Gorge, Tanzania, and Koobi Fora, Kenya. *Journal of Human Evolution*, **15**: 673-690.
- Bunn, H.T. and Kroll, E.M. (1986). Systematic butchery by Plio-Pleistocene hominids at Olduvai Gorge, Tanzania. *Current Anthropology*, **27**: 431-452.
- Ciochon, R.L. (1993). *Evolution of the Cercopithecoid Forelimb—phylogenetic and functional implications from morphometric analyses*. California: University of California Press.
- Clarke, R.J. (1985). *Australopithecus* and early *Homo* in southern Africa. In: Delson E *Ancestors: The Hard Evidence*, pp 171–177. New York: Alan R. Liss.
- Clarke, R.J. (1988). A new *Australopithecus* cranium from Sterkfontein and its bearing on the ancestry of *Paranthropus*. In: Grine F.E. *Evolutionary History of the "Robust" Australopithecines*, pp 285–292. New York: Aldine de Gruyter.

- Clarke, R.J. (1994). On some new interpretations of Sterkfontein stratigraphy. *South African Journal of Science*, **90**: 211-214.
- Clarke, R. J. (1998). First ever discovery of a well preserved skull and associated skeleton of *Australopithecus*. *South African Journal of Science*, **94**: 460 – 463.
- Clarke, R. J. (1999). Discovery of a complete arm and hand of the 3.3 million year old *Australopithecus* skeleton from Sterkfontein. *South African Journal of Science*, **95**: 477-480.
- Clarke, R. J. (2002). Latest information on the Sterkfontein *Australopithecus* skeleton. *South African Journal of Science*, **98**: 523-526.
- Clarke, R. J. (2006). A deeper understanding of the Sterkfontein fossil hominid site. *Transactions of the Royal Society of South Africa*, **61**(2): 111-120.
- Clarke, R.J. (2008). Latest information on Sterkfontein *Australopithecus* skeleton and a new look at *Australopithecus*. *South African Journal of Science*, **104**: 443-449.
- Clarke, R.J. (2013). *Australopithecus* from Sterkfontein Caves, South Africa. In Reed, K.E., Fleagle, J. and Leakey, R.E.F. (eds.). *Palaeobiology of Australopithecus*, pp 105-121. New York; Springer.
- Clarke, R.J. and Tobias, P.V. (1995). Sterkfontein Member 2 foot-bones of the oldest South African hominid. *Science* **269**: 521-524.
- Codron, D., Luyt, J., Lee-Thorp, J., Sponheimer, M., de Ruiter D. and Codron, J. (2005). Utilization of savanna-based resources by Plio-Pleistocene baboons. *South African Journal of Science*, **101**:245-248.

- Conroy, G. C. (1976). Primate postcranial remains from the Oligocene of Egypt. *Contributions to Primatology*, **8**: 1–134.
- Cooke H.B.S. (1990). Taung fossils in the University of California collections. In Sperber, G. (ed.), *From Apes to Angels: Essays in Anthropology in Honor of Phillip Tobias*, pp 119-134. New York: Wiley-Liss.
- Curnoe, D. and Tobias P.V. (2006). Description, new reconstruction, comparative anatomy, and classification of the Sterkfontein StW 53 cranium, with discussions about the taxonomy of other southern African early *Homo* remains. *Journal of Human Evolution*, **50**: 36-77.
- Dart R.A. (1925): *Australopithecus africanus*: The Man-Ape of South Africa. *Nature*, **115**: 195-199.
- Delson, E. (1984). Cercopithecoid biochronology of the African Plio-Pleistocene: correlation among eastern and southern hominid-bearing localities. *Courier Forschungs-Institut Senckenberg*, **69**: 199-218.
- Delson E, and Dean, D. (1993). Are *T. baringensis* R. Leakey, 1969, and *P. quadratiostris* Iwamoto, 1982, species of *Papio* or *Theropithecus*? In Jablonski, N. (ed.). *Theropithecus: the rise and fall of a primate genus*, pp 125-156. Cambridge: Cambridge University Press.
- Delson, E., Eck, G.G., Leakey, M.G. and Jablonski, N.G. (1993). A partial catalogue of fossil remains of *Theropithecus*. In Jablonski, N.G. (ed.). *Theropithecus: The Rise and Fall of a Primate Genus*, pp.499–525. Cambridge University Press, Cambridge.
- Delson, E., Terranova, C. J., Jungers, W. L., Sargis, E. J., Jablonski, N. G. and Dechow, P. C. (2000). Body mass in Cercopithecidae (Primates, Mammalia). *Anthropological Papers of the American Museum of Natural History*, **83**: 1-139

- De Silva, J.M., Steininger, C. and Patel, B.A. (2013). Cercopithecoid primate postcranial fossils from Cooper's D, South Africa. *GeoBios*, **46**:381-394.
- Dominguez-Rodrigo M. (2001). A study of carnivore competition in riparian and open habitats of modern savannas and its implications for hominid behavioral modeling. *Journal of Human Evolution*, **40**:77-98.
- Domínguez-Rodrigo, M. and Piqueras, A. (2003). The use of tooth pits to identify carnivore taxa in tooth-marked archaeofaunas and their relevance to reconstruct hominid carcass processing behaviors. *Journal of Archaeological Science*, **30**: 1385–1391.
- DraPeau, M.S.M. (2008). Articular morphology of the proximal ulna in extant fossil hominoids and hominin. *Journal of Human Evolution*, **55**: 86-102.
- Dunbar, R. 1993. Conservation status of the Gelada. pp. 527-531. In Jablonski, N.G. (ed.) *Theropithecus: The rise and fall of a primate genus*. New York: Cambridge University Press.
- Eck, G.G. (1976). Cercopithecoidea from Omo Group deposits. In Coppens, Y., Howell, F.C., Isaac, G.H. and Leakey, R.E.F. *Earliest Man and Environments in the lake Rudolf Basin*. Chicago: University of Chicago Press.
- Elton, S. (2000). Habitat preference and locomotion in Plio-Pleistocene *Theropithecus* species. *American Journal of Physical Anthropology*, **S30**: 145.
- Elton, S. (2001). Locomotor and habitat classifications of cercopithecoid postcranial material from Sterkfontein Member 4, Bolt's Farm and Swartkrans Members 1 and 2, South Africa. *Paleontologica africana* **37**:115–126.

- Elton, S., Barham, L., Andrews, P. and Sambrook Smith, G. (2003) Pliocene femur of *Theropithecus* from the Luangwa Valley, Zambia. *Journal of Human Evolution* **44**: 133-140.
- Egi, N., Nakatsukasa, M., Kalmykov, N.P., Maschenko, E.N., Takai, M. (2007). Distal humerus and ulna of *Parapresbytis* (Colobinae) from the Pliocene of Russia and Mongolia: phylogenetic and ecological implications based on elbow morphology, *Anthropological Science*, **115**(2): 107-117.
- Eisenhart, W.L. (1974). *Fossil Cercopithecoids of Makapansgat and Sterkfontein*. B.A. thesis, Department of Anthropology, Harvard College.
- El Zaatari, S., Grine, F.E., Teaford, M.F. and Smith, H.F. (2005). Molar microwear and dietary reconstructions of fossil Cercopithecoidea from the Plio-Pleistocene deposits of South Africa. *Journal of Human Evolution*, **49**:180: 205.
- Fleagle, J. G. (1983). Locomotor adaptations of Oligocene and Miocene hominoids and their phyletic implications. In R. L. Ciochon and R. S. Corruccini (eds.). *New Interpretations of Ape and Human Ancestry*. New York: Plenum Press.
- Fleagle, J. G. and Simons, E. L. (1982). Skeletal remains of *Propliopithecus chirobates* from the Egyptian Oligocene. *Folia primatologica*. **39**: 161-177.
- Fleagle, J. G. and Simons, E. L. (1978). *Micropithecus clarki*, a small ape from the Miocene of Uganda. *American Journal of Physical Anthropology*, **49**(4): 427-440.
- Freedman, L. (1957). The fossil Cercopithecoidea of South Africa. *Annals of the Transvaal Museum* **23**: 121-262.
- Freedman, L. (1960). Some new fossil Cercopithecoid specimens from Makapansgat, South Africa. *Palaeontologia Africana* **7**: 7-45.



- Freedman, L. (1961). New Cercopithecoid fossils, including a new species from *Taung*, Cape Province, South Africa. *Annals of the South African Museum*, **46**: 1–14.
- Freedman, L. (1965). Fossil and subfossil primates from the limestone deposits at Taung, Bolt's Farm and Witkrans, South Africa. *Palaeontologia Africana*, **9**: 19-48.
- Freedman, L. (1970) A new check-list of fossil Cercopithecoidea of South Africa, *Palaeontologia africana*, **13**: 109-110.
- Freedman, L. (1976). South African fossil Cercopithecoidea: A re-assessment including a description of new material from Makapansgat, Sterkfontein and Taung. *Journal of Human Evolution*, **5**: 297- 310.
- Freedman, L. and Brain, C.K. (1977). A re-examination of the cercopithecoid fossils from Swartkrans (Mammalia: Cercopithecidae). *Annals of the Transvaal Museum*, **30**: 211-218.
- Freedman, L., and Stenhouse, N. S. (1972). The *Parapapio* species of Sterkfontein, Transvaal, South Africa. *Palaeontologia Africana*, **14**: 93–111.
- Frost, S.R. and Delson, E. (2002). Fossil Cercopithecidae from the Hadar Formation and surrounding areas of the Afar Depression, Ethiopia. *Journal of Human Evolution*, **43**: 687-748.
- Frost, S.R. and Alemseged, Z. (2007). Middle Plesitocene fossil Cercopithecidae from Asbole, Afar Region, Ethiopia. *Journal of Human Evolution*, **53**: 227-259.
- Fulwood, E. (2012). An evaluation of niche separation in the terrestrial primate fauna of Plio-Pleistocene South Africa using biogeochemical data. *Pursuit: The Journal of Undergraduate Research at the University of Tennessee*, **3**: 67-73.

- Gear, J. H. S. (1926). A preliminary account of the baboon remains from Taungs. *South African Journal of Science*, **28**:731–747.
- Gebo, D.L. (1993). *Postcranial Adaptation in nonhuman Primates*. DeKalb: Northern Illinois University Press.
- Gebo, D.L., Beard, C.K., Teaford, M.F., Walker, A., Larson, S.G., Jungers, W.L. and Fleagle, J.G. (1988). A hominoid proximal humerus from the Early Miocene of Rusinga Island, Kenya. *Journal of Human Evolution*, **17**: 393-401.
- Gebo, D.L. and Sargis, E.J. (1994). Terrestrial adaptations in the postcranial skeletons of guenons. *American Journal of Physical Anthropology* **93**: 341-371.
- Geoffroy, E. (1812). Type species: *Cercocebus fuliginosus*. *Annales Muséum National D'Histoire Naturelle*, **19**: 97.
- Gilbert, C.C. (2007). Identification and description of the first *Theropithecus* (Primates: Cercopithecidae) material from Bolt's Farm, South Africa. *Annals of the Transvaal Museum* **44**: 1-10.
- Gilbert, C.C. (2008). *African papionin phylogenetic history and Plio-Pleistocene biogeography*. Ph.D. Dissertation. Stony Brook University: New York
- Gilbert, C.C. (2011). Phylogenetic analysis of the African papionin basicranium using 3-D geometric morphometrics: the need for improved methods to account for allometric effects. *American Journal of Physical Anthropology*, **144**: 60-71.
- Gilbert, C.C. (2013). Cladistic analysis of extant and fossil African papionins using craniodental data. *Journal of Human Evolution*, **64**: 399-433.

- Gilbert, C.C. Goble, E.D. Kingston, J.D. and Hill, A. (2011). Partial skeleton of *Theropithecus brumpti* (Primates, Cercopithecidae) from the Chemeron Formation of the Tugen Hills, Kenya. *Journal of Human Evolution*, **61**: 347-362.
- Gilbert, C., Frost, S.R. and Delson, E. (2015). *Review of Olduvai cercopithecoids reveals a newly recognized taxon and biochronological connection to South Africa*. Poster presented at the 84th Annual Meeting of the American Association of Physical Anthropologists.
- Gilbert C.C., Takahashi M.Q. and Delson E. (2016). Cercopithecoid humeri from Taung support the distinction of major papionin clades in the South African fossil record. *Journal of Human Evolution*, **90**: 88-104.
- Gommery, J., Thackeray, F., S  n  gas, F. Potze, S. and Kgasi, L. (2008). The earliest primate (*Parapapio* sp.) from the Cradle of Humankind World Heritage site (Waypoint 160, Bolt's Farm, South Africa). *South African Journal of Science*, **104**: 405-408.
- Granger, D., Gibbon, R., Kuman, K., Clarke, R.J. and Caffee, M. (2015). New cosmogenic burial ages for Sterkfontein Member 2 *Australopithecus* and Member 5 Oldowan. *Nature*. 522:85-88.
- Grayson, D.K. (1989). Bone transport, bone destruction, and reverse utility curves. *Journal of Archaeological Science*, **16**: 643-652.
- Grine, F.E. and Hendey Q.B. (1981). Earliest primate remains from South Africa. *South African Journal of Science* **77**:374-376.
- Guthrie, E.H. (2011). *Functional Morphology of the morphology of Theropithecus brumpti* (Primates: Cercopithecidae). Oregon: University of Oregon.

- Hammer, Ø, Harper D.A.T. and Ryan, P.D. (2001). PAST: Palaeontological statistics software package for education and data analysis. *Palaeontologia Electronica*, 4 (1): 9pp. [http://palaeo-electronica.org/2001\\_1/past/issue1\\_01.htm](http://palaeo-electronica.org/2001_1/past/issue1_01.htm).
- Hatchett, M.K. (2011). *Creating a chronocline of the diet of Theropithecus from low-magnification stereomicroscopy: how has the diet of Theropithecus changed over time?* Honours Thesis: Georgia State University.
- Halenar, L.B. and Rosenberger, A.L. (2013). A closer look at the '*Protopithecus*' fossil assemblages: New genus and species from Bahia, Brazil. *Journal of Human Evolution*, **65**: 374-390.
- Harrison, T. (1981). New finds of small fossil apes from the Miocene locality at Koru in Kenya. *Journal of Human Evolution*, **10**: 129–137
- Harrison, T. (1989). New postcranial remains of *Victoriapithecus* from the middle Miocene of Kenya. *Journal of Human Evolution*, **18**: 3–54.
- Harrison, T. (1993). Cladistic concepts and the species problem in hominoid evolution. In Kimbel W. H. and Martin, L. B. (eds.), *Species, Species Concepts and Primate Evolution*. New York: Plenum Press.
- Harrison, T. (2011). Cercopithecids. (Cercopithecidae, Primates). In Harrison, T. (ed.). *Paleontology and Geology of Laetoli: Human Evolution in Context. Volume 2: Fossil Hominins and the Associated Fauna, Vertebrate Paleobiology and Paleoanthropology*, pp 83-139. Dordrecht: Springer.
- Harrison, T., and Harris, E. E. (1996). Plio-Pleistocene cercopithecids from Kanam East, Western Kenya. *Journal of Human Evolution*, **30**: 539-561.

- Haynes, G.A. (1983). A guide for differentiating mammalian carnivore taxa responsible for gnaw damage to herbivore limb bones. *Paleoecology*, **9**: 164–172.
- Heaton, J.L. (2006). *Taxonomy of the Sterkfontein Fossil Cercopithecinae: the Papionini of Members 2 and 4 (Gauteng, South Africa)*. Unpublished PhD thesis. Department of Anthropology, Indiana State University.
- Herries, A.I.R., Curnoe, D. and Adams, J.W. (2009). A multi-disciplinary seriation of early *Homo* and *Paranthropus* bearing palaeocaves in southern Africa. *Quaternary International*, **202**: 14-28.
- Herries, A.I.R. and Shaw, J. (2011). Palaeomagnetic analysis of the Sterkfontein palaeocave deposits: Implications for the age of the hominin fossils and stone tool industries. *Journal of Human Evolution*, **60**(5): 523-539.
- Hlusko, L.J. (2007). A new late Miocene species of *Paracolobus* and other cercopithecoidea (Mammalia: Primates) fossils from Lemudong'o, Kenya. *Kirtlandia, The Cleveland Museum of Natural History*, **56**:72–85.
- Hopwood, A. (1934). New fossil mammals from Olduvai, Tanganyika territory. *Annals of the Magazine of Natural History*, **10**: 546-550.
- Hughes, A.R. (1958). Some ancient and recent observations on hyaenas. *Kodoe, Journal of Scientific Research in National Parks South, Africa*, **1**: 1-10.
- Hughes, A.R. and Tobias, P.V. (1977). A fossil skull probably of the genus *Homo* from Sterkfontein, Transvaal. *Nature*, **265**: 310-312.
- Jablonski, N.G. (1993). Introduction. In Jablonski, N.G. (ed.) *Theropithecus: The rise and fall of a primate genus*. New York: Cambridge University Press.

- Jablonski, N.G. Leakey, M.G. Klarey, C. and Antón, M. (2002). A new Skeleton of *Theropithecus brumpti* (Primates: Cercopithecidae) from Lomekwi, West Turkana, Kenya. *Journal of Human Evolution*, **43**: 887–923.
- Jablonski, N.G. and Chaplin, G. (2008) Natural language descriptions and keys of the Koobi Fora monkey fossil species using DELTA. In: Jablonski, N.G. and Leakey, M.G. (eds.). *Koobi Fora Research Project. Volume 6. The Fossil Monkeys*, pp. 301-33. California Academy of Sciences: San Francisco.
- Jablonski, N. G., and Frost, S. (2010). *Cercopithecoidea*. In L. Werdelin and W. J. Sanders (eds.), *Cenozoic Mammals of Africa*, pp. 393-428. California: University of California Press.
- Jablonski, N.G. and Leakey, M.G. (2008). Systematic paleontology of the small colobines. In, Jablonski, N.G. and Leakey, M.G. (eds.). *Koobi Fora Research Project, the Fossil Monkeys, Volume 6*. California: California Academy of Sciences.
- Jablonski, N.G., Leakey, M.G. and Anton, M. (2008). Systematic paleontology of the Cercopithecines. In, Jablonski, N.G. and Leakey, M.G. (eds.). *Koobi Fora Research Project, the Fossil Monkeys, Volume 6*. California: California Academy of Sciences.
- Jones, T.R. (1937). A new fossil primate from Sterkfontein, Krugersdorp, Transvaal. *South African Journal of Science*, **33**: 709-728.
- Jones, S., Pilbeam, D.R. and Martin, R.D. (1992). *The Cambridge Encyclopedia of Human Evolution*. Cambridge: Cambridge University Press.
- Jolly, C. J. (1970). The seed-eaters: A new model of hominid differentiation based on a baboon analogy. *Man*, **5**: 5–26.

- Jolly, C. J. (1972). The classification and natural history of *Theropithecus* (*Simopithecus*) (Andrews, 1916), baboons of the African Plio-Pleistocene. *Bulletin of the British Museum of Natural History (Geology)* **22**: 1–123.
- Jones A.L. (2008). The evolution of brachiation in ateline primates. *American Journal of Physical Anthropology*, **137**(2):123-44.
- Kalb, J. E., Wood, C. B., Smart, C., Oswald, E. B., Mebrate, A., Tebedge, S. and Whitehead, P. (1980). Preliminary geology and palaeontology of the Bodo D'ar hominid site, Afar, Ethiopia. *Palaeogeography, Palaeoclimatology and Palaeoecology*, **30**: 107–120.
- Kibii, J.M. (2000). *The Macrofauna from Jacovec Cavern-Sterkfontein*. Unpublished Master's Thesis, Department of Archaeology, University of the Witwatersrand.
- Kibii, J.M. (2004). *Comparative, Taxonomic, Taphonomic and Palaeoenvironmental Analysis of 4-2.3 Million Year Old Australopithecine Cave Infills at Sterkfontein*. Unpublished PhD Thesis, Department of Archaeology, University of the Witwatersrand.
- Kibii, J.M. and Clarke, R.J. (2003). A reconstruction of the StW 431 *Australopithecus* pelvis based on newly discovered fragments. *South African Journal of Science*, **99**: 225-226.
- Kingdon, J. (1974). *East African Mammals: An Atlas of Evolution in Africa, Vol. 1*. The University of Chicago Press, Chicago.
- Klein, R.G. and Cruz-Urbe, K. (1984). *The Analysis of Animal Bones from Archaeological Sites*. Chicago: University of Chicago Press.

- Klein, R. G., Cruz-Urbe, K., Halkett, D., Hart, T. and Parkington, J. (1999). Paleoenvironmental and Human Behavioral Implications of the Boegoeberg 1 Late Pleistocene Hyena Den, Northern Cape Province, South Africa. *Journal of Archaeological Science*, **52**: 393-403.
- Krentz, H.B. (1993). Postcranial anatomy of extant and extinct species of *Theropithecus*. In Jablonski, N.G. (ed.). *Theropithecus: The Rise and Fall of a Primate Genus*. New York: Cambridge University Press.
- Kuman, K. (1994). The archaeology of Sterkfontein: preliminary findings on site formation and cultural change. *South African Journal of Science*, **90**: 215-219.
- Kuman, K. and Clarke, R.J. (2000). Stratigraphy, artefact industries and hominid associations for Sterkfontein, Member 5. *Journal of Human Evolution*, **38**: 827-847.
- Lam, Y. M. (1992). Variability in the behaviour of spotted *hyaenas* as taphonomic agents. *Journal of Archaeological Science*, **19**: 389-406.
- Lambert, J. (2014). The biology and evolution of Ape and monkey feeding and nutrition. In Henke, W., Tattersall, I., and Hardt, T. (eds.). *Handbook of Palaeoanthropology*, pp 1631-1660. Springer Berlin Heidelberg: Germany.
- Larson, S.G. (1996). Estimating humeral torsion on incomplete fossil anthropoid humeri. *Journal of Human Evolution*, **31**: 239-257.
- Larson, S.G., Stern, J.T. (1986). EMG of scapulohumeral muscles in the chimpanzee during reaching and “arboreal” locomotion. *American Journal of Anatomy*, **176**: 171-190.
- Leakey, L.S.B. (1965). *Olduvai Gorge, 1951-1961*. Cambridge: Cambridge University Press.



- Leakey, M. G. (1993). Evolution of *Theropithecus* in the Turkana Basin. In Jablonski, N. G. (ed.) *Theropithecus: The Rise and Fall of a Primate Genus*, pp. 85–123. Cambridge: Cambridge University Press.
- Leakey, M. G. and Delson, E. (1987). Fossil Cercopithecidae from the Laetoli Beds. In Leakey M. D. and Harris J. M. (eds.). *Laetoli: A Pliocene Site in Northern Tanzania*, pp. 91–107. Clarendon Press, Oxford.
- Leakey, M.G. and Leakey, R.E.F. (1973). Further evidence of *Simopithecus* (Mammalia, Primates) from Olduvai and Olorgesailie. In Savage, R.J.G. and Coryndon, S.C. (eds.). *Fossil Vertebrates of Africa*, vol 4, pp 121-146. New York: Academic Press.
- Luyt, C.J. (2001). *Revisiting palaeoenvironments from the hominid bearing Plio Pleistocene sites: New isotopic evidence from Sterkfontein*. Unpublished M.Sc. thesis, University of Cape Town
- Maier, W. (1970). New fossil Cercopithecoidea from the lower Pleistocene cave deposits of Makapansgat Limeworks, South Africa. *Palaeontologia Africana*, **13**: 69–107.
- Maier, W. (1972). The first complete skull of *Simopithecus darti* from Makapansgat, South Africa, and its systematic position. *Journal of Human Evolution*, **1**: 395–400.
- Maguire, J., Pemberton, D. and Collet, M.H. (1980). The Makapansgat limeworks grey breccia: hominids, hyaenas, hystricids or hillwash. *Palaeontologia Africana* **23**: 75-98.
- McHenry, H.M. (1992). Body size and proportions in early hominids. *American Journal of Physical Anthropology*, **87**: 407–431.
- McKee, J.K. (1993). Taxonomic and evolutionary affinities of *Papio izodi* fossils from Taung and Sterkfontein. *Palaeontologia Africana*, **30**: 43-49.

- McKee, J.K., von Mayer, A. and Kuykendall, K.L. (2011). New species of *Cercopithecoides* from Haasgat, North West Province. South Africa. *Journal of Human Evolution*, **60**: 83-93.
- MacPhee, R.D.E. and Horovitz, I. (2002). *Extinct Quaternary platyrrhines of the Greater Antilles and Brazil*. In Hartwig, W.C. (Ed.). *The Primate Fossil Record*, pp 189-200. Cambridge University Press, Cambridge.
- Mills, M. G. L. and Mills, E. J. M. (1977). An analysis of bones collected at hyena breeding dens in the Gemsbok Nat. Parks. *Annals of the Transvaal Museum*, **30**: 145-155.
- Moggi-Cecchi, J. (2003). The elusive ‘second species’ in Sterkfontein Member 4: the dental metrical evidence. *South African Journal of Science* **99**: 268–270.
- Moggi-Cecchi, J., Tobias, P. V. and Beynon, A. D. (1998). The mixed dentition and associated skull fragments of a juvenile fossil from Sterkfontein, South Africa. *American Journal of Physical Anthropology*, **106**: 425–465.
- Mollett, O. (1947). Fossil mammals from the *Makapansgat* Valley, Potgeitersrust. I. Primates. *South African Journal of Science*, **43**: 95–303
- Nakatsukasa, M. (1994). Morphology of the humerus and femur in African Mangabeys and Guenons: Functional adaptation and implications for the evolution of positional behavior. *African Study Monographs Supplement*, **21**: 1-61.
- Nakatsukasa, M. (1996). Locomotor differentiation and different skeletal morphologies in mangabeys (*Lophocebus* and *Cercocebus*). *Folia Primatologica* **66**: 15-24.

- Napier, J.R. and Napier, P.H. (1967). *A Handbook of Living Primates*. Academic Press: New York.
- Ogola, C.O. (2009). *The Sterkfontein western breccias: stratigraphy, fauna and artefacts*. Unpublished PhD thesis, University of the Witwatersrand: Wits University Press.
- O'Regan, H.J. and Reynolds, S.R. (2009). An ecological reassessment of the southern African carnivore guild: a case study from Member 4, Sterkfontein South Africa. *Journal of Human Evolution*, **57**: 212-222.
- Padian, K. (1995) *Form versus function: the evolution of a dialectic*. pp. 264-277. In Thomason, J.J (ed.). *Functional Morphology in Vertebrate Paleontology*. Cambridge University Press, Cambridge/New York
- Partridge, T.C. (1978). Re-appraisal of lithostratigraphy of Sterkfontein hominid site. *Nature*, **275**: 282-287.
- Partridge T.C. (2000). Hominid-bearing cave and tufa deposits. In: Partridge, T.C. and Maud, R.R. (eds.). *The Cenozoic of southern Africa*, pp 100–125. New York: Oxford University Press.
- Partridge, T. C. and Watt, I. B. (1991). The stratigraphy of the Sterkfontein hominid deposit and its relationship to the underground cave system. *Palaeontologia Africana*, **28**: 35–40.
- Partridge, T.C., Latham, A.G., and Heslop, D. (2000). Appendix on magnetostratigraphy of Makapansgat, Sterkfontein, Taung and Swartkrans. In, Partridge T.C. and Maud R.R. (eds.). *The Cenozoic of southern Africa*, pp 126–129. New York: Oxford University Press.

- Partridge T.C., Granger D.E., Caffee M.W. and Clarke, R.J. (2003). Lower Pliocene hominid remains from Sterkfontein. *Science*, **300**: 607-12.
- Patel, B.A., Wallace, I.J., Boyer, D.M., Granatosky, M.C., Larson, S.G. and Stern, J.T. (2015). Distinct functional roles of primate grasping hands and feet during arboreal quadrupedal locomotion. *Journal of Human Evolution*; **88**:79-84.
- Pickering, T.R. (1999). *Taphonomic Interpretation of the Sterkfontein Early Hominid Site (Gauteng, South Africa) Reconsidered in Light of Recent Evidence*. PhD thesis, University of Wisconsin, Madison.
- Pickering, T. R. (2002). Reconsideration of criteria for differentiating faunal assemblages created by hyenas and hominids. *International Journal of Osteology*, **12**:127-141.
- Pickering, T.R. and Wallis, J. (1997). Bone modifications resulting from captive chimpanzee mastication: implications for the interpretation of Pliocene archaeological faunas. *Journal of Archaeological Science*, **24**: 1115-1127.
- Pickering, T.R., White, T. and Toth, N. (2000). Brief communication: cutmarks on a Plio-Pleistocene hominid from Sterkfontein, South Africa. *American Journal Physical Anthropology*, **111**: 579-584.
- Pickering, T.R., Clarke, R.J. and Heaton, J.L. (2004a). The context of StW 573, an early hominid skull and skeleton from Sterkfontein Member 2: taphonomy and paleoenvironment. *Journal of Human Evolution*, **46**: 279-295.
- Pickering, T.R., Clarke, R.J. and Moggi-Cecchi, J. (2004b). The role of carnivores in the accumulation of the Sterkfontein Member 4 hominid fossil assemblage: a taphonomic reassessment of the complete hominid fossil sample (1936–1999). *American Journal of Physical Anthropology*, **125**: 1-15.

- Pickering, R., and Kramers, J.D. (2010). Re-appraisal of the stratigraphy and determinations of new U-Pb dates for the Sterkfontein hominin site, South Africa. *Journal of Human Evolution*, **59**: 70-86.
- Pickering, T.R. Heaton, J.L., Clarke, R.J., Sutton, M.B., Brain, C.K. and Kuman, K. (2012). New hominid fossils from Member 1 of the Swartkrans formation, South Africa. *Journal of Human Evolution*, **62**: 618-628.
- Plavcan, M.J., Lockwood, C.A., Kimbel, W.H, Lague, M.R. and Harmon, E.H. (2005). Sexual dimorphism in *Australopithecus afarensis* revisited: How strong is the case for a human-like pattern of dimorphism? *Journal of Human Evolution*, **48**: 313–320.
- Reed, K.E. (1997). Early hominid evolution and ecological change through the African Plio-Pleistocene. *Journal of Human Evolution*, **32**: 289-322.
- Reno, P.L., Mendl, R.S., McCollum, M.A. and Lovejoy, C.O. (2003). Sexual dimorphism in *Australopithecus afarensis* was similar to that of modern humans. *Proceedings of the National Academy of Sciences of United States of America*, **100**: 9404–9409.
- Reynolds, S.C. (2000). *Sterkfontein: Exploration of Some Lesser Known Archaeological and Fossil Deposits*. Unpublished Masters thesis, Department of Archaeology, University of the Witwatersrand.
- Reynolds, S.C. (2007). Mammalian body size changes and Plio-Pleistocene environmental shifts: implications for understanding hominin evolution in eastern and southern Africa. *Journal of Human Evolution*, **53**: 528-548.
- Reynolds, S.C., Bailey, G.N. and King, G.C.P. (2007). Landscapes and their relation to hominin habitats: Case studies from *Australopithecus* sites in eastern and southern Africa. *Journal of Human Evolution*, **60**: 281-298.

- Reynolds, S.C., Vogel, J.C., Clarke, R.J. and Kuman, K. (2003). Preliminary results of excavations at Lincoln Cave, Sterkfontein, South Africa. *South African Journal of Science*, **99**: 286-288.
- Reynolds, S.C., Clarke, R. J. and Kuman, K. (2007). The view from the Lincoln Cave: Mid-to Late Pleistocene fossil deposits from Sterkfontein. *Journal of Human Evolution*, **53**: 528-548.
- Reynolds, S.C. and Kibii, J.M. (2011). Sterkfontein at 75: a review of palaeoenvironments, fauna and archaeology from the hominin site of Sterkfontein (Gauteng Province, South Africa). *Palaeontologia africana*, **46**: 59-88.
- Richardson P.R.K. (1980). Carnivore damage to antelope bones and its archaeological implications. *Palaeontologia Africana*, **23**: 109–125.
- Robinson J.T. (1952). The Australopithecine bearing deposits of the Sterkfontein area, *Annals of the Transvaal Museum*, **22**: 1-19.
- Robinson, J.T. (1962). Sterkfontein stratigraphy and the significance of the Extension Site. *South African Archaeological Bulletin*, **17**: 87-107.
- Rose, M.D. (1973). Quadrupedalism in Primates. *Primates*, **14**: 337-357.
- Rose, M.D. (1974). Postural adaptations in New and Old World Monkeys. In Jenkins, F.A (ed.). *Primate locomotion*, pp 201-222. New York: Academic Press.
- Rose, M. D. (1997). “Functional and Phylogenetic Features of the *Forelimb* in *Miocene* Hominoids.” In Begun, D.R., Ward, C.V., Rose, M.D. (eds.). *Function, Phylogeny, and Fossils. Miocene Hominoid Evolution and Adaptations*. New York: Platinum Press.

- Rowe, N. (1996). *The Pictorial Guide to the Living Primates*. Rhode Island and Charleston: Pogonias Press.
- Ruff, C. (2002). Long bone articular and diaphyseal structure in old world monkeys and apes 1: locomotor effects. *American Journal of Physical Anthropology*, **119**(4): 305-342.
- Ruff, C. (2003). Long bone articular and diaphyseal structure in old world monkeys and apes II: estimation of body mass. *American Journal of Physical Anthropology*, **120**: 16-37.
- Selvaggio, M.M. (1994). *Identifying the Timing of Hominid and Sequence of Hominid and Carnivore Involvement with Plio-Pleistocene Bone Assemblages from Carnivore Tooth Marks and Stone tool Butchery Marks on Bone Surfaces*. Rutgers University: New Brunswick.
- Shipman, P. (1981). *Life History of a Fossil: An Introduction to Taphonomy and Palaeoecology*. Cambridge: Cambridge University Press.
- Shipman, P., Bosler, W. and Davis, K.L. (1981). Butchering of giant geladas at an acheulian site. *Current Anthropology*, **22**: 257–68.
- Silcox, M.T., Bloch, J.I. Boyer, D.M., Godinot, M., Ryan, T.M. Spoor F. and Walker, A. (2009). Semicircular canal system in early primates. *Journal of Human Evolution*, **56**: 315-327.
- Simons E.L. (1959). An Anthropoid frontal bone from the Fayum Oligocene of Egypt: the oldest skull fragments of a higher primate. *American Museum Novitates*, **1976**: 1-16.

- Simons, J. W. (1966). The presence of leopard and a study of the food debris in the leopard lairs of the Mt Suswa caves. *Bulletin of the Cave Exploration Group of East Africa*, **1**: 51-69.
- Smith, J. M. and Savage, R. J. G. (1956). Some locomotory adaptations in mammals: *Zoological Journal of the Linnean Society*, **42**: 603–622.
- Spoor, F., Garland, Jr., Krovitz, G., Ryan, M.T. and Walker, A. (2007). The primate semi-circular canal system and locomotion. *Proceedings of the National Academy of Sciences*, **104**: 10808-10812.
- Stevens, N.J., Seiffert, E.R., O'Connor, P.M., Roberts, E.M., Schmitz, M.D., Krause, C., Gorscak, E., Ngasala, S.M., Hieronymus, T.L. and Temu, T.J. (2013). Paleontological evidence for an Oligocene divergence between Old World monkeys and apes. *Nature*, **497**: 611-614.
- Stratford, D. (2009). *A study of newly discovered lithics from earlier Stone Age deposits at Sterkfontein, Gauteng province, South Africa*. Unpublished Masters Thesis, University of the Witwatersrand, Johannesburg.
- Stratford, D. (2012). *The underground central deposits of the Sterkfontein Caves, South Africa*. Unpublished PhD Thesis, University of the Witwatersrand, Johannesburg.
- Szalay, F.S. and Delson, E. (1979). *Evolutionary History of the Primates*. New York: Academic Press.
- Thackeray, J.F. and Kirschvink, J. (2002). Palaeomagnetic analysis of calcified deposits from the Plio-Pleistocene hominid site of Kromdraai, South Africa. *South African Journal of Science* **98**: 537-540



- Thackeray J.F. and Myer S. (2004). *Parapapio broomi* and *Parapapio jonesi* from Sterkfontein: males and females of one species? *Annals of the Transvaal Museum*, **41**: 79–82.
- Tobias, P. V. (1979). The Silberberg Grotto, Sterkfontein, Transvaal, and its importance in palaeoanthropological researches. *South African Journal of Science*, **75**: 161–164.
- Tobias, P.V. (2000). The fossil hominids. In: Partridge, T.C. and Maud, R.R. (eds.). *The Cenozoic of Southern Africa. Oxford Monograph on Geology and Geophysics*, pp. 252-276. Oxford: Oxford University Press.
- Tobias, P. V., and Hughes, A. R. (1969). The new Witwatersrand University excavation at Sterkfontein: progress report, some problems and first results. *South African Archaeological Bulletin*, **24**: 158-169.
- Von Mayer, A. (1999). *A reassessment of Cercopithecoides in Southern Africa*. Unpublished Masters Thesis, University of the Witwatersrand, Johannesburg.
- Williams F.L., Ackermann, R.R. and Leigh, S.R. (2007). Inferring Plio-Pleistocene southern African biochronology from facial affinities in *Parapapio* and other fossil papionins. *American Journal of Physical Anthropology*, **132**: 163-174.
- Wilkinson, M.J. (1973). *Sterkfontein cave system: evolution of a karst form*. Unpublished M.A. thesis. University of the Witwatersrand, Johannesburg.
- Youlatos, D. and Meldrum J. (2011). Locomotor diversification in new world monkeys: running, climbing, or clawing along evolutionary branches. *The Anatomical Record*, **294** (12): 1991-2012.

**STERKFORTEIN FOSSIL CERCOPITHECOIDEA POSTCRANIA CATALOGUE**

Table A1. Catalogue of specimens derived from Jacovec Cavern

Specimen no	Taxon	ElemenDt	Portion	Side	Size	Age
BP/3/22410	<i>Cercopithecoides indet</i>	Radius	prox.	R	Small	Adult
BP/3/22418	<i>Cercopithecoides indet</i>	Patella	Complete	R	Medium	Adult
BP/3/22419	<i>Cercopithecoides indet</i>	Patella	Complete	?	Medium	Adult
BP/3/22446	<i>Cercopithecoides indet</i>	Femur	shaft	R	Small	Adult
BP/3/22456	<i>Cercopithecoides indet</i>	Radius	shaft	L	Small	Adult
BP/3/22470	<i>Cercopithecoides indet</i>	2nd metatarsal	Complete	R	Medium	Adult
BP/3/22493	<i>Cercopithecoides indet</i>	1st Phalanx	Complete	?	Small	Adult
BP/3/22494	<i>Cercopithecoides indet</i>	Radius	shaft	R	Medium	Adult
BP/3/22610	<i>Cercopithecoides indet</i>	Fibula	shaft		Medium	Adult
BP/3/22613	<i>Cercopithecoides indet</i>	Radius	Proximal	L	Medium	Adult
BP/3/22616	<i>Cercopithecoides indet</i>	Clavicle	medial	L	Medium	Adult
BP/3/22661	<i>Cercopithecoides indet</i>	Navicular	Complete	R	Medium	Adult
BP/3/22799	<i>Cercopithecoides indet</i>	3rd metatarsal	Complete	L	Medium	Adult
BP/3/22852	<i>Cercopithecoides indet</i>	Tibia	shaft		Small	Adult
BP/3/22416	<i>Cercopithecoides indet</i>	1st Phalanx	Complete	R	Medium	Adult
BP/3/22518	<i>Cercopithecoides indet</i>	Calcaneus	Complete	R	Small	Adult
BP/3/22617	<i>Cercopithecoides indet</i>	Clavicle	lateral	L	Medium	Adult
BP/3/22669	<i>Papio/Parapapio</i>	Ulna	prox	R	Medium	Adult
BP/3/22789	<i>Cercopithecoides indet</i>	Fifth Metatarsal	Complete	R	Small	Adult

Specimen no	Taxon	Element	Portion	Side	Size	Age
BP/3/22790	<i>Cercopithecoides indet</i>	Fourth Metatarsal	Complete	L	Medium	Adult
BP/3/22794	<i>Cercopithecoides indet</i>	1st Metatarsal	Complete	?	Medium	Juvenile
BP/3/22800	<i>Cercopithecoides indet</i>	Clavicle	Complete	?	Small	Adult
BP/3/22866	<i>Cercopithecoides indet</i>	1st Phalanx	Complete	?	Medium	Adult
BP/3/22873	<i>Cercopithecoides indet</i>	Femur	shaft	L	Medium	Adult
BP/3/18382	<i>Papio/Parapapio</i>	Humerus	distal	L	Small	Adult
BP/3/22413	<i>Cercopithecoides indet</i>	Fibula	shaft	R	Medium	Adult
BP/3/22459	<i>Cercopithecoides indet</i>	Calcaneus	Body	L	Medium	Adult
BP/3/22466	<i>Cercopithecoides indet</i>	Rib	shaft	R	Medium	Adult
BP/3/22471	<i>Cercopithecoides indet</i>	3rd metacarpal	prox.	L	Medium	Adult
BP/3/22495	<i>Cercopithecoides indet</i>	Fibula			Medium	Juvenile
BP/3/22520	<i>Cercopithecoides indet</i>	Tibia	prox.	L	Large	Adult
BP/3/22575	<i>Cercopithecoides indet</i>	Radius	shaft		Medium	Adult
BP/3/22604	<i>Cercopithecoides indet</i>	Tibia	shaft		Small	Adult
BP/3/22624	<i>Cercopithecoides indet</i>	Patella		R	Small	Adult
BP/3/22625	<i>Cercopithecoides indet</i>	1st Phalanx			Medium	Juvenile
BP/3/22645	<i>Cercopithecoides indet</i>	Clavicle	shaft		Small	Adult
BP/3/22660	<i>Cercopithecoides indet</i>	Radius	shaft		Small	Adult
BP/3/22675	<i>Cercopithecoides indet</i>	Pelvis	Acetabulum	R	Small	Adult

Specimen no	Taxon	Element	Portion	Side	Size	Age
BP/3/22710	<i>Cercopithecoidea indet</i>	Femur	prox.	R	Medium	Adult
BP/3/22738	<i>Cercopithecoidea indet</i>	1st Phalanx			Medium	Juvenile
BP/3/22739	<i>Cercopithecoidea indet</i>	1st Phalanx			Medium	Adult
BP/3/22757	<i>papio sp</i>	Humerus	head	L	Medium	Juvenile
BP/3/22758	<i>Cercopithecoidea indet</i>	Femur	prox.	R	Medium	Adult
BP/3/22763	<i>Cercopithecoidea indet</i>	Tibia	dist.	L	Small	Adult
BP/3/22771	<i>Cercopithecoidea indet</i>	Ulna	prox.	R	Small	Adult
BP/3/22773	<i>Cercopithecoidea indet</i>	Humerus	shaft	R	small	Juvenile
BP/3/22775	<i>Cercopithecoidea indet</i>	1st Metatarsal		R	Medium	Adult
BP/3/22776	<i>Cercopithecoidea indet</i>	Second Metatarsal		R	Medium	Adult
BP/3/22777	<i>Cercopithecoidea indet</i>	5th metacarpal		R	Small	Adult
BP/3/22819	<i>Cercopithecoidea indet</i>	Metapodial	condyle		Small	Adult
BP/3/22829	<i>Cercopithecoidea indet</i>	Metapodial			Small	Adult
BP/3/22842	<i>Cercopithecoidea indet</i>	Carpal			Small	Adult
BP/3/22844	<i>Cercopithecoidea indet</i>	Sternum	frag		Medium	Adult
BP/3/22850	<i>Cercopithecoidea indet</i>	Femur	shaft	L	Small	Adult
BP/3/22857	<i>Cercopithecoidea indet</i>	Humerus	Proximal fragment	R	Small	Adult
BP/3/22865	<i>Cercopithecoidea indet</i>	Third Metacarpal		R	Medium	Adult

Specimen no	Taxon	Element	Portion	Side	Size	Age
BP/3/22872	<i>Cercopithecoidea indet</i>	Femur	Proximal	R	Medium	Adult
BP/3/23154	<i>Cercopithecoidea indet</i>	5th metatarsal	Distal and shaft	L	Medium	Adult
BP/3/23191	<i>Cercopithecoidea indet</i>	Radius	shaft		Small	Adult
BP/3/23232	<i>Cercopithecoidea indet</i>	Radius	Shaft Fr	?	Medium	adult
BP/3/23235	<i>Papionina</i>	Radius	Proximal	R	Medium	Adult
BP/3/23237	<i>Cercopithecoidea indet</i>	Radius	shaft		Small	Adult
BP/3/23253	<i>Cercopithecoidea indet</i>	Vertebra	Axis		Small	Adult
BP/3/23257	<i>Papio</i>	Ulna	prox.	R	Medium	adult
BP/3/23259	<i>Cercopithecoidea indet</i>	Sacrum	Vertebra		Medium	Adult
BP/3/23271	<i>Papio/Parapapio</i>	Ulna	prox	L	Medium	Adult
BP/3/23272	<i>Cercopithecoidea indet</i>	2nd metatarsal		L	Medium	Adult
BP/3/23293	<i>Cercopithecoidea indet</i>	Metapodial			Medium	Adult
BP/3/23315	<i>Cercopithecoidea indet</i>	Pelvis	Ilium	L	Large	Adult
BP/3/23331	<i>Cercopithecoidea indet</i>	Pelvis	Acetabulum	?	Medium	Adult
BP/3/23336	<i>Papio/Parapapio</i>	Ulna	Proximal	L	Medium	Adult
BP/3/23357	<i>Papio/Parapapio</i>	Ulna	Prox	?	Medium	Adult
BP/3/23380	<i>Cercopithecoidea indet</i>	Femur	lesser trochanter	R	Medium	Adult
BP/3/23389	<i>Papio</i>	Humerus	Distal and shaft	L	Small	Adult

Specimen no	Taxon	Element	Portion	Side	Size	Age
BP/3/23421	<i>Cercopithecoides indet</i>	Humerus	distal condyles	R	Small	Adult
BP/3/23428	<i>Cercopithecoides indet</i>	Humerus	dist.	L	Small	Adult
BP/3/23453	<i>Papio</i>	Radius	proximal	L	medium	Adult
BP/3/23585	<i>Cercopithecoides indet</i>	Clavicle			Small	Adult
BP/3/23648	<i>Cercopithecoides indet</i>	Femur	head	?R	Medium	Adult
BP/3/23652	<i>Cercopithecoides indet</i>	Rib	head		Small	Adult
BP/3/23653	<i>Cercopithecoides indet</i>	Palmar distal phalanx	Complete	?	Medium	Adult
BP/3/23655	<i>Cercopithecoides indet</i>	palmar distal phalange		?L	Small	Adult
BP/3/23665	<i>Cercopithecoides indet</i>	1st Phalanx			Small	Adult
BP/3/23672	<i>Cercopithecoides indet</i>	metapodial			Medium	Adult
BP/3/23681	<i>Cercopithecoides indet</i>	Femur	prox	L	Small	Adult
BP/3/23684	<i>Cercopithecoides indet</i>	Humerus	dist.	R	Medium	Adult
BP/3/23689	<i>Cercopithecoides indet</i>	1st Phalanx			Small	Adult
BP/3/23692	<i>Cercopithecoides indet</i>	Thoracic Vertebra			Medium	Adult
BP/3/23694	<i>Cercopithecoides indet</i>	Tibia	dist.	R	Medium	Adult
BP/3/23700	<i>Cercopithecoides indet</i>	Scapula		R	Small	Adult
BP/3/23710	<i>Cercopithecoides indet</i>	Femur	prox.	L	Medium	Adult
BP/3/23715	<i>Cercopithecoides indet</i>	Radius	Shaft	?	Medium	Adult



Specimen no	Taxon	Element	Portion	Side	Size	Age
BP/3/23718	<i>Papionina</i>	Ulna	Proximal	R	medium	adult
BP/3/23720	<i>Cercopithecoides indet</i>	Radius	Proximal shaft	L	Medium	Adult
BP/3/23724	<i>Cercopithecoides indet</i>	Pelvis	ilio-pubis ramus	L	medium	adult
BP/3/23733	<i>Cercopithecoides indet</i>	Intermediate hand phalange	Proximal and shaft	R	medium	adult
BP/3/23734	<i>Cercopithecoides indet</i>	Lumbar Vertebra			Small	Adult
BP/3/23737	<i>Cercopithecoides indet</i>	4th metatarsal			Medium	Adult
BP/3/23741	<i>Cercopithecoides indet</i>	Ulna	proximalfr	L	Small	Adult
BP/3/23742	<i>Cercopithecoides indet</i>	Caudal Vertebra	Complete		Small	Adult
BP/3/23746	<i>Cercopithecoides indet</i>	1st Phalanx			Medium	Adult
BP/3/23860	<i>Cercopithecoides indet</i>	1st Phalanx			Medium	Adult
BP/3/23890	<i>Cercopithecoides indet</i>	Proximal foot phalanx	complete	?R	Small	Adult
BP/3/23891	<i>Cercopithecoides indet</i>	phalanx II			Small	Adult
BP/3/23903	<i>Cercopithecoides indet</i>	Fibula	shaft	?	Small	Adult
BP/3/23954	<i>Cercopithecoides indet</i>	palmar intermediate 5th phalange			Small	Adult
BP/3/31153	<i>Cercopithecoides indet</i>	Radius	Proximal fragment	?	Medium	adult
BP/3/31170	<i>Cercopithecoides indet</i>	Ulna	shaft		Medium	Adult

Specimen no	Taxon	Element	Portion	Side	Size	Age
BP/3/31174	<i>Cercopithecoides indet</i>	Femur	shaft	?	Small	Adult
BP/3/31175	<i>Papio/Parapapio</i>	Ulna	prox.	R	Small	Adult
BP/3/31221	<i>Cercopithecoides indet</i>	5th intermediate palmar phalanx		R	small	Juvenile
BP/3/31251	<i>Cercopithecoides indet</i>	Distal palmar phalanx		?	Small	Adult
BP/3/31257	<i>Cercopithecoides indet</i>	Tibia	dist.	L	Medium	Adult
BP/3/31274	<i>Cercopithecoides indet</i>	Fibula	shaft	?	Small	?
BP/3/31282	<i>Cercopithecoides indet</i>	Ulna	shaft		Medium	Adult
BP/3/31305	<i>Cercopithecoides indet</i>	Cervical Vertebra	body	-	small	
BP/3/31312	<i>Cercopithecoides indet</i>	Metacarpal	complete	R	small	
BP/3/31354	<i>Cercopithecoides indet</i>	Radius	shaft	?	Medium	Adult
BP/3/31362	<i>Cercopithecoides indet</i>	Vertebrae	body		small	Sub-adult
BP/3/31380	<i>Cercopithecoides indet</i>	1st Phalanx			small	
BP/3/31381	<i>Cercopithecoides indet</i>	Metapodial	Proximal	?	Medium	Adult
BP/3/31382	<i>Cercopithecoides indet</i>	Radius	shaft		Medium	Adult
BP/3/31384	<i>Cercopithecoides indet</i>	2nd metatarsal	base	R	Medium	Adult
BP/3/31388	<i>Cercopithecoides indet</i>	Radius	shaft	?R	Medium	Adult
BP/3/31389	<i>Cercopithecoides indet</i>	Talus	complete	L	small	

Specimen no	Taxon	Element	Portion	Side	Size	Age
BP/3/31390	<i>Cercopithecoides indet</i>	Clavicle	complete	R	Medium	Adult
BP/3/31423	<i>Cercopithecoides indet</i>	Fibula	shaft		Small	
BP/3/31436	<i>Cercopithecoides indet</i>	phalange	distal	?	Medium	Adult
BP/3/31457	<i>Cercopithecoides indet</i>	Navicular	complete	R	Medium	Adult
BP/3/31458	<i>Cercopithecoides indet</i>	Cervical Vertebra			small	
BP/3/31494	<i>Cercopithecoides indet</i>	Tibia	Distal	?R	Medium	Adult
BP/3/31525	<i>Cercopithecoides indet</i>	palmar intermediate phalange	complete	L	Medium	Adult
BP/3/31527	<i>Cercopithecoides indet</i>	Plantar distal phalange			Medium	Adult
BP/3/31529	<i>Cercopithecoides indet</i>	metapodial	DISTal	?	Small	Sub-adult
BP/3/31550	<i>Cercopithecoides indet</i>	Metapodial	DISTAL FR		Medium	Adult
BP/3/31553	<i>Papionina</i>	Radius	Proximal	L	medium	Juvenile
BP/3/31578	<i>Cercopithecoides indet</i>	Ulna	distal	R	Medium	Adult
BP/3/31590	<i>Cercopithecoides indet</i>	thoracic Vertebra	centrum		Large	Adult
BP/3/31596	<i>Cercopithecoides indet</i>	Pelvis	ILuim	?	Medium	Adult
BP/3/31629	<i>Cercopithecoides indet</i>	5th metacarpal	Distal and shaft	R	Small	Adult
BP/3/31643	<i>Cercopithecoides indet</i>	Ulna	shaft	?R	Small	Adult
BP/3/31647	<i>Cercopithecoides indet</i>	Femur	distal condyle fr	R	Small	juvenile

Specimen no	Taxon	Element	Portion	Side	Size	Age
BP/3/31651	<i>Cercopithecoides indet</i>	Rib			Small	Adult
BP/3/31653	<i>Cercopithecoides indet</i>	Femur	dist.	L	Small	Adult
BP/3/31661	<i>Cercopithecoides indet</i>	talus	complete	R	Small	sub-adult
BP/3/31686	<i>Cercopithecoides indet</i>	Humerus	shaft	R	Small	Sub-adult
BP/3/31691	<i>Papio</i>	Humerus	distal	R	Medium	Sub-adult
BP/3/31697	<i>Cercopithecoides indet</i>	Scapula	Glenoid cavity	L	Small	sub-adult
BP/3/31715	<i>Cercopithecoides indet</i>	5th metacarpal	complete	R	Medium	sub-adult
BP/3/31716	<i>Cercopithecoides indet</i>	Fibula	shaft	?	Small	?
BP/3/31735	<i>Cercopithecoides indet</i>	Tibia	dist.	L	Medium	Adult
BP/3/31800	<i>Cercopithecoides indet</i>	4th metacarpal		L	Small	Adult
BP/3/31805	<i>Cercopithecoides indet</i>	Lateral cuneiform	complete	R	Small	Adult
BP/3/31816	<i>Cercopithecoides indet</i>	Radius	prox	R	Small	Adult
BP/3/31829	<i>Papio sp</i>	Humerus	prox	L	Small	Adult
BP/3/31837	<i>Cercopithecoides indet</i>	2nd metacarpal		L	Small	Adult
BP/3/31872	<i>Cercopithecoides indet</i>	Humerus	capitulum	L	Small	Adult
BP/3/31905	<i>Cercopithecoides indet</i>	Femur	shaft	?	Small	Adult
BP/3/31910	<i>Cercopithecoides indet</i>	thoracic Vertebra			Small	Adult

BP/3/31922	<i>Cercopithecoides indet</i>	Radius	shaft	L	Small	Adult
BP/3/31923	<i>Papio sp</i>	Radius	prox	R	Medium	Adult
BP/3/31945	<i>Cercopithecoides indet</i>	Navicular		L	Medium	Adult
BP/3/31960	<i>Cercopithecoides indet</i>	Scapula	glenoid	R	Small	Adult
BP/3/32006	<i>Cercopithecoides indet</i>	1st phalanx			Small	Adult
BP/3/32007	<i>Cercopithecoides indet</i>	1st phalanx			Small	Adult
BP/3/32008	<i>Cercopithecoides indet</i>	1st phalanx			Small	Adult
BP/3/32009	<i>Cercopithecoides indet</i>	2nd metatarsal	complete	R	medium	Juvenile
BP/3/32045	<i>Cercopithecoides indet</i>	Ulna	shaft		Small	Adult
BP/3/32046	<i>Cercopithecoides indet</i>	1st metatarsal		L	Medium	Adult
BP/3/32047	<i>Cercopithecoides indet</i>	2nd metatarsal		L	Small	Adult
BP/3/32111	<i>Cercopithecoides indet</i>	Clavicle	shaft	?	Medium	Adult
BP/3/32130	<i>Cercopithecoides indet</i>	Ulna	shaft		Medium	Adult
BP/3/32139	<i>Cercopithecoides indet</i>	Humerus	dist.	L	Small	Adult
BP/3/32151	<i>Cercopithecoides indet</i>	Internal cuneiform		L	Medium	Adult
BP/3/32167	<i>Cercopithecoides indet</i>	Ulna	shaft		Medium	Adult
BP/3/32194	<i>Cercopithecoides indet</i>	Navicular		R	Small	Adult
BP/3/32206	<i>Cercopithecoides indet</i>	Scapula		R	Medium	Adult
BP/3/32211	<i>Cercopithecoides indet</i>	Humerus	shaft	R	Small	Juvenile
BP/3/32221	<i>Cercopithecoides indet</i>	Fibula	dist.	L	Medium	Adult

BP/3/32239	<i>Cercopithecoidea indet</i>	5th metacarpal		L	Medium	Adult
BP/3/3119	<i>Cercopithecoidea indet</i>	Scapula	Blade	?	Medium	Adult

Table A2. Catalogue of specimens derived from Silberberg Grotto

<b>Specimen no</b>	<b>Provenance</b>	<b>Taxon</b>	<b>Element</b>	<b>Portion</b>	<b>Side</b>	<b>Size</b>
S94-7211	D20	<i>Cercopithecoidea indet</i>	Talus	complete	R	Medium
SWP 920	D20	<i>Cercopithecoidea indet</i>	Humerus	distal shaft	?	Medium
SWP 921	D20	<i>Cercopithecoidea indet</i>	Humerus	shaft	?	Medium
SWP 1785	D20	<i>Papio/Parapapio</i>	Femur	prox	L	Medium
SWP 1303	D20	<i>Cercopithecoidea indet</i>	Femur	Proximal	R	Medium
SWP 1365	D20	<i>Cercopithecoidea indet</i>	Tibia	Distal	R	Large
SWP 1367	D20	<i>Cercopithecoidea indet</i>	Femur	distal shaft	?	Medium
SWP 1368	D20	<i>Papio/Parapapio</i>	Radius	Proximal	L	Medium
SWP 1383	D20	<i>Cercopithecoidea indet</i>	Femur	Proximalfr	R	Medium
SWP 1384	D20	<i>Papionina</i>	Femur	Proximal	R	Medium
SWP 1385	D20	<i>Papio/Parapapio</i>	Femur	Proximal	L	Medium
SWP 1386	D20	<i>Cercopithecoidea indet</i>	Humerus	distal	?	Medium
SWP 1387	D20	<i>Cercopithecoidea indet</i>	Tibia	Proximal fr	?	Medium
SWP 1388	D20	<i>Cercopithecoidea indet</i>	Humerus	Distal		Medium
SWP 1390	D20	<i>Cercopithecoidea indet</i>	Talus	complete	R	medium
SWP 1391	D20v	<i>Cercopithecoidea indet</i>	Calcaneus		R	Medium
SWP 1403	D20	<i>Cercopithecoidea indet</i>	Ulna	distal	L	Medium
SWP 1404	D20	<i>Cercopithecus sp</i>	Femur	Proximal	R	Medium
SWP 1405	D20	<i>Cercopithecoidea indet</i>	Ulna	Distal shaft	R	Medium
SWP 1406	D20	<i>Papio</i>	Humerus	Proximal	R	Medium
SWP 1408	D20	<i>Cercopithecoidea indet</i>	Metapodial	Proximal	?	Medium
SWP 1410	D20	<i>Papio/Parapapio</i>	Humerus	Distal	L	Medium
SWP 1411	D20	<i>Cercopithecoidea indet</i>	Tibia	Proximal	? L	Medium
SWP 1414	D20	<i>Cercopithecoidea indet</i>	Femur	Proximal	L	Medium
SWP 1416	D20	<i>Papionina</i>	Radius	Proximal	R	Large
SWP 1418	D20	<i>Papio</i>	Radius	Proximal	R	Medium
SWP 1419	D20	<i>Cercopithecoidea indet</i>	Radius	Shaft	?	Medium
SWP 1420	D20	<i>Cercopithecoidea indet</i>	Radius	Proximal shaft	?	Medium
SWP 1532	D20	<i>Papionina</i>	Femur	Distal	R	Medium
<b>Specimen no</b>	<b>Provenance</b>	<b>Taxon</b>	<b>Element</b>	<b>Portion</b>	<b>Side</b>	<b>Size</b>
SWP 1533	D20	<i>Cercopithecoidea indet</i>	Femur	shaft	?	Medium



SWP 1534	D20	<i>Papionina</i>	Femur	Distal	L	Large
SWP 1535	D20	<i>Cercopithecoidea indet</i>	Femur	Distal	R	Medium
SWP 1536	D20	<i>Papionina</i>	Femur	Proximal shaft	R	Large
SWP 1537	D20	<i>Papionina</i>	Femur	Proximal shaft	L	Medium
SWP 1538	D20	<i>Cercopithecoidea indet</i>	Humerus	Proximal shaft	?	Medium
SWP 1539	D20	<i>Papionina</i>	Humerus	capitulum	R	Medium
SWP 1540	D20	<i>Parapapio</i>	Humerus	distal	L	Medium
SWP 1541	D20	<i>Cercopithecoidea indet</i>	Humerus	distal	?	medium
SWP 1542	D20	<i>Cercopithecoidea indet</i>	Humerus	head fr	L	Medium
SWP 1543	D20	<i>Papionina</i>	Humerus	Capitulum and trochlea	L	Medium
SWP 1544	D20	<i>Papionina</i>	Humerus	Distal fr	?	Medium
SWP 1545	D20	<i>Cercopithecoidea indet</i>	Ulna	Shaft	?	Medium
SWP 1546	D20	<i>Cercopithecoidea indet</i>	Tibia	Proximal	L	Medium
SWP 1547	D20	<i>Cercopithecoidea indet</i>	Ulna	Proximal	R	Medium
SWP 1547	D20	<i>Cercopithecoidea indet</i>	Radius	Distal	?	Medium
SWP 1548	D20	<i>Cercopithecoidea indet</i>	Tibia	Proximal fragment	L	Medium
SWP 1550	D20	<i>Cercopithecoidea indet</i>	Metapodial	Distal shaft	?	Medium
SWP 1552	D20	<i>Papio</i>	Radius	proximal	R	Medium
SWP 1554	D20	<i>Cercopithecoidea indet</i>	Ulna	shaft	?	Medium
SWP 1555	D20	<i>Cercopithecoidea indet</i>	Radius	shaft fragment	?	Medium
SWP 1556	D20	<i>Cercopithecoidea indet</i>	Radius	Shaft fragment	?	Medium
SWP 1557	D20	<i>Cercopithecoidea indet</i>	Radius	Shaft fragment	?	Medium
SWP 1560	D20	<i>Papionina</i>	Ulna	Proximal	L	Medium
SWP 1561	D20	<i>Papionina</i>	Ulna	Proximal	R	Medium
SWP 1562	D20	<i>Cercopithecoidea indet</i>	Ulna	proximal	R	Medium
SWP 1566	D20	<i>Papionina</i>	Ulna	Proximal	L	Medium
SWP 1581	D20	<i>Papionina</i>	Humerus	Distal	L	Medium
SWP 1582	D20	<i>Parapapio/Papio</i>	Humerus	Distal	R	Medium
SWP 1583	D20	<i>Papionina</i>	Humerus	Distal	L	Medium
SWP 1584	D20	<i>Papio</i>	Humerus	distal	R	Medium
SWP 1585	D20	<i>Cercopithecoidea indet</i>	Humerus	Distal and prox fragment	R	Medium

<b>Specimen no</b>	<b>Provenance</b>	<b>Taxon</b>	<b>Element</b>	<b>Portion</b>	<b>Side</b>	<b>Size</b>
SWP 1586	D20	<i>Cercopithecoides indet</i>	Humerus	Distal	R	Small
SWP 1587	D20	<i>Cercopithecoides indet</i>	Humerus	Distal		Medium
SWP 1588	D20	<i>Cercopithecoides indet</i>	Humerus	Distal shaft	?	Small
SWP 1589	D20	<i>Parapapio</i>	Humerus	Distal	L	Medium
SWP 1590	D20	<i>Papio/Parapapio</i>	Ulna	Proximal	R	Medium
SWP 1591	D20	<i>Cercopithecoides indet</i>	Ulna	Proximal	R	Medium
SWP 1592	D20	<i>Cercopithecoides indet</i>	Ulna	Shaft	L	Medium
SWP 1593	D20	<i>Cercopithecoides indet</i>	Ulna	Distal shaft	L	Small
SWP 1593	D20	<i>Cercopithecoides indet</i>	Ulna	Proximal fr	?	Medium
SWP 1594	D20	<i>Papio/Parapapio</i>	Ulna	Proximal	L	Small
SWP 1595	D20	<i>Cercopithecoides indet</i>	Ulna	Shaft	L	Large
SWP 1597	D20	<i>Cercopithecoides indet</i>	Tibia	Proximal	L	Medium
SWP 1598	D20	<i>Cercopithecoides indet</i>	Tibia	Proximal	?	Medium
SWP 1601	D20	<i>Cercopithecoides indet</i>	Tibia	Distal	L	Medium
SWP 1602	D20	<i>Cercopithecoides indet</i>	Tibia	Distal	L	Medium
SWP 1603	D20	<i>Cercopithecoides indet</i>	Tibia	Distal	L	Medium
SWP 1604	D18	<i>Papionina</i>	Ulna	proximal	R	Large
SWP 1605	D20	<i>Cercopithecoides indet</i>	Femur	Distal	L	Large
SWP 1606	D20	<i>Cercopithecoides indet</i>	Femur	Head	R	Medium
SWP 1607	D20	<i>Cercopithecoides indet</i>	Femur	Distal	L	Medium
SWP 1608	D20	<i>Cercopithecoides indet</i>	Femur	Distal	L	Medium
SWP 1609	D20	<i>Cercopithecoides indet</i>	Femur	Condyles	L	Medium
SWP 1610	D20	<i>Cercopithecoides indet</i>	femur	distal condyles	L	Medium
SWP 1611	D20	<i>Cercopithecoides indet</i>	Humerus	proximal	R	Medium
SWP 1612	D20	<i>Cercopithecoides indet</i>	Femur	proximal	L	Medium
SWP 1613	D20	<i>Cercopithecoides indet</i>	Femur	Head	L	medium
SWP 1614	D20	<i>Cercopithecoides indet</i>	femur	Head	?	Medium
SWP 1615	D20	<i>Cercopithecoides indet</i>	Femur	Head	?	Medium
SWP 1616 smudged	D20	<i>Cercopithecoides indet</i>	Femur	Proximal	?	Medium
SWP 1617	D20	<i>Cercopithecoides indet</i>	Femur	Proximal	R	Small
SWP 1618	D20	<i>Cercopithecoides indet</i>	Femur	Shaft	?	Medium
SWP 1619	D20	<i>Cercopithecoides indet</i>	Femur	Shaft	?	Medium
SWP 1620	D20	<i>Cercopithecoides indet</i>	Calcaneus	complete	?	Medium

<b>Specimen no</b>	<b>Provenance</b>	<b>Taxon</b>	<b>Element</b>	<b>Portion</b>	<b>Side</b>	<b>Size</b>
SWP 1621	D20	<i>Cercopithecoides indet</i>	1st phalanx	complete	?	Medium
SWP 1622	D20	<i>Cercopithecoides indet</i>	Phalanx	Distal	?	Medium
SWP 1623	D20	<i>Cercopithecoides indet</i>	Metapodial	shaft	?	Medium
SWP 1625	D20	<i>Cercopithecoides indet</i>	Long bone	shaft	?	Small
SWP 1626	D20	<i>Cercopithecoides indet</i>	Talus	complete	L	Medium
SWP 1627	D20	<i>Cercopithecoides indet</i>	Calcaneus	complete	L	Medium
SWP 1628	D20	<i>Cercopithecoides indet</i>	Phalanx	Complete	?	Medium
SWP 1630	D20	<i>Cercopithecoides indet</i>	Pelvis	Os coxa fr	L	Medium
SWP 1631	D20	<i>Cercopithecoides indet</i>	Pelvis	Fragment	?	Medium
SWP 1633	D20	<i>Cercopithecoides indet</i>	Pelvis	Fragment	?	Medium
SWP 1634	D20	<i>Cercopithecoides indet</i>	Pelvis	Acetabulum	?	Medium
SWP 1635	D20	<i>Cercopithecoides indet</i>	Pelvis	Fragment	?	Medium
SWP 1636	D20	<i>Cercopithecoides indet</i>	Pelvis	Ilium	?	Medium
SWP 1697	D20	<i>Theropithecus sp</i>	Femur	prox	R	Medium
SWP 1698	D20	<i>Papio/Parapapio</i>	Femur	prox	L	Medium
SWP 1699	D20	<i>Papionina</i>	Femur	prox	L	Medium
SWP 1700	D20	<i>Papio/Parapapio</i>	Femur	Proximal fr	L	Medium
SWP 1701	D20	<i>Cercopithecoides indet</i>	Femur	head	R	Medium
SWP 1702	D20	<i>Cercopithecoides indet</i>	Femur	head	L	Medium
SWP 1703	D20	<i>Cercopithecoides indet</i>	Femur	head	?	Medium
SWP 1704	D20	<i>Papionina</i>	Femur	Prox	R	Medium
SWP 1705	D20	<i>Cercopithecoides indet</i>	Femur	Proximal	L	Medium
SWP 1706	D20	<i>Papionina</i>	Femur	Shaft	L	Medium
SWP 1707	D20	<i>Cercopithecoides indet</i>	Femur	Proximal	?	Medium
SWP 1708	D20	<i>Cercopithecoides indet</i>	Femur	Proximal fragment	?	Medium
SWP 1709	D20	<i>Cercopithecoides indet</i>	Femur	Proximal fr	L	Medium
SWP 1711	D20	<i>Cercopithecoides indet</i>	femur	Distal	L	Medium
SWP 1712	D20	<i>Cercopithecoides indet</i>	Femur	distal condyles	R	Medium
SWP 1713	D20	<i>Cercopithecoides indet</i>	Femur	distal condyles	?	Medium
SWP 1714	D20	<i>Cercopithecoides indet</i>	Femur	distal condyles	R	Large
SWP 1715	D20	<i>Cercopithecoides indet</i>	Femur	distal condyles	R	Medium
SWP 1716	D20	<i>Cercopithecoides indet</i>	Femur	Distal	?	Medium

<b>Specimen no</b>	<b>Provenance</b>	<b>Taxon</b>	<b>Element</b>	<b>Portion</b>	<b>Side</b>	<b>Size</b>
SWP 1717	D20	<i>Cercopithecoides indet</i>	Femur	distal condyles	R	Medium
SWP 1718	D20	<i>Cercopithecoides indet</i>	Femur	distal condyles	?	Medium
SWP 1719	D20	<i>Cercopithecoides indet</i>	Femur	Shaft	?	Medium
SWP 1720	D20	<i>Cercopithecoides indet</i>	Femur	Shaft	?	Medium
SWP 1721	D20	<i>Cercopithecoides indet</i>	Femur	Shaft	?	Medium
SWP 1722	D20	<i>Cercopithecoides indet</i>	Femur	Shaft	?	Medium
SWP 1724	D20	<i>Cercopithecoides indet</i>	Femur	Distal		Medium
SWP 2349	D20	<i>Cercopithecoides indet</i>	Pelvis	Acetabulum	R	Medium
SWP 2351	D20	<i>Cercopithecoides indet</i>	Pelvis	Fragment	?	Medium
SWP 2352	D20	<i>Cercopithecoides indet</i>	Pelvis	Ilium	?	Medium

Table A3. Catalogue of specimens derived from Member 4

Specimen no	Provenance	Level	Taxon	Element	Portion	Side	Size	Age
BP/3/16533	O43	24'10"-25'10"	<i>Cercopithecoides indet</i>	Pelvis	Ilium	R	Medium	Adult
BP/3/16554	O43	24'10"-25'10"	<i>Cercopithecoides indet</i>	Pelvis	Ilium	?	Small	Adult
BP/3/16617	O40	12'0"-13'0'	<i>Cercopithecoides indet</i>	Femur	Shaft		Small	Adult
BP/3/16624	O42	16'4"-17'-4'	<i>Cercopithecoides indet</i>	Femur	Shaft		Medium	Adult
BP/3/16635	O46	21'10"-22'10'	<i>Cercopithecoides indet</i>	Vertebrae	Lumbar		Small	Adult
BP/3/16652	O42	?	<i>Cercopithecoides indet</i>	Humerus	Condyle	?	Small	Adult
BP/3/16793	O46	28'10"-29'10"	<i>Cercopithecoides indet</i>	Scapula	Glenoid cavity	R	Medium	Adult
BP/3/16816	O46	26'10"-27'10'	<i>Cercopithecoides indet</i>	Femur	Shaft	?	Medium	Adult
BP/3/16847	O46	26'10"-27'10'	<i>Cercopithecoides indet</i>	Ulna	Shaft		Medium	Adult
BP/3/17757	R42	32'8"-33'8"	<i>Cercopithecoides indet</i>	Caudal Vertebra	Complete		Medium	Adult
BP/3/17789	R45	36'3"-37'3"	<i>Cercopithecoides indet</i>	Humerus	Proximal	R	Medium	Adult
BP/3/23004	P46	16'5"-17'5"	<i>Cercopithecoides indet</i>	Humerus	Shaft	R	Small	Adult
BP/3/23008	P43	10'2"-11'6"	<i>Cercopithecoides indet</i>	Tibia	Distal	L	Medium	Adult
BP/3/23009	P42	11'11"-12'6"	<i>Cercopithecoides indet</i>	Talus	Complete	L	Medium	Adult
BP/3/23016	P42	12'6"-13'-1"	<i>Papio/Parapapio</i>	Humerus	Distal condyles	L	Small	Adult
BP/3/23021	P45	14'4"-15'8"	<i>Cercopithecoides indet</i>	Pelvis	Ilium	L	Medium	Adult
BP/3/23022	P45	14'4"-15'8"	<i>Cercopithecoides indet</i>	Pelvis	Acetabulum	L	Medium	Adult
BP/3/23023	P45	14'4"-15'8"	<i>Cercopithecoides indet</i>	Femur	Proximal	R	Medium	Adult
BP/3/23028	P44	14'5"-15'1"	<i>Papionina</i>	Ulna	Proximal	L	Small	Adult
BP/3/23029	P44	14'5"-15'1"	<i>Cercopithecoides indet</i>	Talus	Complete	L	Medium	Adult
BP/3/23048	P44	8'7"-9'7"	<i>Cercopithecoides indet</i>	1st metatarsal	Prox	R	Medium	Adult
BP/3/23049	P44	8'7"-9'7"	<i>Cercopithecoides indet</i>	Pelvis	Ilium	L	Medium	Adult
BP/3/23059	P43	8'3"-9'3"	<i>Cercopithecoides indet</i>	Ulna	Shaft	R	Medium	Adult
BP/3/2306			<i>Papio/Parapapio</i>	Humerus	Distal	L	Small	Adult
BP/3/23064	P44	17'11"-18'11"	<i>Cercopithecoides indet</i>	2nd metatarsal	Proximal	L	Medium	Adult
BP/3/23067	N46	13'5"-14'5"	<i>Cercopithecoides indet</i>	Pelvis	Os coxa	L	Medium	Adult
BP/3/23070	P44	15'1"-16'1"	<i>Cercopithecoides indet</i>	Fibula	Shaft	?	Medium	Adult
BP/3/23071	P44		<i>Cercopithecoides indet</i>	Metapodial	Dist	?	Medium	Adult

Specimen no	Provenance	Level	Taxon	Element	Portion	Side	Size	Age
BP/3/23072	P44	15'1'-16'1'	<i>Cercopithecoides indet</i>	Sternum	Body		Small	Adult
BP/3/23074	P44	8'11'-9'11'	<i>Cercopithecoides indet</i>	Femur	Head	?	Small	Juvenile
BP/3/23088	N46	16'5"-17'5"	<i>Cercopithecoides indet</i>	1st metatarsal	Head	L	Medium	Adult
BP/3/23090	N46	16'5'-17'5'	<i>Cercopithecoides indet</i>	Calcaneus	Head	L	Medium	Adult
BP/3/23091	N46	16'5'-17'5'	<i>Papio sp</i>	Radius	Shaft	L	Medium	Adult
BP/3/23092	N46	16'5'-17'5'	<i>Cercopithecoides indet</i>	Ulna	Proximal	R	Medium	Adult
BP/3/23093	N46	16'5'-17'5'	<i>Papionina</i>	Ulna	Head	L	Medium	Adult
BP/3/23112	P41	10'6'-11'3'	<i>Cercopithecoides indet</i>	5th metatarsal	Proximal	R	Medium	Adult
BP/3/23113	P41	10'6'-11'3'	<i>Cercopithecoides indet</i>	4th metatarsal	Head	L	Medium	Adult
BP/3/23115	P44		<i>Cercopithecoides indet</i>	1st metatarsal	Proximal and shaft	?		Adult
BP/3/23119	?	?	<i>Cercopithecoides indet</i>	2nd phal	Complete	R	Medium	Adult
BP/3/23120	P32	9'9'-10'1'	<i>Cercopithecoides indet</i>	Femur	Proximal	L	Medium	Adult
BP/3/23121	P32	9'9'-10'1'	<i>Cercopithecoides indet</i>	Femur	Shaft	L	Medium	Adult
BP/3/23126	W44		<i>Cercopithecoides indet</i>	Scapula	Glenoid	R	Small	Adult
BP/3/23141	W43	?	<i>Cercopithecoides indet</i>	Vertebra	Atlas fr		Small	Adult
BP/3/23143	W43	?	<i>Cercopithecoides indet</i>	Manus phal	Distal	?	Medium	Adult
BP/3/23145	T44	30'5'-31'5'	<i>Cercopithecoides indet</i>	4th metatarsal	Proximal	L	Medium	Adult
BP/3/23955	N43	13'9'-14'9'	<i>Cercopithecoides indet</i>	Tibia	Distal	R	Medium	Adult
BP/3/23958	N43	13'9'-14'9'	<i>Cercopithecoides indet</i>	Pelvis	Ilium		Medium	Adult
BP/3/23959	N43	13'9'-14'9'	<i>Cercopithecoides indet</i>	Scapula	Glenoid cavity	R	Medium	Adult
BP/3/23964	N46	21'9'-22'9'	<i>Cercopithecoides indet</i>	5th metatarsal	Prox.	R	Small	Adult
BP/3/23966	O44		<i>Cercopithecoides indet</i>	Caudal Vertebra	Complete		Medium	Adult
BP/3/23970	O46	29"10'-30'10'	<i>Cercopithecoides indet</i>	Pelvis	Ilium blade	R	Medium	Adult
BP/3/23979			<i>Cercopithecoides indet</i>	Cerv Vertebra	Spine and body		Medium	Adult
BP/3/23980	P44	30' 7" - 31' 7"	<i>Cercopithecoides indet</i>	4rth metatarsal	Proximal	R	Medium	Adult
BP/3/23984	O44	30' 7" - 31' 7"	<i>Cercopithecoides indet</i>	Talus	Complete	L	Small	Adult
BP/3/24000	N46	17'5"-18'0"	<i>Papio</i>	Humerus	Distal	L	Small	Adult

Specimen no	Provenance	Level	Taxon	Element	Portion	Side	Size	Age
BP/3/24003	N44	15'8"-16'6'	<i>Cercopithecoides indet</i>	proximal phal	Complete	L	Medium	Adult
BP/3/24004	N44	15'8"-16'6'	<i>Cercopithecoides indet</i>	Proximal phal	Complete	R	Medium	Adult
BP/3/24007	N46	15'5"-16'5'	<i>Cercopithecoides indet</i>	Radius	Shaft	?	Medium	Adult
BP/3/24010	N44	12'9"-13'8"	<i>Cercopithecoides indet</i>	Talus	Complete	L	Medium	Adult
BP/3/24011	S43	13' 10" - 14' 10"	<i>Cercopithecoides indet</i>	2nd metatarsal	Complete	R	Medium	Adult
BP/3/24014	P43	35'0"-36'0'	<i>Cercopithecoides indet</i>	Humerus	Head	?	Small	Sub-adult
BP/3/24018	S43	14'10"-15'1'0'	<i>Cercopithecoides indet</i>	Ulna	Shaft	L	Medium	Adult
BP/3/24019	S43	14'10"-15'1'0'	<i>Cercopithecoides indet</i>	Pelvis		L	Medium	Adult
BP/3/24023	Q46	20'10"-21'10"	<i>Cercopithecoides indet</i>	Scapula	Glenoid	L	Small	Adult
BP/3/24033	Q44	9'3"-10'3'	<i>Cercopithecoides indet</i>	Manus 2nd phalanx	Complete	L	Medium	Adult
BP/3/24037	N44	13'8"-14'8"	<i>Cercopithecoides indet</i>	Femur	Prox.	R	Medium	Adult
BP/3/24038	N44	13'8"-14'8"	<i>Papio?</i>	Ulna	Shaft	L	Medium	Adult
BP/3/24042	N45	16'8"-17'8'	<i>Cercopithecoides indet</i>	Femur	Head	L	Medium	Adult
BP/3/24043	N45	16'8"-17'8'	<i>Papio/Parapapio</i>	Radius	Head	L	Medium	Adult
BP/3/24050	N44	11'9"-12'9'	<i>Cercopithecoides indet</i>	2nd phalanx	Complete	L	Small	Adult
BP/3/24051	P42	36'0"-37'0'	<i>Cercopithecoides indet</i>	Ulna	Shaft	R	Small	Adult
BP/3/24053	P42	36'0"-37'0'	<i>Papio/Parapapio</i>	Humerus	Distal	R	Medium	Adult
BP/3/24055	R43	14'3"-15'0'	<i>Cercopithecoides indet</i>	Metapodial			Medium	
BP/3/24056	R43	?	<i>Cercopithecoides indet</i>	2-5phal manus	?	R	Medium	Adult
BP/3/24057	R43	14' 3"- 15' 0"	<i>Cercopithecoides indet</i>	3rd metatarsal	Proximal	R	Medium	Adult
BP/3/24066	24'2"-25'2'	S43	<i>Cercopithecoides indet</i>	Metapodial	Distal		Medium	Adult
BP/3/24070	N42	15'1"-16'1'	<i>Cercopithecoides indet</i>	2-5th pes phal	Proximal	L	Medium	Adult
S94-10344	Q44	10'3"-11'3'	<i>Cercopithecoides indet</i>	Femur	Medial	L	Medium	Adult
S94-10366	Q44	?	<i>Cercopithecoides indet</i>	Tibia	Shaft	?	Small	Adult
S94-10431	Q43	?	<i>Cercopithecoides indet</i>	Patella	Complete	?	Medium	Adult
S94-10431			<i>Cercopithecoides indet</i>	Patella	Complete	?	Medium	Adult



Specimen no	Provenance	Level	Taxon	Element	Portion	Side	Size	Age
S94-10456	Q48	9'2"-10'2'	<i>Cercopithecoides indet</i>	Tibia	Shaft		Medium	Adult
S94-10745	S57	?	<i>Cercopithecoides indet</i>	Tibia	Shaft	?	Small	Adult
S94-10836	S64	N/a	<i>Cercopithecoides sp</i>	Ulna same as 13505	Proximal	R	Small	Adult
S94-10852	Q48	8'6"-9'6'	<i>Cercopithecoides indet</i>	Tibia	Shaft		Medium	Juvenile
S94-10864	Q49	7' 0" - 8' 0"	<i>Cercopithecoides indet</i>	Ulna	Shaft	R	Large	Adult
S94-10865	Q49	7' 0" - 8' 0"	<i>Cercopithecoides indet</i>	Ulna	Shaft	R	Large	Adult
S94-10936	I39	20'5"-21'6'	<i>Cercopithecoides indet</i>	Ulna	Shaft	?	Medium	Adult
S94-10937	I39	20'5"-21'6'	<i>Cercopithecoides indet</i>	Ulna	Shaft		Medium	Adult
S94-10951	I40	22'6"-23'6'	<i>Cercopithecoides indet</i>	Pelvis	Pubis	L	Medium	?
S94-11408	U47	11'5"-12'5"	<i>Cercopithecoides indet</i>	Femur	Shaft	?	Medium	Adult
S94-11409	U47	11'5"-12'5"	<i>Cercopithecoides indet</i>	Femur	Proximal	?	Medium	Adult
S94-11422	U47	17'3"-18'3'	<i>Cercopithecoides indet</i>	Pelvis	Ilium	R	Large	A
S94-11424	U47	17'3"-18'3'	<i>Cercopithecoides indet</i>	Ulna	Proximal	R	Large	Adult
S94-11626	T43	26'11"-27'11'	<i>Cercopithecoides indet</i>	Calcaneus	Head	L	Medium	Adult
S94-11638	T43	27'11"-28'11'	<i>Cercopithecoides indet</i>	Int cuneiform	Complete	L	Medium	Adult
S94-11660	T43	31'11"-32'11'	<i>Cercopithecoides indet</i>	Femur	Distal	L	Medium	Adult
S94-12011	P42	24'0"-25'0'	<i>Cercopithecoides indet</i>	Pelvis	Ilium	L	Medium	Adult
S94-12023	P43	25' 0" - 26' 0"	<i>Cercopithecoides indet</i>	Scapula	Coronoid and glenoid	R	Medium	Adult
S94-12054	P44	22'9"-23'2"	<i>Cercopithecoides indet</i>	Radius	Shaft	R	Medium	Adult
S94-12055	P44	22'7"-23'7"	<i>Cercopithecoides indet</i>	Ulna	Shaft		Medium	Adult
S94-12070	P44	24'7"-25'7"	<i>Cercopithecoides indet</i>	Humerus	Shaft	R	Medium	Adult
S94-12072	P44	24'7"-25'7"	<i>Cercopithecoides indet</i>	Radius	Shaft	L	Small	Adult
S94-12113	P45	?	<i>Cercopithecoides indet</i>	Thoracic Vertebra	Complete		Medium	Adult
S94-12234	R45	25'6"-26'6'	<i>Cercopithecoides indet</i>	1st metacarpal	Shaft		Medium	Adult
S94-12266	R49	17'1"017'6"	<i>Cercopithecoides indet</i>	Ulna	Shaft	R	Small	Adult
S94-12290	P40	11'8"-12'3'	<i>Cercopithecoides indet</i>	Talus	Body	R	Small	Adult

Specimen no	Provenance	Level	Taxon	Element	Portion	Side	Size	Age
S94-12306	P41	16'5'-17'9'	<i>Cercopithecoides indet</i>	Tibia	Distal	L	Medium	Adult
S94-12325	P47	19'1'-20'0'	<i>Cercopithecoides indet</i>	Scapula	Glenoid	R	Small	Adult
S94-12384	P43	17'0'-18'0'	<i>Cercopithecoides indet</i>	Ulna	Shaft	R	Medium	Adult
S94-12485	P44	29'7'-30'7'	<i>Cercopithecoides indet</i>	Tibia	Proximal	R	Small	Juvenile
S94-1256	H40	22'9'-23'5'	<i>Cercopithecoides indet</i>	Sacrum	Body		Medium	Adult
S94-12624		15'4"-16'5"	<i>Cercopithecoides indet</i>	Pelvis	Acetabulum	R	Medium	Adult
S94-12691	P42	13'1'-14'1'	<i>Cercopithecoides indet</i>	Patella	Complete		Medium	Adult
S94-12692	P42	13' 1" - 14' 1"	<i>Cercopithecoides indet</i>	Pelvis	Ischium	L	Medium	Adult
S94-12728	P44	7'7'-8'7'	<i>Cercopithecoides indet</i>	Femur	Shaft		Medium	Adult
S94-12750	P44	14'5'-15'11"	<i>Cercopithecoides indet</i>	Pelvis	Ilium	L	Large	Adult
S94-12824	P47	15'4"-16'5"	<i>Cercopithecoides indet</i>	Pelvis	Acetabulum	R	Medium	Adult
S94-12919	R43	28'10"-29'10"	<i>Cercopithecoides indet</i>	Pelvis	Ischium	R	Medium	Adult
S94-12922	R43	30'10-31'10"	<i>Cercopithecoides indet</i>	Vertebrae	Axis		Medium	Adult
S94-13006	R43	24'6"-25'6"	<i>Cercopithecoides indet</i>	Pelvis	Ilium fr	L	Medium	Adult
S94-13087	O44	11'4'-12'4'	<i>Cercopithecoides indet</i>	Ulna	Shaft	?	Large	Adult
S94-13088	O44	11'4'-12'4'	<i>Cercopithecoides indet</i>	Tibia	Shaft		Large	A
S94-13100	O44	14'10-15'10"	<i>Cercopithecoides indet</i>	Ulna	Shaft	R	Small	Adult
S94-13106	O45	14'3'-15'8"	<i>Cercopithecoides indet</i>	Pelvis	Ischium	R	Small	Adult
S94-13115	O45	15'8'-16'4'	<i>Cercopithecoides indet</i>	Ulna	Shaft	L	Large	Adult
S94-13130	O46	15'3'-16'3'	<i>Cercopithecoides indet</i>	Thoracic Vertebra	Body n spine		Medium	Adult
S94-13140	O45	17'3'-18'3'	<i>Cercopithecoides indet</i>	Femur	Distal		Medium	Adult
S94-13151	O46	17'3'-18'3'	<i>Cercopithecoides indet</i>	Ulna	Shaft	?	Medium	Adult
S94-13152	O46	17'-3"-18'-3"	<i>Papionina</i>	Ulna	Proximal	L	Small	Adult
S94-13215	Q42	18'5'-19'5'	<i>Cercopithecoides indet</i>	Pelvis	Ischium	R	Small	Adult
S94-13218	Q42	18'5'-19'5'	<i>Cercopithecoides indet</i>	Femur	Distal	R	Small	Adult
S94-13505	L42	19' 0" - 20' 40"	<i>Cercopithecoides sp</i>	Ulna	Proximal	L	Large	Adult
S94-13515	P32	9' 9" - 10' 1"	<i>Cercopithecoides indet</i>	Femur	Shaft	L	Large	Adult

Specimen no	Provenance	Level	Taxon	Element	Portion	Side	Size	Age
S94-13625	U51	9'10'-10'10'	<i>Cercopithecoides indet</i>	Pelvis	Ischium	R	Medium	Adult
S94-13626	U51	?	<i>Cercopithecoides indet</i>	Pelvis	Ischium	R	Medium	Adult
S94-13717	O43	12'6'-13'9'	<i>Cercopithecoides indet</i>	Humerus	Shaft	L	Medium	Adult
S94-13727	O43	17' 10" - 18'10"	<i>Cercopithecoides indet</i>	Ulna	Shaft		Medium	Adult
S94-13792	O46	18'3'-19'8'	<i>Cercopithecoides indet</i>	Radius	Distal	L	Medium	Adult
S94-13816	O47	16'11'-17'11"	<i>Cercopithecoides indet</i>	Humerus	Shaft	L	Medium	Adult
S94-13970	Q46	28'6"-29'6"	<i>Cercopithecoides indet</i>	Tibia	Shaft	?	Medium	Adult
S94-14235	S41	9'11'-12'11"	<i>Cercopithecoides indet</i>	Scapula	Glenoid	R	Medium	Adult
S94-14238	S41	9'11"-10'11"	<i>Cercopithecoides indet</i>	Scapula	Glenoid	R	Medium	Adult
S94-14301	S43	28'2'-29'2'	<i>Cercopithecoides indet</i>	Pelvis	Acetabulum	R	Small	Adult
S94-14425	S46	28'8'-29'3'	<i>Cercopithecoides indet</i>	Pelvis	Ischium	R	Small	Adult
S94-1519	W46	27'4'-28'4'	<i>Cercopithecoides indet</i>	Femur	Shaft		Small	Juvenile
S94-1520	W46	27' 4" - 28' 4"	<i>Cercopithecoides indet</i>	Thor Vertebra	Body		Small	Juvenile
S94-1543	W46	28'4'-29'4'	<i>Cercopithecoides indet</i>	Lumbar Vertebra	Body		Medium	Adult
S94-1775	P45	13'-4'-14'4"	<i>Cercopithecoides indet</i>	1st phal	Complete		Small	Adult
S94-2317	P46	8"2'-9"2'	<i>Cercopithecoides indet</i>	Ulna	Shaft	?	Small	Adult
S94-2327	P45	5'5'-6'5'	<i>Cercopithecoides indet</i>	Humerus	Shaft	R		Adult
S94-258	V62	9'5"-10'5"	<i>Cercopithecoides indet</i>	Navicular	Complete	L	Medium	Adult
S94-259	V62	9'5"-10'5"	<i>Cercopithecoides indet</i>	Navicular	Complete	L	Medium	Adult
S94-492	U43	25'0'-26'0'	<i>Cercopithecoides indet</i>	Lumbar Vertebra	Complete		Medium	Adult
S94-8002	Cc47	7' 2" - 8' 2"	<i>Cercopithecoides indet</i>	Pelvis	Pubis		Medium	Adult
S94-8835	V48	4' 0" - 5' 10"	<i>Cercopithecoides indet</i>	Cerv Vertebra	Complete		Small	Adult
S94-8855	V41	4'0'-5'0'	<i>Cercopithecoides indet</i>	Calcaneus	Head	L	Medium	Adult
S94-9076	V49	?	<i>Cercopithecoides indet</i>	Humerus	Shaft	?	Medium	Adult
S94-9257	N32	?	<i>Papionin</i>	Humerus	Proximal	L	Medium	Adult
S94-9291	J42	22'5'-22'10'	<i>Cercopithecoides indet</i>	Tibia	Proximal	R	Large	Adult

Specimen no	Provenance	Level	Taxon	Element	Portion	Side	Size	Age
S94-9493	V61	13'6"-14'7"	<i>Cercopithecoidea indet</i>	Lumbar Vertebra	Body		Medium	Adult
Sf 1365	Q43	8' 5" - 9" 5"	<i>Cercopithecoidea indet</i>	Humerus	Shaft	?	Medium	Adult
Sf 1465	Q42	11' 2" - 12' 10"	<i>Papionina</i>	Ulna	Proximal	R	Large	Adult
Sf 1551	R 41	8'10"-9'10"	<i>Cercopithecoidea indet</i>	Femur	Shaft	L	Medium	Adult
Sf 1553	R41	8'9"-9'10"	<i>Papionina</i>	Radius	Proximal	L	Medium	Adult
Sf 1654	R41	9'10"-10'7"	<i>Cercopithecoidea indet</i>	Metapodial	Distal		Medium	Adult
Sf 2567	S45	22' 6" - 23' 6"	? <i>Colobinae</i>	Radius	Prox	L	Large	Adult
Sf 2689	S46	22' 7" - 23' 7"	<i>Papionina</i>	Radius	Proximal	L	Small	Juvenile
Sf 3418	T45	18' 6" - 19' 6"	<i>Theropithecus</i>	Ulna	Proximal	R	Very large	Adult
Sf 3484	T45	?	<i>Papionina</i>	Radius	Proximal	R	Medium	Adult
Sf 4103	T50	17' 10" - 18'10"	<i>Cercopithecoidea indet</i>	?	?		Large	Adult
Sf 4116	T50	21'10"-22'10"	<i>Cercopithecoidea indet</i>	Radius	Distal	L	Medium	Adult
Sf 4151	T50	19'11"-20'11"	<i>Cercopithecoidea indet</i>	Ulna	Fr		Medium	Adult
Sf 4217	T39	6' 7" - 7' 7"	<i>Cercopithecoidea indet</i>	Radius	Distal with broken shaft	L	Medium	Adult
Sf 4218	T39	6' 7" - 7' 7"	<i>Cercopithecoidea indet</i>	Scapula (?)	Fr	L	Medium	Adult
Sf 4219	T39	6' 7" - 7' 7"	<i>Cercopithecoidea indet</i>	Scapula	Fr	?	Medium	Adult
Sf 4232	T52	13' 10" - 14' 10"	<i>Cercopithecoidea indet</i>	Scapula	Acromion process	L	Medium	Adult
Sf 4284	U47	25'11"-26'11"	<i>Cercopithecoidea indet</i>	Ulna	Prox	R	Very large	Adult
Sf 4417	U47	24'11"-25'11"	<i>Cercopithecoidea indet</i>	Radius	Shaft	L	Very large	Adult
Sf 4552	U52	13'3"-14'3"	<i>Cercopithecoidea indet</i>	Metatarsaliv	Complete	L	Medium	Adult
Sf 4610	U52	14'3"-15'3"	<i>Papionina</i>	Humerus	Distal shaft	R	Medium	Adult
Sf 4611	U52	14'3"-15'3"	<i>Papionina</i>	Ulna	Prox	L	Medium	Adult
Sf 5495	V45	18'6"-19'6"	<i>Cercopithecoidea indet</i>	Pelvis	Ilium	L	Medium	Adult
Sf 5496	V45	18'6"-19'6"	<i>Papio/Parapapio</i>	Femur	Head	L	Medium	Adult
St ?	Type site		<i>Papio/Parapapio</i>	Humerus	Head	L	Medium	Adult
Sts ?	Type site		<i>Cercopithecoidea indet</i>	Radius	Shaft	?	Medium	Adult

<b>Specimen no</b>	<b>Provenance</b>	<b>Level</b>	<b>Taxon</b>	<b>Element</b>	<b>Portion</b>	<b>Side</b>	<b>Size</b>	<b>Age</b>
Sts ?	Type site		<i>Cercopithecoidea indet</i>	Clavicle		L	Medium	Adult
Sts ?	Type site		<i>Cercopithecoidea indet</i>	Humerus	Distal and shaft	L	Medium	Adult
Sts 1069	Type site		<i>Cercopithecoidea indet</i>	Femur	Proximal	R	Medium	Adult
Sts 1089	Type site		<i>Cercopithecoidea indet</i>	Femur	Proximal missing trochanae	L	Medium	Adult
Sts 1092 and 1733	Type site		<i>Cercopithecoidea indet</i>	Femur	Head and neck only	R	Medium	Adult
Sts 1094	Type site		<i>Cercopithecoidea indet</i>	Femur	Proximal femur	R	Small	Adult
Sts 1204	Type site		<i>Cercopithecoidea indet</i>	Tibia	Distal	R	Medium	Adult
Sts 1264	Type site		<i>Papionina</i>	Humerus	Distal and shaft	L	Medium	Adult
Sts 1458	Type site		<i>Cercopithecoidea indet</i>	Humerus	Head	L	Medium	Adult
Sts 146	Type site		<i>Cercopithecoidea indet</i>	Pelvis	Ilium	R	Medium	Adult
Sts 1469	Type site		<i>Cercopithecoidea indet</i>	Femur	Head	?	Medium	Adult
Sts 1504	Type site		<i>Papio/Parapapio</i>	Humerus	Distal	L	Medium	Adult
Sts 1614	Type site		<i>Cercopithecoidea indet</i>	Femur	Distal and shaft	R	Medium	Adult
Sts 1663	Type site		<i>Cercopithecoidea indet</i>	Radius	Distal	?R	Medium	Adult
Sts 1764	Type site		<i>Cercopithecoidea indet</i>	Radius	Distal	L	Small	Adult
Sts 1860	Type site		<i>Cercopithecoidea indet</i>	Tibia	Prox	R	Medium	Adult
Sts 1905	Type site		<i>Cercopithecoidea indet</i>	Femur	Distal	R	Medium	Adult
Sts 1978	Type site		<i>Cercopithecoidea indet</i>	Ulna	Proximal	R	Medium	Adult
Sts 1992	Type site		<i>Cercopithecoidea indet</i>	Femur	Proximal	L	Medium	Adult
Sts 2050	Type site		<i>Cercopithecoidea indet</i>	Femur	Proximal	L	Medium	Adult
Sts 2069	Type site		<i>Cercopithecoidea indet</i>	Femur	Head	?	Medium	Adult
Sts 2074	Type site		<i>Papionina</i>	Humerus	Distal and shaft	L	Small	Adult
Sts 2109	Type site		<i>Cercopithecoidea indet</i>	Femur	Proximal femur	R	Medium	Adult
Sts 2150	Type site		<i>Cercopithecoidea indet</i>	Femur	Head	?	Medium	Adult
Sts 2185	Type site		<i>Papionina</i>	Humerus	Proximal fragment	R	Medium	Adult
Sts 2188	Type site		<i>Cercopithecoidea indet</i>	Femur	Distal	?	Medium	Adult

<b>Specimen no</b>	<b>Provenance</b>	<b>Level</b>	<b>Taxon</b>	<b>Element</b>	<b>Portion</b>	<b>Side</b>	<b>Size</b>	<b>Age</b>
Sts 2201	Type site		<i>Cercopithecoides indet</i>	Humerus	Distal	R	Small	Adult
Sts 2219	Type site		<i>Parapapio</i>	Humerus	Proximal	R	Medium	Adult
Sts 2229	Type site		<i>Cercopithecoides indet</i>	Pelvis	Acetabulum	L	Medium	Adult
Sts 2230	Type site		<i>Cercopithecoides indet</i>	Tibia	Proximal	R	Medium	Adult
Sts 2259	Type site		<i>Cercopithecoides indet</i>	Femur	Head	R	Medium	Adult
Sts 2357	Type site		<i>Cercopithecoides indet</i>	Femur	Head		Medium	Adult
Sts 2474	Type site		<i>Cercopithecoides indet</i>	Tibia	Distal	L	Medium	Adult
Sts 2521	Type site		<i>Cercopithecoides indet</i>	Femur	Head and neck only	R	Medium	Adult
Sts 2562	Type site		<i>Cercopithecoides indet</i>	Tibia	Proximal	L	Medium	Adult
Sts 2563	Type site		<i>Cercopithecoides indet</i>	Tibia	Distal	R	Medium	Adult
Sts 27?	Type site		<i>Papionina</i>	Humerus	Distal shaft only	L	Medium	Adult
Sts 377c	Type site		<i>Parapapio/papio</i>	Humerus	Distal	R	Medium	Adult
Sts 377d	Type site		<i>Parapapio/papio</i>	?Humerus	Shaft		Medium	Adult
Sts 443	Type site		<i>Cercopithecoides indet</i>	Femur	Proximal femur	R	Medium	Adult
Sts 549	Type site		<i>Cercopithecoides indet</i>	Femur	Distal	?	Medium	Adult
Sts unnumbered	Type site		<i>Papionina</i>	Radius	Proximal	R	Medium	Adult
SWP 498	D13	?	<i>Cercopithecoides indet</i>	Tibia	Proximal	L	Medium	Adult
SWP 499	D13		<i>Cercopithecoides indet</i>	Pelvis	Acetabulum	L	Medium	Adult
SWP 500	D13	?	<i>Cercopithecoides indet</i>	Tibia	Distal	R	Medium	Adult
SWP 501	D13	?	<i>Cercopithecoides indet</i>	Tibia	Distal	R	Medium	Adult
SWP 502	D13	?	<i>Cercopithecoides indet</i>	Tibia	Distal	R	Medium	Adult
SWP 503	D13	?	<i>Cercopithecoides indet</i>	Tibia	Distal	R	Medium	Adult
SWP 504	D13		<i>Parapapio</i>	Humerus	Proximal	R	Medium	Adult
SWP 505	D14		<i>Papio</i>	Humerus	Proximal	L	Medium	Adult
SWP 506	D17	?	<i>Papionina</i>	Radius	Proximal	R	Medium	Adult
SWP 507	D13		<i>Papio/Parapapio</i>	Humerus	Distal	R	Medium	Adult

Specimen no	Provenance	Level	Taxon	Element	Portion	Side	Size	Age
SWP 508	D13		<i>Cercopithecoidea indet</i>	Humerus	Distal	R	Medium	Adult
SWP 509	D14		<i>Cercopithecoidea indet</i>	Humerus	Distal	R	Medium	Adult
SWP 510	D13		<i>Cercopithecoidea indet</i>	Humerus	Distal	L	Medium	Adult
SWP 511	D13	?	<i>Papio</i>	Humerus	Distal	L	Medium	Adult
SWP 512	D13		<i>Cercopithecoidea indet</i>	Humerus	Distal	L	Medium	Adult
SWP 513	D13		<i>Cercopithecoidea indet</i>	Radius	Distal	L	Medium	Adult
SWP 514	D13	?	<i>Papio</i>	Radius	Proximal	R	Medium	Adult
SWP 515	D15	?	<i>Parapapio</i>	Radius	Proximal	L	Medium	Adult
SWP 516	D13	?	<i>Papionina</i>	Radius	Proximal	R	Medium	Adult
SWP 517	D13	?	<i>Papio</i>	Radius	Proximal	L	Medium	Adult
SWP 518	D18	?	<i>Papio/Parapapio</i>	Radius	Proximal	L	Medium	Adult
SWP 519	D18	?	<i>Papionina</i>	Radius	Proximal	R	Small	Adult
SWP 520	D13		<i>Papionina</i>	Radius	Proximal	L	Medium	Adult
SWP 522	D13	?	<i>Cercopithecoidea indet</i>	Radius	Head	?	Large	Adult
SWP 523	D13		<i>Parapapio</i>	Ulna	Proximal	R	Medium	Adult
SWP 524	D13		<i>Papio/Parapapio</i>	Ulna	Proximal	R	Medium	Adult
SWP 525	D13		<i>Cercopithecoidea indet</i>	Ulna	Proximal		Medium	Adult
SWP 526	D13		<i>Papio/Parapapio</i>	Femur	Proximal	L	Medium	Sub-adult
SWP 527	D13		<i>Papionina</i>	Femur	Proximal	L	Medium	Adult
SWP 528	D13		<i>Theropithecus</i>	Femur	Proximal	L	Medium	Adult
SWP 529	D14		<i>Papionina</i>	Femur	Proximal	L	Medium	Adult
SWP 530	D13		<i>Papionina</i>	Femur	Proximal	L	Medium	Adult
SWP 531	D13	?	<i>Papio/Parapapio</i>	Femur	Proximal	R	Medium	Sub-adult
SWP 532	D13		<i>Papio/Parapapio</i>	Femur	Proximal	R	Medium	Adult
SWP 533	D13		<i>Papio/Parapapio</i>	Femur	Proximal	R	Medium	Adult
SWP 534	D13	?	<i>Cercopithecoidea indet</i>	Fibula	Distal	?	Medium	Adult
SWP 535	D13		<i>Cercopithecoidea indet</i>	Fibula	Distal	L	Medium	Adult
SWP 536	D13		<i>Cercopithecoidea indet</i>	Fibula	Distal	R	Medium	Adult

Specimen no	Provenance	Level	Taxon	Element	Portion	Side	Size	Age
SWP 537	D18	?	<i>Cercopithecoidea indet</i>	Calcaneus	Complete	L	Large	Adult
SWP 538	D13	?	<i>Cercopithecoidea indet</i>	Calcaneus	Complete	L	Large	Adult
SWP 539	D13	?	<i>Cercopithecoidea indet</i>	Calcaneus	Complete	L	Medium	Juvenile
SWP 540	D13		<i>Cercopithecoidea indet</i>	Calcaneus	Complete	R	Medium	Adult
SWP 541	D13		<i>Cercopithecoidea indet</i>	Talus	Frag	R	Medium	Adult
SWP 543	D13		<i>Cercopithecoidea indet</i>	Talus	Complete	R	Medium	Adult
SWP 543	D13		<i>Cercopithecoidea indet</i>	Talus	Complete	R	Medium	Sub-adult
SWP 544	D13		<i>Cercopithecoidea indet</i>	Talus	Complete	R	Medium	Sub-adult
SWP 545	?	?	<i>Cercopithecoidea indet</i>	Tibia	Distal	R	Medium	Adult
SWP 560	D18	?	<i>Cercopithecoidea indet</i>	Tibia	Proximal	R	Medium	Adult
SWP 561	D15		<i>Papionina</i>	Ulna	Proximal	R	Medium	Adult
SWP 562	D14		<i>Papio/Parapapio</i>	Humerus	Distal	L	Medium	Adult
SWP 563	D18	?	<i>Cercopithecoidea indet</i>	Tibia	Distal	R	Medium	Adult
SWP 568	D13	?	<i>Cercopithecoidea indet</i>	Calcaneus	Posterior	L	Medium	Adult
SWP 570	D13	?	<i>Cercopithecoidea indet</i>	Radius	Fragment	?	Medium	Adult
SWP 577	D18		<i>Cercopithecoidea indet</i>	Vmetatarsal	Complete	R	Medium	Adult
SWP 578	D18	?	<i>Cercopithecoidea indet</i>	Calcaneus	Complete	R	Medium	Adult
SWP 589	D18	?	<i>Cercopithecoidea indet</i>	Humerus	condyle	L	Medium	Adult
SWP 604	D14		<i>Cercopithecoidea indet</i>	Femur	Distal condyles	R	Medium	Adult
SWP 606	D15	?	<i>Cercopithecoidea indet</i>	Humerus	Proximal	L	Medium	Adult
SWP 608	D13		<i>Cercopithecoidea indet</i>	Tibia	Distal	R	Medium	Adult
SWP 693	D13		<i>Cercopithecoidea indet</i>	Pelvis	Acetabulum	R	Medium	Adult
SWP 694	D13		<i>Cercopithecoidea indet</i>	Pelvis	Os coxa	R	Medium	Adult
SWP 695	D13		<i>Cercopithecoidea indet</i>	Pelvis	Ischium	R	Medium	Adult
SWP 696	D13		<i>Cercopithecoidea indet</i>	Pelvis	Ischium	R	Medium	Adult
SWP 697	D13		<i>Cercopithecoidea indet</i>	Pelvis	Ischium	?	Medium	Adult
SWP 698	D13		<i>Cercopithecoidea indet</i>	Pelvis	Ilium	L	Medium	Adult
SWP 699	D13		<i>Cercopithecoidea indet</i>	Pelvis	Ilium	L	Medium	Adult



Specimen no	Provenance	Level	Taxon	Element	Portion	Side	Size	Age
SWP 700	D13		<i>Cercopithecoidea indet</i>	Pelvis	Ilium	L	Medium	Adult
SWP 701	D13		<i>Cercopithecoidea indet</i>	Pelvis	Ilium	L	Medium	Adult
SWP 703	D13		<i>Cercopithecoidea indet</i>	Pelvis	Acetabulum	L	Medium	Adult
SWP 705	D13		<i>Cercopithecoidea indet</i>	Pelvis	Ischium	?	Medium	Adult
SWP 706	D13		<i>Cercopithecoidea indet</i>	Pelvis	Ischium	?	Medium	Adult
SWP 707	D13		<i>Cercopithecoidea indet</i>	Pelvis	Ischium	?	Medium	Adult
SWP 708	D13		<i>Cercopithecoidea indet</i>	Pelvis	Acetabulum fr	?	Medium	Adult
SWP 709	D13		<i>Cercopithecoidea indet</i>	Pelvis	Acetabulum	?	Medium	Adult
SWP 709	D13		<i>Cercopithecoidea indet</i>	Pelvis	Acetabulum	L	Medium	Adult
SWP 719	D13		<i>Cercopithecoidea indet</i>	Tibia	Distal	L	Medium	Adult
SWP 719	D14		<i>Cercopithecoidea indet</i>	Tibia	Distal	L	Medium	Adult
SWP 721	D13		<i>Cercopithecoidea indet</i>	Tibia	Distal	R	Medium	Adult
SWP 722	D13		<i>Cercopithecoidea indet</i>	Tibia and fibula articulated	Distal and shaft	R	Medium	Adult
SWP 723	D13		<i>Cercopithecoidea indet</i>	Tibia	Distal	?	Medium	Adult
SWP 724	D13	?	<i>Cercopithecoidea indet</i>	Tibia	Proximal	R	Medium	Adult
SWP 725	D13		<i>Cercopithecoidea indet</i>	Humerus	Distal shaft	R	Medium	Adult
SWP 726	D13		<i>Papionin</i>	Humerus	Distal and shaft	R	Medium	Adult
SWP 727	D13		<i>Papionin</i>	Humerus	Distal and shaft	L	Medium	Adult
SWP 728	D13		<i>Cercopithecoidea indet</i>	Humerus	Shaft	?	Medium	Adult
SWP 729	D13		<i>Papionin</i>	Humerus	Distal and shaft	L	Medium	Adult
SWP 731	D13		<i>Cercopithecoidea indet</i>	Humerus	Proximal	R	Medium	Adult
SWP 732	D13		<i>Cercopithecoidea indet</i>	Femur	Distal	L	Medium	Adult
SWP 733	D13		<i>Cercopithecoidea indet</i>	Femur	Distal	R	Medium	Adult
SWP 734	D13		<i>Cercopithecoidea indet</i>	Femur	Proximal	R	Medium	Adult
SWP 735	D13		<i>Cercopithecoidea indet</i>	Femur	Proximal	R	Medium	Adult
SWP 736	D13		<i>Cercopithecoidea indet</i>	Femur	Proximal fr	L	Medium	Adult
SWP 737	D13		<i>Cercopithecoidea indet</i>	Femur	Proximal	R	Medium	Adult

Specimen no	Provenance	Level	Taxon	Element	Portion	Side	Size	Age
SWP 738	D13		? <i>Papionina</i>	Femur	Proximal	L	Medium	Adult
SWP 739	D13		<i>Cercopithecoidea indet</i>	Femur	Shaft	R	Medium	Adult
SWP 740	D13		<i>Cercopithecoidea indet</i>	Femur	Shaft	?	Medium	Adult
SWP 741	D13		<i>Cercopithecoidea indet</i>	Femur	Shaft	?	Medium	Adult
SWP 742	D13		<i>Papionina</i>	Femur	Proximal	R	Medium	Adult
SWP 743	D13		<i>Papionina</i>	Femur	Proximal	L	Medium	Adult
SWP 744	D13		<i>Cercopithecoidea indet</i>	Femur	Proximal	?	Medium	Adult
SWP 745	D13		<i>Papionina</i>	Femur	Proximal	R	Medium	Adult
SWP 746	D13		<i>Papio/Parapapio</i>	Femur	Proximal	R	Medium	Adult
SWP 747	D13		<i>Cercopithecoidea indet</i>	Femur	Proximal	R	Medium	Adult
SWP 748	D12		<i>Cercopithecoidea indet</i>	Femur	Proximal	L	Medium	Adult
SWP 749	D13		<i>Cercopithecoidea indet</i>	Femur	Head fragment	L	Large	Adult
SWP 750	D13		<i>Cercopithecoidea indet</i>	Femur	Proximal	R	Medium	Adult
SWP 751	D13		<i>Cercopithecoidea indet</i>	Femur	Proximal	R	Medium	Adult
SWP 752	D13		<i>Cercopithecoidea indet</i>	Femur	Proximal	L	Medium	Adult
SWP 753	D13		<i>Papionina</i>	Femur	Proximal	R	Medium	Adult
SWP 754	D13		<i>Papionina</i>	Femur	Proximal	R	Medium	Adult
SWP 755	D13		<i>Cercopithecoidea indet</i>	Femur	Proximal	?R	Medium	Adult
SWP 756	D13		<i>Cercopithecoidea indet</i>	Femur	Proximal	R	Medium	Adult
SWP 757	D13		<i>Cercopithecoidea indet</i>	Femur	Proximal	? L	Medium	Adult
SWP 758	D13		<i>Cercopithecoidea indet</i>	Radius	Shaft	?	Medium	Adult
SWP 759	D13		<i>Cercopithecoidea indet</i>	Radius	Shaft	?	Medium	Adult
SWP 760	D13		<i>Cercopithecoidea indet</i>	Radius	Shaft	?	Medium	Adult
SWP 761	D13		<i>Cercopithecoidea indet</i>	Radius	Shaft	?	Medium	Adult
SWP 762	D13		<i>Cercopithecoidea indet</i>	Radius	Shaft	?	Medium	Adult
SWP 763	D13		<i>Cercopithecoidea indet</i>	Radius	Shaft	?	Medium	Adult
SWP 764	D13		<i>Cercopithecoidea indet</i>	Radius	Shaft	?	Medium	Adult
SWP 765	D13		<i>Cercopithecoidea indet</i>	Radius	Shaft	?	Medium	Adult

Specimen no	Provenance	Level	Taxon	Element	Portion	Side	Size	Age
SWP 767	D13		<i>Cercopithecoidea indet</i>	Radius	Shaft	?	Medium	Adult
SWP 768	D13		<i>Cercopithecoidea indet</i>	Radius	Shaft	?	Medium	Adult
SWP 769	D13		<i>Cercopithecoidea indet</i>	Radius	Shaft	?	Medium	Adult
SWP 770	D13		<i>Cercopithecoidea indet</i>	Radius	Shaft	?	Medium	Adult
SWP 771	D13		<i>Cercopithecoidea indet</i>	Radius	Shaft	?	Medium	Adult
SWP 772	D13		<i>Cercopithecoidea indet</i>	Radius	Shaft	?	Medium	Adult
SWP 773	D13		<i>Cercopithecoidea indet</i>	Radius	Shaft	?	Medium	Adult
SWP 774	D13		<i>Cercopithecoidea indet</i>	Radius	Shaft	?	Medium	Adult
SWP 775	D13		<i>Cercopithecoidea indet</i>	Radius	Shaft	?	Medium	Adult
SWP 776	D13		<i>Cercopithecoidea indet</i>	Radius	Shaft	?	Medium	Adult
SWP 777	D13	?	<i>Cercopithecoidea indet</i>	Radius	Distal	?	Small	Adult
SWP 778	D13	?	<i>Cercopithecoidea indet</i>	Radius	Distal	?	Small	Adult
SWP 779	D13	?	<i>Cercopithecoidea indet</i>	Radius	Distal	?	Small	Adult
SWP 780	D13	?	<i>Cercopithecoidea indet</i>	Radius	Proximal	?	Medium	Adult
SWP 781	D18	?	<i>Cercopithecoidea indet</i>	Radius	Proximal	L	Medium	Adult
SWP 782	D12		<i>Cercopithecoidea indet</i>	Radius	Proximal	R	Small	Juvenile
SWP 783	D12		<i>Cercopithecoidea indet</i>	Radius	Shaft	?	Medium	Adult
SWP 784	D12		<i>Parapapio</i>	Radius	Proximal	R	Medium	Adult
SWP 785	D13		<i>Cercopithecoidea indet</i>	Radius	Proximal	?	Medium	Adult
SWP 786	D13		<i>Cercopithecoidea indet</i>	Radius	Proximal	?	Medium	Adult
SWP 787	D13	?	<i>Cercopithecoidea indet</i>	Radius	Proximal	?	Small	Adult
SWP 788	D13		<i>Papionini</i>	Radius	Head	?	Medium	Adult
SWP 789	D13	?	<i>Cercopithecoidea indet</i>	Radius	Fragment	?	Large	Adult
SWP 790	D13	?	<i>Cercopithecoidea indet</i>	Radius	Proximal	R	Medium	Adult
SWP 791	D13	?	<i>Papio</i>	Radius	Proximal	L	Small	Adult
SWP 792	D?3	?	<i>Papionina</i>	Radius	Proximal	L	Medium	Adult
SWP 793	?	?	<i>Papio sp</i>	Radius	Proximal	R	Medium	Adult
SWP 794	D13		<i>Cercopithecoidea indet</i>	Radius	Head	?	Medium	Adult

Specimen no	Provenance	Level	Taxon	Element	Portion	Side	Size	Age
SWP 795	D13	?	<i>Cercopithecoidea indet</i>	Radius	Head and neck	?	Medium	Adult
SWP 796	D13		<i>Cercopithecoidea indet</i>	Ulna	Proximal	?	Medium	Adult
SWP 797	D13	?	<i>Papionina</i>	Radius	Head	?	Medium	Adult
SWP 798	D12	?	<i>Parapapio</i>	Radius	Proximal	R	Small	Adult
SWP 799	D13		<i>Papionina</i>	Radius	Proximal	R	Medium	Adult
SWP 800	D13	?	<i>Cercopithecoidea indet</i>	Radius	Head	?	Medium	Adult
SWP 801	D13	?	<i>Cercopithecus sp</i>	Radius	Proximal	L	Medium	Adult
SWP 802	D13	?	<i>Parapapio</i>	Radius	Proximal	R	Medium	Adult
SWP 803	D13	?	<i>Papio</i>	Radius	Proximal	R	Medium	Adult
SWP 804 / 904	D13		<i>Cercopithecoidea indet</i>	Radius	Proximal	?	Medium	Adult
SWP 805	D13		<i>Cercopithecoidea indet</i>	Radius	Proximal	?	Medium	Adult
SWP 806	D13	?	<i>Papionina</i>	Radius	Proximal	L	Medium	Adult
SWP 808	D13	?	<i>Papionina</i>	Radius	Proximal	L	Medium	Adult
SWP 809	D13		<i>Cercopithecoidea indet</i>	Radius	Distal	L	Medium	Adult
SWP 810	D13		<i>Cercopithecoidea indet</i>	Radius	Distal	R	Medium	Adult
SWP 811	D13		<i>Cercopithecoidea indet</i>	Tibia	Distal	?	Medium	Adult
SWP 812	D13		<i>Cercopithecoidea indet</i>	Ulna	Distal	?	Medium	Adult
SWP 813	D13		<i>Papionina</i>	Ulna	Proximal	R	Medium	Adult
SWP 814	D13		<i>Papio</i>	Ulna	Proximal	R	Medium	Adult
SWP 815	D13		<i>Papionina</i>	Ulna	Proximal	R	Medium	Adult
SWP 816	D13		<i>Papionina</i>	Ulna	Proximal	R	Large	Adult
SWP 817	D13		<i>Theropithecus</i>	Ulna	Proximal	L	Large	Adult
SWP 819	D13		<i>Cercopithecoidea indet</i>	Ulna	Proximal	R	Medium	Adult
SWP 820	D13		<i>Cercopithecoidea indet</i>	Ulna	Proximal	L	Medium	Adult
SWP 821	D13		<i>Cercopithecoidea indet</i>	Ulna	Prox	R	Medium	Adult
SWP 822	D13		<i>Theropithecus</i>	Ulna	Prox	L	Medium	Sub-adult
SWP 824	D13		<i>Papio</i>	Ulna	Proximal	R	Medium	Adult
SWP 825	D13		<i>Theropithecus</i>	Ulna	Proximal	R	Large	Adult

Specimen no	Provenance	Level	Taxon	Element	Portion	Side	Size	Age
SWP 826	D13		<i>Cercopithecoidea indet</i>	Ulna	Shaft	?	Medium	Adult
SWP 827	D13		<i>Cercopithecoidea indet</i>	Ulna	Shaft	?	Medium	Adult
SWP 828	D13		<i>Cercopithecoidea indet</i>	Ulna	Shaft	?	Medium	Adult
SWP 829	D13		<i>Cercopithecoidea indet</i>	Ulna, radius	Shaft	?	Medium	Adult
SWP 830	D13		<i>Papio</i>	Ulna, radius, humerus	Proximal with shaft	R	Medium	Adult
SWP 831	D13		<i>Cercopithecoidea indet</i>	Femur	Shaft	?	Medium	Adult
SWP 832	D13		<i>Cercopithecoidea indet</i>	Femur	Shaft	?	Medium	Adult
SWP 833	D13		<i>Cercopithecoidea indet</i>	Femur	Shaft	?	Medium	Adult
SWP 834	D13		<i>Cercopithecoidea indet</i>	Femur	Shaft		Medium	Adult
SWP 835	D13		<i>Cercopithecoidea indet</i>	Femur	Shaft		Medium	Adult
SWP 836	D13		<i>Cercopithecoidea indet</i>	Femur	Shaft		Medium	Adult
SWP 837	D13		<i>Cercopithecoidea indet</i>	Femur	Shaft		Medium	Adult
SWP 838	D13		<i>Cercopithecoidea indet</i>	Femur	Shaft		Medium	Adult
SWP 839	D13		<i>Cercopithecoidea indet</i>	Femur	Shaft	?	Medium	Adult
SWP 840	D13		<i>Cercopithecoidea indet</i>	Femur	Shaft	?	Medium	Adult
SWP 841	D13		<i>Cercopithecoidea indet</i>	Femur	Shaft	?	Medium	Adult
SWP 842	D13		<i>Cercopithecoidea indet</i>	Femur	Shaft	?	Medium	Adult
SWP 843	D13		<i>Cercopithecoidea indet</i>	Femur	Shaft	?	Medium	Adult
SWP 845	D13		<i>Cercopithecoidea indet</i>	Femur	Shaft	?	Medium	Adult
SWP 846	D13		<i>Cercopithecoidea indet</i>	Femur	Shaft	?	Medium	Adult
SWP 847	D13		<i>Cercopithecoidea indet</i>	Femur	Shaft	?	Medium	Adult
SWP 848	D13		<i>Cercopithecoidea indet</i>	Femur	Shaft	?	Medium	Adult
SWP 849	D13		<i>Cercopithecoidea indet</i>	Femur	Shaft	?	Medium	Adult
SWP 850	D13		<i>Cercopithecoidea indet</i>	Femur	Shaft	?	Medium	Adult
SWP 851	D13		<i>Cercopithecoidea indet</i>	Femur	Shaft	?	Medium	Adult
SWP 852	D13		<i>Cercopithecoidea indet</i>	Femur	Shaft	?	Medium	Adult
SWP 853	D13		<i>Papio/Parapapio</i>	Ulna	Proximal	R	Medium	Adult

Specimen no	Provenance	Level	Taxon	Element	Portion	Side	Size	Age
SWP 853	D13		<i>Cercopithecoides indet</i>	Femur	Shaft	?	Medium	Adult
SWP 854	D13		<i>Cercopithecoides indet</i>	Long bone	Shaft		Medium	Adult
SWP 855	D13		<i>Cercopithecoides indet</i>	Long bone	Shaft		Medium	Adult
SWP 856	D13		<i>Cercopithecoides indet</i>	Femur	Shaft	?	Medium	Adult
SWP 857	D13		<i>Cercopithecoides indet</i>	Humerus	Shaft	?	Medium	Adult
SWP 858	D13		<i>Cercopithecoides indet</i>	Femur	Shaft	?	Medium	Adult
SWP 859	D13		<i>Cercopithecoides indet</i>	Femur	Shaft	?	Medium	Adult
SWP 860	D13		<i>Cercopithecoides indet</i>	Femur	Shaft	?	Medium	Adult
SWP 861	D13		<i>Cercopithecoides indet</i>	Femur	Shaft	?	Medium	Adult
SWP 862	D13		<i>Cercopithecoides indet</i>	Femur	Shaft	?	Medium	Adult
SWP 863	D13		<i>Cercopithecoides indet</i>	Femur	Shaft	?	Medium	Adult
SWP 864	D13		<i>Cercopithecoides indet</i>	Femur	Shaft	?	Medium	Adult
SWP 865	D13		<i>Cercopithecoides indet</i>	Humerus	Shaft	?	Medium	Adult
SWP 866	D13		<i>Cercopithecoides indet</i>	Femur	Shaft	?	Medium	Adult
SWP 867	D13		<i>Cercopithecoides indet</i>	Femur	Distal condyle	?L	Medium	Adult
SWP 868	D13		<i>Cercopithecoides indet</i>	Femur	Distal condyle	?	Medium	Adult
SWP 869	?	?	<i>Cercopithecoides indet</i>	Femur	Head	?	Medium	Adult
SWP 870	D13		<i>Cercopithecoides indet</i>	Femur	Head	?L	Medium	Adult
SWP 871	D13		<i>Cercopithecoides indet</i>	Femur	Head	?L	Medium	Adult
SWP 872	D13		<i>Cercopithecoides indet</i>	Femur	Head	R	Medium	Adult
SWP 873	D13		<i>Cercopithecoides indet</i>	Femur	Head	L	Medium	Adult
SWP 874	M4		<i>Cercopithecoides indet</i>	Femur	Head		Medium	Juvenile
SWP 875	D13		<i>Cercopithecoides indet</i>	Femur	Head	?		Juvenile
SWP 876			<i>Cercopithecoides indet</i>	Femur	Head	?	Medium	Sub-adult
SWP 877		?	<i>Cercopithecoides indet</i>	Femur	Head	R	Small	Sub-adult
SWP 878	D13		<i>Cercopithecoides indet</i>	Femur	Proximal	L	Medium	Adult
SWP 879	M4		<i>Cercopithecoides indet</i>	Femur	Head	?	Large	Juvenile
SWP 880	D13		<i>Cercopithecoides indet</i>	Femur	Head	L	Medium	Adult

Specimen no	Provenance	Level	Taxon	Element	Portion	Side	Size	Age
SWP 881	D13		<i>Cercopithecoides indet</i>	Femur	Proximalshaft	?	Medium	Adult
SWP 882	D13		<i>Cercopithecoides indet</i>	Femur	Prox	?	Medium	Adult
SWP 883	D13		<i>Cercopithecoides sp</i>	Femur	Proximal	L	Medium	Adult
SWP 884	D13		<i>Cercopithecoides indet</i>	Femur	Head	?	Medium	Adult
SWP 885	D13		<i>Cercopithecoides indet</i>	Femur	Proximal	R	Medium	Adult
SWP 886	M4	?	<i>Cercopithecoides indet</i>	Femur	Head	?	Medium	Juvenile
SWP 887	D13		<i>Cercopithecoides indet</i>	Femur	Head	?	Medium	Juvenile
SWP 888	D13		<i>Cercopithecoides indet</i>	Femur	Proximal	?L	Medium	Adult
SWP 889	D13		<i>Cercopithecoides indet</i>	Femur	Proximal fr	?	Medium	Adult
SWP 890	D13		<i>Cercopithecoides indet</i>	Femur	Head	?	Med	Juvenile
SWP 891	M4	?	<i>Cercopithecoides indet</i>	Femur	Head	L	Large	Adult
SWP 892	M4		<i>Cercopithecoides indet</i>	Femur	Head	?	Medium	Adult
SWP 893	D13		<i>Cercopithecoides indet</i>	Femur	Head	?	Medium	Adult
SWP 894	D13		<i>Cercopithecoides indet</i>	Femu	Head	?	Medium	Adult
SWP 895	M4		<i>Cercopithecoides indet</i>	Femur	Head	?	Med	Juvenile
SWP 896	D13		<i>Cercopithecoides indet</i>	Femur	Head	L	Med	Sub-adult
SWP 897	D13		<i>Cercopithecoides indet</i>	Femur	Head	?R	Medium	Adult
SWP 898	D13		<i>Cercopithecoides indet</i>	Femur	Head fr	?	Medium	Adult
SWP 899	D13		<i>Cercopithecoides indet</i>	Femur	Proximal	R	Medium	Adult
SWP 900	D13		<i>Papionina</i>	Femur	Proximal	R	Medium	Adult
SWP 901	D13		<i>Cercopithecoides indet</i>	Femur	Prox	?	Medium	Adult
SWP 902	D13		<i>Cercopithecoides indet</i>	Femur	Proximal fr	?	Medium	Adult
SWP 903	D13		<i>Cercopithecoides indet</i>	Femur	Proximal fr	?	Medium	Adult
SWP 904	D13		<i>Cercopithecoides indet</i>	Femur	Proximal	?	Medium	Adult
SWP 905	D17		<i>Papionina</i>	Femur	Proximal	R	Medium	Adult
SWP 906	D13		<i>Cercopithecoides indet</i>	Humerus	Distal shaft	?	Medium	Adult
SWP 907	D13		<i>Cercopithecoides indet</i>	Humerus	Distal	?	Medium	Adult
SWP 908	D13		<i>Cercopithecoides indet</i>	Humerus	Distal	R	Medium	Adult

Specimen no	Provenance	Level	Taxon	Element	Portion	Side	Size	Age
\SWP 909	D13		<i>Cercopithecoides indet</i>	Humerus	Distal		Medium	Adult
SWP 910	D13		<i>Cercopithecoides indet</i>	Humerus	Distal	L	Medium	Adult
SWP 911	D13		<i>Papio</i>	Humerus	Distal	R	Medium	Adult
SWP 912	D13		<i>Papio/Parapapio</i>	Humerus	Distal condyle	R	Medium	Sub-adult
SWP 913	D13		<i>Cercopithecoides indet</i>	Humerus	Distal condyle	R	Medium	Sub-adult
SWP 914	D13		<i>Cercopithecoides indet</i>	Humerus	Distal	L	Medium	Adult
SWP 915	D13		<i>Cercopithecoides indet</i>	Humerus	Distal	?	Medium	Adult
SWP 916	D13		<i>Cercopithecoides indet</i>	Humerus	Distal	L	Medium	Adult
SWP 917	D13		<i>Cercopithecoides indet</i>	Humerus	Distal	?	Medium	Adult
SWP 918	D13		<i>Cercopithecoides indet</i>	Humerus	Distal shaft	?	Medium	Adult
SWP 919	D13		<i>Cercopithecoides indet</i>	Humerus	Distal shaft	?	Medium	Adult
SWP 922	D13		<i>Cercopithecoides indet</i>	Humerus	Distal shaft	L	Medium	Adult
SWP 923	D13		<i>Cercopithecoides indet</i>	Humerus	Distal condyle		Medium	Adult
SWP 924	D13		<i>Cercopithecoides indet</i>	Humerus	Distal condyle	L	Medium	Adult
SWP 925	D13		<i>Cercopithecoides indet</i>	Humerus	Distal	?	Medium	Adult
SWP 926	D13		<i>Cercopithecoides indet</i>	Humerus	Distal	R	Medium	Adult
SWP 927	D13		<i>Cercopithecoides indet</i>	Humerus	Distal	?	Medium	Adult
SWP 928	D13		<i>Cercopithecoides indet</i>	Humerus	Shaft	?	Medium	Adult
SWP 929	D13		<i>Cercopithecoides indet</i>	Humerus	Shaft	?	Medium	Adult
SWP 930	D13		<i>Cercopithecoides indet</i>	Humerus	Shaft	?	Medium	Adult
SWP 931	D13		<i>Cercopithecoides indet</i>	Ulna	Shaft		Medium	Adult
SWP 932	D13		<i>Cercopithecoides indet</i>	Humerus	Shaft		Medium	Adult
SWP 933	D13		<i>Cercopithecoides indet</i>	Humerus	Shaft		Medium	Adult
SWP 934	D13		<i>Cercopithecoides indet</i>	Ulna	Shaft		Medium	Adult
SWP 935	D13		<i>Cercopithecoides indet</i>	Humerus	Shaft		Medium	Adult
SWP 936	D13		<i>Cercopithecoides indet</i>	Humerus	Shaft		Medium	Adult
SWP 937	D13		<i>Cercopithecoides indet</i>	Humerus	Shaft		Medium	Adult
SWP 938	D13		<i>Cercopithecoides indet</i>	Radius	Shaft		Medium	Adult



Specimen no	Provenance	Level	Taxon	Element	Portion	Side	Size	Age
SWP 939	D13		<i>Cercopithecoidea indet</i>	Humerus	Shaft		Medium	Adult
SWP 940	D13		<i>Cercopithecoidea indet</i>	Humerus	Shaft		Medium	Adult
SWP 941	D13		<i>Cercopithecoidea indet</i>	Humerus	Shaft		Medium	Adult
SWP 942	D13		<i>Cercopithecoidea indet</i>	Humerus	Shaft		Medium	Adult
SWP 943	D13		<i>Cercopithecoidea indet</i>	Long bone	Shaft		Medium	Adult
SWP 944	D13		<i>Cercopithecoidea indet</i>	Femur	Shaft		Medium	Adult
SWP 945	D13		<i>Cercopithecoidea indet</i>	Radius	Shaft		Medium	Adult
SWP 946	D13		<i>Cercopithecoidea indet</i>	Humerus	Shaft		Medium	Adult
SWP 947	D13		<i>Cercopithecoidea indet</i>	Radius	Shaft		Large	Adult
SWP 948	D13		<i>Cercopithecoidea indet</i>	Humerus	Shaft		Medium	Adult
SWP 949	D13		<i>Cercopithecoidea indet</i>	Femur	Shaft		Medium	Adult
SWP 950	D13		<i>Cercopithecoidea indet</i>	Humerus	Shaft	?	Medium	Adult
SWP 952	D13		<i>Cercopithecoidea indet</i>	Humerus	Shaft		Small	Adult
SWP 953	D13		<i>Cercopithecoidea indet</i>	Humerus	Shaft		Medium	Adult
SWP 954	D13		<i>Cercopithecoidea indet</i>	Humerus	Shaft		Medium	Adult
SWP 955	D13		<i>Cercopithecoidea indet</i>	Humerus	Shaft		Medium	Adult
SWP 956	D13		<i>Cercopithecoidea indet</i>	Ulna	Shaft		Medium	Adult
SWP 957	D13		<i>Cercopithecoidea indet</i>	Humerus	Shaft	?	Medium	Adult
SWP 958	D13		<i>Cercopithecoidea indet</i>	Humerus	Head	?	Medium	Adult
SWP 959	D13		<i>Parapapio</i>	Humerus	Head	R	Medium	Adult
SWP 960	D13	?	<i>Papio sp</i>	Humerus	Proximal	L	Medium	Adult
SWP 961	D13		<i>Cercopithecoidea indet</i>	Humerus	Proximal	?	Medium	Sub-adult
SWP 962	D13		<i>Parapapio</i>	Humerus	Proximal	R	Medium	Adult
SWP 963	D13		<i>Papionina</i>	Humerus	Proximal	L	Medium	Sub-adult
SWP 964	M4		<i>Cercopithecoidea indet</i>	Humerus	Proximal	L	Medium	Adult
SWP 965	D18		<i>Papionina</i>	Humerus	Proximal	L	Medium	Adult
SWP 966	D13		<i>Cercopithecoidea indet</i>	Humerus	Proximal	R	Medium	Adult
SWP 967	D13		<i>Papio sp</i>	Humerus	Proximal	R	Medium	Adult

Specimen no	Provenance	Level	Taxon	Element	Portion	Side	Size	Age
SWP 968	D15	?	<i>Cercopithecoidea indet</i>	Fibula	Proximal	L	Medium	Adult
SWP 971	D14	?	<i>Cercopithecoidea indet</i>	Radius	Shaft	?	Medium	Adult
SWP 972	D14	?	<i>Papionina</i>	Radius	Proximal	R	Medium	Adult
SWP 973	D14	?	<i>Cercopithecoidea indet</i>	Radius	Shaft	?	Medium	Adult
SWP 974	D13		<i>Cercopithecoidea indet</i>	Thoracic Vertebra	Body		Small	Adult
SWP 975	D13		<i>Cercopithecoidea indet</i>	Vertebra	Axis		Small	Adult
SWP 976	D13		<i>Cercopithecoidea indet</i>	Cervical Vertebra	Complete		Small	Adult
SWP 977	D13		<i>Cercopithecoidea indet</i>	Cervical Vertebra	Complete		Small	Adult
SWP 978	D13		<i>Cercopithecoidea indet</i>	Vertebra	Body		Medium	Adult
SWP 980	D10		<i>Cercopithecoidea indet</i>	Humerus	Shaft	?	Medium	Adult
SWP 981	D10		<i>Cercopithecoidea indet</i>	Radius	Shaft	?	Medium	Adult
SWP 982	D10		<i>Cercopithecoidea indet</i>	Humerus	Proximal	R	Medium	Adult
SWP 983	D10		<i>Cercopithecoidea indet</i>	Ulna	Shaft	R	Medium	Adult
SWP 984	D15		<i>Cercopithecoidea indet</i>	Tibia	Shaft	L	Medium	Adult
SWP 985	D15		<i>Cercopithecoidea indet</i>	Tibia	Shaft		Medium	Adult
SWP 986	D15		<i>Cercopithecoidea indet</i>	Bone Fragment	Fragment		Medium	Adult
SWP 987	D15		<i>Cercopithecoidea indet</i>	Humerus	Distal fragment	L	Medium	Adult
SWP 989	D15		<i>Cercopithecoidea indet</i>	Humerus	Shaft	?	Medium	Adult
SWP 990	D15		<i>Cercopithecoidea indet</i>	Humerus	Shaft	?	Medium	Adult
SWP 991	D15		<i>Cercopithecoidea indet</i>	Humerus	Shaft	?	Medium	Adult
SWP 992	D15		<i>Cercopithecoidea indet</i>	Humerus	Shaft	?	Medium	Adult
SWP 993	D14		<i>Papionina</i>	Humerus	Proximal	R	Medium	Adult
SWP 994	D14		<i>Cercopithecoidea indet</i>	Humerus	Shaft		Medium	Adult
SWP 995	D14		<i>Papio/Parapapio</i>	Humerus	Distal	L	Medium	Adult
SWP 996			<i>Cercopithecoidea indet</i>	Tibia	Shaft		Medium	Adult
SWP 997	D14		<i>Cercopithecoidea indet</i>	Femur	Distal	?	Medium	Adult

Specimen no	Provenance	Level	Taxon	Element	Portion	Side	Size	Age
SWP 998	D14		<i>Cercopithecoides indet</i>	Humerus	Shaft	?	Medium	Adult
SWP 999	D14		<i>Cercopithecoides indet</i>	Humerus	Shaft	?	Medium	Adult
SWP 979	D10	?	<i>Papionina</i>	Radius	Proximal	R	Medium	Adult
SWP 179	?		<i>Papionina</i>	Ulna	Proximal	L	Medium	Adult
SWP 1000	D14		<i>Cercopithecoides indet</i>	Radius	Shaft	?	Medium	Adult
SWP 1001	D14		<i>Cercopithecoides indet</i>	Femur	Shaft	?	Medium	Adult
SWP 1002	D14		<i>Cercopithecoides indet</i>	Femur	Proximal fr	?	Medium	Adult
SWP 1003	D14		<i>Cercopithecoides indet</i>	Femur	Shaft	?	Medium	Adult
SWP 1004	D14		<i>Cercopithecoides indet</i>	Femur	Shaft	?	Medium	Adult
SWP 1005	D14		<i>Cercopithecoides indet</i>	Femur	Shaft	?	Medium	Adult
SWP 1006	D14		<i>Cercopithecoides indet</i>	Femur	Head	?	Medium	Adult
SWP 1007	D14		<i>Cercopithecoides indet</i>	Femur	Head fr	?	Medium	Adult
SWP 1008	D14		<i>Papio/Parapapio</i>	Femur	Proximal	R	Medium	Adult
SWP 1009	D14		<i>Cercopithecoides indet</i>	Femur	Proximal	L	Medium	Adult
SWP 1010	D14		<i>Cercopithecoides indet</i>	Femur	Shaft		Medium	Adult
SWP 1011	D14		<i>Cercopithecoides indet</i>	Femur	Proximal	L	Medium	Adult
SWP 1015	D13	?	<i>Cercopithecoides indet</i>	Tibia	Distal	L	Medium	Adult
SWP 1016	D13		<i>Papio/Parapapio</i>	Humerus	Distal	R	Medium	Adult
SWP 1103	D13		<i>Cercopithecoides indet</i>	Ulna	Shaft			
SWP 1104	T46	9' 10" - 10' 10"	<i>Theropithecus</i>	Ulna	Proximal	L	Large	Adult
SWP 1105	S/48	13' 6" - 14' 5"	<i>Cercopithecoides indet</i>	Ulna	Shaft	?	Large	Adult
SWP 1107	Dd48	10' 6" - 11' 8"	<i>Cercopithecoides indet</i>	Femur	Proximal	R	Medium	Adult
SWP 1108/9?	U44	10' 10" - 11' 10"	<i>Cercopithecoides indet</i>	Humerus	Distal	?	Medium	Adult
SWP 1110	Aa 48	4' 1" - 5' 1"	<i>Theropithecus</i>	Ulna	Proximal	L	Large	Adult
SWP 1113	M61	12' 8" - 13' 8"	<i>Cercopithecoides indet</i>	Tibia	Distal	L	Medium	Adult
SWP 1114	D17		<i>Cercopithecoides indet</i>	Femur	Proximal	L	Medium	Adult
SWP 1115	M4		<i>Cercopithecoides indet</i>	Humerus	Head fr	?	Medium	Adult
SWP 1116	D17		<i>Cercopithecoides indet</i>	Femur	Proximalfr	?	Medium	

Specimen no	Provenance	Level	Taxon	Element	Portion	Side	Size	Age
SWP 1117	D17		<i>Cercopithecoidea indet</i>	Femur	Proximalfr	?	Medium	
SWP 1118	D17		<i>Cercopithecoidea indet</i>	Femur	Proximalfr	?	Medium	Adult
SWP 1125	O45	13' 3" - 13' 11"	<i>Papionina</i>	Radius	Proximal	R	Medium	Adult
SWP 1126	Aa 44	6' 7" - 7' 10"	<i>Cercopithecoidea indet</i>	Femur	Proximal	L	Medium	Adult
SWP 1127	Aa 44	6' 7" - 7' 10"	<i>Cercopithecoidea indet</i>	Femur	Proximal shaft	R	Small	Adult
SWP 1128	V49	13' 10" - 14' 10"	<i>Cercopithecoidea indet</i>	Tibia	Distal	L	Medium	Adult
SWP 1132	D13		<i>Cercopithecoidea indet</i>	Femur	Proximal	L	Medium	Adult
SWP 1137	U57	10'5"-11'5"	<i>Parapapio</i>	Humerus	Distal	?	Medium	Adult
SWP 1138	T57	11' 1" - 12' 1"	<i>Cercopithecoidea indet</i>	Talus	Complete	L	Medium	Adult
SWP 1139	T45	6'0"-7'0"	<i>Cercopithecoidea indet</i>	Radius	Shaft	R	Small	Juvenile
SWP 1140	W46	3'11"-4'11"	<i>Papio/Parapapio</i>	Humerus	Distal	R	Medium	Adult
SWP 1141	W46	3'11"-4'11"	<i>Papio/Parapapio</i>	Humerus	Distal	R	Medium	Adult
SWP 1142	U48	7' 6" - 8' 6"	<i>Cercopithecoidea indet</i>	Clavicle	Complete	L		
SWP 1143	U48	7' 6" - 8' 6"	<i>Cercopithecoidea indet</i>	Metatarsal	Third	L	Medium	Adult
SWP 1144	U48	7' 6" - 8' 6"	<i>Parapapio</i>	Ivmetatarsal	Complete	R	Medium	Adult
SWP 1145	U48	7' 6" - 8' 6"	<i>Cercopithecoidea indet</i>	Metapodial	Distal	?	Medium	Adult
SWP 1146	U49	7'6"-8'6"	<i>Cercopithecoidea indet</i>	Calcaneus	Complete	L	Medium	Adult
SWP 1147	U49	7'6"-8'6"	<i>Cercopithecoidea indet</i>	Patella	Complete	L	Medium	Adult
SWP 1148	Q46	8' 8" - 9' 8"	<i>Theropithecus</i>	Ulna	Proximal	R	Large	Adult
SWP 1149	P49	10' 6" - 11' 6"	<i>Cercopithecoidea indet</i>	Tibia	Distal	R	Medium	Adult
SWP 1150	P46	10' 2" 11' 2"	<i>Cercopithecoidea indet</i>	Femur	Proximal fragment	R	Medium	Adult
SWP 1151	P46	10'2"-11'2"	<i>Cercopithecoidea indet</i>	Metapodial	Distal	?	Medium	Adult
SWP 1152	P45	13' 4" - 14' 4"	<i>Cercopithecoidea indet</i>	Femur	Proximal	L	Medium	Adult
SWP 1155	R46	6'2"-7'2"	<i>Papio</i>	Ulna	Olecranon	L	Medium	Adult
SWP 1156	T49	8'8" - 9' 8"	<i>Theropithecus</i>	Ulna	Proximal fragment	L	Medium	Adult
SWP 1157	V47	8' 4" - 9' 4"	<i>Cercopithecoidea indet</i>	Calcaneus	Complete	L	Medium	Adult

Specimen no	Provenance	Level	Taxon	Element	Portion	Side	Size	Age
SWP 1158	S48	9'8"-10'8"	<i>Cercopithecoidea indet</i>	Phalanx	Proximal manus	?	Medium	Adult
SWP 1159	S48	9'8"-10'8"	<i>Cercopithecoidea indet</i>	Metatarsal	Complete	?	Medium	Adult
SWP 1160	S49	9'8"-10'8"	<i>Cercopithecoidea indet</i>	Phalanx	Proximal manus	?	Medium	Adult
SWP 1161	T47	9' 4" - 10' 4"	<i>Cercopithecoidea indet</i>	Calcaneus	Complete	R	Medium	Adult
SWP 1162	V53	10'9"-11'9"	<i>Papionina</i>	Radius	Proximal	?	Large	Adult
SWP 1164	X54	9' 3" - 10' 3"	<i>Cercopithecoidea indet</i>	Tibia	Distal	R	Medium	Adult
SWP 1165	U52	12' 3" - 13' 3"	<i>Parapapio</i>	Humerus	Distal	R	Medium	Adult
SWP 1166	P47	6' 2"-7' 2"	<i>Cercopithecoidea indet</i>	Ulna	Proximal	R	Medium	Adult
SWP 1171	V47	5' 10" - 6' 10"	<i>Papio/Parapapio</i>	Femur	Proximal	L	Medium	Adult
SWP 1172	S46	5' 8" - 6' 8"	<i>Cercopithecoidea indet</i>	Pelvis	Os coxa fr	L	Medium	Adult
SWP 1173	T49	6'8"-7'8"	<i>Cercopithecoidea indet</i>	Humerus	Proximal	?	Medium	Juvenile
SWP 1174	V48	6' 10" - 7' 10"	<i>Cercopithecoidea indet</i>	Tibia	Distal	R	Medium	Adult
SWP 1175	U48	6'6"-7'6"	<i>Cercopithecoidea indet</i>	Femur	Distal	R	Medium	Sub-adult
SWP 1176	U48	6'6"-7'6"	<i>Papio</i>	Humerus	Distal	L	Medium	Adult
SWP 1197	T63	3'5"-4'5"	<i>Papionina</i>	Ulna	Proximal	L	Medium	Adult
SWP 1198	V57	10' 3" - 11' 0"	<i>Papionina</i>	Radius	Proximal	L	Medium	Adult
SWP 1199	V57	10' 3" - 11' 0"	<i>Papio/Parapapio</i>	Humerus	Proximal	R	Medium	Adult
SWP 1200	W57	9' 2" - 10' 2"	<i>Papio</i>	Ulna	Proximal	L	Medium	Adult
SWP 1201	W57	9' 2" - 10' 2"	<i>Papio</i>	Humerus	Proximal	L	Medium	Adult
SWP 1205	U57	5'2"-6'2"	<i>Papio/Parapapio</i>	Humerus	Shaft	?	Medium	Adult
SWP 12059	P44	22'7"-23'7"	<i>Cercopithecoidea indet</i>	Scapula	Glenoid cavity	R	Small	Adult
SWP 1206	Jj35	8'6"-9'5"	<i>Papio/Parapapio</i>	Femur	Head	L	Medium	Sub-adult
SWP 1207	W56	9' 10" - 10' 10"	<i>Cercopithecoidea indet</i>	Calcaneus	Complete	R	Medium	Adult
SWP 1208	V63	8' 6" - 9' 6"	<i>Papio</i>	Ulna	Proximal	L	Medium	Adult
SWP 1209	T61	23'1"-24'1"	<i>Cercopithecoidea indet</i>	Radius	Fr			
SWP 1210	T62	23'1"-24'1"	<i>Cercopithecoidea indet</i>	Pes proximalphal	Complete	?	Medium	Adult
SWP 1211	R65	14'8"-15'8"	<i>Parapapio</i>	Humerus	Distal		Medium	Adult

Specimen no	Provenance	Level	Taxon	Element	Portion	Side	Size	Age
SWP 1212	O59	13' 6" - 14' 6"	<i>Cercopithecoides indet</i>	Tibia	Shaft	?	Large	Adult
SWP 1213	R65	10' 8" - 11' 8"	<i>Papionina</i>	Ulna	Proximal	R	Medium	Sub-adult
SWP 1214	U50	10' 8" - 11' 8"	<i>Cercopithecoides indet</i>	Humerus	Distal	R	Medium	Adult
SWP 1215	T62	16' 1" - 17' 1"	<i>Cercopithecoides indet</i>	Radius	Proximal	L	Medium	Adult
SWP 1219	V47	7' 10" - 8' 10"	<i>Parapapio</i>	Radius	Proximal	L	Medium	Adult
SWP 1222	V47	7' 10" - 8' 10"	<i>Cercopithecoides indet</i>	Manus	Proximal	?	Medium	Adult
SWP 1223	V47	7'10"-8'10"	<i>Cercopithecoides indet</i>	Manus	Proximal	?	Medium	Adult
SWP 1225	V47	7' 10" - 8' 10"	<i>Cercopithecoides indet</i>	Femur	Proximal	L	Medium	Adult
SWP 1262	T59	9'5"-10'5"	<i>Parapapio</i>	Humerus	Distal	L	Medium	Adult
SWP 1263	Hh 38	8'10"-9'10"	<i>Papio/Parapapio</i>	Femur	Proximal and shaft	L	Medium	Sub-adult
SWP 1266	Ii 36	14'4"-15'4"	<i>Cercopithecoides indet</i>	Femur	Head	?	Medium	Juvenile
SWP 1267	V63	6' 9" - 7' 9"	<i>Cercopithecoides indet</i>	Metapodial		?	Large	Adult
SWP 1268	W47	6'6"-7'6"	<i>Cercopithecoides indet</i>	Humerus	Condyle	L	Medium	Sub-adult
SWP 1269	R49	10' 2" - 11' 2"	<i>Cercopithecoides indet</i>	Phalanx	Indet.	?	Medium	Adult
SWP 1270	V63	4' 9" - 5' 9"	<i>Cercopithecoides indet</i>	Metapodial	Proximal and shaft	R	Medium	Adult
SWP 1271	W57	7' 5" - 8' 5"	<i>Papio/Parapapio</i>	Humerus	Distal	R	Medium	Sub-adult
SWP 1273	T46	8' 6" - 9' 6"	<i>Cercopithecoides indet</i>	Calcaneus	Complete	L	Medium	Adult
SWP 1274	T48	8' 6" - 9' 6"	<i>Cercopithecoides indet</i>	Femur	Distal	L	Medium	Adult
SWP 1275	V44	10'10"-11'10"	<i>Cercopithecoides indet</i>	Humerus	Distal	R	Medium	Adult
SWP 1276	T60		<i>Papio</i>	Humerus	Prox	?	Medium	Adult
SWP 1277	T67	14' 7" - 15' 9"	<i>Cercopithecoides indet</i>	Tibia	Shaft	L	Large	Adult
SWP 1286	U61	14' 2" - 15' 1"	<i>Cercopithecoides indet</i>	Tibia	Distal	R	Medium	Adult
SWP 1287	W58	14'11"-15'11"	<i>Parapapio</i>	Humerus	Distal		Medium	Adult
SWP 1291	V62	7' 5" - 8' 5"	<i>Papionina</i>	Ulna	Proximal	R	Medium	Adult
SWP 1300	V62	16'8"-17'8"	<i>Parapapio</i>	Femur	Proximal and shaft	L	Medium	Adult
SWP 1301	V62	8' 5" - 9' 5"	<i>Cercopithecoides indet</i>	Femur	Distal condyle	?	Medium	Adult

Specimen no	Provenance	Level	Taxon	Element	Portion	Side	Size	Age
SWP 1305	T60	18' 2" - 19' 2"	<i>Cercopithecoides indet</i>	Patella	Complete	?L	Small	Adult
SWP 1339	Cc49	7' 7" - 8' 6"	<i>Cercopithecoides indet</i>	Metatarsal	2nd	R	Medium	Adult
SWP 1340	Dd47	4'8"-5'8"	<i>Cercopithecoides indet</i>	Metatarsal	Fr	?	Medium	Adult
SWP 1341	Ee46	5' 7" - 6' 7"	<i>Cercopithecoides indet</i>	Phalanx	Complete		Medium	Adult
SWP 1342	Ee46	5' 7" - 6' 7"	<i>Cercopithecoides indet</i>	Vertebraebra	Cervical		Medium	Adult
SWP 1343	Ee46	5' 7" - 6' 7"	<i>Cercopithecoides indet</i>	Clavicle	Complete	L	Medium	Juvenile
SWP 1344	Cc42	4' 6" - 5' 6"	<i>Cercopithecoides indet</i>	Vertebraebra	Atlas		Medium	Adult
SWP 1350	Cc43	3' 7" - 4' 7"	<i>Cercopithecoides indet</i>	Femur	Distal	?	Medium	Juvenile
SWP 1351	Ee44	3' 5" - 4' 5"	<i>Cercopithecoides indet</i>	Femur	Proximal	R	Small	Juvenile
SWP 1352	Bb54	7' 2" - 8' 2"	<i>Cercopithecoides indet</i>	Femur	Proximal	R	Medium	Adult
SWP 1353	Dd49	12'6"-13'-6"	<i>Cercopithecoides indet</i>	Femur	Proximal	R	Medium	Adult
SWP 1355	Aa50	6' 9" - 7' 9"	<i>Papionina</i>	Femur	Shaft	R	Medium	Adult
SWP 1356	Cc 50	9' 4" - 10' 4"	<i>Cercopithecoides indet</i>	Tibia	Proximal fragment	?	Medium	Adult
SWP 1357	Aa 50	5' 9" - 6' 9"	<i>Cercopithecoides indet</i>	Tibia	Distal	R	Medium	Adult
SWP 1374	Ee50	8' 10" - 9' 10"	<i>Cercopithecoides indet</i>	Scapula	Fr	L	Medium	Adult
SWP 1375	Ee50	8' 10" - 9' 10"	<i>Cercopithecoides indet</i>	Metatarsal	Complete	R	Medium	Adult
SWP 1376	Ee 50	8' 10" - 9' 10"	<i>Cercopithecoides indet</i>	Humerus	Proximal	R	Medium	Adult
SWP 1421			<i>Cercopithecinae</i>	Radius	Head	?	Medium	Adult
SWP 1507	D17	?	<i>Cercopithecoides indet</i>	Radius	Shaft		Medium	Adult
SWP 1508	D13		<i>Cercopithecoides indet</i>	Humerus	Condyles		Medium	Adult
SWP 1509	D13		<i>Cercopithecoides indet</i>	Femur	Distal	?	Medium	Adult
SWP 1510	D18	?	<i>Cercopithecoides indet</i>	Humerus	Distal	L	Medium	Adult
SWP 1511	D18	?	<i>Cercopithecoides indet</i>	Tibia	Distal	L	Medium	Adult
SWP 1512	D18	?	<i>Cercopithecoides indet</i>	Calcaneus	Proximal head	L	Medium	Adult
SWP 1513	D18		<i>Papionina</i>	Ulna	Proximal	L	Medium	Adult
SWP 1514	D18		<i>Papionina</i>	Femur	Proximal	R	Medium	Adult

Specimen no	Provenance	Level	Taxon	Element	Portion	Side	Size	Age
SWP 1515	D18	?	<i>Cercopithecoidea indet</i>	Radius	Proximal	R	Medium	Adult
SWP 1516	D18	?	<i>Cercopithecoidea indet</i>	Metapodial	Distal	?	Medium	Adult
SWP 1517	D18	?	<i>Cercopithecoidea indet</i>	Phalanx	Complete	?	Medium	Adult
SWP 1518	D18		<i>Cercopithecoidea indet</i>	Humerus	Distal	R	Medium	Adult
SWP 1519	D18		<i>Papio/Parapapio</i>	Radius	Proximal		Medium	Adult
SWP 1520	D13	?	<i>Cercopithecoidea indet</i>	Radius	Proximal	L	Medium	Adult
SWP 1520	D18		<i>Cercopithecoidea indet</i>	Humerus	Distal	R	Medium	Adult
SWP 1521	D18		<i>Cercopithecoidea indet</i>	Radius	Proximal	?	Medium	Adult
SWP 1522	D18	?	<i>Cercopithecoidea indet</i>	Radius	Proximal	L	Small	Adult
SWP 1523	D18		<i>Cercopithecoidea indet</i>	Femur	Distal	?	Medium	Adult
SWP 1524	D18		<i>Cercopithecoidea indet</i>	Humerus	Distal		Medium	Adult
SWP 1525	D18		<i>Cercopithecoidea indet</i>	Humerus	Capitulum	L	Medium	Adult
SWP 1525	D18		<i>Cercopithecoidea indet</i>	Femur	Head	?	Medium	Adult
SWP 1526	D18		<i>Cercopithecoidea indet</i>	Humerus	Distal condyles	L	Medium	Adult
SWP 1528	D18		<i>Cercopithecoidea indet</i>	Fibula	Distal	R	Medium	Adult
SWP 1529	D18		<i>Cercopithecoidea indet</i>	Humerus	Distal condyles	R	Medium	Adult
SWP 1530	D18		<i>Cercopithecoidea indet</i>	Radius	Shaft	?	Medium	Adult
SWP 1531	D18	?	<i>Cercopithecoidea indet</i>	Ulna	Proximal	L	Medium	Adult
SWP 1540	D14	?	<i>Cercopithecoidea indet</i>	Calcaneus	Complete	R	Medium	Adult
SWP 1553	R41	8' 10" - 9' 10"	<i>Cercopithecoidea indet</i>	Radius	Prox	L	Medium	Adult
SWP 1563	D18		<i>Papionina</i>	Ulna	Proximal	R	Medium	Adult
SWP 1564	?		<i>Cercopithecoidea indet</i>	Ulna	Shaft	?	Medium	Adult
SWP 1565	D18		<i>Cercopithecoidea indet</i>	Ulna	Shaft	?	Medium	Adult
SWP 1567	D18		<i>Papionina</i>	Ulna	Proximal	L	Medium	Adult
SWP 1568	D18		<i>Papio/Parapapio</i>	Ulna	Proximal	R	Medium	Adult
SWP 1569	D18		<i>Papio/Parapapio</i>	Ulna	Proximal	L	Medium	Adult
SWP 1570	D18		<i>Papio/Parapapio</i>	Ulna	Proximal	R	Medium	Adult
SWP 1571	D18		<i>Papio/Parapapio</i>	Ulna	Proximal	R	Medium	Adult



Specimen no	Provenance	Level	Taxon	Element	Portion	Side	Size	Age
SWP 1572	D18		<i>Papio</i>	Ulna	Proximal			
SWP 1573	D18	?	<i>Papionina</i>	Ulna	Proximal	R	Large	Adult
SWP 1574	D18		<i>Papionina</i>	Ulna	Proximal	R	Medium	Adult
SWP 1575	?		<i>Papionina</i>	Ulna	Proximal	L	Medium	Adult
SWP 1576	D18		<i>Papio/Parapapio</i>	Ulna	Proximal	R	Medium	Adult
SWP 1577	D18		<i>Papio</i>	Ulna	Proximal	L	Medium	Adult
SWP 1578	D18		<i>Theropithecus</i>	Ulna	Proximal	R	Medium	Adult
SWP 1580	D18		<i>Papio/Parapapio</i>	Ulna	Proximal	R	Medium	Adult
SWP 1596	?	?	<i>Cercopithecoidea indet</i>	Tibia	Proximal	R	Medium	Adult
SWP 1608	D15		<i>Cercopithecoidea indet</i>	Tibia	Distal and shaft	R	Medium	Adult
SWP 1629	?		<i>Cercopithecoidea indet</i>	Metatarsal	Proximal	?	Medium	Adult
SWP 1723	D13	?	<i>Cercopithecoidea indet</i>	Tibia	Proximal and shaft	?	Medium	Adult
SWP 2308	T33		<i>Cercopithecoidea indet</i>	Fibula	Distal	R	Medium	Adult
SWP 2357a,b (2 pieces)			<i>Cercopithecoidea indet</i>	2 ulna	Shaft fragment	?	Medium	Adult
SWP 2537			<i>Papio/Parapapio</i>	Humerus	Distal		Medium	Adult
SWP 255	V47	?	<i>Papionina</i>	Radius	Head	?	Medium	Adult
SWP 2713	S48	25'7"-26'7"	<i>Cercopithecoidea indet</i>	Ulna	Olecranon process	R	Medium	Adult
SWP 2746	T39	7'7"-8'7"	<i>Cercopithecoidea indet</i>	Ulna		R	Medium	Adult
SWP 2747	T39	7'7"-8'7"	<i>Cercopithecoidea indet</i>	Tibia	Shaft		Medium	Adult
SWP 2804	T60	10'2"-11'2"	<i>Cercopithecoidea indet</i>	Tibia	Prox	R	Small	Juvenile
SWP 2807	V46	15'11"-16'11"	<i>Cercopithecoidea indet</i>	Calcaneus	Prox	L	Medium	Adult
SWP 2808	Q43	31'9"-32'9"	<i>Cercopithecoidea indet</i>	Sacrum	Complete		Medium	?
SWP 2809	V49	4'10"-5'10"	<i>Cercopithecoidea indet</i>	Pelvis	Ilium	L	Small	Adult
SWP 2810	W47	18'10"-19'7"	<i>Papio</i>	Humerus	Disal and shaft fr	L	Medium	Adult
SWP 2811	Q49	13'4"-14'4"	<i>Cercopithecoidea indet</i>	Pelvis	Ilium	L	Medium	Adult
SWP 2812	W46	27'4"-28'4"	<i>Cercopithecoidea indet</i>	Rib	Shaft	L	Medium	Adult

Specimen no	Provenance	Level	Taxon	Element	Portion	Side	Size	Age
SWP 2813	Q44	35'7"-36'7"	<i>Papionina</i>	Ulna	Prox	R	Medium	Adult
SWP 2814	V45	5'11"-6'11"	<i>Cercopithecoidea indet</i>	Manus 1st phal	Complete		Medium	Adult
SWP 2816	H39	21'8"-22'8"	<i>Papio/Parapapio</i>	Humerus	Distal	R	Medium	Adult
SWP 29d	D15	?	<i>Cercopithecoidea indet</i>	Tibia	Distal condyle	L	Medium	Adult
SWP 4000	D18	?	<i>Cercopithecoidea indet</i>	Radius	Proximal	R	Small	Adult
SWP 4001	D18		<i>Theropithecus</i>	Ulna	Proximal	R	Large	Adult
SWP 4002	T45	13'4"-14' 4"	<i>Cercopithecoidea indet</i>	Femur	Lesser trochnater	L	Medium	Adult
SWP 4003			<i>Cercopithecoidea indet</i>	Femur	Lat. Condyle	R	Small	
SWP 4004	P49	26'3"-27'3"	<i>Cercopithecoidea indet</i>	Hamate	Complete	L	Small	Adult
SWP 4005	?	?	<i>Papionina</i>	Radius	Head			
SWP 4006	?	?	<i>Parapapio</i>	Humerus	Distal	?	Medium	Adult
SWP 4007	N45	31' 0" - 32' 0"	<i>Papio/Parapapio</i>	Ulna	Proximal	?	Medium	Adult
SWP 4008	N45	31' 0" - 32' 0"	<i>Papio/Parapapio</i>	Ulna	Proximal and shaft	L	Medium	Adult
SWP 4009	S45	6' 3" - 7' 3"	<i>Cercopithecoidea indet</i>	Radius	Shaft	?	Medium	Adult
SWP 4010	X36	3' 2" – 4' 9"	<i>Cercopithecoidea indet</i>	Ulna	Shaft	R	Medium	Adult
SWP 4011	S45	6' 3" - 7' 3"	<i>Cercopithecoidea indet</i>	Ulna	Shaft	?	Medium	Adult
SWP 4012	X36	3' 2" - 4' 9"	<i>Cercopithecus sp</i>	Radius	Proximal		Medium	Adult
SWP 4013	S45	6' 3" - 7' 3"	<i>Cercopithecoidea indet</i>	Ulna	Shaft	?	Medium	Adult
SWP 4014	S45	6' 3" - 7' 3"	<i>Cercopithecoidea indet</i>	Ulna	Shaft	?	Medium	Adult
SWP 4015	N45	29' 1" - 30' 1"	<i>Papionina</i>	Ulna	Proximal	L	Large	Adult
SWP 4016	N45	29' 1" - 30' 1"	<i>Papio/Parapapio</i>	Ulna	Proximal	L	Medium	Adult
SWP 4017	W37	4' 2"- 5' 2"	<i>Cercopithecoidea indet</i>	Femur	Shaft	?	Medium	Adult
SWP 4018	V37	5' 0" - 6' 9"	<i>Cercopithecoidea indet</i>	Femur	Shaft	R	Medium	Adult
SWP 4019	N46	28' 0" - 29' 0"	<i>Cercopithecoidea indet</i>	Humerus	Distal	R	Medium	Adult
SWP 4020	X 36	3' 2" – 4' 9"	<i>Cercopithecoidea indet</i>	Femur	Shaft	?	Medium	Adult
SWP 4021	V37	5' 0" - 6' 9"	<i>Cercopithecoidea indet</i>	Femur	Shaft	?	Medium	Adult
SWP 4022	N46	28' 0" - 29' 0"	<i>Cercopithecoidea indet</i>	Radius	Proximal		Medium	Adult

Specimen no	Provenance	Level	Taxon	Element	Portion	Side	Size	Age
SWP 4023	N46	28' 0" - 29' 0"	<i>Cercopithecoides indet</i>	Radius	Proximal	R	Medium	Adult
SWP 4024	V37	5' 0" - 6' 9"	<i>Cercopithecoides indet</i>	Femur	Shaft	?	Medium	Adult
SWP 4025	N46	28' 0" - 29' 0"	<i>Cercopithecoides indet</i>	Humerus	Shaft	?	Medium	Adult
SWP 4026	X36	3' 2" - 4' 9"	<i>Cercopithecoides indet</i>	Tibia	Distal	L	Medium	Adult
SWP 4027	X36	3' 2" - 4' 9"	<i>Cercopithecoides indet</i>	Humerus	Head fragment	?R	Medium	Adult
SWP 4028	W37	4' 2" - 5' 2"	<i>Cercopithecoides indet</i>	Ulna	Shaft	?	Medium	Adult
SWP 4029	X36	3' 2" - 4' 9"	<i>Cercopithecoides indet</i>	Ulna	Shaft	R	Medium	Adult
SWP 4030	W37	4' 2" - 5' 2"	<i>Cercopithecoides indet</i>	Radius	Shaft	?	Medium	Adult
SWP 4031	N47	25' 5" - 26' 5"	<i>Cercopithecoides indet</i>	Femur	Shaft	?	Large	Adult
SWP 4032	?	?	<i>Cercopithecoides indet</i>	Femur	Proximal	R	Large	Adult
SWP 4033	?N49	25' 3" - 26' 3"	<i>Cercopithecoides indet</i>	Femur	Distal	R	Medium	Sub-adult
SWP 4034	N49	25' 3" - 26' 3"	<i>Cercopithecoides indet</i>	Femur	Shaft	?	Medium	Adult
SWP 4035	W37	4' 5" - 5' 2"	<i>Papionina</i>	Femur	Proximal	L	Medium	Adult
SWP 4036	X36	3' 2" - 4' 9"	<i>Parapapio</i>	Humerus	Distal and shaft	R	Medium	Adult
SWP 4037	N49	25' 3" - 26' 3"	<i>Cercopithecoides indet</i>	Femur	Distal	L	Medium	Sub-adult
SWP 4038	V37	5' 0" - 6' 0"	<i>Parapapio/papio</i>	Humerus	Distal	L	Medium	Adult
SWP 4039	N49	25' 3" - 26' 3"	<i>Theropithecus sp</i>	Femur	Proximal	L	Medium	Adult
SWP 4040	V37	5' 0" - 6' 9"	<i>Cercopithecoides indet</i>	Femur	Proximal	L	Medium	Adult
SWP 4041	N45	31' 0" - 32' 0"	<i>Parapapio/papio</i>	Humerus	Distal	L	Medium	Adult
SWP 4042	W37	4' 5" - 5' 0"	<i>Papio</i>	Radius	Proximal	L	Medium	Adult
SWP 4043	N46	28' 0" - 29' 0"	<i>Cercopithecoides indet</i>	Ulna	Proximal	R	Medium	Adult
SWP 4044	W37	4' 5" - 5' 2"	<i>Cercopithecoides indet</i>	Femur	Shaft	?	Medium	Adult
SWP 4045	W37	4' 5" - 5' 2"	<i>Cercopithecoides indet</i>	Femur	Proximal	L	Large	Adult
SWP 4046	V37	5' 0" - 6' 9"	<i>Cercopithecoides indet</i>	Humerus	Distal shaft	?	Medium	Adult
SWP 4047	W37	4' 5" - 5' 2"	<i>Parapapio</i>	Humerus	Distal	R	Medium	Adult
SWP 4048	V37	5' 0" - 6' 0"	<i>Cercopithecoides indet</i>	Femur	Proximal	R	Medium	Adult
SWP 4049	V37	5' 0" - 6' 9"	<i>Cercopithecoides indet</i>	Ulna	Shaft	?	Medium	Adult
SWP 4050	W37	4' 5" - 5' 2"	<i>Cercopithecoides indet</i>	Femur	Shaft	?	Medium	Adult

Specimen no	Provenance	Level	Taxon	Element	Portion	Side	Size	Age
SWP 4051	N48	32' 0" - 33' 4"	<i>Cercopithecoidea indet</i>	Scapula	Corocoid and glenoid cavity			
SWP 4052	V37	5' 9" - 6' 9"	<i>Cercopithecoidea indet</i>	Tibia	Shaft	?	Medium	Adult
SWP 4053	W37	4' 5" - 5' 2"	<i>Cercopithecoidea indet</i>	Femur	Shaft (2)	L	Medium	Adult
SWP 4055	N49	25' 3" - 26' 3"	<i>Cercopithecoidea indet</i>	Femur	Shaft	?	Medium	Adult
SWP 4056	N47	35' 9" – 36' 9"	<i>Cercopithecoidea indet</i>	Rib	Head	R	Medium	Adult
SWP 4057	N48	15' 11" - 16' 11"	<i>Cercopithecoidea indet</i>	Lunate	Complete	L	Medium	Adult
SWP 4058	N48	15' 11" - 16' 11"	<i>Cercopithecoidea indet</i>	?Hamate	Complete	?L	Medium	Adult
SWP 4059	P49	28' 0" – 29' 0"	<i>Papionina</i>	Radius	Proximal fragment	?	Medium	Adult
SWP 4060	N47	31' 9" - 32' 9"	<i>Cercopithecoidea indet</i>	Proximal foot phalanx	Complete	?	Medium	Adult
SWP 4061	N49	26' 0" - 27' 0"	<i>Cercopithecoidea indet</i>	Coccyx	Complete		Medium	Juvenile
SWP 4062	S49	8' 6" - 9' 6"	<i>Cercopithecoidea indet</i>	Iii metatarsal	Complete	R	Medium	Adult
SWP 4063	P 45	32' 1" - 33' 1"	<i>Papionina</i>	Radius	Proximal	L	Small	Juvenile
SWP 4064	V37	5' 0" - 6' 9"	<i>Cercopithecoidea indet</i>	Scapula	Body	L	Medium	Adult
SWP 4065	N49	25' 3"- 26' 3"	<i>Cercopithecoidea indet</i>	Long bone	Shaft fr	?	Medium	Adult
SWP 4066	N49	25' 3"- 26' 3"	<i>Cercopithecoidea indet</i>	Long bone	Shaft fr	?	Medium	Adult
SWP 4067	N49	25' 3"- 26' 3"	<i>Cercopithecoidea indet</i>	Long bone	Shaft fr	?	Medium	Adult
SWP 4068	N49	25' 3"- 26' 3"	<i>Cercopithecoidea indet</i>	Long bone	Shaft fr	?	Medium	Adult
SWP 4069	N49	25' 3"- 26' 3"	<i>Cercopithecoidea indet</i>	Long bone	Shaft fr	?	Medium	Adult
SWP 4070	N49	25' 3"- 26' 3"	<i>Cercopithecoidea indet</i>	Long bone	Shaft fr	?	Medium	Adult
SWP 4071	N49	25' 3"- 26' 3"	<i>Cercopithecoidea indet</i>	Long bone	Shaft fr	?	Medium	Adult
SWP 4072	N49	25' 3"- 26' 3"	<i>Cercopithecoidea indet</i>	Long bone	Shaft fr	?	Medium	Adult
SWP 4073	N49	25' 3"- 26' 3"	<i>Cercopithecoidea indet</i>	Long bone	Shaft fr	?	Medium	Adult
SWP 4074	N49	25' 3"- 26' 3"	<i>Cercopithecoidea indet</i>	Long bone	Shaft fr	?	Medium	Adult
SWP 4075	N49	25' 3"- 26' 3"	<i>Cercopithecoidea indet</i>	Long bone	Shaft fr	?	Medium	Adult
SWP 4076	N49	25' 3"- 26' 3"	<i>Cercopithecoidea indet</i>	Long bone	Shaft fr	?	Medium	Adult
SWP 4077	N49	25' 3"- 26' 3"	<i>Cercopithecoidea indet</i>	Long bone	Shaft fr	?	Medium	Adult

Specimen no	Provenance	Level	Taxon	Element	Portion	Side	Size	Age
SWP 4078	W37	4' 2" - 5' 2"	<i>Cercopithecoidea indet</i>	Femur	Head	L	Small	Adult
SWP 4079	V37	5' 0" - 6' 9"	<i>Cercopithecoidea indet</i>	Pelvis	Ilium	R	Medium	Adult
SWP 4080	V37	5' 0" - 6' 9"	<i>Cercopithecoidea indet</i>	Calcaneus	Complete	R	Medium	Adult
SWP 4081	V37	5' 0" - 6' 9"	<i>Parapapio</i>	Humerus	Distal with extensive shaft	L	Medium	Adult
SWP 4082	V37	5' 0" - 6' 9"	<i>Cercopithecoidea indet</i>	Calcaneus	Complete	L	Large	Adult
SWP 4083	W37	4' 5" - 5' 2"	<i>Cercopithecoidea indet</i>	Long bone	Shaft fr	?	Medium	Adult
SWP 4084	W37	4' 5" - 5' 2"	<i>Papio/Parapapio</i>	Ulna	Proximal	R	Medium	Adult
SWP 4085	X36	3' 2" – 4' 9"	<i>Cercopithecoidea indet</i>	Humerus	Shaft	?	Large	Adult
SWP 4086	X36	3' 2" – 4' 9"	<i>Cercopithecoidea indet</i>	Femur	Head	L	Medium	Adult
SWP 4087	W37	4' 5" - 5' 2"	<i>Papionina</i>	Radius	Proximal	L	Medium	Adult
SWP 4088	W37	4' 5" - 5' 2"	<i>Cercopithecoidea indet</i>	Femur	Proximal fragment	R	Medium	Adult
SWP 4089	V37	5' 0" - 6' 9"	<i>Cercopithecoidea indet</i>	Femur	Shaft fr	?	Medium	Adult
SWP 4090	W37	4' 5" - 5' 2"	<i>Cercopithecoidea indet</i>	Ulna	Shaft	?	Medium	Adult
SWP 4091	V37	5' 0" - 6' 9"	<i>Cercopithecoidea indet</i>	Long bone	Shaft fr	?	Medium	Adult
SWP 4092	V37	5' 0" - 6' 9"	<i>Cercopithecoidea indet</i>	Femur	Shaft	R	Medium	Adult
SWP 4093	X36	3' 2" – 4' 9"	<i>Cercopithecoidea indet</i>	Long bone	Shaft fr	?	Medium	Adult
SWP 4094	V37	5' 0" - 6' 9"	<i>Cercopithecoidea indet</i>	Long bone	Shaft fr	?	Medium	Adult
SWP 4095	X36	3' 2" – 4' 9"	<i>Cercopithecoidea indet</i>	Long bone	Shaft fr	?	Medium	Adult
SWP 4096	V37	5' 0" - 6' 9"	<i>Cercopithecoidea indet</i>	Femur	Shaft	L	Medium	Adult
SWP 4097	X36	3' 2" – 4' 9"	<i>Cercopithecoidea indet</i>	Ulna	Proximal	L	Medium	Adult
SWP 4098			<i>Papionina</i>	Ulna	Proximal	R	Medium	Adult
SWP 4099	V37	5' 0" - 6' 9"	<i>Papionina</i>	Humerus	Distal lateral epicondyle	L	Medium	Adult
SWP 4100	W37	4' 5" - 5' 2"	<i>Cercopithecoidea indet</i>	Tibia	Distal and shaft fr	L	Medium	Adult
SWP 4101	V37	5' 0" - 6' 9"	<i>Cercopithecoidea indet</i>	Tibia	Distal and shaft fragment	R	Medium	Adult
SWP 4102	V37	5' 0" - 6' 9"	<i>Cercopithecoidea indet</i>	Long bone	Shaft fr	?	Medium	Adult

Specimen no	Provenance	Level	Taxon	Element	Portion	Side	Size	Age
SWP 4103	V37	5' 0" - 6' 9"	<i>Papio/Parapapio</i>	Femur	Proximal	L	Medium	Adult
SWP 4104	X36	3' 2" – 4' 9"	<i>Cercopithecoides indet</i>	Femur	Head	L	Medium	Adult
SWP 4105	V37	5' 0" - 6' 9"	<i>Cercopithecoides indet</i>	Tibia	shaft fr	R	Medium	Adult
SWP 4106	X36	3' 2" – 4' 9"	<i>Cercopithecoides indet</i>	Femur long bone	Distal shaft	?	Medium	Adult
SWP 4107	W37	4' 5" - 5' 2"	<i>Cercopithecoides indet</i>	Femur long bone	Distal shaft	?	Medium	Adult
SWP 4108	V37	5' 0" - 6' 9"	<i>Cercopithecoides indet</i>	Femur long bone	Distal shaft	?	Medium	Adult
SWP 4109	V37	5' 0" - 6' 9"	<i>Cercopithecoides indet</i>	Long bone	Shaft fragment	?	Medium	Adult
SWP 4110	V37	5' 0" - 6' 9"	<i>Cercopithecoides indet</i>	Femur	Head fragment	?	Medium	Adult
SWP 4111	U51	4' 5" - 5' 2"	<i>Cercopithecoides indet</i>	Patella	Complete	R	Medium	Adult
SWP 4112	S49		<i>Cercopithecoides indet</i>	3metatarsal	Complete	R	Medium	Adult
SWP 4113	N50		<i>Cercopithecoides indet</i>	?Metatarsal	Prox	?	Medium	Adult
SWP 4114	S45		<i>Cercopithecoides indet</i>	Femur	Lateral condyle	R	Medium	Adult
SWP 4115	S45		<i>Cercopithecoides indet</i>	Ulna	Fr	?	Medium	Adult
SWP 4116	?		<i>Cercopithecoides indet</i>	Ulna	Fr	?	Medium	Adult
SWP 4117	S45	6'3" - 7'3"	<i>Cercopithecoides indet</i>	Ulna	Shaft	?	Medium	Adult
SWP 4118	S45	6'3" - 7'3"	<i>Cercopithecoides indet</i>	Ulna	Shaft	?	Medium	Adult
SWP 4119	N46	28'0"-29'0"	<i>Cercopithecoides indet</i>	Ulna	Prox		Medium	Adult
SWP 4120	N47	31'9"-32'9"	<i>Cercopithecoides indet</i>	2nd phalanx pes	Proximal	?	Medium	Adult
SWP 4121	N48	15'11"-16'11"	<i>Cercopithecoides indet</i>	Scaphoid	Complete	L	Medium	Adult
SWP 4122	S45	8'5"-9'5"	<i>Cercopithecoides indet</i>	Caudal Vertebra	Complete	?	Medium	Adult
SWP 4123	P49	26'3"-27'3"	<i>Cercopithecoides indet</i>	Hamate	Complete	L	Medium	Adult
SWP 4124	N48	32'0"-33'4"	<i>Cercopithecoides indet</i>	Scapula	Coronoid process and glenoid fossa	R	Medium	Adult
SWP 4125	N50	20'5"-21'5"	<i>Cercopithecoides indet</i>	Navicular	Complete	R	Medium	Adult
SWP 4126	N47	35'9"-36'9"	<i>Cercopithecoides indet</i>	Vertebra	Body	?	Medium	Adult
SWP 4127	N47	35'9"-36'9"	<i>Cercopithecoides indet</i>	2nd rib	Body	L	Medium	Adult

Specimen no	Provenance	Level	Taxon	Element	Portion	Side	Size	Age
SWP 4128	N47	35'9"-36'9"	<i>Cercopithecoides indet</i>	Vertebra	Wing	?	Medium	Adult
SWP 4129	N45	29'1"-30'1"	<i>Cercopithecoides indet</i>	Ulna	Olecranon	R	Medium	Adult
SWP 4130	P49	28'0"-29'0"	<i>Cercopithecoides indet</i>	Radius	Head	?	Small	Adult
SWP 4132	N49	26'0"-27'0"	<i>Cercopithecoides indet</i>	Caudal Vertebra	Complete	?	Medium	Adult
SWP 4133	N48	15'11"-16'11"	<i>Cercopithecoides indet</i>	Rib	Head and shaft	R	Medium	Adult
SWP 4134	N46	28'0"-29'0"	<i>Cercopithecoides indet</i>	Humerus	Distal condyle	L	Medium	Adult
SWP 4135	N46	28'0"-29'0"	<i>Cercopithecoides indet</i>	Radius	Proximal and shaft	L	Medium	Adult
SWP 4136	N46	28'0"-29'0"	<i>Cercopithecoides indet</i>	Radius	Shaft	?	Medium	Adult
SWP 4137	S44	5'3" - 6'3"	<i>Cercopithecoides indet</i>	Ulna	Shaft	R	Medium	Adult
SWP 4138	S44	5'3" - 6'3"	<i>Cercopithecoides indet</i>	Ulna	Shaft	?	Medium	Adult
SWP 4139	S44	5'3" - 6'3"	<i>Cercopithecoides indet</i>	Caudal Vertebra	Complete		Medium	Adult
SWP 4140	W37	4'5"-5'2"	<i>Cercopithecoides indet</i>	Femur	Shaft	L	Medium	Adult
SWP 4141	X36	3'2"-9'9"	<i>Cercopithecoides indet</i>	Humerus	Distal and shaft	R	Medium	Adult
SWP 4142	W37	4'5"-5'2"	<i>Cercopithecoides indet</i>	Ulna	Shaft	L	Medium	Adult
SWP 4143	W37	4'5"-5'2"	<i>Cercopithecoides indet</i>	Ulna	Shaft	R	Medium	Adult
SWP 4144	W37	4'5"-5'2"	<i>Cercopithecoides indet</i>	Femur	Head and shaft	L	Medium	Adult
SWP 4145	W37	4'5"-5'2"	<i>Cercopithecoides indet</i>	Femur	Shaft	L	Medium	Adult
SWP 4146	W37	4'5"-5'2"	<i>Cercopithecoides indet</i>	Radius	Proximal and shaft	R	Medium	Adult
SWP 4147	W37	4'5"-5'2"	<i>Cercopithecoides indet</i>	Femur	Head	?	Medium	Adult
SWP 4148	W37	4'5"-5'2"	<i>Cercopithecoides indet</i>	Humerus	Distal and shaft	L	Medium	Adult
SWP 4149	V37	5'0"-6'9"	<i>Cercopithecoides indet</i>	Breccia block skull & 3 long bones			Small	Sub-adult
SWP 4150	N49	25'3"-26'3"	<i>Cercopithecoides indet</i>	Femur	Prox	L	Medium	Adult
SWP 4151	N49	25'3"-26'3"	<i>Cercopithecoides indet</i>	Femur	Distal	?	Medium	Adult
SWP 4152	N49	25'3"-26'3"	<i>Cercopithecoides indet</i>	Femur	Shaft	?	Medium	Adult
SWP 4153	N49	25'3"-26'3"	<i>Theropithecus sp</i>	Femur	Proximal	R	Medium	Adult

Specimen no	Provenance	Level	Taxon	Element	Portion	Side	Size	Age
SWP 4154	N49	25'3"-26'3"	<i>Cercopithecoides indet</i>	Femur	Shaft and distal condyle	R	Medium	Adult
SWP 4155	N49	25'3"-26'3"	<i>Cercopithecoides indet</i>	Femur	Fr	?	Medium	Adult
SWP 4156	N49	25'3"-26'3"	<i>Cercopithecoides indet</i>	Femur	Fr	?	Medium	Adult
SWP 4157	N49	25'3"-26'3"	<i>Cercopithecoides indet</i>	Femur	Fr	?	Medium	Adult
SWP 4158	N49	25'3"-26'3"	<i>Cercopithecoides indet</i>	Femur	Fr	?	Medium	Adult
SWP 4159	N49	25'3"-26'3"	<i>Cercopithecoides indet</i>	Femur	Fr	?	Medium	Adult
SWP 4160	N49	25'3"-26'3"	<i>Cercopithecoides indet</i>	Femur	Fr	?	Medium	Adult
SWP 4161	N49	25'3"-26'3"	<i>Cercopithecoides indet</i>	Femur	Fr	?	Medium	Adult
SWP 4162	N49	25'3"-26'3"	<i>Cercopithecoides indet</i>	Femur	Fr	?	Medium	Adult
SWP 4163	N49	25'3"-26'3"	<i>Cercopithecoides indet</i>	Femur	Fr	?	Medium	Adult
SWP 4164	N49	25'3"-26'3"	<i>Cercopithecoides indet</i>	Femur	Fr	?	Medium	Adult
SWP 4165	N49	25'3"-26'3"	<i>Cercopithecoides indet</i>	Femur	Shaft fr	?	Medium	Adult
SWP 4166	N49	25'3"-26'3"	<i>Cercopithecoides indet</i>	Femur	Fr	?	Medium	Adult
SWP 4167	N49	25'3"-26'3"	<i>Cercopithecoides indet</i>	Femur	Fr	?	Medium	Adult
SWP 4168	N49	25'3"-26'3"	<i>Cercopithecoides indet</i>	Femur	Fr	?	Medium	Adult
SWP 4169	N49	25'3"-26'3"	<i>Cercopithecoides indet</i>	Femur	Fr	?	Medium	Adult
SWP 4170	N50	20'5"-21'5"	<i>Cercopithecoides indet</i>	Cuneiform	Fr	R	Medium	Adult
SWP 4171	N50	20'5"-21'5"	<i>Cercopithecoides indet</i>	Metacarpal 3	Distal	R	Medium	Adult
SWP 4172	S46	22'7"-23'7"	<i>Cercopithecoides indet</i>	Radius	Prox	?	Small	Juvenile
SWP 4173	W37	4'5"-5'2"	<i>Cercopithecoides indet</i>	Femur	Shaft	?	Medium	Adult
SWP 4174	W37	4'5"-5'2"	<i>Cercopithecoides indet</i>	Ulna	Shaft	?	Medium	Adult
SWP 4175	W37	4'5"-5'2"	<i>Cercopithecoides indet</i>	Tibia	Shaft	?	Medium	Adult
SWP 4176	U51	4'5"-5'2"	<i>Cercopithecoides indet</i>	Patella	Shaft	R	Medium	Adult
SWP 4177	W37	4'5"-5'2"	<i>Cercopithecoides indet</i>	Tibia	Distal	L	Medium	Adult
SWP 4178	W35	4'5"-5'2"	<i>Cercopithecoides indet</i>	Ulna	Shaft	?	Medium	Adult
SWP 4179	W35	4'5"-5'2"	<i>Cercopithecoides indet</i>	Fibula	Prox	?	Medium	Adult
SWP 4180	W35	4'5"-5'2"	<i>Cercopithecoides indet</i>	Humerus	Shaft	?	Medium	Adult



Specimen no	Provenance	Level	Taxon	Element	Portion	Side	Size	Age
SWP 4181	W35	4'5"-5'2"	<i>Cercopithecoides indet</i>	Humerus	Shaft	?	Medium	Adult
SWP 4182	V37	5'0"-6'9"	<i>Cercopithecoides indet</i>	Humerus	Distal shaft	L	Medium	Adult
SWP 4183	V37	5'0"-6'9"	<i>Cercopithecoides indet</i>	Calcaneus	Complete	L	Medium	Adult
SWP 4184	W37	4'5"-5'2"	<i>Cercopithecoides indet</i>	Calcaneus	Complete	R	Small	Adult
SWP 4185	V37	5'0"-6'9"	<i>Cercopithecoides indet</i>	Femur	Prox	L	Medium	Adult
SWP 4186			<i>Cercopithecoides indet</i>	Ulna	Proximal	R	Medium	Adult
SWP 4187	V37	5'0"-6'9"	<i>Cercopithecoides indet</i>	Femur	Head	?	Medium	Adult
SWP 4188	W37	4'5"-5'2"	<i>Cercopithecoides indet</i>	Tibia	Distal	R	Medium	Adult
SWP 4189	V37	5' 0" - 6' 9"	<i>Cercopithecoides indet</i>	Femur	Distal condyles	R	Medium	Adult
SWP 4190	W37	4'5"-5'2"	<i>Cercopithecoides indet</i>	Radius	Proximal shaft	L	Medium	Adult
SWP 4191	V37	5'0"-6'9"	<i>Cercopithecoides indet</i>	Tibia	Distal shaft	R	Medium	Adult
SWP 4192	V37	5'0"-6'9"	<i>Cercopithecoides indet</i>	Femur	Shaft	?	Medium	Adult
SWP 4193	V37	5'0"-6'9"	<i>Cercopithecoides indet</i>	Humerus	Shaft	?	Medium	Adult
SWP 4194	V37	5'0"-6'9"	<i>Cercopithecoides indet</i>	Long bone	Shaft	?	Medium	Adult
SWP 4195	V37	5'0"-6'9"	<i>Cercopithecoides indet</i>	Femur	Shaft	?	Medium	Adult
SWP 4196	V37	5'0"-6'9"	<i>Cercopithecoides indet</i>	Femur	Shaft	?	Medium	Adult
SWP 4197	V37	5'0"-6'9"	<i>Cercopithecoides indet</i>	Femur	Shaft	?	Medium	Adult
SWP 4198	V37	5'0"-6'9"	<i>Cercopithecoides indet</i>	Femur	Shaft	?	Medium	Adult
SWP 4199	V37	5'0"-6'9"	<i>Cercopithecoides indet</i>	Femur	Shaft	?	Medium	Adult
SWP 4200	V37	5'0"-6'9"	<i>Cercopithecoides indet</i>	Humerus	Distal shaft	L	Medium	Adult
SWP 4201	V37	5'0"-6'9"	<i>Cercopithecoides indet</i>	Femur	Distal shaft	?	Medium	Adult
SWP 4202	V37	5'0"-6'9"	<i>Cercopithecoides indet</i>	Humerus	Distal	L	Medium	Adult
SWP 4203	V37	5'0"-6'9"	<i>Cercopithecoides indet</i>	Femur	Shaft	R	Medium	Adult
SWP 4204	V37	5'0"-6'9"	<i>Cercopithecoides indet</i>	Femur	Proximal	L	Medium	Adult
SWP 4205	V37	5'0"-6'9"	<i>Cercopithecoides indet</i>	Humerus	Distal shaft	L	Medium	Adult
SWP 4206	V37	5'0"-6'9"	<i>Cercopithecoides indet</i>	Femur	Shaft fr	R	Medium	Adult
SWP 4207	V37	5'0"-6'9"	<i>Cercopithecoides indet</i>	Femur	Distal shaft	R	Medium	Adult
SWP 4208	V37	5'0"-6'9"	<i>Cercopithecoides indet</i>	Humerus	Distal shaft	?	Small	Adult

Specimen no	Provenance	Level	Taxon	Element	Portion	Side	Size	Age
SWP 4209	V37	5'0"-6'9"	<i>Cercopithecoides indet</i>	Femur	Proximal shaft	R	Medium	Adult
SWP 4210	V37	5'0"-6'9"	<i>Cercopithecoides indet</i>	Ulna	Proximalshaft	?	Medium	Adult
SWP 4211	V37	5'0"-6'9"	<i>Cercopithecoides indet</i>	Tibia	Proximalshaft	?	Medium	Adult
SWP 4212	V37	5'0"-6'9"	<i>Cercopithecoides indet</i>	Femur	Proximalshaft	L	Medium	Adult
SWP 4213	V37	5'0"-6'9"	<i>Cercopithecoides indet</i>	Femur	Shadft	?	Medium	Adult
SWP 4214	V37	5'0"-6'9"	<i>Cercopithecoides indet</i>	Femur	Shaft	?	Medium	Adult
SWP 4215	X36	3'2"-4'9"	<i>Cercopithecoides indet</i>	Femur	Shaft	?	Medium	Adult
SWP 4216	X36	3'2"-4'9"	<i>Cercopithecoides indet</i>	Humerus	Shaft	?	Medium	Adult
SWP 4217	X36	3'2"-4'9"	<i>Cercopithecoides indet</i>	Radius	Shaft	?	Medium	Adult
SWP 4218	X36	3'2"-4'9"	<i>Cercopithecoides indet</i>	Ulna	Shaft	R	Medium	Adult
SWP 4219	X36	3'2"-4'9"	<i>Cercopithecoides indet</i>	Radius	Shaft	R	Small	Adult
SWP 4220	X36	3'2"-4'9"	<i>Cercopithecoides indet</i>	Femur	Head	R	Medium	Adult
SWP 4221	X36	3'2"-4'9"	<i>Cercopithecoides indet</i>	Femur	Head	?	Medium	Adult
SWP 4222	X36	3'2"-4'9"	<i>Cercopithecoides indet</i>	Femur	Distal shaft	?	Medium	Adult
SWP 4223	X36	3'2"-4'9"	<i>Cercopithecoides indet</i>	Femur	Distal shaft	?	Medium	Adult
SWP 4224	X36	3'2"-4'9"	<i>Cercopithecoides indet</i>	Humerus	Shaft	?	Medium	Adult
SWP 4225	X36	3'2"-4'9"	<i>Cercopithecoides indet</i>	Tibia	Shaft	L	Medium	Adult
SWP 4226	X36	3'2"-4'9"	<i>Cercopithecoides indet</i>	Humerus	Head	?R	Medium	Adult
SWP 4227	X36	3'2"-4'9"	<i>Cercopithecoides indet</i>	Ulna	Shaft	?	Medium	Adult
SWP 4228	X36	3'2"-4'9"	<i>Cercopithecoides indet</i>	Iv metatarsal	Distal fra	L	Medium	Adult
SWP 4229	X36	3'2"-4'9"	<i>Cercopithecoides indet</i>	Iii metatarsal	Distal	L	Medium	Adult
SWP 4230	X36	3'2"-4'9"	<i>Cercopithecoides indet</i>	Metapodial	Shaft	?	Medium	Adult
SWP 4231	W37	4'5"-5'2"	<i>Cercopithecoides indet</i>	Ulna	Proximalshaft	R	Medium	Adult
SWP 4232	W37	4'5"-5'2"	<i>Cercopithecoides indet</i>	Long bone	Shaft	?	Medium	Adult
SWP 4233	W37	4'5"-5'2"	<i>Cercopithecoides indet</i>	Femur	Distal shaft	?	Small	Adult
SWP 4234	W37	4'5"-5'2"	<i>Cercopithecoides indet</i>	Radius	Shaft	?	Medium	Adult
SWP 4235	W37	4'5"-5'2"	<i>Cercopithecoides indet</i>	Ulna	Shaft	?	Medium	Adult
SWP 4236	W37	4'5"-5'2"	<i>Cercopithecoides indet</i>	Ulna	Shaft	?	Medium	Adult

<b>Specimen no</b>	<b>Provenance</b>	<b>Level</b>	<b>Taxon</b>	<b>Element</b>	<b>Portion</b>	<b>Side</b>	<b>Size</b>	<b>Age</b>
SWP 4237	W37	4'5"-5'2"	<i>Cercopithecoidea indet</i>	Long bone	Shaft	?	Medium	Adult
SWP 4238	W37	4'5"-5'2"	<i>Cercopithecoidea indet</i>	Femur	Shaft	?L	Medium	Adult
SWP 4239	W50	23'5"-24'5"	<i>Cercopithecoidea indet</i>	Humerus	Distal	R	Medium	Adult
SWP 4240	W50	25'6"-26'6"	<i>Cercopithecoidea indet</i>	Phalanx	Complete	?	Medium	Adult
SWP 4241	W37	4'5"-5'2"	<i>Cercopithecoidea indet</i>	Femur	Proximal	R	Medium	Adult
SWP 4242	N45	31'10"-32'10"	<i>Cercopithecoidea indet</i>	Ulna	Proximal	L	Medium	Adult
SWP 4243	N45	31'10"-32'10"	<i>Parapapio</i>	Radius	Proximal	R	Medium	Adult
SWP 4244	N45	31'10"-32'10"	<i>Cercopithecoidea indet</i>	Humerus	Distal	L	Medium	Adult
SWP 4245	N45	31'10"-32'10"	<i>Cercopithecoidea indet</i>	Radius	Proximal	R	Small	Adult
SWP 4246	D18	?	<i>Papio</i>	Humerus	Distal	R	Medium	Adult
SWP 4246	D18	?	<i>Parapapio</i>	Humerus	Distal	R	Medium	Adult
SWP 4246	D18	?	<i>Parapapio</i>	Humerus	Distal	L	Medium	Adult

Table A4. Catalogue of specimens derived from StW 53

Specimen no	Provenance	Level	Taxon	Element	Portion	Side	Size	Age
S94-6405	V60	9'5"-10'9"	<i>Cercopithecoides indet</i>	Patella	Complete	R	Medium	Adult
SWP 1163	X53	12'10"-13'2"	<i>Colobinae indet</i>	Femur	Proximal fr	L	Medium	Adult
SWP 1198	V57	10' 3" - 11' 0"	<i>Theropithecus</i>	Radius	proximal	L	Medium	Adult
SWP 1199	V57	10' 3" - 11' 0"	<i>Parapapio</i>	Humerus	Proximal	R	Medium	Adult
SWP 1202	V 60	15'0"-16'0"	<i>Cercopithecoides indet</i>	Rib	?	?	Medium	Adult
SWP 1203	V/W 60	12'8"-14'0"	<i>Papio/Parapapio</i>	Femur	Proximal	L	Medium	Adult
SWP 1204	V/W 60	12'8"-14'0"	<i>Parapapio</i>	radius	proximal	L	Medium	Adult
SWP 1261	W59	7' 6' - 8' 6"	<i>Cercopithecoides indet</i>	Phalanx	Complete	?	Medium	Adult
SWP 1261	W59	7' 6' - 8' 6"	<i>Cercopithecoides indet</i>	Phalanx	Complete	?	Medium	Adult
SWP 1272	W59	8'5"-9'5"	<i>Cercopithecoides indet</i>	Ulna	proximal	R	Medium	Sub-adult
SWP 1278	V59	11'0"-12'0"	<i>Cercopithecoides indet</i>	Humerus	prox	?	Medium	Adult
SWP 1279	V59	9'0"-10'0"	<i>Cercopithecoides indet</i>	Radius	proximal	?	Medium	Adult
SWP 1287	W58	14'11"-15'11"	<i>Parapapio</i>	humerus	Distal		Medium	Adult
SWP 1304	V60	10' 0" - 11' 0"	<i>Cercopithecoides indet</i>	Metatarsal	Complete	L	Medium	Adult
SWP 1306	W59	10'5"-11'5"	<i>Papionina</i>	Radius	Proximal	R	Medium	Adult
SWP 1307	V60	12' 0" - 13' 0"	<i>Cercopithecoides indet</i>	Calcaneus	Complete	L	Medium	Adult
SWP 1308	V60	12' 0" - 13' 0"	<i>Papionina</i>	Radius		L	Small	Juvenile
SWP 2357a,b			<i>Cercopithecoides indet</i>	2 Ulnae		?	Medium	Adult
SWP 2375	V60	13'0"-14'0"	<i>Cercopithecoides indet</i>	Lumbar Vertebra	complete	?	Medium	Adult
SWP 2376	V60	13'0"-14'0"	<i>Cercopithecoides indet</i>	Tibia	shaft	?	Medium	Juvenile
SWP 2377	V60	13'0"-14'0"	<i>Cercopithecoides indet</i>	Tibia	prox	?	Small	Juvenile
SWP 2378	V60	13'0"-14'0"	<i>Cercopithecoides indet</i>	Calcaneus	almost complete	R	Medium	Adult
SWP 2382	V60	13'0"-14'0"	<i>Cercopithecoides indet</i>	Tibia	Prox	r	Medium	juvenile
SWP 2383	V60	13'0"-14'0"	<i>Cercopithecoides indet</i>	Calcaneus	complete	L	Medium	Adult
SWP 2384	V60	13'0"-14'0"	<i>Cercopithecoides indet</i>	Tibia	shaft	?	Medium	Adult
SWP 2385	V60	13'0"-14'0"	<i>Papio</i>	humerus	head	R	Medium	Adult
SWP 2386	V60	13'0"-14'0"	<i>Cercopithecoides indet</i>	Rib	head	?	Medium	Adult
SWP 2387	V60	13'0"-14'0"	<i>Cercopithecoides indet</i>	Metapodial	shaft	?	Medium	juvenile
SWP 2400	V59	10'0"-10'9"	<i>Cercopithecoides indet</i>	Calcaneus	complete	L	Medium	Adult
SWP 2401	V59	10'0"-10'9"	<i>Cercopithecoides indet</i>	Metapodial	distal	?	Medium	Adult
SWP 2537	V60		<i>Papio/Parapapio</i>	humerus	distal		Medium	Adult

Specimen no	Provenance	Level	Taxon	Element	Portion	Side	Size	Age
SWP 2677	V60	14'0"-15'0"	<i>Cercopithecoidea indet</i>	Lumbar Vertebra	complete	?	Medium	adult
SWP 2796	W59	7'5"-8'5"	<i>Cercopithecoidea indet</i>	Ulna	proximal	R	Small	Adult
SWP 2797	W59	9'6"-10'6"	<i>Cercopithecoidea indet</i>	Tibia	distal	R	Medium	Sub-adult
SWP 2798	W59	9'6"-10'6"	<i>Cercopithecoidea indet</i>	Tibia	proximal	R	Medium	Adult
SWP 2800	V60	13'5"-14'5"	<i>Cercopithecoidea indet</i>	Caudal Vertebra	Complete		Medium	Adult
SWP 2801	V60	13'5"-14'5"	<i>Cercopithecoidea indet</i>	Rib	Shaft	R	Medium	Adult
SWP 2802	V60	13'5"-14'5"	<i>Cercopithecoidea indet</i>	Rib	Shaft	?	Medium	Adult
SWP 2676	V60	17'0"-17'5"	<i>Cercopithecoidea indet</i>	ulna	shaft	?	Small	Adult

Table A5. Catalogue of specimens derived from the Oldowan Infill

Specimen no	Provenance	Level	Taxon	Element	Portion	Side	Size	Age
BP/3/18380	S54	25'7"-26'7"	<i>Cercopithecoides indet</i>	Rib	prox	L	Medium	Adult
BP/3/18382	S54	25'7"-26'7"	<i>Papio/Parapapio</i>	Humerus	distal	L	Medium	Adult
BP/3/23015	P54	32'10" - 34'10"	<i>Cercopithecoides indet</i>	Fibula	Shaft	?	Medium	Adult
S94-13415	Q51	31'4"-32'4"	<i>Cercopithecoides indet</i>	Tibia	Proximal	R	Medium	Adult
S94-13416	Q51	31'4"-32'4"	<i>Cercopithecoides indet</i>	Tibia	Shaft	R	Medium	Adult
S94-2420	Q56	29'2"-30'2"	<i>Cercopithecoides indet</i>	Vertebrae	Axis		Medium	Adult
S94-2924	Q55	26'7"-27'7"	<i>Cercopithecoides indet</i>	Scapula	Fragment	R	Medium	Adult
S94-3142	Q51	30'4"-31'4"	<i>Cercopithecoides indet</i>	Rib	Head	R	Medium	Adult
S94-3143	Q51	30'4"-31'4"	<i>Cercopithecoides indet</i>	Rib	head	R	Medium	Adult
S94-3144	Q51	30'4"-31'4"	<i>Cercopithecoides indet</i>	Rib	head	L	Medium	Adult
S94-3145	Q51	30'4"-31'4"	<i>Cercopithecoides indet</i>	Rib	head	R	Medium	Adult
S94-3146	Q51	30'4"-31'4"	<i>Cercopithecoides indet</i>	Rib	Shaft	R	Medium	Adult
S94-3147	Q51	30'4"-31'4"	<i>Cercopithecoides indet</i>	Rib	shaft	R	Medium	Adult
S94-3149	Q51	30'4"-31'4"	<i>Cercopithecoides indet</i>	Caudal Vertebra	complete		Medium	Adult
S94-3276	Q51	29'4"-30'4"	<i>Cercopithecoides indet</i>	Rib	Shaft	?	Medium	Adult
S94-3277	Q51	29'4"-30'4"	<i>Cercopithecoides indet</i>	Rib	Shaft	?	Medium	Adult
S94-3278	Q51	29'4"-30'4"	<i>Cercopithecoides indet</i>	RIB	body		Medium	Adult
S94-3279	Q51	29'4"-30'4"	<i>Cercopithecoides indet</i>	Rib	body	?	Medium	Adult
S94-3281	Q51	29'4"-30'4"	<i>Cercopithecoides indet</i>	Rib	Shaft	?	Medium	Adult
S94-3282	Q51	29'4"-30'4"	<i>Cercopithecoides indet</i>	Rib	prox		Medium	Adult
S94-3283	Q51	29'4"-30'4"	<i>Cercopithecoides indet</i>	thoracic Vertebra	Fragment		Medium	Adult
S94-3284	Q51	29'4"-30'4"	<i>Cercopithecoides indet</i>	thoracic Vertebra	Fragment		Medium	Adult
S94-6263	R51	28'8"-29'8"	<i>Cercopithecoides indet</i>	Rib	Neck	L	Medium	Adult
S94-6264	R51	28'8"-29'8"	<i>Cercopithecoides indet</i>	Rib	shaft	?	Medium	Adult
S94-6266	R51	28'8"-29'8"	<i>Cercopithecoides indet</i>	thoracic Vertebra	Fragment		Medium	Adult
S94-6267	R51	28'8"-29'8"	<i>Cercopithecoides indet</i>	Lumbar Vertebra	Complete		Medium	Adult
S94-6268	R51	28'8"-29'8"	<i>Cercopithecoides indet</i>	thoracic Vertebra	body		Medium	Adult



Specimen no	Provenance	Level	Taxon	Element	Portion	Side	Size	Age
S94-6269	R51	28'8"-29'8"	<i>Cercopithecoides indet</i>	Lumbar Vertebra	body		Medium	Adult
S94-6289	R51	27'8"-28'8"	<i>Cercopithecoides indet</i>	Rib	Neck	R	Medium	Adult
S94-6290	R51	27'8"-28'8"	<i>Cercopithecoides indet</i>	Rib	Shaft	?	Medium	Adult
S94-6291	R51	27'8"-28'8"	<i>Cercopithecoides indet</i>	Caudal Vertebra	Body		Medium	Adult
S94-6292	R51	27'8"-28'8"	<i>Cercopithecoides indet</i>	thoracic Vertebra	body		Medium	Adult
S94-6307	R51	26'8"-27'8"	<i>Cercopithecoides indet</i>	thoracic Vertebra	Body		Medium	Adult
S94-6309	R51	26'8"-27'8"	<i>Cercopithecoides indet</i>	thoracic Vertebra	Body		Medium	Adult
S94-6310	R51	26'8"-27'8"	<i>Cercopithecoides indet</i>	Rib	shaft	R	Medium	Adult
S94-6341	R51	29'4"-30'4"	<i>Cercopithecoides indet</i>	thoracic Vertebra	Complete		Medium	Adult
S94-6342	R51	29'4"-30'4"	<i>Cercopithecoides indet</i>	thoracic Vertebra	Fragment		Medium	Adult
S95-6344	R51	29'4"-30'4"	<i>Cercopithecoides indet</i>	Rib	head	R	Medium	Adult
S95-6354	R51	30'8"-31'8"	<i>Cercopithecoides indet</i>	Rib	shaft	?	Medium	Adult
S95-6355	R51	30'8"-31'8"	<i>Cercopithecoides indet</i>	Rib	shaft	?	Medium	Adult
SWP 1120	R56	10' 9" - 11' 9"	<i>Papio</i>	Humerus	Distal	R	Medium	Adult
SWP 1154	U58	11' 0" - 12' 0"	<i>Papionina</i>	Humerus	Proximal fr	L	Medium	Adult
SWP 1167	R55	15' 1" - 16' 1"	<i>Cercopithecoides indet</i>	Tibia	Distal	R	Small	Adult
SWP 2109	Q57	25'8"-26'8"	<i>Cercopithecoides indet</i>	Pelvis	ilium	R	Medium	Adult
SWP 2144	O58	21'11"-22'11"	<i>Cercopithecoides indet</i>	humerus	Shaft	R	Medium	Adult
SWP 2177	P54	26'1" - 27'1"	<i>Papio/Parapapio</i>	Radius	proximal	r	Medium	Adult
SWP 2184	P54	32'10" - 34'10"	<i>Cercopithecoides indet</i>	Ulna	Olecranon	L	Medium	Adult
SWP 2185	P53	24'6"-25'6"	<i>Cercopithecoides indet</i>	Calcaneus	complete	L	Medium	Adult
SWP 2193	Q56	28'2"-29'2"	<i>Cercopithecoides indet</i>	Ulna	Proximal	R	Medium	Adult
SWP 2194	Q51	28'4"-29'4"	<i>Cercopithecoides indet</i>	Ulna	prox	R	Medium	Adult
SWP 2195	Q51	28'4"-29'4"	<i>Cercopithecoides indet</i>	thoracic Vertebra	body	?	Medium	Adult
SWP 2196	Q51	28'4"-29'4"	<i>Cercopithecoides indet</i>	Caudal	body	?	Medium	Adult

				Vertebra				
Specimen no	Provenance	Level	Taxon	Element	Portion	Size	Size	Age
SWP 2197	Q51	28'4"-29'4"	<i>Cercopithecoides indet</i>	1st phalanx	complete	?	Medium	Adult
SWP 2199	Q57	25'8"-26'8"	<i>Cercopithecoides indet</i>	Pelvis	ilium	R	Medium	Adult
SWP 2200	Q56	23'2"-24'2"	<i>Papio</i>	Radius	proximal	R	Medium	Adult
SWP 2203	s55	24'8"-25'8"	<i>Cercopithecoides indet</i>	2nd metacarpal	proximal	L	Medium	Adult
SWP 2294	R53	26'2"-27'2"	<i>Cercopithecoides indet</i>	1st phalanx	complete	?	Medium	Adult
SWP 2295	R53	26'2"-27'2"	<i>Cercopithecoides indet</i>	Second Phalanx	proximal	?	Medium	Adult
SWP 2296	S54	22'7"-23'7"	<i>Papio/Parapapio</i>	Ulna	proximal	R	Medium	Adult
SWP 2297	S55	25'8"-26'8"	<i>Cercopithecoides indet</i>	Calcaneus	Complete	R	Medium	Adult
SWP 2302	R55	32'4" - 33'4"	<i>Cercopithecoides indet</i>	3rd Metacarpal	complete	R	Medium	Adult
SWP 2409	Q51	30'4" 31'4"	<i>Cercopithecoides indet</i>	3rd metatarsal	distal	R	Medium	Juvenile
SWP 2423	Q56	32'2" - 33'2"	<i>Cercopithecoides indet</i>	1st phalanx	complete	?	Medium	Adult
SWP 2426	Q54	25'0"-26'0"	<i>Cercopithecoides indet</i>	Calcaneus	complete	L	Medium	Adult
SWP 2437	R55	25'4"-26'4"	<i>Cercopithecoides indet</i>	2nd metacarpal	complete	R	Medium	Adult
SWP 2438	Q55	31'4" 32'4"	<i>Cercopithecoides indet</i>	Ulna	Distal	L	Medium	Adult
SWP 2439	Q55	34'4" 35'4"	<i>Cercopithecoides indet</i>	fifth metacarpal	proximal	R	Medium	Adult
SWP 2442	R55	19'4"-20'4"	<i>Cercopithecoides indet</i>	1st phalanx	complete	L	Medium	Adult
SWP 2445	Q54	28'0"-29'0"	<i>Cercopithecoides indet</i>	Talus	Fragment	L	Medium	Adult
SWP 2458	Q50	28'11"-29'11"	<i>Cercopithecoides indet</i>	Cerv Vertebra	Fragment		Medium	Adult
SWP 2459	Q50	28'11"-29'11"	<i>Cercopithecoides indet</i>	Caudal Vertebra	Complete		Medium	Adult
SWP 2467	Q50	27'11"-28'11"	<i>Cercopithecoides indet</i>	Cerv Vertebra	body		Medium	Adult
SWP 2469	Q51	30'4"-31'4"	<i>Cercopithecoides indet</i>	Fourth metacarpal	Complete	r	Medium	Adult
SWP 2470	R51	27'8"-28'8"	<i>Cercopithecoides indet</i>	1st phalanx	Proximal	?	Medium	Adult
SWP 2473	R51	29'8"-30'8"	<i>Cercopithecoides indet</i>	Femur	Med condyle	R	Medium	Adult
Specimen no	Provenance	Level	Taxon	Element	Portion	Size	Size	Age
SWP 2474	R51	29'8"-30'8"	<i>Cercopithecoides indet</i>	Tibia	Distal	L	Medium	Adult

SWP 2475	R51	28'8"-29'8"	<i>Cercopithecoides indet</i>	Hamate	complete	L	Medium	Adult
SWP 2475	R51	28'8"-29'8"	<i>Cercopithecoides indet</i>	2nd metacarpal	Proximal and shaft	R	Medium	Juvenile
SWP 2476	R51	28'8"-29'8"	<i>Cercopithecoides indet</i>	Hamate	complete	R	Medium	Adult
SWP 2477	R51	28'8"-29'8"	<i>Cercopithecoides indet</i>	Talus	complete	L	Small	Adult
SWP 2478	R51	30'8"-31'8"	<i>Cercopithecoides indet</i>	thoracic Vertebra	body		Medium	Adult
SWP 2479	R51	30'8"-31'8"	<i>Cercopithecoides indet</i>	thoracic Vertebra	Fragment		Medium	Adult
SWP 2480	R51	30'8"-31'8"	<i>Cercopithecoides indet</i>	thoracic Vertebra	Fragment		Medium	Adult
SWP 2481	R51	30'8"-31'8"	<i>Cercopithecoides indet</i>	5th metatarsal	Proximal and shaft	R	Medium	Juvenile
SWP 2482	R51	30'8"-31'8"	<i>Cercopithecoides indet</i>	thoracic Vertebra	Fragment		Medium	Adult
SWP 2483	R51	30'8"-31'8"	<i>Cercopithecoides indet</i>	thoracic Vertebra	Fragment		Medium	Adult
SWP 2573	P53	31'6"-32'6"	<i>Cercopithecoides indet</i>	Humerus	distal	L	Medium	Adult
SWP 2779	S51	26'11"-27'11"	<i>Cercopithecoides indet</i>	4th metacarpal	proximal	R	Large	Adult
SWP 2784	R56	25'4"-26'4"	<i>Cercopithecoides indet</i>	Femur	shaft	R	Medium	Adult
SWP 2785	R56	24'4"-25'4"	<i>Cercopithecoides indet</i>	Calcaneus	distal art	L	Medium	Adult
SWP 2786	R56	24'4"-25'4"	<i>Cercopithecoides indet</i>	proximal phalange	complete	r	Medium	Adult
SWP 2788	R57	22'4"-23'4"	<i>Papio</i>	Ulna	Olecranon	R	Medium	Adult
SWP 2792	S53	22'7"-23'7"	<i>Papio/Parapapio</i>	humerus	proximal	R	Medium	Adult
SWP 6267	R51	28'8"-29'8"	<i>Cercopithecoides indet</i>	Vertebrae	Lumbar		Medium	Adult
SWP 6269	R51	28'8"-29'8"	<i>Cercopithecoides indet</i>	Lumbar Vertebra	body		Medium	Adult

Table A6. Catalogue of specimens derived from the Member 5 West

Specimen no	Provenance	Level	Taxon	Element	Portion	Size	Size	Age
S94-10778	S63	10'1-11'1'	<i>Cercopithecoidea indet</i>	Femur	Shaft		Medium	Adult
S94-10798	S63	10' 1" - 11' 1"	<i>Cercopithecoidea indet</i>	Humerus	Complete	L	Medium	Adult
S94-8291	O62	17'9" - 18'9"	<i>Cercopithecoidea indet</i>	Calcaneus	Fragment		Medium	Adult
SWP 1119	Q59	14'0"-15'0"	<i>Parapapio</i>	Humerus	Distal	?	Medium	Adult
SWP 1154	U58	11' 0" - 12' 0"	<i>Papionina</i>	Femur	Proximal fr	L	Medium	Adult
SWP 1177	O62	15' 9" - 16' 9"	<i>Cercopithecoidea indet</i>	Tibia	Proximal	?	Medium	Adult
SWP 1282	U60	12' 5" - 13' 5"	<i>Cercopithecoidea indet</i>	Phalanx	Complete	?	Medium	Adult
SWP 1284	U60	9' 5" - 10' 5"	<i>Cercopithecoidea indet</i>	Talus	Complete	L	Small	Adult
SWP 2140	Q61	15'5"-16'5"	<i>Cercopithecoidea indet</i>	Sternum	Body		Medium	Adult
SWP 2141	Q61	15'5"-16'5"	<i>Cercopithecoidea indet</i>	Sternum	Body		Medium	Adult
SWP 2669	N64	12'8"-13'8"	<i>Cercopithecoidea indet</i>	Caudal Vertebra	Complete		Medium	Adult
SWP 2680	N64	12'8"-13'8"	<i>Cercopithecoidea indet</i>	Ulna	Olecranon	R	Medium	Adult
SWP 2741	O62	17'9" - 18'9"	<i>Cercopithecoidea indet</i>	Calcaneus	Fragment	L	Medium	Adult
SWP 2742	R61	15'4"-16'10"	<i>Cercopithecoidea indet</i>	Calcaneus	Distal	L	Medium	Adult
SWP 2800	U60	13'5"-14'5"	<i>Cercopithecoidea indet</i>	Caudal Vertebra	Complete		Medium	Adult
SWP 2805	U60	12'5"-13'5"	<i>Cercopithecoidea indet</i>	Talus	Art facet	L	Small	Adult
SWP 1014	D11		<i>Cercopithecoidea indet</i>	Tibia	Distal	?	Medium	Adult

Table A7. Catalogue of specimens derived from the Member 6 and Post member 6

Specimen no	Provenance	Level	Taxon	Element	Portion	Side	Size	Age
BP/3/19236	P59	8'1" - 9'1"	<i>Cercopithecoides indet</i>	Tibia		L	Medium	Juvenile
BP/3/31470	L63	15'6" - 16'6"	<i>Cercopithecus sp</i>	Humerus	Distal	L	Small	Adult
BP/3/32426	J62	19'10" - 20'10"	<i>Cercopithecoides indet</i>	Cervical Vertebra	Fragment		Medium	Adult
BP/3/32871	N59	21'0" - 22'0"	<i>Cercopithecoides indet</i>	Tibia	Shaft	R	Medium	Adult
BP/3/33082	N59	21'0" - 22'0"	<i>Cercopithecoides indet</i>	Tibia	Shaft	R	Medium	Adult
BP/3/33411	L62	14'5" - 15'5"	<i>Cercopithecoides indet</i>	Thoracic Vertebra	Complete		Medium	Adult
BP/3/33457	M60	15'2" - 16'2"	<i>Cercopithecoides indet</i>	Pelvis	Ilium	R	Medium	Adult
BP/3/33537	H62	21'10" - 22'10"	<i>Cercopithecoides indet</i>	Ulna	Shaft	L	Medium	Adult
BP/3/33605	L62	14'5" - 15'5"	<i>Cercopithecoides indet</i>	Ulna	Shaft		Medium	Adult
S94-10064	N60	13'9" - 14'9"	<i>Papio</i>	Humerus	Proximal	R	Small	Juvenile
S94-7694	M61	12'8" - 13'8"	<i>Cercopithecoides indet</i>	Calcaneus	Fragment	L	Medium	Adult
SE 2046			<i>Cercopithecoides indet</i>	Humerus	Shaft	R	Medium	Adult
SE 731			<i>Cercopithecoides indet</i>	1st Phalanx	Complete	L	Medium	Adult
SWP 1111	P60	16'4"-16'6"	<i>Cercopithecus sp</i>	Humerus	Distal	L	Small	Adult
SWP 1112	O61	15'8"-16'8"	<i>Cercopithecus sp</i>	Ulna	Proximal	R	Small	Adult
SWP 1212	O59	13' 6" - 14' 6"	<i>Cercopithecoides indet</i>	Tibia	Shaft	?	Large	Adult
SWP 1258	O63	13'0"-14'0"	<i>Cercopithecoides</i>	Ulna	Proximal	R	Medium	Adult
SWP 1281	Q58	14' 6" - 15' 3"	<i>Cercopithecoides indet</i>	Humerus	Distal shaft	R	Medium	Adult
SWP 1285	O61	16'8"-17'8"	<i>Cercopithecus sp</i>	Ulna	Proximal	L	Small	Adult
SWP 2140	Q61	15'5"-16'5"	<i>Cercopithecoides indet</i>	Sternum	Body		Medium	Adult
SWP 2141	Q61	15'5"-16'5"	<i>Cercopithecoides indet</i>	Sternum	Body		Medium	Adult
SWP 2149	O61	18'8"- 19'1"	<i>Cercopithecoides indet</i>	Talus	Complete	L	Medium	Adult
SWP 4054	O61	18'8" - 19' 1"	<i>Cercopithecoides indet</i>	Scapula	Glenoid cavity and acromion		Medium	Adult
SWP 4131	O61	18'8"19'1"	<i>Cercopithecoides indet</i>	Scapula	Glenoid cavity	?	Medium	Adult

## APPENDIX B

### TABLES B1-B20. QUANTITATIVE ANALYSIS OF COMPARATIVE SAMPLES FROM THE UNIVERSITY OF THE WITWATERSRAND AND THE DITSONG MUSEUM OF NATURAL HISTORY

Table B1. Measurements derived from *Papio* sp humerus

SPECIMEN NO	Za1227	Za1226	Za 1228	BP1/C 541	Za 1360	Za 1299	Za 740	Za 1232	Za 1357	Za 1231
Length(maximum dist from the most proximal point on the head to the most distal point)	195	181	194	210	205	242	182	186	182	184
Proximal medio-lateral dimension	29.9	27.6	32.9	27.1	27.5	34	31	28	25	27
Bi-epicondylar breadth	35.5	33.89	34.9	33.2	32	44	33	37.1	31	32
Greater tuberosity diameter	18.4	15.02	15.8	19.8	17.9	22	17	16.1	15	15
Medial trochlear flange length	16.9	17	17.26	16.9	18.9	23	16	18.9	16	17
Lateral epicondyle to medial edge of trochlea	34.9	29.3	33.9	30	31	36	30	32	28	28
Distal articular breadth	24.1	24.89	26.26	23.4	26.1	30	29	24.1	24	23.4
Proximal distal height of capitulum	14.9	14.5	13,69	14.4	16	18	14	16	14	14
Humeral head diameter.	22	12.69	21	18	24	26	21	24.5	24	22.2



Anterior-posterior length of humeral head	26	24.2	24.02	24.8	28	31	24	23	23	24.5
Maximum medio-lateral length of olecranon fossa	13.4	13.07	13.771	15	12.1	26.2	14	13	13	
Maximum proximo-distal length of olecranon fossa	11	10.32	10.44	9.8	10.5	19	9		13	14.9
Angle of medial epicondyle relative to axis of distal articular surface	35	30	40	40	40	40	35	40	40	40

Table B2. Measurements derived from *Papio* sp ulna

<b>SPECIMEN NO</b>	<b>ZA 1227</b>	<b>Za 1226</b>	<b>Za 1228</b>	<b>Za 1299</b>	<b>Za 740</b>	<b>Za 1357</b>	<b>Za 1232</b>	<b>Za 1231</b>
Ulna length	215	198	218	293	205	207	210	219
Antero-posterior length of olecranon process	24.9	24.04	25.67	34	26	24	25	22
Proximo distal height of olecranon process	14.1	11.03	16.15	7.9	12	10	16	9
Medio-lateral breadth of olecranon process	12.5	13.61	11.76	15	13	12	14	11
Proximo distal height of trochlear notch	16.6	18.9	18.11	19.9	17	16.5	15	14.2
Anterior posterior length of distal end	13.7	12.9	13.76	19.5	12	11	12	12
Medio-lateral breadth of distal end	9.6	8.43	9.64	12.1	14	14.5	19	12.3
Proximo distal height of styloid process	4.9	10.1	7.05	7	7	7.8	7	6.9

Table B3.Measurements derived from *Papio* sp radius

SPECIMEN NO	Za 1227	Za 1226	Za 1228	BPI/C 541	Za 1360	Za 740	Za 1357	Za 1232	Za 1231
Radial length	196	180	199		224	189		186	188
Maximum diameter of radial head	17.7	16.5	17.44	16	18	17.2	14.2	16	14.9
Perpendicular breadth of radial head	16.8	15.83	16.36	14.9	16	14.9	9.5	15	16.2
Proximo distal height of radial neck	6.9	7.05	6.51	4.9	6	8	6.2	6	7
Proximo distal height of radial neck and head	12.4	13.99	15.41	12	13.1	13.1	12	12	12
Anterior posterior width of radius neck	10	9	9.3		9.6	9.9	14	7.8	9.1
Medio-lateral breadth of radius neck	11.1	10.9	11.9		12	12	12.5	11.9	11

Table B4. Measurements derived from *Papio* sp tibia

SPECIMEN NO	ZA 1227	ZA 1226	Za 228	Za 1360	Za 1299	Za 740	Za 1357	Za 1232	Za 1231
Tibia length		176	193	208	241	180	181	188	182
Proximal-distal length of proximal tibia condyle	22.11	27.18	25.6	9	13	10.1	9	12.8	122
Medio-lateral breadth of lateral facet	18.5	16.2	16.85	16	18.2	19	9	17	16.2
Proximal distal breath of lateral facet	6.54	9.29	8.15	6	9	7	6	8.5	9.2
Medio-lateral breadth of medial facet	16.22	15.67	14.98	15.1	19	17	9	15.3	15
Proximo-distal breadth of medial facet	6.73	7.77	9.01	9	12	8	6	7	9.2
Maximum medio lateral length of distal tibia	23.4	21.3	22.15	21.9	27	22	18	22	21
Maximum proximo distal length of distal tibia (medial malleolus projection)	10.16	9.98	10.65	10.5	13	9.2	10	9.8	14

Table B5. Measurements derived from *Papio* sp femur

SPECIMEN NO	BPI/C 541	ZA 1227	Za 1226	Za 1228	Za 1360	Za 1299	Za 740	Za 1357	Za 1232	Za1231
Length	235	223	228	219	238	287	210	205	220	214
Anterior-posterior head diameter	21.1	22	21.03	20.19	22	24	25	25	21	20.9
Medio-lateral breadth of femur head	18.6	18	17.9	18.09	19.8	22	17.9	19	18.6	17.5
Proximo-distal height of femur head		20.9	20.1	19.9	22	25	19.3	19	21	21.5
Greater trochanter projection/height	11.6	11	10.1	10.69	13	14	9.8	9.5	12	12
Neck diameter	18.2	15.9	12.96	9.11	17.8	21	15.5	16.2	17	15
Medio-lateral neck	12.1	4	8.04	8.7	11	9.2	5.9	9.5	7	9
Bi-epicondylar breadth/width	33.3	40	33.86	35.21	35.9	42	35	28.5	36	35
Patella surface rim height	22	22	20.35	20.13	19	33	17.5	19	21	21
Femoral length	235	223	228	219	238	287	210	205	220	214
Neck-shaft angle	120	120	125	128	129	120	130	140	145	130
Medial condyle width	12	12	12.72	13.52	18	14	12	11	6.2	11
Lateral condyle width	10	9.9	10.7	11.1	12	12	9	8	9.7	9.8

Table B6. Measurements derived from *Cercopithecus aethiops* humerus

<b>SPECIMEN NO</b>	V33	Za 968	Za 129	Za 1224	Za 864	Za 862
Length(maximum dist from the most proximal point on the head to the most distal point)	135	132	139	129	188	114
Proximal medio-lateral dimension	17.7	18.2	18.1	16.9	15	16.2
Bi-epicondylar breadth	23.06	19.9	22.3	23.1	17	19.4
Greater tuberosity diameter	11.99	10.5	11.8	11.8	9	9.1
Medial trochlear flange length	10.91	10	12.1	10.1	8	10
Lateral epicondyle to medial edge of trochlea	17.89	18.2	18.9	19.4	14.7	16.2
Distal articular breadth	15.31	12.2	12.3	14	11	13.1
Proximal distal height of capitulum	9.4	9	9.1	9	12	7
Humeral head diameter.	13	14.9	12.5	13	12	14
Anterior-posterior length of humeral head	14.55	15.5	15	14.9	13	14
Maximum medio-lateral length of olecranon fossa	11.15	14.2	10.9	10.1	13	14
Maximum proximo-distal length of olecranon fossa	8.53	6.9		7	4.9	6
Angle of medial epicondyle relative to axis of distal articular surface	40	38	40	39	39	35

Table B7. Measurements derived from *Cercopithecus aethiops* ulna

SPECIMEN NO	V33	Za 973	Za 968	Za 1224	Za 864	Za 862
Ulna length	143	136	145	141.4	123	130
Antero-posterior length of olecranon process	13.78	13.52	11.8	9	11.2	12
Proximo distal height of olecranon process	10.82	9.05	6.9	6.1	13	6
Medio-lateral breadth of olecranon process	9.48	7.74	7.9	8	7.9	7.4
Proximo distal height of trochlear notch	10.34	11.82	9	8.9	9.8	7.6
Anterior posterior length of distal end	8.21	8.09	5.1	7	6	3
Medio-lateral breadth of distal end	6.38	6.67	4.9	6	5	4.9
Proximo distal height of styloid process	4.71	4.37	4.36	4.2		4

Table B8. Measurements derived from *Cercopithecus aethiops* radius

SPECIMEN NO	V33	Za 973	BPI/C 294	Za 12s	Za 968	Za 1244	Za 864	Za 862
Radial length	131	122		125	126	131	118	
Maximum diameter of radial head	9.89	10.02	10	8.9	9.1	10	8.5	9.1
Perpendicular breadth of radial head	9.37	8.98	9	8.2	9	8.9	7.8	8
Proximo distal height of radial neck	6.65	4.27	8.5	4.5	6	6.1	6	4
Proximo distal height of radial neck and head	9.08	9.31	13	9.9	8.9	10	8	7.1
Anterior posterior width of radius neck	4	4.6		4.1	4.8	5.2	3.9	3
Medio-lateral breadth of radius neck	6.2	6		6.3	6.9	7	4.9	5



Table B9. Measurements derived from *Cercopithecus aethiops* femur

SPECIMEN NO	BPI/C/295	Za12s	v33	Za 1129	Za 968	Za 1244	Za 864	Za 862
Length		147	160	140	155	163	139	138
Anterior-posterior head diameter	14	12.82	13.23	11.89	13	12.1	10.9	11
Medio-lateral breadth of femur head	12.1	10.72	10.6	10.98	10.9	10.2	8.2	10
Proximo-distal height of femur head	8.2	12	12.9		12	11.1	10.7	11
Greater trochanter projection/height	6.2	4.61	7.97	4.78	6.8	6.3	5.1	4.6
Neck diameter		9.74	7.31	7.88	7.9	8	9.4	3.8
Medio-lateral neck	12.6	7.33	5.71	4.03	5	4	4.9	4
Bi-epicondylar breadth/width		22.38	22.21	19.85	20.5	22	18	20.1
Patella surface rim height	15	14.92	14.76	13.22	11.3	15	9.9	13
Femoral length	150.39	147	160	140	155	163	139	138
Neck-shaft angle	100	112	114	110	110	110	140	145
Medial condyle width	7.5	7.67	8.54	7.11	7	7.1	7.4	5.5
Lateral condyle width	6.9	6.8	7.97	6.42	6	6.2	5	7

Table B10. Measurements derived from *Cercopithecus aethiops* tibia

SPECIMEN NO	V33	Za 973	Za 968	Za 129	Za 1244	Za 864	Za 864
Tibia length	155	145	155	155	154	125	138
Proximal-distal length of proximal tibia condyle	14.88	14.79	6.1	8.1	8	9/6/	13/7.2
Medio-lateral breadth of lateral facet	11.71	10.01	9.8	11	10.1	8.7	9.6
Proximal distal breath of lateral facet	5.74	5.54	6.1	6.9	6	4.9	3.9
Medio-lateral breadth of medial facet	10.05	10.6	9.1	10	9	8.9	9
Proximo-distal breadth of medial facet	6.62	5.92	5.9	4.1	5	6	3
Maximum medio lateral length of distal tibia	15.54	14.62	15	13	15.9	12.9	13
Maximum proximo distal length of distal tibia (medial malleolus projection)	6.37	5.91	6.2	6.1	5.9	5	5

Table B11. Measurements derived from *Colobus* humerus

SPECIMEN NO	A2/981	A2/1437	A2/ 807	A2/155
Length(maximum dist from the most proximal point on the head to the most distal point)	181	174.9	154.9	161
Proximal medio-lateral dimension	26	23.8	20	24.9
Bi-epicondylar breadth	31.9	28.3	26	34.9
Greater tuberosity diameter	12.9	13.1	16.4	15.2
Medial trochlear flange length	12.3	11.2	9.1	11.7
Lateral epicondyle to medial edge of trochlea	26.1	28	21	25
Distal articular breadth	20.5	24.9	17.1	19.6
Proximal distal height of capitulum	10.2	14.9	8	9.9
Humeral head diameter.	18	19.9	15.5	19.8
Anterior-posterior length of humeral head	20.1	18.1	17	21
Maximum medio-lateral length of olecranon fossa	14	14.1	14.2	11
Maximum proximo-distal length of olecranon fossa	11	9.8	8	8
Angle of medial epicondyle relative to axis of distal articular surface	25	23	30	30

Table B12. Measurements derived from *Colobus* ulna

<b>SPECIMEN NO</b>	A2 981	A2 1437	A2/807	A2/155
Ulna length	184.9	182	163	180
Antero-posterior length of olecranon process	15	16	9.1	18
Proximo distal height of olecranon process	16.1	14.9	7.4	12.4
Medio-lateral breadth of olecranon process	11.8	9.5	10.9	10.8
Proximo distal height of trochlear notch	14.1	11.2	12	12
Anterior posterior length of distal end	12.8	6.8	10.1	11.8
Medio-lateral breadth of distal end	7.9	7.2	7.1	9.9
Proximo distal height of styloid process	4.9	6	4	6

Table B13. Measurements derived from *Colobus* radius

SPECIMEN NO	Az/981	Az 1437	Az 807	A2/155
Radial length	166.1	163.3	148	154
Maximum diameter of radial head	16	14.9	7.9	14.4
Perpendicular breadth of radial head	13.4	12	11	11.5
Proximo distal height of radial neck	13.3	6	6.1	6.1
Proximo distal height of radial neck and head	15	7.2	9.4	11
Anterior posterior width of radius neck	6	6.1	8.1	12
Medio-lateral breadth of radius neck	10.2	8.4	4.9	13.9

Table B14. Measurements derived from *Colobus* femur

SPECIMEN NO	A2/981	A2/1437	A2/807	A2/155
Length	234	222	205	212
Anterior-posterior head diameter	17.8	16.9	16	17.5
Medio-lateral breadth of femur head	13.8	13.8	12.8	15.7
Proximo-distal height of femur head	17	15.1	15.8	17
Greater trochanter projection/height	9.1	6.8	6.5	6
Neck diameter	15	14	9	16
Medio-lateral neck	8.9	13.2	6,5	6.5
Bi-epicondylar breadth/width	32.5	30.9	28	31
Patella surface rim height	22.4	20.9	20.1	24
Femoral length	234	222	205	212
Neck-shaft angle	135	140	130	127
Medial condyle width	11.6	10.8	8.1	11
Lateral condyle width	10.6	11	8.1	11

Table B15. Measurements derived from *Colobus* tibia

SPECIMEN NO	Az/1437	Az 981	Az/ 807	A2/155
Tibia length	205	215	187.9	204
Proximal-distal length of proximal tibia condyle	23.9/11.8	21/12.3	22.2	22.3/9.7
Medio-lateral breadth of lateral facet	13.1	14.9	11.4	10.3
Proximal distal breath of lateral facet	8.2	8.2	7.1	9.4
Medio-lateral breadth of medial facet	12	12	11.1	12.1
Proximo-distal breadth of medial facet	8.1	8.1	6.1	12.1
Maximum medio lateral length of distal tibia	16.8	17.9	14	17.8
Maximum proximo distal length of distal tibia (medial malleolus projection)	8	7.8	7	8

Table B16. Measurements derived from *Mandrillus sphinx* humerus

SPECIMEN NO	A2/1971
Length(maximum dist from the most proximal point on the head to the most distal point)	195
Proximal medio-lateral dimension	26.6
Bi-epicondylar breadth	33
Greater tuberosity diameter	13
Medial trochlear flange length	13.2
Lateral epicondyle to medial edge of trochlea	26
Distal articular breadth	22.6
Proximal distal height of capitulum	11
Humeral head diameter.	21
Anterior-posterior length of humeral head	22.6
Maximum medio-lateral length of olecranon fossa	12.3
Maximum proximo-distal length of olecranon fossa	11
Angle of medial epicondyle relative to axis of distal articular surface	40



Table B17. Measurements derived from *Mandrillus sphinx* ulna

SPECIMEN NO	A2/1971	A2/1972
Ulna length	218	5
Antero-posterior length of olecranon process	21.2	21
Proximo distal height of olecranon process	10.3	6
Medio-lateral breadth of olecranon process	11	10.2
Proximo distal height of trochlear notch	13	13
Anterior posterior length of distal end	10	15
Medio-lateral breadth of distal end	13.5	15
Proximo distal height of styloid process	5	

Table B18. Measurements derived from *Mandrillus sphinx* radius

SPECIMEN NO	A2/1971	A2/1972
Radial length	202	197
Maximum diameter of radial head	15.2	15
Perpendicular breadth of radial head	14	13.1
Proximo distal height of radial neck	5.9	7
Proximo distal height of radial neck and head	12	12
Anterior posterior width of radius neck	10	8
Medio-lateral breadth of radius neck	10	10.5

Table B19. Measurements derived from *Mandrillus sphinx* femur

SPECIMEN NO	Az 1972	Az 1971
length	219	210
anterior-posterior head diameter	17.5	17.9
medio-lateral breadth of femur head	14.9	19.9
proximo-distal height of femur head	12.9	17.8
greater trochanter projection/height	6.6	7.4
neck diameter	9	8.7
medio-lateral neck	6	7
Bi-epicondylar breadth/width	31.3	29
patella surface rim height	23	19
femoral length	219	210
neck-shaft angle	135	125
medial condyle width	13	17.5
lateral condyle width	8.2	9.7

Table B20. Measurements derived from *Mandrillus sphinx* tibia

SPECIMEN NO	A2/1972
Tibia length	199
Proximal-distal length of proximal tibia condyle	10.4
Medio-lateral breadth of lateral facet	12.3
Proximal distal breath of lateral facet	13.6
Medio-lateral breadth of medial facet	13.5
Proximo-distal breadth of medial facet	5.5
Maximum medio lateral length of distal tibia	17.5
Maximum proximo distal length of distal tibia (medial malleolus projection)	8.1

**TABLES B21- B53. MEASUREMENTS OF MODERN MONKEY TAXA DERIVED FROM THE PRIMATE  
MORPHOMETRICS ONLINE (PRIMO) DATABASE OF THE NEW YORK CONSORTIUM IN EVOLUTIONARY  
PRIMATOLOGY (NYCEP)**

Table B21. List of abbreviations used in the PRIMO NYCEP database

<b>ABBREVIATION</b>	<b>TRAIT</b>
HLHDCP	Humeral head to capitulum
HLGTCP	Humeral greater tuberosity to capitulum
HHDWAP	Humeral head anterior to posterior
HHDWTR	Medio-lateral length of humeral head
HDTRWX	Width distal humerus
HDTRWA	Width distal humeral articulation
HDTRWT	Width humeral trochlea
HDLENT	Proximodistal length humeral trochlea
HDAPWX	Anterior posterior length of distal humerus
HDTROW	Transverse width of olecranon fossa
HBRFAP	Humerus anterior to posterior at brachioradialis flange
HBRFTR	Medio-lateral breadth of humerus at brachioradialis flange
HBRFLC	Humeral brachioradialis flange to capitulum
HBRFLH	Humeral brachioradialis flange to head
HADCAPW	Humerus anterior to posterior at anteriormost deltoid crest
HADCTRW	Humerus medio-lateral at anteriormost deltoid crest
HADCLHD	Humerus anteriormost deltoid crest to head
HADCLGT	Humerus anteriormost deltoid crest to greater tuberosity
HADCLCP	Humerus anteriormost deltoid crest to capitulum
HDDAAPW	Humerus anterior to posterior at distal end of deltoid articulation
HDDATTRW	Humerus medio-lateral at distal end of deltoid articulation
HDDALCP	Humerus distal end of deltoid articulation to capitulum
HDDALHD	Humerus distal end of deltoid articulation to head
HWMXDEL	Maximum width of humeral deltoid plane
ULCBAS	Ulnar olecranon to head
ULCSTY	Ulnar olecranon to styloid
ULASTY	Ulnar coronoid to styloid
ULPXAB	Ulnar coronoid to anterior proximal trochlear notch
ULPXAC	Ulnar coronoid to olecranon

ULPXBC	Ulnar olecranon to anterior proximal trochlear notch
ULPXDE	Ulnar anterior to posterior thickness in trochlear notch
ULPXDC	Ulnar olecranon to trochlear notch
ULPXAR	Diameter of ulnar radial notch
ULPXFG	"Major axis" of ulnar trochlear articular surface
ULPXFH	Medial length of ulnar trochlear articular surface
ULPXRG	Lateral length of ulnar radio-trochlear articular surface
ULPXRF	Distal width of ulnar radio-trochlear articular surface
ULPXAH	"Minor axis" of ulnar trochlear articular surface
UOLTRW	medio-lateral breadth of ulnar olecranon
UOLAPW	Anterior posterior length of ulnar olecranon
UOLDEP	Depth of ulnar trochlear notch
URADEP	Depth of ulnar radial notch
ULANGL	Proximal ulnar angle
UDSTYH	Length of ulnar styloid process
UDWXAP	anterior to posterior length of ulnar head
UDWXTR	Medio-lateral breadth of ulnar head
RNECKAP	Radial neck anterior to posterior
RNECKML	Medio-lateral breadth of radial neck
RTUBWID	medio-lateral breadth of radial shaft at tuberosity
RSHAFTAP	Anterior to posterior length of radius at midshaft
RSHAFTML	Medio-lateral length of radial midshaft
RLENBAS	Radial head to base
RLENSTY	Radial head to styloid
FHEADAP	Anterior to posterior length of femoral head
FHEADML	Medio-lateral breadth of femoral head
FHEADPD	Proximo-distal length of femoral head
FMAXML	Femoral head to greater trochanter
FAP	Femoral midshaft anterior to posterior
FTR	Femoral midshaft medio-lateral
FLENGTR	Femur greater trochanter to lateral condyle
FLEN	Femur head to medial condyle

FLENFOS	Femur fovea capitis to medial condyle
---------	---------------------------------------



Table B22a and b. Measurements derived from *Colobus* humeri

<i>Taxon</i>	Sexno	Hlhdcp	Hlgtcp	Hhdwap	Hhdwtr	Hdtrwx	Hdtrwa	Hdtrwt	Hdlent	Hdapwx	Hdtrow	Hbrfap	Hbrftr
<i>Colobus guereza occidentalis</i>	1	148.3	148	20.9	20.5	27.3	17.3	10.2	10.5	14.9	11.6	8.9	10.1
<i>Colobus guereza occidentalis</i>	2	146.3	145.2	21.3	20.9	25.8	17.3	9.6	11.6	15.1	12.1	8.1	9.8
<i>Colobus guereza occidentalis</i>	1	158.96	158.6	22.05	23.58	31.55	24	13.78	12.73	16.55	12.66	10.47	11.37
<i>Colobus guereza kikuyuensis</i>	9	138.66	139.42	19.18	19.88	25.16	16.46	7.9	10.79	13.7	10.26	8.38	9.45
<i>Colobus angolensis cottoni</i>	2	142.68	142.47	21.43	21.48	25.51	19.61	11.46	10.22	14.23	11.63	8.64	12.07
<i>Colobus angolensis cottoni</i>	1	161.67	162.26	20.15	19.88	26.34	20.24	12.35	12.14	14.59	12.91	9.49	11.31
<i>Colobus angolensis cottoni</i>	1	152.51	152.16	22.71	22.69	28.77	21.3	12.87	13.29	15.81	11.89	9.77	10.06
<i>"Colobus" freedmani</i>	4	136.8	137.08	19.76	19.86	24.74	15.99	9.18	11.32	13.55	10.26	8.2	9.86

<i>Colobus guereza occidentalis</i>	1	Hbrflc	Hbrflh	Hadcapw	Hadctrw	Hadclhd	Hadclgt	Hadclcp	Hddaapw	Hddatrw	Hddalcp	Hddalhd	Hwmxdel
<i>Colobus guereza occidentalis</i>	2	41.1	105.9	12.1	10.8	43.1	40.2	109.8	11.1	10.7	82.8	67	10.77
<i>Colobus guereza occidentalis</i>	1	39.3	107.5	11.9	12	51.9	49.1	97.3	10.3	10.4	81.5	65.5	9.77
<i>Colobus guereza kikuyuensis</i>	9	54.01	103.12	13.34	13.03	59.07	57.98	104.96	12.01	11.59	86.28	76.42	12.62
<i>Colobus angolensis cottoni</i>	2	51.36	86.87	12.05	10.41	46.16	46.63	91.23	9.03	9.95	71.03	71.68	11.55
<i>Colobus angolensis cottoni</i>	1	40.2	105.05	12.12	12.5	51.02	52.16	93.26	10.91	10.97	82.2	62.73	12.03
<i>Colobus angolensis cottoni</i>	1	49.66	113.87	12.72	11.26	54.38	53.44	108.87	11.23	10.91	87.74	74.5	12.25

<i>"Colobus"</i> <i>freedmani</i>	4	62.03	91.52	12.71	11.38	54.01	52.64	101.5	11.35	10.37	86.26	68.43	12.46
--------------------------------------	---	-------	-------	-------	-------	-------	-------	-------	-------	-------	-------	-------	-------

Table B23a and b. Measurements derived from *Colobus ulnae*

TAXON	ULCBAS	ULCSTY	ULASTY	ULPXAB	ULPXAC	ULPXBC	ULPXDE	ULPXDC	ULPXAR
<i>Colobus guereza occidentalis</i>	163.6	167.9	147.3	11.4	22.2	12.5	9.1	14.9	11.3
<i>Colobus guereza occidentalis</i>	144.9	149.6	128.9	13	22.5	11.2	9.5	13	11.4

TAXON	ULPXFG	ULPXFH	ULPXRG	ULPXRF	ULPXAHA	UOLTRW	UOLAPW	UOLDEP	URADEP	ULANGL
<i>Colobus guereza occidentalis</i>	17.2	15.4	16.2	12.8	14.4	5.2	8.3	6.5	1.4	22
<i>Colobus guereza occidentalis</i>	17.7	15.3	17	14.4	16.1	5.3	8	6.7	2.4	34

Table B24. Measurements derived from *Colobus* radii

TAXON	RNECKAP	RNECKML	RTUBWID	RSHAFTAP	RSHAFTML	RLENBAS	RLENSTY
<i>Colobus guereza occidentalis</i>	5.3	7.5				148.2	152
<i>Colobus guereza occidentalis</i>	5.5	7.4				131.3	136.1

Table B25. Measurements derived from *Colobus* femora

TAXON	FHEADML	FHEADPD	FAP	FTR	FLENGTR	FLEN	FLENFOS
<i>Colobus guereza occidentalis</i>	15.8	15.3	12.6	11.8	202	199	193
<i>Colobus guereza occidentalis</i>	16.2	16	11.3	12.1	188	187	180
<i>Colobus guereza matschiei</i>			12.6	12.3		205	
<i>Colobus guereza matschiei</i>			11.5	11		193.3	
<i>Colobus guereza matschiei</i>			14	13		212.2	
<i>Colobus guereza matschiei</i>			10.5	10.5		173.2	
<i>Colobus guereza matschiei</i>			13.3	12.2		192	
<i>Colobus guereza matschiei</i>			14	12.8		206.8	
<i>Colobus guereza matschiei</i>			12	11.7		199.5	
<i>Colobus guereza matschiei</i>			12.3	11.3		187.8	
<i>Colobus guereza matschiei</i>			13.7	12.2		203	
<i>Colobus guereza matschiei</i>			12.5	11.4		189	
<i>Colobus guereza matschiei</i>			12.3	12.1		184.5	
<i>Colobus guereza matschiei</i>			12.9	12.4		185.2	
<i>Colobus guereza matschiei</i>			13.3	13.1		206.6	
<i>Colobus guereza matschiei</i>			12.1	11.4		190.2	

<i>Colobus guereza matschiei</i>			11.8	11.4		184.2	
<i>Colobus guereza dodingae</i>			12.9	11.8		195.7	
<i>Colobus guereza guereza</i>			13.6	14.3		208.5	
<i>Colobus polykomos</i>			12	11.7		204.1	
<i>Colobus angolensis palliatus</i>			10.5	10.8		192.6	
<i>Colobus angolensis palliatus</i>			13.7	12.3		206.5	
<i>Colobus angolensis palliatus</i>			12.7	12.8		206.5	

Table B26a and b. Measurements derived from *Procolobus humeri*

TAXON	HLGTC P	HHDWA P	HHDWTR	HDTRWX	HDTRWA	HDTRWT	HDLENT	HDAPWX	HDTROW	HBRFAP	HBRFTR
<i>Procolobus badius oustaleti</i>	152.7	152.2	21.7	20.4	28.7	18.3	10.9	10.8	14.2	12.7	8.5
<i>Procolobus badius oustaleti</i>	163.6	162.5	23.9	22.4	19.4	11.4	14.9	12.2	15.1	12.8	9.9
<i>Procolobus badius temmincki</i>	132.13	132.65	18.52	19.55	24.62	19.48	8.93	12.15	13.37	10.37	8.42
<i>Procolobus badius temmincki</i>	141.6	142.6	19.32	19.76	25.52	19.84	10.25	10.93	13.38	10.85	7.94

<i>Procolobus badius oustaleti</i>	HBRFL C	HBRFLH	HADCAP W	HADCTR W	HADCLH D	HADCLG T	HADCLC P	HDDAAP W	HDDATR W	HDDALC P	HDDALH D
<i>Procolobus badius oustaleti</i>	31	122.6	13.7	11	41.7	38.8	116.5	9.9	10.5	92	62.5
<i>Procolobus badius tephrosceles</i>	34	130	14.9	12.5	51.2	48	117.7	11.3	12.4	93.4	72.2
<i>Procolobus badius temmincki</i>	48.62	83.73	12.21	12.09	40.52	40.4	95.97	9.87	10.8	77.98	60.81

Table B27 a and b. Measurements derived from *Procolobus ulnae*

TAXON	ULCBAS	ULCSTY	ULASTY	ULPXAB	ULPXAC	ULPXBC	ULPXDE	ULPXDC	ULPXAR	ULPXFG	ULPXFH
<i>Procolobus badius oustaleti</i>	162	166.5	146.5	12.5	22.1	11.1	8.7	13.4	11.3	18	13.9
<i>Procolobus badius oustaleti</i>	176	181.8	158.1	14.3	24.7	12.9	9	15.9	12.1	20.4	16.3
<i>Procolobus badius temmincki</i>	139.15	143.66	127.55	11.42	19.1	10.09	8.79	10.69	11.24	15.33	12.57
<i>Procolobus badius temmincki</i>	151.11	155.31	134.15	10.7	22.64	14.73	9.84	14.21	10.93	16.96	11.48

TAXON	ULPXRG	ULPXRF	ULPXA	UOLTRW	UOLAPW	UOLDEP	URADEP	ULANGL	UDSTYH	UDWXAP	UDWXTR
<i>Procolobus badius oustaleti</i>	20.1	14.8	15.1	5.6	7.6	7	1.7	30			
<i>Procolobus badius oustaleti</i>	19.6	15.3	16.1	7.2	8.9	7.6	1.7	22			
<i>Procolobus badius temmincki</i>	13.57	12.86	12.78	7.09	8.53	4.95	1.42		8.27	9.99	8.43
<i>Procolobus badius temmincki</i>	13.97	12.32	13.27	7.34	11.37	6.29	1.48		9.3	11.01	8.52



Table B28. Measurements derived from *Procolobus* radii

TAXON	RNECKAP	RNECKML	RTUBWID	RSHAFTAP	RSHAFTML	RLENBAS	RLENSTY
<i>Procolobus badius oustaleti</i>	6.3	8.2				146.2	150.2
<i>Procolobus badius oustaleti</i>	7.3	8.2				156.7	162.5
<i>Procolobus badius oustaleti</i>	7.45	8.65	8.05	6.82	7	156.72	160.92
<i>Procolobus badius tholloni</i>	5.55	6.15	7.19	5.48	6.53	135.49	138.42
<i>Procolobus badius temmincki</i>	5.44	7.92	6.51	5.91	6.78	127.87	132.29
<i>Procolobus badius temmincki</i>	5.31	7.08	8.05	5.68	6.71	136.75	138.15

Table B29. Measurements derived from the *Procolobus* femora

TAXON	FHEADAP	FHEADML	FHEADPD	FMAXML	FAP	FTR	FLENGTR	FLEN	FLENFOS
<i>Procolobus verus</i>					8.8	8.5		154	
<i>Procolobus verus</i>					9.9	8.9		153.1	
<i>Procolobus verus</i>					8.7	8		149.6	
<i>Procolobus badius oustaleti</i>		16.2	15.7		10.2	10.8	189	187	181
<i>Procolobus badius oustaleti</i>		17.7	17.6		12.1	12.5	199	205	200
<i>Procolobus badius tephrosceles</i>					11.3	10.3		175.5	
<i>Procolobus badius tholloni</i>	14.82	11.55	14.12	29.22	9.37	10.18	177.66	176.58	170.29
<i>Procolobus badius temmincki</i>	14.8	11.54	13.11	28.39	10.08	10.34	178.14	177.1	171.29

Table B30. Measurements derived from *Paracolobus humeri*

TAXON	HDTRWX	HDTRWA	HDTRWT	HDLENT	HDAPWX	HDTROW	HBRFAP	HBRFTR	HBRFLC
<i>Paracolobus chemeroni</i>	44.5	32.1	19.7	23	27.8	21	17.2	19.5	92.6
<i>Cf. Paracolobus mutiwa</i>	44	32.3	18.5		20	17			
<i>Paracolobus mutiwa</i>	48.26	32.05	18.31	17.73	22.57	17.88	15.46	18.5	82.5

Table 31. Measurements derived from *Paracolobus* femur

TAXON	FAP	FTR	FLEN
<i>Paracolobus chemeroni</i>	23	20.9	270

Table B32. Measurements derived from *Rhinocolobus* humeri

TAXON	HDTRWX	HDTRWA	HDTRWT	HDLENT	HDAPWX	HDTROW	HBRFAP	HBRFTR	HBRFLC
Cf. <i>Rhinocolobus turkanaensis</i>	51	37	22	23	24.5	20	14	27	55
Cf. <i>Rhinocolobus turkanaensis</i>	53	34.5	22	22					
<i>Rhinocolobus turkanaensis</i>	45.5	31	19.2	19.5	24.5	20.3	14.2	25.1	65

Table B33. Measurements derived from *Cercopithecoides humeri*

Taxon	Hlhdcp	Hlgtcp	Hhdwap	Hhdwtr	Hdtrwx	Hdtrwa	Hdtrwt	Hdlent	Hdapwx	Hdtrow	Hbrfap	Hbrftr
Cf. Cercopithecoides williamsi	215	215.5	32	28	44	31.5	18	21	28	21	15	25
Cercopithecoides meaveae			31.5	29	35.8	23.8	14.2	18.5	19.5	18.8		
Cercopithecoides meaveae					31.3	19.7	11	14.6	17.7	14.5		

	Hbrflc	Hbrflh	Hadcapw	Hadctrw	Hadclhd	Hadclgt	Hadclcp	Hddaapw	Hddatrw	Hddalcp	Hddalhd	Hwmxdel
Cf. Cercopithecoides williamsi	50	164	22	21	71	69	152	18.5	18	109	112.5	22.13

Table B34a and b. Measurements derived from *Cercopithecoides* ulnae

TAXON	ULCBAS	ULCSTY	ULPXAB	ULPXAC	ULPXBC	ULPXDE	ULPXDC	ULPXAR	ULPXFG	ULPXFH
Cf. <i>Cercopithecoides williamsi</i>	208	215	23.5	40	23.5	18.5	24	22	38.5	27.5
<i>Cercopithecoides meaveae</i>			19	32	18	15	16	17.8	27.8	23

TAXON	ULPXRG	ULPXRF	ULPXAHA	UOLTRW	UOLAPW	UOLDEP	URADEP	ULANGL	UDWXAP	UDWXTR
Cf. <i>Cercopithecoides williamsi</i>	28	26.5	25.5	15	21	11.5	4.5	90	17	12.5
<i>Cercopithecoides meaveae</i>	21	21.8	22.3	13	17	9.7	5			

Table B35 a and b. Measurements derived from *Chlorocebus* humeri

Taxon	Hlhdcp	Hlgtcp	Hhdwap	Hhdwtr	Hdtrwx	Hdtrwa	Hdtrwt	Hdlent	Hdapwx	Hdtrow	Hbrfap	Hbrftr
<i>Chlorocebus aethiops pygerythrus</i>	140.5	141.7	21.4	21.6	25.8	16.2	10.4	13.6	16.5	11.9	7.5	10.9
<i>Chlorocebus aethiops pygerythrus</i>	147.3	146	20.8	22	25.6	14.6	7.9	12.4	13.8	11.7	8.4	11.2
<i>Chlorocebus aethiops pygerythrus</i>	117.17	117.55	17.94	17.29	20.63	13.83	7.93	8.93	12.22	9.44	6.81	9.48

	Hbrflc	Hbrflh	Hadcapw	Hadctrw	Hadclhd	Hadclgt	Hadclcp	Hddaapw	Hddatrw	Hddalcp	Hddalhd	Hwmxdel
<i>Chlorocebus aethiops pygerythrus</i>	33.8	107	13.3	13.8	45.6	44.2	101	12.7	10.2	80.5	59.8	11.42
<i>Chlorocebus aethiops pygerythrus</i>	38.7	107.2	13.5	12.3	46.1	42.2	107.1	11.5	10.6	81.4	65.3	11.5
<i>Chlorocebus aethiops pygerythrus</i>	26.91	88.51	9.25	10.26	44.29	43.37	73.68	8.21	10.29	57.15	61.22	8.09



Table B36. Measurements derived from *Chlorocebus* radius

TAXON	RNECKAP	RNECKML	RLENBAS	RLENSTY
<i>Chlorocebus aethiops pygerythrus</i>	5	7.8	130.8	134.7
<i>Chlorocebus aethiops pygerythrus</i>	5.4	7	145.8	144.4

Table B37 a and b. Measurements derived from *Chlorocebus ulnae*

TAXON	ULCBAS	ULCSTY	ULASTY	ULPXAB	ULPXAC	ULPXBC	ULPXDE	ULPXDC	ULPXAR	ULPXFG
<i>Chlorocebus aethiops pygerythrus</i>	145.4	148.8	132.8	11.1	23.3	15.5	10	15	11.6	21.1
<i>Chlorocebus aethiops pygerythrus</i>	161.9	166.2	146.1	12.3	23.4	14.6	9.5	14.4	11.6	18.9

TAXON	ULPXFH	ULPXRG	ULPXRF	ULPXAHA	UOLTRW	UOLAPW	UOLDEP	URADEP	ULANGL
<i>Chlorocebus aethiops pygerythrus</i>	16	17.7	14.8	13.1	5.8	7.1	6.8	2.9	42
<i>Chlorocebus aethiops pygerythrus</i>	14.3	17	15.4	13.7	5.7	8	7	2.2	34

Table 38. Measurements derived from *Chlorocebus* femur

TAXON	FHEADML	FHEADPD	FAP	FTR	FLENGTR	FLEN
<i>Chlorocebus aethiops</i> <i>pygerythrus</i>	14.4	14.3	10.6	11.2	173	168
<i>Chlorocebus aethiops</i> <i>pygerythrus</i>	15.6	15.7	12.3	12	196	188
<i>Chlorocebus aethiops</i> <i>pygerythrus</i>			10.4	10.6		163.8

Table B39. Measurements derived from *Cercopithecus humeri*

<i>Taxon</i>	Hlhdcp	Hlgtcp	Hhdwap	Hhdwtr	Hdtrwx	Hdtrwa	Hdtrwt	Hdlent	Hdapwx	Hdtrow	Hbrfap	Hbrftr
<i>Cercopithecus aethiops</i>	130.56	130.91	19.05	19.04	23.42	16.29	9.31	9.83	13.5	8.94	7.09	10.16
<i>Cercopithecus mitis kandti</i>	113.24	112.69	14.83	16.34	19.22	12.52	6.96	7.48	10.69	7.76	5.25	7.32
<i>Cercopithecus mitis kandti</i>	120.88	120.08	16.54	16.54	20.71	13.39	7.45	8.8	11.23	8.22	5.35	7.78
<i>Cercopithecus mitis stuhlmani</i>	146.84	145.45	18.37	19.29	23.28	13.59	7.14	10.04	12.18	9.04	5.48	7.99
<i>Cercopithecus mitis stuhlmani</i>	119.66	118.8	14.12	14.33	19.71	12.03	5.71	6.95	9.88	6.36	4.16	5.62
<i>Cercopithecus albogularis kolbi</i>	116.63	116.74	16.59	16.82	18.99	12.9	7.76	7.44	11.36	6.56	6.56	8.17
<i>Cercopithecus ascanius katangae</i>	126.92	126.71	19.58	18.78	22.84	15.68	7.83	10.63	13.99	8.67	7.02	10.15
<i>Cercopithecus neglectus (uelensis)</i>	130.18	128.23	18.79	17.13	22.76	15.58	8.92	8.29	10.95	4.96	5.61	9.46
<i>Cercopithecus neglectus (uelensis)</i>	138.02	137.99	20.78	20.63	25.26	16.77	9.99	12.6	15.35	10	7.77	11.21
<i>Cercopithecus diana</i>	110.45	110.62	15.91	15.74	19.29	12	6.52	9.14	11.72	7.07	6.5	7.47
<i>Cercopithecus cephus</i>	123.11	122.3	16.07	17.22	19.96	13.38	8	9.95	11.83	7.98	6.72	8.75

<i>cephus</i>												
<i>Cercopithecus hamlyni</i>	120.06	120.96	17.62	16.61	20.76	14.76	8.54	9.08	12.27	6.32	6.7	9.44
<i>Cercopithecus erythrotis</i>	124.57	125.25	19.11	19.5	25.67	16.28	9.15	9.28	13.01	7.46	7.23	9.87
<i>Cercopithecus pogonias denti</i>	111.05	110.24	13.37	14.58	17.27	11.33	6.27	7.18	9.75	5.93	4.02	6.61
<i>Cercopithecus pogonias denti</i>	113.07	111.67	13.61	13.28	17.71	11.56	5.74	6.28	8.77	4.97	5.65	5.33
<i>Taxon</i>	HBRFL C	HBRFL H	HADCAP W	HADCTR W	HADCL HD	HADCL GT	HADCL CP	HDDAAP W	HDDATR W	HDDAL CP	HDDAL HD	HWMXD EL
<i>Cercopithecus pogonias denti</i>	29.32	75.99	6.13	6.59	36.17	34.02	75.29	5.09	5.36	55.58	55.38	6.43
<i>Cercopithecus aethiops</i>	31.53	100.75	10.89	10.32	44.11	43.49	87.87	8.37	9.87	71.14	62.89	10.07
<i>Cercopithecus mitis kandi</i>	22.73	84.01	7.45	7.65	40.54	38.92	75.3	6.61	7.52	56.89	58.93	8.19
<i>Cercopithecus mitis kandi</i>	30.79	92.65	8.8	8.28	40.57	39.41	80.66	7.1	7.98	64.99	57.12	8.04
<i>Cercopithecus mitis stuhlmani</i>	32.68	108.73	9.16	9.22	49.16	47.86	94.75	6.67	8.03	74.49	68.53	8.61
<i>Cercopithecus mitis stuhlmani</i>	25.44	89.99	7.2	6.74	33.87	31.78	82.82	4.54	5.87	57.25	58.8	6.62
<i>Cercopithecus albogularis kolbi</i>	28.66	90.91	8.53	8.26	39.69	38.51	79.64	7.33	8.75	59.52	61.25	8.72
<i>Cercopithec</i>	35.77	94.2	10.52	11.17	44.79	42.81	83.6	8.16	10.16	67.15	64.8	10.6

<i>us ascanius katangae</i>												
<i>Cercopithecus neglectus (uelensis)</i>	32.18	92.27	9.72	11.13	49.49	46.57	79.88	6.81	8.82	57.42	70.27	12.48
<i>Cercopithecus neglectus (uelensis)</i>	37.6	100.52	12.27	12.18	45.58	44.77	92.75	11.23	11.72	79.21	59.65	11.73
<i>Cercopithecus diana</i>	28.03	81.36	8.36	9.93	39.14	72.6	73.65	7.37	8.74	59.29	56.46	9.65
<i>Cercopithecus cephus cephus</i>	33.09	90.39	9.64	9.27	41.26	39.49	83.88	7.93	8.85	65.27	60.13	8
<i>Cercopithecus hamlyni</i>	35.27	85.38	9.91	10.25	44.76	43.78	75.59	8.64	9.12	56.19	66.66	11.32
<i>Cercopithecus erythrotis</i>	54.04	74.68	10.8	9.02	44.3	42.58	82.73	7.65	10.01	57.88	68.49	10.73
<i>Cercopithecus pogonias denti</i>	26.74	80.21	6.52	6.95	34.4	32.05	74.86	5.36	5.79	54.85	54.14	6.66

Table B40 a and b. Measurements derived from *Cercopithecus ulnae*

TAXON	ULCBAS	ULCSTY	ULASTY	ULPXAB	ULPXAC	ULPXBC	ULPXDE	ULPXDC	ULPXAR	ULPXFG	ULPXFH
<i>Cercopithecus mitis kandti</i>	108.69	112.49	96.78	7.65	16.53	9.28	6.42	10.41	8.16	13.82	10.04
<i>Cercopithecus mitis kandti</i>	117.04	120.82	105.06	7.43	16.77	9.41	6.5	10.62	8.8	14.54	9.55
<i>Cercopithecus mitis stuhlmanni</i>	156.53	162.08	141.83	9.38	20.5	10.76	9.16	13.73	12.18	19.14	14.22
<i>Cercopithecus mitis stuhlmanni</i>	152.83	157.07	136.09	10.84	22.89	12.99	8.66	14.22	10.69	17.84	13.69
<i>Cercopithecus ascanius schmidt</i>	131.9	136.08	119.94	8.47	17.83	9.89	7.45	10.69	9.21	15.12	11.05
<i>Cercopithecus ascanius schmidt</i>	134.76	137.99	121.67	8.81	18.3	10.64	7.4	11.46	8.69	16.65	12.18
<i>Cercopithecus ascanius katangae</i>	120.37	123.84	109.21	9.36	16.44	8.26	6.66	9.59	8.83	14.19	10.85
<i>Cercopithecus diana</i>	119.14	123.14	108.34	9.12	15.96	8.62	7.89	9.28	8.92	14.09	10.39
<i>Cercopithecus cephus cephus</i>	138.33	140.52	123.22	9.08	18.85	10.42	7.41	12.01	8.29	15.22	12.19
<i>Cercopithecus hamlyni</i>	137.1	140.62	125.53	7.24	15.62	8.42	7.48	10.43	9.35	15.13	10.93
<i>Cercopithecus erythrotis</i>	146.07	149.65	131.21	9.24	20.23	12.1	8.96	12.96	10.06	15.76	11.52
<i>Cercopithecus pogonias denti</i>	125.78	128.39	112.48	8.85	16.65	9.9	6.6	10.94	8.45	14.8	11.74
<i>Cercopithecus mona denti</i>	128.34	131.24	115.61	7.61	16.43	9.01	6.45	10.32	7.67	14.2	10.03

TAXON	ULPXRG	ULPXRF	ULPXA	UOLTRW	UOLAPW	UOLDEP	URADEP	ULANGL	UDSTYH	UDWXAP	UDWXTR
<i>Cercopithecus mitis kandti</i>	11.75	9.94	9.4	7.56	7.48	4.5	1.7	36	4.92	6.78	4.67
<i>Cercopithecus mitis kandti</i>	10.69	11.45	9.96	6.97	9.73	5.7	3	34	5.71	6.96	5.05
<i>Cercopithecus mitis stuhlmanni</i>	15.56	14.08	12.86	9.82	11.2	6.7	1.9	31	7.49	9.23	7.38
<i>Cercopithecus mitis stuhlmanni</i>	14.23	13.04	13.17	8.74	10.72	6.3	2	35	6.71	8.99	6.58
<i>Cercopithecus ascanius schmidt</i>	12.09	10.93	11.45	7.88	9.91	4.9	1.7	35	5.25	7.41	5.26
<i>Cercopithecus ascanius schmidt</i>	14.04	10.03	11.3	7.54	9.45	5.2	1.3	34	5.81	7.24	5.44
<i>Cercopithecus ascanius katangae</i>	12.93	10.84	11.26	6.87	8.97	5.1	1.4	37	5.72	7.43	5.59
<i>Cercopithecus diana</i>	12.65	11.38	10.08	7.58	10.28	5.11	2.7	39	5.07	7.26	4.96
<i>Cercopithecus cephus cephus</i>	13.31	11.54	12.01	7.6	10.09	5.3	1.81	39	5.64	7.72	5.48
<i>Cercopithecus hamlyni</i>	11.01	11.88	11.1	7.55	9.73	5.1	2.1	33	5.86	7.69	5.71
<i>Cercopithecus erythrotis</i>	14.81	11.54	10.57	8.91	9.71	4.6	2	34	7.01	8.68	5.73
<i>Cercopithecus pogonias denti</i>	12.67	10.27	11.5	7.31	9.52	4.81	1.4	37	5.74	7.98	5.59
<i>Cercopithecus mona denti</i>	11.37	9.92	11.52	7.02	9.9	4.4	1.3	30	6.05	7.54	5.75

Table B41. Measurements derived from *Cercopithecus* femora

TAXON	FAP	FTR	FLEN
<i>Cercopithecus aethiops pygerythrus</i>	8.6	9.2	141.5
<i>Cercopithecus aethiops pygerythrus</i>	11.4	11.7	171.6
<i>Cercopithecus aethiops pygerythrus</i>	8.9	9.1	151.4
<i>Cercopithecus aethiops pygerythrus</i>	8.6	9.2	137.7
<i>Cercopithecus aethiops pygerythrus</i>	8.9	9.1	137.2
<i>Cercopithecus aethiops pygerythrus</i>	8.9	8.3	126.8
<i>Cercopithecus aethiops pygerythrus</i>	8.8	7.5	139.6
<i>Cercopithecus aethiops pygerythrus</i>	8	7.4	138.1
<i>Cercopithecus aethiops pygerythrus</i>	8.5	8.4	140.7
<i>Cercopithecus aethiops pygerythrus</i>	10.3	11.4	163.6
<i>Cercopithecus mitis</i>	10.1	11.1	172.8
<i>Cercopithecus mitis</i>	11	11	181.2
<i>Cercopithecus mitis</i>	10.8	11	160.8
<i>Cercopithecus mitis</i>	10.1	10.9	167.5
<i>Cercopithecus mitis</i>	9.5	8.4	141.3
<i>Cercopithecus mitis</i>	8.4	8.1	139.4
<i>Cercopithecus mitis</i>	9.7	9.1	149.5
<i>Cercopithecus mitis</i>	12.2	11	182
<i>Cercopithecus mitis</i>	11	12.6	177.8
<i>Cercopithecus mitis</i>	10.6	10.4	172
<i>Cercopithecus mitis</i>	9.1	8.3	138.5
<i>Cercopithecus mitis</i>	9.1	8.2	143.9
<i>Cercopithecus mitis</i>	8.6	8	148
<i>Cercopithecus ascanius</i>	9.6	9.3	155.7
<i>Cercopithecus ascanius</i>	8.3	7.9	128.8
<i>Cercopithecus ascanius</i>	9.3	9	155
<i>Cercopithecus ascanius</i>	9.1	8.6	159.5
<i>Cercopithecus ascanius</i>	9.8	8.5	160.7
<i>Cercopithecus neglectus</i>	9	9.4	137.8



<i>Cercopithecus neglectus</i>	8.7	8.6	132.2
<i>Cercopithecus neglectus</i>	10.6	10.4	156.3
<i>Cercopithecus neglectus</i>	10.9	10.6	160.3
<i>Cercopithecus neglectus</i>	8.8	8.1	124.7
<i>Cercopithecus cephus</i>	7.8	8.1	131.8
<i>Cercopithecus cephus</i>	8.6	8.5	141.5
<i>Cercopithecus cephus</i>	10	9.4	114.9
<i>Cercopithecus cephus</i>	9	8.7	150.2
<i>Cercopithecus cephus</i>	7	7.5	128.5
<i>Cercopithecus cephus</i>	6.6	6.7	118

Table B42. Measurements derived from *Papio* humeri

Taxon	Hlhdcp	Hlgtcp	Hhdwap	Hhdwtr	Hdtrwx	Hdtrwa	Hdtrwt	Hdlent	Hdapwx	Hdtrow	Hbrfap	Hbrftr
<i>Papio hamadryas hamadryas</i>	204	206	31.8	27.1	32.3	23.4	13.1	15.6	23.2	15	12.1	11.5
<i>Papio hamadryas hamadryas</i>	198.56	201.47	32.16	28.65	33.84	24.69	13.54	19.15	22.87	13.76	11.66	12.88
<i>Papio hamadryas kindae</i>	173.48	174.16	25.58	25.12	35.8	22.5	11.78	17.44	22.61	12.12	10.37	11.24
<i>Papio h. Cynocephalus</i>	239.78	242.93	40.94	32.51	43.95	32.11	17.89	22.54	27.6	15.92	14.81	17.19
<i>Papio h. Anubis</i>	192.62	193.84	28.51	26.39	35.07	25.87	14.23	17.06	22.22	14.57	13.07	13.66
<i>Papio h. Anubis</i>	242.8	244.85	38.16	36.81	45.93	30.9	16.26	24.76	27.72	17.62	15.64	15.45
<i>Papio hamadryas anubis ?"neumann i"</i>	238.26	239.47	37.23	34.41	44.91	29.05	15.83	22.67	28	17.85	14.66	16.23
Taxon	Hbrflc	Hbrflh	Hadcapw	Hadctrw	Hadclhd	Hadclgt	Hadclcp	Hddaapw	Hddatrw	Hddalcp	Hddalhd	Hwmxdel
<i>Papio hamadryas hamadryas</i>	73.1	131.3	16.5	12.2	73	71.7	135.6	10.5	14.3	110.9	95.1	14.71
<i>Papio hamadryas hamadryas</i>	66.47	132.06	15.99	13.44	50.32	52.48	149.37	13.12	12.7	100.08	94.58	14.21
<i>Papio hamadryas kindae</i>	57.99	114.05	13.02	10.94	64.56	65.43	111.17	13.44	10.37	91.61	81.54	11.06
<i>Papio h. Cynocephalus</i>	90.68	146.98	23.02	18.03	91.06	93.74	157.2	18.86	15.69	138.67	105.05	21.27

<i>lus</i>												
<i>Papio h. Anubis</i>	62.17	134.55	16.76	15.53	78.31	77.11	122.78	15.58	14.4	100.74	89.53	15.77
papio h. anubis	81.65	160.41	21.64	17.57	75.73	77.66	167.04	18.71	16.71	127.33	116.79	17.72
papio hamadryas anubis ?"neumann i"	71.88	158.5	20.12	14.43	107.62	108.85	135.5	18.98	14.17	119.54	122.67	19.67
TAXON	HLHD CP	HLGT CP	HHDWA P	HHDWT R	HDTRW X	HDTRW A	HDTRW T	HDLENT	HDAPW X	HDTRO W	HBRFAP	HBRFTR
Papio hamadryas ursinus	215.32	217.87	29.51	28.45	34.13	23.18	13.46	17.9	22.17	14.39	12.26	15.42
Papio hamadryas ursinus	194.81	196.26	30	26.15	33.57	24.08	13.28	17.5	20.74	12.17	11.32	11.92
Papio hamadryas ursinus	225	228.16	36.32	32.97	42.54	28.97	16	22.6	25.16	15.25	15.99	16.91
Papio hamadryas ursinus	253.53	257.47	41.14	36.72	46.52	31.12	20.06	21.86	27.75	17.88	14.47	17.23
Cf. Parapapio cf. jonesi					42	29.5	18.4	17.3	23.8	16.1	14.7	21
	HBRFL C	HBRF LH	HADCAP W	HADCTR W	HADCL HD	HADCL GT	HADCL CP	HDDAA PW	HDDAT RW	HDDAL CP	HDDAL HD	HWMXD EL
Papio hamadryas ursinus	64.98	150.16	16.63	13.84	67.2	68.56	151.11	14.22	15	118.91	94.94	15.19
Papio hamadryas ursinus	67.58	126.37	16.91	13.06	67.9	63.38	128.88	15.24	11.98	112.36	84.95	14.13

Papio hamadryas ursinus	75.81	150.64	21.77	17.73	96.47	99.09	129.35	18.5	15.7	118.56	111.52	20.3
Papio hamadryas ursinus	82.07	166.6	21.01	19.64	103.82	104.63	166.31	17.71	16.78	139.77	112.7	18.58
Cf. Parapapio cf. jonesi	52.5											
TAXON	HLHD CP	HLGT CP	HHDWA P	HHDWT R	HDTRW X	HDTRW A	HDTRW T	HDLENT	HDAPW X	HDTRO W	HBRFAP	HBRFTR
Papio hamadryas ursinus	215.32	217.87	29.51	28.45	34.13	23.18	13.46	17.9	22.17	14.39	12.26	15.42
Papio hamadryas ursinus	194.81	196.26	30	26.15	33.57	24.08	13.28	17.5	20.74	12.17	11.32	11.92
Papio hamadryas ursinus	225	228.16	36.32	32.97	42.54	28.97	16	22.6	25.16	15.25	15.99	16.91
Papio hamadryas ursinus	253.53	257.47	41.14	36.72	46.52	31.12	20.06	21.86	27.75	17.88	14.47	17.23
Papio hamadryas ursinus	64.98	150.16	16.63	13.84	67.2	68.56	151.11	14.22	15	118.91	94.94	15.19
Papio hamadryas ursinus	67.58	126.37	16.91	13.06	67.9	63.38	128.88	15.24	11.98	112.36	84.95	14.13
Papio hamadryas ursinus	75.81	150.64	21.77	17.73	96.47	99.09	129.35	18.5	15.7	118.56	111.52	20.3
Papio hamadryas ursinus	82.07	166.6	21.01	19.64	103.82	104.63	166.31	17.71	16.78	139.77	112.7	18.58

Table B43. Measurements derived from *Papio* radii

TAXON	RNECKAP	RNECKML	RTUBWID	RSHAFTAP	RSHAFTML	RLENBAS	RLENSTY
<i>Papio hamadryas hamadryas</i>	6.7	11.4	11.11	6.51	10.89	200	207
<i>Papio hamadryas hamadryas</i>	6.9	10.5				210	217
<i>Papio hamadryas kindae</i>	11.15	7.85	11.46	8.91	6.15	192	197
<i>Papio h. cynocephalus</i>	9.89	13.42	15.1	10.6	12.65	258.79	262.66
<i>Papio hamadryas anubis [heuglini]</i>	8.9	12.18	13.5	9.5	12.65	227	232
<i>Papio hamadryas anubis</i>	9.74	13.66	15.27	9.6	15.19	248	256?
<i>Papio hamadryas anubis</i>	9.29	11.54	12.4	8.54	11.13	194	198
<i>Papio hamadryas ursinus</i>	8.19	10.38	10.45	8.08	10.55	206.82	210.69
<i>Papio hamadryas ursinus</i>	9.77	13.08	13.99	10.21	15.3	228.57	236.01

Table B43 a and b. Measurements derived from *Papio ulnae*

TAXON	ULCBAS	ULCSTY	ULASTY	ULPXAB	ULPXAC	ULPXBC	ULPXDE	ULPXDC	ULPXAR
<i>Papio hamadryas hamadryas</i>	215	221	201	18.7	31.7	17.8	13.2	19.2	16
<i>Papio h. cynocephalus</i>	275.67	282.48	256.26	25.24	41.29	29.38	20.03	28.56	22.7
<i>Papio hamadryas anubis [heuglini]</i>				22	39	25	17.2	24.6	21.5
<i>Papio h. anubis</i>	210.27	216.13	192.7	17.72	31.82	18.35	14.3	19.49	18.31
<i>Papio h. anubis</i>	274.85	284.34	253.74	22.17	44.81	28.91	18.09	28.51	21.67
<i>Papio hamadryas anubis ?"neumanni"</i>	256.38	264.02	237.72	18.29	38.69	24.25	17.73	28.81	21.23
<i>Papio hamadryas ursinus</i>	224.16	230.6	207.5	15.8	29.72	17.14	13.06	19.28	17.64
<i>Papio hamadryas ursinus</i>	250.65	257.48	230.38	18.48	36.97	22.73	18.13	24.46	20.81

TAXON	ULPXF G	ULPXF H	ULPXR G	ULPXR F	ULPXA H	UOLTR W	UOLAP W	UOLDE P	URADE P	UDSTY H	UDWXA P	UDWXT R
<i>Papio hamadryas hamadryas</i>	28.4	22.4	26	20.8	20.2	11	17.2	8.3	5	11.15	12.36	8.56
<i>Papio h. cynocephalus</i>	33.6	28.68	28.01	29.36	21.92	15.56	17.83	10.9	6.1	11.66	16.14	11.83
<i>Papio hamadryas anubis [heuglini]</i>	37.3	27	32.8	26.5	22.6	13.9	19	11.5	4.7			
<i>Papio h. anubis</i>	26.09	21.33	21.9	22.87	19.05	10.57	15.56	8.55	5.5	12.62	10.82	7.93
<i>Papio h. anubis</i>	40.15	26.95	31.84	26.9	25.11	12.78	14.04	12.4	6.4	9.24	15.79	11.86
<i>Papio hamadryas anubis ?"neumanni"</i>	35.63	25.35	29.65	25.24	21.72	12.45	17.36	11.2	6.3	12.03	15.24	10.82
<i>Papio</i>	28.8	21.6	23.93	22.37	18.03	10.84	12.27	8.3	6.73	11.59	12.16	8.91

<i>hamadryas</i> <i>ursinus</i>												
<i>Papio</i> <i>hamadryas</i> <i>ursinus</i>	37.62	26.96	29.6	27.61	22.16	13.68	17.96	12.03	6.07	13.4	15.17	10.71

Table 45. Measurements derived from *Papio* femora

TAXON	FHEADAP	FHEADML	FHEADPD	FMAXML	FAP	FTR	FLENGTR	FLEN	FLENFOS
<i>Papio hamadryas hamadryas</i>	19.77	20.1	20	39.02	12.5	12.9	227	222	213.17
<i>Papio hamadryas hamadryas</i>		20.5	20		14	13.4	218	209	
<i>Papio hamadryas hamadryas</i>					15.3	15.5		242.8	
<i>Papio hamadryas hamadryas</i>					15.6	14.3		215.3	
<i>Papio hamadryas hamadryas</i>					15.8	15.1		227.6	
<i>Papio hamadryas hamadryas</i>					15.2	16.4		243.2	
<i>Papio hamadryas kindae</i>	19.1	16.53	18.34	41.13	10.77	11.09	216	211	200
<i>Papio h. cynocephalus</i>	24.19	23.18	24.08	58.47	16.87	17.74	302	289.5	278.61
<i>Papio hamadryas cynocephalus</i>					16.2	16.3		279.8	
<i>Papio hamadryas cynocephalus</i>					16.3	14.4		248.3	
<i>Papio hamadryas cynocephalus</i>					13.4	12.3		196.4	
<i>Papio hamadryas cynocephalus--Darajani</i>					19.4	18.1		281.2	
<i>Papio hamadryas cynocephalus--Darajani</i>					16.9	16.6		258.1	
<i>Papio hamadryas cynocephalus--Darajani</i>					17.1	16.9		277.2	
<i>Papio hamadryas cynocephalus--Darajani</i>					16	15.5		235	
<i>Papio hamadryas cynocephalus--Darajani</i>					16.3	17.7		251.7	
<i>Papio hamadryas cynocephalus--Darajani</i>					16	15.5		246.5	
<i>Papio hamadryas cynocephalus--Darajani</i>					16.5	16.4		250.7	
<i>Papio hamadryas cynocephalus--Darajani</i>					15.8	16.4		244.6	
<i>Papio hamadryas cynocephalus--Darajani</i>					15.4	16.6		258.3	
<i>Papio hamadryas</i>					15.9	16.8		256.2	



<i>cynocephalus--Darajani</i>									
<i>Papio hamadryas cynocephalus--Darajani</i>					16	15.7		257.3	
<i>Papio hamadryas cynocephalus--Darajani</i>					15.8	16.8		269.8	
<i>Papio hamadryas cynocephalus--Darajani</i>					12.6	12.8		209.2	
<i>Papio hamadryas cynocephalus--Darajani</i>					13.1	12		212.2	
<i>Papio hamadryas cynocephalus--Darajani</i>					13.7	13		200.7	
<i>Papio hamadryas cynocephalus--Darajani</i>					14.1	12.8		217.1	
<i>Papio hamadryas cynocephalus--Darajani</i>					12.9	13		204.8	
<i>Papio hamadryas cynocephalus--Darajani</i>					13	11.9		204.5	
<i>Papio hamadryas cynocephalus--Darajani</i>					13.9	13.2		210	
<i>Papio hamadryas cynocephalus--Darajani</i>					13.8	12.9		223.5	
<i>Papio hamadryas cynocephalus--Darajani</i>					14	13.7		226	
<i>Papio hamadryas cynocephalus--Darajani</i>					13.7	12.9		217	
<i>Papio hamadryas anubis [heuglini]</i>	24.45	20.17	24.47	50.33	15.5	17.43			
<i>Papio hamadryas anubis</i>	25.1	20.83	24.36	56.17	16.47	18.12			
<i>Papio hamadryas anubis</i>	20.1	16.64	20.38	43.44	14.54	13.26	219	215	205
<i>Papio hamadryas anubis "neumanni"</i>					13.5	14.3		198.3	
<i>Papio hamadryas anubis</i>					17.3	17.4		255	
<i>Papio hamadryas anubis</i>					18.6	18.1		254	
<i>Papio hamadryas anubis "neumanni"</i>					15.9	15.3		228.5	

<i>Papio hamadryas anubis</i> <i>"neumanni"</i>					18.2	16.1		246.5	
<i>Papio hamadryas anubis</i> <i>"neumanni"</i>					15.9	15		215.8	
<i>Papio hamadryas anubis</i> <i>"neumanni"''''</i>					16.5	15.7		226.2	
<i>Papio hamadryas anubis</i> <i>"neumanni"</i>					15	13.5		220.3	
<i>Papio hamadryas ursinus</i>					12.7	13.8		208.3	
<i>Papio hamadryas ursinus</i>					13.9	15.6		221	
<i>Papio hamadryas ursinus</i>					16.4	17.2		254	
<i>Papio hamadryas ursinus</i>					16.9	18.1		221	
<i>Papio hamadryas ursinus</i>	19.44	18.06	19.64	40.32	13.02	13.17	227.24	222.02	215.1
<i>Papio hamadryas ursinus</i>	23.55	19.49	23.08	49.66	15.53	17.7	263.41	253.41	242.58

Table B46a and b. Measurements derived from *Mandrillus humeri*

Taxon	Sexno	Hlhdc p	Hlgtcp	Hhdwap	Hhdwtr	Hdtrwx	Hdtrwa	Hdtrwt	Hdlent	Hdapwx	Hdtrow	Hbrfap	Hbrftr
<i>Mandrillus sphinx</i>	2	178.5	178.5	26.1	25.7	31.6	22	13.1	14.2	18.6	12.4	12.5	10
<i>Mandrillus sphinx</i>	1	259	261	38.9	36.2	44.3	28.5	16.1	21.4	27.7	13.1	20.4	15.2
<i>Mandrillus sphinx</i>	1	221.19	220.43	33.88	32.66	40.66	29.24	16.56	20.62	24.13	14.01	15.59	16.86
<i>Mandrillus sphinx</i>	2	174.98	174.2	21.45	23.3	28.26	21.83	12.23	13.48	17.3	10.76	11.6	12.95
<i>Mandrillus sphinx</i>	2	188.07	186.78	27.6	25.45	32.87	23.13	12.6	17.28	20.87	13.09	11.73	13.15
<i>Mandrillus sphinx</i>	1	253.32	250.64	40.92	39.57	49.94	33.44	18.01	25.48	27.58	16.19	16.61	22.78
<i>Mandrillus sphinx</i>	1	288	265.76	39.26	36.2	44	28.3	14.7	22.3	28	14	16.5	21
<i>Mandrillus sphinx</i>	2	184.38	183.96	25.72	24.86	29.05	20.98	10.8	16.26	18.76	12.19	10.8	14.05
<i>Mandrillus sphinx</i>	2	233.78	232.81	33.22	32.68	41.7	29	17.6	21.8	27.5	18	14.14	17.92
<i>Mandrillus cf sphinx</i>	5	240.23	241.23	36.73	36.26	47.19	31.14	14.71	22.21	30.95	16.76	17.87	22.96
<i>Mandrillus ?leucophaeus</i>	1	219.88	221.36	39.71	33.86	43.93	28.41	16.22	19.35	24.98	16.59	14.31	19.54
<i>Mandrillus ?leucophaeus</i>	1	175.66	180.26	29.63	31.63	41.5	26.91	15.15	19.6	23.66	14.14	14.56	16.57
		Hbrflc	Hbrflh	Hadcap w	Hadctrw	Hadclhd	Hadclgt	Hadclcp	Hddaap w	Hddatrw	Hddalcp	Hddalhd	Hwmxdel
<i>Mandrillus</i>	2	57.7	114.5	12.3	12.6	53.3	56.6	111.2	12.2	9.8	89.4	88.9	

<i>sphinx</i>													
<i>Mandrillus sphinx</i>	1	87	177.5	22.4	18.2	85.5	82	181.5	19.5	19.3	135.2	134.5	22.38
<i>Mandrillus sphinx</i>	1	74.39	145.24	21.44	17.67	78.99	80.18	140.15	16.19	15.85	103.75	114.15	17.87
<i>Mandrillus sphinx</i>	2	60.72	118.21	14.15	14.16	70.49	67.48	110.53	11.34	12.6	78.6	98.64	13.39
<i>Mandrillus sphinx</i>	2	66.14	119.75	14.62	13.41	51.91	49.67	138.54	12.02	13.05	91.99	93.66	13.18
<i>Mandrillus sphinx</i>	1	86.8	164.85	26.09	26.51	97.42	97.65	154.23	21.58	22.48	137.09	115.17	26.17
<i>Mandrillus sphinx</i>	1	94.55	172.89	26.55	25.36	87.12	89.38	179.78	19.7	22.9	138.57	132.01	28.33
<i>Mandrillus sphinx</i>	2	64.47	120.26	16.57	14.93	55.36	54.19	128.7	13.08	14.26	106.04	76.03	14.71
<i>Mandrillus sphinx</i>	2	84.16	151.27	22.61	17.51	87.51	86.57	148.01	17.64	15.12	117.29	115.8	19.83
<i>Mandrillus cf sphinx</i>	5	84.84	153.61	29.65	27.35	91.39	94.98	148.18	23.96	21.39	123.67	119.03	23.54
<i>Mandrillus ?leucophaeus</i>	1	68.5	143.03	25.11	18.78	86.33	83.48	146.54	23.81	17.9	127.3	91.79	23.56
<i>Mandrillus ?leucophaeus</i>	1	71.88	106.56	22.05	22.14	66.56	68.87	112.88	19.99	19.82	99.09	83.14	22.03

Table B47. Measurements derived from *Mandrillus* radii

TAXON	RNECKAP	RNECKML	RTUBWID	RSHAFTAP	RSHAFTML	RLENBAS	RLENSTY
<i>Mandrillus sphinx</i>	7	8				179.5	184.3
<i>Mandrillus sphinx</i>	9.5	13.1	10.98	9.96	14.31	265	273
<i>Mandrillus sphinx</i>	7.17	8.49	9.73	7.08	9.21	186.06	190.92
<i>Mandrillus sphinx</i>	8.12	8.89	8.06	7.06	9.3	195.96	200.97
<i>Mandrillus sphinx</i>	11.86	15.18	11.66	11.47	16.74	248.4	255.84
<i>Mandrillus sphinx</i>	11.7	10.99	15.23	10.81	16.46	269.23	274.56
<i>Mandrillus sphinx</i>	8.24	8.63	9.96	6.97	10.5	185.64	188.34
<i>Mandrillus sphinx</i>	10.83	13.41	13.67	9.42	13.97	233.71	237.05
<i>Mandrillus cf sphinx</i>	12.49	16.19	15.71	13.12	18.21	247.31	260.09
<i>Mandrillus ?leucophaeus</i>	11.88	12.81	12.31	10.2	14.62	197.43	201.98

Table B48 a and b. Measurements derived from *Mandrillus ulnae*

TAXON	ULCBAS	ULCSTY	ULASTY	ULPXAB	ULPXAC	ULPXBC	ULPXDE	ULPXDC	ULPXAR	ULPXFG	ULPXFH
<i>Mandrillus sphinx</i>	192	197	182	12.7	22.9	14.7	11.7	13.3	14.7	23.7	17.2
<i>Mandrillus sphinx</i>	286	294	271	17	37.5	25.8	17.8	24.2	20.3	33.6	24.8
<i>Mandrillus sphinx</i>	198.11	203.91	185.72	12.68	23.07	15.19	11.58	15.07	13.71	17.63	16.39
<i>Mandrillus sphinx</i>	206.57	213.07	195.54	14.99	24.97	15.32	12.7	14.88	15.33	24.45	18.75
<i>Mandrillus sphinx</i>	266.34	274.93	247.68	19.76	38.1	26.12	18.68	25.03	23.84	36.37	26.21
<i>Mandrillus sphinx</i>	287.34	294.76	271.64	18.3	34.2	24.4	17.8	20.6	19.2	33.6	23.9
<i>Mandrillus sphinx</i>	197.54	203.53	183.81	15.26	25.64	14.77	11.62	15.61	15.26	25.45	20.77
<i>Mandrillus sphinx</i>				18.8	37.2	23.1	17.6	23.3	20.4	35.6	26.3
<i>Mandrillus sphinx</i>	251.22	252.97	226.99	18.8	37.2	23.1	17.6	23.3	20.4	35.6	26.3
<i>Mandrillus cf sphinx</i>	272.04	279.62	252.2	23.38	39.18	23.69	19.59	26.37	22.88	35.63	27.91
<i>Mandrillus ?leucophaeus</i>	208.76	215.81	191.11	16.7	30.29	20.43	15.05	20.94	18.74	29.91	23.13

TAXON	ULPXRG	ULPXRF	ULPXAH	UOLTRW	UOLAPW	UOLDEP	URADEP	ULANGL	UDSTYH	UDWXAP	UDWXTR
<i>Mandrillus sphinx</i>	22.5	18	15.7	8.2	10.2	6.9	2.7	50	8.6	12	7.3
<i>Mandrillus sphinx</i>	33.2	22.8	20.9	10.2	14.2	10.2	4.2	54	13.01	16.51	11.13
<i>Mandrillus sphinx</i>	18.95	15.78	13.92	8.61	13.46	7.58	3.15		8.79	9.75	7.15
<i>Mandrillus sphinx</i>	18.5	16.89	16.84	9.47	14.35	7.14	2.36		10.35	10.26	8.52
<i>Mandrillus sphinx</i>	29.53	25.96	22.93	15.09	20.35	10.44	6.5		11.2	17.56	11.68
<i>Mandrillus sphinx</i>	32.6	24.3	20.3	15.2	17	10.3	4.7		14.11	17.14	10.89
<i>Mandrillus sphinx</i>	20.29	18	18.49	9.47	12.18	6.77	3.8		9.01	11.35	7.78
<i>Mandrillus sphinx</i>	29.8	27.8	21.4	14.6	21.5	11.5	6.7				
<i>Mandrillus sphinx</i>	29.8	27.8	21.4	14.6	21.5	11.5	6.7		6.39	15.39	9.17
<i>Mandrillus cf sphinx</i>	28.06	27.77	22.56	14.66	16.44	12.84	8.46		8.91	16.21	11.84
<i>Mandrillus ?leucophaeus</i>	24.44	23.49	17.54	12.09	18.26	10.29	6.14		8.04	15.35	12.79

Table B49. Measurements derived from *Mandrillus* femora

TAXON	FHEADAP	FHEADML	FHEADPD	FMAXML	FAP	FTR	FLENGTR	FLEN	FLENFOS
<i>Mandrillus sphinx</i>		18.3	18.2		11.5	11.4	207	201	
<i>Mandrillus sphinx</i>	24.59	25	24.3	56.73	19.2	18.3	297	290	279.75
<i>Mandrillus sphinx</i>	16.59	15.34	16.5	34.23	12.73	13.74	203.41	200.28	193.77
<i>Mandrillus sphinx</i>	18.78	17.39	18.19	35.97					
<i>Mandrillus sphinx</i>	28.12	25.21	27.04	58.57	19.06	19.84	288.51	282.16	269.83
<i>Mandrillus sphinx</i>	25.58	22.39	24.62	55.69	21.81	20.93	299.3	293	281.19
<i>Mandrillus sphinx</i>	17.38	14.31	17.11	35.71	13.52	13.99	208.76	208.27	200.93
<i>Mandrillus sphinx</i>	23.22	19.34	23.05	55.73	17.61	16.33	278.69	270.93	259.83
<i>Mandrillus sphinx</i>					20.2	18.6		288	
<i>Mandrillus cf sphinx</i>	24.86	20.02	23.82	55.16	17.7	20.63	283.18	279.71	267.92
<i>Mandrillus ?leucophaeus</i>	20.92	19.06	20.67	47.87	16.06	16.17	215.93	212.67	202.08

Table B50. Measurements derived from *Theropithecus humeri*

Taxon	Hlhdcp	Hlgtcp	Hhdwap	Hhdwtr	Hdtrwx	Hdtrwa	Hdtrwt	Hdlent	Hdapwx	Hdtrow	Hbrfap	Hbrftr
<i>Theropithecus gelada</i>	166.14	168.03	27.03	24.4	30.99	23.3	12.51	16.08	20	10.9	13.58	12.25
<i>Theropithecus gelada</i>	200	202	32.5	22.84	35	22.9	13.7	16.6	23.2	13.8	12.4	11.4
<i>Theropithecus gelada</i>	201.2	202	32	27.5	34	25	14	17.7	22.5	13	11.5	13
<i>Theropithecus gelada</i>	172	172.5	26	23.5	29.6	20.4	12.2	15.3	18.7	12	10	12
<i>Theropithecus gelada</i>	203.2	205	32	28	35	23.5	14	17.5	23	13	12	14.2
<i>Theropithecus gelada</i>	205.66	205.81	31.86	28.93	36.83	23.08	13.84	18.01	23.05	12.77	12.75	14.51
<i>Theropithecus oswaldi oswaldi</i>						31.65	18.38	18.82	27.05			
<i>Theropithecus oswaldi</i>					46.5	34	22.5	26	29	21		
<i>Theropithecus oswaldi</i>					47	32	20	22	28	18	17	21
<i>Theropithecus oswaldi</i>	264	267.5			54	39	23	26	32	21	19	25
<i>Theropithecus oswaldi cf. leakeyi</i>					52.5	34	21.5	23.5	30	20		
<i>Theropithecus oswaldi cf. darti</i>					29.2	19.7	12.2	14.5	18.3	10.4	11	12.1
<i>Theropithecus oswaldi cf. darti</i>					36	23.5	14	19.5	23	13	12.5	15.5



<i>Theropithecus oswaldi</i> <i>cf. darti</i>					35.2	23.3	13.8	19.5	23	12.7	14	16.2
<i>Theropithecus oswaldi</i> <i>cf. darti</i>					38	26.5	14.5	18	24	15		
<i>Theropithecus oswaldi</i> <i>cf. Darti</i>					35.5	25	16	21	24	16.5	14.8	17
<i>Theropithecus oswaldi</i> <i>cf. darti</i>	166	166	24	24	28.3	19.5	12.5	16.5	18	11	10.5	
<i>Theropithecus oswaldi</i> <i>cf. darti</i>					29.5	21	12.3	17	18			12.5
<i>Theropithecus oswaldi</i> <i>cf. darti</i>					33.7	21.8	12.7	16.8	19			
<i>Theropithecus oswaldi</i> <i>cf. darti</i>					36	26	15.5	19	24	14.5	12.5	16
<i>Cf. Theropithecus brumpti</i>					45.5	30.5	19	26	31	18.5	17.5	23
<i>Cf. Theropithecus brumpti</i>					40	25.5	17	21.5	24.5	17	15.5	20
<i>Theropithecus</i> ( <i>Omopithecus</i> ) <i>brumpti</i>	220.87	219.64	31.11	36.53	46.52	32.53	19.44	17.46	30.95	16.79		
	HBRF LC	HBRF LH	HADCA PW	HADCT RW	HADCL HD	HADCL GT	HADCL CP	HDDAA PW	HDDAT RW	HDDAL CP	HDDAL HD	HWMXD EL
<i>Theropithecus gelada</i>	57.21	108.64	17.03	12.64	43.88	43.34	123.94	14.06	12.47	86.1	80.23	13.06
<i>Theropithecus</i>	62.5	135	15.6	12.1	69.3	66.1	135.1	11.6	13.2	92.3	109.9	13.93

<i>cus gelada</i>												
<i>Theropithecus gelada</i>	61	139	17.5	13	72	69	134	15.5	12	99	107	
<i>Theropithecus gelada</i>	52	118.5	15	11.2	61	59.3	116.5	12.5	10.5	79	94	11.6
<i>Theropithecus gelada</i>	59	142	18	14	67	65	137	14	13	96	108	16.2
<i>Theropithecus gelada</i>	59.71	146.96	17.84	13.76	58.32	56.03	161.77	15.21	13.52	100.26	106.91	16.62
<i>Theropithecus oswaldi oswaldi</i>								20	17.5			
<i>Theropithecus oswaldi cf. leakeyi</i>								26	23			
<i>Theropithecus oswaldi</i>	84.5	179	29	27	102.5	98.5	172	25	25	129.5	140	
<i>Theropithecus oswaldi cf. darti</i>	47.7							13.1	14.9	83.3		
<i>Theropithecus oswaldi cf. darti</i>	56	109	16.2	15	53.5	52	114	13.5	14.5	86	84	16.2
<i>Theropithecus oswaldi cf. darti</i>	56		22	20			138	17.5	17	105		
<i>Cf. Theropithecus brumpti</i>	67		24.5	21			126	21.5	18	95		
<i>Theropithecus (Omopithecus) brumpti</i>			22.47	20.69	74.91	73.47	148.56		25.14	122.29	95.86	20.85

Table B51. Measurements derived from *Theropithecus gelada* radius

TAXON	RNECKAP	RNECKML	RTUBWID	RSHAFTAP	RSHAFTML	RLENBAS	RLENSTY
<i>Theropithecus gelada</i>	6.94	9.1	11.06	7.45	9.44	179.61	186.38

Table B52 a and b. Measurements derived from *Theropithecus ulnae*

TAXON	ULCBAS	ULCSTY	ULASTY	ULPXAB	ULPXAC	ULPXBC	ULPXDE	ULPXDC	ULPXAR	ULPXFG	ULPXFH
<i>Theropithecus gelada</i>	223	240	215	14.8	32.2	20.8	13.2	22.2	16.1	29.9	22.2
<i>Theropithecus gelada</i>	230.5	233	213	16	31	19.5	14.3	21.5	16.5	30.5	21
<i>Theropithecus gelada</i>	197	203	182	15.3	26.8	15.3	11.2	16.5	14.6	26.3	19.8
<i>Theropithecus gelada</i>	237	242.5	216.5	16.5	32.5	19.5	14	20	16.7	28.5	21.5
Cf. <i>Theropithecus oswaldi</i>				17.8	33.1	19.3	16	20	19.2	31.5	23
Cf. <i>Theropithecus oswaldi</i>				22.2	41.6	25	16.9	25.5	21.2	37.7	27.8
<i>Theropithecus oswaldi</i>				20.5	35	17	17	20.5	24	40	27
<i>Theropithecus oswaldi</i>				21.5	27	20.5	15.5	24.5	22.5	35.5	26.5
<i>Theropithecus oswaldi cf. leakeyi</i>				20	46	33	23	30	26	46	30
<i>Theropithecus oswaldi cf. darti</i>				13.9	24.9	15.4	12.6	15.2	13.7	22	15.1
<i>Theropithecus oswaldi cf. darti</i>				18	30	16.5	14	18.2	15.5	28.2	21
<i>Theropithecus oswaldi cf. darti</i>				12	34.2	20.3	14	21.2	18	30	21.2
<i>Theropithecus oswaldi cf. darti</i>				13.5	26	14	11	16	14	25	18
<i>Theropithecus oswaldi cf. darti</i>				16	27.5	15		16.5		25.5	18.5
<i>Theropithecus oswaldi cf. darti</i>						18.2	14.1	17.5			
<i>Theropithecus oswaldi cf. darti</i>				17			13		16.5	25	19.5
Cf. <i>Theropithecus brumpti</i>				17.5	32.7	20.7	16	18.9	18.7	30	23.4

TAXON	ULPXRG	ULPXRF	ULPXA	UOLTRW	UOLAPW	UOLDEP	URADEP	UDSTYH	UDWXAP	UDWXTR
<i>Theropithecus gelada</i>	26	21.3	16.8	13	19	9.4	5.5			
<i>Theropithecus gelada</i>	26.2	23.7	17.6	14	18.5	8.5	4.8	5.8	13.4	9.5
<i>Theropithecus gelada</i>	22.2	18.9	15.9	10.8	14.2	7.4	4.2	4.9	11	8.1
<i>Theropithecus gelada</i>	23	22.5	18	13.5	19	8.5	4.3	5.5	12.5	9.4
Cf. <i>Theropithecus oswaldi</i>	28	24	20	12	17.3	9.4	4.3			
Cf. <i>Theropithecus oswaldi</i>	31.9	26	26.1	16	22.3	12.5	3.5			
<i>Theropithecus oswaldi</i>	34	30	24			11	5.5			
<i>Theropithecus oswaldi</i>	32	28	25.5	15	20.5	12				
<i>Theropithecus oswaldi cf. leakeyi</i>	40	31	24.5	18	26	13	5		18.5	14

<i>Theropithecus oswaldi cf. darti</i>	19.5	17	16.1	9.8	14.1	6.9	2.7			
<i>Theropithecus oswaldi cf. darti</i>	27	18	20	12.5	16.7	7.7	3.5			
<i>Theropithecus oswaldi cf. darti</i>	26.3	21.5	21	12	18.7	10	4.5			
<i>Theropithecus oswaldi cf. darti</i>	21	17.5	22	10.2	13.2	7.4	3.5			
<i>Theropithecus oswaldi cf. darti</i>			19.5	10		6.7				
<i>Theropithecus oswaldi cf. darti</i>	24.4			12	17.8					
<i>Theropithecus oswaldi cf. darti</i>	24.5	25	18.5			9.1	3			
<i>Cf. Theropithecus brumpti</i>	26.8	23	25.8	12.1	21.2	8.9	3.3			

Table B53. Measurements derived from *Theropithecus* femora

TAXON	FHEADAP	FHEADML	FHEADPD	FMAXML	FAP	FTR	FLENGTR	FLEN	FLENFOS
<i>Theropithecus gelada</i>	17.9	15.83	17.87	35.56	12.03	14.24	179.28	173.79	165.51
<i>Theropithecus gelada</i>					14	13.4		209	
<i>Theropithecus oswaldi cf. Leakeyi</i>					26	25		284	

## **QUANTITATIVE ANALYSIS OF THE STERKFORTEIN FOSSIL CERCOPITHECOIDEA POSTCRANIA**

Table B54. Measurements derived from *Parapapio* humeri

SPECIMEN NO	SWP 504	SWP 959	SWP 962	SWP1137	SWP 1165	SWP 1211	SWP 1262	SWP 1287	SWP 1540	SWP 4006	SWP 4047
SQUARE	D13	D13		U57	?	?	U52	?	?		
LEVEL				10'5"- 11'5"	?	?	12' 3" - 13' 3"		?		
Proximal medio-lateral dimension	27.93	32.92	27.88				?				
Humeral head diameter.	15.86	15.01	17.35								
Anterior-posterior length of humeral head	17.69	19.26	20.94								
Bio-epicondylar breadth	0		0		28.61	28.39	27.09	35.36	28	33.04	31.32
Greater tuberosity diameter	17.73	20.68	16.39	29.31	?	?	?	?	?		?
Medial trochlear flange length	0			16.89	14.27	10.27	15.15	19.27	16.22	17.57	19.34
Lateral epicondyle to medial edge of trochlea	0				25.6	26.4	25.2	33.24	26.87	27.32	26.24
Distal articular breadth	0			22.35	18.52	18.54	18.74	24.55	22.3	23.11	22.24
Proximal distal height of capitulum	0		0	12.76	12.38	12.82	?	15.79	14.86	13.03	12.76
Maximum medio-lateral length of olecranon fossa			0	12.86	11.23	12.56		15.79	13.39	13.2	12.69
Maximum proximo-distal length of olecranon fossa				8.86	7.02	10.02		10.89	11.51	11.62	8.71
Angle of medial epicondyle relative to			0	32	36	36		38	46	40	25



<b>axis of distal articular surface</b>											
<b>Medial epicondyle projection</b>				31	20.5	41	16.97	27	14	27	26

Table B55. Measurements derived from *Parapapio* radii

SPECIMEN NO	SWP 515	SWP 798	SWP 802	SWP 1139	SWP 1204	SWP 1219
SPQUARE	D15	D18	D13			V47
LEVEL						7' 10" - 8' 10"
Maximum diameter of radial head	17.73	14.26	17.19		14.28	16.13
Perpendicular breadth of radial head	15.4				12.74	15.24
Proximo distal height of radial neck	11.14	6	8.58	4.72	6.64	9.57
Proximo distal height of radial neck and head	17.65	11.75	15.59		11.81	16.19

Table B56. Measurements derived from *Parapapio* femora

<b>Specimen no</b>	<b>SWP 1300 (L)</b>
<b>Square</b>	<b>V62</b>
<b>Level</b>	<b>8'5"-9'5"</b>
<b>Anterior-Posterior head diameter</b>	18.99
<b>Medio-lateral breadth of femur head</b>	16.89
<b>Greater trochanter projection/height</b>	8.32
<b>Neck diameter</b>	18.15
<b>Femoral length</b>	
<b>Neck-shaft angle</b>	101
<b>Medial condyle width</b>	
<b>Lateral condyle width</b>	
<b>Lesser trochanter shape and direction</b>	

Table B57a and b. Measurements derived from *Papio* humeri

SPECIMEN NO	BP1/C 541	BP/3/23389	BP/3/24000	BP/3/31691	SWP 511	SWP 911	SWP 960	SWP967
SPQUARE		JAC	N46	JAC	D13	D13	D13	D13
LEVEL			17'5"-18'0"	Pp				
Length(maximum dist from the most proximal point on the head to the most distal point)	210				0	0		0
Proximal medio-lateral dimension	27.1				0	0		21.03
Bio-epicondylar Breadth	33.2		28.1		33.4	0		0
Greater tuberosity diameter	19.8			24.5	0	0	21.74	0
Medial trochlear flange length	16.9	13.6			16.95	0		0
Lateral epicondyle to medial edge of trochlea	30			13	31.69	0		0
Distal articular breadth	23.4	20.1		20.37	23.08	0		0
Fossa above capitulum	NO		no	15.34	no	0		0
Proximal distal height of capitulum	14.4	12.6	12.1	10.5	13.71	13.07	deep	0
Humeral head diameter.	18							8.73
Anterior-posterior length of humeral head	24.8						23.62	
Maximum medio-lateral length of olecranon fossa	15	12.5	14.5		13.39	15.5		0

Maximum proximo-distal length of olecranon fossa	9.8	9.4	9.5	11.9	7.65	9.3		0
Projection of greater tuberosity above the head	well above			10.05		0	slightly above	slightly above
Angle of medial epicondyle relative to axis of distal articular surface	40	38	9		17	0		0

SPECIMEN NO	SWP1137	SWP 1176	SWP 1201	SWP 1276	SWP 1406	SWP 1584	SWP 2810	SWP 4246
SPQUARE	U57	W46	W57	M4	D20	D20	D18	W57
LEVEL	10'5"-11'5"	3'11"-4'11"	9'2"-10'2"					7'5"-8'5"
Proximal medio-lateral dimension			23.59	27.56				0
Bio-epicondylar Breadth	29.31	35.81	0			31.44	28.3	28.14
Greater tuberosity diameter	0	0		16.4				0
Medial trochlea flange length	16.89	18.5				16.3		19.03
Lateral epicondyle to medial edge of trochlea	22.35	25.64				29.96	25.4	23.41

Distal articular breadth	25.08	20.28					17.7	20.04
Fossa above capitulum	depression	0				depression	NO	no
Proximal distal height of capitulum	12.76	10.87					12.8	0
Shaft curvature (weak or marked)	weak							weak
Humeral head diameter.			12.08		15.77			
Anterior-posterior length of humeral head			18.7	20.27	25.33			
Maximum medio-lateral length of olecranon fossa	12.86	10.02				14.8	11.6	13.04
Maximum proximo-distal length of olecranon fossa	8.86	4.41				9.77	8	9.21
Projection of greater tuberosity above the head	0	0	well above	above	well above			0
Angle of medial epicondyle relative to axis of distal articular surface	32	33				31		41

Table B58. Measurements derived from *Papio* radii

<b>SPECIMEN NO</b>	<b>BPI/C 541</b>	<b>SWP 514</b>	<b>SWP 517</b>	<b>SWP 791</b>	<b>SWP 793</b>	<b>SWP 803</b>	<b>SWP 1418</b>	<b>SWP 1552</b>
<b>SPQUARE</b>		<b>D13</b>	<b>D13</b>	<b>D18</b>		<b>D13</b>	<b>D20</b>	<b>D20</b>
<b>Maximum diameter of radial head</b>	16	15.81	14.68	13.3	18.06	16.01	15.5	17.73
<b>Perpendicular breadth of radial head</b>	14.9	13.97	13.88		14.12	13.55	15.29	15.87
<b>Proximo distal height of radial neck</b>	4.9	6.83	6.72	5.4	6.26	8.65	7.16	9.74
<b>Proximo distal height of radial neck and head</b>	12	10.58	13.87	10.31	12.74	14.61	11.8	16.15

Table B59. Measurements derived from *Papio* ulnae

<b>SPECIMEN NO</b>	<b>BP/3/23257</b>	<b>SWP 814</b>	<b>SWP 824</b>	<b>SWP 1155</b>	<b>SWP 1572</b>	<b>SWP 1577</b>
<b>SPQUARE</b>	JAC	<b>D13</b>	<b>D13</b>		D18	<b>D18</b>
Antero-posterior length of olecranon process	26.50	19	23.14		23.39	17.01
Proximo distal height of olecranon process	12.8	6.81	8.74		10.02	7.07
Medio-lateral breadth of olecranon process	10.5	10.55	9.11		11.71	9.75
Proximo distal height of trochlear notch	17.2	13.66	14.69		15.86	13.84



Table B60a. Measurements derived from *Papio/Parapapio* humeri

SPECIMEN NO	BP/3/23016	BP/3/23389	SWP 441	SWP 4038	SWP 1584	SWP 1199	SWP 1582	SWP 1542	sts 154
SPQUARE		JAC	N45	V37	D2	V57	D2	D2	
LEVEL	12' 6"- 13' 1"		31' 0" - 32' 0"	5' 0" 6'9"		10'3"-11'0"			
Proximal medio-lateral dimension						22.35			
Bio-epicondylar Breadth			28.36	28.6	31.44	17.45			
Greater tuberosity diameter						15.57			
Medial trochlear flange length	14.1	13.6	15.32	13.7	16.3				17
Lateral epicondyle to medial edge of trochlea	27.1		27.92	21.46	29.96		29.94		
Distal articular breadth	19.3	20.1	22..55	15.58			22.8		22
Fossa above capitulum	yes		no	no					
Proximal distal height of capitulum	12	12.6	12.13	12.09			13.34		1
Anterior-posterior length of humeral head						14.95			
Maximum medio-lateral length of olecranon fossa		12.5	12.63		14.8		12.77		
Maximum proximo-distal length of olecranon fossa		9.4	13.36		9.77				
Angle of medial epicondyle relative to axis of distal articular surface	38	38	28	28	31				1

Table B60b. Measurements derived from *Papio/Parapapio* humeri

SPECIMEN NO	BP/3/23016	SWP 4041	SWP 1199	SWP 1582	SWP 1542	SWP 1410	SWP 562	STS 377C	SWP 507
SPQUARE		N45	V57	D20	D20	D20	D14		D13
LEVEL	12' 6"- 13' 1"	31' 0" - 32' 0"	10'3"- 11'0"						
Length(maximum dist from the most proximal point on the head to the most distal point)									
Proximal medio-lateral dimension			22.35						
Bio-epicondylar Breadth		28.36				27.57	30.26	27	27.71
Greater tuberosity diameter			15.57						
Medial trochlear flange length	14.1	15.32				13.9	18.31	14	12.29
Lateral epicondyle to medial edge of trochlea	27.1	27.92		29.94		24.03	29.01	25	25.07
Distal articular breadth	19.3	22..55		22.8		19	26.74	15	18.74
Fossa above capitulum	yes	no							no
Proximal distal height of capitulum	12	12.13		13.34		12.03	11.9	9.9	8.92
Depth of bicipital groove			deep						
Humeral head diameter.			10						
Anterior-posterior length of humeral head			14.95						
Maximum medio-lateral length of olecranon fossa		12.63		12.77		1.7	11.5	14	10.6
Maximum proximo-distal length of olecranon fossa		13.36				11.91	12.26	11	10.6

Angle of medial epicondyle relative to axis of distal articular surface	38	28				35	27	25	45
---	----	----	--	--	--	----	----	----	----

Table B60c. Measurements derived from *Papio/Parapapio* humeri

SPECIMEN NO	SWP 1140	SWP 1141	SWP 995	SWP 912	SWP 1016	BP/3/18382	sts 1504	SWP 4038
SPQUARE	W46		D14	D13	D8	S54		
LEVEL	3'11"-4'11"							
Proximal medio-lateral dimension								
Bio-epicondylar Breadth	35.81			26.77	29.82	26		28.6
Greater tuberosity diameter								
Medial trochlear flange length	18.5			11.33	19.78		17	13.07
Lateral epicondyle to medial edge of trochlea	33.64			22.25	29.65	23		21.46
Distal articular breadth	20.28			18.67	18.57	20.5	22	15.58
Proximal distal height of capitulum	10.87		7.07	11.15	15.12	10.6	10	12.09
Shaft curvature (weak or marked)			weak					
Maximum medio-lateral length of olecranon fossa	10.02		8.01	10.71	12.87	10.5		
Maximum proximo-distal length of olecranon fossa	4.41		8.01	8.47	10.12	10.5		
Angle of medial epicondyle relative to axis of distal articular surface	33		18	19	40			28

Table B61a and b. Measurements derived from *Papio/Parapapio* ulna

<b>SPECIMEN NO</b>	<b>BP/3/23336</b>	<b>SWP 1569</b>	<b>SWP 524</b>	<b>SWP 853</b>	<b>SWP 1568</b>	<b>SWP 1570</b>	<b>SWP 1571</b>
<b>SQUARE</b>	<b>JAC</b>	<b>D18</b>	<b>D13</b>	<b>D13</b>	<b>D18</b>	<b>D18</b>	<b>D18</b>
Antero-posterior length of olecranon process				19.46		18.34	
Proximo distal height of olecranon process			8.35	9.31		8.94	3.98
Medio-lateral breadth of olecranon process	10		10.44	10.06	10.12	7.16	8.69
Proximo distal height of trochlear notch		15.83	14.73	13.68	11.37	12.91	12.87

<b>SPECIMEN NO</b>	<b>SWP 1576</b>	<b>SWP1580</b>	<b>SWP 1590</b>	<b>BP/3/31175</b>	<b>SWP 4008</b>	<b>SWP 4084</b>	<b>SWP 4015</b>
<b>SQUARE</b>	<b>D18</b>	<b>D18</b>	<b>D20</b>	<b>Jacovec Cavern</b>	<b>N45</b>	<b>W37</b>	<b>N45</b>
<b>LEVEL</b>					31' 0" - 32' 0"	4' 5" - 5' 2"	29' 1" - 30' 1"
Antero-posterior length of olecranon process			23.97			24.51	24.08
Proximo distal height of olecranon process		5.86				10.17	8.04
Medio-lateral breadth of olecranon process		9.16	11.94	11.78	10.9	11.06	10.46
Proximo distal height of trochlear notch	14.43	12.99	15.65	17.25	12.35	20.36	16.93

Anterior posterior length of distal end							
Medio-lateral breadth of distal end							
Proximo distal height of styloid process							

Table B21. Measurements derived from *Papio/Parapapio* radii

<b>SPECIMEN NO</b>	<b>SWP 518</b>	<b>SWP 1368</b>	<b>SWP 1519</b>	<b>SWP 255</b>	<b>SWP 506</b>
<b>SQUARE</b>	<b>D13</b>	<b>D20</b>	<b>D18</b>	<b>D13</b>	<b>D18</b>
Maximum diameter of radial head	15.61			17.08	14.74
Perpendicular breadth of radial head	14.6			15.31	13.15
Proximo distal height of radial neck			8.16		
Proximo distal height of radial neck and head			10.22		

Table B63a. Measurements derived from *Papio/Parapapio* femora

SPECIMEN NO	SWP 1700	SWP526	SWP 746	SWP 1085	SWP 1171	SWP 1203
<b>SQUARE</b>		<b>D13</b>	<b>D13</b>	<b>D20</b>	<b>V47</b>	
<b>LEVEL</b>					<b>5'10"-6'10"</b>	
<b>Anterior-Posterior head diameter</b>		18.62		19		18.16
<b>Medio-lateral breadth of femur head</b>		16.55		17.18		16.54
<b>Greater trochanter projection/height</b>	8.35			8.52		
<b>Neck diameter</b>	15.11	7.07		5.96		14.33
<b>Neck-shaft angle</b>	115	108		120		104
<b>Medial condyle width</b>						
<b>Lateral condyle width</b>	11					

Table B63b. Measurements derived from *Papio/Parapapio* femora

SPECIMEN NO	SWP 1263	SWP 531	SWP 1532 ®	SWP 533	SWP 1008	SWP 1206	SWP 1698	SWP 4103	SF5496
<b>SQUARE</b>		<b>D13</b>	<b>D20</b>	<b>D13</b>	<b>D14</b>	<b>T35</b>		<b>V37</b>	
<b>LEVEL</b>						<b>8'6"-9'5"</b>		<b>5' 0" - 6' 9:</b>	
<b>Anterior- Posterior head diameter</b>	18.73	18		18.57	17.53	18.04		18.93	16.1
<b>Medio-lateral breadth of femur head</b>	13.82	17.77		16.42	14.97		15.18	16.27	14.9
<b>Greater trochanter projection/height</b>							8.8		9



<b>Neck diameter</b>	16.99	15.52		17.53	13.87		14.44	17.01	11.8
<b>Bi-epicondylar breadth/width</b>			34.83						
<b>Patella surface rim height</b>			22.45						
<b>Position and shape of fovea capitus</b>	posterior oval	distal and oval		anterior rounded	Posterior oval	Posterior, oval	oval	oval elongated	
<b>Femoral length</b>									
<b>Neck-shaft angle</b>	114	125		118				110	
<b>Medial condyle width</b>			11.65						
<b>Lateral condyle width</b>			14.23						
<b>Lesser trochanter shape and direction</b>	medially	medial		medial					L

Table B64. Measurements derived from *Theropithecus* ulnae

SPECIMEN NO	SWP 1148	SWP 1578	SWP 1604	SWP 4001	SWP 1104	SWP 1110	SWP 1156	SF 3418	SWP 4084	SWP 822	SWP 825
SQUARE	Q46	D18	D18	d18	T46	Aa 48	T49	T45	W37	D13	D13
LEVEL	8'8"-9'8"				9'10 - 10'10"	4' 1" - 5' 1"	8'8"- 9'8"	18' 6" - 19' 6"	4' 5" - 5' 2"		
Antero-posterior length of olecranon process		20.26	27.32	28.03	25.92	25.88	18.23	25.45	24.51	19.37	15.91
Proximo distal height of olecranon process	8.3	10.38		13.61	14.34	13.75	7.38	7.14	10.17	8.77	6.44
Medio-lateral breadth of olecranon process	11.37	10.2		11.46	11.97	14.41	10.02	10.85	11.06	12.68	6.23
Proximo distal height of trochlear notch	16.82	15.34		16.52	16.62	8.07	13.65	15.52	20.36	11.66	11.21

Table B65. Measurements derived from *Theropithecus* femur

<b>SPECIMEN NO</b>	<b>SWP 1536</b>	<b>SWP 1697</b>	<b>SWP 4039</b>	<b>SWP 528</b>	<b>SWP1537</b>
<b>SQUARE</b>	<b>D20</b>	<b>D20</b>	<b>N49</b>	<b>D13</b>	<b>D20</b>
<b>LEVEL</b>			<b>25' 3" - 26' 3</b>		
Anterior-Posterior head diameter		19.23	19.19	18.86	22.27
Medio-lateral breadth of femur head		16.94	17.43	18.8	21.28
Greater trochanter projection/height	10.33	12.3	13.06	12.14	11.1
Neck diameter		16.69	16.8	16.93	19.17
Neck-shaft angle		110	100	100	106

## Papionina

Table B66. Measurements derived from *Papionina* humerus

SPECIMEN NO	SWP 1539	SWP 1543	SWP 1581	SWP 4099
SPQUARE	D20	D20	D20	V37
LEVEL				5' 0" - 6' 9"
Medial trochlear flange length		15.11		
Proximal distal height of capitulum	12.57	5.68	12.08	15.02
Angle of medial epicondyle relative to axis of distal articular surface		21		

Table B67. Measurements derived from *Papionina* humerus

<b>SPECIMEN NO</b>	<b>SF 1465</b>	<b>SWP 816</b>	<b>SWP 817</b>	<b>SWP 179</b>	<b>SWP 1213</b>	<b>SWP 1285</b>	<b>SWP 1561</b>	<b>SWP 1567</b>	<b>SWP 1575</b>	<b>SWP 4015</b>
<b>SQUARE</b>	<b>Q42</b>	<b>D13</b>			<b>R65</b>		<b>D20</b>	<b>D18</b>		<b>N45</b>
<b>LEVEL</b>	<b>11' 2" -12' 10"</b>				10'8- 11'8"					<b>29' 1" - 30' 1"</b>
Antero-posterior length of olecranon process			25.31			19.24	19.54			24.08
Proximo distal height of olecranon process			10.38			6.03				8.04
Medio-lateral breadth of olecranon process	11.94	11.40	10.84	9.72		11.28	10.80			10.46
Proximo distal height of trochlear notch	15.86		17.00		12.89	13.01	11.31	13.17	10.15	16.93

Table B68a. Measurements derived from *Papionina* radius

<b>SPECIMEN NO</b>	<b>STS Unnumbered</b>	<b>SWP 255</b>	<b>SWP 506</b>	<b>SWP 516</b>	<b>SWP 519</b>	<b>SWP 520</b>	<b>SWP 1553</b>	<b>SWP 792</b>	<b>SWP 797</b>	<b>SWP 799</b>
<b>SQUARE</b>		<b>D13</b>	<b>D18</b>	<b>D13</b>	<b>D18</b>	<b>D20</b>	<b>MYR 41</b>	<b>D3</b>	<b>D13</b>	
<b>LEVEL</b>							8' 10" - 9' 10"			
<b>Maximum diameter of radial head</b>	17	17.08	14.74	17.93	13.25	14.99	14.96	15.8	15.79	16.75
<b>Perpendicular breadth of radial head</b>	15	15.31	13.15	16.16	12.28	13.37				
<b>Proximo distal height of radial neck</b>	9			8.62	7.76	6.93		9.16		5
<b>Proximo distal height of radial neck and head</b>	15			14.87	11.64	11.78		15.04		10.69

Table B68b. Measurements derived from *Papionina* radius continued

<b>SPECIMEN NO</b>	<b>SWP 806</b>	<b>SWP 808</b>	<b>SWP 972</b>	<b>SWP 979</b>	<b>SWP 1125</b>	<b>SWP 1139</b>	<b>SWP 1198</b>	<b>SWP 1306</b>	<b>SWP 1416</b>	<b>SWP 4059</b>	<b>SWP 4063</b>	<b>SWP 4087</b>	<b>SF 2689</b>
<b>SQUARE</b>	<b>D13</b>	<b>D13</b>	<b>D13</b>	<b>D13</b>	<b>O45</b>		<b>V57</b>	<b>W59</b>	<b>D20</b>	<b>p49</b>	<b>P 45</b>	<b>W37</b>	<b>S46</b>
<b>LEVEL</b>					<b>13' 3"- 13' 11"</b>					<b>28' 0" – 29' 0</b>	<b>32' 1" - 33' 1"</b>	<b>4' 5" - 5' 2"</b>	<b>22' 7" - 23' 7"</b>
<b>Maximum diameter of radial head</b>		16.38	17.14	15.06	16.42			18.02	19.52	13.62			
<b>Perpendicular breadth of radial head</b>			15.58	13.35						12.88			
<b>Proximo distal height of radial neck</b>	9.44	6.27	9.55	7.95	8.89	4.72	5.43	8.46	10.41		5.05	7.19	5.06
<b>Proximo distal height of radial neck and head</b>	13.71	12.91	17.28	12.39	13.95			15.04	15.81			12.52	

Table B69. Measurements derived from *Papionina* femur

SPECIMEN NO	SWP 527	SWP 529	SWP530	SWP 1384	SWP 1532	SWP 1534	SWP 1699	SWP 1704	SWP 4035
SQUARE	D13	D14	D13	D20	D20	D20	D20	D20	W37
LEVEL				R					4' 5" - 5' 2"
Anterior-posterior head diameter		19.43		17.3			17.49	16.41	18.31
Medio-lateral breadth of femur head	13.43	14.79	17.93	12.22			16.18	13.54	17.68
Greater trochanter projection/height								7.73	
Neck diameter	15	15.39	17.21				17	13.49	13.33
Bi-epicondylar breadth/width					34.83	36.9			
Patella surface rim height					22.45	27.5			
Neck-shaft angle	120								112
Medial condyle width					11.65				
Lateral condyle width					14.23	13			



*Cercopithecus sp*

Table B70. Measurements derived from *Cercopithecus sp* radius

SPECIMEN NO	BPI/C 294	SWP 4012
SQUARE		X36
LEVEL		3' 2" - 4' 9"
Maximum diameter of radial head	10	13.99
Perpendicular breadth of radial head	9	9.35
Proximo distal height of radial neck	8.5	4.21
Proximo distal height of radial neck and head	13	8.11

*Cercopithecoides* sp

Table B71. Measurements derived from *Cercopithecoides* femur

SPECIMEN NO	SWP 883
SQUARE	D13
Anterior-Posterior head diameter	18
Medio-lateral breadth of femur head	15.63
Greater trochanter projection/height	
Neck diameter	8.61

**TABLES**

Table C1 Fossil cercopithecoid taxa identified in the Sterkfontein deposits based on post crania.

Taxa	Jacovec	Silberberg	M4	StW53	Oldowan	M5West	M6
<i>Papio</i>	x	x	x	x	x		x
<i>Parapapio</i>		x	x	x		x	
<i>Papio/Parapapio</i>	x	x	x	x	x		
<i>cf. Theropithecus</i>			x	x			
<i>Cercopithecus sp</i>		x	x				x
<i>Cercopithecus aethiops</i>			x				x
<i>Cercopithecoides</i>			x				
<i>Colobinae indet</i>			x	x			
<i>Colobus sp</i>							

TABLES C2-C18. Sterkfontein caves skeletal element frequencies, NISP/MNE/cMNI.

Legend

cMNI	cumulative Minimum Number of Individuals
M	Medium
MNE	Minimum Number of Elements
NISP	Number of Identified Specimens
S	Small
Vert	Vertebrae

Table C2. Sterkfontein Caves combined skeletal frequencies, NISP

Element	NISP
Humerus	<b>228</b>
Ulna	<b>181</b>
Radius	<b>167</b>
Femur	<b>349</b>
Tibia	<b>98</b>
Fibula	<b>18</b>
Rib	<b>35</b>
Vert	<b>71</b>
Scapula	<b>24</b>
Pelvis	<b>66</b>
Patella	<b>11</b>
Sternum	<b>5</b>
Clavicle	<b>10</b>
Metacarpal	<b>17</b>
Metatarsal	<b>41</b>
Metapodial	<b>22</b>
Phalanges	<b>20</b>
Talus	<b>39</b>
Calcaneus	<b>79</b>
Carpals	<b>2</b>
Tarsals	<b>13</b>
Long bones	<b>34</b>
<b>Total</b>	<b>1510</b>

Table C3. Jacovec Cavern skeletal frequencies, current study.

Element	NISP	MNE	cMNI
Humerus	14	10	9
Ulna	16	9	5
Radius	22	17	10
Femur	14	11	8
Tibia	8	7	4
Fibula	8	7	4
Rib	4	3	2
Vert	10	10	4
Scapula	5	5	3
Pelvis	5	5	3
Patella	3	3	2
Sternum	2	1	1
Clavicle	7	6	3
Metacarpal	9	9	4
Metatarsal	14	14	5
Metapodial	7	6	3
Phalanges	24	24	3
Talus	2	2	2
Calcaneus	2	2	2
Carpals			
Tarsals	6	6	3

Table C4. Jacovec Cavern skeletal frequencies (after Kibii 2004).

Element	NISP (M/S)	MNE (M/S)E	cMNI (M/S)
Humerus	3/6	2/4	1/3
Ulna	11/3	8/2	4/1
Radius	10/7	6/5	4/3
Femur	7/5	5/5	3/3
Tibia	3/4	3/3	2/2
Fibula	0/4	0/2	0/1
Rib	0	0	0
Vert	0/5	0/5	0/1
Scapula	1/3	1/3	½
Pelvis	1/1	1/1	1/1
Patella	2/1	2/1	1/1
Sternum	0	0	0
Clavicle	/3	/3	/2
Metacarpal	4/5	4/5	1/3
Metatarsal	11/1	11/1	4/1
Metapodial			
Phalanges	9/14	9/13	1/1
Talus	/2	/2	/1
Calcaneus	1/1	1/1	1/1
Carpals			
Tarsals	4/2	4/2	2/1

Table C5. Silberberg Grotto skeletal frequencies, current study

Element	NISP	MNE	cMNI
Humerus	23	19	12
Ulna	18	12	8
Radius	10	9	7
Femur	55	28	13
Tibia	10	4	4
Fibula	0	0	0
Rib	0	0	0
Vert	0	0	0
Scapula	0	0	0
Pelvis	9	7	4
Patella	0	0	0
Sternum	0	0	0
Clavicle	0	0	0
Metacarpal	0	0	0
Metatarsal	0	0	0
Metapodial	3	2	2
Phalanges	3	3	2
Talus	3	3	2
Calcaneus	3	3	1
Carpals	0	0	0
Tarsals	0	0	0

Table C6. Member 2 Main excavation skeletal frequencies by Pickering *et al.* (2004)

Element	NISP	MNE	cMNI
Humerus	8	7	6
Ulna	1	1	1
Radius	1	1	1
Femur	9	6	4
Tibia	7	4	3
Fibula	0	0	0
Rib	3	3	1
Vert	7	7	2
Scapula	0	0	0
Pelvis	8	7	4
Patella	0	0	0
Sternum	0	0	0
Clavicle	1	1	1
Metacarpal	0	0	0
Metatarsal	3	3	1
Metapodial	0	0	0
Phalanges	0	0	0
Talus	0	0	0
Calcaneus	5	5	1
Carpals			
Tarsals	5	5	5



Table C7. Member 4 deposit skeletal frequencies, current study.

Element	NISP	MNE	cMNI
Humerus	173	86	46
Ulna	131	82	45
Radius	128	74	40
Femur	274	89	52
Long bone	34		
Tibia	64	42	26
Fibula	9	6	4
Rib	4	4	1
Vert	25	22	3
Scapula	16	11	9
Pelvis	49	26	17
Patella	7	7	4
Sternum	1	1	1
Clavicle	3	3	3
Metacarpal	2	2	1
Metatarsal	24	23	5
Metapodial	10	8	2
Phalanges	10	10	7
Talus	21	21	14
Calcaneus	19	18	2
Carpals	4	4	2
Tarsals	5	5	2

Table C8. Member 4 deposit skeletal frequencies by Kibii (2004).

Element	NISP	MNE	cMNI
Humerus	14	8	7
Ulna	18	11	7
Radius	7	6	5
Femur	14	10	6
Long bone	?	?	?
Tibia	10	8	6
Fibula	2	2	2
Rib	0	0	0
Vert	11	11	9
Scapula	8	8	7
Pelvis	22	19	14
Patella	2	2	1
Sternum	0	0	0
Clavicle	0	0	0
Metacarpal	7	7	4
Metatarsal	8	8	6
Metapodial	0	0	0
Talus	5	5	4
Calcaneus	4	4	4
Phalanges	11	11	3
Carpals			
Tarsals	2	2	2

Table C9. StW 53 Infill skeletal frequencies, current study

Element	NISP	MNE	cMNI
Humerus	5	3	2
Ulna	4	3	2
Radius	5	5	4
Femur	1	1	1
Tibia	6	4	3
Fibula	0	0	0
Rib	4	2	1
Vert	4	3	1
Scapula	0	0	0
Pelvis	0	0	0
Patella	1	1	1
Sternum	0	0	0
Clavicle	0	0	0
Metacarpal	0	0	0
Metatarsal	1	1	1
Metapodial	2	1	1
Phalanges	0	0	0
Talus	4	4	3
Calcaneus	2	2	1
Carpals	0	0	0
Tarsals	0	0	0

Table C10. StW 53 infill skeletal frequencies by Pickering 1999

Element	NISP	MNE	cMNI
Humerus	2	2	1
Ulna	2	1	1
Radius	0	0	0
Femur	0	0	0
Tibia	6	2	1
Fibula	0	0	0
Rib	0	0	0
Vert	3		
Scapula	0	0	0
Pelvis	0	0	0
Patella	1	1	1
Sternum	0	0	0
Clavicle	0	0	0
Metacarpal	0	0	0
Metatarsal	0	0	0
Metapodial	2	2	2
Phalanges	2	2	2
Talus	3	3	2
Calcaneus	0	0	0
Carpals	0	0	0
Tarsals	1	1	1

Table C11. Oldowan Infill skeletal frequencies, current study.

Element	NISP	MNE	cMNI
Humerus	6	4	3
Ulna	7	6	5
Radius	2	2	2
Femur	3	2	1
Tibia	4	3	2
Fibula	1	1	1
Rib	21	9	1
Vert	26	19	1
Scapula	1	1	1
Pelvis	1	1	1
Patella	0	0	0
Sternum	0	0	0
Clavicle	0	0	0
Metacarpal	6	6	3
Metatarsal	2	2	2
Metapodial	0	0	0
Phalanges	2	2	2
Talus	5	5	3
Calcaneus	7	7	1
Carpals	0		
Tarsals	2	2	1

Table C12. Oldowan Infill skeletal frequencies by Pickering 1999

Element	NISP	MNE	cMNI
Humerus	3	2	2
Ulna	6	6	5
Radius	3	3	2
Femur	2	2	2
Tibia	4	3	2
Fibula	1	1	1
Rib	22	10	1
Vert	26	19	1
Scapula	1	1	1
Pelvis	1	1	1
Patella	0	0	0
Sternum	0	0	0
Clavicle	0	0	0
Metacarpal	0	0	0
Metatarsal	2	2	1
Metapodial	10	6	1
Phalanges	2	2	2
Talus	4	4	3
Calcaneus	0	0	0
Carpals	0	0	0
Tarsals	1	1	1

Table C13. Member 5 West deposit skeletal frequencies, current study.

Element	NISP	MNE	cMNI
Humerus	2	2	1
Ulna	1	1	1
Radius	0	0	0
Femur	2	1	1
Tibia	1	1	1
Fibula	0		
Rib	2	1	1
Vert	4	4	1
Scapula	0		
Pelvis	0		
Patella	1	1	1
Sternum	0		
Clavicle	0		
Metacarpal	0		
Metatarsal	0		
Metapodial	0		
Phalanges	2	2	2
Talus	2	2	2
Calcaneus	1	1	1
Carpals			
Tarsals			

Table C14. Member 5 West deposit skeletal frequencies by Pickering (1999).

Element	NISP	MNE	cMNI
Humerus	0	0	0
Ulna	1	1	1
Radius			
Femur			
Tibia	1	1	1
Fibula			
Rib	2	1	1
Vert	1	1	1
Scapula			
Pelvis			
Patella			
Sternum			
Clavicle			
Metacarpal			
Metatarsal			
Metapodial			
Phalanges	1	1	1
Talus	2	2	2
Calcaneus			
Carpals			
Tarsals			

Table C15. Member 6 skeletal frequencies, current study

Element	NISP	MNE	cMNI
Humerus	1	1	1
Ulna	0	0	0
Radius	0	0	0
Femur	0	0	0
Tibia	0	0	0
Fibula	0	0	0
Rib	0	0	0
Vert	0	0	0
Scapula	0	0	0
Pelvis	0	0	0
Patella	0	0	0
Sternum	0	0	0
Clavicle	0	0	0
Metacarpal	0	0	0
Metatarsal	0	0	0
Metapodial	0	0	0
Phalanges	1	1	1
Talus	0	0	0
Calcaneus	0	0	0
Carpals	0	0	0
Tarsals	0	0	0

Table C16. Member 6 skeletal frequencies by Ogola (2009)

Element	NISP	MNE	cMNI
Humerus	0	0	0
Ulna	0	0	0
Radius	0	0	0
Femur	0	0	0
Tibia	0	0	0
Fibula	0	0	0
Rib	0	0	0
Vert	0	0	0
Scapula	0	0	0
Pelvis	0	0	0
Patella	0	0	0
Sternum	0	0	0
Clavicle	0	0	0
Metacarpal	0	0	0
Metatarsal	0	0	0
Metapodial	0	0	0
Phalanges	1	1	1
Talus	0	0	0
Calcaneus	0	0	0
Carpals	0	0	0
Tarsals	0	0	0

Table C17. Post Member 6 skeletal frequencies, current study

Element	NISP	MNE	cMNI
Humerus	4	3	3
Ulna	5	4	4
Radius	0	0	0
Femur	0	0	0
Tibia	4	4	3
Fibula	0	0	0
Rib	0	0	0
Vert	2	2	1
Scapula	0	0	0
Pelvis	1	1	1
Patella	0	0	0
Sternum	2	1	1
Clavicle	0	0	0
Metacarpal	0	0	0
Metatarsal	0	0	0
Metapodial	0	0	0
Phalanges	0	0	0
Talus	3	3	3
Calcaneus	1	1	1
Carpals	0	0	0
Tarsals	0	0	0

Table C18. Post Member 6 skeletal frequencies, Ogola, 2009.

Element	NISP	MNE	cMNI
Humerus	2	2	2
Ulna	2	2	2
Radius	0	0	0
Femur	0	0	0
Tibia	3	3	3
Fibula	0	0	0
Rib	0	0	0
Vert	2	2	2
Scapula	0	0	0
Pelvis	1	1	1
Patella	0	0	0
Sternum	0	0	0
Clavicle	0	0	0
Metacarpal	0	0	0
Metatarsal	0	0	0
Metapodial	0	0	0
Phalanges	0	0	0
Talus	3	3	3
Calcaneus	0	0	0
Carpals	0	0	0
Tarsals	0	0	0

Table C19. Sterkfontein fossil cercopithecoid postcrania carnivore modification tooth pit dimensions

		SF4217		SF 1465	SWP 377d			SWP 526	SWP 531			SWP 756	SWP 896	SWP 1351	SWP 1416
<b>Pit</b>	<b>Epiphysis</b>														
	Length	4.73	4.98	5.68							3.44				
	Breadth	4.3	4.39	4.88							2.43				
	<b>Diaphysis</b>														
	Length				2.9	2.1	5	3.74	2.95	3.42			8.46	5.9	7.25
	Breadth				2.2	1.9	3.5	2.18	2.83	2.56			1.45	4.34	6.66
<b>Score</b>	<b>Epiphysis</b>														
	Length	7.54													
	Breadth	4.77													
	<b>Diaphysis</b>														
	Length											9.06			
	Breadth											5.67			

Table C19 continued.

		<b>SWP 1104</b>			<b>SWP 1119</b>	<b>SWP 1137</b>		<b>SWP 1140</b>			<b>SWP 1206</b>		<b>SWP 1263</b>	<b>SWP 1271</b>	
<b>Pit</b>	<b>Epiphysis</b>														
	Length				3.94	5.94	6.99	7.01	6.99	7.99	7.63	5.66	6.13	6.18	7.01
	Breadth				2.2	4.99	4.02	5.02	5.02	5.01	5.66	1.66	4.86	5.09	4.98
	<b>Diaphysis</b>														
	Length	7.76	4.51	5.34											
	Breadth	4.51	3.74	4.47											
<b>Score</b>	<b>Epiphysis</b>														
	Length														
	Breadth														
	<b>Diaphysis</b>														
	Length														
	Breadth														



Table C20. Sterkfontein fossil cercopithecoid postcrania tooth pit true population mean

	<b>Epiphysis</b>		<b>Diaphysis</b>	
<b>Statistics</b>	<b>Length</b>	<b>Breadth</b>	<b>Length</b>	<b>Breadth</b>
<b>mean</b>	6.02	4.3	4.94	3.36
<b>Standard deviation</b>	1.320	1.212	2.064	1.477
<b>95 % confidence interval</b>	$\pm 0.67$	$\pm 0.61$	$\pm 1.17$	$\pm 0.84$
<b>True population mean</b>	5.35-6.69	3.69-4.91	3.77-6.11	2.52-4.2

Table C21. Ordinary Least Squares Regression: maximum medio-lateral width of olecranon fossa (HDTROW) and width distal humeral articulation (HDTRWA)

Slope a:	0.49362	Std. error a:	0.024689
Intercept b:	1.9193	Std. error b:	0.57779
95% bootstrapped confidence intervals (N=1999):			
Slope a:	(0.43933, 0.55081)		
Intercept b:	(0.60318, 3.1963)		
Correlation:			
r:	0.87531		
r <sup>2</sup> :	0.76616		
t:	19.993		
p (uncorr.):	2.621E-40		
Permutation p:	0.0001		

Table C22. Ordinary Least Squares Regression: humeral head diameter/medio-lateral width (HHDWTR) and humeral head anterior-posterior length (HHDWAP).

Slope a:	0.77561	Std. error a:	0.041235
Intercept b:	4.7615	Std. error b:	1.0656
95% bootstrapped confidence intervals (N=1999):			
Slope a:	(0.71407, 0.84452)		
Intercept b:	(2.9419, 6.429)		
Correlation:			
r:	0.90309		
r <sup>2</sup> :	0.81558		
t:	18.809		
p (uncorr.):	4.214E-31		
Permutation p:	0.0001		

Table C23. Ordinary Least Squares Regression: Maximum medio-lateral length of olecranon fossa-Maximum proximo-distal length of olecranon fossa

Slope a:	0.37746	Std. error a:	0.1271
Intercept b:	5.1001	Std. error b:	1.6041
95% bootstrapped confidence intervals (N=1999):			
Slope a:	(0.040741, 0.66999)		
Intercept b:	(1.2525, 9.6418)		
Correlation:			
r:	0.42944		
r <sup>2</sup> :	0.18442		
t:	2.9696		
p (uncorr.):	0.0050795		
Permutation p:	0.0059		

Table C24. Ordinary Least Squares Regression: HDTRWA-HDTRWT

Slope a:	0.59901	Std. error a:	0.018844
Intercept b:	-0.60208	Std. error b:	0.44309
95% bootstrapped confidence intervals (N=1999):			
Slope a:	(0.55373, 0.6567)		
Intercept b:	(-2.0053, 0.46189)		
Correlation:			
r:	0.94922		
r <sup>2</sup> :	0.90102		
t:	31.788		
p (uncorr.):	1.4204E-57		
Permutation p:	0.0001		

Table C25. Ordinary Least Squares Regression: HDTRWX-HDTRWA

Slope a:	0.74738	Std. error a:	0.02241
Intercept b:	-2.35	Std. error b:	0.7259
95% bootstrapped confidence intervals (N=1999):			
Slope a:	(0.71724, 0.77882)		
Intercept b:	(-3.5043, -1.3251)		
Correlation:			
r:	0.95277		
r <sup>2</sup> :	0.90777		
t:	33.35		
p (uncorr.):	2.5666E-60		
Permutation p:	0.0001		

Table C26. Ordinary Least Squares Regression: Antero-posterior length of olecranon process and proximo distal height of olecranon process

Slope a:	-0.32169	Std. error a:	0.13669
Intercept b:	18.808	Std. error b:	2.6477
95% bootstrapped confidence intervals (N=1999):			
Slope a:	(-0.55955, -0.079748)		
Intercept b:	(13.254, 24.371)		
Correlation:			
r:	-0.33437		
r <sup>2</sup> :	0.1118		
t:	-2.3534		
p (uncorr.):	0.023134		
Permutation p:	0.0237		

Table C27. Ordinary Least Squares Regression: Proximo-distal height of olecranon process and proximo-distal height of trochlea notch

Slope a:	-0.0001224	Std. error a:	0.057614
Intercept b:	12.344	Std. error b:	1.7584
95% bootstrapped confidence intervals (N=1999):			
Slope a:	(-0.09163, 0.073469)		
Intercept b:	(10.081, 14.418)		
Correlation:			
r:	-0.00030045		
r2:	9.0271E-08		
t:	-0.0021245		
p (uncorr.):	0.99831		
Permutation p:	0.998		

Table C28. Ordinary Least Squares Regression: Femur head anterior posterior length and femur medio-lateral width

Ordinary Least Squares Regression: FHEADAP-FHEADML			
Slope a:	0.65642	Std. error a:	0.10077
Intercept b:	3.9572	Std. error b:	1.9649
95% bootstrapped confidence intervals (N=1999):			
Slope a:	(0.4153, 0.92826)		
Intercept b:	(-1.0237, 8.7607)		

Correlation:  
r: 0.62555  
r2: 0.39132  
t: 6.5139  
p (uncorr.): 1.1743E-08  
Permutation p: 0.0001